SHORT PAPERS IN—

Economic geology

Geochemistry

Geochronology

Ground water

Hydrologic techniques

Limnology

Mineralogy

Paleontology

Petrology

Quality of water

Sedimentation

Stratigraphy

Structural geology

Surface water

Volcanology

GEOLOGICAL SURVEY RESEARCH 1972

Chapter D

GEOLOGICAL SURVEY PROFESSIONAL PAPER 800–D

GEOLOGICAL SURVEY RESEARCH 1972

Chapter D

GEOLOGICAL SURVEY PROFESSIONAL PAPER 800–D

Scientific notes and summaries of investigations in geology, hydrology, and related fields

UNITED STATES GOVERNMENT PRINTING OFFICE, WASHINGTON: 1972

UNITED STATES DEPARTMENT OF THE INTERIOR

ROGERS C. B. MORTON, Secretary

GEOLOGICAL SURVEY

V. E. McKelvey, Director

For sale by the Superintendent of Documents, U.S. Government Printing Office, Washington, D.c. 20402 - Price $4.50 (paper cover)

Stock Number 2401-00255

CONTENTS

GEOLOGIC STUDIES

HYDROLOGIC STUDIES

INDEXES

GEOLOGICAL SURVEY RESEARCH 1972

This collection of 30 short papers is the third published chapter of "Geological Survey Research 1972." The papers report on scientific and economic results of current work by members of the Geologic and Water Resources Divisions of the U.S. Geological Survey.

Chapter A, to be published later in the year, will present a summary of significant results of work done in fiscal year 1972, together with lists of investigations in progress, cooperating agencies, and Geological Survey offices.

"Geological Survey Research 1972" is the thirteenth and last volume of the annual series Geological Survey Research. The short-papers chapters (B, C, and D) will be replaced in 1973 by the "Journal of Research of the U.S. Geological Survey," and the summary chapter (A) will be published as a separate professional paper. The twelve volumes already published are listed below, with their series designations.

Geological Survey Research	*Prof. Paper*
1960	400
1961	424
1962	450
1963	475
1964	501
1965	525
1966	550
1967	575
1968	600
1969	650
1970	700
1971	750

GRAVINA-NUTZOTIN BELT—TECTONIC SIGNIFICANCE OF AN UPPER MESOZOIC SEDIMENTARY AND VOLCANIC SEQUENCE IN SOUTHERN AND SOUTHEASTERN ALASKA

By H. C. BERG, D. L. JONES; and D. H. RICHTER,
Menlo Park, Calif.; Anchorage, Alaska

Abstract.—Rocks of the Gravina-Nutzotin belt in southern and southeastern Alaska consist dominantly of marine flyschlike argillite and graywacke, minor nonmarine strata, and interbedded andesitic volcanic rocks. Fossils from the belt range in age from Late Jurassic (Oxfordian) to late Early Cretaceous (Albian), although some may be as old as Bajocian. The volcanic rocks comprise thick lenses that intertongue with and overlie both the oldest and youngest sedimentary beds known in the belt. Gravina-Nutzotin strata depositionally overlie upper Paleozoic and Triassic rocks (Taku-Skolai terrane) in the northwestern and central parts of the belt, and lower Paleozoic to Triassic rocks (Alexander terrane) in the central and southeastern parts. They are in fault contact with metamorphosed Paleozoic rocks (Yukon terrane) along the Denali fault. Rocks in the northern part of the belt are moderately deformed and relatively unmetamorphosed. In the southeastern part they are intensely folded and regionally metamorphosed, and probably overthrust by older rocks of the Taku-Skolai terrane. Upper Mesozoic and Cenozoic granitic plutons and zoned ultramafic complexes have intruded the belt and adjacent terranes. The Gravina-Nutzotin belt is part of a deformed upper Mesozoic magmatic arc. In southern Alaska, partly coeval shallow-marine (Matanuska-Wrangell terrane) and deep-marine (younger Chugach terrane) sedimentary rocks may correspond respectively to an arc-trench gap assemblage formed on the continental shelf and slope and an oceanic trench assemblage formed at the continental margin. The relatively strong deformation of the Gravina-Nutzotin belt in southeastern Alaska may be the result of northeastward movement of the Alexander terrane, a displaced fragment of older continental crust.

A narrow belt of Middle(?) Jurassic to middle-Cretaceous sedimentary and volcanic rocks extends almost continuously from southeastern Alaska to the eastern Alaska Range, a distance of over 700 miles. This belt, herein called the Gravina-Nutzotin belt after geographic features at its presently known extremities, comprises a thick prism of flyschlike sedimentary rocks, subordinate andesitic volcanic and volcaniclastic rocks, and minor granitic and ultramafic rocks. Rocks throughout the belt are moderately to intensely deformed and, in the southeastern part, metamorphosed in the greenschist facies.

The existence of this belt in southeastern Alaska has long been known (Buddington and Chapin, 1929; Brew and others, 1966), but its continuation across the Chatham Strait fault through the southwest corner of Yukon Territory and into the eastern Alaska Range hitherto has not been recognized. The near continuity of this belt from southeastern Alaska to the Alaska Range thus is highly important in linking the geologic history of these large areas that had previously been treated as separate geologic provinces.

This report describes the sedimentary and volcanic rocks of the Gravina-Nutzotin belt in several places in order to document their gross similarity throughout the belt, compares these rocks with two other upper Mesozoic terranes of coeval, but dissimilar, bedded rocks in nearby parts of southern and southeastern Alaska, and, finally, speculates on the origin and relations of these three sequences in terms of plate-tectonic theory.

During our analysis of the late Mesozoic history of this region, it became apparent that great differences exist in the character and age of basement rocks that underlie or abut the Gravina-Nutzotin belt. In order to express these differences more clearly, we have found it useful to organize these rocks into discrete tectonic units. In the first part of this report, we summarize the salient features of these subjacent terranes and speculate briefly on their origin; in the second part, we consider their significance in the evolution of the three upper Mesozoic superjacent terranes.

This report is a direct outgrowth of a reconnaissance by Berg and Jones in 1971 of Mesozoic and upper Paleozoic rocks from Ketchikan to Juneau and also draws on detailed work by Berg in the Ketchikan area, by A. B. Ford and D. A. Brew in the Juneau area, by E. M. MacKevett, Jr., and G. D. Robinson near Haines, and by Richter and Jones in the eastern Alaska Range.

SUBJACENT TERRANES

Upper Mesozoic rocks of the Gravina-Nutzotin belt were deposited on two different basement terranes and are in fault contact with a third terrane. Those in depositional contact are

herein informally designated the Taku-Skolai terrane and the Alexander terrane. The third is called the Yukon terrane. Distribution of these terranes is shown on figure 1.

Taku-Skolai terrane.—Upper Paleozoic (mainly Permian) andesitic and minor basaltic volcanic and volcaniclastic rocks are the oldest known in the Taku-Skolai terrane. They have been extensively studied by Richter (1971a, 1971b, and unpub. data) in the eastern Alaska Range and by Smith and MacKevett (1970) in the adjoining Wrangell Mountains. These volcanic rocks are associated with abundant mafic and alpine-type ultramafic rocks in the central Alaska Range (Clark and others, 1972) and in the Kluane Ranges in Canada (Muller, 1967) and have been interpreted by Richter and Jones (1972b) as vestiges of an upper Paleozoic island arc formed directly on oceanic crust.

Overlying the Permian volcanic rocks is a thick sequence of Permian sedimentary rocks and Triassic volcanic and sedimentary (mainly calcareous) rocks (MacKevett, 1970, 1971; Richter, 1971a, 1971b). Similar rocks crop out to the southeast near Kluane Lake (Muller, 1967) and Dezadeash Lake (Kindle, 1953), and they probably occur in the Squaw Creek—Rainy Hollow area (Watson, 1948).

Distribution and character of the Taku-Skolai terrane in southeastern Alaska are poorly known. The presence there of this terrane is substantiated by Permian and Triassic fossils associated with volcanic rocks, argillite, and marble in a number of localities (fig. 1) along the eastern margin of the Gravina-Nutzotin belt. Throughout much of this region, however, intense deformation and metamorphism have obliterated the preorogenic history.

Metamorphosed bedded and intrusive rocks of late(?) Paleozoic or early Mesozoic age on southern Duke, Annette, and Gravina Islands in southeastern Alaska (figs. 1 and 2) are provisionally assigned to the Taku-Skolai terrane because they are grossly similar in lithology to other rocks of this terrane. The Gravina Island occurrence is too small to show on figure 1.

A depositional contact between Gravina-Nutzotin rocks and the Taku-Skolai terrane can be observed in the northwest part of the belt (Richter and Schmoll, 1972) but cannot be demonstrated in the southeast part where Late Cretaceous or Cenozoic deformation has emplaced older rocks on top of Gravina-Nutzotin rocks in what may be an eastward-dipping thrust zone (fig. 1).

Alexander terrane.—The Alexander terrane, well exposed throughout the Alexander Archipelago of southeastern Alaska, comprises an extremely heterogeneous assemblage of sedimentary, volcanic, and metamorphic rocks ranging in age from Ordovician, or older, to Late Triassic. It contains granitic plutons at least as old as Silurian, indicating that it was by then a terrane of continental crust. It is also intruded by numerous other granitic bodies of Paleozoic, Mesozoic, and Cenozoic age (Lanphere and others, 1965; Loney and others, 1967), and near its southern terminus, by ultramafic plutons of Silurian and Ordovician age (M. A. Lanphere, oral commun., 1971).

In many places rocks of the Alexander terrane are gently folded and only slightly metamorphosed. Locally, however, they are complexly folded and have undergone at least two periods of metamorphism, one of which is probably of early Paleozoic age (A. L. Clark and G. D. Eberlein, oral commun., 1971). Structure of the terrane is still poorly known and is undoubtedly complex. On southern Prince of Wales and Dall Islands, and probably elsewhere in the terrane, juxtaposition of roughly coeval bedded rocks of contrasting structure and metamorphic grade may be due to large-scale thrust faulting (Berg, 1972b).

The oldest fossiliferous rocks in the Alexander terrane are Lower Ordovician graptolitic chert and shale exposed on western Prince of Wales and nearby islands (Eberlein and Churkin, 1970). These beds, whose base has not been seen, are in the lowermost part of a well-preserved, nearly continuous sequence of Ordovician to Pennsylvanian marine sedimentary and volcanic rocks at least 35,000 feet thick. Partly correlative rocks have also been mapped on Kuiu and Kupreanof (Muffler, 1967), Annette and Gravina (Berg, 1972a,c), Chichagof (Loney and others, 1963), and Admiralty (Lathram and others, 1965) Islands, in the Chilkat Mountains (Lathram and others, 1959), and in the St. Elias Mountains in Yukon Territory (Muller, 1967).

On Kuiu, Kupreanof, and southern Admiralty Islands, Permian marine sedimentary and minor volcanic rocks depositionally overlie lower and middle Paleozoic rocks and in turn are unconformably overlain by Upper Triassic marine strata, the youngest bedded rocks assigned to the Alexander terrane.

Upper Mesozoic sedimentary rocks of the Gravina-Nutzotin belt in unconformable contact with Paleozoic and lower Mesozoic rocks of the Alexander terrane have been observed in several places along the present western margin of the belt in southeastern Alaska, and in the St. Elias Mountains west of Dezadeash Lake in Yukon Territory (Kindle, 1953). Although several workers (Monger and Ross, 1972; Jones and others, 1972; Monger and others, 1972) have proposed that rocks of the Alexander terrane are allochthonous, the deposition of Gravina-Nutzotin belt rocks by this terrane establishes that it was contiguous to the belt by late Mesozoic time.

Yukon terrane.—The region north of the Denali fault is underlain by phyllite, quartz-mica schist, marble, and other metasedimentary and metavolcanic rocks. Upper Mesozoic and lower Tertiary granitic rocks locally are abundant. These poorly known rocks have been called the Yukon Complex in Canada. Greenschist-facies metamorphism prevails in south-central Alaska and adjoining Yukon Territory, and in Alaska the rocks may grade northward into the higher grade rocks formerly called the Birch Creek Schist (now abandoned).

Paleontological evidence for the age of much of the Yukon terrane is scant. Tabulate and rugose corals (*Cladopora*, *Favosites*, *Thamnopora*, *Acanthophyllum*) collected from

rocks in the eastern Alaska Range indicate that some are of Devonian age (Richter, unpub. data), and Muller (1967, p. 24) suggests that some may be pre-Ordovician. The time of regional metamorphism is also poorly known, although several episodes seem likely (Muller, 1967, p. 25). Mesozoic potassium-argon ages cited by Muller probably record only the latest period of intense deformation.

Upper Mesozoic rocks of the Gravina-Nutzotin belt are nowhere in depositional contact with rocks of the Yukon terrane, although the presence of Yukon terrane detritus in Gravina-Nutzotin conglomerate (p. D9, this report) indicates that the belt may originally have overlapped the terrane. In the eastern Alaska Range and in the Kluane Ranges, they are in fault contact along the Denali fault.

SUPERJACENT TERRANES

The Gravina-Nutzotin belt is distinct from two other belts of upper Mesozoic bedded rocks in southern and southeastern Alaska, which are herein informally called the Matanuska-Wrangell terrane and the Chugach terrane. After describing the Gravina-Nutzotin rocks, we compare the lithology and geologic histories of these three coeval sequences.

Gravina-Nutzotin Belt

The Gravina-Nutzotin belt comprises a distinctive suite of rocks distributed in a narrow, linear, nearly continuous inland belt that parallels the Pacific coast in southeastern Alaska, but which diverges from the arcuate coast near long 140° W. The southern part of the belt is less than 100 miles from the edge of the continental shelf, whereas the northern part is over 200 miles distant from it. The western boundary of the belt is an erosional edge complicated in places by faults that separate it from Alexander and Taku-Skolai terrane basement rocks. The eastern boundary in south-central Alaska, Yukon, and British Columbia is the Denali and related faults. In southeastern Alaska, we arbitrarily place the eastern boundary between phyllite and greenstone lithically akin to the less metamorphosed Gravina-Nutzotin belt rocks, and mica schist, amphibolite, and marble, some of which are known to be of late Paleozoic and early Mesozoic age. These older rocks appear to overlie structurally the younger Gravina-Nutzotin rocks, and we presume that major imbricate thrust faulting has produced the inverted sequence. Other geologists, however, have postulated that this relation is due to a large overturned synclinorium (Chapin, 1918, p. 87; Buddington and Chapin, 1929, p. 240), but the strikingly different nature of the eastern (Taku-Skolai terrane) and western (Alexander terrane) "limbs" does not support this hypothesis.

DESCRIPTIONS OF SELECTED AREAS

Ketchikan area

The Gravina-Nutzotin belt has been recognized in Alaska as far south as the United States–Canada boundary (fig. 1). Metamorphosed Jurassic(?) sedimentary and volcanic rocks near Prince Rupert (Hutchison, 1967) may represent a southward continuation of the belt.

Gravina-Nutzotin belt rocks near Ketchikan (figs. 1 and 2; Berg, 1972a, c) consist mainly of two structurally juxtaposed sequences of roughly coeval bedded rocks–the Gravina Island Formation and an unnamed unit–that differ in lithology, depositional environment, metamorphism, and structure.

Gravina Island Formation.–This widespread bedded unit consists of andesitic metavolcanic rocks and flyschlike metasedimentary rocks. They are highly deformed, commonly phyllitic, and metamorphosed to greenschist facies. Complex folds with gently eastward-dipping axial surfaces are prevalent. Neither the base nor top of this formation has been observed.

On eastern Gravina and northeastern Annette Islands, at least 2,000 feet of fragmental metaandesite overlies and locally intertongues with dark-gray argillite and phyllitic siltstone, graywacke, and conglomerate. Fossils (*Cylindroteuthis* sp. and *Entolium* sp.) are locally abundant in siltstone beds; *Buchia* is conspicuously absent. A late Middle or early Late Jurassic age seems possible for this assemblage.

The metavolcanic rocks range from thinly laminated phyllite to thick competent beds with crude, indistinct schistosity. Most consist of green and gray porphyritic metatuff and agglomerate containing euhedral phenocrysts of light-gray plagioclase and dark-greenish-black clinopyroxene. The groundmass is fine grained and contains clinopyroxene, amphibole, epidote-clinozoisite, chlorite, albite, quartz, muscovite, prehnite, and calcite. The clinopyroxene commonly is altered to hornblende and pale-green amphibole, and the plagioclase to fine-grained albite and clinozoisite. The abundance and relative proportions of phenocrysts vary markedly; typically, they make up 10 to 15 percent of the rock.

Unnamed unit.–An unnamed bedded unit, known in the Ketchikan area only on western Gravina Island, consists of *Buchia*-bearing siltstone, argillite, and conglomerate of Late Jurassic age. In contrast to the Gravina Island Formation, this unit is characterized by relatively simple folds, slaty cleavage, and only slight metamorphism. It unconformably overlies older Mesozoic and Paleozoic rocks of the Alexander terrane; its top has not been observed.

The lower part of the unit is an elongate lens of conglomerate as much as 350 feet thick; the upper part comprises at least 500 feet of thinly interbedded, locally fossiliferous siltstone and argillite, and subordinate limestone, grit, and pebbly to cobbly mudstone. Clasts in the conglomerate were derived mainly from underlying Mesozoic and Paleozoic rocks on western Gravina Island. The strong contrast of this unit with the nearby Gravina Island Formation indicates large-scale

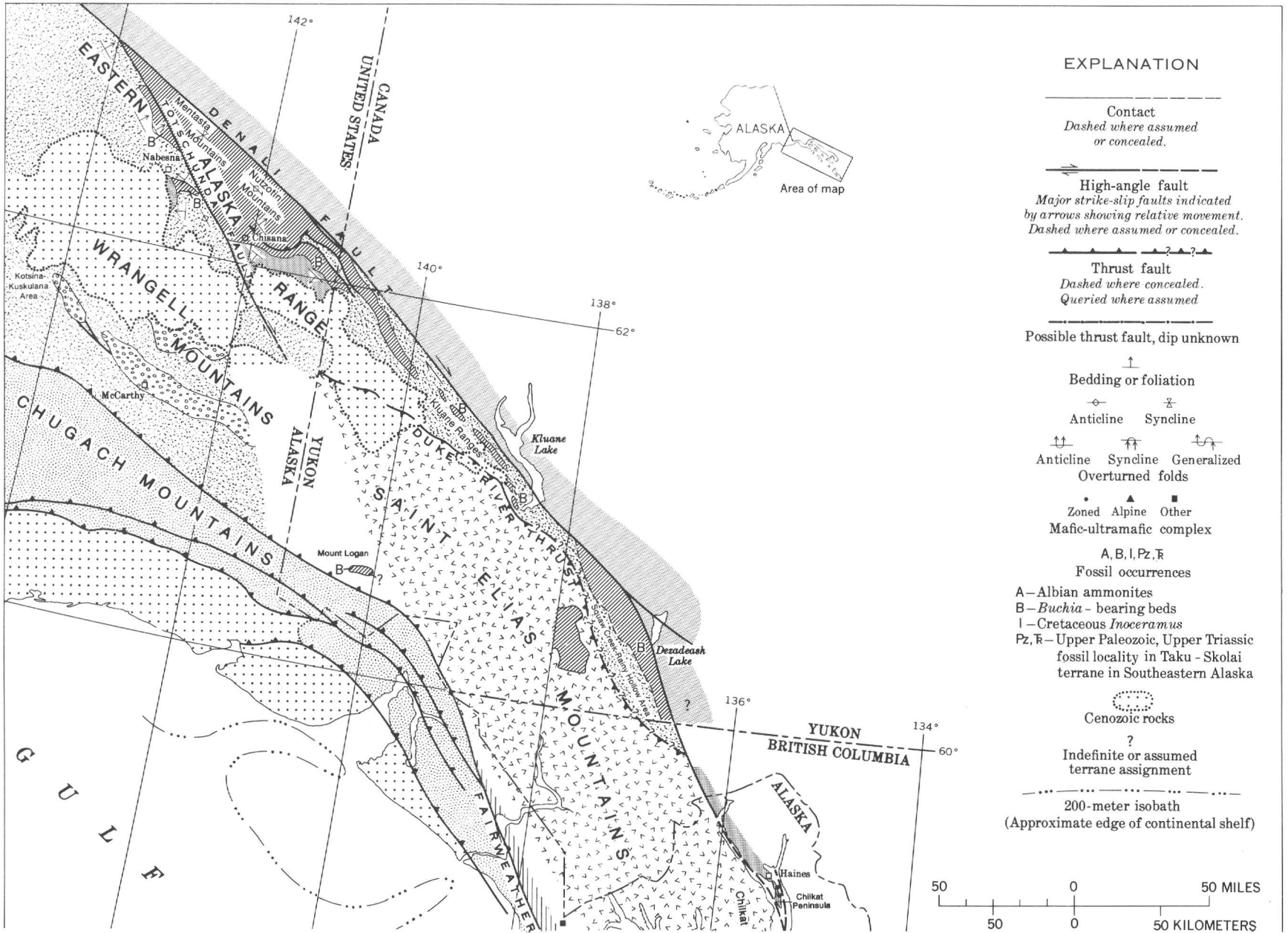
142°
140°
138°
136°
134°
62°
60°
CANADA
UNITED STATES
YUKON
BRITISH COLUMBIA
ALASKA
Area of map
EASTERN ALASKA RANGE
DENALI FAULT
WRANGELL MOUNTAINS
CHUGACH MOUNTAINS
SAINT ELIAS MOUNTAINS
DUKE RIVER THRUST
FAIRWEATHER
G U L F
Mentasta Mountains
Tok-Chisana Mountains
Nutzotin Mountains
Nabesna
Chisana
Kotsina-Kuskulana Area
McCarthy
Mount Logan
Kluane Ranges
Kluane Lake
Dezadeash Lake
Snag-Klutlan Area
Haines
Chilkat Peninsula
Chilkat
50 0 50 MILES
50 0 50 KILOMETERS
EXPLANATION
Contact
Dashed where assumed or concealed.
High-angle fault
Major strike-slip faults indicated by arrows showing relative movement. Dashed where assumed or concealed.
Thrust fault
Dashed where concealed. Queried where assumed
Possible thrust fault, dip unknown
Bedding or foliation
Anticline
Syncline
Anticline
Syncline
Generalized
Overturned folds
Zoned
Alpine
Other
Mafic-ultramafic complex
A, B, I, Pz, Tr
Fossil occurrences
A—Albian ammonites
B—Buchia - bearing beds
I—Cretaceous Inoceramus
Pz, Tr—Upper Paleozoic, Upper Triassic fossil locality in Taku - Skolai terrane in Southeastern Alaska
Cenozoic rocks
?
Indefinite or assumed terrane assignment
200-meter isobath
(Approximate edge of continental shelf)

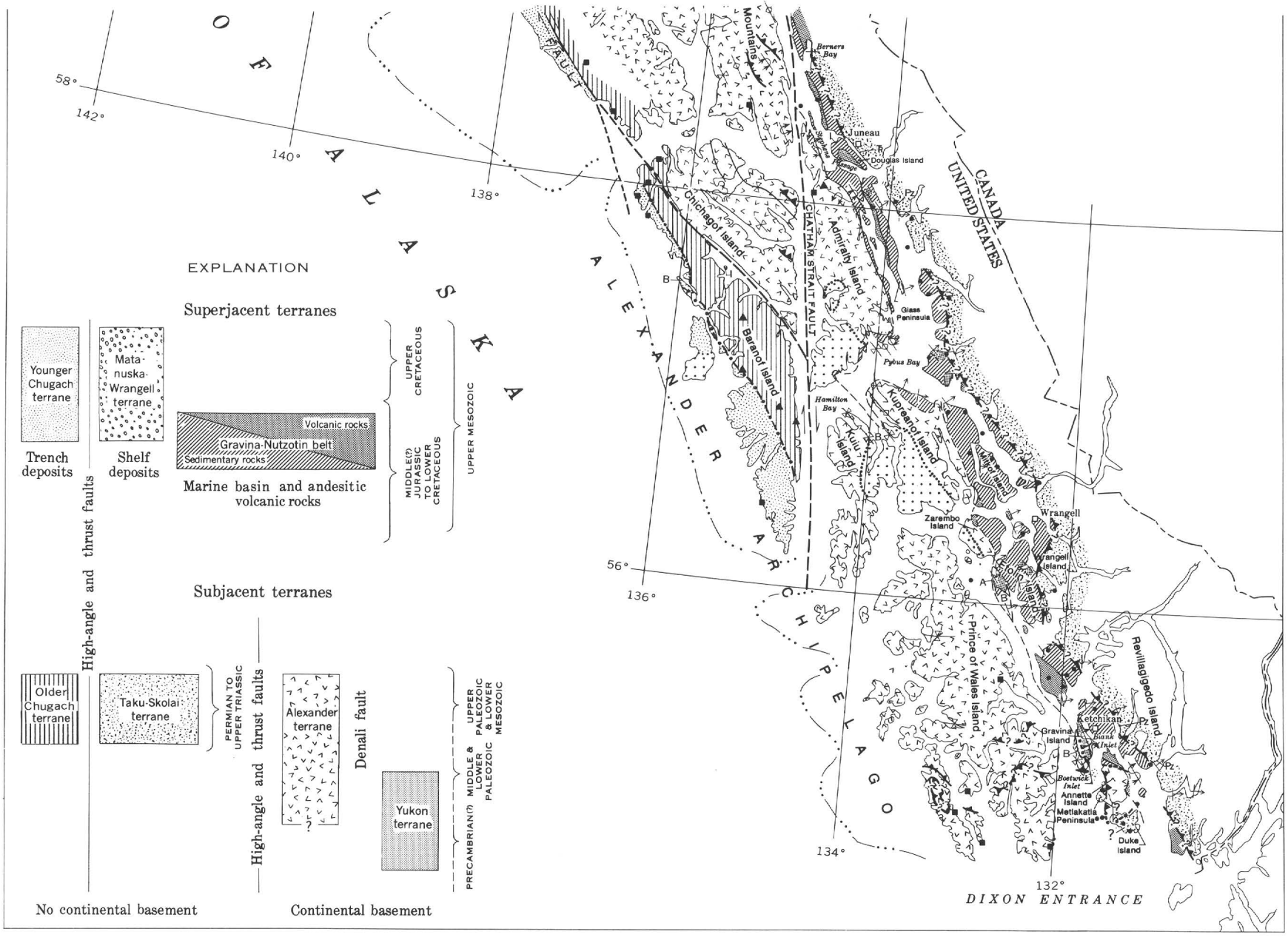

Figure 1.—Generalized geologic map of southern and southeastern Alaska, showing Gravina-Nutzotin belt and other superjacent terranes, subjacent terranes, and selected structural features and granitic intrusive rocks. Compiled in part from Buddington and Chapin (1929), Brew and others (1966), Kindle (1953), Muller (1967), and Taylor and Noble (1969).

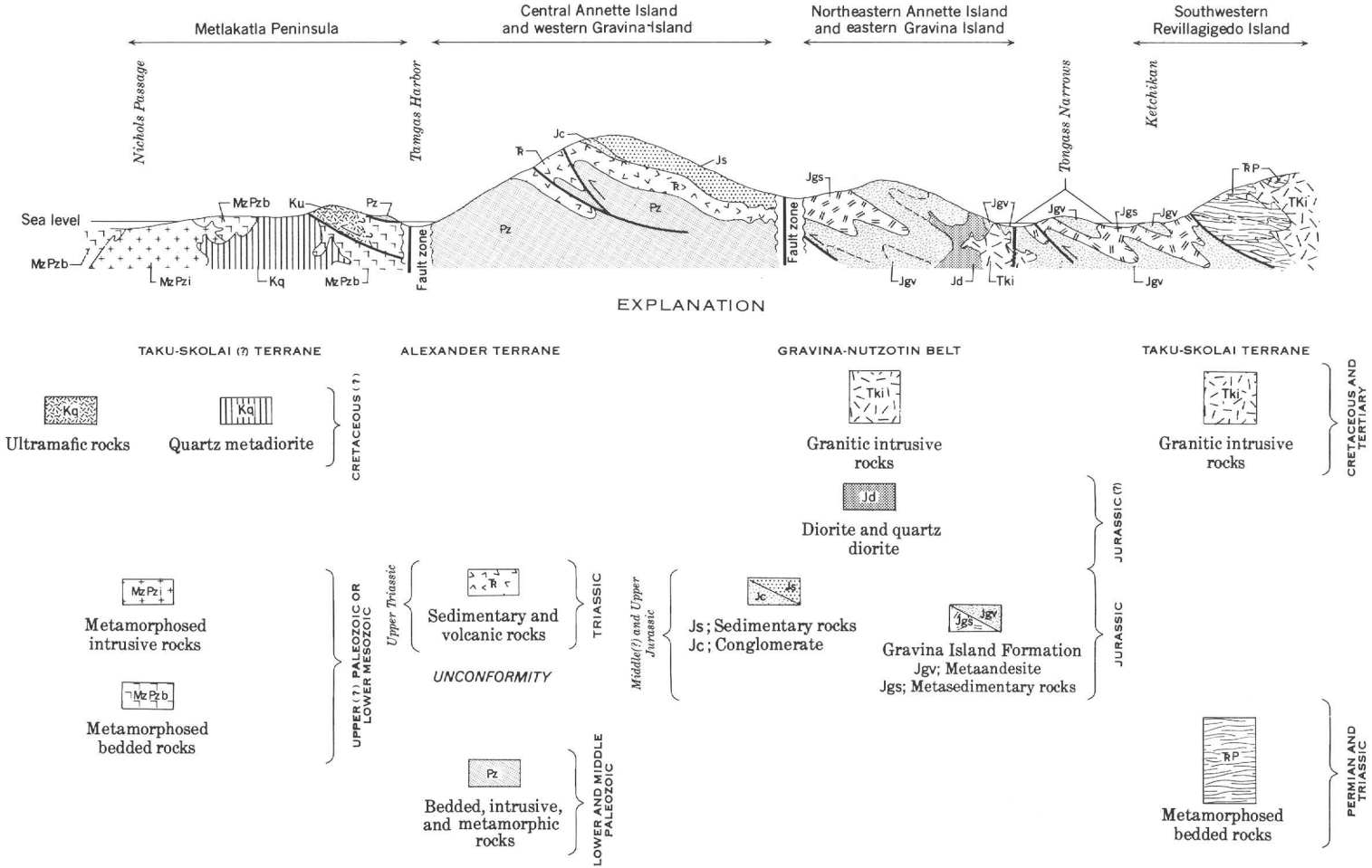

Figure 2.– Diagrammatic composite section of Ketchikan and Annette-Gravina areas, showing inferred structural and stratigraphic relations within the Gravina-Nutzotin belt and between the belt and subjacent terranes. Length of section about 25 miles; otherwise not to scale. Queried contact may be intrusive or a fault.

internal structural juxtaposition within the Gravina-Nutzotin belt.

Etolin-Kupreanof area

Upper Mesozoic bedded rocks assigned to the Gravina-Nutzotin belt crop out on Etolin and Kupreanof Islands, and on several smaller intervening islands.

On western Etolin Island, these rocks are folded and faulted, but only slightly recrystallized; primary sedimentary and volcanic textures are well preserved. The sedimentary beds commonly have pronounced slaty cleavage, whereas competent volcanic units are massive and jointed. The youngest bedded rocks known anywhere in the belt are on Marsh Island, just off the coast of westernmost Etolin Island, where about a 50-foot-thick section of thinly interbedded argillite, siltstone, volcanogenic sandstone, and andesite tuff contains scattered ammonites of early Albian age.

The tuff typically is a mottled green fragmental rock containing angular to subrounded clasts of clinopyroxene and plagioclase (An_{11-30}) porphyry and minor black argillite in a matrix of minute porphyritic fragments, individual clinopyroxene and feldspar crystals, hydrothermal alteration products, and locally a little very finely disseminated potassium feldspar. The porphyry clasts average less than 1 foot in maximum dimension; bedding ranges from less than 1 inch to 6 to 8 feet.

The Albian beds grade downward into *Buchia*-bearing siltstone, argillite, and minor conglomerate and limestone of Late Jurassic and Early Cretaceous age and upward into a very thick unit of andesitic crystallithic tuff, flows, and volcaniclastic rocks with minor argillite and graywacke lenses. Neither the base nor top of this sequence has been observed, nor is its thickness known.

Central and eastern Etolin Island, and Woronkofski, Wrangell, and eastern Zarembo, Mitkof, and Kupreanof Islands are composed mostly of granitic plutons (Buddington and Chapin, 1929, pl. 1), but also present are small tracts of unfossiliferous phyllite, graywacke semischist, greenschist, and greenstone (primarily metaandesite), which we assume from their lithology to be regionally metamorphosed equivalents of at least part of the western Etolin section. Near some plutons, these rocks are thermally metamorphosed to schist and hornfels locally containing garnet, andalusite, and staurolite. The bedded rocks are complexly deformed, most commonly into isoclinal overturned to recumbent folds with gently eastward-dipping axial surfaces.

Fossiliferous, thin-bedded lithic sandstone and mudstone of Early Cretaceous age near Hamilton Bay on northwestern Kupreanof Island (Muffler, 1967, p. C44–C45) disconformably overlie Upper Triassic strata. These rocks, about 1,000 feet thick, are simply folded, locally slaty, and, near the contact of a Tertiary gabbro pluton, converted to hornfels. They lack the flyschlike character of most of the Gravina-Nutzotin rocks, and we interpret them to be shallow-water marginal deposits.

Unfossiliferous, complexly folded, and dynamically metamorphosed graywacke, argillite, and conglomerate crop out on the coast of north-central Kupreanof Island. Although these rocks may be partly coeval with the beds near Hamilton Bay, they differ from them in lithology, structure, and metamorphism and instead resemble the Seymour Canal Formation of Admiralty Island (Muffler, 1967, p. C44; Loney, 1964, p. 55–69; Lathram and others, 1965, p. R22–R27). Contacts between these rocks and Alexander terrane rocks on northern Kupreanof Island are obscured by faults, but we infer original depositional relations from the presence of conglomerate clasts derived from middle and lower Paleozoic rocks nearby on Kupreanof and Kuiu Islands.

Admiralty Island

Upper Mesozoic strata on Admiralty Island include a lower unit of flyschlike sedimentary rocks and an upper unit of augite-bearing volcanic flow-breccia and tuff, with minor graywacke and slate. The entire assemblage (see table 1) constitutes the Stephens Passage Group (Lathram and others, 1965, p. R22), including the predominantly sedimentary Seymour Canal Formation (Loney, 1964, p. 55) and two overlying formations, the Douglas Island Volcanics (Lathram and others, 1965, p. R23; Barker, 1957) and Brothers Volcanics (Loney, 1964, p. 69).

The Seymour Canal Formation has two phases that differ in structure and metamorphism. The less-deformed phase is mainly near Pybus Bay on southeastern Admiralty Island and comprises fossiliferous (*Buchia*-bearing) argillite, graywacke, and conglomerate. It is faulted and complexly folded, but relatively unmetamorphosed.

The more deformed phase, on eastern Admiralty Island, is unfossiliferous slate, phyllite, and semi-schistose siltstone, graywacke, and conglomerate. The beds are regionally deformed into tight to isoclinal northwest-trending folds with both eastward- and westward-dipping axial surfaces.

The Seymour Canal Formation conformably underlies the Douglas Island and Brothers Volcanics. It disconformably overlies Upper Triassic strata near Pybus Bay, but its stratigraphic relations to older Mesozoic and Paleozoic formations elsewhere on the island are obscured by faulting. Loney (1964, p. 57) estimated 4,000 to 8,000 feet of Seymour Canal strata in the Pybus Bay area, and Lathram and others (1965, p. R26) report an approximately 3,500-foot-thick lens of conglomerate in the formation on northern Admiralty Island.

The Douglas Island Volcanics, mapped mainly on Glass Peninsula, consists mostly of dark-green andesitic flow breccia and tuff containing conspicuous augite and subordinate hornblende crystals as much as ½-inch in diameter. Near the base, the volcanic rocks intertongue with slate and graywacke, which also occur sporadically throughout the formation. Bedding commonly is thick and massive without conspicuous layering or foliation, but on eastern Glass Peninsula the rocks are schistose. The top of the formation has not been observed.

The Brothers Volcanics occurs only on islands near Pybus Bay and consists of at least 2,000 feet of well-bedded, dark-hued andesitic flows, breccia, and minor volcanogenic sedimentary rocks. According to Loney (1964, p. 71–72), the andesite typically is porphyritic, with phenocrysts of plagioclase (An_{25-48}), clinopyroxene, and hornblende set in a very fine grained groundmass of plagioclase, chlorite, calcite, and opaque minerals. The rocks are folded and only slightly altered, with locally well developed fracture cleavage, and thus are structurally like the less deformed phase of the Seymour Canal Formation.

Fossils have not been found in either of these volcanic units; Loney (1964, p. 71) and Lathram and others (1965, p. R28) assigned both formations a Jurassic and Cretaceous age mainly because they conformably overlie and also appear to intertongue laterally with the Seymour Canal Formation.

Juneau area

Upper Mesozoic bedded rocks similar to those on Admiralty Island are widespread on the islands and mainland west and north of Juneau. They crop out in a wedge-shaped belt along the east side of Lynn Canal from Stephens Passage to beyond Berners Bay. The belt, nearly 10 miles wide near Juneau, narrows northwestward, where it is encroached by granitic intrusive rocks.

As on Admiralty Island, the Gravina-Nutzotin belt near Juneau consists of an upper unit principally of volcanic rocks and a lower unit mainly of sedimentary rocks. The rocks are moderately to strongly deformed and variably recrystallized in the greenschist facies. Structure of the belt is still poorly known, and undoubtedly there is tectonic repetition of some units. This deformation, coupled with regional metamorphism, has obscured original stratigraphic relations, not only internally but also between the belt and the adjoining mostly higher rank and probably older metamorphic rocks to the east. Metamorphic grade increases eastward through a typically Barrovian metamorphic zonal sequence from biotite through sillimanite isograds (Forbes, 1959) between Juneau and the western margin of the Coast Range batholithic complex. The biotite isograd generally is about 1 to 2 miles east of Douglas Island (D. A. Brew and A. B. Ford, unpub. data), and the belt near Juneau thus is entirely within the chlorite zone.

Permian and Triassic rocks structurally overlie the Gravina-Nutzotin rocks, but the actual contact, which may be a thrust fault, has not been observed. Fossils of Permian and late Triassic age (Buddington and Chapin, 1929, p. 119; Martin, 1926, p. 94) occur locally in the rocks adjoining the batholithic complex, but the extent of these older rocks is largely unknown. Because both the younger and older rocks are poorly fossiliferous and are grossly similar in lithology, they cannot be readily discriminated, particularly in the more metamorphosed areas. Hence, the boundary between the Gravina-Nutzotin belt and the Taku-Skolai terrane is arbitrarily placed at the easternmost known occurrences of Jurassic or Cretaceous rocks.

A number of formal rock-stratigraphic names have been applied to Gravina-Nutzotin belt rocks of the Juneau area, some of which are conflicting or duplicative (see table 1). The metasedimentary rocks underlying and locally intertonguing with the Douglas Island Volcanics (Martin, 1926; Lathram and others, 1965) are probably correlative with parts or all of the Berners Formation of Knopf (1911), the Treadwell Slate of Martin (1926), the Symonds and Shelter Formations of Barker (1957), and the Seymour Canal Formation as used by Lathram and others (1965).

The Douglas Island Volcanics near Juneau comprises a thick pile of greenstone, mostly of fragmental volcanic origin, interlayered in places with varied volcaniclastic metasedimentary rocks. The greenstone, called augite melaphyre by Knopf (1912), is characterized by an abundance of dark-green clinopyroxene crystals, commonly 3 to 5 mm and rarely 10 mm across, set in a dense, recrystallized matrix of chlorite, pale- to dark-green amphiboles, epidote, and generally minor sodic plagioclase, quartz, and calcite.

The greenstones structurally and probably stratigraphically overlie a thick metasedimentary section that includes mainly argillite, slate, and graywacke. Original thicknesses are indeterminable, but the sedimentary and volcanic rock sequences must each have been at least several thousand feet thick. The only fossils known are Jurassic or Early Cretaceous plants found in argillite east of Berners Bay (Knopf, 1911, p. 17) and deformed specimens of *Inoceramus* in slaty argillite interlayered with metagraywacke a few miles northwest of the town of Douglas (J. G. Smith and A. B. Ford, unpub. data). Mafic and felsic dikes and small dioritic masses intruded the sedimentary rocks prior to or contemporaneously with Late Cretaceous(?) deformation and regional metamorphism. This deformation predates emplacement of the nearby Coast Range batholithic complex, at least part of which is of Eocene age (Forbes and Engels, 1970).

Haines area

Greenstone, slate, and graywacke similar to the rocks of the Gravina-Nutzotin belt in the Juneau area crop out southeast of Haines near the tip of the Chilkat Peninsula (Buddington and Chapin, 1929, pl. 1; Brew and others, 1966, p. 164 and fig. 2a). Fossils have not been found in these beds, and we assign them to the Gravina-Nutzotin belt solely on the basis of lithology.

Northwest of Haines, bedded rocks metamorphosed to amphibolite and schist are provisionally assigned to the Gravina-Nutzotin belt. The premetamorphic age of these rocks is uncertain, but according to E. M. MacKevett, Jr. (oral commun., 1972), they may be late Mesozoic and hence part of the belt.

Yukon Territory

A thick sequence of upper Mesozoic sedimentary rocks, known as the Dezadeash Group (Kindle, 1953; Muller, 1967), is exposed intermittently between Dezadeash Lake and the Alaska-Yukon border. Near Dezadeash Lake, where the rocks are extensively exposed, Kindle reports more than 12,000 feet of slate, graywacke, argillite, quartzite, chert, impure limestone, grit, conglomerate, tuffaceous sandstone, and bedded volcanic tuff. Locally, 200 to 500 feet of conglomerate occurs at the base and rests on "reddish-hued andesite". A few thin beds of coal occur in this conglomerate and also in carbonaceous slate and argillite. In places, these rocks are strongly deformed and metamorphosed to quartz-mica and cordierite schists.

To the northwest, in the Kluane Lake area, Dezadeash rocks occur in small patches within the Kluane Ranges, where they disconformably overlie Triassic rocks of the Mush Lake Group, in places with a basal conglomerate (Muller, 1967, p. 56). These rocks comprise a sequence of dull, dark-gray to black argillite, graywacke, and sparse tuffaceous beds. Graded bedding is common where bedding features are preserved. The thickness of Dezadeash rocks observed by Muller barely exceeds 1,000 feet.

Eastern Alaska Range

The eastern Alaska Range affords the most widespread and thickest sequences of Gravina-Nutzotin rocks within the presently known extent of the belt. Folded Upper Jurassic and Lower Cretaceous marine strata form the entire Mentasta and Nutzotin Mountains, the two principal mountain masses in the eastern Alaska Range. Although most of the Gravina-Nutzotin belt is structurally terminated at the junction of the Denali and Totschunda fault systems (fig. 1), isolated remnants of it just southwest of the Totschunda and flyschlike sedimentary rocks of late Mesozoic age in the less-known central Alaska Range suggest that the original terrane may have been considerably more extensive.

Two thick and very distinct lithologic sequences constitute most of the Gravina-Nutzotin belt in the eastern Alaska Range. A variety of shallow- and deep-water deposits, informally and collectively referred to as the Nutzotin Mountains sequence, are the stratigraphically lowest rocks in the belt. Lying above these, but probably in part coeval, is the Chisana Formation (Richter and Jones, 1972b), a thick sequence of andesitic fragmental rocks, flows, and volcaniclastics. A third sequence of nonmarine sedimentary rocks, very restricted in extent, occurs between the Chisana Formation and the Nutzotin Mountains sequence. The minimum cumulative thickness of the entire assemblage is about 20,000 feet. In contrast to the Gravina-Nutzotin rocks in southeastern Alaska, those in the eastern Alaska Range are relatively unmetamorphosed and only moderately deformed. However, original lithology and depositional characteristics of rocks at the two extremes of the belt are similar.

The age span of the Gravina-Nutzotin belt in the eastern Alaska Range is fairly well established. On the basis of fossils, the oldest rocks are Late Jurassic (Oxfordian) in age, and the youngest are Early Cretaceous (Barremian); all rocks are cut by middle Cretaceous (110 m.y.) granitic plutons (M. A. Lanphere and D. H. Richter, unpub. data).

Nutzotin Mountains sequence.—The Nutzotin Mountains sequence comprises both shallow and deep marine sedimentary rocks that apparently intertongue. They were deposited in a linear marine basin that developed largely on Taku-Skolai terrane but, as suggested by provenance studies, may have overlapped onto Yukon terrane. Shallow-marine facies rocks marking the southern margin of the basin are exposed locally throughout the eastern Alaska Range; none occur along the north side of the belt where the Denali fault juxtaposes deeper marine sedimentary rocks of the basin with rocks of the Yukon terrane. The inferred stratigraphic and structural relations of some of the units of the Nutzotin Mountains sequence are shown diagrammatically in figure 3.

Homoclinal structures with broad gentle folds characterize both the marine sedimentary rocks and the subjacent terrane along the southern margin of the basin. Deformation increases in intensity toward the center of the basin, where folds commonly are isoclinal and locally overturned, and thrust and high-angle reverse faults are present. Axial surfaces and fault planes trend northwestward, parallel to the long axis of the basin, and generally dip steeply to the northeast.

Shallow-marine sedimentary rocks occur at the base of the Nutzotin Mountains sequence. North of Nabesna they consist chiefly of 3,000 feet of dark-gray argillite and minor siltstone, mudstone, graywacke, and impure limestone (unit Ja, fig. 3). Conspicuous clasts of light-gray Triassic(?) limestone, ranging in size from cobbles to house-size boulders, occur sporadically through the lower part of the argillite. Sparse remains of the pelecypod *Buchia concentrica* indicate a Late Jurassic (Oxfordian) age.

Southeast of Nabesna, massive beds of shallow-water pebble to cobble conglomerate as much as 100 feet thick are interbedded with dark-gray siltstone and argillite (unit Jcs, fig. 3) that locally contain fragments of coalified wood and other carbonaceous debris, as well as the pelecypod *Buchia rugosa* of Late Jurassic (Kimmeridgian) age. Clasts in the conglomerate are well-rounded volcanic and volcaniclastic rocks, limestone, chert, and crystalline igneous rocks derived from the underlying Taku-Skolai terrane. Very conspicuous clasts of white quartz and subordinate metamorphic rocks that strongly suggest derivation from the Yukon terrane are also locally abundant. This unit, as much as 5,000 feet thick, is conformably overlain by, and is possibly gradational with, an unnamed sequence of nonmarine sedimentary rocks.

Turbidite deposits (unit KJgb, figs. 3 and 4*A*) constitute a major part of the Nutzotin Mountains sequence. They consist

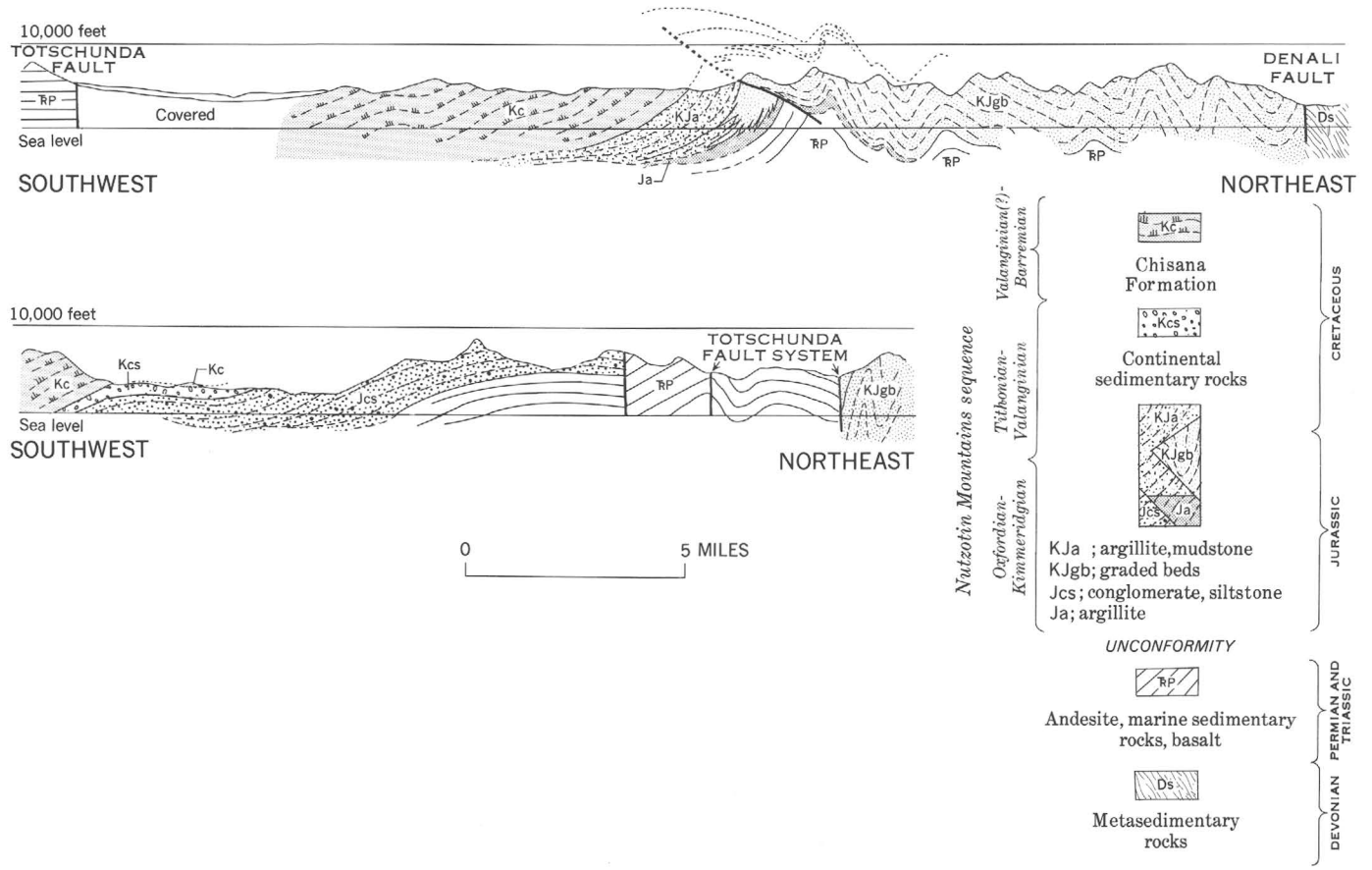

Figure 3.—Generalized sections through parts of the eastern Alaska Range near Chisana (above) and Nabesna (below), showing some inferred structural and stratigraphic relations within the Gravina-Nutzotin belt and between the belt and subjacent terranes.

chiefly of rhythmically alternating graded beds of gray to dark-gray argillite, siltstone, and graywacke in thick sections that locally alternate with massive beds of pebble to cobble conglomerate, pebbly graywacke, graywacke, and argillite. Zones of graded beds, with rhythmic sequences ranging from less than 1 inch to more than 15 inches in thickness occur throughout thousands of feet of uninterrupted section. The massive units may be as much as 500 feet thick and generally lack discernible bedding. The conglomerates are polymictic, similar to those in the shallow-water conglomerate-siltstone unit, with rounded clasts probably derived from both the Taku-Skolai and Yukon terranes. Fossils are extremely rare in these beds; a few specimens of *Buchia* collected at one locality northwest of Chisana indicate a Late Jurassic (Oxfordian to Kimmeridgian) age.

The upper part (KJa, figs. 3 and 4*B*) of the Nutzotin Mountains sequence is exposed between Chisana and the international boundary and consists of about 3,000 feet of graded argillite and graywacke overlain by 600 to 1,500 feet of mudstone. Tuffaceous beds near the top are conformably overlain by massive andesite breccias of the Chisana Formation. Several species of *Buchia* are abundant throughout the unit and indicate an age span from Late Jurassic (Tithonian) to Early Cretaceous (Valanginian).

Nonmarine sedimentary rocks.—Nonmarine clastic sedimentary rocks about 1,000 feet thick (unit Kcs, fig. 3) are exposed in the isolated Gravina-Nutzotin belt remnant southeast of Nabesna (fig. 1). There, carbonaceous thin-bedded to massive, drab brown and gray sandstone, siltstone and shale with minor grit and conglomerate conformably overlie, and probably grade into, the conglomerate and siltstone in the basal part of the Nutzotin Mountains sequence. Fragmental volcanic rocks of the Chisana Formation conformably overlie these deposits. Wood and other plant debris are abundant, but no age-diagnostic fossils have been found.

Chisana Formation.—Interlayered submarine and subaerial andesitic fragmental volcanic rocks, volcanic flows, and volcaniclastic rocks exposed near Nabesna and throughout the Chisana area (fig. 1) have been named the Chisana Formation (Richter and Jones, 1972b). In the type locality near Chisana, at least 10,000 feet of these rocks is estimated to overlie conformably shallow marine sedimentary rocks of the Nutzotin Mountains sequence (fig. 3). Coarse clastic terrigenous deposits of Late(?) Cretaceous age locally overlie the

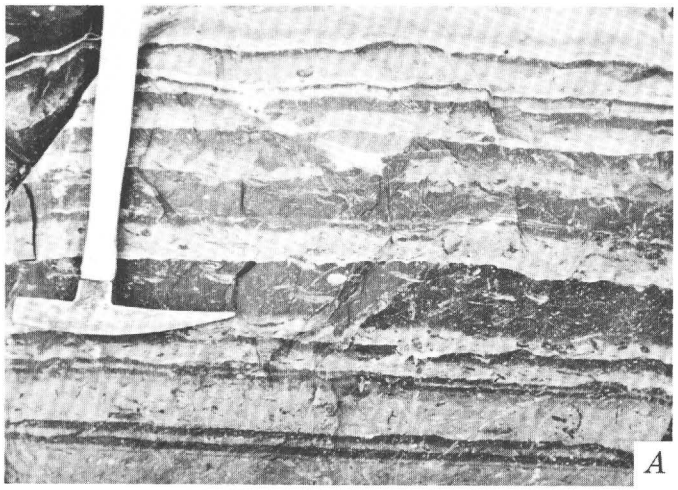

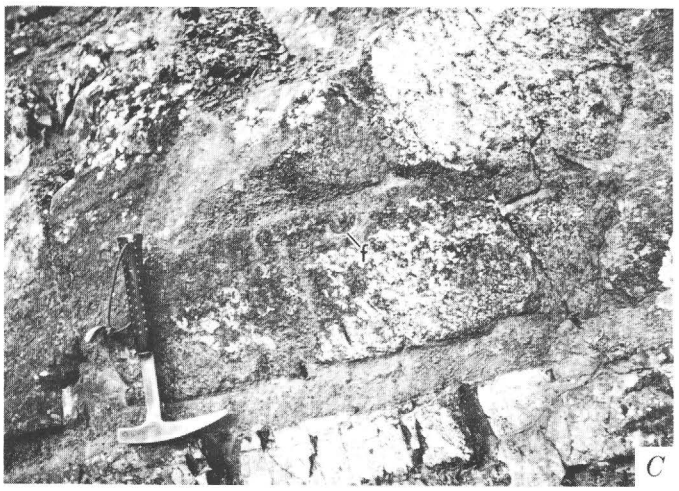

Figure 4.—Upper Mesozoic bedded rocks of the eastern Alaska Range.
A. Graded beds of very fine grained graywacke (light beds) and limy argillite (unit KJgb, fig. 3), lower part of Nutzotin Mountains sequence.
B. Argillite and mudstone (unit KJa, fig. 3), Nutzotin Mountains sequence near Chisana.
C. Bedded andesite crystal tuff, Chisana Formation (unit Kc, fig. 3). Note fossil fragment (f) in center of photograph.

volcanic rocks with slight angular unconformity; elsewhere, Cenozoic rocks overlie them with marked angular unconformity.

The Chisana Formation consists mostly of massive lahar and submarine avalanche deposits—dark gray to gray-green fragmental volcanic units as much as 300 feet thick. The rocks consist of angular to subrounded clasts of effusive volcanic rock and of crystal fragments of plagioclase and clinopyroxene set in a dense, dark fine-grained volcanic mud matrix. Clasts of intraformational sedimentary rock and lignitized wood are locally abundant near the exposed top of the formation. Interlayered with the fragmental volcanics are dense, dark-green porphyritic flows, maroon to dark-green amygdaloidal flows, thin-bedded terrigenous green and maroon volcaniclastics ranging from conglomerate to mudstone, and minor buff to dark-gray vitric and crystal tuffs (fig. 4*C*). Thin-bedded shaly argillite, graywacke, and mudstone of shallow-marine origin occur sparsely in the lower part of the formation.

The volcanic flows and volcanic clasts in the fragmental units consist of a variety of andesitic porphyritic rocks, the most prevalent of which (fig. 5) contain conspicuous phenocrysts of zoned plagioclase (An_{30-45}) or both plagioclase and diopsidic augite in a fine-grained groundmass of plagioclase microlites, minute stubby prisms of clinopyroxene, and scattered opaque minerals. All the rocks show the effects of low-grade chemical alteration. The feldspar is commonly saussuritized and the clinopyroxene replaced in various degrees by amphibole and chlorite. Similar alteration products are locally abundant in the groundmass. Quartz forms veinlets and amygdules where it generally is associated with calcite and chalcedony.

Fragments of *Inoceramus* are locally abundant in the sparse mudstone and argillite in lower parts of the Chisana Formation that overlie the *Buchia*-bearing beds of the Nutzotin Mountains sequence. Higher in the formation, a few scattered remains of the ammonite *Shasticrioceras* indicate an Early Cretaceous (Barremian) age.

FOSSILS AND AGE

Fossils are rare throughout most of the Gravina-Nutzotin belt, but they have been found in abundance in a few places (table 1). Depth of water throughout much of the marine basin was probably too great to allow growth of abundant shelly faunas, and subsequent deformation and metamorphism, especially in southeastern Alaska, have obliterated some fossil remains. The most abundant fossils are several species of *Buchia*, ranging in age from late Oxfordian to Valanginian, from scattered localities throughout the belt. In southeastern Alaska, these localities are in the western part of

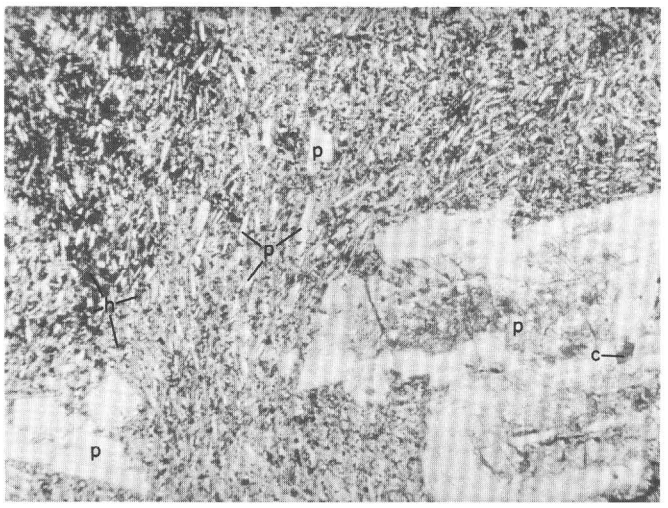

A

0.5mm

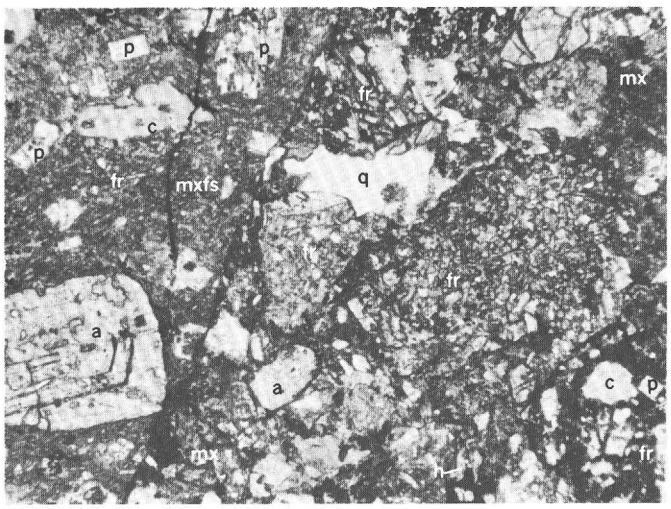

B

0.5mm

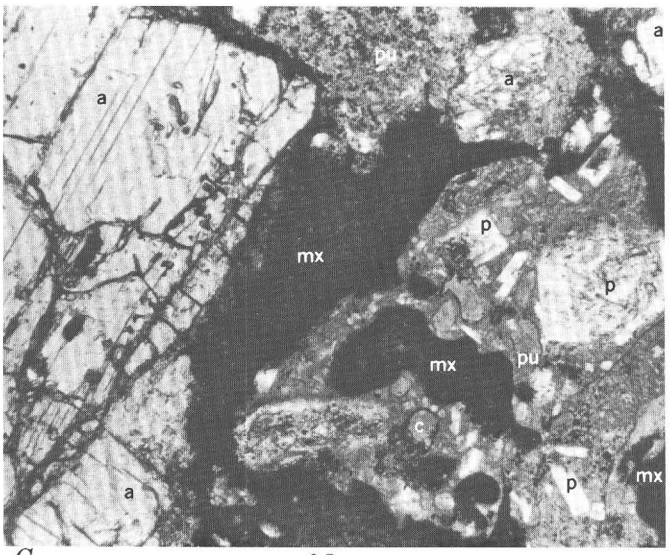

C

0.5mm

Figure 5.—Photomicrographs of volcanic rocks of the Chisana Formation.

A. Maroon amygdaloidal andesite. Plagioclase (p) phenocrysts are zoned from An_{45} (core) to An_{35} (rim); microlites in trachytic groundmass are An_{35}. Sparse grains of green pleochroic chlorite(?) (c), and of augite with magnetite rims (out of field). Abundant opaque material, including fine-grained hematite (h). Sample No. 68AMn266A. Crossed nicols.

B. Fragmental andesite. Densely packed fragments (fr) of porphyritic andesite in a comminuted crystal matrix (mx). Fragments all consist of plagioclase (An_{30}) (p) and diopsidic augite (a) in a matrix of feldspar microlites (mxfs). Minor chlorite (c), quartz (q), and brown hornblende (h). Sample No. 68ARh94. Plane polarized light.

C. Waterlain crystal-vitric tuff. Abundant crystals of diopsidic augite (a) and fragments of pumice (pu) with plagioclase (An_{35}) (p) in a dense, dark, very fine grained volcanilutite matrix (mx). Minor chlorite (c). Sample No. 69ARh301. Plane polarized light.

		Buchia "sublaevis" (Imlay)
	Valanginian	
		B. crassicollis solida
Early Cretaceous		
	-----?-----?-----	*B.* n. sp. cf. *B. tolmatschowi*
	Berriasian	*B. okensis*
Jurassic	Tithonian	*B. fischeriana*

the belt, which presumably represents a marginal, shallow depositional environment, in contrast to the deeper marine environment of the central and eastern parts. Places where Buchias are fairly abundant are designated on figure 1. The most complete and richly fossiliferous sequence of *Buchia*-bearing beds studied by the writers is in the Nutzotin Mountains (Richter and Jones, 1972b). There, sparse specimens of *Buchia concentrica* and *B. rugosa* near the base of the sequence document the presence of upper Oxfordian and Kimmeridgian strata. The overlying Tithonian, Berriasian, and Valanginian rocks locally are abundantly fossiliferous and are characterized by the following species:

From the Kluane Ranges of Yukon Territory, Jeletzky (*in* Muller, 1967, p. 57, 58) identified several species of *Buchia* from the Dezadeash Group, including *B. okensis*, *B. fischeri* (= *B. fischeriana*), and other forms indicating a latest Jurassic or earliest Cretaceous age. In similar strata farther south near Dezadeash Lake, Jeletzky (*in* Kindle, 1953, p. 36) records several *Buchia* species of Early Cretaceous (Neocomian) age.

Strata that locally contain abundant *Buchia* are widespread in southeastern Alaska. On southern Admiralty Island, *Buchia rugosa* is abundant in Pybus Bay (Loney, 1964, p. 96), and *B.* n. sp. cf. *B. tolmatschowi* is found at several nearby localities. Poorly preserved specimens of *Buchia* that may be *B.*

Table 1.—*Summary of fossil occurrences and stratigraphic nomenclature, Gravina-Nutzotin belt*

(10) Thickness in thousands of feet. ——— Conformable contact ~~~ Unconformity or disconformity - - - - - Fault, intrusive or indeterminate contact

			East Alaska Range (Nutzotin Mountains)	Yukon Territory: Kluane Lake	Yukon Territory: Dezadeash Lake	Juneau area (Douglas Island)	Admiralty Island (Pybus Bay)	North Kupreanof Island (Hamilton Bay)	West Etolin Island (Johnson Cove)	West Etolin Island (Rocky Bay)	West Gravina Island (Bostwick Inlet)	East Gravina Island (Blank Inlet)
CRETACEOUS	Upper	Cenomanian-Maestrichtian										
	Lower	Albian				*Inoceramus* sp. (age uncertain)			*Arthoplites belli* (McLearn) *Grantziceras* sp.	Unnamed volcanic rocks		
		Aptian				3				Unnamed sedimentary rocks		
		Barremian	*Shasticrioceras* sp. *Pseudolimea* sp. *Anchura* sp.			2						
		Hauterivian	*Inoceramus* sp.									
		Valanginian	*B. sublaevis* *B. crassicollis solida*		*Buchia* spp.	1				*B. pacifica* (?)		
		Berriasian	*B.* n. sp. cf. *B. tolmatschowi* *B. okensis*	*B. okensis*			*B.* n. sp. cf. *B. tolmatschowi*	*B. keyserlingi* (?) *B. subokensis* (?)	*B. okensis* (?)			
JURASSIC	Upper	Tithonian	*B. fischeriana*	*B. fischeriana*								
		Oxfordian-Kimmeridgian	*B. rugosa* *B. concentrica*				*B. rugosa*				*Buchia* cf. *B. rugosa*	
		Callovian										
	Middle	Bajocian-Bathonian										*Cylindroteuthis* sp. *Entolium* sp.

Chisana Formation (10+) — Nutzotin Mountains sequence (10+) — Dezadeash Group (12+) — Seymour Canal Formation (Berners Formation, Shelter Formation, Symonds Formation, Treadwell Slate) (4–8) — Douglas Island Volcanics; Brothers Volcanics (3+) — Stephens Passage Group (10+) — Seymour Canal Formation — Unnamed sedimentary rocks — Gravina Island Formation (2+)

[1] Of Knopf (1911). [2] Of Barker (1957). [3] Of Martin (1926). [4] Unnamed sedimentary rocks (1). [5] Unnamed sedimentary rocks (.85+).

subokensis or *B. keyserlingi* occur near Hamilton Bay on northern Kupreanof Island (Muffler, 1967, p. C45). Buchias have been collected on and near Etolin Island, but most specimens are too poorly preserved for positive identification. Small, coarsely ribbed specimens from the Johnson Cove area on the western part of the island may be *B. okensis*, and a single specimen from Rocky Bay at the southern end may be *B. pacifica* of Valanginian Age. The southernmost occurrence of Buchias in the Gravina-Nutzotin belt is at Bostwick Inlet on western Gravina Island, where poorly preserved specimens of *Buchia* cf. *B. rugosa* are locally abundant.

Fossils from Blank Inlet on southern Gravina Island may be the oldest known from the Gravina-Nutzotin belt (Berg, 1972c), but unfortunately, an unequivocal age determination cannot be established. The fossils consist of abundant belemnites of the genus *Cylindroteuthis* (J. A. Jeletzky and V. N. Saks, oral commun., 1971) and large pelecypods of the genus *Entolium*. In North America *Cylindroteuthis* is abundant in Jurassic strata, commencing in middle Bajocian time and extending into the Tithonian (Stevens, 1965). Although it has not been found in North American Cretaceous strata, Saks (1960) recorded it from the Lower Cretaceous (Neocomian) of northern Siberia. According to Stevens (1965, p. 175) this is the only known Cretaceous occurrence of this genus.

Belemnites are abundant in Hauterivian and Berremian beds in southern Alaska and elsewhere along the Pacific coast of North America (Jones and Detterman, 1966), but these belong mainly to the genus *Acroteuthis*, a form notably absent from Gravina Island. Likewise, the very large specimens of *Entolium*, some measuring 6 to 8 inches in diameter, are unknown from Cretaceous deposits along the Pacific coast of North America.

The evidence thus afforded by both the belemnites and pelecypods supports a late Middle to Late Jurassic age for the enclosing strata, but neither form has a sufficiently short range nor is well enough preserved to permit a more precise age determination.

A negative, but extremely important, factor bearing on the age of the Gravina Island Formation is the striking absence of Buchias. We know of no place along the west coast of North America where fossiliferous strata of late Oxfordian to Tithonian Age do not contain a fauna dominated by, or at least containing, *Buchia*. Such an absence from the Gravina Island suggests to us that these beds may be of pre-*Buchia* age, perhaps somewhere in the range of middle Bajocian to middle Oxfordian.

The youngest fossils from the Gravina-Nutzotin belt are ammonites of early Albian Age collected from argillite interbedded with andesite breccia and tuff on westernmost Etolin Island (locality A on fig. 1). These ammonites are *Arcthoplites belli* (McLearn) (fig. 6) and a crushed specimen that probably is *Grantziceras* sp.; both types are well known from lower Albian strata of the Wrangell Mountains (Imlay, 1960; Jones, 1967) and also occur on the Queen Charlotte Islands to the south.

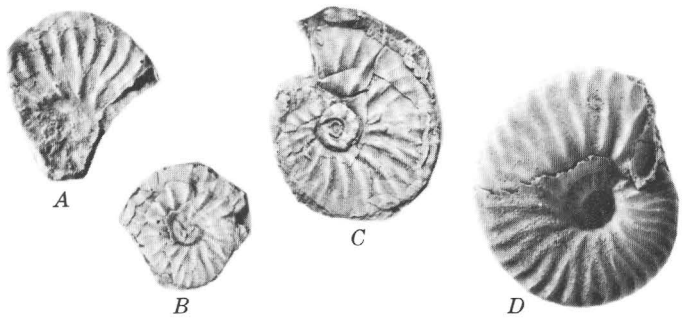

Figure 6.—*Arcthoplites belli* (McLearn). Natural size.
A, *B*, and *C* are rubber casts of crushed specimens from USGS Mesozoic loc. M5835, northern end of Marsh Island, off the northwest coast of Etolin Island. Casts are made from exterior molds in black argillite interbedded with andesite breccia and crystal tuff. USNM No. 183770a, 183770b, 183770c, respectively.
D is specimen from USGS Mesozoic loc. M1339, Kennicott Formation, lower Albian (zone of *Brewericeras hulenense*), McCarthy A-4 quadrangle, Wrangell Mountains. Lat 61°12.3′ N., long 142°19.8′ W. USNM 183771. Well-preserved specimen is illustrated to document the occurrence of the same early Albian fossils in both the Gravina-Nutzotin belt and the Matanuska-Wrangell terrane.

Large specimens of *Inoceramus* collected from argillite on Douglas Island near Juneau (J. G. Smith and A. B. Ford, unpub. data) may be middle Cretaceous in age. Although numerous, these fossils are strongly deformed and cannot be specifically identified. Also, near Chisana in the southern Nutzotin Mountains, large but indeterminable fragments of *Inoceramus* have been found in shaly argillite interbedded with Chisana Formation andesite that overlies upper Valanginian beds (fig. 4*C*). Much higher in the Chisana volcanic sequence, rare fossils, including among others, *Shasticrioceras* sp., *Pseudolimea* sp., and *Anchura* sp. indicate a probable Early Cretaceous (Barremian) age.

In summary, the fossil evidence establishes that sedimentation in the Gravina-Nutzotin belt may have commenced in Middle Jurassic (Bajocian) time in the southernmost part of the belt and somewhat later in the Late Jurassic (Oxfordian) elsewhere in the belt. Except for presumably local interruptions, deposition was evidently continuous until near the end of Early Cretaceous (Albian) time. Volcanism was episodic, as volcanic rocks occur with the presumed oldest beds in southeastern Alaska and lie above the youngest marine beds in the eastern Alaska Range and on Etolin Island. Significantly, no volcanic rocks have been found intercalated with the *Buchia*-bearing beds (upper Oxfordian through Valanginian). Hence, it appears that the bulk of volcanic activity occurred during post-Valanginian time.

CHEMISTRY AND CLASSIFICATION OF THE VOLCANIC ROCKS

Table 2 summarizes the major-oxide chemistry of 27 specimens of volcanic materials from the Gravina-Nutzotin

belt. Of these, 26 (table 2, cols. 1a–1c) are metavolcanic rocks from the Gravina Island Formation, near Ketchikan, where the belt has been strongly deformed and its rocks regionally metamorphosed in the greenschist facies. The remaining specimen (table 2, col. 2c) is relatively unaltered flow rock from the Chisana Formation in the Nutzotin Mountains.

The Gravina Island rocks vary considerably in composition; individual analyses range in SiO_2 content and normative An ratio between those of basalt (Nockolds, 1954, p. 1021) and dacite (Chayes, 1969, p. 2; and 1970, p. 179), with most

Table 2.—*Analyses, in weight percent, of volcanic rocks in the Gravina-Nutzotin belt, Alaska*

[All analyses performed in U.S. Geological Survey rapid rock analysis laboratory under Leonard Shapiro. Analysts: P. L. D. Elmore, G. W. Chloe, James Kelsy, H. Smith, Lowell Artis, and J. L. Glen]

	1 Gravina Island Formation (Berg, 1972c)			[1]2 Chisana Formation (Richter and Jones, 1972b)	3 Andesite (Nockolds, 1954, p. 1019)	4 Cenozoic andesite (Chayes, 1969, p. 2)
	a	b	c			
Chemical analyses						
SiO_2	44.0 –59.8	51.36	53.19	61.90 (51.7)	54.20	58.17
Al_2O_3	16.2 –19.5	18.12	18.79	17.00 (17.1)	17.17	17.26
Fe_2O_3	1.60– 4.90	3.66	3.75	3.10 (2.2)	3.48	3.07
FeO	2.30– 9.80	5.47	5.61	2.70 (6.2)	5.49	4.17
MgO	1.70– 7.20	4.52	4.74	1.40 (5.0)	4.36	3.23
CaO	5.10–11.50	8.76	9.17	4.50 (7.9)	7.92	6.93
Na_2O	.81– 5.80	2.70	2.77	4.10 (2.8)	3.67	3.21
K_2O	.34– 2.20	.89	.93	1.70 (.91)	1.11	1.61
H_2O+	1.30– 4.20	2.71	.....	1.60 (3.3)	.86	1.24
TiO_2	.44– 1.20	.73	.75	.77 (.83)	1.31	.80
P_2O_5	.04– 0.54	.17	.17	.42 (.31)	.28	.20
MnO	.08– 0.35	.16	.17	.12 (.13)	.15	.....
CO_2	.00– 3.20	[2].39	.....	.39 (.23)	.....	.....
Total		99.64	100.04	99.70	100.00	99.89
CIPW norms						
Q	0–20.42 (22)	6.65	6.21	21.52	5.7	13.63
C	0– 6.27 (4)	.....	.....	2.15	.....	.....
or	2.0 –12.85	5.28	5.49	10.08	6.7	9.52
ab	6.91–49.11	22.93	23.43	34.80	30.9	27.19
an	9.51–46.25	34.82	36.08	17.17	27.2	27.96
ne	0– 2.18 (1)	.....	.....	.....	.....	.....
wo	0– 9.11 (22)	2.17	3.46	.....	4.2	2.15
en	1.26–17.75	11.30	11.80	3.50	10.9	8.05
fs	0–15.41 (25)	6.14	6.28	1.35	5.3	3.80
fo	0– 8.20 (4)	.....	.....	.....	.....	.....
fa	0– 7.87 (4)	.....	.....	.....	.....	.....
mt	2.30– 7.14	5.33	5.44	4.51	5.1	4.46
il	.48– 2.30	1.39	1.42	1.47	2.4	1.52
ap	.10– 1.26	.40	.40	1.00	.7	.47
cc	0– 7.19 (14)	.89	.....	.89	.....	.....
Normative an ratio.		60.3	60.6	33.0	46.8	50.7

1. Summary of rapid rock chemical analyses of 26 samples of greenschist facies regionally metamorphosed volcanic rock from the Gravina Island Formation, Annette and Gravina Islands, Alaska.
   a. Range of values in the 26 analyses. Number in parentheses in normative analyses indicates number of samples in which constituent is reported.
   b. Average of the 26 analyses. CIPW norm is calculated from this average.
   c. Average of the 26 analyses recalculated to 100.00 percent on a volatile-free basis.
2. Amygdaloidal flow, Chisana Formation, Nutzotin Mountains, Alaska.
3. Average of 49 analyses of andesite.
4. Average of 1,775 analyses of Cenozoic andesite.

[1] The average of three additional chemical analyses of Chisana Formation volcanic rocks was added to column 2 at time of proof. We believe that this average, shown in parentheses, which closely approximates that of the Gravina Island samples, is more representative of the Chisana Formation than the single analysis reported.

[2] Reported in 14 samples.

falling in the range of basalt-andesite (Williams and others, 1954, p. 43; Coats, 1968, p. 693–717). Doubtless, variability is the combined result of compositional variation in the original lavas and of alteration and metamorphic transfer (Smith, 1968). The distance and magnitude of transfer is unknown, but we assume that element redistribution was largely confined to the volcanic pile. Therefore, although any individual analysis is not representative of original lava composition, we believe that the average of many analyses (table 2, col. 1b) approximates the bulk composition of the parent rocks.

A precise classification of Gravina Island metavolcanic rocks depends on the effects of the volatile constituents, mainly H_2O, which can only be arbitrarily assigned. Recalculated on a water-free basis, and assuming that all H_2O was introduced—an assumption not wholly justified because the original lava may have contained a hydrous phase such as hornblende—the average Gravina Island rock (table 2, col. 1c) can be classed as basaltic andesite (Williams and others, 1954; Coats, 1968). The andesitic nature of these rocks shows well on an ACF diagram (fig. 7), where they plot along the margin of the basalt field of D. S. Coombs (after Smith, 1968), distant from Nockolds' (1954, p. 1021) tholeiitic and "central" basalts, and proximate to average andesite of Chayes (1969; table 2, col. 4 of the present report) and Nockolds (1954, p. 1019; table 2, col. 3 of the present report), and to average island-arc andesite of McBirney (1969, p. 503).

The analysis of the Nutzotin Mountains specimen shows more SiO_2, higher normative quartz, and a lower An ratio than any of the Gravina Island samples, but nevertheless is well within the range commonly reported in andesitic volcanic suites (Dickinson, 1970, p. 818). (See footnote 1, table 2, for additional chemical analyses.)

Gravina-Nutzotin volcanic rocks vary considerably in alkali content, but the regional variation in alkalis has not been established.

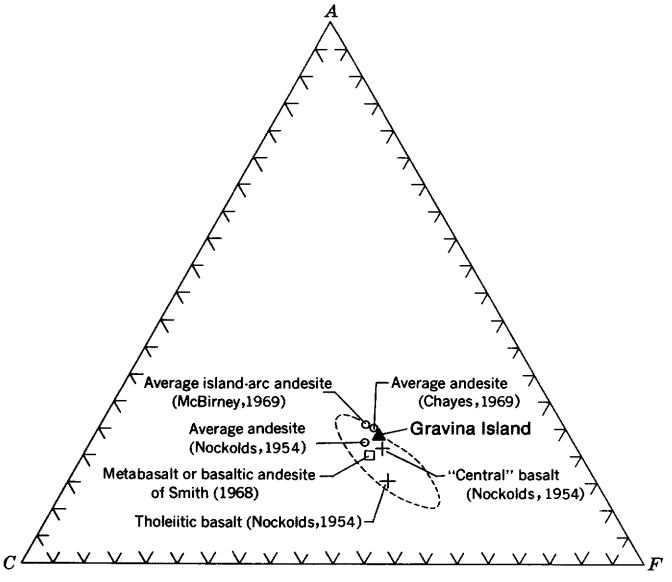

Figure 7.—ACF diagram comparing average Gravina Island metavolcanic rocks (table 2, col. 1b) with average basalt and andesite. Dashed line shows basalt field of D. S. Coombs (after Smith, 1968).

COGENETIC GRANITIC ROCKS

Rocks of the Gravina-Nutzotin belt and adjacent terranes are intruded by numerous granitic plutons ranging in size from dikes a few feet thick to batholiths. Only a few of the plutons, however, have been precisely dated by stratigraphic or radiometric methods. Those that are late Mesozoic and Tertiary in age postdate formation of the Gravina-Nutzotin belt and are not discussed further. Those known to have formed during Late Jurassic to middle Cretaceous time, and thus assumed to be cogenetic with the Gravina-Nutzotin volcanic rocks, are described in this section.

In the eastern Alaska Range and adjoining Kluane Ranges in Canada, more than 15 plutons ranging in size from small stocks to complex batholiths intrude rocks of the Gravina-Nutzotin belt. Reconnaissance K-Ar radiometric studies indicate an age of 110–112 m.y. for the Alaskan plutons (M. A. Lanphere, unpub. data), which is consistent with a post-Barremian–pre-Late Cretaceous age deduced from fossil and field evidence. In the Kluane Ranges, Muller (1967) has bracketed the age of the plutons between Early Cretaceous and early Tertiary on the basis of contact relations.

The Alaskan plutons are principally granodiorite but include quartz monzonite, quartz diorite, diorite, and syenodiorite as locally abundant variants. Less common are trondjhemite, pyroxene monzonite, and biotite gabbro. The rocks are nonfoliate, medium to coarse grained, and in thin section exhibit a subhedral equigranular texture.

The plutons in the eastern Alaska Range generally have sharp intrusive contacts with the country rocks and contain abundant xenoliths. A thermal metamorphic aureole, as much as 1 mile wide, surrounds many of the plutons.

In southeastern Alaska, Gravina-Nutzotin bedded rocks are intruded by numerous granitic plutons (Buddington and Chapin, 1929), but only one, on northern Annette Island, has been recognized as clearly coeval with the andesitic metavolcanic rocks.

This pluton is a crudely tabular diorite to quartz diorite stock, with contacts that strike approximately parallel to the regional northwesterly trend of the enclosing Gravina Island Formation. There is some local baking of the metasedimentary beds along the diorite contact, but thermal effects in the metavolcanic rocks have not been observed. The pluton is moderately foliated and hydrothermally altered and grades outward from an equigranular core of feldspar, amphibole, and minor quartz to a porphyritic border zone containing relict phenocrysts of feldspar and amphibole. The border zone, in turn, grades imperceptibly into feldspar-, amphibole-, and pyroxene-crystal-bearing andesitic metatuff.

The similarity in composition and texture of the diorite border phase and adjoining Gravina-Nutzotin metavolcanic rocks, together with the absence of thermal effects at the intrusive contact and close spatial association of the two rock types, strongly suggests that the pluton is a hypabyssal variant of the precursive andesitic extrusives.

Several granitic plutons that intrude rocks of the terranes adjacent to the Gravina-Nutzotin belt (fig. 1) have been dated as Early and middle Cretaceous by other workers (Loney and others, 1967; E. M. MacKevett, Jr., and J. G. Smith, oral commun., 1972). Although coeval upper Mesozoic volcanic rocks are not known to occur in these terranes, we assume that the plutons were subjacent to andesitic extrusive rocks, all traces of which have been removed by erosion.

ZONED ULTRAMAFIC COMPLEXES

Concentrically zoned ultramafic complexes that ideally grade outward from a core of dunite, through successive shells of peridotite and (clino)pyroxenite, to peripheral hornblendite and gabbro are abundant in southeastern Alaska (Taylor, in Wyllie, 1967, p. 97–121). Of the 35 such complexes that have been reported (Taylor and Noble, 1969), 24 are in the Gravina-Nutzotin belt, and 11 lie within 10 miles of the belt.

The zoned ultramafics are partly serpentinized and, along with the enclosing country rocks, are more or less deformed and dynamically metamorphosed. In addition, the country rocks near several of them are contact metamorphosed to granulite, hornfels, schist, and gneiss containing pyroxene, hornblende, biotite, and garnet (Taylor, 1967, p. 99, 104).

Several of the ultramafic complexes in and near the Gravina-Nutzotin belt have been dated radiometrically by K-Ar methods (Lanphere and Eberlein, 1966). Their ages range from 90 to 110 m.y. and average about 100 m.y., an age closely comparable with that of the faunally dated Albian andesitic volcanic rocks on western Etolin Island (p. D7).

The significance of the zoned ultramafic complexes in southeastern Alaska, a type known to be abundant elsewhere only in the Ural Mountains of Russia (Taylor and Noble, 1969), is uncertain. However, their contemporaneity with Gravina-Nutzotin belt andesite, combined with isotopic (Lanphere, 1968) and petrologic (Irvine, 1967) data suggest that they may be fractional crystallization products in floored magma chambers that fed the andesitic vents.

Matanuska-Wrangell Terrane

An extensive belt of upper Mesozoic rocks extends for nearly 1,000 miles in a sinuous arc from the Wrangell Mountains to near Port Moller on the Alaska Peninsula (see fig. 8). This belt, termed the Matanuska geosyncline by Miller, Payne, and Grye (1959), consists of thick sequences of Lower Jurassic sedimentary and volcanic rocks and Middle Jurassic through uppermost Cretaceous shallow marine deposits. Fossils are locally very abundant, and they have been the subject of numerous paleontologic and biostratigraphic studies.

Of particular significance for this report is the character of the Upper Jurassic (Oxfordian) through Lower Cretaceous (Albian) part of the sequence in the eastern part of the belt. These strata are very different from those of the nearby Gravina-Nutzotin belt and have been studied extensively by MacKevett (1970, 1971) in the McCarthy region of the Wrangell Mountains. There, Upper Jurassic (Oxfordian and Kimmeridgian) rocks, characterized by *Buchia rugosa* and *Buchia concentrica*, of the Root Glacier Formation (MacKevett, 1969, 1971) include 3,000 to 4,000 feet of mudstone and siltstone, and minor amounts of shale, sandstone, and conglomerate. Graded bedding is rare, and MacKevett suggests that deposition occurred in moderately shallow water. The Root Glacier Formation and older rocks are overlain unconformably by the shallow marine Kennicott Formation of Albian Age (Jones and MacKevett, 1969); strata of Tithonian through Aptian Age are missing. Farther to the west, in the Kotsina-Kuskulana area of the Wrangell Mountains, the Root Glacier Formation and lower Neocomian strata are absent, and fossiliferous strata of Hauterivian and Barremian Age underlie those of Albian Age (Grantz and others 1966; Jones, unpub. data).

A nearly complete Upper Cretaceous sequence overlies the Kennicott Formation near McCarthy (Jones and MacKevett, 1969), and similar rocks are widely exposed in the Talkeetna Mountains to the west (Grantz and Jones, 1960). In both places, these rocks are richly fossiliferous (Jones, 1963, 1967; Imlay, 1960) and were deposited in relatively shallow marine waters; volcanic rocks are absent. The degree of deformation of the sedimentary rocks is slight except near several large fault zones.

The rocks of the Matanuska-Wrangell belt differ markedly from those of the Gravina-Nutzotin belt. These differences, which are summarized in table 3, indicate that the two belts have very different geologic histories, even though they are now only a few tens of miles apart.

Chugach Terrane

The Chugach Mountains are underlain by a great thickness of Mesozoic and upper Paleozoic rocks consisting of graywacke, argillite, slate, conglomerate, volcanic rocks, chaotic melanges, and granitic plutons. The rocks are complexly deformed and have been subjected to low-grade regional metamorphism. Similar rocks, which may represent the southernmost exposures of the Chugach terrane, occur on Baranof and Chichagof Islands in southeastern Alaska.

We have subdivided the rocks of this terrane into two units (fig. 1) that appear to differ in age. The older unit (older Chugach terrane) consists of a regionally metamorphosed and multiply deformed assemblage of phyllite, metagraywacke, quartzite, metachert, greenstone, amphibolite, and ultramafic rocks exposed along the southern margin of the St. Elias

Table 3.—*Comparison of Upper Jurassic and Cretaceous rocks of the Gravina-Nutzotin belt and Matanuska-Wrangell terrane*

	Gravina-Nutzotin belt	Matanuska-Wrangell terrane
Time of deposition.	Probably continuous from Middle(?) Jurassic into Albian.	Oxfordian-Kimmeridgian, with local major folding and deep erosion during Tithonian to early Neocomian; deposition resuming in late Neocomian (but Aptian deposits not identified) and extending into Maestrichtian.
Conditions of deposition.	Predominantly deep marine in trough bordering volcanic arc with minor shallow marine and nonmarine facies. Flysch-type rocks predominate; fossils rare.	Shallow marine on an unstable continental shelf, with rapid facies changes and many local disconformities; flysch-type rocks rare; fossils common.
Volcanic activity.	Abundant submarine and subaerial andesitic fragmental volcanic rocks and volcaniclastic rocks; rare flows.	None.
Basement rocks.	Upper Paleozoic to Triassic rocks of Taku-Skolai terrane.	Taku-Skolai and Lower and Middle Jurassic sedimentary and volcanic rocks.
Tectonic activity.	Moderate to intense regional deformation. Local large-scale thrusting and tight-to-isoclinal folding with gently dipping axial surfaces. Contact aureoles near granitic plutons. Vertical uplift at least 10,000 feet.	Minor folding, thrusting, and normal faulting; vertical uplift at least 8,000 feet.

Range and on Baranof and Chichagof Islands. The assemblage locally is intruded by Middle Jurassic and younger granitic plutons. Studied only in reconnaissance, the rocks may be as old as Triassic and Permian (Loney and others, 1963, 1964), but definitive evidence is lacking. We have considered the possibility that these older Chugach terrane rocks may be part of the Taku-Skolai terrane, which they appear to resemble. However, because the age of the older Chugach rocks is uncertain, and because their continuity with the Taku-Skolai terrane has not been demonstrated, we believe it more appropriate to describe them here, along with the neighboring younger Chugach rocks.

Rocks of the younger Chugach terrane include the Sitka Graywacke of Baranof and Chichagof Islands (Loney and others, 1963, 1964), the Yakutat Group in the Gulf of Alaska region (Plafker, 1967), and the Valdez Group and an unnamed formation in the Prince William Sound–Cook Inlet area (S. H. B. Clark, 1972). Fossils are very rare in these rocks, but in a few places sufficiently well preserved forms have been found to establish a range in age from probable Late Jurassic to Late Cretaceous (Maestrichtian). Parts of the Sitka Graywacke and the Yakutat Group are coeval with some of the rocks of the Gravina-Nutzotin belt, as similar *Buchia* assemblages occur in both terranes. Much of the Yakutat and Valdez Groups, however, are younger (Campanian and Maestrichtian) than any rocks known in the Gravina-Nutzotin belt. An unconformity between Sitka Graywacke–Yakutat Group rocks and older Chugach terrane rocks has been mapped on northern Baranof Island (Berg and Hinckley, 1963, p. O11), and inferred on southwestern Chichagof Island (R. A. Loney, oral commun., 1971) and in the Gulf of Alaska region (George Plafker, oral commun., 1972), but in most places, the present contact appears to be a major fault (Loney and others, 1964; Plafker, 1971, p. 122–123, 130; S. H. B. Clark, 1972).

The rocks of the younger Chugach terrane were apparently deposited in a deep marine trench. Rocks in the older Chugach terrane may have accumulated on oceanic crust as indicated by the presence locally of alpine-type ultramafic rocks in association with chert, greenstone, amphibolite, and gabbro.

At least three episodes of deformation can be inferred: one in pre-Late Jurassic time presumably resulted in at least partial accretion of older Chugach terrane rocks to the continent; another, in late Mesozoic and Tertiary time, produced regional metamorphism and thrusting of the younger oceanic trench deposits against and beneath the continental margin (Jones and others, 1971). Lastly, Plafker (1972, p. 30, and oral commun.) believes that rocks of the Chugach terrane in the St. Elias Range may once have been contiguous with those on Baranof and Chichagof Islands and were moved into their present position by about 150 miles of Cenozoic right-lateral slip on the Fairweather fault.

A depositional contact between the older Chugach terrane (probably formed largely on oceanic crust) and the Paleozoic Alexander terrane (composed of older continental crust) seems unlikely. Instead, we postulate that these terranes of wholly dissimilar age and origin were juxtaposed along a major fault and that rocks of the Alexander terrane do not depositionally underlie any part of the Chugach terrane to the west.

HISTORY AND TECTONIC SIGNIFICANCE OF THE GRAVINA-NUTZOTIN BELT

The three upper Mesozoic lithologic and structural belts that rim southern and southeastern Alaska (fig. 8) satisfy many of the geologic criteria for an ancient tripartite arc-trench system (Dickinson, 1970, 1971a, b). In plate-tectonic theory, the three elements of such a system—the trench, arc-trench gap, and magmatic (volcanoplutonic) arc—are interrelated features produced at converging plate margins through the process of plate consumption in subduction zones.

The deep-marine origin of the slate and graywacke of the younger Chugach terrane has long been recognized (for example, see Burk, 1965, p. 69; and Moore, 1969, p. 30), and accumulation in an oceanic trench at the continental margin seems to be the most reasonable interpretation of its depositional environment (Jones and others, 1971; Moore, 1972). The shallow-water, fossiliferous, and only slightly deformed

Matanuska-Wrangell terrane formed on an unstable continental shelf and upper continental slope and is the near-shore correlative of the deep-water Chugach trench deposits. The Gravina-Nutzotin belt, innermost of the three partly coeval terranes, with its thick lenses of andesitic volcanic rocks and cogenetic plutons, thus apparently corresponds to at least part of the magmatic arc, analogous to modern arcs such as the Aleutians (Coats, 1962) or the older arcs of Japan (Matsuda and Uyeda, 1971). However, the presence of granitic plutons coeval with Gravina-Nutzotin rocks in the older terranes adjacent to the Gravina-Nutzotin belt suggests that the arc originally extended beyond the present borders of the belt. Furthermore, certain features of the belt, especially its great thickness of flyschlike turbidite deposits derived in part from older, external terranes, suggest that it was not a typical magmatic arc (see table 4), and might instead more appropriately be termed a "basinal" arc.

This interpretation of a late Mesozoic arc-trench system in southern and southeastern Alaska fits quite nicely the region near long 142° W., just west of the international boundary (fig. 9). There, the three belts occur in proper sequence, but both to the west and southeast the tripartite arrangement breaks down, and the genetic and spatial relations of the parts are not so evident.

To the west, and extending on to the southwest down the Alaska Peninsula, both the Matanuska-Wrangell and Chugach terranes are well developed, but the Gravina-Nutzotin belt has not been recognized beyond the central part of the Alaska Range. Neither the characteristic flyschlike rocks, the fragmental andesitic rocks, nor granitic rocks approximately 100 to 120 m.y. old have been identified.

To the southeast the arc-trench gap deposits of the Matanuska-Wrangell terrane terminate near the border of the much older Alexander terrane (figs. 1 and 8). Farther to the

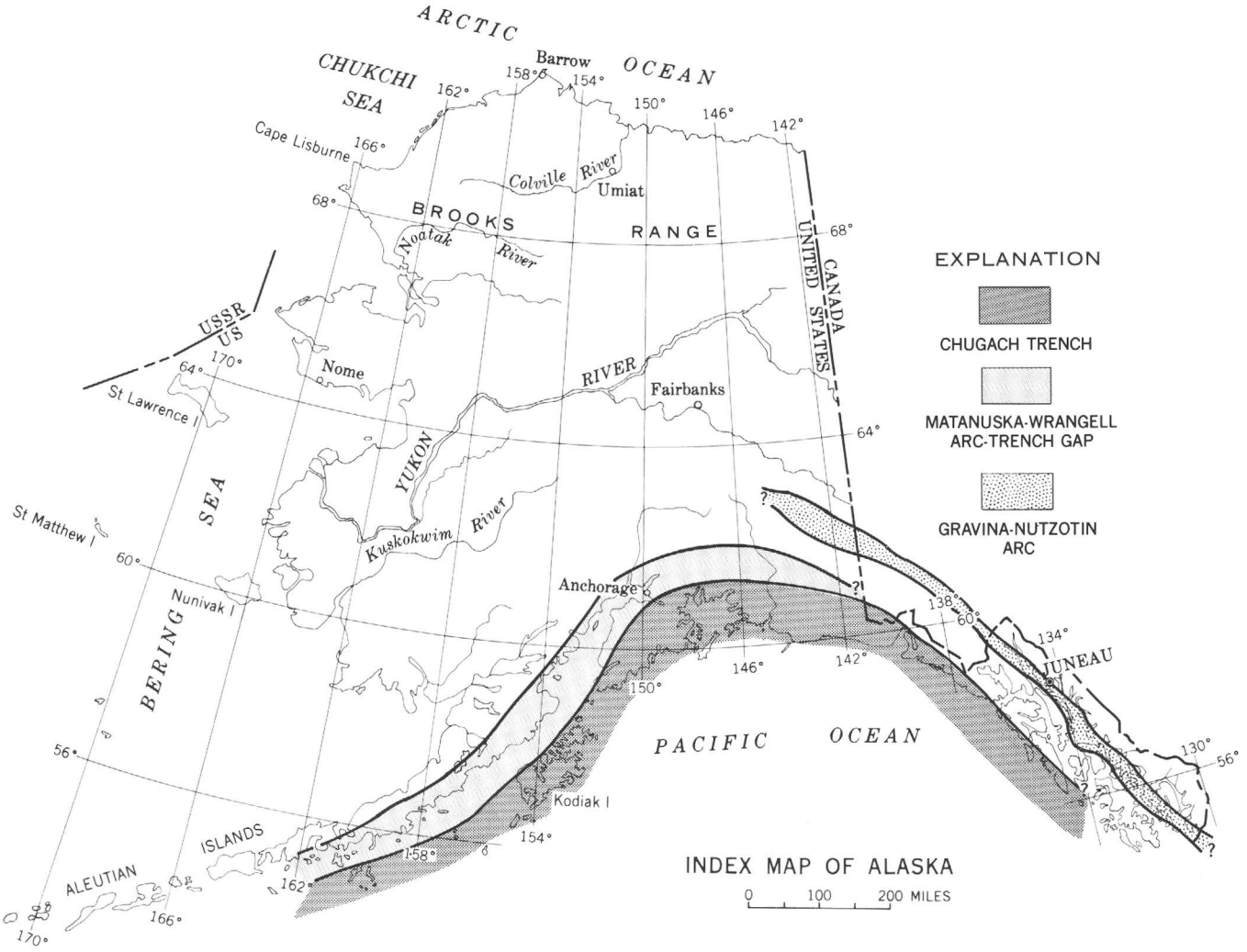

Figure 8.—Sketch map showing inferred extent of upper Mesozoic terranes in southern and southeastern Alaska.

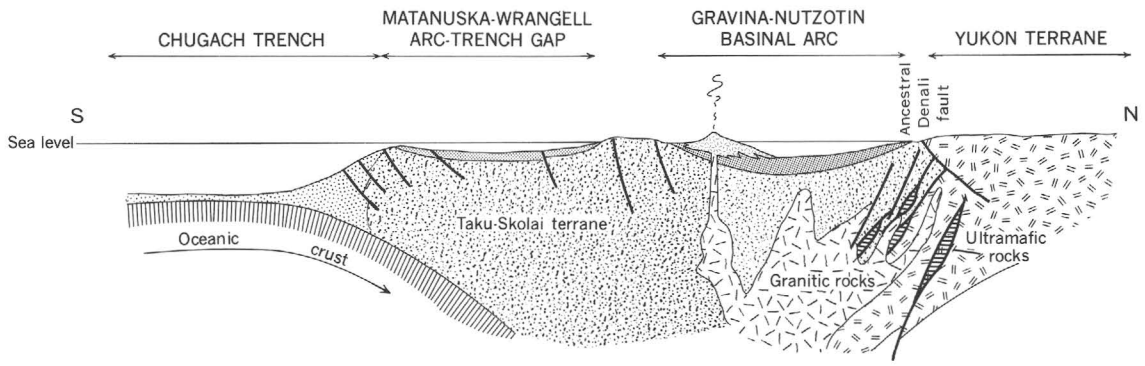

Figure 9.—Interpretation of Upper Jurassic and Lower Cretaceous tectonic elements along long 142° W., southern Alaska (adapted from Richter and Jones, 1972a).

southeast, along the present continental margin, the trench and oceanic crustal deposits of both Chugach terranes also terminate at the Alexander terrane. Such old rocks are not found elsewhere along the Pacific rim in southern Alaska or adjoining British Columbia, and the Alexander terrane may represent an allochthonous fragment of continental crust (Jones and others, 1972) emplaced prior to the development of the late Mesozoic arc-trench system. Thus, a tectonic interpretation of southeastern Alaska (fig. 10) in late Mesozoic time differs from one in southern Alaska in the absence of an arc-trench gap assemblage. Instead, the Alexander and older Chugach terranes were evidently emergent, shedding detritus eastward into the Gravina-Nutzotin basinal arc and probably westward into the Chugach trench.

Reasons for the absence of parts of the tripartite system elsewhere in southern and southeastern Alaska are obscure. In places, they may be present, but incomplete or inadequate mapping so far precludes their recognition. In addition, large-scale tectonic dislocations during late Mesozoic and early Tertiary times may have destroyed or displaced once-existing parts of the system.

Our view that the Gravina-Nutzotin belt represents an ancient volcanoplutonic arc genetically linked with subduction in the Chugach trench faces some difficulty due mainly to differences between the belt and other modern and ancient magmatic arcs (table 4). The deep-marine deposition of most of the Gravina-Nutzotin sedimentary rocks and their great thickness imply rapid depression of a long, linear belt. Moreover, the striking similarity of sedimentary structures and bedding features of the flyschlike deposits in the belt to those in the trench implies a gross similarity in depositional environment for these supposedly different petrotectonic suites. Hence, much of the belt was primarily a negative feature, not positive as expected in a volcanic arc. Anomalous also are the very large ratio of sedimentary to volcanic rock (estimated to be at least 10 to 1) and the external source of most of the sediment. Much of the identifiable debris in the Gravina-Nutzotin sedimentary rocks consists of Paleozoic and lower Mesozoic bedded and intrusive rocks, crystalline igneous and metamorphic rocks, and vein quartz, none of which could have been shed from an active volcanic arc but instead must have been derived from older terranes.

The occurrence of thick deposits of upper Mesozoic marine sedimentary rocks in many places throughout the Gravina-Nutzotin belt suggests the presence of one or more marine basins proximal to chains of andesitic volcanoes within the belt. In the eastern Alaska Range, the thousands of feet of mainly nonvolcanogenic sedimentary rocks north of thick

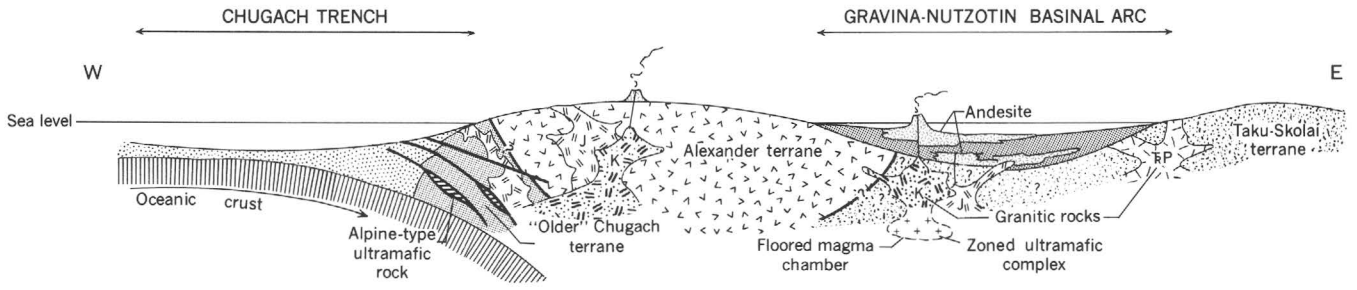

Figure 10.—Interpretation of upper Mesozoic tectonic elements along lat 58° N., southeastern Alaska. Not to scale. K, middle Cretaceous; J, Middle and (or) Upper Jurassic; ₹P, Triassic and Permian.

Table 4.—*Comparison of Gravina-Nutzotin belt and "typical" magmatic arc (Dickinson, 1970, 1971a, b)*

Gravina-Nutzotin belt	Typical magmatic arc
1. Andesitic volcanic rocks.	1. Andesitic volcanic rocks.
2. Several cogenetic granitic plutons in southern and southeastern Alaska, dated at 100–110 m.y.	2. Granitic plutons cogenetic with volcanic rocks.
3. Regional variation in alkalis not yet established.	3. Systematic increase in alkali content of volcanic and associated plutonic rocks toward hinterland.
4. Mainly deep-water (flyschlike) sedimentary rocks (= "basinal" arc).	4. Mainly shallow-water sedimentary rocks.
5. Significant amounts of sedimentary detritus derived from older, external terranes.	5. Primarily volcanogenic sedimentary detritus originating within the arc.
6. Sedimentary rocks much more abundant than volcanic rocks (>10:1).	6. Volcanic rocks more abundant than sedimentary rocks.
7. Arc-trench gap assemblage missing in southeastern Alaska.	7. Coeval arc-trench gap and trench assemblages.
8. Zoned intrusive ultramafic complexes in southeastern Alaska approximately coeval with volcanic rocks.	8. Alpine-type ultramafics may be present if arc forms on oceanic crust.
9. High T-P metamorphism in southeastern Alaska.	9. High T-P metamorphism.

deposits of partly coeval volcanic rocks probably accumulated in a marine basin between the andesitic arc and the main continent mass lying to the north. The deep and rapid subsidence of this trough may have resulted from incipient southward arc migration, similar to that suggested by Karig (1971) and Packham and Falvey (1971) for other arcs bordering marginal seas and interarc basins, but with insufficient movement to break the continental crust and permit generation of new oceanic crust in the widening gap.

Indeed, the great volume (more than 10,000 cubic miles in southern Alaska) of Middle and (or) Late Triassic tholeiitic basalt erupted prior to the development of the Gravina-Nutzotin belt may reflect a weakened and distended continental crust. Moreover, as suggested by Richter and Jones (1972a) the withdrawal of this volume of apparent mantle material may have played a dominant role in initiating trough subsidence in this region.

In our view also, the differences between present models of magmatic arcs and the Gravina-Nutzotin belt, especially that part east of long 142° W., may be due to the presence there of the Alexander terrane, an anomalous block of old continental rocks whose movement probably played a major role in the late Mesozoic tectonic history of the region. The details of this history are still very obscure, and the following paragraphs outline only the major features as presently viewed.

Deposition of Gravina-Nutzotin belt rocks began during the Middle and Late Jurassic, perhaps in Bajocian to early Oxfordian time in the southeast, and late Oxfordian time in the northwest, presumably in a relatively narrow and elongate, rapidly subsiding basin. The main source of sediment in the northwestern part was from the Yukon terrane lying to the north—a source indicated by the lithology of cobbles in conglomerates and by imbrication of cobbles that shows southward sediment transport. A source from the Alexander terrane, on the basis of conglomerate cobble lithology, seems likely for the southeastern part of the basin, at least along its western edge.

Sometime during the Kimmeridgian to Albian interval, rocks in the Wrangell Mountains were folded, uplifted, and deeply eroded. Possibly sediments were shed northward from this uplifted terrane into the Gravina-Nutzotin trough, but no clastic wedge or coarsening of the sedimentary rock sequence in the Nutzotin Mountains has been observed to document this event.

Andesitic volcanism, here interpreted as being genetically related to subduction in the Chugach trench, appears to have started very early in the southeastern end of the trough, but certainly the greatest volcanic activity was during the Early Cretaceous. The development of the Gravina-Nutzotin trough probably was roughly contemporaneous with deposition of the younger sequence of sedimentary rocks in the Chugach terrane. The history of these trench deposits, however, is still so obscure that any further speculation as to possible historic links between the two terranes seems unwarranted.

Major compressional deformation of Gravina-Nutzotin belt rocks probably began in post-early Albian time, after deposition of the youngest strata known in the belt. Significant pre-Albian deformation seems ruled out by the absence of any recognizable structural or stratigraphic breaks in the bedded sequence.

In the northern part of the belt, this deformation produced relatively simple folds and some thrusts and was accompanied or closely followed by emplacement of numerous granitic plutons. In southeastern Alaska, its effects ranged from relatively mild folding and fracturing along the western margin of the belt to intense penetrative deformation and recrystallization in the central and eastern parts, including probable underthrusting of the eastern edge beneath rocks of the Taku-Skolai terrane. This deformation was roughly contemporaneous with intrusion of zoned ultramafic complexes and with emplacement of an as yet undetermined number of granitic plutons.

Significant compressional deformation of Gravina-Nutzotin belt rocks apparently ended during the Late Cretaceous as relatively undeformed Upper Cretaceous and Tertiary continental sedimentary and volcanic rocks unconformably overlie the older rocks.

One relation that appears very significant to us is that the Gravina-Nutzotin belt is bounded on the west throughout 90 percent of its length by the old continental crustal rocks of the Alexander terrane. As pointed out by Jones, Irwin, and Ovenshine (1972), this crustal block is anomalous in that it appears to lie outboard of younger rocks formed directly on oceanic crust (see also Richter and Jones, 1971, 1972a, b; Monger and Ross, 1971). The implication of this relation is that the Alexander terrane is an allochthon that has undergone large-scale tectonic transport. It thus seems reasonable to suppose that the initiation, filling, and final collapse of the Gravina-Nutzotin trough were intimately tied to postulated movements of this terrane. This supposition is supported by the degree of deformation exhibited by Gravina-Nutzotin belt rocks, which is much greater in southeastern Alaska where they are contiguous to the Alexander terrane, than in the Nutzotin Mountains, where they lie beyond its northwestern terminous. This suggests that the Gravina-Nutzotin trough was folded and finally destroyed by lateral compression produced by the block of Alexander terrane being driven northeastward.

Another feature that deserves comment is that the Gravina-Nutzotin belt shows little offset across the Chatham Strait fault. Others (St. Amand, 1957; Twenhofel and Sainsbury, 1958; Brew and others, 1966; and Ovenshine and Brew, 1972) have speculated that this right-lateral fault is a continuation of the Denali fault. As Lathram (1964) and Ovenshine and Brew have shown, the Chatham Strait fault exhibits at least 120 miles of right-lateral separation, on the basis of reconstruction of displaced geologic features. No record of comparable displacement can be observed for the Gravina-Nutzotin belt, although some disruption of the basin could have occurred before the period of intense compression. Certainly, no evidence is seen to support significant postdeformation offset.

This relation suggests that the Chatham Strait fault is either (1) an old structure that predates the Gravina-Nutzotin belt or (2) confined for the most part to the Alexander terrane and not related to the Denali fault, except perhaps for recent minor movements along the reactivated fault trace.

ACKNOWLEDGMENTS

We thank our colleague, A. B. Ford, who wrote the description of the Juneau area and parts of the section "Chemistry and Classification of the Volcanic Rocks." For their constructive comments and suggestions, we are also grateful to E. H. Lathram, E. M. MacKevett, Jr., L. J. P. Muffler, A. T. Ovenshine, George Plafker, and J. G. Smith, of the U.S. Geological Survey, and to J. W. H. Monger and Jan Muller, of the Geological Survey of Canada.

REFERENCES

Barker, Fred, 1957, Geology of the Juneau B-3 quadrangle, Alaska: U.S. Geol. Survey Geol. Quad. Map GQ-100, scale 1:63,360.

Berg, H. C., 1972a, Geologic map of Annette Island, Alaska: U.S. Geol. Survey Misc. Geol. Inv. Map I-684, scale 1:63,360.

—— 1972b, Recognition of large-scale thrust faults and locally related mineral deposits, southeastern Alaska: [abs.], *in* Faults, fractures, lineaments and related mineralization in the Canadian Cordillera: Geol. Assoc. Canada Cordilleran Sec. Programme and abstracts, Feb. 4–5, 1972, p. 8.

—— 1972c, Geology of Gravina Island, Alaska: U.S. Geol. Survey Bull. 1373. [In press]

Berg, H. C., and Hinckley, D. W., 1963, Reconnaissance geology of northern Baranof Island, Alaska: U.S. Geol. Survey Bull. 1141-O, 24 p.

Brew, D. A., Loney, R. A., and Muffler, L. J. P., 1966, Tectonic history of southeastern Alaska, *in* A symposium on tectonic history and mineral deposits of the western Cordillera in British Columbia and neighbouring parts of the United States: Canadian Inst. Mining and Metallurgy Spec. Vol. 8, p. 149–170.

Buddington, A. F., and Chapin, Theodore, 1929, Geology and mineral deposits of southeastern Alaska: U.S. Geol. Survey Bull. 800, 398 p.

Burk, C. A., 1965, Geology of the Alaska Peninsula-Island arc and continental margin (part 1): Geol. Soc. America Mem. 99 (part 1), 250 p.

Chapin, Theodore, 1918, The structure and stratigraphy of Gravina and Revillagigedo Islands, Alaska: U.S. Geol. Survey Prof. Paper 120-D, p. 83–100.

Chayes, F., 1969, The chemical composition of Cenozoic andesite, *in* McBirney, A. R., ed., Proceedings of the Andesite Conference: Oregon Dept. Geology and Mineral Industries Bull. 65, p. 1–11.

——1970, Experimentation on the electronic storage and manipulation of large numbers of rock analyses: Carnegie Inst. Yearbook 68, p. 174–187.

Clark, A. L., Clark, S. H. B., and Hawley, C. C., 1972, Significance of upper Paleozoic oceanic crust in the upper Chulitna district, west-central Alaska Range, *in* Geological Survey Research 1972: U.S. Geol. Survey Prof. Paper 800-C, p. C95–C101.

Clark, S. H. B., 1972, Reconnaissance bedrock geologic map of the Chugach Mountains near Anchorage, Alaska: U.S. Geol. Survey Misc. Field Inv. Map MF-350, scale 1:250,000.

Coats, R. R., 1962, Magma type and crustal structure in the Aleutian arc, *in* MacDonald, G. A., and Kuno, Hisashi, eds., The crust of the Pacific Basin: Am. Geophys. Union Mon. 6, p. 92–109.

——1968, Basaltic andesites, *in* Hess, H. H., and Poldervaart, Arie, eds., Basalts—The Poldervaart treatise on rocks of basaltic composition, v. 2: New York, John Wiley and Sons, p. 689–736.

Dickinson, W. R., 1970, Relations of andesites, granites, and derivative sandstones to arc-trench tectonics: Rev. Geophysics and Space Physics, v. 8, no. 4, p. 813–860.

——1971a, Clastic sedimentary sequences deposited in shelf, slope, and trough settings between magmatic arcs and associated trenches: Pacific Geology, no. 3 (1971), p. 15–30.

——1971b, Plate tectonic models of geosynclines: Earth and Planetary Sci. Letters, no. 10, p. 165–174.

Eberlein, G. D., and Churkin, Michael, 1970, Paleozoic stratigraphy in northwest coastal area of Prince of Wales Island, southeastern Alaska: U.S. Geol. Survey Bull. 1284, 67 p.

Forbes, R. B., 1959, The bedrock geology and petrology of the Juneau ice field area, southeastern Alaska: Washington Univ., Seattle, Ph. D. thesis, 265 p.

Forbes, R. B., and Engels, J. C., 1970, K^{40}/Ar^{40} age relations of the Coast Range batholith and related rocks of the Juneau ice field area, Alaska: Geol. Soc. America Bull., v. 81, no. 2, p. 579–584.

Grantz, Arthur, and Jones, D. L., 1960, Stratigraphy and age of the Matanuska Formation, south-central Alaska: Art. 159 *in* U.S. Geol. Survey Prof. Paper 400-B, p. B347–B350.

Grantz, Arthur, Jones, D. L., and Lanphere, M. A., 1966, Stratigraphy, paleontology, and isotopic ages of upper Mesozoic rocks in southwestern Wrangell Mountains, Alaska, *in* Geological Survey Research 1966: U.S. Geol. Survey Prof. Paper 550-C, p. C39–C47.

Hutchison, W. W., 1967, Prince Rupert and Skeena map-area, British Columbia: Canada Geol. Survey Paper 66-33, 27 p.

Imlay, R. W., 1960, Early Cretaceous (Albian) ammonites from the Chitina Valley and Talkeetna Mountains, Alaska: U.S. Geol. Survey Prof. Paper 354-D, p. 87–114.

Irvine, T. N., 1967, The Duke Island ultramafic complex, southeastern Alaska, *in* Wyllie, P. J., ed., Ultramafic and related rocks: New York, John Wiley and Sons, p. 84–97.

Jones, D. L., 1963, Upper Cretaceous (Campanian and Maestrichtian) ammonites from southern Alaska: U.S. Geol. Survey Prof. Paper 432, 53 p.

——1967, Cretaceous ammonites from the lower part of the Matanuska Formation, southern Alaska: U.S. Geol. Survey Prof. Paper 547, 49 p.

Jones, D. L., and Detterman, R. L., 1966, Cretaceous stratigraphy of the Kamishak Hills, Alaska Peninsula, *in* Geological Survey Research 1966: U.S. Geol. Survey Prof. Paper 550-D, p. D53–D58.

Jones, D. L., Irwin, W. P., and Ovenshine, A. T., 1972, Southeastern Alaska–A displaced continental fragment?, *in* Geological Survey Research 1972: U.S. Geol. Survey Prof. Paper 800-B, p. B211–B217.

Jones, D. L., and MacKevett, E. M., Jr., 1969, Summary of Cretaceous stratigraphy in part of the McCarthy quadrangle, Alaska: U.S. Geol. Survey Bull. 1274-K, p. K1–K19.

Jones, D. L., MacKevett, E. M., Jr., and Plafker, George, 1971, Speculations on late Mesozoic tectonic history of part of southern Alaska: Am. Assoc. Petroleum Geologists, Second Internat. Symposium on Arctic Geology, Program abstracts, p. 30.

Karig, D. C., 1971, Structural history of the Mariana Island arc system: Geol. Soc. America Bull., v. 82, p. 323–344.

Kindle, E. D., 1953, Dezadeash map area, Yukon Territory: Canada Geol. Survey Mem. 268, 68 p.

Knopf, Adolph, 1911, Geology of the Berners Bay region, Alaska: U.S. Geol. Survey Bull. 446, 58 p.

——1912, The Eagle River region, southeastern Alaska: U.S. Geol. Survey Bull. 502, 61 p.

Lanphere, M. A., 1968, Sr-Rb-K and Sr isotopic relationships in ultramafic rocks, southeastern Alaska: Earth and Planetary Sci. Letters, no. 4, p. 185–190.

Lanphere, M. A., and Eberlein, G. D., 1966, Potassium-argon ages of magnetite-bearing ultramafic complexes in southeastern Alaska: Geol. Soc. America Spec. Paper 87, p. 94.

Lanphere, M. A., Loney, R. A., and Brew, D. A., 1965, Potassium-argon ages of some plutonic rocks, Tenakee area, Chichagof Island, southeastern Alaska, *in* Geological Survey Research 1965: U.S. Geol. Survey Prof. Paper 525-B, p. B108–B111.

Lathram, E. H., 1964, Apparent right-lateral separation on Chatham Strait fault, southeastern Alaska: Geol. Soc. America Bull., v. 75, no. 3, p. 249–252.

Lathram, E. H., Loney, R. A., Condon, W. H., and Berg, H. C., 1959, Progress map of the geology of the Juneau quadrangle, Alaska: U.S. Geol. Survey Misc. Geol. Inv. Map I-303, scale 1:250,000.

Lathram, E. H., Pomeroy, J. S., Berg, H. C., and Loney, R. A., 1965, Reconnaissance geology of Admiralty Island, Alaska: U.S. Geol. Survey Bull. 1181-R, 48 p.

Loney, R. A., 1964, Stratigraphy and petrography of the Pybus-Gambier area, Admiralty Island, Alaska: U.S. Geol. Survey Bull. 1178, 103 p.

Loney, R. A., Berg, H. C., Pomeroy, J. S., and Brew, D. A., 1963, Reconnaissance geologic map of Chichagof Island and northwestern Baranof Island, Alaska: U.S. Geol. Survey Misc. Geol. Inv. Map I-388, scale 1:250,000.

Loney, R. A., Brew, D. A., and Lanphere, M. A., 1967, Post-Paleozoic radiometric ages and their relevance to fault movements, northern southeastern Alaska: Geol. Soc. America Bull., v. 78, no. 4, p. 511–526.

Loney, R. A., Pomeroy, J. S., Brew, D. A., and Muffler, L. J. P., 1964, Reconnaissance geologic map of Baranof and Kruzof Islands, Alaska: U.S. Geol. Survey Misc. Geol. Inv. Map I-411, scale 1:250,000.

McBirney, A. R., 1969, Andesitic and rhyolitic volcanism of orogenic belts, *in* Hart, P. J., ed., Earth's crust and upper mantle: Am. Geophys. Union Mon. 13, p. 501–507.

MacKevett, E. M., Jr., 1969, Three newly named Jurassic formations in the McCarthy C-5 quadrangle, *in* Changes in stratigraphic nomenclature by the U.S. Geological Survey 1967: U.S. Geol. Survey Bull. 1274-A, p. A35–A49.

——1970, Geology of the McCarthy B-4 quadrangle, Alaska: U.S. Geol. Survey Bull. 1333, 31 p.

——1971, Stratigraphy and general geology of the McCarthy C-5 quadrangle, Alaska: U.S. Geol. Survey Bull. 1323, 35 p.

Martin, G. C., 1926, The Mesozoic stratigraphy of Alaska: U.S. Geol. Survey Bull. 776, 493 p.

Matsuda, T., and Uyeda, S., 1971, On the Pacific-type orogeny and its model-extension of the paired belts concept and possible origin of marginal seas: Tectonophysics, v. 11, p. 5–27.

Miller, D. J., Payne, T. G., and Gryc, George, 1959, Geology of possible petroleum provinces in Alaska: U.S. Geol. Survey Bull. 1094, 131 p.

Monger, J. W. H., and Ross, C. A., 1971, Distribution of fusulinaceans in the western Canadian cordillera: Canadian Jour. Earth Sci., v. 8, no. 2, p. 259–278.

Monger, J. W. H., Souther, J. G., and Gabrielse, H., 1972, Evolution of the Canadian cordillera–A plate-tectonic model: Am. Jour. Sci. v. 272, no. 7, p. 577–602.

Moore, G. W., 1969, New formations on Kodiak and adjacent islands, Alaska, *in* Changes in stratigraphic nomenclature by the U.S. Geological Survey 1967: U.S. Geol. Survey Bull. 1274-A, p. A27–A35.

Moore, J. C., 1972, Southwestern Alaska–Bering Shelf edge: Science, v. 175, no. 4026, p. 1103–1105.

Muffler, L. J. P., 1967, Stratigraphy of the Keku Islets and neighboring parts of Kuiu and Kupreanof Islands, southeastern Alaska: U.S. Geol. Survey Bull. 1241-C, 52 p.

Muller, J. E., 1967, Kluane Lake map-area, Yukon Territory: Canada Geol. Survey Mem. 340, 137 p.

Nockolds, S. R., 1954, Average chemical compositions of some igneous rocks: Geol. Soc. America Bull., v. 65, p. 1007–1032.

Ovenshine, A. T., and Brew, D. A., 1972, Separation and history of the Chatham Strait fault, southeastern Alaska, North America [abs.]: Internat. Geol. Cong., 24th, Montreal, Canada, Proc. [In press]

Packham, G. H., and Falvey, D. H., 1971, An hypothesis for the formation of marginal seas in the western Pacific: Tectonophysics, v. 11, p. 79–109.

Plafker, George, 1967, Geologic map of the Gulf of Alaska Tertiary Province, Alaska: U.S. Geol. Survey Misc. Geol. Inv. Map I-484, scale 1:500,000.

——1971, Possible future petroleum resources of Pacific-margin Tertiary basin, Alaska, *in* Cram, I. H., ed., Future petroleum provinces of the United States: Am. Assoc. Petroleum Geologists Mem. 15, p. 120–135.

——1972, New data on Cenozoic displacements along the Fairweather fault system, Alaska, *in* Faults, fractures, lineaments, and related mineralization in the Canadian cordillera: Geol. Assoc. Canada, Cordilleran Section, Programme and abstracts, p. 30.

Richter, D. H., 1971a, Reconnaissance geologic map and section of the

Nabesna A-3 quadrangle, Alaska: U.S. Geol. Survey Misc. Geol. Inv. Map I-655, scale 1:63,360.

Richter, D. H., 1971b, Reconnaissance geologic map and section of the Nabesna A-4 quadrangle, Alaska: U.S. Geol. Survey Misc. Geol. Inv. Map I-656, scale 1:63,360.

Richter, D. H., and Jones, D. L., 1971, Structure and stratigraphy of eastern Alaska Range, Alaska: Am. Assoc. Petroleum Geologists, Second Internat. Symposium on Arctic Geology, Program abstracts, p. 45.

——1972a, Structure and stratigraphy of eastern Alaska Range, Alaska: Am. Assoc. Petroleum Geologists, Second Internat. Symposium on Arctic Geology Proc. [In press]

——1972b, Reconnaissance geologic map and sections of the Nabesna A-2 quadrangle, Alaska: U.S. Geol. Survey Misc. Geol. Inv. Map I-749, scale 1:63,360. [In press]

Richter, D. H., and Schmoll, H. R., 1972, Reconnaissance geologic map and sections of the Nabesna C-5 quadrangle, Alaska: U.S. Geol. Survey Geol. Quad. Map GQ-1062, scale 1:63,360. [In press]

Saks, V. N., 1960, On the problem of the distribution and stratigraphic role of Lower Cretaceous Belemnites in the north of Siberia [In Russian]: Akad. Nauk SSSR Doklady, v. 131, p. 640–642 [English translation in March, 1961, Am. Geol. Inst.].

Smith, J. G., and MacKevett, E. M., Jr., 1970, The Skolai Group in the McCarthy B-4, C-4, and C-5 quadrangles, Wrangell Mountains, Alaska: U.S. Geol. Survey Bull. 1274-Q, p. Q1–Q26.

Smith, R. E., 1968, Redistribution of major elements in the alteration of some basic lavas during burial metamorphism: Jour. Petrology, v. 9, p. 191–219.

St. Amand, Pierre, 1957, Geological and geophysical synthesis of the tectonics of portions of British Columbia, the Yukon Territory, and Alaska: Geol. Soc. America Bull., v. 68, p. 1343–1370.

Stevens, J. R., 1965, The Jurassic and Cretaceous belemnites of New Zealand and a review of the Jurassic and Cretaceous belemnites of the Indo-Pacific region: New Zealand Geol. Survey, Paleont. Bull. 36, 283 p.

Taylor, H. P., Jr., 1967, The zoned ultramafic intrusions of southeastern Alaska, *in* Wyllie, P. J., ed., Ultramafic and related rocks: New York, John Wiley and Sons, p. 97–121.

Taylor, H. P., Jr., and Noble, J. A., 1969, Origin of magnetite in the zoned ultramafic complexes of southeastern Alaska: Econ. Geology Mon. 4, p. 209–230.

Twenhofel, W. S., and Sainsbury, C. L., 1958, Fault patterns in southeastern Alaska: Geol. Soc. America Bull., v. 69, p. 1431–1442.

Watson, K. D., 1948, The Squaw Creek–Rainy Hollow area, northern British Columbia: British Columbia Dept. Mines and Petroleum Resources Bull. 25, 74 p.

Williams, Howell, Turner, F. J., and Gilbert, C. M., 1954, Petrography: San Francisco, W. H. Freeman and Co., 406 p.

A SMALL-SCALE THRUST FAULT ASSOCIATED WITH LOW-AMPLITUDE FLEXURAL-SLIP FOLDING, GREENE COUNTY, SOUTHWEST PENNSYLVANIA

By JOHN B. ROEN, Beltsville, Md.

Abstract.—Small faults are known to exist in Washington and Greene Counties, Pa.; however, exposures that permit detailed mapping are practically nonexistent, and as a result, the genesis of these structures and their relation to the regional structure are unknown. A recently excavated railroad cut west of Waynesburg, Pa., exposes in detail one of these small faults. The fault is a thrust that strikes parallel to the regional folds and dips toward a synclinal axis. The geometry of the fault surface and its orientation indicate that it resulted from the compressional stress that produced the low-amplitude regional folds.

The geologic structure in Washington and Greene Counties, Pa., consists primarily of northeast-trending low-amplitude folds of large wavelength. Faults are known to exist, but they have been generally overlooked and not described because of poor exposure and small displacement. The few known faults are exposed in single elevation views such as roadcuts; at some places they are suggested by slight stratigraphic displacement, as interpreted from a combination of drill-hole and surface data. Exposures of or data on these faults have been insufficient to determine their orientation precisely. Because poor exposure precludes delineation of fault geometry, the genesis of the few recognized faults and their relation to other structural features of southwest Pennsylvania is unknown.

A recently excavated vertical railroad cut at East View in the Waynesburg 7½-minute quadrangle, Greene County, Pa. (figs. 1 and 2), provides excellent exposures of a low-angle thrust fault and associated wedging on both sides of the cut. This unique exposure of a small thrust fault permits description of the fault geometry and provides evidence of its origin and relation to regional folding.

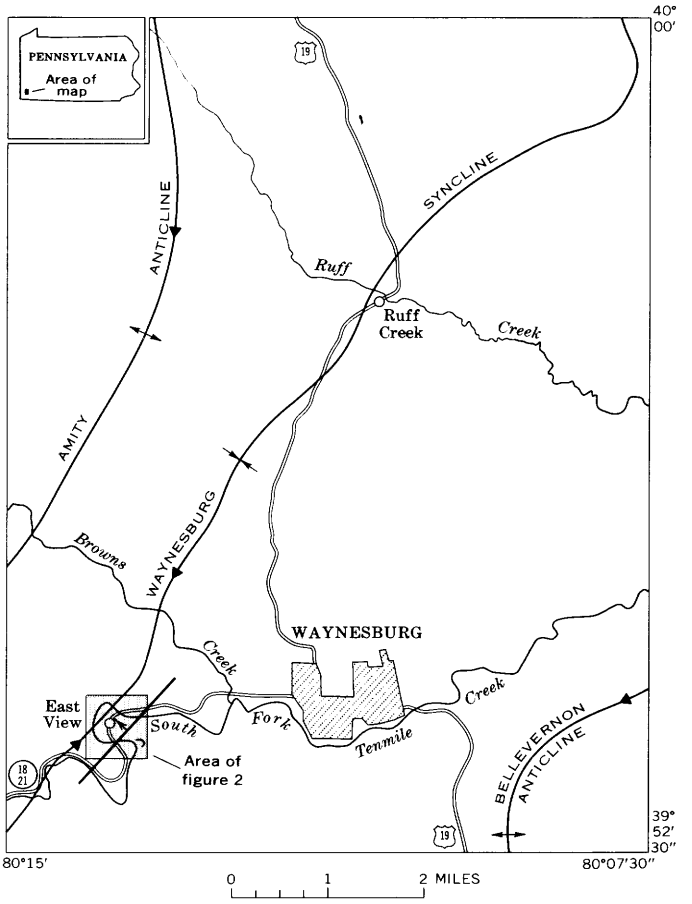

Figure 1.—Index map of the Waynesburg 7½-minute quadrangle, southwest Pennsylvania, showing the strike and direction of dip of the thrust fault surface and its relation to regional fold axes.

FIELD RELATIONS

The rocks exposed in the railroad cut are part of the Washington and Greene Formations (Permian). The lowermost strata exposed are medium-dark-gray shale and clay and gray siltstone of the middle member of the Washington Formation. Above the middle member is the upper limestone member consisting of two very light gray weathering, olive-gray argillaceous limestone units 4–9 feet thick separated by about 18–19 feet of medium-dark-gray shale. The base of the overlying Greene Formation is about 6 feet below the lip of the vertical cut. The Greene Formation here consists of shale, silty shale, sandstone, limestone, and coal. The Ten Mile coal

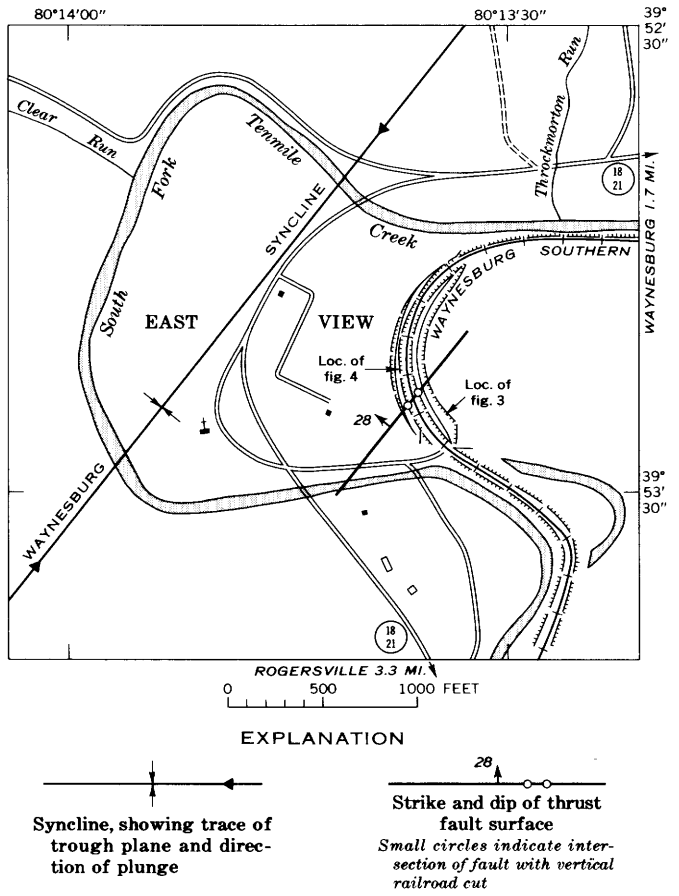

Figure 2.—Detailed map of the railroad cut at East View, east of Waynesburg, Pa., showing the location of fault exposure and relation of fault strike to the axial trend of the Waynesburg syncline.

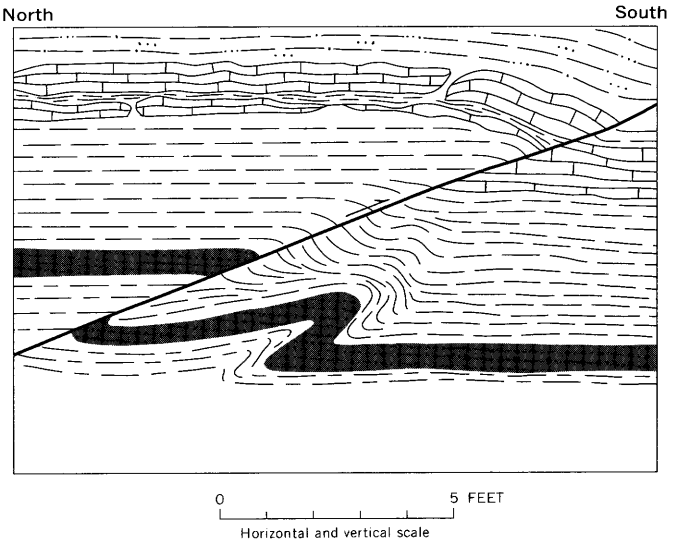

Figure 3.—Sketch showing the dislocation of the Ten Mile coal bed of Clapp (1907) on the east side of the railroad cut. Note the difference in deformation between the competent limestone and the less competent coal and shale.

bed of Clapp (1907) (fig. 3) is 27 feet above the top of the upper limestone member of the Washington Formation.

On both sides of the excavation, the thrust fault displaces the upper limestone member of the Washington Formation. The displacement of the beds cut by the fault is about 3 feet in terms of stratigraphic throw, an amount not detectable in areas of extensive cover. On the east side of the cut, the break is clearly defined; it dislocates not only the upper limestone member, but also the beds above and below. On the west wall the thrust is clearly defined except where the fault follows a bedding plane on top of the lower limestone unit of the upper limestone member (fig. 4). The fault follows the bedding plane for about 30 feet and then passes into the lower limestone unit. At this point the rupture changes from a thrust to a wedging movement (fig. 4) in which limestone beds of the lower plate wedge into and split the limestone beds of the upper plate. The fault does not completely cut the lower limestone unit, and wedging takes up the displacement in the higher beds. Below the limestone beds, this wedging has produced an incipient fault and fracture zone inclined opposite to the thrust.

The strike of the fault is N. 42° E. and was determined by finding the average bearing of two level lines on the fault surface. The surface is concave upward; however, an average dip of 28° was determined graphically from three points of known elevation at the extreme ends of the exposed surface.

With respect to the regional folding, the thrust fault is about 1,000 feet southeast of, and parallel to, the trace of the trough plane of the Waynesburg syncline (fig. 2). Both the syncline and fault trend N. 42° E. The fault surface dips down into the

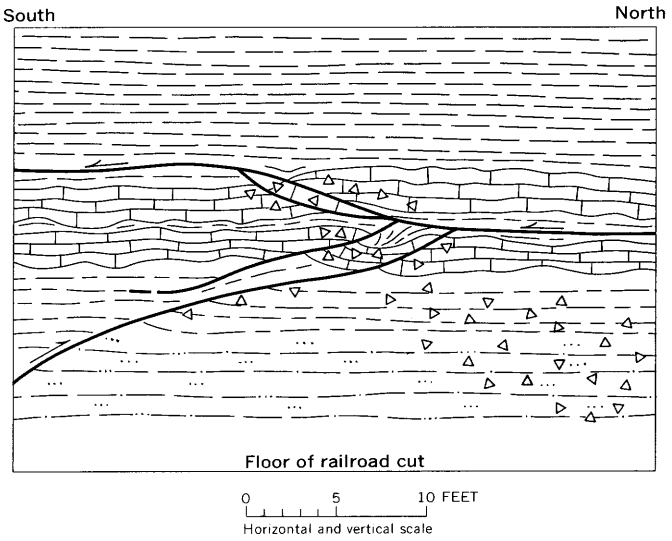

Figure 4.—Sketch of part of the west wall of the railroad cut, showing wedging in the lower limestone unit of the upper limestone member of the Washington Formation. Small triangles indicate brecciation.

synclinal trough. The fault is about 4.5 miles northwest of the Bellevernon anticline (fig. 1) and is approximately parallel to the general trend of the anticline.

DISCUSSION

The strike and dip of the concave-upward fault surface at East View is compatible with folding and faulting in theoretical models in which concave-upward rupture surfaces are inclined about 30° to the greatest principal stress axis and strike normal to it (Hubbert, 1951; Hafner, 1951). Because the strike of the fault and the fold trends are approximately parallel, the direction of maximum principal stress that produced each was undoubtedly about the same. It seems reasonable to assume that the same forces were involved in both the faulting and the folding, and that the thrust and associated wedging resulted from shortening and lack of space in the synclinal core during the folding.

REFERENCES

Clapp, F. G., 1907, Economic geology of the Amity quadrangle, eastern Washington County, Pennsylvania: U.S. Geol. Survey Bull. 300, 145 p.

Hafner, Willy, 1951, Stress distributions and faulting: Geol. Soc. America Bull., v. 62, no. 4, p. 373–398.

Hubbert, M. K., 1951, Mechanical basis for certain familiar geologic structures: Geol. Soc. America Bull., v. 62, no. 4, p. 355–372.

SIGNIFICANCE OF LOWER ORDOVICIAN EXOTIC BLOCKS IN THE HAMBURG KLIPPE, EASTERN PENNSYLVANIA

By JACK B. EPSTEIN, ANITA G. EPSTEIN, and STIG M. BERGSTRÖM[1],
Beltsville, Md., Washington, D.C., Columbus, Ohio

Abstract.—Limestone slide blocks in the Hamburg klippe near Lenhartsville, eastern Pennsylvania, contain Early Ordovician North Atlantic province conodonts. Similar lithic types and conodonts are unknown in correlative autochthonous rocks of the Beekmantown Group in the Great Valley of eastern Pennsylvania. The character of the fauna and the host rocks suggest that these limestones were (1) deposited on a northwest-facing bank in the "proto-Atlantic" ocean east of their present location, (2) remobilized and transported partly by turbidity currents and as slumps onto a slope, and (3) subsequently broken up into blocks that slid into deeper water. These rocks were later displaced northwestward to their present position by thrusting during Taconic tectonism.

An assemblage of rocks of at least Early Ordovician and possibly Cambrian to Middle Ordovician age in eastern Pennsylvania, south of Shochary Ridge (fig. 1) and extending westward to the Susquehanna River, were considered by Stose (1946) to be a remnant of the "Taconic sequence." Stose believed that this assemblage is similar to rocks in New York and New England and was thrust from an eastern basin westward onto the Martinsburg Formation (Ordovician) and older carbonate rocks, an idea earlier expressed by Kay (1941). Stose named this thrust sheet the Hamburg klippe. The boundary of the Hamburg klippe as used in this report is taken from Stose (1946; fig. 1).

Rock types unknown in the Martinsburg Formation of the slate belt to the east characterize the klippe. The klippe contains many slump blocks either emplaced in pelite and graywacke of the Martinsburg Formation, as suggested by Platt and others (1972), or emplaced in a different host rock and later thrust on top of the Martinsburg as one large structurally complex sheet. We favor the latter hypothesis, that the rocks of the klippe are not indigenous to the Martinsburg depositional basin, because (1) preliminary examination of some of the graywackes in the Hamburg klippe suggests that they are significantly different petrographically from Martinsburg graywacke and (2) reconnaissance by A. A. Drake, Jr., and J. B. Epstein (U.S. Geological Survey, 1971, p. A27) has indicated a major structural break between the klippe and rocks of the Martinsburg. This structural break was also inferred from paleontologic data by J. B. Epstein (U.S. Geological Survey, 1970, p. A26).

The Hamburg klippe includes a variety of rock types: gray, red, and green shale; graywacke; argillaceous, arenaceous, aphanitic to coarsely crystalline, laminated to massive limestone; dolomite; intraformational limestone conglomerate; quartz-, chert-, and limestone-pebble conglomerate; massive sandstone and pebbly orthoquartzite; radiolarian chert; altered tuffaceous sediments; and basalt and diabase (Gordon, 1921; Stose and Jonas, 1927; Behre, 1933; Willard, 1939, 1943; Moseley, 1950).

Many of the rock types in the Hamburg klippe are demonstrably nearshore shelf deposits. These rocks are in discontinuous or fault-bounded bodies suggesting, along with the presence of boulder conglomerates and wildflysch, emplacement into deeper water as submarine slides (McBride, 1962; MacLachlan and Root, 1966; Aldrich, 1967; Platt, 1968; Alterman, 1969; Myers, 1969; Platt and others, 1969; Bird and Dewey, 1970). The host for these submarine slides is shale and graywacke interpreted to be deepwater deposits. Red shales, although believed by Willard (1939, 1943) to be continental in origin, along with sponge-spicule-bearing siliceous shale and radiolarian chert, are regarded by McBride (1962, p. 46) to be very deepwater (abyssal) deposits.

AGE OF THE ROCKS IN THE HAMBURG KLIPPE AND SURROUNDING TERRANE

All rocks in the part of the Hamburg klippe shown on figure 1 were mapped as Martinsburg Formation on the geologic map of Pennsylvania (Gray and others, 1960) and regarded to be of Middle and Late Ordovician age. Willard (1943, p. 1101) reported graptolites in rocks of the klippe which were determined by Rudolf Ruedemann and E. O. Ulrich to be of Early Ordovician (Deepkill) age, but Willard was somewhat reluctant to accept these graptolite-bearing rocks as being as

[1] Department of Geology, The Ohio State University.

U.S. GEOL. SURVEY PROF. PAPER 800-D, PAGES D29-D36

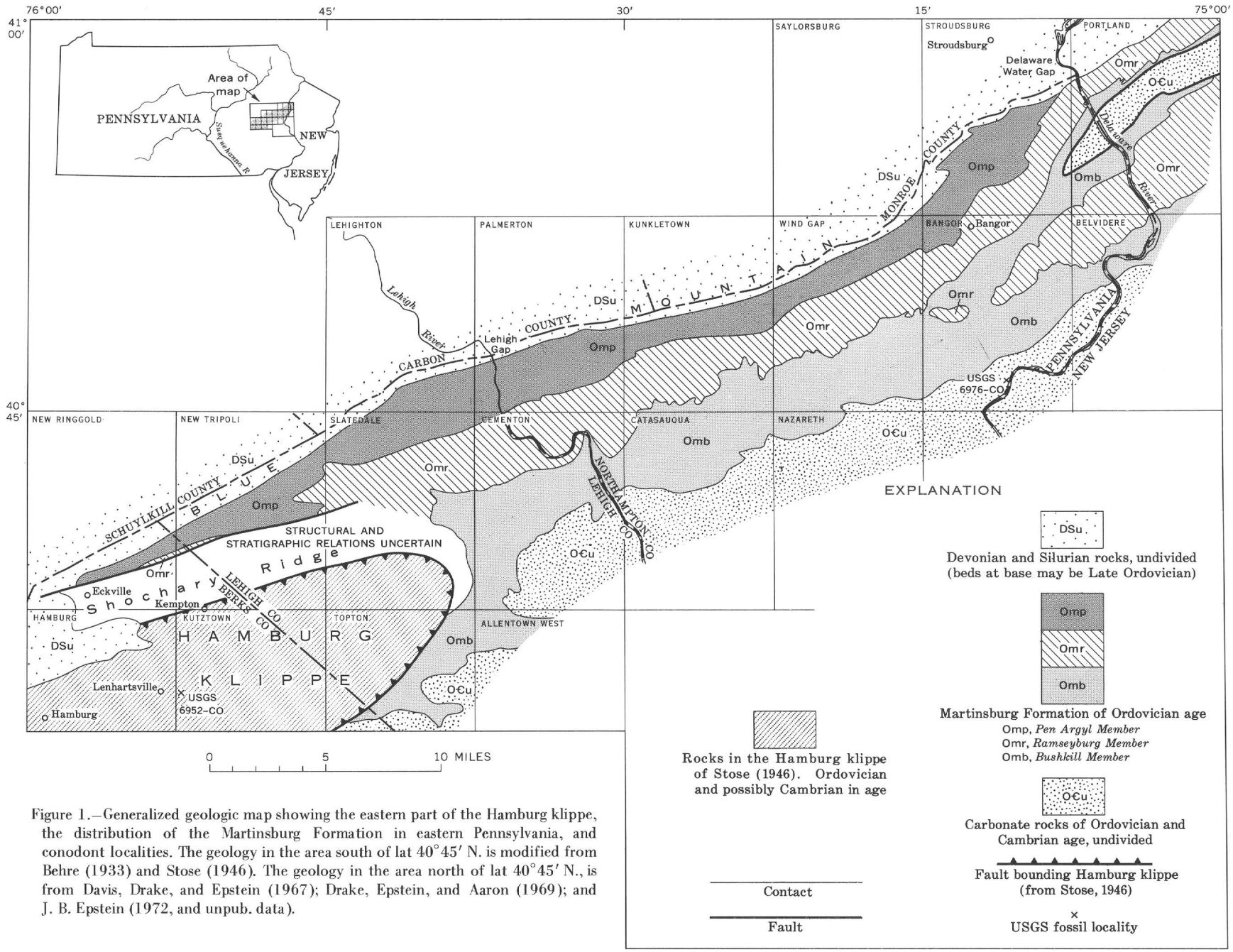

Figure 1.—Generalized geologic map showing the eastern part of the Hamburg klippe, the distribution of the Martinsburg Formation in eastern Pennsylvania, and conodont localities. The geology in the area south of lat 40°45′ N. is modified from Behre (1933) and Stose (1946). The geology in the area north of lat 40°45′ N., is from Davis, Drake, and Epstein (1967); Drake, Epstein, and Aaron (1969); and J. B. Epstein (1972, and unpub. data).

old as Early Ordovician. Stose (1946) suggested that these rocks of the "Taconic sequence" in Pennsylvania were Early Cambrian and Ordovician in age. Gray and Willard (1955) were not entirely convinced that the rocks in Stose's Hamburg klippe were part of a large overthrust and suggested that these rocks might be a facies of rocks to the east. They also claimed that perhaps the stratigraphic ranges of the graptolites from the Hamburg klippe were incompletely known. Platt (1968) reported Early Ordovician graptolites in a sequence of interbedded limestone and shale and limestone-pebble conglomerate in the Hamburg klippe near Harrisburg, Pa. A review of the sparse fauna reported from klippe rocks is given by Platt and others (1972).

Trilobites and brachiopods were collected from the Hamburg klippe at Swatara Gap (34 miles west of Lenhartsville) by J. B. Epstein in 1969 from yellowish-orange- and olive-gray-weathering shale just below the Shawangunk Formation in new roadcuts along U.S. Interstate Route 81 (USGS loc. D2185-CO). The fossils were identified by W. T. Dean, Geological Survey of Canada (written commun., 1970), who reported that the dominant trilobite is most probably *Cryptolithus lorettensis* Foerste (not *C. bellulus* as reported by Stose, 1930, and Whittington, 1968, from the same locality), which is generally believed to indicate an early Barneveldian Age (lower part of the lower subzone of Zone 13 of Berry, 1970, the Shermanian of Sweet and Bergström, 1971). This is the age of the oldest Martinsburg or youngest Jacksonburg Limestone in the slate belt area to the east. In eastern Pennsylvania, the oldest rock truncated by the Taconic unconformity has been equated to graptolite Zone 14 (Pavlides and others, 1968). Thus, the rocks at Swatara Gap represent the greatest hiatus ascribable to the Taconic unconformity in eastern Pennsylvania that has been documented to date.

The age of the rocks in Shochary Ridge (fig. 1) is generally given as late Edenian to early Maysvillian (for example, Twenhofel and others, 1954) on the basis of an abundant shelly fauna initially identified by Ulrich (in Stose, 1930, p. 648–649). Behre (1933) mapped the rocks in Shochary Ridge as the Martinsburg Formation (chiefly the Ramseyburg Member of fig. 1). However, preliminary field and microscopic examination of these rocks by A. A. Drake, Jr. (oral commun., 1971), and J. B. Epstein shows that many of the rocks in Shochary Ridge are petrographically, paleontologically, and sedimentalogically distinct from those of the Martinsburg Formation in the slate belt and differ in stratigraphic succession and tectonic style as well. Therefore, it is possible that Shochary Ridge is tectonically separated from rocks in the slate belt to the east and north and may be a part of the Hamburg klippe, or lies within a fault block north of the klippe. Thus, the stratigraphic and structural relations in the Shochary Ridge area are shown as uncertain on figure 1.

The Martinsburg Formation in the slate belt east of the Hamburg klippe is late Middle Ordovician to early Late Ordovician (Edenian to early Maysvillian or upper subzone of graptolite Zone 13) in age on the basis of graptolites from the Pen Argyl Member of the Martinsburg at Lehigh Gap (Epstein and Berry, 1972) and conodonts in the underlying Jacksonburg Limestone (Barnett, 1965). Thus, it appears that some of the rocks in the Hamburg klippe are older than rocks in the Martinsburg Formation immediately to the east.

Conclusive conodont evidence that the Hamburg klippe contains blocks of rock that are older than the Martinsburg Formation of the slate belt to the east and that correlate with Lower Ordovician carbonate rocks underlying the Martinsburg in easternmost Pennsylvania is given by Bergström, Epstein, and Epstein (1972) (p. D37–D44, this chapter). Whereas, other carbonate blocks and conglomerates of Cambrian and Ordovician age in the northern Appalachians are demonstrably slumps emplaced from a carbonate bank on the west into deepwater pelites to the east (for example, Rodgers, 1968), the rocks discussed here were derived from a source that probably lay to the east.

LIMESTONE SLIDE BLOCKS

The limestone blocks from which the conodonts were recovered are in a roadcut on old U.S. Route 22, 0.9 mile east of Lenhartsville, Pa. (fig. 1). Details of the exposures and location of samples are shown in figure 2.

One limestone block is at least 80 feet long and consists of medium-gray to medium-dark-gray, light-gray- to medium-dark-gray-weathering calcisiltite in ripple lenses isolated by laminated medium-dark-gray shale and moderate-yellowish-brown-weathering calcareous shale (fig. 3). The starved ripples are about 1 to 12 inches long and many merge to form discontinuous beds, especially higher in the block where the rock is more evenly bedded. In most of the exposure, the ripples in the limestone are accentuated by pelitic material that extends from the surrounding shale through the limestone (fig. 4*A*) showing that the limestone and shale were deposited at the same time. Soon after deposition, some of the ripple lenses may have become detached or acted as rigid barriers to the moving muds around them, because in several samples the ripple laminae do not pass through the lenses into the surrounding shale but end at the border of the limestone (fig. 4*B*). Some limestone intraclasts within the lenses likewise terminate abruptly at the limestone-shale interface, which also suggests that there was some erosion of the lenses soon after their deposition. The presence of intraclasts indicates that there was some reworking of consolidated or semiconsolidated limestone prior to final deposition. Sample 1 (fig. 2) was collected from the limestone lenses in this block.

The block of rippled limestone and shale is surrounded by greenish-gray to medium-greenish-gray and grayish-red mudstone, as far as can be deduced from the limited exposures. The greenish mudstone contains abundant clasts and broken discontinuous beds of limestone (fig. 5). The clasts are generally tabular and angular, but some are subrounded. They are medium to light gray and bluish gray and weather very

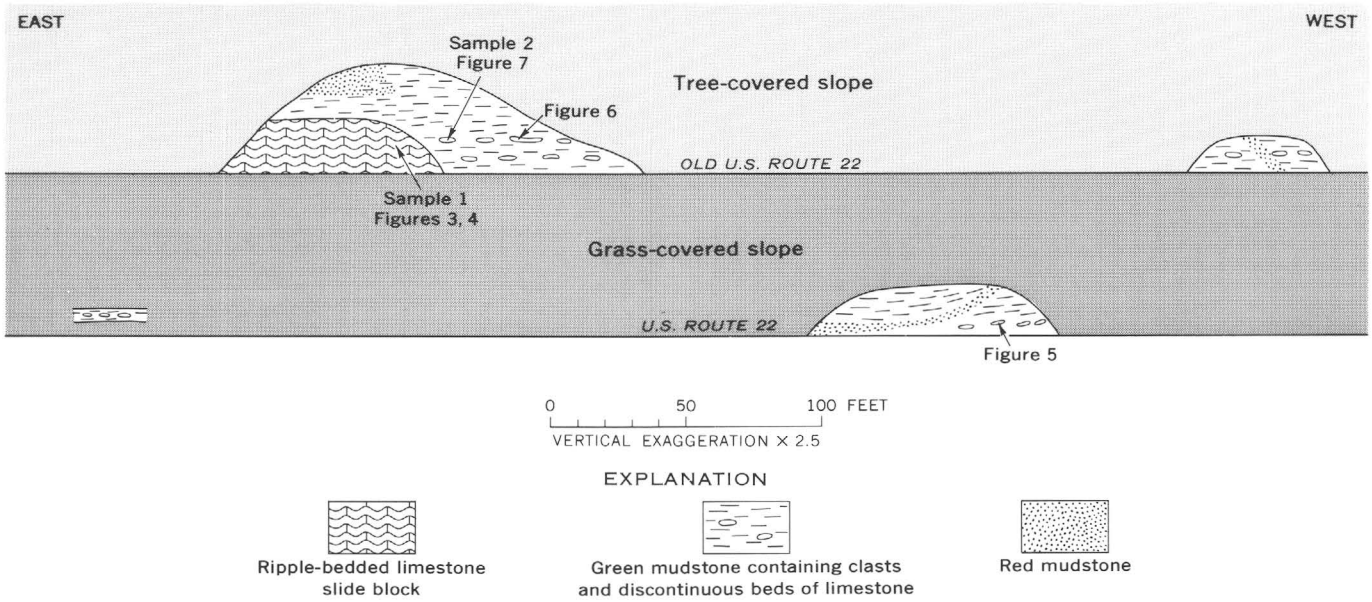

Figure 2.—Sketch showing roadcuts containing limestone blocks in green and red mudstone near Lenhartsville, Pa., and location of conodont-bearing samples (USGS loc. 6952-CO).

light gray to white. Along U.S. Route 22, the clasts are ¼–1 inch thick and ¼–7 inches long, but on old U.S. Route 22 some boulders are 3 feet long. Many of the clasts are laminated and others are crosslaminated (fig. 6). The crosslaminated clasts are lithically identical with the large ripple-bedded limestone block. Many of the clasts have been pulled apart along irregular surfaces, and flowage of mud over these clasts indicates that the limestone was deposited in a semiconsolidated state (fig. 6). Because limy sediments are known to consolidate relatively rapidly, it is possible that the conodonts in the limestone date the surrounding shale as well.

Figure 3.—Outcrop of ripple-bedded calcisiltite (light lenses) and calcareous shale, 0.9 mile east of Lenhartsville, Pa., along old U.S. Route 22.

Some of the limestone clasts exposed along old U.S. Route 22 are graded conglomeratic limestone (fig. 7). One such clast, about 15 feet west of the large ripple-bedded block, supplied the conodonts in sample 2 (fig. 2). It is approximately 3 feet long and 10 inches high, consists of light-gray to medium-light-gray sparrudite to intrasparite, and is surrounded by greenish-gray laminated mudstone. Other clasts are from 0.2 to at least 40 mm long, tabular with rounded corners, and are chiefly micrite and, to a lesser degree, pelsparite. Most are laminated or crosslaminated. Many of the clasts contain silt-sized to very fine sand sized quartz and small grains of plagioclase. Disarticulated crinoid columnals, brachiopod fragments, rounded quartz grains (as much as 0.8 mm in diameter), and rare rounded to irregularly shaped collophane nodules (averaging approximately 4 mm in diameter) form the remainder of the framework grains.

The limestone clasts are similar to limestone in the Bernville, Pa., area, about 15 miles southwest of Lenhartsville.[1] Besides massive limestone- and sandstone-pebble conglomerate with a quartz-sandstone matrix which is not found in the Lenhartsville exposure, the rocks near Bernville consist of conglomeratic limestone in beds as much as 3 feet thick with angular and subrounded tabular limestone and sandstone clasts as much as 6 inches long, and thin-bedded, laminated, and ripple-bedded limestone, sandy limestone, and gray shale.

[1] For example, 2½ miles southeast of the borough boundary of Bernville on State Route 183 at the intersection with Church Road and 1 mile north of the borough boundary of Bernville on Shartlesville Road, just south of the intersection with Berger School Road.

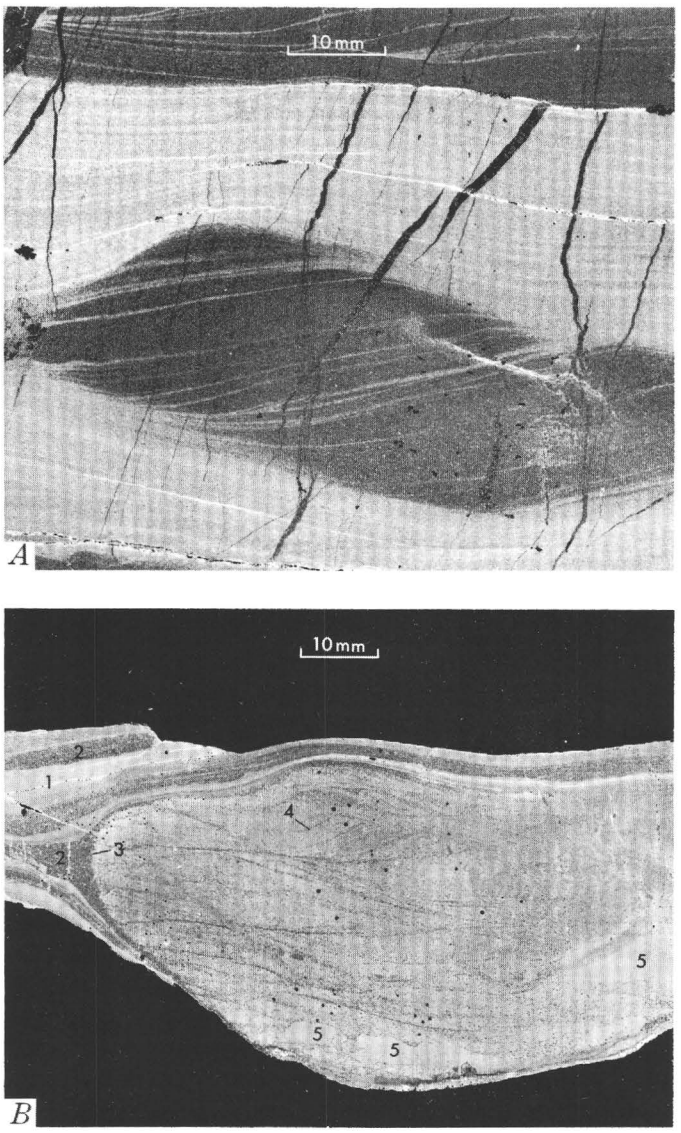

Figure 4.—Negative prints of—

A. Acetate peel showing rippled calcisiltite (dark) and laminated shale and calcareous shale (light). The laminae of shale pass through the limestone lens. Sample collected from outcrop shown in figure 3.

B. Acetate peel showing isolated limestone rippled lens from about 10 feet east of outcrop shown in figure 3. Laminae of shale (1) and calcareous shale (2) terminate against the fuzzy border of the limestone (as at 3). The lens contains small-scale cross-bedding clearly illustrated by grains of quartz and possibly dolomite and feldspar (4). Note smaller sharply defined micrite intraclasts (5). Small black spots are air bubbles. Specimen stained with Alizarin Red S.

Figure 5.—Tabular limestone clasts, as much as 7 inches long and averaging about 1 inch in length, in greenish-gray mudstone. Many of the clasts are laminated (at arrows; many laminations do not show in the photograph). The rocks here have two cleavages: a slaty cleavage, about parallel to the bedding, along which there has been some flowage of material, and a slip cleavage that crenulates the earlier slaty cleavage. Many limestone clasts have been pulled apart (boudinaged) along the slaty cleavage.

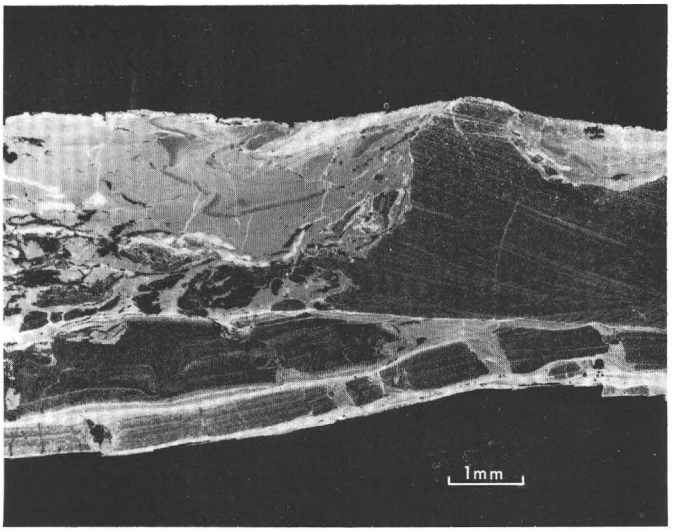

Figure 6.—Negative print of acetate peel showing disrupted cross-laminated limestone (dark) in mudstone. The limestone has been pulled apart along an irregular border, and the fragments have been rotated. Note flow folds above the limestone, suggesting that the limestone was semiconsolidated during deposition. Specimen stained with Alizarin Red S.

Load casts, small contemporaneous slumps, soft-rock pull aparts, small-scale crossbedding, flame structures, and graded bedding are common. These rocks are partly in fining-upward sequences, and it is likely that they were deposited by a combination of subaqueous slumping and turbidity currents. This interpretation was also reached by P. B. Myers, Jr. (oral commun., 1972), who has mapped in the Bernville area. The sandstone pebbles in the conglomerates are orthoquartzites and may be calcareous. The limestone pebbles are laminated to massive and may be quartzose. The pebbles indicate derivation from a well-winnowed carbonate-orthoquartzite shelf environment, and the rocks formed from repeated movement of rock

Figure 7.—Negative print of acetate peel of graded intrasparrudite boulder from near Lenhartsville, Pa. Note crossbedding in many of the intraclasts which is similar to crossbedding in the limestone block shown in figure 3.

fragments and individual grains from the bank into deeper water, most likely onto the continental slope.

The ripple-bedded limestone (fig. 3) and graded conglomeratic limestone (fig. 7) at the Lenhartsville exposure are similar to limestones in the Bernville area, suggesting that the Lenhartsville blocks experienced multicycle transport; that is, sediments originally on a shelf were remobilized and came to rest on an intermediary slope and were later detached as large blocks and small fragments and slid into somewhat deeper water.

AGE OF LIMESTONE SLIDE BLOCKS

Early Early Ordovician conodonts were recovered from two limestone blocks (USGS loc. 6952-CO, fig. 1; samples 1 and 2, fig. 2). They are virtually identical with conodonts of the *Prioniodus elegans* Zone (early Arenigian) of the Balto-Scandic succession. They are the first Early Ordovician North Atlantic province conodonts reported from eastern United States and are unlike those of the North American Midcontinent province. North American Midcontinent province conodonts have been found in nearby autochthonous rocks of the Beekmantown Group in eastern Pennsylvania (USGS loc. 6976-CO, fig. 1) and in three other collections from the Beekmantown Group of central Pennsylvania and Maryland. Details of the faunal provincialism and paleontology are given in Bergström, Epstein, and Epstein (1972) (p. D37–D44, this chapter).

STRUCTURAL SIGNIFICANCE

The exotic blocks bearing North Atlantic province conodonts in the Hamburg klippe near Lenhartsville are faunally and lithically distinct from correlative rocks in the autochthonous Beekmantown Group of the Great Valley of eastern Pennsylvania. The proximity of these two rock types suggests structural telescoping of once distant rocks from two faunal realms. The site of deposition for the Hamburg klippe sediments is unknown, but there can be little doubt, on the basis of the fauna, that the sediments were derived from a southeastern or eastern source. Paleocurrent data collected in the Bernville, Pa., area by P. B. Myers, Jr. (oral commun., 1972), corroborate the proposal that the sediments in the klippe were transported from the southeast. The evidence presented in this report indicates that the exotic blocks were transported from a shelf and deposited as slumps and turbidites on a slope where subsequently small and large fragments from these beds slid into deeper water. Evidence presented here does not favor an east-facing carbonate bank along the North American continental margin as the source for the exotic blocks in the Hamburg klippe of eastern Pennsylvania.

Alternatively, it might be argued that the blocks were derived from near the North American bank edge, but that edge is no longer available for study because of erosion and destruction during continental plate consumption (for example, Bird and Dewey, 1970, fig. 7). However, if this were true, and if future conodont collections show that there are no North Atlantic conodonts in the Beekmantown Group and only North Atlantic conodonts are found in rocks of the Hamburg klippe, then the boundary between the faunal provinces was narrow and lay on the carbonate bank itself. It is difficult to envision this situation without mixing of the two faunas. Furthermore, Bergström's (1972) and Sweet and Bergström's (1972) conclusion that the two faunas developed separately in low and high latitudes makes it even less likely that they could have coexisted on the same carbonate bank. Thus, it is likely that the faunal barrier was a water body of considerable size, perhaps oceanic in magnitude.

Wilson (1966), Ross and Ingham (1970), and Bird and Dewey (1970) believe that Cambrian and Early Ordovician brachiopod and trilobite faunal realms were separated by a proto-Atlantic ocean. Such faunal provincialism has been used to date periods of oceanic expansion (Dewey, 1969, p. 126; Bird and Dewey, 1970, p. 1049–1050). If the plate-tectonic model can also be used to explain conodont provincialism, then continental drift can account for the initial juxtaposition

of Lower Ordovician rocks of the North Atlantic and Midcontinent provinces. The source of the carbonate slump blocks may have been shelf sediments on an uplifted continental rise in the proto-Atlantic ocean or in carbonate banks fringing oceanic island arcs. Thrusting of the Hamburg klippe during the Taconic orogeny resulted in the emplacement of these exotic rocks in eastern Pennsylvania into their present position.

ACKNOWLEDGMENTS

We wish to thank Ina B. Alterman, Avery A. Drake, Jr., Paul B. Myers, Jr., and Lucien B. Platt for their helpful suggestions on the original manuscript, and William T. Dean for identifying the trilobites at Swatara Gap, Pa.

REFERENCES

Aldrich, M. J., Jr., 1967, Cambrian dolomite in the Martinsburg Formation, eastern Pennsylvania: Pennsylvania Acad. Sci. Proc., v. 41, p. 133–140.

Alterman, I. B., 1969, An Ordovician boulder conglomerate at the base of the Hamburg klippe, east-central Pennsylvania [abs.]: Geol. Soc. America Abstracts with Programs, 1969, [v. 1] pt. 1, p. 1–2.

Barnett, S. G., III, 1965, Conodonts of the Jacksonburg Limestone (Middle Ordovician) of northwestern New Jersey and eastern Pennsylvania: Micropaleontology, v. 11, p. 59–80.

Behre, C. H., Jr., 1933, Slate in Pennsylvania: Pennsylvania Geol. Survey, 4th ser., Bull. M16, 400 p.

Bergström, S. M., 1972, Ordovician conodont biogeography, *in* Hallam, A., ed., Atlas of paleobiogeography: Amsterdam, Elsevier. [In press]

Bergström, S. M., Epstein, A. G., and Epstein, J. B., 1972, Early Ordovician North Atlantic province conodonts in eastern Pennsylvania, *in* Geological Survey Research 1972: U.S Geol. Survey Prof. Paper 800-D, p. D37–D44.

Berry, W. B. N., 1970, Review of late Middle Ordovician graptolites in eastern New York and Pennsylvania: Am. Jour. Sci., v. 269, p. 304–313.

Bird, J. M., and Dewey, J. F., 1970, Lithosphere plate-continental margin tectonics and the evolution of the Appalachian orogen: Geol. Soc. America Bull., v. 81, p. 1031–1060.

Davis, R. E., Drake, A. A., Jr., and Epstein, J. B., 1967, Geology of the Bangor quadrangle, Pennsylvania-New Jersey: U.S. Geol. Survey Geol. Quad. Map GQ-665.

Dewey, J. F., 1969, Evolution of the Appalachian/Caledonian orogen: Nature, v. 222, p. 124–129.

Drake, A. A., Jr., Epstein, J. B., and Aaron, J. M., 1969, Geologic map and sections of parts of the Portland and Belvidere quadrangles, New Jersey-Pennsylvania: U.S. Geol. Survey Misc. Geol. Inv. Map I-552.

Epstein, J. B., 1972, Geologic map of the Stroudsburg quadrangle, Pennsylvania-New Jersey: U.S. Geol. Survey Geol. Quad. Map GQ-1047. [In press]

Epstein, J. B., and Berry, W. B. N., 1972, Graptolites from the Martinsburg Formation, Lehigh Gap, easternmost Pennsylvania: U.S. Geol. Survey Jour. Research, v. 1, no. 1. [In press]

Gordon, S. G., 1921, Ordovician basalts and quartz diabases in Lebanon County, Pennsylvania: Acad. Nat. Sci. Philadelphia Proc., v. 72, p. 354–357.

Gray, Carlyle, and Willard, Bradford, 1955, Stratigraphy and structure of lower Paleozoic rocks in eastern Pennsylvania, *in* Pittsburgh Geol. Soc., Field guidebook of Appalachian geology, Pittsburgh to New York: Pittsburgh, Pittsburgh Geol. Soc., p. 53–55, 87–92.

Gray, Carlyle, and others, 1960, Geologic map of Pennsylvania: Pennsylvania Geol. Survey, 4th ser., scale 1:250,000.

Kay, G. M., 1941, Taconic allochthone and the Martic thrust: Science new ser., v. 94, p. 73.

McBride, E. F., 1962, Flysch and associated beds of the Martinsburg Formation (Ordovician), central Appalachians: Jour. Sed. Petrology, v. 32, p. 39–91.

MacLachlan, D. B., and Root, S. I., 1966, Comparative tectonics and stratigraphy of the Cumberland and Lebanon Valleys, Field Conference of Pennsylvania Geologists, 31st, Harrisburg, Guidebook: Harrisburg, Pa., Pennsylvania Geol. Survey, 90 p.

Moseley, J. R., 1950, The Ordovician-Silurian contact near Kempton, Pa.: Pennsylvania Acad. Sci. Proc., v. 24, p. 176–187.

Myers, P. B., Jr., 1969, Development of the Hamburg klippe in the Bernville-Strausstown area, Pennsylvania [abs.]: Geol. Soc. America, Abstracts with Programs, 1969, [v. 1] pt. 4, p. 55–56.

Pavlides, Louis, Boucot, A. J., and Skidmore, W. B., 1968, Stratigraphic evidence for the Taconic orogeny in the northern Appalachians, *in* Zen, E-an, White, W. S., Hadley, J. B., and Thompson, J. B., Jr., eds., Studies of Appalachian geology—Northern and maritime: New York, John Wiley and Sons, p. 61–82.

Platt, L. B., 1968, Geology, *in* Carswell, L. D., Hollowell, J. R., and Platt, L. B., Geology and hydrology of the Martinsburg Formation in Dauphin County, Pennsylvania: Pennsylvania Geol. Survey, 4th ser., Bull. W24 (Ground Water Rept.), p. 9–16.

Platt, L. B., Loring, R. B., Papaspyros, Athanasios, and Stephens, G. C., 1972, The Hamburg klippe reconsidered: Am. Jour. Sci., v. 272, p. 305–318.

Platt, L. B., Loring, R. B., and Stephens, G. C., 1969, Taconic events in the Hamburg 15′ quadrangle, Pennsylvania [abs.]: Geol. Soc. America, Abstracts with Programs, 1969, [v. 1] pt. 1, p. 48–49.

Rodgers, John, 1968, The eastern edge of the North American continent during the Cambrian and Early Ordovician, *in* Zen, E-an, White, W. S., Hadley, J. B., and Thompson, J. B., Jr., eds., Studies of Appalachian geology—Northern and maritime: New York, John Wiley and Sons, p. 141–149.

Ross, R. J., Jr., and Ingham, J. K., 1970, Distribution of the Toquima-Table Head (Middle Ordovician Whiterock) faunal realm in the Northern Hemisphere: Geol. Soc. America Bull., v. 81, p. 393–408.

Stose, G. W., 1930, Unconformity at the base of the Silurian in southeastern Pennsylvania: Geol. Soc. America Bull., v. 41, p. 629–658.

——1946, The Taconic sequence in Pennsylvania: Am. Jour. Sci., v. 244, p. 665–696.

Stose, G. W., and Jonas, A. I., 1927, Ordovician shale and associated lava in southeastern Pennsylvania: Geol. Soc. America Bull., v. 38, p. 505–536.

Sweet, W. C., and Bergström, S. M., 1971, The American Upper Ordovician standard. XIII. A revised time-stratigraphic classification of North American upper Middle and Upper Ordovician rocks: Geol. Soc. America Bull., v. 82, p. 613–628.

——1972, Provincialism exhibited by Ordovician conodont faunas [abs.]: Am. Assoc. Petroleum Geologists Bull., v. 56, p. 657.

Twenhofel, W. H., and others, 1954, Correlation of the Ordovician formations of North America: Geol. Soc. America Bull., v. 65, p. 247–298.

U.S. Geological Survey, 1970, Geological Survey Research 1970, chapter A: U.S. Geol. Survey Prof. Paper 700-A, 426 p.

——1971, Geological Survey Research 1971, chapter A: U.S. Geol. Survey Prof. Paper 750-A, 418 p.

Whittington, H. B., 1968, *Cryptolithus* (Trilobita)—Specific characters and occurrence in Ordovician of eastern North America: Jour. Paleontology, v. 42, p. 702–714.

Willard, Bradford, 1939, Ordovician shales of southeastern Pennsylvania: Pennsylvania Acad. Sci. Proc., v. 13, p. 126–133.

——1943, Ordovician clastic sedimentary rocks in Pennsylvania: Geol. Soc. America Bull., v. 54, p. 1067–1121.

Wilson, J. T., 1966, Did the Atlantic close and then re-open?: Nature, v. 211, p. 676–681.

EARLY ORDOVICIAN NORTH ATLANTIC PROVINCE CONODONTS IN EASTERN PENNSYLVANIA

By STIG M. BERGSTRÖM[1], ANITA G. EPSTEIN, and JACK B. EPSTEIN,
Columbus, Ohio, Washington, D.C., Beltsville, Md.

Abstract.—Abundant conodonts of North Atlantic province type have been recovered from limestone slide blocks in the Hamburg klippe in eastern Pennsylvania and from rocks at South Catcher Pond, Newfoundland. The faunas are very different from all other Ordovician faunas described from the United States, but they are virtually indentical with faunas characteristic of the *Prioniodus elegans* Zone of the lower Arenigian (lower Lower Ordovician) in the Balto-Scandic area. The discovery of North Atlantic province conodont faunas in rocks as old as Early Ordovician in two widely separated areas in eastern North America is of considerable interest because it provides, among other things, evidence that the striking provincial differentiation of Ordovician conodont faunas in the northern hemisphere may be traced back to at least early Arenigian time.

Early Ordovician conodonts of North Atlantic province type were recovered from carbonate slide blocks in the Hamburg klippe, Lenhartsville, Pa. (see fig. 1, Epstein and others, 1972, p. D29–D36, this chapter), and from South Catcher Pond, Newfoundland. These conodonts are unlike those of the North American Midcontinent faunal province found in autochthonous carbonates of the Appalachians. They are virtually identical with conodonts of the *Prioniodus elegans* Zone at the boundary between the Hunnebergian and Billingenian Substages of the Latorpian Stage in the lower Arenigian (lower Lower Ordovician) of the Balto-Scandic succession. The Hamburg klippe collection is of interest because it contains the only known North Atlantic province conodonts of this age in the United States and is the most extensive such collection in North America to date.[2] The distribution of the two faunal provinces is useful in interpreting the complex structural history that characterizes Taconic deformation in the northern Appalachians.

The petrography of the carbonate slide blocks from the Hamburg klippe and their geologic setting are given in Epstein, Epstein, and Bergström (1972) (p. D29–D36, this chapter).

CONODONT FAUNAS

Approximately 30 pounds (14 kg) each of ripple-bedded calcisiltite and graded conglomeratic limestone (see fig. 2, Epstein and others, 1972) was dissolved in dilute acetic acid and about 1,100 specimens of generally well preserved, although dark-colored, conodonts were obtained from the insoluble residues. A list of the species identified in each sample as well as the number of specimens of each form is given in table 1. In addition, conodonts from rocks at South Catcher Pond, Newfoundland, which appear to be in the same geologic situation as rocks in the Hamburg klippe, are also listed. A number of selected species are illustrated in figure 1.

Table 1 shows that the conodont faunas of the two Hamburg klippe samples are very similar, and there is little doubt that the samples are of about the same age. The faunas are quite characteristic of a narrow stratigraphic interval in the Balto-Scandic sequence, and there is no clear indication of the presence of specimens of younger or older stratigraphic age.

These conodont faunas are of unusual interest for at least two reasons: (1) They are the first large North Atlantic province faunas found in the Lower Ordovician of North America, and (2) they provide an exceptionally precise correlation of the limestone blocks near Lenhartsville with the Lower Ordovician sequence of the Balto-Scandic area in northwestern Europe.

BIOGEOGRAPHIC SIGNIFICANCE

With one possible exception, all the Early Ordovician conodont faunas thus far described from North America (summarized in Clark and Ethington, 1971) are strikingly

[1] Department of Geology, The Ohio State University.

[2] In a paper published after the completion of this study, R. L. Ethington ("Lower Ordovician (Arenigian) conodonts from the Pogonip Group, central Nevada", in Geologica et Palaeontologica SB 1, p. 17–28, 1972) reported the presence of Balto-Scandic-type conodonts of the *Prioniodus elegans* Zone in the Ninemile Formation (Lower Ordovician) in central Nevada. Although the presence of faunas in the Western United States similar to ours in the Hamburg klippe is of considerable biogeographic interest, it does not affect the conclusions presented in this paper, apart from the fact that the Hamburg klippe fauna is not the first but the second of this type reported from the United States.

Table 1.—*Conodont multielement species in collections from the Hamburg klippe, Pennsylvania, and South Catcher Pond, Newfoundland*

[In addition to the forms listed, the samples contain some specimens that cannot be classified as to genus or species at present. The occurrence of the species in the *Prioniodus elegans* Zone in the Baltic area is mainly based on unpublished data of S. M. Bergström]

Conodont multielement species	Number of specimens			Occurrence in *Prioniodus elegans* Zone beds, Baltic area
	Hamburg klippe, Pennsylvania		South Catcher Pond, Newfoundland	
	Sample 1	Sample 2		
Drepanodus arcuatus Pander?				
drepanodiform element	3	3	1	X
scandodiform element	...	8	...	X
Drepanoistodus cf. *forceps* (Lindström)				
oistodiform element	4	6	...	cf.
Drepanodids indet.	122	138	24	X
"*Oistodus*" *elongatus* Lindström	5	6	1	X
"*Oistodus*" spp. indet.	9	8	5	X
Paltodus inconstans Lindström	2	...	...	X
Paracordylodus gracilis Lindström				
paracordylodiform element	11	1	29	X
oistodiform element	15	1	6	X
Paroistodus parallelus (Pander)				
drepanodiform element	2	...	3	X
Paroistodus proteus (Lindström)				
drepanodiform element	44	11	2	X
oistodiform element	7?	29	...	X
Prioniodus elegans Pander				
belodiform element	67	59	10	X
falodiform element	44	56	4	X
hibbardelliform element	16	7	1	X
prioniodoform element	165	119	41	X
tetraprioniodiform element	47	11	4	X
Protopanderodus arcuatus (Lindström)	31	20	...	X
Protopanderodus cf. *P. rectus* (Lindström)				
acontiodiform element	...	1	16	cf.
scolopodiform element	...	...	5	cf.
Rhipidognathus? n. sp.	...	2	...	...
Scolopodus rex Lindström	...	10	...	X
Stolodus stola (Lindström)	6	3	...	X
N. gen. and sp. 1	...	...	5	X
N. gen. and sp. 2	1	8	...	X

different from the Hamburg klippe collections. The one exception may be a small collection from Bed 10 of the Cow Head Group of western Newfoundland (Fåhraeus, 1970), which apparently includes only three forms representing two multielement species. These multielement species are, however, highly diagnostic stratigraphically, and it appears likely that the fauna of Bed 10 is of the same age or slightly younger than the Hamburg klippe collections.

Recently, S. M. Bergström, through the courtesy of Dr. A. J. Boucot (Oregon State University), studied a large collection of Early Ordovician conodonts found in limestone in an unnamed volcanic-clastic unit near South Catcher Pond, north-central Newfoundland (Dean, 1970). This collection, which is being studied in detail by Bergström, is very similar in overall species composition, as well as in frequency of individual species, to the Hamburg klippe collections, and it is apparently of the same age (table 1). The Hamburg klippe and South Catcher Pond collections, as well as the one from Bed 10 of the Cow Head, are all dominated by conodont species currently unknown in other parts of North America but quite common in, and highly characteristic of, an interval in the Lower Ordovician sequence in the Balto-Scandic area.

Conodont faunas of Middle Ordovician age similar to those in northwestern Europe, on the other hand, are known from many localities in the eastern part of the Appalachians (Bergström, 1971). These faunas belong to the North Atlantic of European conodont faunal province (Sweet and Bergström, 1962; Bergström and Sweet, 1966; Bergström, 1971, 1972; Lindström 1969). The very different faunas in the western Appalachians and the North American midcontinent region form the basis of the concept of the Midcontinent faunal province (Sweet and others, 1959; Bergström, 1972). Although there were occasional invasions of some North Atlantic province faunal elements into the Midcontinent, especially during the late Middle Ordovician, and similar invasions of Midcontinent elements into some areas in northwestern Europe during the Middle and Late Ordovician, by and large the two types of faunas have very little in common and represent an example of early Paleozoic biogeographic differentiation fully comparable to the more well known Cambrian trilobite faunal provinces.

The discovery of North Atlantic province conodont faunas in rocks as old as Early Ordovician in two widely separated areas in eastern North America is of considerable interest,

because it provides, among other things, evidence that the striking provincial differentiation of Ordovician conodont faunas in the northern hemisphere may be traced back to at least early Arenigian time.

Unfortunately, our knowledge of the distribution of the Early Ordovician conodont faunas and faunal realms in North America is still very fragmentary because of the few conodont faunas of that age that have been described on this continent. In Pennsylvania, Early Ordovician conodonts have been reported previously from the shelf carbonate rocks of the Stonehenge and Rockdale Run Formations of the Beekmantown Group (Lower Ordovician) near Chambersburg (Hass, *in* Sando, 1958). Hass' collection, which has never been described in detail, contains, judging from his illustrations, *Loxodus bransoni* Furnish, "*Scolopodus*" *quadraplicatus* Branson and Mehl, *Acanthodus* sp., and *Cordylodus* sp., as well as a number of unrevised simple cone forms, and represents a typical Midcontinent province assemblage. Goodwin (1972) and Tipnis and Goodwin (1972) reported Midcontinent conodont faunas from the Stonehenge and Axemann Formations (Beekmantown Group) of Pennsylvania-Maryland and central Pennsylvania, respectively. There is very little, if any, similarity between the Beekmantown faunas and those of the Hamburg klippe, and there is no doubt that these faunas represent different faunal realms. During this study, another sample from the Beekmantown Group in eastern Pennsylvania was collected and processed for conodonts. It is from the Epler Formation in a railroad cut 0.9 mile south of Martins Creek and 1.1 miles northwest of Sandt's Eddy, Bangor quadrangle (USGS loc. 6976, see fig. 1, Epstein and others, 1972). Relatively poorly preserved specimens of "*Drepanodus*" cf. *subarcuatus* Furnish, *Drepanoistodus* sp., "*Scolopodus*" *quadraplicatus* Branson and Mehl, and "*Sc.*" cf. *sulcatus* Furnish along with representatives of a number of other unrevised simple cone species of Midcontinent province type were found. None of the forms present in the Epler collection can be positively identified with a species present in the Ordovician of the Balto-Scandic area, but very similar forms have been described from the Prairie du Chien Group (Lower Ordovician) of the Upper Mississippi Valley (Furnish, 1938). Although the Epler collection contains few, if any, stratigraphically important species, there is no doubt that it is Early Ordovician in age, and it is clearly of Midcontinent province type. The same is true for similar conodont faunas from the March and Oxford Formations of southeastern Ontario described by Greggs and Bond (1971).

The only other early Early Ordovician conodont faunas thus far described from eastern North America come from the St. George Formation of northernmost Newfoundland (Barnes and Tuke, 1970). The exact age of that collection in terms of the standard Canadian Series is still somewhat uncertain, but the available megafossil evidence, which is not extensive, suggests that it is at least comparable to that of Bed 10 of the Cow Head Group (Whittington, 1968). As is the case with the Beekmantown conodonts near Martins Creek, the St. George conodont fauna is entirely different from the faunas of the Hamburg klippe carbonate blocks and from Bed 10 of the Cow Head, and, as noted by Barnes and Tuke (1970), it is dominated by forms typical of the Midcontinent province. Although Barnes and Tuke (1970) claim that some of the St. George species are in common with Baltic faunas, we feel that this statement needs to be confirmed by investigation of larger collections because practically all so-called "European" elements illustrated in their paper do not appear entirely conspecific with species known from the Lower Ordovician of the Balto-Scandic area.

As previously noted, Early Ordovician conodont faunas similar to those from the Hamburg klippe and South Catcher Pond have previously been reported mainly from the Balto-Scandic area. A slightly younger fauna of the same type is also known from the Southern Uplands of Scotland (Lamont and Lindström, 1957). Although admittedly the incompleteness of the available information about the distribution of Early Ordovician Midcontinent and North Atlantic province conodont faunas makes it difficult at present to produce an accurate map of their areal distribution, we have, nevertheless, summarized the pertinent data in figure 2. The North Atlantic province faunas in North America are all (at least in their present tectonic position) found within the area of the Appalachian geosyncline, whereas the European localities are within the Caledonian geosynclinal area (Scotland) and on the Russian platform (Sweden, western U.S.S.R.). Further, the geographic position of the border between the Midcontinent and North Atlantic conodont faunal realms in Early Ordovician time, although still poorly known, appears to be approximately the same as that prevailing during a large part of Middle Ordovician time (Bergström, 1971).

BIOSTRATIGRAPHIC SIGNIFICANCE

The Hamburg klippe faunas can be dated with extraordinary precision in terms of the Balto-Scandic Lower Ordovician sequence and, hence, provide clear evidence of the age of their host sediments which have not been accurately dated before. Extensive recent work on Early Ordovician conodonts in the Balto-Scandic area has made it possible to establish a detailed conodont zonation (Lindström, 1955, 1957, 1971; Sergeeva, 1962, 1963, 1964; Viira, 1967, 1970; Bergström, 1968). The identified species in the collections from the Hamburg klippe and South Catcher Pond, as well as those of the small Cow Head collection mentioned above, are characteristic of a very restricted stratigraphic interval in the lower part of the lower Arenigian of Sweden (fig. 3). The presence of *Prioniodus elegans* Pander, in particular, and *Paroistodus proteus* (Lindström) and *P. parallelus* (Pander) indicates beyond any doubt that the rocks which yielded these condonts belong in the *Prioniodus elegans* Zone at the boundary between the Hunnebergian and Billingenian Substages of the Latorpian Stage in the early Arenigian of the Balto-Scandic succession (fig. 4). In the Baltic Basin area, conodont faunas of this type

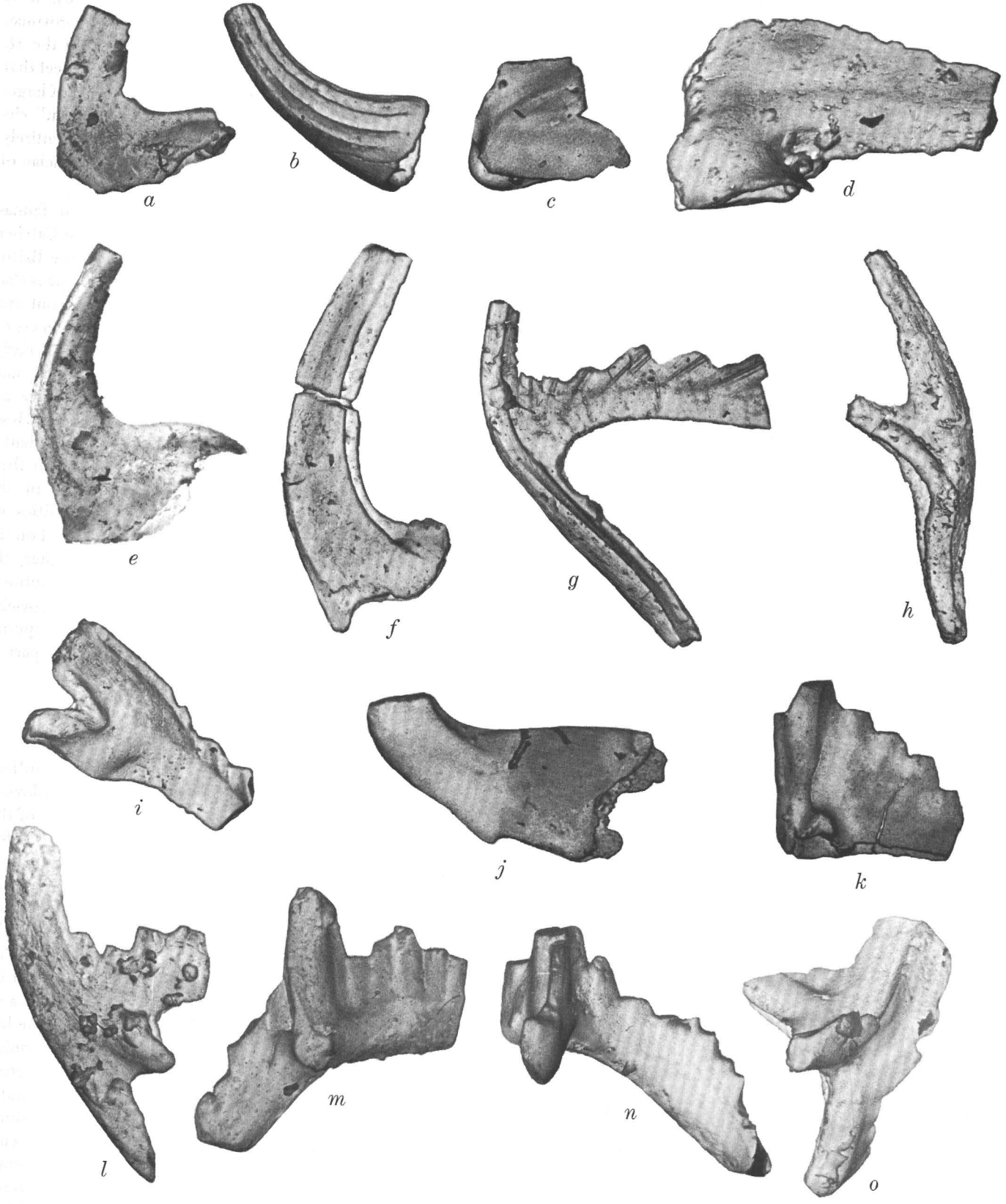

Figure 1.

are restricted to an obviously very condensed sequence of glauconitic limestones, poorly consolidated sandstones, and green shales containing scattered limestone lenses. This stratigraphic interval, which clearly is a lag concentrate at least locally, is generally less than 1 to 100 cm thick. In southwestern Sweden, the corresponding stratigraphic interval is a dark shale (Lindström, 1957), and the *Prioniodus elegans* Zone there attains a thickness of a few meters. The strata belonging to this conodont zone have yielded numerous megafossils, including graptolites of the *Didymograptus balticus* and the lower part of the *Phyllograptus densus* Zones of the standard Balto-Scandic graptolite zonation (Bergström, 1968).

Although the age of the Hamburg klippe and the South Catcher Pond collections can be confidently dated with extraordinary precision in terms of the Balto-Scandic sequence, the collections can be fitted with much less certainty into the North American Standard Lower Ordovician sequence, and the conodonts themselves provide no help in dating the collections in terms of the Canadian Series. The graptolites associated with *Prioniodus elegans* zonal conodonts in Sweden also offer little help because opinions differ whether the *Didymograptus balticus* and *Phyllograptus densus* Zones correspond to part of the North American *Tetragraptus fruticosus* Zone (Berry, 1967, 1968; Erdtmann, 1971) or to the whole of this zone as well as the succeeding *Didymograptus protobifidus* Zone (Skevington, 1968; Jackson, 1964). Whittington (1968, table 4-1) refers Bed 10 of the Cow Head Group, that is, strata yielding conodonts that probably belong to the *Prioniodus elegans* Zone, to the lower Cassinian Stage of the Canadian Series, but he indicated difficulties in dating the unit exactly. In the same paper, Whittington (1968, table 4-2) correlates these strata with upper Latorpian and lowermost Volkhovian beds in the Balto-Scandic sequence, which, how-

Figure 1.—Scanning electron photomicrographs of elements of selected conodont species from Lower Ordovician limestone blocks in the Hamburg klippe. All illustrated specimens are from sample 2 (USGS loc. 6952–CO). All figures × 100 except *c*, *j*, and *k* which are × 50. All figured specimens are reposited in the U.S. National Museum (USNM); the rest of the collection is reposited in the Orton Museum of the Ohio State University, Columbus, Ohio.

a, *c*, *d*, *e*. *Paroistodus proteus* (Lindström). *a*. Lateral view of drepanodiform element, USNM 182589. *c*, *d*. Lateral views of oistodiform elements, USNM 182591, 182592. *e*. Lateral view of drepanodiform element, USNM 182593. Hamburg klippe specimens are very similar to elements of this species from the lower part of the *Prioniodus elegans* Zone in Sweden with which they have been compared directly.

b. *Scolopodus rex* Lindström, Lateral view of hypotype, USNM 182590. Several very closely related species of *Scolopodus* (s.s.) have been described from the Lower Ordovician, and the genus is in need of modern taxonomic revision. The few elements of this type in the Hamburg klippe collections are all fragmentary, but they are similar to specimens of *S. rex* in important respects and are herein referred to that species pending further studies.

f. *Protopanderodus* cf. *P. rectus* (Lindström). Lateral view of acontiodiform element, USNM 182594. Hamburg klippe specimens differ from typical elements of this species, which they resemble otherwise, in the development of a conspicuous notch in the anterior part of the basal margin.

g, *h*. *Paracordylodus gracilis* Lindström. *g*. Lateral view of cordylodiform element, USNM 182595. Note conspicuous striations on cusp, denticles, and anterior process. *h*. Lateral view of oistodiform element, USNM 182596. Hamburg klippe elements of this species have been compared directly with Lindström's 1955 Swedish types (see Lindström, 1954) and no obvious difference was noted.

i, *l–o*. *Prioniodus elegans* Pander. *i*. Lateral view of falodiform element, USNM 182597. *l*. Lateral view of belodiform element, USNM 182600. *m*. Lateral view of prioniodiform element with incomplete anterior process, USNM 182601. *n*. Posterior view of prioniodiform element with most of anterior and posterior processes missing, USNM 182602. *o*. Lateral view of prioniodiform element with incomplete lateral and posterior processes, USNM 182606. Hamburg klippe elements of the present species have been compared directly with elements from the *Prioniodus elegans* Zone in Sweden and they appear to fall within the range of variation exhibited by the Swedish specimens.

j. *Protopanderodus arcuatus* (Lindström). Lateral view of acontiodiform element, USNM 182598. Hamburg klippe elements referred to this species are quite similar to Lindström's 1955 Swedish types (Lindström, 1954) with which they have been compared directly.

k. *Rhipidognathus*? n. sp. Posterior view of element missing one of the lateral processes, USNM 182599. Hamburg klippe elements of this type exhibit close similarity to specimens of the Middle and Late Ordovician genus *Rhipidognathus* Branson, Mehl, and Branson, but it is not certain if these are homeomorphs. However, the Hamburg klippe form is clearly a new species.

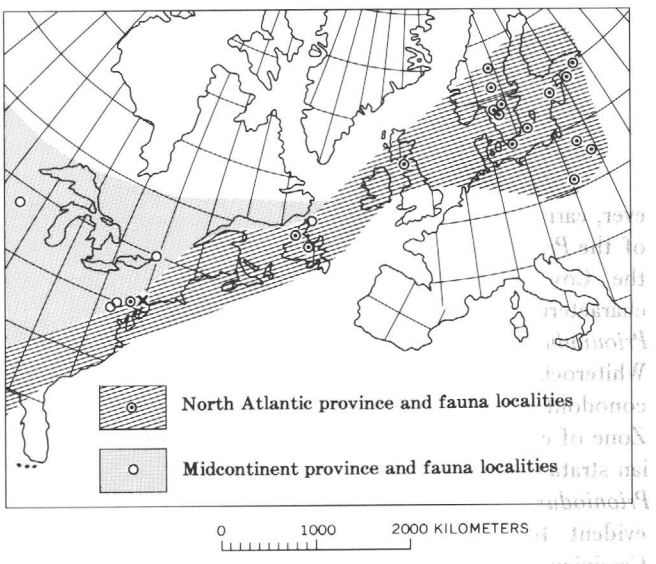

Figure 2.—Sketch map showing the distribution of early Early Ordovician conodont faunas of the North American Midcontinent province and North Atlantic province. For additional information about these faunas, see Clark and Ethington (1971) and Lindström (1971); Midcontinent fauna in Ontario from Greggs and Bond (1971); ×, Early Ordovician Midcontinent province conodont fauna from the Epler Formation (USGS loc. 6976). Base from Bullard, Everett, and Smith (1965).

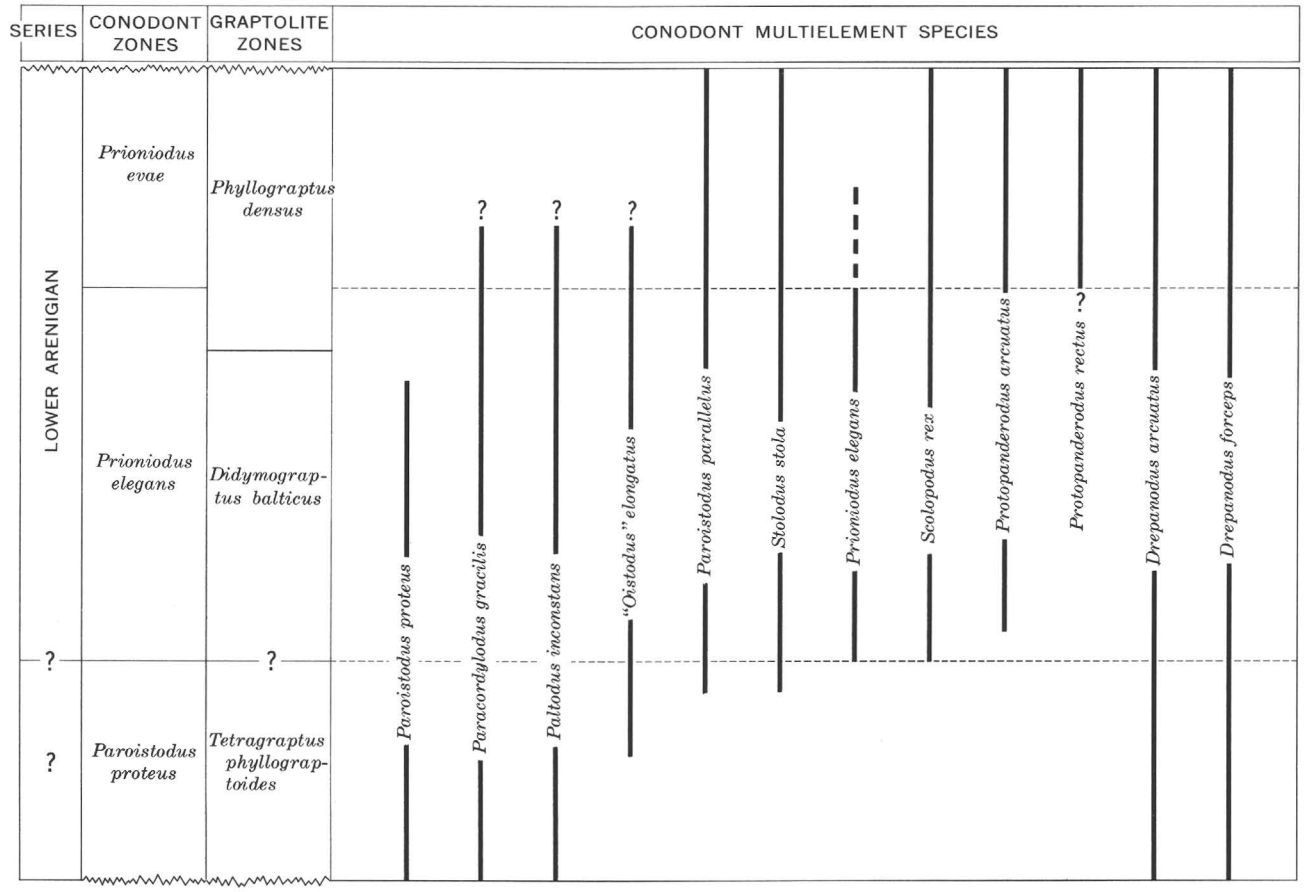

Figure 3.—Stratigraphic range of conodont species from the Hamburg klippe and South Catcher Pond collections in the Lower Ordovician of Sweden. The ranges of individual species, as well as the correlation between conodont and graptolite zones, are largely based on the Talubäcken section at Skattungbyn, central Sweden (Bergström, 1968; and unpub. data). As seen in table 1, some of the forms from North America are identified with a particular Balto-Scandic species only with reservation.

ever, carry conodont faunas that are clearly younger than that of the *Prioniodus elegans* Zone. Further, he places Bed 11 of the Cow Head sequence, which has yielded conodonts characteristic of the *Prioniodus evae* and, probably, the *Prioniodus navis* Zones (Fåhraeus, 1970) in the basal Whiterockian Stage (Whittington, 1968, table 4-2). Studies of conodont collections from the basal Whiterockian *Orthidiella* Zone of central Nevada suggest, however, that the Whiterockian strata are definitely younger than the *Prioniodus evae* and *Prioniodus navis* Zones (Bergström, unpub. data), and it is evident that much additional work on the Jeffersonian-Cassinian faunas is needed before their correlation with the Balto-Scandic sequence is safely established. However, it can be concluded that regardless of their exact age in terms of the North American Standard Early Ordovician succession, the carbonate blocks investigated in the Hamburg klippe and South Catcher Pond sequences must be coeval with part of the Beekmantown Group, although rocks of this lithic type are unknown in the Beekmantown of eastern Pennsylvania.

CONCLUSIONS

The proximity in eastern North America of North Atlantic province conodonts and of Midcontinent faunas without apparent mixing suggests that the boundary between these faunal realms must have been a distributional barrier powerful enough to prevent noteworthy faunal exchange. On the basis of the distribution of these faunas and on Ordovician paleogeography, Bergström (1972), and Sweet and Bergström (1972) concluded that the Midcontinent and North Atlantic faunas developed in low latitudes (tropic and subtropic waters) and high latitudes (colder waters), respectively. The location of the sedimentary basin in which the conodont-bearing sediments of the Hamburg klippe were originally deposited is unknown, although there can be no doubt that the sediments were derived from an eastern source. Red shales, radiolarian cherts, and graywackes, which form important parts of the deposits in the Hamburg klippe, are characteristic rock types in the Lower Ordovician of some areas in the British Isles,

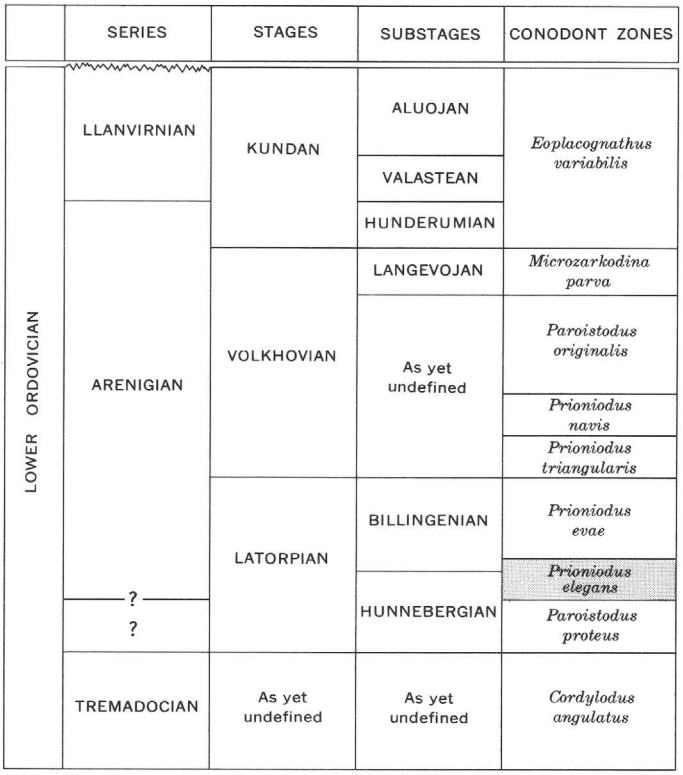

Figure 4.—Stratigraphic age of the Hamburg klippe and South Catcher Pond conodont collections in terms of the Balto-Scandic Early Ordovician biostratigraphic units. The *Prioniodus elegans* Zone bears conodont faunas of the same type as those from the Hamburg klippe and South Catcher Pond. The conodont zonal succession is that used by Lindström (1971). Note that the age of the *Paroistodus proteus* Zone cannot be expressed in terms of the British Standard series because, judging from the faunal successions in the type Tremadocian and Arenigian in Wales, this zone is apparently post-Tremadocian but pre-Arenigian in age. In terms of the standard stadial subdivision of the Canadian Series (see Whittington, 1968), the *Prioniodus elegans* Zone is probably approximately middle Jeffersonian in age. The shaded zone is the interval bearing a conodont fauna of the same type as those of the Hamburg klippe and South Catcher Pond.

especially southwestern Scotland. However, the only Lower Ordovician carbonate deposit of noteworthy areal extent in that area is the Durness Limestone of northernmost Scotland on the foreland platform northwest of the Caledonian geosyncline. No early Arenigian conodont faunas have so far been reported from that unit, but the late Arenigian to early Llanvirnian conodonts described from the Durness (Higgins, 1967), as well as those known from broadly equivalent calcareous rocks in the Loch Mask region of northwestern Ireland (Bergström, unpub. data), are not closely similar to coeval faunas in the Balto-Scandic area. As pointed out by several authors, the Durness Limestone exhibits similarities both in lithology and faunas with the shelf carbonates of the St. George Group, Newfoundland, which are clearly different from those of the Hamburg klippe. Hence, there is no obvious source for the Hamburg klippe boulders in the Lower Ordovician of the British Isles, or for that matter, anywhere in northwesternmost Europe.

Wilson (1966), Ross and Ingham (1970), and Bird and Dewey (1970) believe that the Cambrian and Early Ordovician brachiopod and trilobite faunal realms were separated by a proto-Atlantic ocean. Such faunal provincialism has been used to date periods of oceanic expansion (Dewey, 1969, p. 126; Bird and Dewey, 1970, p. 1049–1050). At the present stage of our knowledge, it might be reasonable to suggest that the conodont-bearing blocks in the Hamburg klippe were parts of shelf sediments, on an uplifted continental rise of a proto-Atlantic ocean, that slid into the host pelitic deposits which in turn were later emplaced by faulting and (or) submarine sliding into their present position. Available information about the rocks yielding the *Prioniodus elegans* faunas in the South Catcher Pond and Cow Head successions of Newfoundland indicates that a similar explanation may well be applied to those "exotic" carbonate rocks with their remarkable faunas.

ACKNOWLEDGMENTS

Appreciation is extended to V. Jaanusson and J. W. Huddle for their critical reading of the manuscript. We are also indebted to Prof. Erik Jarvik, Dr. Tor Ørvig, and Mr. Göran Blom, of Naturhistoriska Riksmuseet, Stockholm, Sweden, for permission to use their scanning electron microscope facilities.

REFERENCES

Barnes, C. R., and Tuke, M. F., 1970, Conodonts from the St. George Formation (Ordovician), northern Newfoundland: Canada Geol. Survey Bull. 187, p. 79–97.

Bergström, S. M., 1968 Biostratigraphy of the lower Ordovician sequence at Skattungbyn, Dalarna [abs.]: Geol. Fören. Stockholm Förh., v. 90, pt. 3, no. 534, p. 454.

—— 1971, Conodont biostratigraphy of the Middle and Upper Ordovician of Europe and eastern North America, *in* Sweet, W. C., and Bergström, S. M., eds., Symposium on conodont biostratigraphy: Geol. Soc. America Mem. 127, p. 83–157.

—— 1972, Ordovician conodont biogeography, *in* Hallam, A., ed., Atlas of paleobiogeography: Amsterdam, Elsevier. [In press]

Bergström, S. M., and Sweet, W. C., 1966, Conodonts from the Lexington Limestone (Middle Ordovician) of Kentucky, and its lateral equivalents in Ohio and Indiana: Bulls. Am. Paleontology, v. 50, no. 229, p. 271–441.

Berry, W. B. N., 1967, Comments on the correlation of the North American and British Lower Ordovician: Geol. Soc. America Bull., v. 78, p. 419–427.

—— 1968, British and North American Lower Ordovician correlation—Reply: Geol. Soc. America Bull., v. 79, p. 1265–1272.

Bird, J. M., and Dewey, J. F., 1970, Lithosphere plate-continental margin tectonics and the evolution of the Appalachian orogen: Geol. Soc. America Bull., v. 81, p. 1031–1060.

Bullard, E. C., Everett, J. E., and Smith, A. G., 1965, The fit of the continents around the Atlantic: Royal Soc. London Philos. Trans., v. 258, ser. A, p. 41–51.

Clark, D. L., and Ethington, R. L., 1971, Lower Ordovician conodonts in North America, *in* Sweet, W. C., and Bergström, S. M., eds.,

Symposium on conodont biostratigraphy: Geol. Soc. America Mem. 127, p. 63–82.

Dean, W. T., 1970, Lower Ordovician trilobites from the vicinity of South Catcher Pond, northeastern Newfoundland: Canada Geol. Survey Paper 70–44, 15 p.

Dewey, J. F., 1969, Evolution of the Appalachian/Caledonian orogen: Nature, v. 222, p. 124–129.

Epstein, J. B., Epstein, A. G., and Bergström, S. M., 1972, Significance of Lower Ordovician exotic blocks in the Hamburg klippe, eastern Pennsylvania, *in* Geological Survey Research 1972: U.S. Geol. Survey Prof. Paper 800-D p. D29–D36.

Erdtmann, B.-D., 1971, Ordovician graptolite zones of western Newfoundland in relation to paleogeography of the North Atlantic: Geol. Soc. America Bull., v. 82, p. 1509–1528.

Fåhraeus, L. E., 1970, Conodont-based correlations of Lower and Middle Ordovician strata in western Newfoundland: Geol. Soc. America Bull., v. 81, p. 2061–2076.

Furnish, W. M., 1938, Conodonts from the Prairie du Chien beds of the upper Mississippi Valley: Jour. Paleontology, v. 12, p. 318–340.

Goodwin, P. W., 1972, Lower Ordovician conodonts from the Axemann Limestone in central Pennsylvania [abs.]: Geol. Soc. America Abs. with Programs, v. 4, no. 5, p. 322.

Greggs, R. G., and Bond, I. J., 1971, Conodonts from the March and Oxford Formations in the Brockville area, Ontario: Canadian Jour. Earth Sci., v. 8, p. 1455–1471.

Higgins, A. C., 1967, The age of the Durine Member of the Durness Limestone Formation at Durness: Scottish Jour. Geology, v. 3, p. 382–388.

Jackson, D. E., 1964, Observations of the sequence and correlation of Lower and Middle Ordovician graptolite faunas of North America: Geol. Soc. America Bull., v. 75, p. 523–534.

Lamont, Archie, and Lindström, Maurits, 1957, Arenigian and Llandeilian cherts identified in the Southern Uplands of Scotland by means of conodonts, etc.: Edinburgh Geol. Soc., Trans., v. 17, p. 60–70.

Lindström, Maurits, 1954, Conodonts from the lowermost Ordovician strata of south-central Sweden: Geol. Fören. Stockholm Förh., v. 76, p. 517–614. [1955]

—— 1957, Two Ordovician conodont faunas found with zonal graptolites: Geol. Fören. Stockholm Förh., v. 79, p. 161–178.

—— 1969, Faunal provinces in the Ordovician of the North Atlantic areas: Nature, v. 225, p. 1158–1159.

—— 1971, Lower Ordovician conodonts of Europe, *in* Sweet, W. C., and Bergström, S. M., eds., Symposium on conodont biostratigraphy: Geol. Soc. America Mem. 127, p. 21–61.

Ross, R. J., Jr., and Ingham, J. K., 1970, Distribution of the Toquima-Table Head (Middle Ordovician Whiterock) faunal realm in the Northern Hemisphere: Geol. Soc. America Bull., v. 81, p. 393–408.

Sando, W. J., 1958, Lower Ordovician section near Chambersburg, Pennsylvania: Geol. Soc. America Bull., v. 69, p. 837–854.

Sergeeva, S. P., 1962, Stratigraphic distribution of conodonts in the Lower Ordovician of the Leningrad region: Akad. Nauk SSSR Doklady, v. 146, p. 1393–1395 [In Russian].

—— 1963, Conodonts from the Lower Ordovician of the Leningrad region: Akad. Nauk SSSR, Paleont. Jour., 1963, p. 93–108 [In Russian].

—— 1964, On the stratigraphic significance of the Lower Ordovician conodonts in the Leningrad region: Leningrad Univ. Vestnik, Ser. Geologiya i Geografii, no. 12, vip. 2, p. 56–60 [In Russian].

Skevington, David, 1968, British and North American Lower Ordovician correlation—Discussion: Geol. Soc. America Bull., v. 79, p. 1259–1264.

Sweet, W. C., and Bergström, S. M., 1962, Conodonts from the Pratt Ferry Formation (Middle Ordovician) of Alabama: Jour. Paleontology, v. 36, p. 1214–1252.

—— 1972, Provincialism exhibited by Ordovician conodont faunas [abs.]: Am. Assoc. Petroleum Geologists Bull., v. 56, p. 657.

Sweet, W. C., Turco, C. A., Warner, E., and Wilkie, L. C., 1959, The American Upper Ordovician standard. I. Eden conodonts from the Cincinnati region of Ohio and Kentucky: Jour. Paleontology, v. 33, p. 1029–1068.

Tipnis, R. S., and Goodwin, P. W., 1972, Lower Ordovician conodonts from the Stonehenge Formation of Pennsylvania and Maryland [abs.]: Geol. Soc. America Abs. with Programs, v. 4, no. 5, p. 352.

Viira, Viive, 1967, Ordovician conodont succession in the Ohesaare core: Eesti NSV Tead, Akad. Toimetised, Voide 16, p. 319–329.

—— 1970, [Baltic Ordovician conodonts]: Acad. Sci. Estonian SSR, Dissertation autoreferate, 24 p. [In Russian].

Whittington, H. B., 1968, Zonation and correlation of Canadian and Early Mohawkian series, *in* Zen, E-an, White, W. S., Hadley, J. B., and Thompson, J. B., Jr., eds., Studies of Appalachian geology—Northern and maritime: New York, John Wiley and Sons, p. 49–60.

Wilson, J. T., 1966, Did the Atlantic close and then re-open?: Nature, v. 211, p. 676–681.

NEW NEPHRITICERATIDAE (NAUTILOIDEA) FROM THE DEVONIAN OF MARYLAND, PENNSYLVANIA, AND INDIANA

By ROUSSEAU H. FLOWER[1] and MACKENZIE GORDON, JR.,
Socorro, N. Mex., Washington, D.C.

Abstract.—The nautiloid family Nephriticeratidae occurs in Devonian rocks and seems to be limited almost entirely to the Western Hemisphere. This paper describes and figures three species, each belonging in a different genus. Two of the species are new and come from Middle and Upper Devonian rocks in the vicinity of the Maryland-Pennsylvania State line. *Rhadinoceras atlas* n. sp. is the largest and youngest example of its genus on record. *Nephriticerina cornucopia* n. sp. is a moderate-sized longitudinally lirate and somewhat cancellate species. A third form, *Lyrioceras sampsoni* (Nettleroth), from the Middle Devonian of southernmost Indiana, was originally described as a straparollid gastropod (*Euomphalus*). This strongly longitudinally lirate form is recognized here as a rhadinoceratid nautiloid for the first time. In reviewing the genera to which these species are referred, several changes in assignment of other nephriticeratid species are suggested.

Five unusual coiled nautiloids of Middle and early Late Devonian age are the subject of this report. Two of them belong in two new species and were found at localities a little more than 7 miles apart. Both localities are in the Devonian outcrop belt that constitutes part of the warp of the Allegheny Mountains and strikes northeast across western Maryland and southwestern Pennsylvania. The other three specimens are from southern Indiana.

The nautiloids represent three different genera belonging to the same family, which occurs in rocks of Devonian age and seems to be limited almost entirely to the Western Hemisphere. The family Nephriticeratidae constituted the sole representation of the Order Barrandeocerida during Devonian time and was therefore an important though not overly abundant group of nautiloids. Our main purpose in writing this paper is to place these relatively well preserved examples on record. This has permitted us also to suggest some changes in generic assignments for several members of this nautiloid family.

Rhadinoceras atlas n. sp. is by far the largest member of the genus known. It was found in 1955 by Wallace deWitt, Jr., of the U.S. Geological Survey, in Allegany County, Md., during his studies of the Devonian belt.

[1] New Mexico State Bureau of Mines and Mineral Resources.

Nephriticerina cornucopia n. sp. was found in 1958 by the late A. G. Perdew on the Hazen Road in Bedford County, Pa., just across the State line from Allegany County and roughly 5½ miles northeast of Cumberland, Md. Mr. Perdew presented the specimen to the U.S. National Museum.

Lyrioceras sampsoni (Nettleroth) was described originally as a gastropod and for this reason seems to have been neglected by cephalopod specialists. The primary types, in the collection of the U.S. National Museum, are from Clark County, Ind.

SYSTEMATIC PALEONTOLOGY

Phylum MOLLUSCA
Class CEPHALOPODA
Subclass NAUTILOIDEA
Order BARRANDEOCERIDA
Family NEPHRITICERATIDAE

Genus RHADINOCERAS Hyatt, 1884

Rhadinoceras contains relatively smooth Nephriticeratidae (in contrast to lirate genera) that are coiled symmetrically and develop an impressed zone. It differs from *Nephriticeras*, which has broad whorls throughout, in that the anterior whorl is circular or slightly compressed in cross section.

Rhadinoceras cornulum (Hall), the type species, and *R. ellipticum* (Rowley) are the only previously described species that can be placed properly in *Rhadinoceras*. Kindle and Miller (1939), however, assigned *Gyroceras eryx* Cleland and *G. clarkei* Cleland, both of the Milwaukee Formation of Wisconsin, and *Gyroceras validum* Hall of the Schoharie Formation of New York to *Rhadinoceras*. Restudy of these species by Flower (1945, p. 716) showed that they have marginal siphuncles with actinosiphonate deposits, so they were placed in a new genus, *Gyronaedyceras* Flower.

Rhadinoceras atlas n. sp.

Figures 1; 2, *g*, *h*

Description.—The type and only known specimen is a coiled shell 222 mm in diameter, retaining a phragmocone of one

U.S. GEOL. SURVEY PROF. PAPER 800-D, PAGES D45-D50

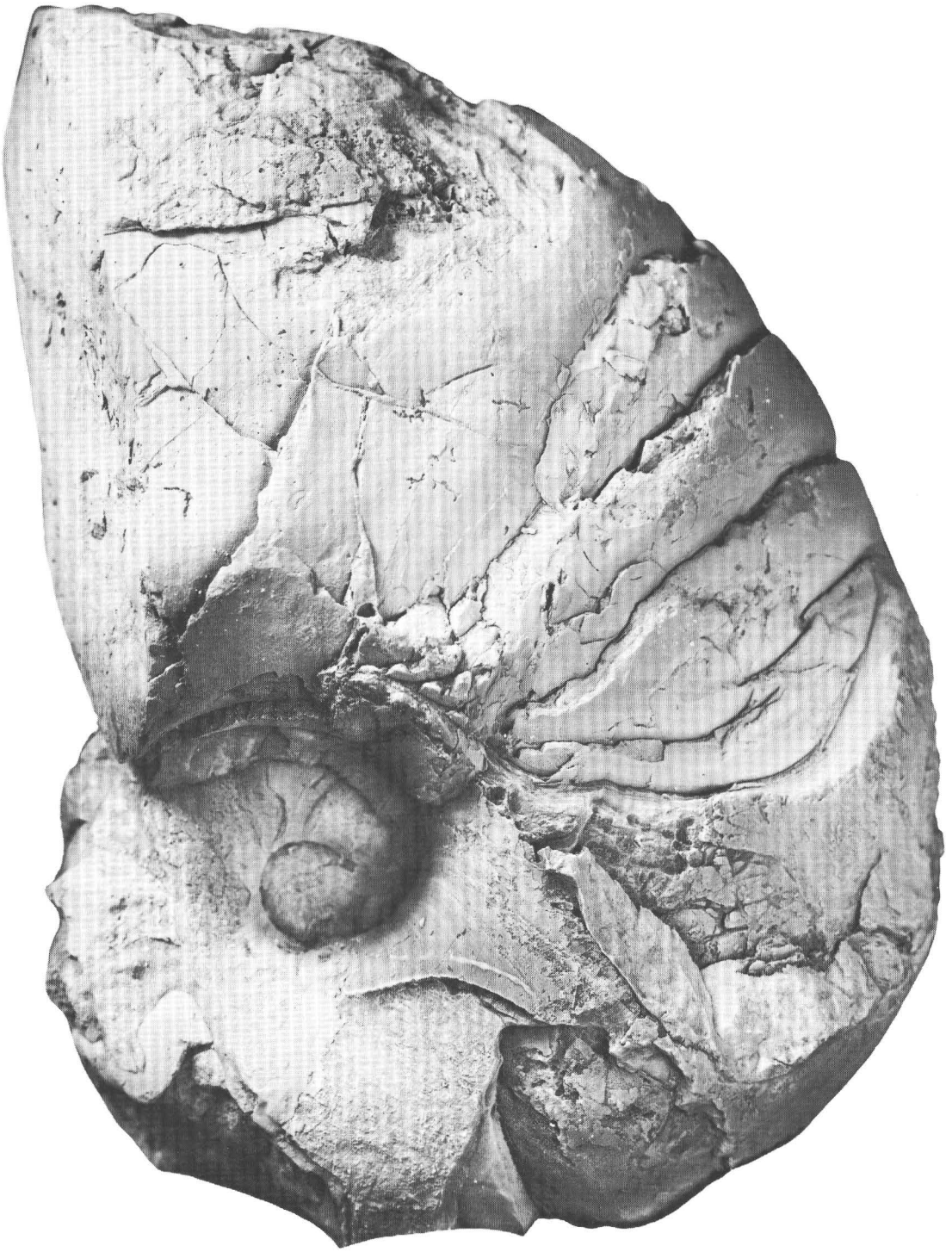

Figure 1.—*Rhadinoceras atlas* Flower and Gordon, n. sp. Holotype, USNM 174017, side view, natural size.

volution and the basal part of a living chamber. The slightly restored whorl measures 108 mm high and 110 mm wide. Some of the shell, about 3 mm thick, is preserved in the region of the relatively small and rather deep umbilical perforation which can also be seen in cross section (fig. 2 *g*). Little more than the last whorl is preserved, but an early missing part would bring the shell to two whorls or even slightly more. The cross section shows successive half-whorl intervals with the measurements as listed in table 1.

The whorl in the earliest stage preserved is evenly rounded, is broader than high, has its greatest width at midheight, and the sides are equally rounded above and below the point of

Table 1.—*Measurements, in millimeters, of four successive half-whorl intervals of* Rhadinoceras atlas *n. sp.*

[Figures 1; 2, *g*; 2, *h*]

	1	2	3	4
Diameter	[1]194	94	46	25
Whorl:				
Width	108	65	37	21
Height	104	[1]55	26	[1]13
Impressed zone:				
Width	35	20	9.5	...
Height	10	8	4.5	...
Siphuncle:				
Diameter	(Living chamber)	10	5.0	...
Distance to venter		[1]19	10.5	...
Distance to dorsum		18	6.0	...
Umbilical perforation diameter	31	14	[1]7	...

[1] Estimated.

greatest width. The impressed zone is narrow, rather deep, and about one-fourth the greatest width of the whorl. In the next half volution the dorsal surface is slightly flattened on either side of the impressed zone, strongly rounded over the umbilical shoulder, shows slight ventrolateral flattening, and is more strongly rounded midventrally. The whorl is still wider than high.

In the last half whorl the impressed zone is proportionately shallower than in the earlier part, the dorsal faces on the sides are appreciably flattened, the umbilical shoulder is strongly rounded, and the lateral faces are gently convex and merge into a more narrowly rounded venter. It is only in the last half whorl that the height becomes subequal to the width; the sides become considerably flattened, giving the shell the aspect of being narrower than it really is.

Parts of the shell preserved within the umbilicus show fine straight transverse growth lirae crossed by wider spaced faint longitudinal lirae on the umbilical wall; eight or nine of these longitudinal lirae occur in a space of 5 mm. Sutures are poorly shown, but appear to be straight and transverse. The last three adoral camerae measure 19, 21, and 18 mm, respectively, on the venter.

Discussion.—This species is a giant among its few congeners, being more than twice the size of *Rhadinoceras cornulum* (Hall) which comes from the Hamilton beds (almost certainly from the Skaneateles Shale of the Hamilton Group) near Cazenovia, N.Y. Moreover, it is four times the size of *R. ellipticum* (Rowley) of the Sellersburg Limestone of southern Indiana.

Hall (1879 p. 416) described from the "Hamilton" of Cumberland, Md., *Nautilus cavus*, a species that has the aspect of a *Nephriticeras*. Interestingly, commensurate parts of the present species also have the broad whorl of *Nephriticeras* rather than of *Rhadinoceras*, but the species are distinct, as *Nephriticeras cavum* (Hall) shows an impressed zone that is about one-sixth instead of one-fourth of the width of the whorl.

R. atlas was collected in rocks presently believed to be of very early Frasnian age and is therefore the youngest and only Late Devonian *Rhadinoceras* on record.

Holotype.—USNM 174017.

Occurrence.—Harrell Shale (Upper Devonian), 30 feet above the Mahantango-Harrell contact, in Milkhouse Hollow, a tributary of Town Creek, 7,100 feet south of lat 39°40′ N., 4,200 feet east of long 78°35′ W., Allegany County, Md. Collector, Wallace deWitt, Jr., 1955.

Genus NEPHRITICERINA Foerste, 1927

Species that clearly belong in *Nephriticerina* Foerste include, besides the type species *N. alpenensis* Foerste from the Alpena Limestone (Middle Devonian) of Michigan, *N. hyatti* (Hall) from the Hamilton Group at Cumberland, Md., and *N. juvenis* (Hall) from the Hamilton of New York.

Hall (1879) figured two other specimens that show a surface pattern suggesting *Nephriticerina.* One is a small length of shell with fine lirae illustrated as *Cyrtoceras liratum* Hall (1879, pl. 95, fig. 1), upon which was based the species *Lyrioceras dubium* Miller (1932). This specimen shows very fine close longitudinal markings and seems better assigned to *Nephriticerina* than to *Lyrioceras*.

Some specimens of *Nephriticeras* show fine cancellate markings approaching those of *Nephriticerina*, notably *Nephriticeras subliratum* (Hall) (1879, pl. 57, fig. 7) and a specimen figured as *N. bucinum* (Hall, 1879, pl. 107, figs. 4, 5). Some intergradation exists between *Nephriticeras*, as commonly understood, and *Nephriticerina*. Indeed, there is some confusion as to what constitutes *Nephriticeras bucinum.* Specimens assigned to this species vary from those showing only faint growth lines to those with finely cancellate surfaces, whereas the holotype of *N. bucinum* from the Cherry Valley Limestone Member of the Marcellus Shale has distinct gentle longitudinal carinations on its dorsum.

Kindle and Miller (1939) transferred to *Nephriticerina* some species that belong elsewhere. These are: *Cyrtoceras metula* Hall, *C. nevadense* Walcott, *C. occidentale* Whiteaves, and *C. belus* Billings. *Cyrtoceras metula* Hall from the Onondaga Limestone of New York is a small cyrtocone, quite slender, simple in aspect. On the basis of similar forms from the Onondaga of Ontario, Canada, this species is believed to be based upon the phragmocone of an *Ecdyceras* or a small *Breviococeras. Cyrotoceras nevadense* Walcott from the Nevada Formation is a slender shell showing bases of frills; it is either a *Goldringia* or a species of *Centrolitoceras. Cyrtoceras occidentale* Whiteaves from the Winnipegosis Limestone of Manitoba, Canada, belongs to *Alpenoceras*, a genus of the Discosorida (Flower and Teichert, 1957).

Cyrtoceras belus Billings, from either the Bois Blanc or the Onondaga of Ontario has never been figured and is of uncertain taxonomic position; as its siphuncle is said to be extremely close to the venter, the assignment of this species to *Nephriticerina* cannot be correct.

Nephriticerina cornucopia n. sp.

Figures 2, *a*, *b*

Description.—The type is an external mold of a curved shell

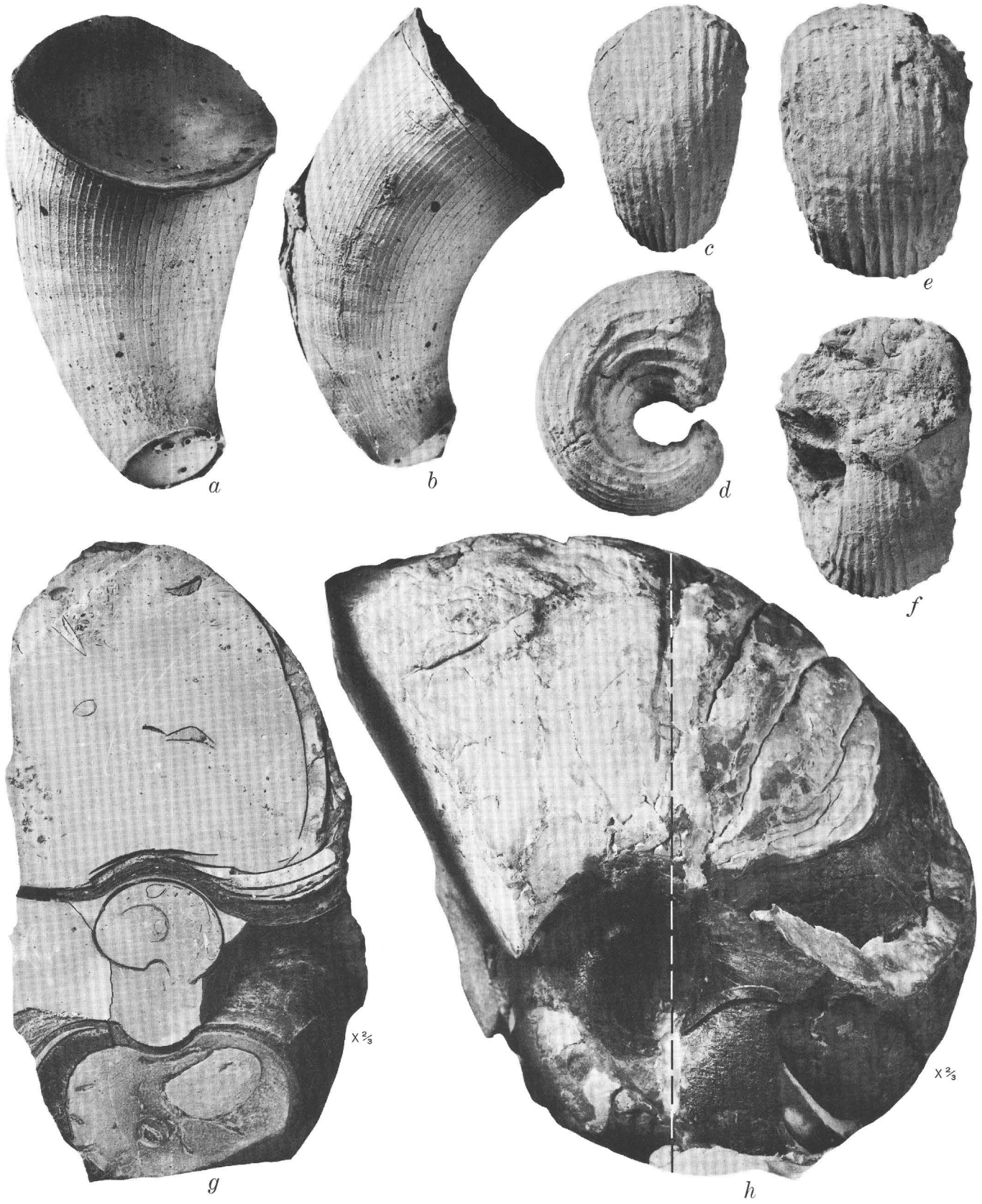

Figure 2.

80 mm long, which expands uniformly from a height of 16 mm and width of 21 mm to a height of 42 mm and width of 50 mm. The radius of curvature of the venter increases from 60 to 80 mm; that of the dorsum increases from 45 to 60 mm. A septum at the base shows a cross section having the sides strongly and evenly rounded, the dorsum slightly more flattened than the venter. The siphuncle is 1 mm across and is 8 mm from the dorsum and 9 mm from the venter.

The surface of the conch is ornamented by narrow rounded longitudinal lirae separated by broad flat interspaces and by finer closely spaced transverse threads interrupted by the longitudinal lirae. The longitudinal lirae, approximately 85 in all, are spaced so that five interspaces occur in a width of 10 mm on the dorsum near the broad end of the specimen and seven in an equal space on the venter and sides. Between the lirae some very fine faint longitudinal threads are also present locally in the interspaces. The transverse growth lines average 13 to 15 in a length of 5 mm. Adapically they are fairly even, adorally they are thicker, higher, and more conspicuous in two bands 4 mm long and 5 mm apart. The growth lirae are transverse ventrally; there is no indication of a hyponomic sinus.

The sides of the shell, only one of which is preserved, show vestigial lateral expansions and contractions; they are too faint to be measured properly, but the last two are each 4 mm long and are 16 mm apart.

Discussion.—This species is characterized by the rather gentle and uniform expansion of its conch and by the proportions of the surface markings. *N. alpeńensis* Foerste is a much larger and more rapidly expanding species in which fine vestigial transverse markings are present between the longitudinal lirae. Our species differs further in the absence of a hyponomic sinus, as demonstrated by the clearly preserved growth lines of the venter.

N. hyatti (Hall) from the Middle Devonian of Cumberland, Md., though known originally from an incomplete and somewhat crushed example, is certainly much more rapidly expanding than our shell and shows lirae on the dorsum that at a similar diameter have three instead of five interspaces in a width of 10 mm.

N. juvenis (Hall) from the Hamilton of New York has a shell that initially expands rapidly but becomes very slender after attaining a shell width of 32 mm.

Figure 2.—Nephriticeratidae. All figures natural size unless otherwise indicated.

a, b, Nephriticerina cornucopia Flower and Gordon, n. sp., holotype, USNM 137644, oblique dorsal and side views, from silicone cast.

c–f, Lyrioceras sampsoni (Nettleroth):

c, d, lectotype, USNM 51259, back and side views;

e, f, paralectotype, USNM 179137, back and front views.

g, h, Rhadinoceras atlas Flower and Gordon, n. sp., holotype, USNM 174017:

g, cross section;

h, side view, dashed line shows position of cross section.

Holotype.—USNM 137644.

Occurrence.—Middle Devonian (Mahantango Formation, according to Wallace deWitt, Jr.) from the Hazen Road, just north of the Maryland State line, Evitt's Creek quadrangle, in the valley of Evitt's Creek, east of Pine Ridge, Bedford County, Pa. Collector, A. G. Perdew, 1958.

Genus LYRIOCERAS Foerste, 1927

In addition to the type species *L. liratum* (Hall), species regarded as belonging in this genus include *L. hindshawi* (Ehlers and Hussey) and *L. sampsoni* (Nettleroth). The first two species were described originally as nautiloids of the genera *Gyroceras* and *Nephriticeras*, respectively. *L. sampsoni*, however, was regarded as a gastropod by its author and assigned to *Euomphalus*. It is to correct this erroneous referral that the types of *Lyrioceras sampsoni* (Nettleroth) are redescribed and refigured in this paper.

Gyroceras subliratum Hall was originally included in *Lyrioceras* by Foerste (1927, p. 193), an assignment later followed by Kindle and Miller (1939, p. 70). We believe, however, that this species is more correctly referred to *Nephriticerina*.

Lyrioceras dubium Miller (1932, p. 331) was proposed as a new name to replace *Aploceras* (*Cyrtoceras*) *liratum* Hall (1862 [1861], p. 64), which Miller regarded as a secondary homonym of *Gyroceras liratum* Hall (1860, p. 104), as he included both species in *Lyrioceras*. We believe that *Lyrioceras dubium* Miller also is more correctly referred to *Nephriticerina*. As the rejection and replacement of Hall's *Aploceras* (*Cyrtoceras*) *liratum* was effected prior to 1961, it is not necessary to return to the use of Hall's name for this species, according to Article 59C of the International Code of Zoological Nomenclature (1961, p. 56, 57).

Lyrioceras sampsoni (Nettleroth)

Figure 2, *c–f*

Euomphalus sampsoni Nettleroth, 1889, p. 182, 183, pl. 24, figs. 3, 4; Kindle, 1901, p. 718, 719.

Description.—The shell is thick discoidal, the number of whorls not known but probably about two; the whorls are in contact but lack an impressed zone. The outer volution is depressed, oval in cross section, increasing rapidly in width, about 1 mm in 5 mm measured along the venter, and increasing slightly in degree of depression adorally. In the lectotype, which is slightly less than one volution and has a diameter of 45.8 mm, the whorls increase from a height of 10.0 mm and width 11.9 mm to 23.5 and 29.0 mm, respectively.

The shell is ornamented by 26 to 28 prominent longitudinal ridges having broad concave interspaces. The ridges are narrowly rounded, increase in strength adorally, and are slightly closer spaced over the venter and ventrolateral zones than on the flanks and dorsum; they diverge orad on the dorsum. Transverse sculpture consists of fine raised incre-

mental lirae crossing the ridges and interspaces, slightly retractive on the flanks but fairly straight across the venter. Present also on the first volution are somewhat irregularly spaced faint annulations, strongest over the flanks where they are fairly straight to somewhat retractive. The septa and siphuncle are not exposed in the primary types.

Discussion.—Although the absence of visible septa led Nettleroth to regard this as the shell of a gastropod, he pointed out that it resembles *Nautilus liratus* Hall, later designated as the type species of *Lyrioceras*. Nettleroth's types in the collection of the U.S. National Museum consist of three specimens (USNM 51259), two of them found among the gastropod types and turned over to us by E. L. Yochelson, and the third in the nautiloid collection. All three specimens have been used in preparing the description. The specimen figured by Nettleroth (1889, pl. 21, figs. 3, 4) is hereby designated the lectotype. The lectotype is figured photographically for the first time (fig. 2, *c*, *d*) together with one of the two paralectotypes (fig. 2, *e*, *f*) which is slightly crushed so that the coiling is asymmetrical. The three primary types have been placed in the U.S. National Museum nautiloid type collection.

L. sampsoni possesses all the surface characters of typical *Lyrioceras*, including the strong longitudinal ribs, the fine threadlike transverse lirae, and the weak annulations in the early part of the conch. We have not been able to compare it with Hall's types of *Lyrioceras liratum*, but, judging from the original description of that species (Hall, 1879, p. 407, 408, pl. 57, fig. 3, pl. 60, figs. 8, 9), it has fewer longitudinal ribs than *L. sampsoni*, and these become obsolete anteriorly over the venter. Similar obsoletion has not been observed in the primary types of *L. sampsoni*.

Types.—Lectotype USNM 51259; paralectotypes USNM 179137 and 179138.

Occurrence.—Middle Devonian, Silver Creek Limestone Member of the Sellersburg Limestone ("cherty layers superimposed upon the hydraulic limestone," according to Nettleroth (1889, p. 183) which are assigned to the Silver Creek by Campbell, 1942, p. 1062), Watson's Station, Clark County, Ind., about 6 miles from the Falls of the Ohio River.

REFERENCES

Campbell, Guy, 1942, Middle Devonian stratigraphy of Indiana: Geol. Soc. America Bull., v. 53, no. 7, p. 1055–1072, 2 text figs.

Flower, R. H., 1945, Classification of Devonian nautiloids: Am. Midland Naturalist, v. 33, no. 3, p. 675–724, 5 pls.

Flower, R. H., and Teichert, Curt, 1957, The cephalopod order Discosorida: Kansas Univ. Paleont. Contrib. [no. 21], Mollusca, Art. 6, 144 p., 43 pls., 34 text figs.

Foerste, A. F., 1927, Devonian cephalopods from Alpena in Michigan: Michigan Univ., Mus. Geology Contr., v. 2, no. 9, p. 189–208, pls. 1–5.

Hall, James, 1860, Notes and observations upon the fossils of the Goniatite Limestone in the Marcellus Shale of the Hamilton Group in . . . New York and those of the Goniatite beds of Rockford, Ind.; with some analagous forms from the Hamilton Group proper: New York State Cabinet Ann. Rept. 13, p. 95–112.

—— 1862, Descriptions of new species of fossils from the Upper Helderberg, Hamilton, and Chemung groups: New York State Cabinet Ann. Rept. 15, p. 29–80. (Advance pub. 1861.)

—— 1879, Descriptions of the Gastropoda, Pteropoda, and Cephalopoda of the Upper Helderberg, Hamilton, Portage, and Chemung groups: New York Geol. Survey, Palaeontology, v. 5, pt. 1, 492 p., pt. 2, 113 pls.

Hyatt, Alpheus, 1883–84, Genera of fossil cephalopods: Boston Soc. Nat. History Proc., v. 22, p. 253–338 (p. 253–272, Dec., 1883; p. 273–338, Jan., 1884).

International Commission on Zoological Nomenclature, 1961, International code of zoological nomenclature adopted by the XV International Congress of Zoology: London, 176 p.

Kindle, E. M., 1901, Devonian fossils and stratigraphy of Indiana: Indiana Dept. Geology and Nat. Resources Ann. Rept. 25, p. 529–758, 773–775, pls. 1–31.

Kindle, E. M., and Miller, A. K., 1939, Bibliographic index of North American Devonian Cephalopoda: Geol. Soc. America Spec. Paper 23, 179 p.

Miller, A. K., 1932, New names for Devonian cephalopod homonyms: Am. Jour. Sci., 5th ser., v. 24, p. 330–331.

Nettleroth, Henry, 1889, Kentucky fossil shells; a monograph of the fossil shells of the Silurian and Devonian rocks of Kentucky: Kentucky Geol. Survey, 245 p., 36 pls.

LATE PLEISTOCENE GLACIATION AND POLLEN STRATIGRAPHY IN NORTHWESTERN NEW JERSEY

By LESLIE A. SIRKIN[1], and JAMES P. MINARD,
Garden City, Long Island, N.Y., Washington, D.C.

Abstract.—Study of pollen from a peat bog on Kittatinny Mountain, Sussex County, N.J., allows correlation of the late Pleistocene pollen stratigraphy of the bog with that of the Wallkill Valley to the north, New England to the northeast, and Long Island to the east. The bog (here called Saddle Bog) is in a saddle in the summit ridge of the mountain and is partly dammed by an end moraine of late Wisconsin age. Radiocarbon dating gives an age of 12,300 years B.P. at a depth of 5.50–5.65 m. The bog was cored to a depth of 7.65 m; commercial quality peat extends from near the surface to a depth of 4.75 m. The lower peat of the bog contains spruce, pine, and birch pollen, and willow, alder, grass, sedge, and composite pollen, which may represent park-tundra vegetation, that is, the herb pollen zone (T). The spruce maximum occurs in the A1 subzone, even though pine is more abundant. Pine pollen peaks in the B1 subzone, accompanied by abundant birch, and oak pollen rises in the B2 subzone. Oak-hemlock and oak-hickory-hemlock pollen associations characterize the C1 and C2 subzones, whereas both spruce and birch pollen rise in the C3 subzone. Sedimentation in the bog may have begun sometime between 15,000 and 18,300 years ago as deglaciation of the area began.

The area of study, here called Saddle Bog, is on Kittatinny Mountain in the north-central part of Sussex County, N.J., at 41°14′08″ N. and 74°42′10″ W. (fig. 1). The bog is about 200 m wide (northwest-southeast) and about 300 m long (northeast-southwest) and amounts to about 10 acres in surface extent.

Samples of peat from Saddle Bog have been studied for pollen and dated by radiocarbon techniques to learn more about the time and duration of withdrawal of the ice sheet from this area. The location of the bog is significant in reconstruction of late Pleistocene deglaciation in the northeastern United States, specifically as related to the recession of the Wallkill Valley–Hudson Valley glacial lobe (Connally and Sirkin, 1970, 1972). Pollen stratigraphy and radiocarbon dates of bog sediments provide additional detail on late-glacial environments in the vicinity of the end moraine of Wisconsin age in northwestern New Jersey.

Acknowledgments.—The authors are indebted to Dr. G. Gordon Connally, Staten Island Community College, New York, and Jack B. Epstein, U.S. Geological Survey, for their assistance in coring the bog and to Meyer Rubin, U.S. Geological Survey, for the radiocarbon dates.

[1] Adelphi University.

PREVIOUS INVESTIGATIONS

Studies of the glacial geology of this area have been made by Minard (1961, 1969) and Minard and Rhodehamel (1969). Minard's (1961) description of end moraines across Kittatinny Mountain filled the previous gap between mapped moraines in the valleys to the east and west (fig. 1). A detailed map of the moraines was prepared by Minard (1969), and the moraines were described and two radiocarbon dates were cited by Minard and Rhodehamel (1969, p. 283, 297, 299, fig. 22). One sample from a depth of 3 m, about 30 m from the southeast edge of the bog, was dated at 6,260±300 years B.P. (Meyer Rubin, written commun., 1968, U.S. Geol. Survey radiocarbon lab. sample W-2200). A second sample, taken within 16.5 m of the core described in this report and from a depth of 5.5 m, was dated at 7,800±650 years (Meyer Rubin, written commun., 1968, U.S. Geol. Survey radiocarbon lab. sample W-2236).

PHYSIOGRAPHY AND GLACIAL HISTORY

The bog is in a saddle in the summit ridge of Kittatinny Mountain. This ridge is underlain by the resistant quartzite conglomerate of the Shawangunk Formation of Ordovician(?) and Silurian age. The bog occupies a depression as much as 8 m deep. The lower part of the depression is a bedrock basin in the quartzite; the upper part is dammed by the end of one of the recessional moraines lying across the westward drainageway from the saddle. The relationship between bedrock and drift was recently revealed in a drainage ditch. The ditch cut through several feet of moraine and several feet of the underlying quartzite. The bog had previously been partly drained by an old hand-dug ditch which is still evident on the northwest side. That ditch dates from near the end of the 19th century when the bog had been partly cleared for farming.

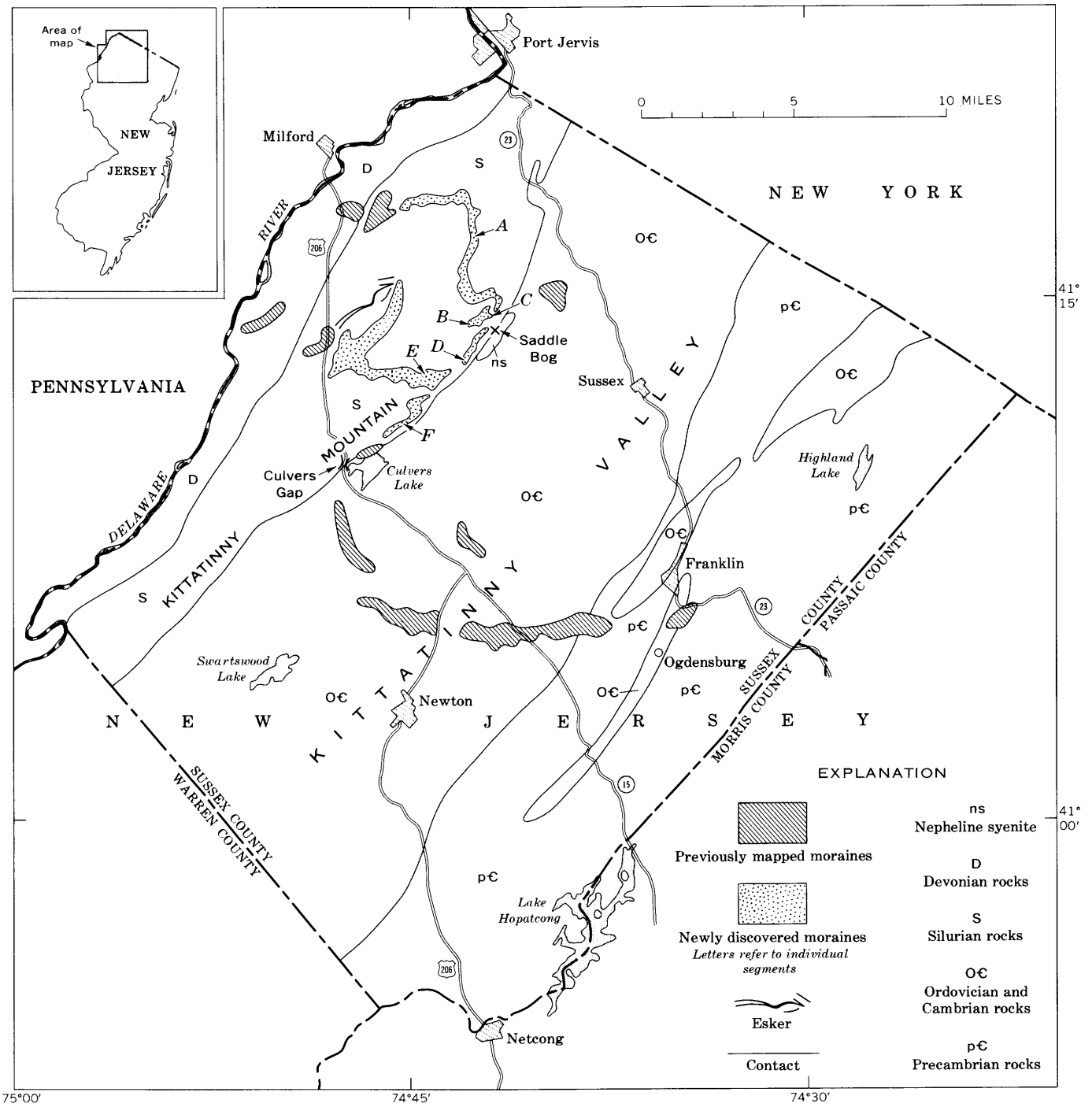

Figure 1.—Map of Sussex County, N.J., showing location of end moraines and eskers on Kittatinny Mountain and their relationship to moraines in the valley on either side. Saddle Bog (X) is at the north end of moraine D. After Minard (1961).

The basin may have been initially scoured in bedrock by a tongue of ice which flowed westward from the main ice lobe in Kittatinny Valley through the saddle and down the slope of the intermontane valley (fig. 1). The end of the tongue came to rest on an end moraine (B, fig. 1) which had been deposited at the base of the slope by a prior ice lobe. That lobe had occupied the intermontane valley just west of Kittatinny Mountain and had deposited moraines A and E (fig. 1). A steep-sided arcuate end moraine (C, fig. 1) was subsequently deposited by the ice tongue on top of moraine B (Minard, 1969; Minard and Rhodehamel, 1969, p. 297, 299, fig. 22). The lithology of the underlying moraine (B) is that of the

ridge and intermontane valley (Silurian quartzite, sandstone, and shale), whereas the upper moraine (C) includes these lithologies plus rocks from Kittatinny Valley, such as nepheline syenite and Ordovician Martinsburg Shale (fig. 1).

During and after withdrawal of the ice tongue, a lateral moraine was deposited by the edge of the ice lobe in Kittatinny Valley as a narrow ridge along the crest of Kittatinny Mountain (fig. 1, moraine D). The north end of this moraine dammed the west side of the bedrock basin (Minard and Rhodehamel 1969, p. 299, and fig. 22) and provided additional closure. The origin of moraine D is similar to that of moraine F which also was deposited along the ridge crest and across a saddle by the main ice lobe (fig. 1).

CHRONOLOGY AND STRATIGRAPHY

Samples for pollen analysis were retrieved by a Davis-type peat sampler from a core hole in the bog (Saddle Bog core hole 3) after probing had located the deepest sedimentary section. Sediments from the base of the organic section at 5.50–5.65 m were submitted for radiocarbon dating (table 1 and fig. 2). Relative pollen frequencies for dominant forms are shown as percentages except between 6.37 and 7.37 m where bars indicate the actual number of pollen grains counted (fig. 2). Absolute pollen data are shown as pollen per gram of sediment in a curve superimposed on the arboreal pollen (AP) curve.

Herb pollen zone T

Although pollen is sparse in the lower 1.50 m of the core, the basal samples (7.50, 7.65 m) contain significant amounts of pine, spruce, and birch pollen, including possible shrub varieties of pine and birch, and pollen of willow, alder, grass, sedge, and the composites. A few pollen grains of *Thalictrum*, *Shepherdia*, Ranunculaceae, and *Dryas*, and other rosaceous forms, occur in the general pollen assemblage which may be traced from 7.65 m up to 6.12 m. This association of pollen forms, and by inference, plants, many of which have cold or boreal affinities, may have been derived from a tundralike vegetation. The nonarboreal pollen (NAP) maximum of 52 percent of the pollen at 6.12 m lends further support for placing the basal part of the core in the late Pleistocene herb pollen zone.

Table 1.—*Sedimentary log of Saddle Bog core hole 3*

Depth (cm)	*Material*
0–25	Peat, rich in coarse forest humus.
25–175	Peat, rich in sphagnum fibers.
175–225	Peat, very wet, top of water table.
225–250	Woody layer in peat.
250–275	Peat, rich in sphagnum fibers.
275–450	Peat, fine-grained.
450–475	Peat, very fine grained, cohesive.
475–565	Peat, silty, grayish-green to grayish-brown.
565–625	Clay, gray, silty at base.
625–650	Clay, bluish-gray.
650–725	Clay, bluish-gray, cohesive but containing thin sand layers.
725–760	Sand and clay, bluish-gray, banded.
760–765	Silt, medium-gray.

Spruce pollen zone A

The spruce pollen rise occurs rather abruptly at 6.0 m and is accompanied by increases in pine and alder and by decreasing but still significant NAP. The spruce maximum occurs at 5.75 m, even though pine is the most abundant pollen in this zone. The abundance of NAP in lower zone A (subzone A1) suggests the presence of a spruce park, whereas the subsequent spruce maximum and NAP decline (subzone A4) might signify forest conditions. Oak is also abundant in the upper subzone, which has been dated at 12,300±300 years B.P. (Meyer Rubin, written commun., 1971, U.S. Geol. Survey radiocarbon lab. sample W-2562). The incursion of oak into the pollen record may indicate the proximity of the oak forest to the spruce forest at that time.

Pine pollen zone B

The percentage of pine pollen increases substantially in subzone A4 and peaks in the lower B zone (subzone B1) at nearly 75 percent. Birch and alder pollen are also relatively abundant. Oak pollen increases markedly in subzone B2, whereas pine and birch pollen decrease. The NAP decreases to less than 1.0 percent of the pollen in this zone.

Oak pollen zone C

The oak pollen rise continues in this zone until the oak pollen represents 80 percent of the total pollen. Subzone C1 contains an oak-hemlock association, whereas C2 is composed of oak, hickory, and hemlock. In both the B zone and subzones C1 and C2, NAP represents less than 6 percent of the pollen. Pollen of beech, hickory, and elm also appear in subzone C1, and the pollen of these trees and that of the Ericaceae increase in subzone C2. Chestnut pollen appears late in that subzone. Subzone C3 is marked by both spruce and composite pollen rises, the birch maximum, increases in pine and alder, and decreases in oak and hemlock.

REGIONAL CORRELATIONS

The pollen stratigraphy in this bog correlates closely with that of areas studied in southern New York, particularly to the north in the Wallkill Valley (Connally and Sirkin, 1970) and to the east in Long Island (Sirkin, 1967a,b). The herb pollen zone, although not consistently well represented in numbers of pollen grains, compares favorably in taxa with herb and shrub pollen represented elsewhere in this zone. The pollen assemblages reinforce the inferred existence of late Pleistocene tundra vegetation as described in the Wallkill and Long Island studies (table 2).

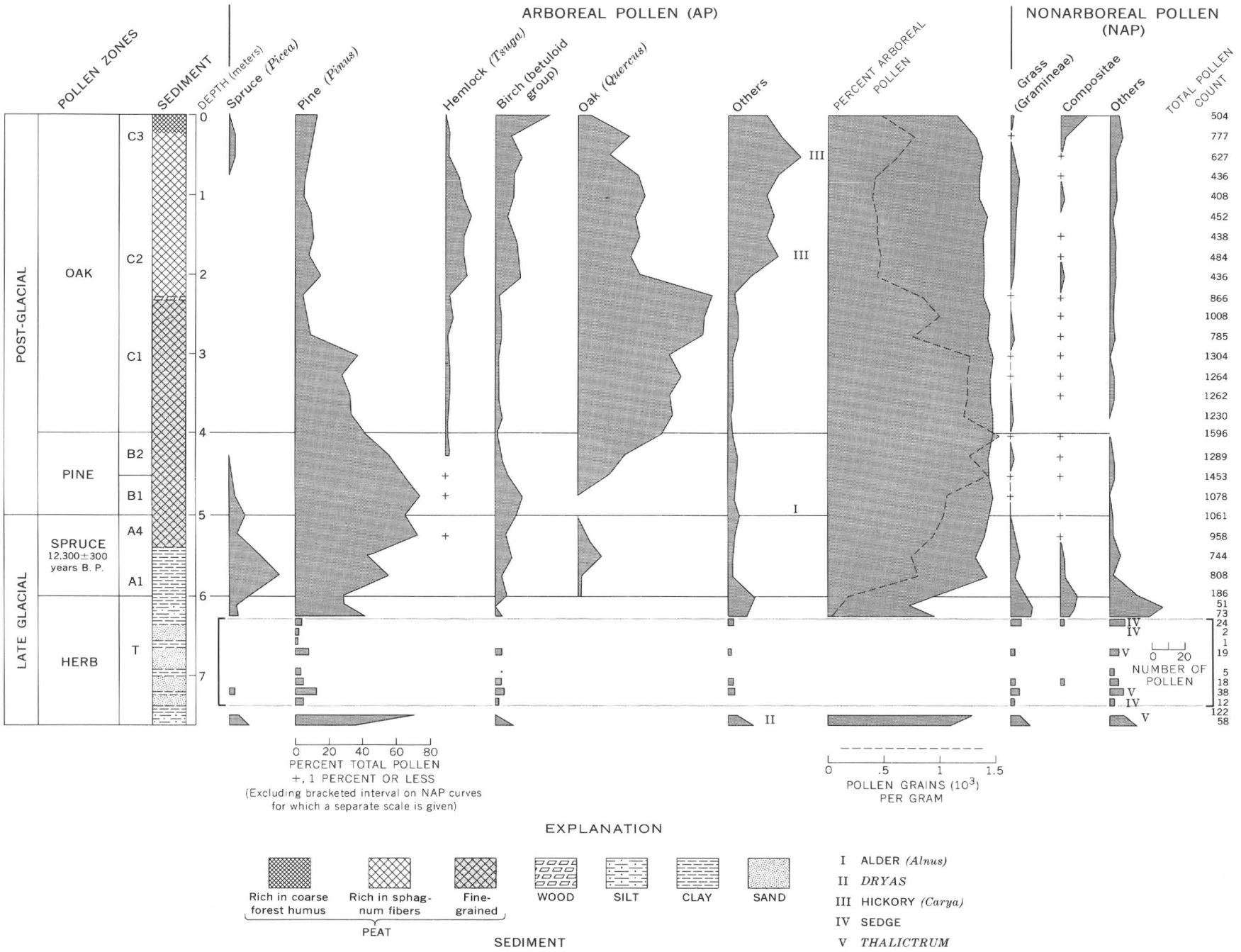

Figure 2.–Pollen diagram for Saddle Bog core hole 3, Kittatinny Mountain, Sussex County, N.J.

Table 2.—*Correlation of late Pleistocene and Holocene radiocarbon-dated pollen stratigraphy, pollen assemblages, and inferred vegetation from northwestern New Jersey, upper Wallkill Valley, N.Y., southern New England, western Long Island, and central New Jersey*

[Compiled from Connally and Sirkin (1970); Deevey (1958); Davis (1969); Sirkin and others (1970)]

	Pollen Zonation		Age (yrs B.P., approx)	Northwestern New Jersey	Upper Wallkill Valley, N.Y.	Southern New England	Western Long Island, N.Y.	Central New Jersey
Postglacial	C3	Oak		C3, Birch, oak, spruce rise	C3, Oak, hemlock, chestnut	C3, Spruce rise, oak	C3, Oak, chestnut, birch, hemlock, holly	C3, Oak, chestnut, alder
	C2	Oak		C2, Oak, hickory, hemlock	C2, Oak, hemlock, hickory, elm	C2, Oak, hickory,	C2, Oak, hickory	C2, Oak, hickory
	C1	Oak		C1, Oak, hemlock	C1, Oak, hemlock	C1, Oak, hemlock	C1, Oak, hemlock	C1, Oak, hemlock
	B2	Pine	7,000	B2, Pine, oak	B2, Pine, oak	B2, Pine	B2, Pine, oak	
	B1	Pine	10,000	B1, Pine, birch	B1, Pine	A4, Spruce returns	B1, Pine	B, Pine
	A4	Spruce		A3, A4, Pine, spruce, oak (12,300±300 yrs B.P.)	A3, A4, Spruce returns, pine, spruce, oak (12,850±250 yrs B.P.)	A3, Pine, spruce, oak A1, A2, Birch, spruce (12,150 yrs B.P.)	A4, Spruce, pine	
	A3	Spruce						
	A1, A2	Spruce		A1, A2, Pine, spruce, NAP (Spruce park)	A1, A2, Pine, spruce	T3, Birch, park tundra	A1–A3, Pine, spruce	A1, A2, Pine, spruce
Glacial/Late glacial					T3, pine, spruce, birch	T2, Spruce, park tundra	T3, Pine, spruce, NAP	
	T	Herb			T2, Spruce, pine, fir	T1, Tundra (14,300 yrs B.P.)	T2, Spruce rise	T, Pine, spruce
		Herb	15,000		T1, Pine, birch, tundra	Glaciated	T1, Park tundra	
	W	Herb	17,000	W, Park tundra Glaciated	Glaciated		W, Tundra	W, Park tundra
			20,000				Glaciated	

It may also be significant that this record persists through the basal 1.65 m (6.0–7.65 m) of the core. On the basis of a sediment column of 2.15 m (5.5–7.65 m), deposition rates of 0.036 cm/year and 0.08 cm/year for fine clastic sediments in a late-glacial lake sequence (Davis and Deevey, 1964, p. 1293; Davis, 1969, p. 411, respectively), and on the mean radiocarbon age of 12,300 years B.P. at a depth of 5.50–5.65 m, sedimentation in Saddle Bog could have begun between about 18,300 and 15,000 years ago. Accordingly, the period represented by herb pollen zone T (6.0–7.65 m) would have lasted about 4,600 to 2,100 years. The older and longer age range would be in keeping with the greater age of the more southerly moraines and would provide a tentative maximum age of about 18,600 years B.P. (18,300+300) for the Ogdensburg-Culvers Gap moraine more than 12 miles south of the bog site. Thus, the bog site could have been ice free and occupied by tundra vegetation at the latest about 15,000 years ago.

An age of 18,600 years B.P. for the Ogdensburg-Culvers Gap moraine would provide a closer correlation between the time of emplacement of the moraine and the readvance of the ice sheet in southern New England and New York, and the time when the Roslyn till was deposited on Long Island (Sirkin, 1971). This age would also bracket the age of the New Hampton moraine in the Wallkill Valley, more than 25 miles north of the Odgensburg-Culvers Gap moraine. Deposition of the New Hampton moraine has been placed at more than 15,000 years B.P., the postulated age for the basal bog sediments in the New Hampton bog (Connally and Sirkin, 1970, p. 3302). The age of 18,600 years for the end moraine and the persistence of the glacier within 25 miles of the study site for a minimum of 2,100 years (the minimum duration of tundra at this site) is in keeping with the age of 16,700 years for park-tundra vegetation in the Delaware Valley south of the terminal moraine (Sirkin and others, 1970, p. D83–D84, figs. 2–4). This age was previously used as a minimum age for the establishment of the tundra in the end moraine region. The age also serves to substantiate the "rate of glacial recession" curve in which deglaciation of the Hudson-Wallkill lobe from the western Long Island–Staten Island–New Jersey terminus is postulated to have begun prior to 17,000 years B.P. (Connally and Sirkin, 1972).

ECONOMIC ASPECTS

As a conservative estimate, Saddle Bog has an average thickness of 10 feet (3 m) of commercial quality peat over a surface area of 10 acres (40,050 m^2); this constitutes a probable economic deposit. Use of the term "commercial quality peat" is in accordance with the standard classification of the American Society for Testing and Materials (1969). On the basis of 200 short tons of air-dried peat per acre foot (Cameron, 1970b, p. B19) and an average price of $10.73 per ton (Cameron, 1970a, p. A43), the bog contains about 20,000 tons of air-dried peat worth about $214,600.

REFERENCES

American Society for Testing and Materials, 1969, Standard classification of peats, mosses, humus, and related products, ASTM Designation D 2607–69; Philadelphia, Pa., 1 p.

Cameron, C. C., 1970a, Peat deposits of northeastern Pennsylvania: U.S. Geol. Survey Bull. 1317-A, 90 p.

—— 1970b, Peat deposits of southeastern New York: U.S. Geol. Survey Bull. 1317-B, 32 p.

Connally, G. G., and Sirkin, L. A., 1970, Late glacial history of the upper Wallkill Valley, New York: Geol. Soc. America Bull., v. 81, no. 11, p. 3297–3305.

—— 1972, Wisconsinan history of the Hudson-Champlain lobe: Geol. Soc. America Mem. 136 [In press]

Davis, M. B., 1969, Climatic changes in southern Connecticut recorded by pollen deposition at Rogers Lake: Ecology, v. 50, no. 3, p. 409–422.

Davis, M. B., and Deevey, E. S., Jr., 1964, Pollen accumulation rates–Estimates from late-glacial sediment of Rogers Lake: Science, v. 145, no. 3638, p. 1293–1295.

Deevey, E. S., Jr., 1958, Radiocarbon-dated pollen sequences in eastern North America: Zurich, Geobot. Inst. Rübel Veröff., no. 34, p. 30–37.

Minard, J. P., 1961, End moraines on Kittatinny Mountain, Sussex County, New Jersey: Art. 172 *in* U.S. Geol. Survey Prof. Paper 424-C, p. C61–C64.

—— 1969, Geologic map of part of Kittatinny Mountain, Sussex County, New Jersey: U.S. Geol. Survey open-file rept., scale 1:24,000.

Minard, J. P., and Rhodehamel, E. C., 1969, Quaternary geology of part of northern New Jersey and the Trenton area, *in* Subitzky, Seymour, ed., Geology of selected areas in New Jersey and eastern Pennsylvania and guidebook of excursions: New Brunswick, N.J., Rutgers Univ. Press, p. 279–313.

Sirkin, L. A., 1967a, Correlation of late glacial pollen stratigraphy and environments in the northeastern United States: Rev. Palaeobotany and Palynology, v. 2, nos. 1–4, p. 205–218.

—— 1967b, Late-Pleistocene pollen stratigraphy of western Long Island and eastern Staten Island, New York, *in* Cushing, E. J., and Wright, H. E., Jr., eds., Quaternary paleoecology–Internat. Assoc. Quaternary Research, 7th Cong., 1965, Proc., v. 7: New Haven, Conn., Yale Univ. Press, p. 249–274.

—— 1971, Surficial glacial deposits and postglacial pollen stratigraphy in central Long Island, New York: Pollen et Spores, v. 13, no. 1, p. 93–100.

Sirkin, L. A., Owens, J. P., Minard, J. P., and Rubin, Meyer, 1970, Palynology of some upper Quaternary peat samples from the New Jersey coastal plain, *in* Geological Survey Research 1970: U.S. Geol. Survey Prof. Paper, 700-D, D77–D87.

UNCONFORMITIES WITHIN THE FRONTIER FORMATION, NORTHWESTERN CARBON COUNTY, WYOMING

By E. A. MEREWETHER and W. A. COBBAN, Denver, Colo.

Abstract.—The Upper Cretaceous Frontier Formation in northwestern Carbon County, Wyo., consists of marine clastic rocks that are divided into three parts by two unconformities. The parts are herein called, in ascending order, the Belle Fourche Shale Member, the unnamed member, and the Wall Creek Sandstone Member. This sequence is represented in the Black Hills region of northeastern Wyoming by the Belle Fourche Shale, Greenhorn Formation, and Carlile Shale. The lower hiatus is represented in the Black Hills by about 300 feet of strata in the Greenhorn Formation and the lower part of the Carlile Shale. The upper hiatus is equivalent to about 100 feet of beds in the middle of the Carlile Shale. At most outcrops, beds above and below the unconformities appear parallel; however, at one locality on the Rawlins uplift they seem to be slightly discordant. At this locality there is scanty evidence of local folding during deposition of the Frontier.

In northwestern Carbon County, Wyo. (fig. 1), two unconformities divide the Upper Cretaceous Frontier Formation into three members which are called here, in ascending order, the Belle Fourche Shale Member, an unnamed member, and the Wall Creek Sandstone Member (table 1). Unconformities within the Frontier were first recognized by Cobban and Reeside (1951) at Grenville dome, south of Sinclair, Wyo. These rocks and hiatuses are represented in the Black Hills region of northeastern Wyoming by the Belle Fourche Shale, Greenhorn Formation, and Carlile Shale. Fossil data (table 1) show that the lower unconformity is represented in the Black Hills by about 300 feet of beds comprising most of the Greenhorn Formation and the lower part of the Carlile Shale (Cobban and Reeside, 1951, p. 63). The upper unconformity is equivalent to about 100 feet of strata in the lower part of the Turner Sandy Member of the Carlile Shale. The upper unconformity occurs in both areas but the hiatus represents a much thinner sequence of beds in the Black Hills.

Unconformities and facies changes within the Frontier probably influence the distribution of oil and gas in this important petroleum-producing formation. During the years prior to 1972, petroleum was discovered in the formation at more than 90 fields in Wyoming. In 1970, the Frontier and equivalent rocks produced more than 600,000 barrels of oil and more than 23 billion cubic feet of gas, and may have ranked second among the gas-producing formations of Wyoming (Wyoming Oil and Gas Conserv. Comm., 1971).

FRONTIER FORMATION

The Frontier Formation in northwestern Carbon County (fig. 1) crops out on the southern slopes of the Ferris and Seminoe Mountains and on the flanks of the Rawlins uplift and the Grenville dome. Many wells drilled for oil and gas in the area have penetrated these rocks. The Frontier has been described in detail by Fath and Moulton (1924, p. 21–23), Dobbin, Hoots, and Dane (1928, p. 182–183), Cobban and Reeside (1951, p. 60–65), and Berry (1960, p. 20–21 and 64). The formation consists of shale, siltstone, sandstone, and bentonite, and was deposited in shallow-marine environments. Soft concretion-bearing shale of the lowest member of the Frontier conformably overlies siliceous shale of the Lower Cretaceous Mowry Shale. The top of the Mowry is a bentonite bed 3–5 feet thick. The Frontier is conformably overlain by dark-gray noncalcareous concretion-bearing shale that is similar in lithology and stratigraphic position to the Sage Breaks Member of the Carlile Shale in the Black Hills. The upper part of the Frontier intertongues with the lower part of this unnamed shale. The upper contact of the Frontier is placed at the top of the uppermost sandstone or siltstone bed beneath a thick shale unit which includes the unnamed shale and the overlying Niobrara Formation and Steele Shale.

The thickness of the Frontier decreases irregularly from north to south in northwestern Carbon County; it is as much as 1,000 feet along the southwestern flank of the Ferris Mountains (Fath and Moulton, 1924, p. 21; Reynolds, 1968a), and about 900 feet on the southern slope of the Seminoe Mountains (Merewether, 1972b). Near well 1 (fig. 1) on the Lost Soldier anticline, thicknesses determined from well logs range from 935 to 1,230 feet (uncorrected for dip). At outcrops on the Rawlins uplift and Grenville dome, the thickness ranges from 723 to 912 feet (fig. 2); however, at sections 2 and 4, where the formation is best exposed, the thickness is about 840 and 815 feet, respectively. Along a line

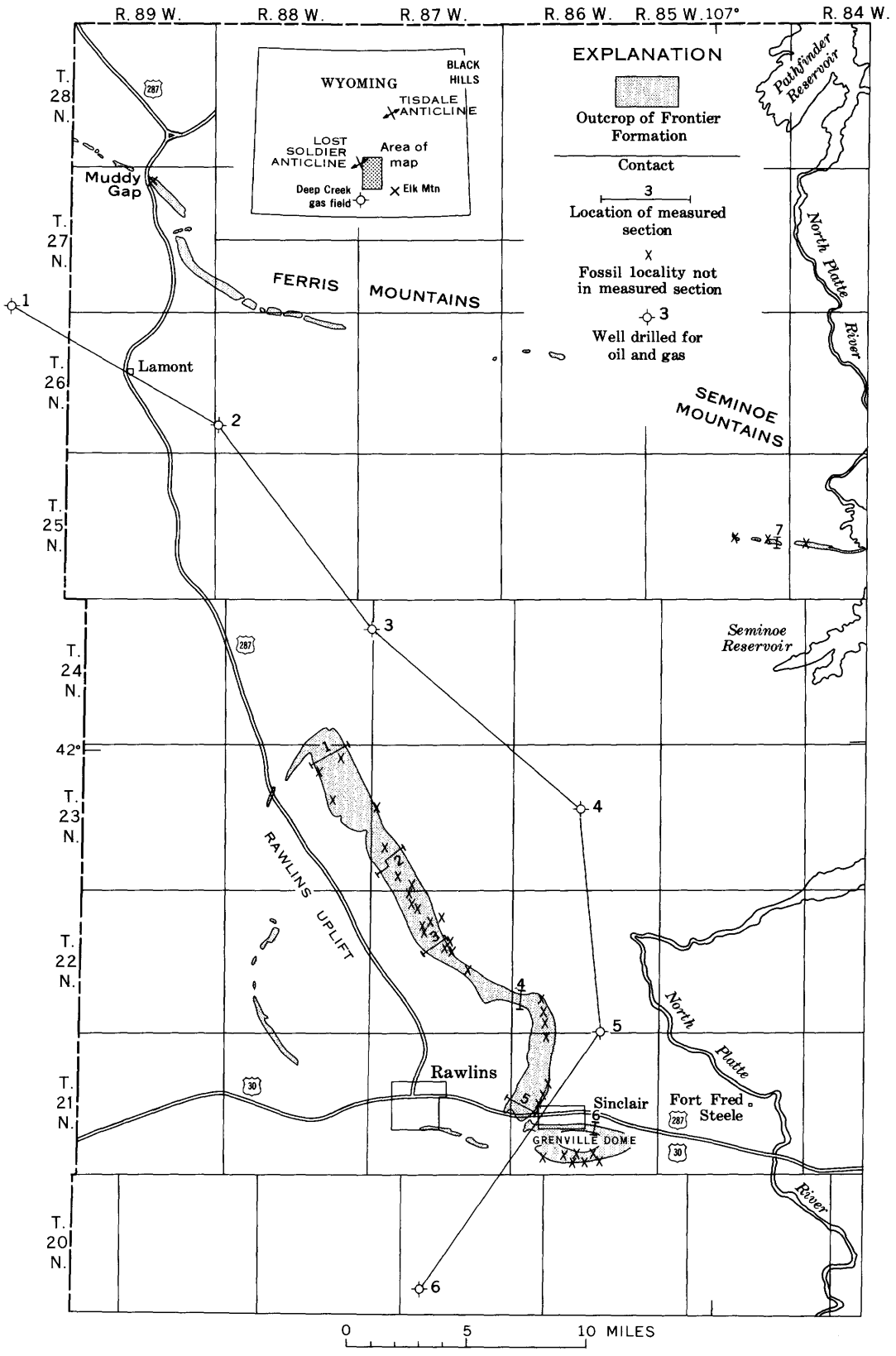

Figure 1.—Map of northwestern Carbon County, Wyo., showing outcrops of Frontier Formation, locations of measured sections, fossil localities not in measured sections, and selected wells drilled for oil and gas. From Weitz and Love (1952).

Table 1.—*Correlation of the Frontier Formation of northwestern Carbon County and Upper Cretaceous rocks of the Black Hills region, Wyoming*

Upper Cretaceous stages	Characteristic mollusks of the northern Great Plains; numbers refer to fossil collections shown on figure 2.	Northern end of Black Hills uplift		Northwestern Carbon County
Turonian	20 *Inoceramus deformis* Meek, *Inoceramus inconstans* Woods, *Scaphites preventricosus* Cobban, *Baculites mariasensis* Cobban			Unnamed noncalcareous shale
	19 *Inoceramus erectus* Meek, *Scaphites frontierensis* Cobban, *Scaphites preventricosus* Cobban, *Scaphites mariasensis* Cobban			
	18 *Inoceramus* cf. *I. problematicus* (Schlotheim), *Prionocyclus reesidei* Sidwell, *Scaphites corvensis* Cobban			
	17 *Inoceramus* cf. *I. incertus* Jimbo, *Prionocyclus quadratus* Cobban, *Scaphites corvensis* Cobban	Carlile Shale	Sage Breaks Member	Wall Creek Sandstone Member
	16 *Inoceramus perplexus* Whitfield, *Inoceramus lamarcki* Woods, *Scaphites nigricollensis* Cobban		Turner Sandy Member	
	15 *Inoceramus perplexus* Whitfield, *Scaphites whitfieldi* Cobban, *Prionocyclus wyomingensis elegans* Haas			
	14 *Inoceramus perplexus* Whitfield, *Scaphites ferronensis* Cobban, *Prionocyclus wyomingensis* Meek			
	13 *Inoceramus dimidius* White, *Scaphites warreni* Meek and Hayden, *Prionocyclus macombi* Meek		?	
	12 *Inoceramus howelli* White, *Scaphites carlilensis* Morrow, *Prionocyclus hyatti* (Stanton)		Pool Creek Shale Member	Unnamed member
	11 *Inoceramus cuvieri* Sowerby, *Collignoniceras woollgari* (Mantell), *Scaphites larvaeformis* Meek and Hayden			
	10 *Inoceramus labiatus* (Schlotheim), *Mammites nodosoides* (Schlotheim)	Greenhorn Formation	Chiefly limestone equivalent to Bridge Creek Limestone Member	Frontier Formation
	9 *Inoceramus labiatus* (Schlotheim), *Vascoceras stantoni* Reeside			
Cenomanian	8 *Inoceramus pictus* Sowerby, *Sciponoceras gracile* (Shumard), *Metoicoceras whitei* Hyatt, *Allocrioceras annulatum* (Shumard)			
	7 *Dunveganoceras albertense* (Warren), *Dunveganoceras conditum* Haas, *Metoicoceras muelleri* Cobban, *Metoicoceras defordi* Young		Chiefly shale equivalent to Hartland Shale Member	
	6 *Inoceramus pictus* Sowerby (early flat form), *Dunveganoceras pondi* Haas, *Calyoceras? canitaurinum* Haas		Chiefly limestone equivalent to Lincoln Limestone Member	
	5 *Inoceramus pictus* Sowerby (early flat form), *Plesiacanthoceras wyomingense* (Reagan)	Belle Fourche Shale		Belle Fourche Shale Member
	4 *Inoceramus rutherfordi* Warren, *Ostrea beloiti* Logan, *Acanthoceras amphibolum* Morrow			
	3 *Inoceramus arvanus* Stephenson, *Ostrea beloiti* Logan, *Acanthoceras alvaradoense* Stephenson			
	2 *Inoceramus dunveganensis* McLearn, *Acanthoceras* aff. *A. pepperense* Moreman			
	1 *Inoceramus dunveganensis* McLearn, *Calycoceras leonense* (Adkins), *Acanthoceras* spp.			
	No molluscan fossil record			

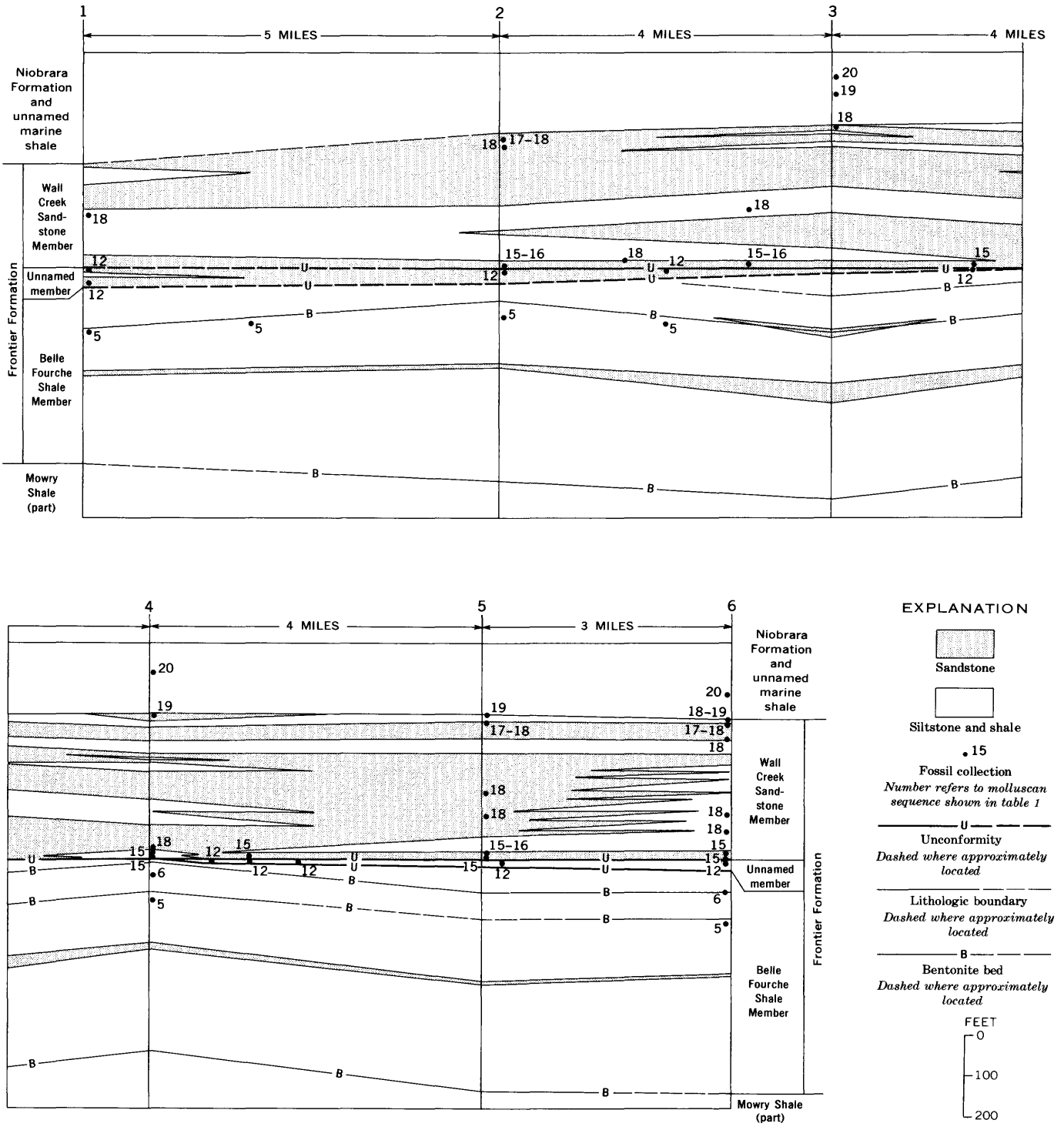

Figure 2.–Stratigraphic diagram showing intertonguing relations and unconformities in the Frontier Formation in outcrops along the northeastern flank of the Rawlins uplift. Location of sections shown on figure 1.

approximately parallel to the axis of the Rawlins uplift (fig. 3), the thickness penetrated by wells decreases southward from about 830 feet at well 3 to about 725 feet at well 6. Southeast of the report area, near Elk Mountain, the formation in the subsurface has thinned to 500–600 feet; south of the report area, at the Deep Creek gas field, it is as thin as 500 feet.

BELLE FOURCHE SHALE MEMBER

The name of the basal member of the Frontier Formation in this area as herein assigned is the Belle Fourche Shale Member. The name comes from the Belle Fourche River in northeastern Wyoming (Collier, 1922, p. 83) and has been applied in Montana and in Wyoming to rocks of similar lithology and age as a member of the Cody Shale (Knechtel and Patterson, 1956, p. 17–21), as a member of the Colorado Shale (Schmidt and others, 1964), and as a formation (Reeside, 1944). In northwestern Carbon County the Belle Fourche generally underlies long narrow valleys and is poorly exposed.

On the Rawlins uplift the Belle Fourche Shale Member is about 425–475 feet thick and consists of about 60 percent shale, 35 percent siltstone, and 5 percent sandstone and bentonite. The shale is dark gray, soft, and partly silty; in the lower 80 feet of the member the shale contains brownish-gray to dark-bluish-gray ironstone concretions, and in the upper 150 feet it contains brownish-gray calcareous concretions which are partly septarian and commonly fossiliferous. The siltstone in the member is medium gray to dark gray to dark olive gray, and clayey to sandy. In the upper part of the member the siltstone contains brownish-gray calcareous concretions. On the Rawlins uplift, Grenville dome, and along the Seminoe Mountains a thin ridge-forming sandstone is present near the middle of the member. The sandstone is medium gray to light brownish gray, very fine to fine grained, silty, irregular bedded, platy to flaggy, and contains burrows. Beds of bentonite, mostly less than 1 foot thick, are abundant in the lower and upper parts of the member.

The thinning of the Frontier toward the south is mostly the result of depositional thinning of the Belle Fourche Shale Member. The thickness of the member as determined from well logs (uncorrected for dip) decreases from about 855 feet (well 1, figs. 1, 3) to about 420 feet (well 6). On the southern flank of the Seminoe Mountains the Belle Fourche Member is 600 feet thick, and at outcrops on the Rawlins uplift (fig. 2, sections 1, 2, and 4) it is 425–475 feet thick.

Marine invertebrate fossils were collected from only the upper part of the Belle Fourche Member (fig. 2). The fossils, of Cenomanian age, are restricted to zones 4 through 7 (table 1) and include species characteristic of the upper part of the Belle Fourche Shale and the basal part of the Greenhorn Formation in the Black Hills region. In northwestern Carbon County the oldest fossils were collected from the sandstone in the middle of the Belle Fourche Member and are probably from the zone of *Acanthoceras amphibolum* (zone 4).

Fossils and distinctive beds in the upper part of the Belle Fourche Member provide evidence that the top of the member is an erosional surface. The most easily recognized bed is a dark-gray silty shale or siltstone which underlies a bed of bentonite and contains abundant brownish-gray fossiliferous concretions and small black chert pebbles. Fossils in the concretions are from the zone of *Plesiacanthoceras wyomingense* (zone 5). The thickness of the Belle Fourche strata overlying the bentonite varies locally—it is 100 feet at section 1 (W. A. Cobban and J. B. Reeside, Jr., unpub. data; Dobbin and others, 1928, p. 183), about 40 feet at section 2, as much as 140 feet at section 3, about 75 feet at section 4, and about 120 feet at section 6 (Cobban and Reeside, 1951, p. 60–62). These strata also contain fossils at a few localities. On the southwestern flank of the Ferris Mountains near Muddy Gap (NW¼SW¼ sec. 3, T. 27 N., R. 89 W.), fossils representing the zone of *Dunveganoceras conditum* and *D. albertense* (zone 7) were found about 50 feet below the top of the Belle Fourche Member. On the Rawlins uplift along section 4, older fossils, from the zone of *Dunveganoceras pondi* (zone 6), were obtained from concretions about 35 feet below the top of the member. *D. pondi* was also found on the Grenville dome (section 6) in concretions about 50 feet below the top of the member.

UNNAMED MIDDLE MEMBER

The unnamed middle member of the Frontier is a thin sequence of marine sandstone, siltstone, and shale of early Carlile age, which unconformably overlies the Belle Fourche Shale Member and separates the upper and lower unconformities. At one locality (section 5) the basal bed is a thin fine- to coarse-grained sandstone which contains small black chert pebbles and fish teeth.

On the southern flank of the Seminoe Mountains the unnamed middle member consists of brownish-gray carbonaceous unfossiliferous siltstone and shale about 10 feet thick. The lower and upper contacts are sharp. These rocks are not fossiliferous but are underlain by fossil-bearing marine shale of the Belle Fourche Member and overlain by fossil-bearing marine sandstone of the Wall Creek Member. On the Rawlins uplift at sections 1, 2, and 3, the member is mainly sandstone which pinches out southward between sections 3 and 4. At section 1 the member is mostly flaggy to slabby very fine grained sandstone at least 40 feet thick and contains marine fossils of early Carlile age. The upper contact has not been precisely located. The member at section 2 consists of about 38 feet of silty very fine grained sandstone. It overlies a thick sandy siltstone in the Belle Fourche Member and underlies a fossiliferous sandstone in the Wall Creek Member. At section 3 the member consists of about 11 feet of friable very fine grained sandstone; it unconformably overlies a sandy siltstone and sharply underlies a well-cemented sandstone.

The unnamed middle member has been removed by erosion at section 4, and there the Belle Fourche Member is

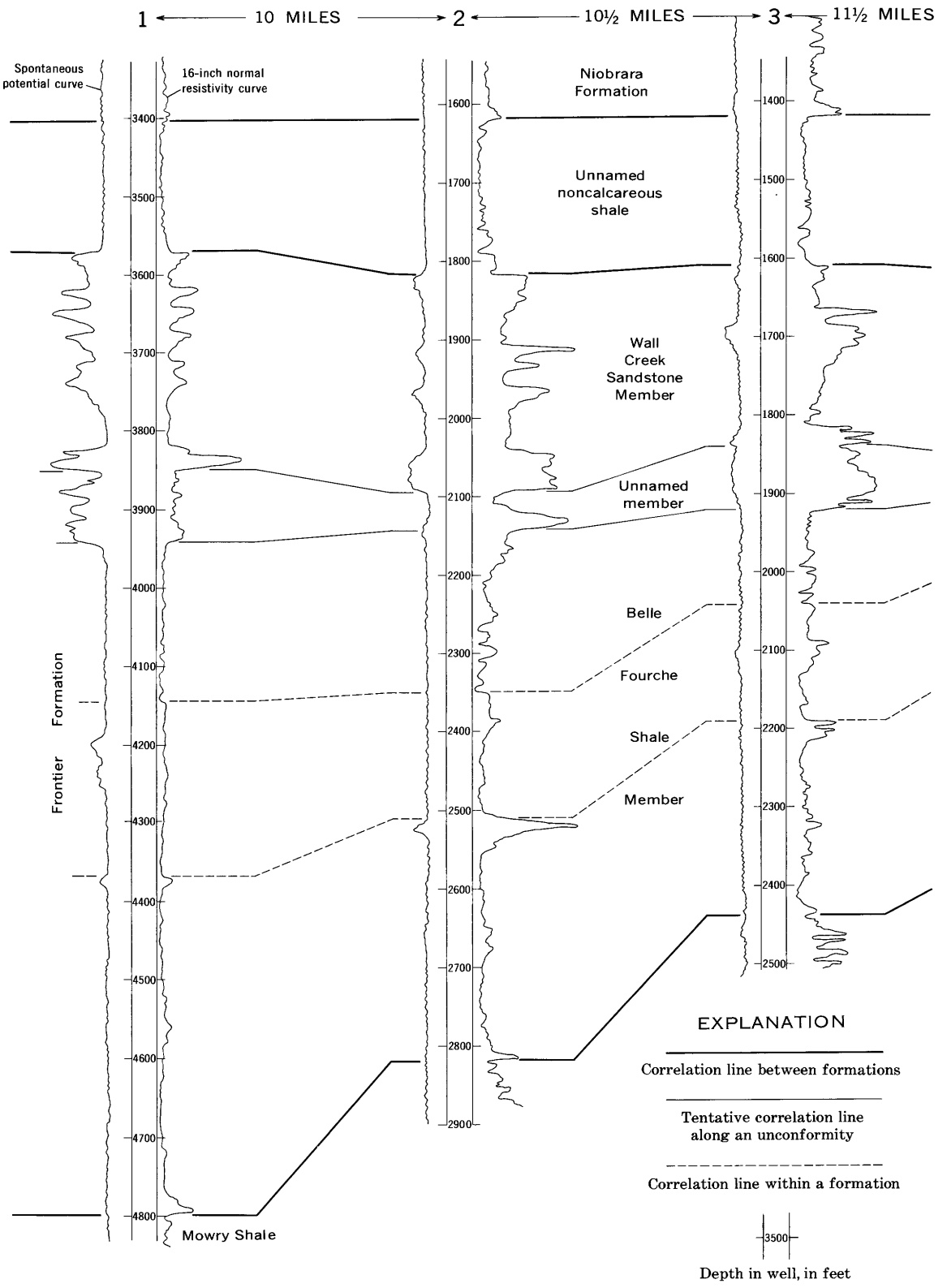
1
10 MILES
2
10½ MILES
3
11½ MILES
Spontaneous potential curve
16-inch normal resistivity curve
Niobrara Formation
Unnamed noncalcareous shale
Wall Creek Sandstone Member
Unnamed member
Belle Fourche Shale Member
Frontier Formation
Mowry Shale
3400
3500
3600
3700
3800
3900
4000
4100
4200
4300
4400
4500
4600
4700
4800
1600
1700
1800
1900
2000
2100
2200
2300
2400
2500
2600
2700
2800
2900
1400
1500
1600
1700
1800
1900
2000
2100
2200
2300
2400
2500
EXPLANATION
Correlation line between formations
Tentative correlation line along an unconformity
Correlation line within a formation
3500
Depth in well, in feet

Figure 3.

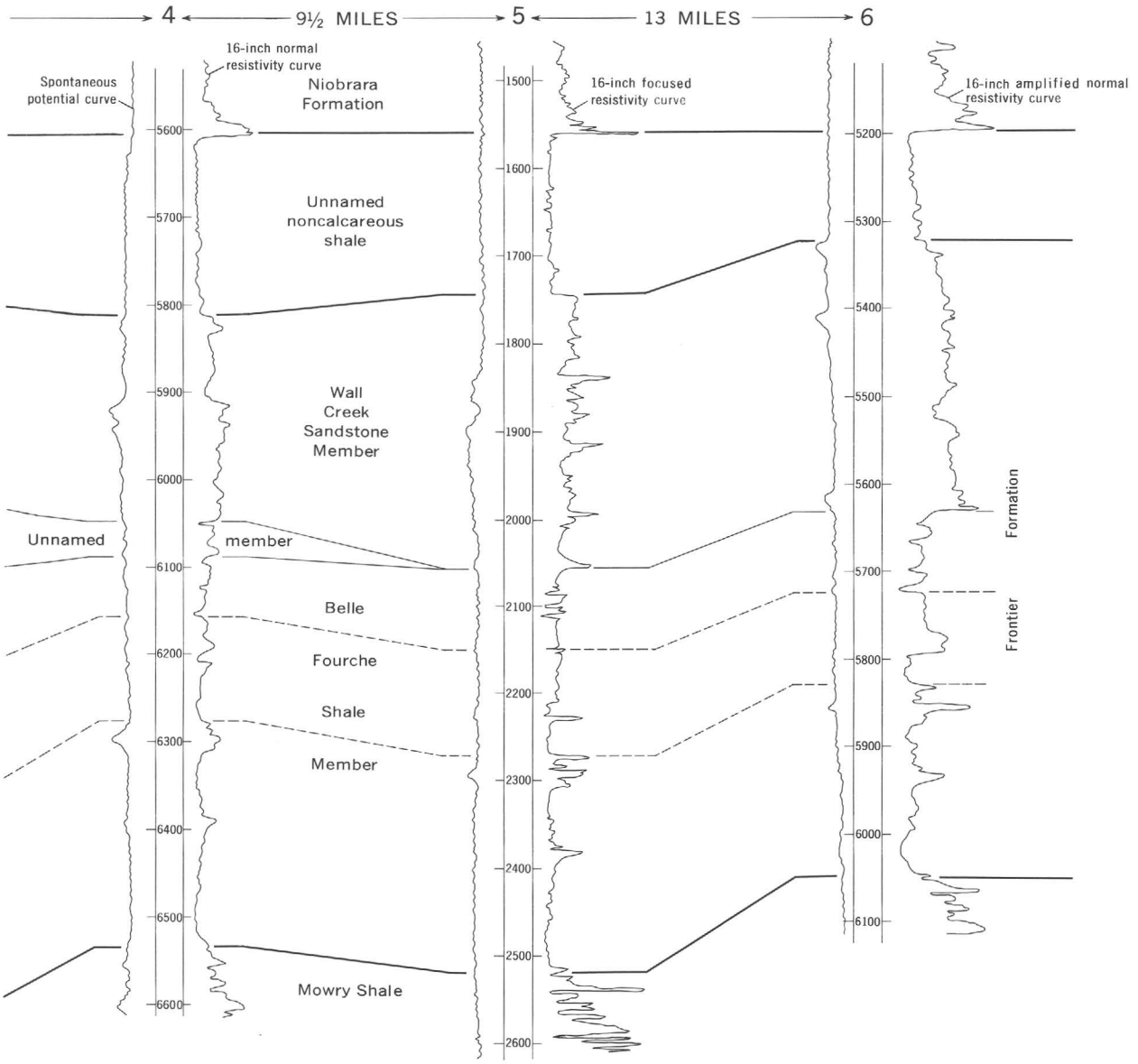

WELL	OPERATOR	NAME AND NUMBER	LOCATION		
			SEC.	T. N.	R. W.
1	Deep Rock Oil Co	Federal Lands "A" 1-x	34	27	90
2	Superior Oil Co	Government 27-30	30	26	88
3	Amax Petroleum Corp	Government-Rosen 12-1	12	24	88
4	Superior Oil Co	Haystack Unit 33-16	16	23	86
5	Colorado Oil and Gas Corp	Government 1	34	22	86
6	Sun Oil Co	Government Grindstone 1	30	20	87

Figure 3.—Electric logs showing correlation of beds in the Frontier Formation in northwestern Carbon County. Location of wells shown on figure 1.

unconformably overlain by the Wall Creek Sandstone Member. The unnamed middle member, siltstone in section 5 and shale in section 6, thickens southward from a featheredge between sections 4 and 5 to 17 feet at section 5 and 26 feet at section 6. At section 5 the base of the member consists of a 6-inch-thick well-cemented fine- to coarse-grained sandstone that contains scattered fish teeth and small black chert pebbles. The shale at section 6 is dark gray, sandy, and massive, and contains fossiliferous septarian sandy limestone concretions.

Where tentatively identified on well logs (fig. 3), the unnamed middle member is as much as 90 feet thick in well 1 and is absent or very thin in wells 5 and 6. The thickness seems to vary locally in the subsurface. Sparse evidence from electric logs and outcrops suggests that these rocks are probably absent south and east of the report area.

Marine invertebrate fossils were collected from the unnamed middle member of the Frontier on the Rawlins uplift and Grenville dome at sections 1, 2, 5, and 6, and at localities between these sections. The fossils, of Turonian age, are typical of the lower part of the Carlile Shale. Near the Black Hills the upper part of the Pool Creek Member of the Carlile contains the same fauna. Fossils found in the member represent the zone of *Scaphites carlilensis* (zone 12). *Inoceramus howelli* of this zone is perhaps the most abundant species.

WALL CREEK SANDSTONE MEMBER

The upper one-fourth to one-half of the Frontier Formation is a sequence of mostly sandstone herein called the Wall Creek Sandstone Member. The name, originally the Wall Creek Sandstone Lentil of the Benton Shale (Wegemann, 1911, p. 43, 45), is extended to this area from the Tisdale anticline in Natrona County, Wyo. As used in this report, the Wall Creek Sandstone Member includes all the sandstone beds in the upper part of the Frontier except those in the thin unnamed middle member; it is not restricted to the uppermost sandstone bed of the formation as indicated by Wegemann.

In northwestern Carbon County, sandstone, siltstone, and shale of the Wall Creek Member form a succession of ridges and narrow valleys. The ridge-forming basal sandstone unconformably overlies softer rocks in the unnamed middle member of the Frontier. In the NW¼ sec. 32, T. 22 N., R. 86 W., and at sections 5 and 6, the lowest bed of the Wall Creek Member, a conglomeratic sandstone as much as 2 feet thick, fills shallow channels in the siltstone and shale of the unnamed member (figs. 4 and 5). Along the Rawlins uplift the Wall Creek Member is about 350 feet thick and consists of about 63 percent sandstone, 23 percent siltstone, and 14 percent shale. Most of the sandstone is light gray to brownish gray, very fine to fine grained, silty, platy to slabby, and irregularly bedded. Burrows, including *Ophiomorpha*, are abundant, and fossilifer-

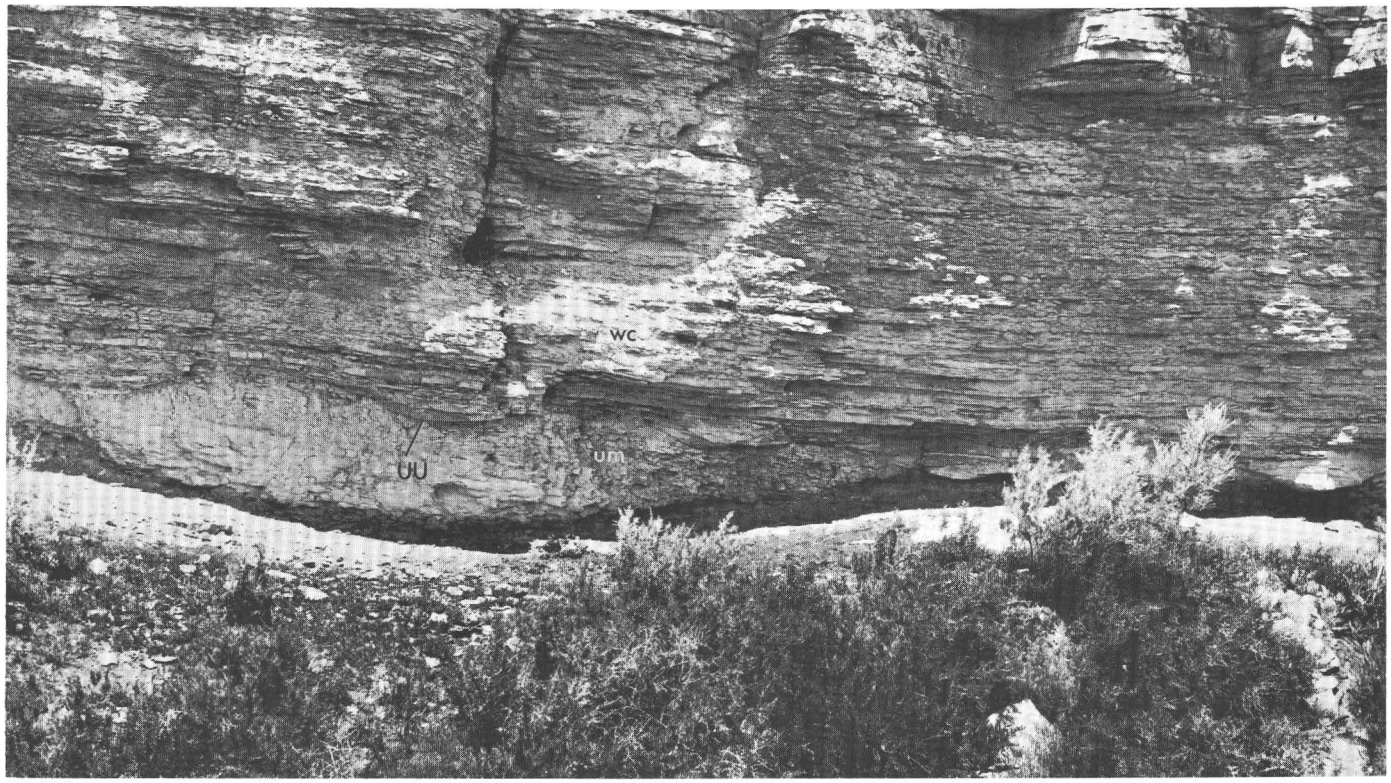

Figure 4.—Upper part of unnamed middle member (um) and basal sandstone of Wall Creek Sandstone Member (wc) in SW¼ sec. 32, T. 22 N., R. 86 W., Carbon County, Wyo. UU, upper unconformity.

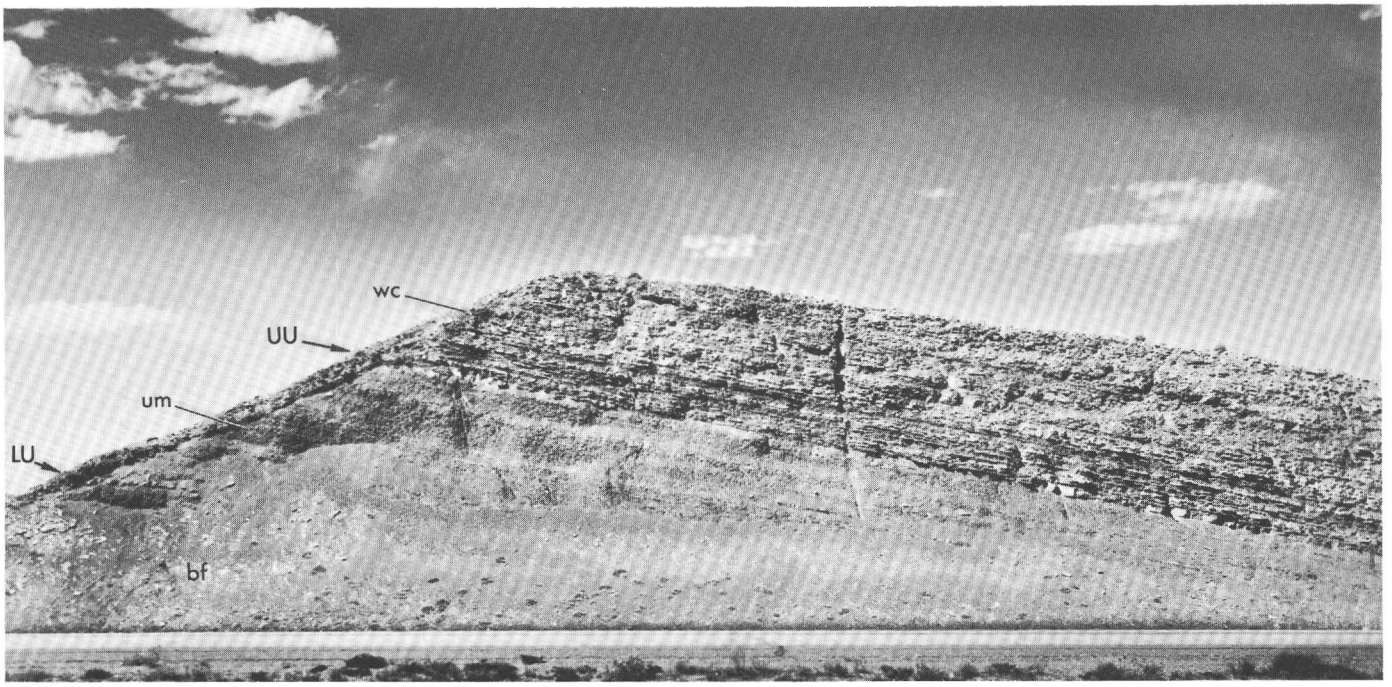

Figure 5.—Upper part of Belle Fourche Shale Member (bf), unnamed middle member (um), and basal sandstone of Wall Creek Sandstone Member (wc) in N½ sec. 19, T. 21 N., R. 86 W., Carbon County, Wyo. LU, lower unconformity; UU, upper unconformity. Basal sandstone of Wall Creek Member is 18 feet thick.

ous concretions are common. Composite sets of sandstone strata in the upper part of the member are generally very fine grained and slightly irregularly bedded at the base and fine to medium grained and crossbedded at the top. The uppermost beds of these sets commonly contain scattered coarse grains, granules, pebbles, and a few fossils. In general, the maximum grain size of sandstones in the member increases from the base to the top of the member. The contact of the member with the overlying rocks is recognized by the abrupt decrease in grain size. The siltstones are medium gray to dark gray to brownish gray, clayey to sandy, and laminated to very thin bedded. Shales are medium gray to dark gray to brownish gray, sandy and silty, and poorly indurated. They commonly contain fossiliferous yellowish-gray limestone concretions.

The thickness of the Wall Creek Sandstone Member ranges from about 230 feet at well 3 to about 350 at section 5. It seems to vary irregularly throughout the area but decreases to the east and south.

Fossils collected from these beds are late Turonian in age and represent zones 15 through 19 of table 1. Rocks of equivalent age near the Black Hills include the upper part of the Turner Sandy Member of the Carlile Shale and the overlying Sage Breaks Member. The basal beds of the Wall Creek Member are commonly sandstone and generally contain *Inoceramus perplexus* (zones 14–16); at a few localities they also contain *Scaphites whitfieldi* (zone 15). At section 4, the basal beds are concretionary siltstone. Most of the younger rocks in the member seem to have been deposited during the time of *Inoceramus* cf. *I. problematicus* (zone 18), a common species. The uppermost bed of the Wall Creek Sandstone Member generally contains *Inoceramus erectus* (zone 19) and interfingers locally with the overlying shale. At section 3 the uppermost bed contains fossils from zone 18, and the overlying shale contains *I. erectus* (zone 19).

UNCONFORMITIES

The two unconformities within the Frontier Formation were described by Cobban and Reeside (1951, p. 63; 1952, p. 1942–1946) at the Grenville dome. Recent work along the southern slopes of the Ferris Mountains (Reynolds, 1968a,b) and Seminoe Mountains (Merewether, 1972b) and on the eastern flank of the Rawlins uplift (Merewether, 1972a) provided additional evidence which supports the interpretations of Cobban and Reeside.

The lower unconformity, which separates the Belle Fourche Shale Member and the unnamed member, represents a large and widespread break in sedimentation which is difficult to identify at most outcrops. At section 5, the unconformity is at the base of a thin well-cemented sandstone which contains small chert pebbles and fish teeth (fig. 5). The youngest fossiliferous rocks below the unconformity are of early Greenhorn age, and the oldest fossiliferous rocks above the unconformity are of early Carlile age. The unconformity may encompass five or six ammonite zones. On the Rawlins uplift at sections 2 and 4 the uppermost beds of the Belle Fourche

Member are as old as the zone of *Dunveganoceras pondi* (zone 6); however, at Muddy Gap, near the Ferris Mountains, the uppermost beds may lie in the zone of *Dunveganoceras albertense* and *D. conditum* (zone 7). Fossils collected from the unnamed middle member represent the zone of *Prionocyclus hyatti* (zone 12). In the Black Hills, strata of the Greenhorn and Carlile that are equivalent to the hiatus in northwestern Carbon County are as much as 300 feet thick (Cobban and Reeside, 1951, p. 63). These strata include, in ascending order, rocks correlative with part of the Lincoln Limestone Member, part of the Hartland Shale Member, and all of the Bridge Creek Limestone Member of the Greenhorn Formation, and with part of the Pool Creek Shale Member of the Carlile Shale.

The lower hiatus may be represented by either a disconformity with moderate relief or an angular unconformity. Evidence is provided by the variation in thickness of upper Belle Fourche rocks between a distinctive bentonite and the unconformity as well as by the changes in the fauna of the uppermost Belle Fourche. If local preunconformity uplift can be inferred from the rocks at sections 3, 4, and 5 (fig. 2) on the Rawlins uplift, the unconformity is slightly angular at places.

The upper unconformity separating the unnamed middle member of the Frontier from the Wall Creek Sandstone Member can be located in most of the report area but seems to converge with the lower unconformity toward the east. The two unconformities cannot be differentiated in wells 5 and 6 (fig. 3). The upper unconformity at most places represents two fossil zones (13 and 14). It is generally underlain by rocks of early Carlile age containing *Inoceramus howelli* (zone 12) and is overlain by sandstone of late Carlile age containing *I. perplexus* and *Scaphites whitfieldi* (zone 15). The basal bed of the Wall Creek Member is a thin fossiliferous sandstone containing small chert pebbles and fish teeth and filling shallow channels in the upper surface of the unnamed middle member in the SW¼ sec. 32, T. 22 N., R. 86 W. (fig. 4), and at sections 5 (fig. 5) and 6. Rocks of the Black Hills region that represent the upper unconformity of northwestern Carbon County probably include the uppermost part of the Pool Creek Member and the lower part of the Turner Sandy Member of the Carlile Shale. These strata are as much as 100 feet thick (Cobban and Reeside, 1951, p. 63).

The upper unconformity is a disconformity in most of the report area. At all localities the underlying middle member contains the same fossils (zone 12), and the basal part of the overlying Wall Creek Member contains one fauna (zone 15). However, at section 4 on the Rawlins uplift the sequence is slightly different. Here the middle member of the Frontier is missing and the unconformity is between the Belle Fourche and Wall Creek Members. At this locality, eight zones are missing (zones 7–14). The uppermost part of the Belle Fourche Member is probably represented by the zone of *Dunveganoceras pondi* (zone 6). The basal beds of the Wall Creek Member contain the usual fossils (zone 15) but are composed of siltstone instead of sandstone.

Section 4 was measured near the crest of a small west-trending anticline which appears to be better developed in the formations underlying the Frontier than in the Frontier and the overlying formations. The thinning of the upper part of the Belle Fourche Member, the absence of the middle member, the convergence of the two unconformities, and the lithologic difference in the basal part of the Wall Creek Member at this locality may be the result of local folding and erosion during deposition of the Frontier.

REFERENCES

Berry, D. W., 1960, Geology and ground-water resources of the Rawlins area, Carbon County, Wyoming: U.S. Geol. Survey Water-Supply Paper 1458, 74 p.

Cobban, W. A., and Reeside, J. B., Jr., 1951, Frontier formation near Sinclair, Carbon County, Wyoming, *in* Wyoming Geol. Assoc. Guidebook 6th Ann. Field Conf., south-central Wyoming: p. 60–65.

—— 1952, Frontier formation, Wyoming and adjacent areas: Am. Assoc. Petroleum Geologists Bull., v. 36, no. 10, p. 1913–1961.

Collier, A. J., 1922, The Osage oil field, Weston County, Wyoming: U.S. Geol. Survey Bull. 736-D, p. 71–110.

Dobbin, C. E., Hoots, H. W., and Dane, C. H., 1928, Geology and oil and gas possibilities of the Bell Springs district, Carbon County, Wyoming: U.S. Geol. Survey Bull. 796-D, p. 171–197.

Fath, A. E., and Moulton, G. F., 1924, Oil and gas fields of the Lost Soldier-Ferris district, Wyoming: U.S. Geol. Survey Bull. 756, 55 p.

Knechtel, M. M., and Patterson, S. H., 1956, Bentonite deposits in marine Cretaceous formations of the Hardin district, Montana and Wyoming: U.S. Geol. Survey Bull. 1023, 116 p.

Merewether, E. A., 1972a, Geologic map of the Rawlins NW quadrangle, Carbon County, Wyoming: U.S. Geol. Survey Geol. Quad. Map GQ-1010.

—— 1972b, Geologic map of the Seminoe Dam SW quadrangle, Carbon County, Wyoming: U.S. Geol. Survey Geol. Quad. Map GQ-1017.

Reeside, J. B., Jr., 1944, Maps showing thickness and general character of the Cretaceous deposits in the western interior of the United States: U.S. Geol. Survey Oil and Gas Inv. Prelim. Map 10.

Reynolds, M. W., 1968a, Geologic map of the Muddy Gap quadrangle, Carbon County, Wyoming: U.S. Geol. Survey Geol. Quad. Map GQ-771.

—— 1968b, Geologic map of the Whiskey Peak quadrangle, Carbon, Fremont, and Sweetwater Counties, Wyoming: U.S. Geol. Survey Geol. Quad. Map GQ-772.

Schmidt, R. G., Pecora, W. T., and Hearn, B. C., Jr., 1964, Geology of the Cleveland quadrangle, Bearpaw Mountains, Blaine County, Montana: U.S. Geol. Survey Bull. 1141-P, p. P1–P26.

Wegemann, C. H., 1911, The Salt Creek oil field, Wyoming, *in* The Lander and Salt Creek oil fields, Wyoming: U.S. Geol. Survey Bull. 452, p. 37–83.

Weitz, J. L., and Love, J. D., 1952, Geologic map of Carbon County, Wyoming: U.S. Geol. Survey.

Wyoming Oil and Gas Conservation Commission, [1971?], Wyoming oil and gas statistics 1970: Casper, Wyo., 89 p.

ELEMENTAL SULFUR EXTRACTED FROM RECENT SEDIMENTS—INDIGENOUS OR ARTIFICIALLY PRODUCED

By JAMES G. PALACAS and ALONZA H. LOVE, Denver, Colo.

Abstract.—Elemental (free) sulfur is present in most unconsolidated recent marine sediments. Accurate determinations of in situ free sulfur, however, are critically dependent upon careful field and laboratory treatment of sediment samples. For example, air-dried samples of quartzose sands and silty muds collected from Choctawhatchee Bay, Fla., yielded an average of about three times more benzene-extractable free sulfur than did freeze-dried samples. The increase in free sulfur is caused by oxidation chiefly of unstable FeS.

During the study of benzene-soluble organic substances in the bottom sediments of Choctawhatchee Bay, Fla. (fig. 1), rather large amounts of yellow crystalline substances were obtained—as much as 94 percent of the benzene extracts (Palacas and others, 1968). Microscopic examination and X-ray diffraction analysis showed that these crystals were composed of free sulfur. Because of the variable but large amount of free sulfur in the extracts we suspected that perhaps some, if not most, of the free sulfur was formed during field handling and laboratory preparation of the samples. Evidence for such a suspicion was the observation that dark-gray to black-stained quartz sand, collected in the shoaly areas of the bay, dramatically turned light gray after several hours of exposure to air. We interpreted that the black material was, in part, some form of unstable iron sulfide, which upon oxidation was altered to iron oxide and free sulfur. This interpretation was supported by the work of previous investigators, such as Berner (1962; 1967, p. 271), who warned about the possible formation of free sulfur by air oxidation of unstable FeS (hydrotroilite), and by the recent laboratory studies of Prokopovich, Cole, and Nishi (1971). To determine the actual amounts of free sulfur that formed, through exposure to air, in sediment samples that had been removed from their original habitat the various field and laboratory experiments reported herein were conducted.

Acknowledgments.—We thank Dr. R. A. Berner, Yale University, for his review of the paper. We also thank A. J. Gude III, who provided the X-ray diffraction analyses on free sulfur; T. G. Ging, Jr., who freeze dried all the samples; and R. D. McIver, Esso Production Research Co., who provided the copper-amalgam method.

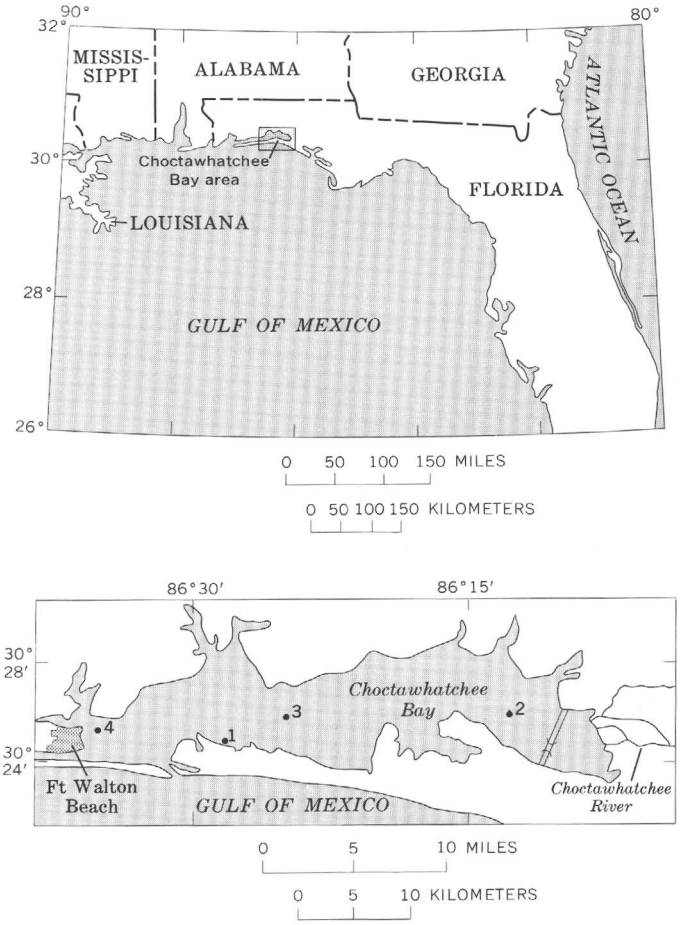

Figure 1.—Maps showing location of Choctawhatchee Bay, Fla., and the four sites in the bay where samples were collected.

FIELD AND LABORATORY METHODS

Two large samples of black-stained sand were collected in water 0.6 m deep in Choctawhatchee Bay at locality 1 (fig. 1). Here, the surface veneer of sand, about 1 cm thick, is oxidized white to very light gray and is underlain by discontinuous lenses or patches of very dark gray sand to a depth of at least 1.2 m. The dark-colored sand was sampled by repeatedly

U.S. GEOL. SURVEY PROF. PAPER 800-D, PAGES D67-D69

pushing a plastic tube, 5 cm in diameter, into the bottom sediment over an area of about 100 sq m, and manually extruding only the dark-stained sand into polyethylene bags. The sand-filled bags were immediately sealed and frozen in a box containing dry ice. The samples were kept frozen until analyzed. For comparative purposes, three mud samples were collected (locs. 2, 3, and 4, fig. 1) with a clamshell grab sampler from water depths of 3–10 m, and were similarly frozen.

In the laboratory, each frozen sample was split into two parts—one part was air dried for about 2 to 3 days in a forced-air oven at a temperature of 40°C, and the other part was freeze dried. Because the mud samples "caked" during air drying they were ground to a size of 0.13 mm or less (115 mesh size) in order to approximate the particle size of the freeze-dried sediment.

Sediment samples were extracted by shaking the sample, at room temperature, in redistilled benzene initially for 24 hours followed by three additional half-hour shakings, using 4 ml of solvent for 1 g of sample. The benzene solutions were combined and concentrated by rotoevaporation at 35°C, evaporated to dryness under a stream of dry nitrogen, and the extract was brought to constant weight. The extract was then redissolved in benzene, placed on a copper-amalgam column, and eluted with benzene (the sulfur in solution reacts with and is trapped in the copper amalgam). The amount of sulfur is determined by evaporating the eluate to dryness, weighing the residue to constant weight, and subtracting its weight from the weight of the original benzene extract.

The assumption is made that most, if not all, of the sulfur that reacts with the copper amalgam is free sulfur. However, any sulfur-containing substances solubilized by benzene would also react with the amalgam and would contribute to the total free sulfur content. Among these soluble substances are the organic sulfur compounds, but they are probably very sparse. The remaining sulfur-bearing substances are predominantly in the form of sulfate-sulfur compounds and iron sulfides, such as pyrite (Kaplan and others, 1963), which are virtually insoluble in benzene.

RESULTS AND DISCUSSION

The results of the experiment (table 1) show that all the air-dried or oxidized samples yielded more free sulfur than did the freeze-dried or nonoxidized samples. In both the sands and muds the oxidized samples produced 1.7 to 4.6 or an average of about 3 times more free sulfur than did the freeze-dried samples.

Because of the conditions of the experiment, the additional free sulfur produced during air drying must be due to oxidation of unstable or reactive sulfur compounds, most likely unstable FeS (commonly referred to as hydrotroilite), and also to oxidation of H_2S or HS^- (Berner, 1962, 1967). The possibility that H_2S is also a source for some of the free sulfur is indicated by the fact that most of the muds and even some of the sands give off an H_2S odor.

In the sedimentary sulfides (unstable FeS, H_2S, or HS^-), sulfur, according to the belief of most investigators, is predominantly derived from the bacterial reduction of sulfate sulfur dissolved in the overlying and interstitial waters. Most free sulfur extracted from freeze-dried sediment, however, is believed to be derived from in situ inorganic chemical oxidation of sedimentary sulfides, although some may also be a product of aerobic or photosynthetic sulfur-oxidizing bacteria (Berner, 1967).

Sulfur isotope analyses were also made on free sulfur crystals in the hope that some diagnostic evidence could be obtained to determine which mechanism—bacterial or inorganic—was responsible for the formation of in situ free sulfur. Published data suggest that little or no isotopic

Table 1.—*Sulfur and carbon in bottom sediments of Choctawhatchee Bay, Fla.*

[All analyses reported on dry-weight basis. Organic carbon and total sulfur analyses by I. C. Frost]

Sample No.	Sediment type	Depth of water (meters)	Drying method[1]	Dried sample weight (grams)	Organic carbon (percent)	Total sulfur (percent)	Free sulfur (percent)	Free sulfur (ratio AD/FD[1])
1a	Clean quartz sand.	0.6	AD	2,100	0.12	0.03	0.0050	3.1
			FD	966	.12	.04	.0016	
1b	..do...	.6	AD	1,550	.10	.05	.0039	3.0
			FD	1,750	.08	.04	.0013	
2	Silty mud.	3.4	AD	535	2.63	2.04	.0078	4.6
			FD	385	2.86	2.02	.0017	
3	..do...	8.5	AD	120	3.53	1.72	.0300	2.2
			FD	120	3.38	1.73	.0135	
4	Clayey mud.	10.1	AD	270	5.56	2.19	.0813	1.7
			FD	315	5.44	1.98	.0488	

[1] AD, air dried; FD, freeze dried.

fractionation occurs during inorganic oxidation of sulfides to sulfur (Nissenbaum and Rafter, 1967), but significant fractionation (S^{34} of −6 per mil) can occur during bacterial oxidation of sulfides (Schoen and Rye, 1970).

Most of the air-dried free sulfur, which was formed artificially in the laboratory, is assumed to have been produced by inorganic means. Consequently, any significant deviations observed in the isotopic ratios for the freeze-dried or in situ free sulfur could be attributed to bacterial processes. Free sulfur crystals were isolated by fractional crystallization from the benzene extracts in separate experiments and then analyzed isotopically by Jan Monster, McMaster Univ., Hamilton, Ontario. The analyses showed that the average δS^{34} value for air-dried sulfur was $-24.0^{\circ}/_{oo}$ (per mil) (range -23.2 to $-24.7^{\circ}/_{oo}$) and for freeze-dried sulfur, $-24.4^{\circ}/_{oo}$ (range -24.2 to $24.6^{\circ}/_{oo}$). As indicated, the isotope data failed to show any significant differences between the two types of sulfur and hence no definite conclusions were warranted. Major isotopic fractionations were observed, however, between free sulfur and sulfate sulfur which was collected from the interstitial waters of the sediments. The average δS^{34} for sulfate sulfur was $+22.4^{\circ}/_{oo}$, and the total fractionation between sulfate sulfur and free sulfur was slightly greater than $46^{\circ}/_{oo}$. All data are relative to the δS^{34} value for the standard Canyon Diablo troilite.

Besides the effects of field and laboratory handling of sediment samples, the kind of solvent and method of extraction also affect the amount of free sulfur extracted. For example, analysis of a representative mud sample from Choctawhatchee Bay (A. H. Love and J. G. Palacas, unpub. data) indicated that a solvent mixture of benzene-methanol (3:1, v/v) extracted nearly twice as much free sulfur as did pure benzene. Certainly, different single solvents such as chloroform, acetone, and carbon disulfide would also extract different amounts of sulfur. Also, comparison of two benzene extraction methods, Soxhlet versus shaking, showed that the Soxhlet method removed about twice as much free sulfur as did the shaking method (Love and Palacas, unpub. data).

Treatment of sediment samples with acid before solvent extraction may also profoundly affect the amount of free sulfur extracted. Berner (1964) reported that samples of bottom sediment from the Gulf of California, when leached with hot HCl prior to acetone extraction, yielded at least eight times more free sulfur than did samples not treated with HCl.

In a very recent study, Berner (1972) confirmed the fact that extraction after acidification of sediment samples results in larger values for elemental sulfur. In this study, he attributed the formation of part of the free sulfur to the oxidation of H_2S by Fe^{+3}. Both H_2S and Fe^{+3} are liberated during the acidification treatment—H_2S from the unstable iron monosulfides and Fe^{+3} from other iron-bearing minerals.

Although free sulfur is a minor constituent in recent sediments and commonly makes up only a few percent of the total sulfur content, the amounts and distribution of free sulfur are a clear indicator of early diagenesis (Palacas and others, 1968; Swanson and others, 1972). Therefore, knowledge of the formation and subsequent fate of free sulfur in the sedimentary cycle should be an aid in better understanding the formation of metal sulfides, complex organic sulfur substances, and possibly free sulfur deposits.

The results of this study show quantitatively the effects of oxidation, and clearly indicate that accurate measurements of in situ free sulfur require extraordinary caution in the field collection and the laboratory treatment of sediment samples. The samples must not be exposed to air but must be kept always under nonoxidizing conditions. Furthermore, as other published data have shown, to prevent formation of free sulfur artifacts, acid treatment of sediment samples prior to solvent extraction must be avoided.

REFERENCES

Berner, R. A., 1962, Tetragonal iron sulfide: Science, v. 137, no. 3531, p. 669.

—— 1964, Distribution and diagenesis of sulfur in some sediments from the Gulf of California: Marine Geology, v. 1, p. 117–140.

—— 1967, Diagenesis of iron sulfide in recent marine sediments, p. 268–272, *in* Lauff, G. H., ed., Estuaries: Am. Assoc. Adv. Sci. Pub. 83, 757 p.

—— 1972, Iron sulfides in the Pleistocene deep Black Sea sediments and their paleo-oceanographic significance, *in* The Black Sea: Am. Assoc. Petroleum Geologists Mem. [In press]

Kaplan, I. R., Emery, K. O., and Rittenberg, S. C., 1963, The distribution and isotopic abundance of sulphur in recent marine sediments off southern California: Geochim. et Cosmochim. Acta, v. 27, no. 4, p. 297–331.

Nissenbaum, Arie, and Rafter, T. A., 1967, Sulfur isotopes in altered pyrite concretions from Israel: Jour. Sed. Petrology, v. 37, no. 3, p. 961–962.

Palacas, J. G., Swanson, V. E., and Love, A. H., 1968, Organic geochemistry of Recent sediments in the Choctawatchee Bay area, Florida—A preliminary report, *in* Geological Survey Research 1968: U.S. Geol. Survey Prof. Paper 600-C, p. C97–C106.

Prokopovich, N. P., Cole, R. C., and Nishi, C. K., 1971, Alteration of sediments by natural gases in western Merced County, California: Am. Assoc. Petroleum Geologists Bull., v. 55, no. 6, p. 826–832.

Schoen, Robert, and Rye, R. O., 1970, Sulfur isotope distribution in solfataras, Yellowstone National Park: Science, v. 170, no. 3962, p. 1082–1084.

Swanson, V. E., Love, A. H., and Frost, I. C., 1972, Geochemistry and diagenesis of tidal-marsh sediment, northeastern Gulf of Mexico: U.S. Geol. Survey Bull. 1360, 83 p.

POSSIBLE ECONOMIC VALUE OF TRONA-LEONARDITE MIXTURES

By VERNON E. SWANSON and TOM G. GING, Denver, Colo.

Abstract.—Experiments indicate that simple addition of water to mixtures of untreated trona and otherwise insoluble leonardite yields a rich, black, slightly alkaline solution of concentrated humic substances. Prices of both trona ($Na_2CO_3 \cdot NaHCO_3 \cdot 2H_2O$) from Wyoming and leonardite (naturally oxidized coal) from South Dakota and Wyoming are very similar, \$10–\$30 per ton. The dissolved mixture could be used, for example, as a liquid soil conditioner or leaf spray-micronutrient fertilizer with desired chelate-elements added, or as a leach solution for secondary recovery of ore metals or for capture of toxic metals from industrial wastes.

Leonardite is the term commonly given to naturally weathered, oxidized coal that is readily soluble in slightly alkaline water (Fowkes and Frost, 1960; Freeman and Fowkes, 1968). Several tens of thousands of tons of leonardite is produced annually in North Dakota and Wyoming from Tertiary lignite and Upper Cretaceous subbituminous coal, mainly for use as a drilling-mud additive, as a base for soil conditioners or micronutrient fertilizers, or as an organic, combustible binder for taconite-iron ore. The characteristics of value in these uses of leonardite are its water solubility and its hydrophyllic and metal-sorptive properties.

Trona, a saline mineral with the composition $Na_2CO_3 \cdot NaHCO_3 \cdot 2H_2O$, exists in huge bedded deposits in the Eocene Green River Formation of southwestern Wyoming (Culbertson, 1966). Nearly 4 million tons of trona is mined annually in Wyoming, mainly for production of soda ash that is used in the manufacture of glass, paper, and detergents, and also in many processes of the chemical and petroleum industries.

Both leonardite and trona are cheaply produced in great quantities, with prices of each in the range of \$10–\$30 per ton.

The amount of leonardite that is readily soluble in ordinary water is variable, but it is generally less than 5 percent. If the water is made slightly alkaline, however, the amount that is readily soluble increases greatly, to as much as 90 percent of the raw leonardite. Generally, relatively expensive chemicals such as ammonia or sodium hydroxide are added to the water to increase alkalinity for leonardite solubilization. Such chemicals can be dangerous and difficult to handle, and these drawbacks have limited some of the uses of leonardite, but we suggest here that these limiting factors can be overcome by crude mixtures of trona and leonardite. Addition of available water to the mixture yields a rich black solution of sodium-humic substances that may be adapted or processed for a variety of additional uses.

With this possibility for potentially increased use of leonardite, a series of experiments was run to establish the controlling factors on the relative amounts of trona and leonardite needed to result in maximum solubility of leonardite and optimum pH values.

SOURCE OF SAMPLE MATERIAL

Some 55 samples of weathered lignite and subbituminous coal containing leonardite were collected in 1968 and 1969 in North Dakota and Wyoming. Many of these samples were subsequently analyzed to determine solubility in distilled and alkaline water, and to determine the organic and inorganic composition of the original sample and its soluble products. For this study, a representative sample of leonardite produced in each of the two States was used. The North Dakota sample (No. P-7) was collected in Bowman County (SW¼SE¼ sec. 33, T. 131 N., R. 99 W.) from the Peerless strip mine, which produces about 20,000 tons of leonardite per year. We are grateful to Herman Oster, mine superintendent, for his assistance and cooperation in collecting samples. The Tertiary geology and the coal reserves of Bowman and Slope Counties, N. Dak. have been described by Kepferle and Culbertson (1955).

The Wyoming leonardite sample (No. PPL-1) was collected from the leonardite storage pile at the strip mine (NE¼ sec. 10, T. 35 N., R. 75 W.) which provides the coal for the Pacific Power and Light Co.'s electricity generating plant at Glenrock, Converse County. The leonardite is selectively mined from the outcrop and back 20–50 feet along the coal bed during the stripping operation. Enough leonardite to fill several railroad cars is mined and shipped each month. Another sample, of low-grade leonardite (No. PPL-2), was collected at the mine at a site where the coal bed was under about 25 feet of overburden. The assistance of W. L. Potter, mine superintendent, during collecting of samples was greatly appreciated. The geology of the Glenrock coal field was described by Shaw (1909).

Several samples of trona were collected in 1971 from mines near Green River, Sweetwater County, Wyo. The sample used in this study from that collection was of the "maple-sugar" type, representative of trona mined from the Lower Big Island bed of economic usage at a depth of 730 feet in the Stauffer Chemical Co.'s mine (sec. 15, T. 20 N., R. 109 W.). Dr. L. E. Mannion, the company's chief geologist, guided and assisted us while we were at the mine. An excellent and complete description of the geology, mineralogy, and mining of trona in southwestern Wyoming has been presented by Parker and Mannion (1971).

The sample of nahcolite ($NaHCO_3$), which was used to test its solubility characteristics with those of leonardite and water, was collected by John R. Dyni from the Mahogany zone of the Green River Formation at the Anvil Points mine (SW¼ sec. 12, T. 6 S., R. 95 W.) in Garfield County, Colo. The general geologic relations and resources of nahcolite in northwest Colorado were described by Hite and Dyni (1967).

The samples of leonardite, trona, and nahcolite that were used in the laboratory experiments were crushed to pea size or smaller, but otherwise were untreated.

EXPERIMENTS AND RESULTS

A preliminary set of experiments established that leonardite was readily soluble in water solutions of trona. Using 200 ml of triply distilled water and varying the amount of trona needed to dissolve the maximum amount of 1.0 g of leonardite (P-7), we obtained the following results:

Ratio, trona: leonardite	*Percentage leonardite dissolved*
0:1	0.4
1:10	7.1
1:2	65.9
1:1	85.4
1:0.33	84.7

As indicated by this set of experiments, less than 1 percent of the leonardite is soluble in distilled water, and the maximum percentage of leonardite is dissolved in a mixture of 1 part trona to 1 part leonardite.

For comparison, 86.6 percent of this North Dakota leonardite (P-7) and 69.7 percent of the Wyoming leonardite (PPL-1) were dissolved when the standard laboratory method using ammonium hydroxide (0.1 *N* NH_4OH) was followed. For ease of comparing the results of the experiments, the weight ratios of trona (or nahcolite) to leonardite have been converted to 1 part trona (or nahcolite) to different amounts of leonardite. All analyses were run at room temperature (22°C) with triply distilled water.

In a second set of experiments, variable amounts of leonardite were mixed into a prepared solution of 1 g of trona per 300 ml of water, producing these results:

Leonardite sample No.	*Ratio, trona: leonardite*	*Percentage leonardite dissolved*
P-7	1:1.2	75.6
	1:0.6	79.4
	1:0.3	80.4
PPL-1	1:1.2	43.4
	1:0.6	51.4
	1:0.3	55.2

In a third set of experiments, the same procedure was followed using a nahcolite solution, which yielded the following results:

Leonardite sample No.	*Ratio, nahcolite: leonardite*	*Percentage leonardite dissolved*
P-7	1:2	23.4
	1:1	34.2
	1:0.5	45.6
PPL-1	1:2	9.8
	1:1	15.8
	1:0.5	22.4

The second and third sets of experiments indicated that the North Dakota leonardite (P-7) is more soluble than the Wyoming leonardite (PPL-1), and that when using slightly less trona than leonardite (1:1.2 trona-leonardite mixture), about 75 percent of the leonardite dissolves. Nahcolite proved to be far less efficient than trona in solubilizing leonardite; even with twice as much nahcolite as leonardite (1:0.5), only one-third to one-half of the amount of leonardite that is soluble in a 0.1 *N* NH_4OH solution is soluble in a nahcolite solution.

A fourth set of experiments, in which dry mixtures of 0.5 g of leonardite (P-7) and variable amounts of trona were added to 150 ml of water and stirred, yielded the following results:

Ratio, trona: leonardite	*Percentage leonardite dissolved*
1:3	38.9
1:1.25	76.6
1:1	78.2
1:0.87	78.2

The solutions turned a dark brownish black within a few minutes after the dry mixtures were added and slowly stirred. Again, the results indicated that almost the maximum amount of leonardite, 76.6 percent, is dissolved in solutions in which trona is slightly less than leonardite.

The lack of precise regularity in the percentages of leonardite dissolved in the trona solutions is explained by the fact that both types of sample material, which were crushed to pea size or smaller, were not wholly homogeneous.

The pH of trona solutions, as determined from other data obtained during the experiments, ranged from 9.84 to 10.11 and averaged 10.0. These solutions ranged in concentration from 2.5 g of trona in 50 ml of water to 0.5 g of trona in 500 ml of water. The addition and mixing of leonardite in the trona solutions lowered the pH of the solutions as follows:

Ratio, trona: leonardite	*pH of trona-leonardite solution*
1:0.6	9.6
1:1	9.3
1:1.25	9.1
1:1.5	8.9
1:2	8.3
1:10	7.0
0:1	5.2

Thus, the alkalinity of a trona solution is lowered when leonardite is added. The optimum trona-leonardite mixture—the one with least alkaline pH and high leonardite solubility—appears to be about 1 part trona to 1½ parts leonardite. This mixture in water dissolves about 75 percent of the leonardite and leaves a solution of pH 8.9.

As with other soluble humic substances (Swanson and Palacas, 1965, p. 13–17), the dissolved leonardite can be readily precipitated from the trona-leonardite solution as a dark-brownish-black gel by adding hydrochloric or sulfuric acid to lower the pH of the solution to about 3. Allowed to settle, the overlying solution is clear and colorless or clear and very slightly yellow. The precipitate can be centrifuged, washed, and dried, resulting in a black, glistening brittle coallike material that has a very low ash content (average of 11 samples, 2.4 percent). The average composition of this material, calculated on a moisture- and ash-free basis, is 58.5 percent carbon, 3.3 percent hydrogen, 37.1 percent oxygen (by difference), and 1.1 percent nitrogen. The dried precipitate can, of course, be totally and readily redissolved in a trona solution.

The original ash content of the North Dakota leonardite (P-7) was 6.3 percent, and of the Wyoming leonardite (PPL-1) 16.7 percent. This ash content represents about one-half the insoluble material of both leonardite samples in a trona solution, the remaining half being coal that is insufficiently oxidized to become soluble.

As indicated, the North Dakota and Wyoming leonardites are not totally soluble. The natural process of conversion of subsurface lignite and subbituminous coal to leonardite is presumably a function of wetting and drying under oxidizing conditions in an arid climate. This process was simulated in the laboratory using a sample of low-grade leonardite (PPL-2) from Wyoming that was 16.3 percent soluble in 0.1 *N* NH_4OH. Five grams of this sample was placed in a flat-bottom dish in a laboratory hood under an infrared lamp positioned to keep the sample at a temperature of 55°–60°C. The sample was kept wet with distilled water for 12 hours and allowed to dry for 12 hours each day for 7 days, under a constant stream of air in the hood. At the end of the 7 days, a fraction of the completely dried sample was analyzed and determined to be 35.4 percent soluble. The test was continued for another 2 weeks on the remaining sample, but subsequent analysis showed that solubility was not measurably increased. Nevertheless, the experiment does suggest that the solubility of mined leonardite would be significantly increased if newly mined leonardite is spread out on the ground in the sun and intermittently dampened.

CONCLUSIONS AND POTENTIAL USES

Trona readily goes into solution in water, the solution having a pH of 9.8–10.1. Whereas less than 1 percent of North Dakota leonardite is soluble in distilled water, 78–85 percent is dissolved in water containing 1 part trona and 1 part leonardite; the resulting solution has a pH of about 9.3. When a mixture of 2 parts trona to 3 parts leonardite is added to water, about 75 percent of the leonardite is dissolved, producing a black solution having a pH of 8.9. Addition of very small amounts of mineral acids such as sulfuric, hydrochloric, or nitric acid readily produces a neutral solution, pH 7.0.

The sole major cation in a trona-leonardite solution is sodium, which is generally nontoxic to animals and nondeleterious to plants. Furthermore, sodium is the most easily replaced cation in ion-exchange or metal-sorption reactions in this humic acid-type solution. The solution thus lends itself to a variety of uses dependent upon these biologic and chemical factors.

Seemingly, the low cost of materials and the ease and speed of preparation would make the trona-leonardite mixture attractive for many applications and processes. A 100-pound bag of a 2:3 trona-leonardite mix costing $1–$2 could be simply added to 1,000 gallons of water to produce a rich, black solution that would serve as a very inexpensive base for the following uses:

A. A soil conditioner or leaf spray. Water-soluble metal salts could be easily added in desired amounts, and the micronutrient metals would be chelated by the dissolved leonardite in a form readily available to plants (Martell, 1957; Swanson and others, 1966, p. C176; Wallace, 1971). More generally, agriculturalists have long recognized the necessity of maintaining an adequate concentration of humate material in productive soils, but the difficulty and expense of application of this material have frequently restricted its use (Burdick, 1965). The trona-leonardite mix could well be the product to overcome these restrictive factors.

B. A leach solution for ionic metal capture. The sodium-organic bond in the trona-leonardite solution is very weak, and as a result the sodium is readily displaced by a large number of metals, for example cobalt, copper, mercury, nickel, lead, uranium, or zinc. Such a leach solution could be applied to secondary recovery of metal from ore dumps (Mining Engineering, 1971), concentration of deleterious or toxic metals from industrial wastes, or addition to acid mine water to simultaneously neutralize the acidity and remove toxic metals.

C. A spray for chemical stabilization of acid mine tailings and simultaneous stimulative for vegetative restoration of tailings (Dean and others, 1971).
D. A spray dye for any water-absorbing material.
E. A surfactant additive to improve secondary recovery of oil.

REFERENCES

Burdick, E. M., 1965, Commercial humates for agriculture and the fertilizer industry: Econ. Botany, v. 19, no. 2, p. 152–156.

Culbertson, W. C., 1966, Trona in the Wilkins Peak Member of the Green River Formation, southwestern Wyoming, *in* Geological Survey Research 1966: U.S. Geol. Survey Prof. Paper 550-B, p. B159–B164.

Dean, K. C., Havens, Richard, and Valdez, E. G., 1971, USBM finds many routes to stabilizing mineral wastes: Mining Eng., v. 23, no. 12, p. 61–63.

Fowkes, W. W., and Frost, C. M., 1960, Leonardite, a lignite byproduct: U.S. Bur. Mines Rept. Inv. 5611, 12 p.

Freeman, P. G., and Fowkes, W. W., 1968, Coal-derived humus, plant growth effects: U.S. Bur. Mines Rept. Inv. 7203, 16 p.

Hite, R. J., and Dyni, J. R., 1967, Potential resources of dawsonite and nahcolite in the Piceance Creek basin, northwest Colorado, *in* Symposium on oil shale: Colorado School Mines Quart., v. 62, no. 3, p. 25–38.

Kepferle, R. C., and Culbertson, W. C., 1955, Strippable lignite deposits, Slope and Bowman Counties, North Dakota: U.S. Geol. Survey Bull. 1015-E, p. 123–182.

Martell, H. J., 1957, The chemistry of metal chelates in plant nutrition: Soil Sci., v. 84, p. 13–26.

Mining Engineering, 1971, Australian breakthrough in metals extraction [using brown coal]: Mining Eng., v. 23, no. 10, p. 68.

Parker, R. B., and Mannion, L. E., eds., 1971, Trona issue: Wyoming Univ. Contr. Geology, v. 10, no. 1, 72 p.

Shaw, E. W., 1909, The Glenrock coal field, Wyoming, *in* Coal fields of Wyoming: U.S. Geol. Survey Bull. 341-B, p. 151–164.

Swanson, V. E., Frost, I. C., Rader, L. F., Jr., and Huffman, Claude, Jr., 1966, Metal sorption by northwest Florida humate, *in* Geological Survey Research 1966: U.S. Geol. Survey Prof. Paper 550-C, p. C174–C177.

Swanson, V. E., and Palacas, J. G., 1965, Humate in coastal sands of northwest Florida: U.S. Geol. Survey Bull. 1214-B, 29p.

Wallace, Arthur, 1971, Regulation of micronutrient status of plants by chelating agents and other factors: Los Angeles, pub. by author (printed by Edwards Bros., Inc., Ann Arbor, Mich.), 309 p.

GEOLOGY AND METASOMATIC IRON DEPOSITS OF THE SAMLI REGION, BALIKESIR PROVINCE, WESTERN TURKEY

By GERHARD W. LEO, Washington, D.C.

Abstract.—In the Şamli area in Balikesir province, western Turkey, one or more lower Miocene granitic plutons intrude Upper Jurassic(?) limestone, Upper Triassic(?) sandstone, Lower Tertiary(?) diabase and metadiabase, and subordinate extrusive volcanic rocks. The limestone forms chaotically scattered blocks which probably represent remnants of an extensive thrust plate or gravity slide. The contact metamorphism has recrystallized limestone to marble and has selectively converted the mafic rocks to calc-silicate hornfels and skarn. Several types of iron deposits are distributed along the southern margin of the granitic intrusions, and three different modes of origin are apparent. On Bakirlik Tepe, magnetite-martite lenses follow primary or metamorphically induced planar structures in metadiabase converted to hornfels and skarn, the iron apparently having been supplied by mobilization of magnetite (and ilmenite?) in the host rocks in response to metamorphism. At Kocaçal Tepe, hematite ore is found at the contact between crystalline limestone and a tabular(?) diabase intrusion. Elsewhere in the region, magnetite deposits are related to contacts between granite and limestone.

The Şamli area was studied in 1968 as part of a joint project between the Mineral Research and Exploration Institute (MTA) of Turkey and the U.S. Geological Survey, sponsored by the Government of Turkey and the Agency for International Development, U.S. Department of State. Şamli was included in the project because of the possibility of finding additional iron deposits; the area appeared promising because aeromagnetic and ground magnetometer surveys in 1966–67 showed magnetic anomalies along the southern margin of a large granitic pluton, partly coinciding with long-known but only intermittently exploited magnetite deposits on Bakirlik Tepe.[1]

After the magnetic surveys, about 40 holes were drilled during 1967–69, mostly around Bakirlik Tepe; an unknown number of holes have been drilled since. The latest borehole data available for this study date from early 1969.

The present paper is not concerned with the economic aspects of the deposits, which have been discussed elsewhere (Leo and Genç, 1972). Instead, it presents the geologic framework of the region, followed by some consideration of the nature and probable genesis of the iron deposits, particularly those on Bakirlik Tepe, where the iron appears to have been derived from the enclosing mafic metavolcanic rocks by mobilization related to contact metamorphism.

Acknowledgments.—J. E. Gair improved the manuscript at various stages by careful and thorough reviews. Thanks are also due Harry Klemic for a review and discussions.

LOCATION AND TERRAIN

The village of Şamli is in Balikesir province in western Turkey about 18 km north of the regional capital of Balikesir (fig. 1). The iron deposits discussed here are about 1 km north of Şamli in an east-west belt about 7 km wide.

The Şamli region has gently rolling topography and sparse vegetation. The maximum relative relief is about 200 m, and the highest point, Kocaçal Tepe (fig. 2), is 548 m above sea level. Rock exposures are generally poor. The only well-exposed unit is crystalline limestone; others are represented by float and rare outcrops.

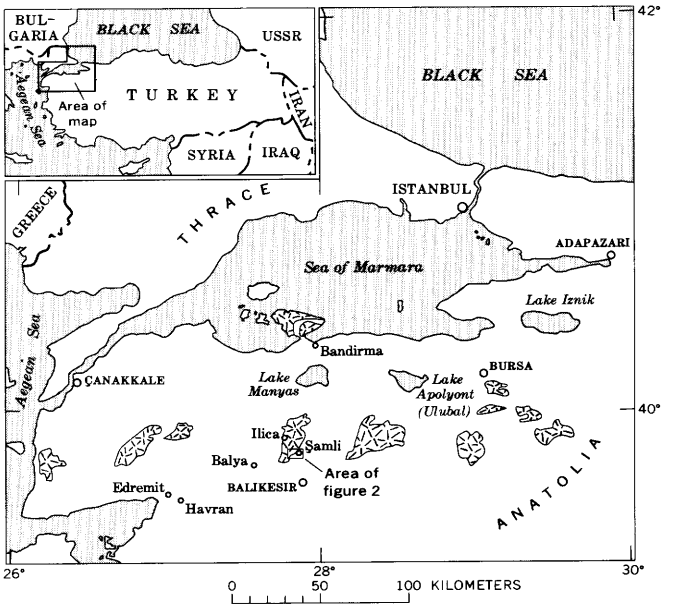

Figure 1.—Index map of western Turkey. Patterned areas are major granitic intrusions.

[1] Tepe, hill.

U.S. GEOL. SURVEY PROF. PAPER 800-D, PAGES D75-D87

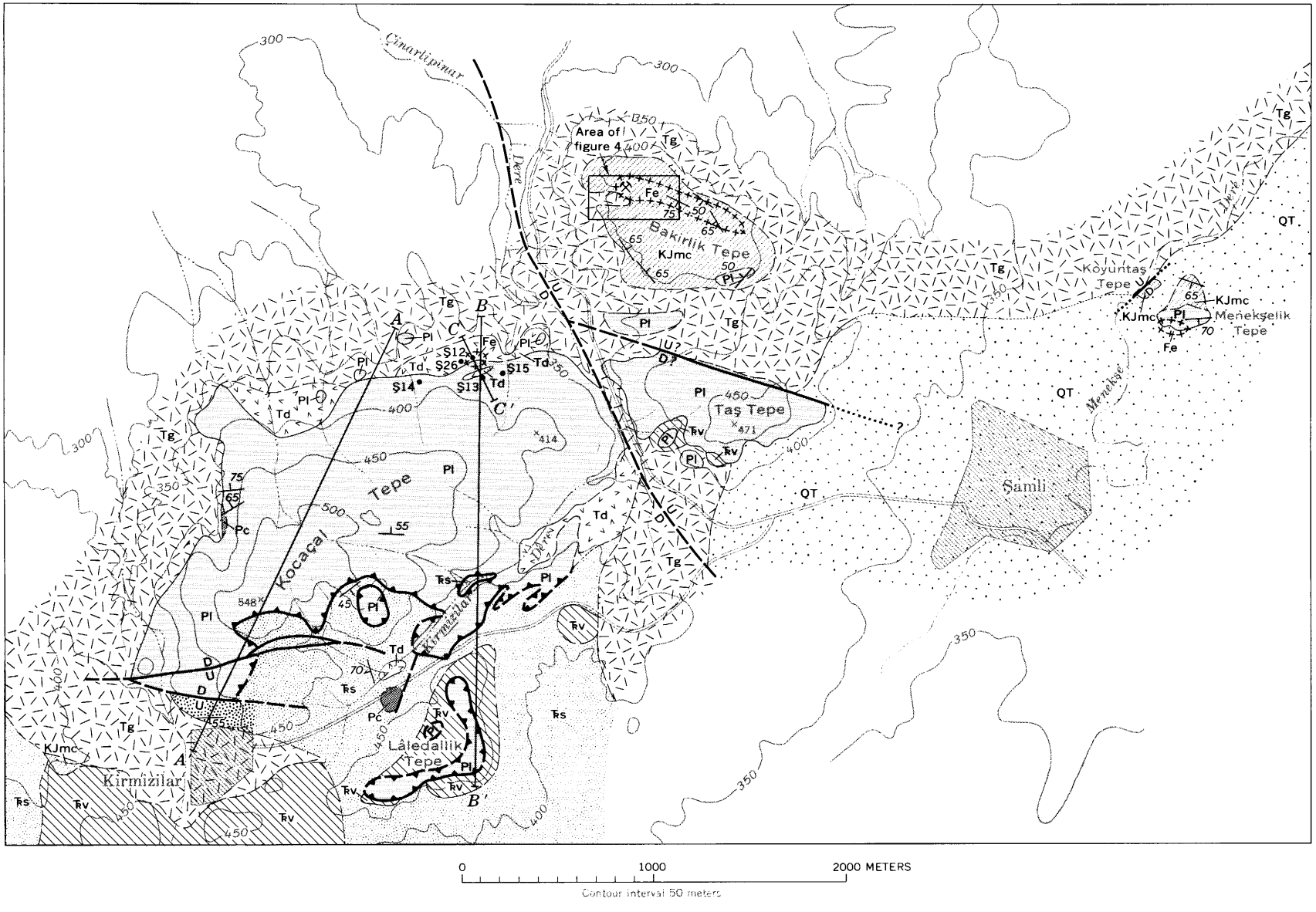
Çınartipinar
Area of figure 4
Bakirlik Tepe
KJmc
Koyuntaş Tepe
Menekşelik Tepe
Taş Tepe
Şamli
Kocaçal Tepe
Kirmizilar
Kirmizilar
Láledallik Tepe
Menekşe
Tg
QT
Pl
Td
Fe
Pc
Trs
Trv
KJmc
A
A'
B
B'
C
C'
S12
S26
S15
S14
S13
0
1000
2000 METERS
Contour interval 50 meters

Figure 2.

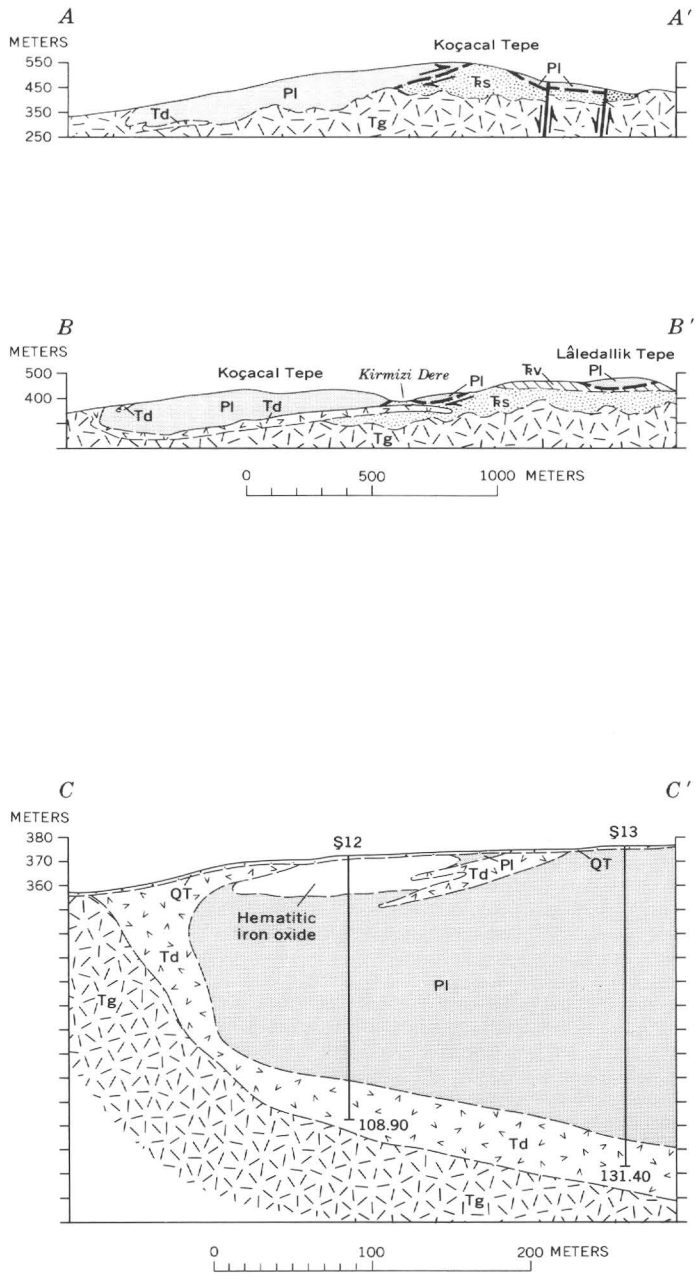

EXPLANATION

QT — Quaternary colluvium and upper Tertiary (Neogene) sedimentary rocks
Shown on map only where thicker than 3 m
(TERTIARY AND QUATERNARY)

Td — Diabase
Generally slightly metamorphosed

Tg — Granitic rocks, mostly granodiorite, less commonly quartz diorite, quartz monzonite, and syenite
Miocene
(TERTIARY)

KJmc — Metadiabase, hornblende-plagioclase amphibolite; commonly gradational to calc-silicate hornfels and skarn with associated magnetite
(POST-TRIASSIC TO PRE-TERTIARY(?))

Tv — Volcanic rocks including tuff

Ts — Graywacke gradational to arkose
Probably Halilar Formation of Krushensky and others (1972); coarsely stippled where silicified
(TRIASSIC(?))

Pl, Pc — Pl, crystalline limestone remnants of a thrust plate
Probably limestone of Kocaçal Tepe of Krushensky and others (1972)
Pc, calc-silicate rocks derived from limestone
(PERMIAN(?))

Contact
Dashed where approximately located; dotted where concealed or inferred

Fault
Dashed where approximately located; dotted where concealed or inferred. U, upthrown side; D, downthrown side

Thrust fault
Dashed where approximately located. Sawteeth on upper plate

75 — Strike and dip of bedding or compositional banding

Fe — Open pit
Major area of surface or subsurface iron mineralization

S13 — Diamond drill hole
Depth given in meters in sections

Figure 2.—Generalized geologic map and sections of the Şamli area.

DEFINITIONS OF TERMS

Several descriptive rock names used in this paper are defined here to avoid ambiguity.

The terms "granitic rocks" or "granitic pluton" refer to one, or possibly several, intrusive masses in the Şamli region whose composition is mostly granodiorite to quartz diorite, and locally diorite, granite, and syenite.

Mafic rocks all have a generally basaltic composition, on the basis of petrographic criteria, and field relations suggest that they are intrusive, not flows. Textures are holocrystalline, subophitic or intergranular, locally porphyritic. The least altered of such rocks are referred to as "diabase" or "slightly metamorphosed diabase." "Metadiabase" is used to designate higher grade metamorphic rocks consisting dominantly of hornblende and intermediate plagioclase (microamphibolite) with clearly recognizable volcanic textures. "Calc-silicate hornfels" denotes fine-grained calcic plagioclase-diopside-(garnet) rocks in which relict volcanic textures may or may not be recognizable. "Skarn" refers to coarser grained, irregularly textured calc-silicate rocks commonly containing abundant garnet and magnetite. Pods and crosscutting veins of epidote are common in both hornfels and skarn.

The opaque material in thin sections of the diabase and its metamorphic derivatives is mostly black by reflected light and is assumed to be magnetite. However, in a few sections of the diabase, fringes and patches of leucoxene adjacent to opaque minerals indicate that either the magnetite is titaniferous or that ilmenite, and possibly ulvöspinel, may be present. In the absence of more specific data, the term magnetite is used collectively for the opaque minerals in the mafic rocks.

GENERAL GEOLOGY

The iron deposits of the Şamli area are near the southern margin of a granitic pluton of batholithic size, which is in an east-trending belt of generally similar intrusions in western Turkey (fig. 1). All but the westernmost of these intrusions, near the Aegean coast, have until recently been regarded as pre-Mesozoic (Kaaden, 1971, fig. 4 and p. 205). However, newly determined potassium-argon ages of hornblende and biotite from granitic rocks near Şamli and Edremit are about 22 m.y. to 25 m.y. (fig. 1; John Obradovich, written commun., 1971), hence early Miocene; ages of biotite and hornblende from a sample of the Şamli intrusion were determined as 22.1±0.6 and 21.7±0.7 m.y., respectively.

The regional structure is incompletely known, and is evidently complex. Some of the most prominent features are limestone blocks which are irregularly distributed between Havran and Bursa, a distance of more than 160 km (fig. 1), and possibly beyond. These bodies appear to be unrooted and to represent remnants of one or more thrust plates (gravity slides?) (Aygen, 1956; Leo and Genç, 1972; Krushensky and others, 1972). East of Edremit, and some 60 km southwest of Şamli, Krushensky and others (1972) have identified two separate limestone allochthons related to one or two episodes of post-Triassic thrusting. In the smaller and less conspicuous allochthon, identified as such by fossils only, Permian limestone (informally named "limestone of Ayakli") overlies Upper Triassic sandstone (Halilar Formation). In the other, more extensive allochthon, marked by basal breccia, discordant attitudes in the upper and lower plates, and other structural features indicative of tectonic emplacement, Upper Jurassic limestone (informally named "limestone of Kocaçal Tepe[1]") also overlies the Halilar Formation. A similar thrust contact between the two units is also found at Balya (Aygen, 1956), about 20 km southwest of Şamli (fig. 1).

North of Şamli, several hills, including Kocaçal Tepe and Taş Tepe (fig. 3) are underlain by white, coarsely crystalline

Figure 3.—View of Şamli from the southeast. Taş Tepe, in the background, is capped by an irregular plate of crystalline limestone (white) surrounded by Quaternary deposits and granitic rocks (see fig. 2). Outcrop pattern of this limestone thrust remnant is typical of this region.

limestone which probably can be correlated with the limestone of Kocaçal Tepe, as described by Krushensky and others (1972). Surface and borehole data indicate that at least some of these blocks are subhorizontal plates resting unconformably on younger rocks, and that some of them are buried almost entirely by Tertiary and Quaternary sediments. Locally developed basal breccia of angular limestone fragments in a sandstone matrix, and highly contorted and sheared limestone in its southernmost exposures on Lâledallik Tepe (fig. 2) are further indications of tectonic emplacement.

The autochthonous rock in the Şamli area is predominantly a buff to brown, coarse, highly indurated, massively bedded to structureless sandstone which varies over short distances

[1] A fortuitous identity of names for two different hills, one in the Edremit area, the other near Şamli and discussed in this paper.

between arkose feldspathic graywacke and is correlated with the Halilar Formation (Krushensky and others, 1972). This rock is overlain by dense, white to tan, slightly metamorphosed silicic tuff exposed mostly south of Kocaçal Tepe. Small patches of dacite and andesite of uncertain extent and relationship overlie the silicic tuff and underlie the crystalline limestone.

Two mafic volcanic units are of special interest relative to the genesis of the iron deposits. The older of the two units, exposed on Bakirlik Tepe and eastward, is metadiabase selectively recrystallized to calc-silicate hornfels and skarn with associated magnetite. Most of the recrystallization is obviously related to the granitic intrusions, but some probably resulted from earlier low-grade metamorphism; hence, the metadiabase evidently is older than the slightly metamorphosed volcanic units mentioned in the last paragraph, but their mutual relations could not be determined. This metadiabase is more fully described below.

The other mafic unit, which crops out discontinuously along much of the northern and southern margins of Kocaçal Tepe, and forms at least one sill cutting the contact aureole of Bakirlik Tepe, is slightly metamorphosed diabase. It consists of albitized plagioclase, augitic pyroxene, epidote, chlorite, carbonate and (or) zeolites, and 3 to 8 percent dusty magnetite (fig. 5*A*). Locally this mafic unit has been recrystallized to sodic plagioclase and green hornblende which are indicative of higher grade metamorphism (lower amphibolite facies if regional metamorphism, hornblende hornfels facies if contact metamorphism). Higher grade, distinctly contact-metamorphic effects typical of the metadiabase on Bakirlik Tepe are lacking. Thus, as granitic rocks directly underlie the Kocaçal Tepe area, this diabase must be younger than the metadiabase of Bakirlik Tepe and may have been emplaced between crystalline limestone and granodiorite soon after intrusion of the latter (about 20 m.y. ago?), becoming slightly to moderately recrystallized in the waning stages of contact metamorphism.

The region has been affected by block faulting. Some faults cut granitic rocks around Taş Tepe, and others on Bakirlik Tepe offset magnetite bodies; hence, some of the faulting is post-early Miocene. A silicified zone in the Triassic sandstone north of Kirmizilar village (fig. 2) is related to a normal fault, and silicified sandstone was found near faults in the Kayalar area, about 20 km west of Şamli. No economic iron deposits are related to the normal faults.

BAKIRLIK TEPE

The gently sloping surface of Bakirlik Tepe is underlain by a wedge-shaped roof pendant of contact-metamorphosed rocks encased in one or more granitic intrusive bodies (figs. 2, 4). The south and west parts of the hill are underlain by granodiorite and quartz diorite of a major pluton; tabular quartz diorite bodies thought to be mostly sills cut the contact aureole. Rocks of more felsic composition, including granite, quartz monzonite, and, locally, syenite are sparsely distributed on the north flank of the hill and may represent a separate intrusion or intrusions. The contact aureole itself consists dominantly of metadiabase, calc-silicate hornfels and skarn, and scattered lenses of crystalline limestone. A small amount of skarn may be derived from the limestone lenses, but most of it has come from metadiabase.

Granitic rocks

Rock of the major pluton is typically light gray and medium grained and has the following estimated composition: about 50 percent conspicuously tabular, mostly zoned, plagioclase (An_{45-60}); 10 to 30 percent quartz; 0 to 20 percent K-feldspar; and 5 to 20 percent green hornblende and partly chloritized biotite. Sphene and magnetite are the most abundant accessories; apatite, zircon, and allanite(?) are less common. Thus, the rocks are granodiorite and quartz diorite (for some chemical analyses see Krushensky and others, 1972, table 5), but the relative abundance and distribution of the two is unknown. In the one locality where the contact with hornfels is clearly exposed, the granodiorite grades in a distance of about 30 m to diorite porphyry with about 70 percent plagioclase phenocrysts (An_{55-72}) plus hornblende and biotite, and less than 5 percent quartz and K-feldspar. The quartz diorite sills commonly contain 60 to 70 percent plagioclase (andesine-labradorite) phenocrysts plus quartz, hornblende, and (or) biotite, and less than 5 percent K-feldspar.

Three random specimens of poorly exposed granitic rock on the north side of Bakirlik Tepe span the range from quartz monzonite to syenite. One specimen of float consists of about 45 percent orthoclase microperthite, 30 percent strongly zoned oligoclase-andesine, 20 percent quartz, and 5 percent biotite; another contains about 70 percent microperthite, 5 percent oligoclase, 20 percent quartz, and 5 percent pale amphibole; and a third consists nearly entirely of orthoclase microperthite with interstitial pockets of microgranite. These rocks may represent separate intrusions, possibly late differentiates of the granodiorite-quartz diorite pluton.

Contact aureole

Much of the contact aureole bordering the granitic pluton consists of dark and dense rock with conchoidal fracture and a megascopically discernible fabric of very finely felted amphibole needles. The rock consists mostly of acicular to prismatic amphiboles (bright- to pale-green hornblende or colorless to blue-green tremolite-actinolite, or both) and subordinate plagioclase (commonly andesine-labradorite, more rarely oligoclase). The texture is distinctly diabasic, owing mainly to the lathlike habit of relict plagioclase; granoblastic recrystallization of plagioclase is rare at this relatively low metamorphic grade. The amphiboles have recrystallized in part from original augite, as shown by intermediate stages of such replacement observed in a few thin sections (fig. 5*A*). Replacement textures

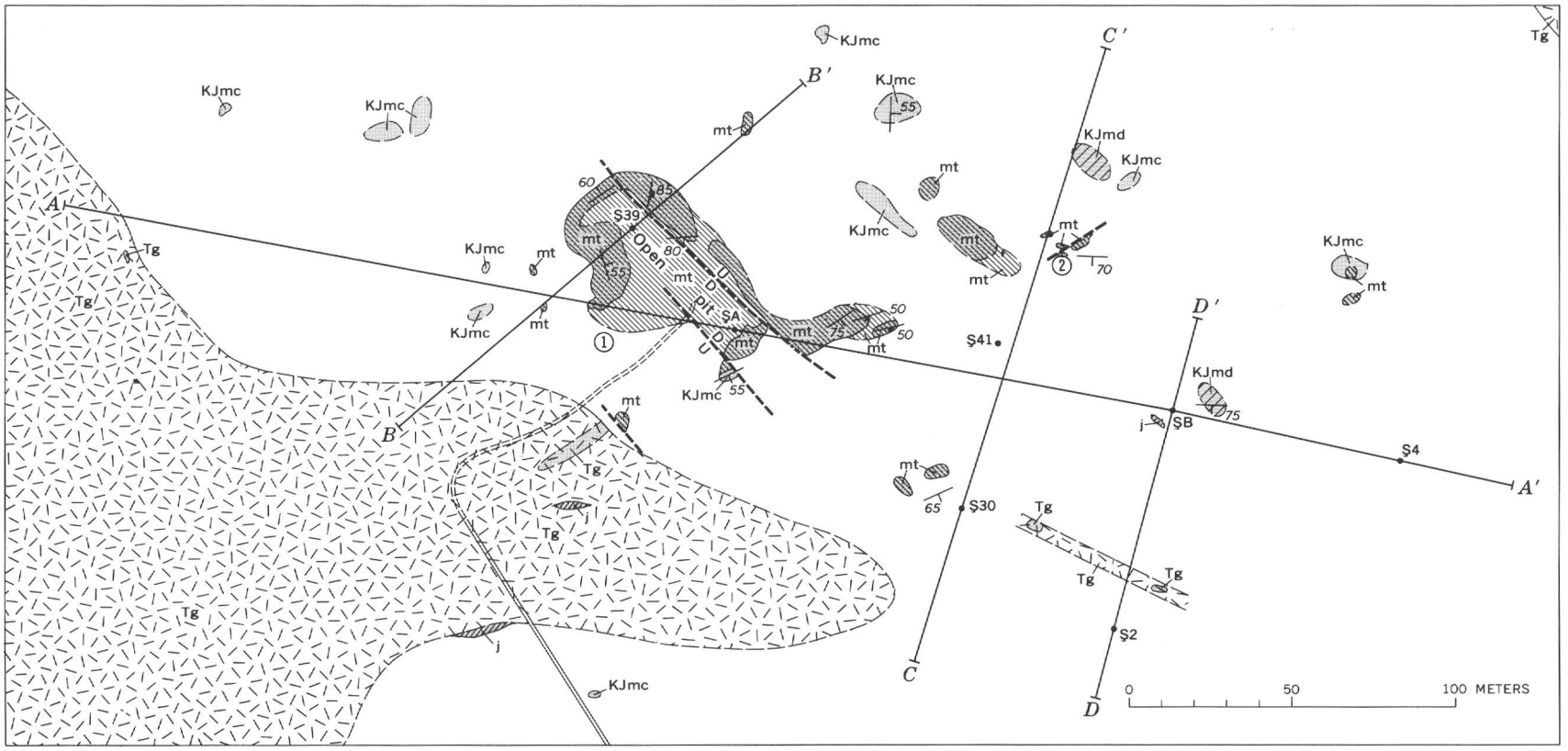

EXPLANATION

Colluvium or rubble
Covers most of the map area; shown in sections only

QUATERNARY

Miocene

Granitic rocks
Granodiorite and quartz diorite

TERTIARY

KJmd, metadiabase, mostly hornblende-plagioclase amphibolite

KJmc, metadiabase, mostly recrystallized to calc-silicate hornfels or skarn

Contact between KJmc *and* KJmd *is gradational and irregular; contact between these two units in sections is largely schematic*

j, more or less pure jasper

mt, enclosed iron oxide, mostly magnetite and subordinate hematite and jasper

In sections, extension of at least 20 m from drill hole assumed parallel to layering

POST-TRIASSIC TO PRE-TERTIARY(?)

Bedrock outcrop

Contact
Dashed where approximately located

Inferred fault
U, *upthrown side;* D, *downthrown side*

75
Strike and dip of compositional layering or schistosity

50
Strike and dip of joint

S30
On map
S30 — 94.40
In sections
Diamond drill hole
Depth given in meters in sections

1
Photo locality
(see fig. 7)

Figure 4.

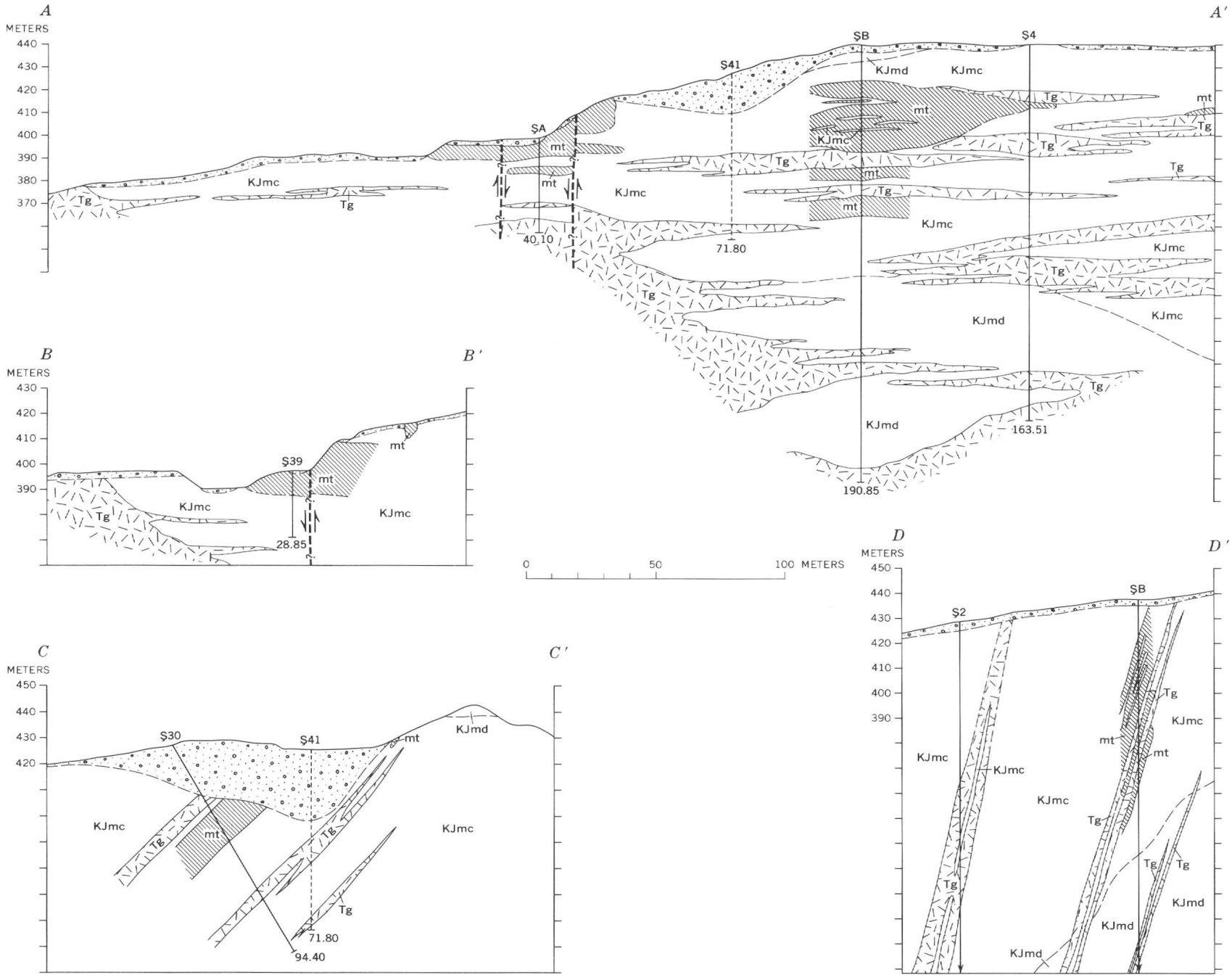

Figure 4.—Geologic map and sections of the area around the open pit, Bakirlik Tepe.

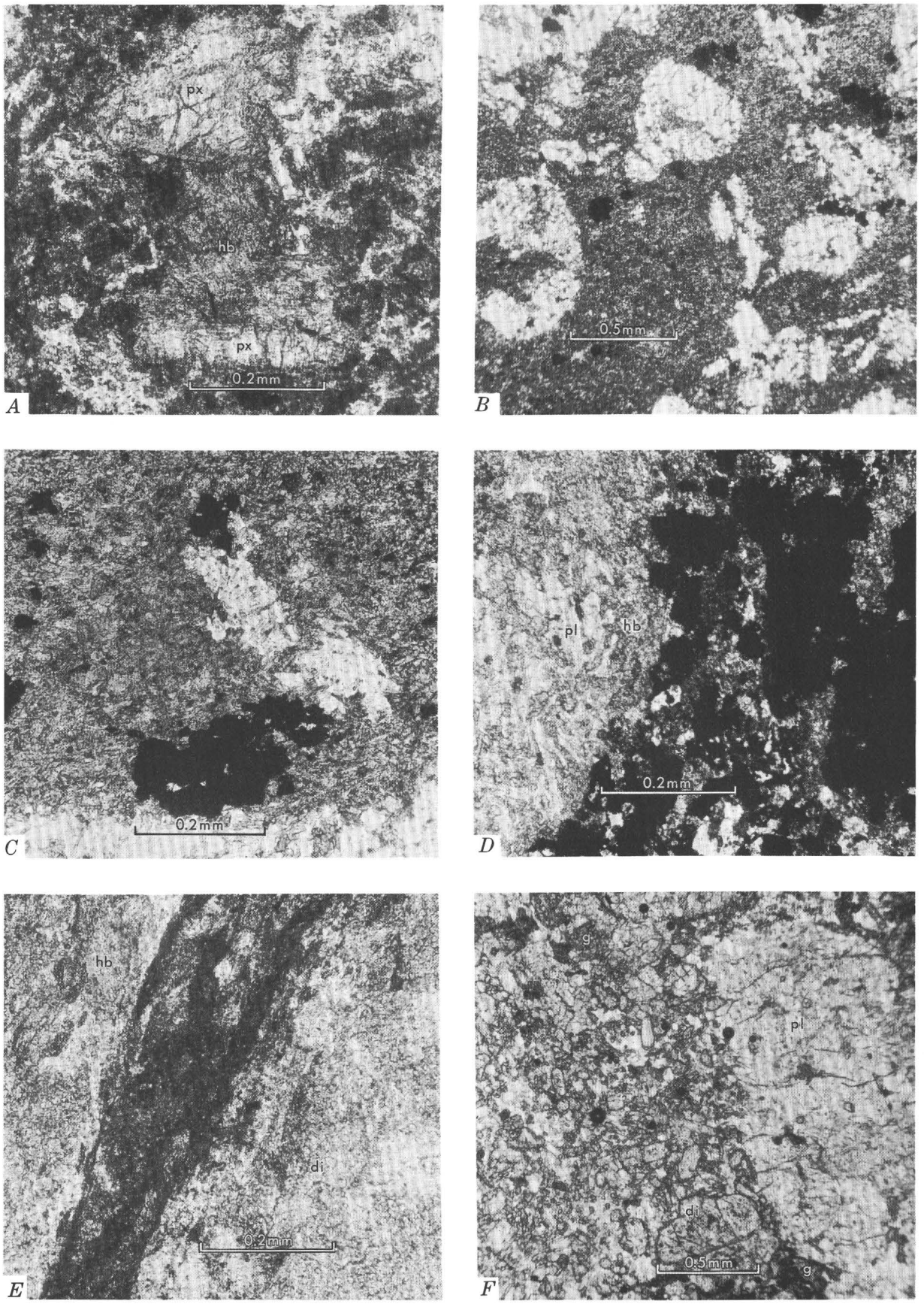
px
hb
px
0.2mm
A
0.5mm
B
0.2mm
C
pl
hb
0.2mm
D
hb
di
0.2mm
E
g
pl
di
0.5mm
g
F

Figure 5.

including scalloped margins of hornblende plates against partly replaced plagioclase laths, and tiny needles or granules of new amphibole within plagioclase indicate that plagioclase contributed to the late growth of amphibole. Green or brown biotite and (or) late epidote veins are present in some sections. Magnetite typically constitutes an estimated 3 to 5 percent by volume but may attain 10 percent. In contrast to the dusty and evenly disseminated magnetite in the slightly metamorphosed diabase of Kocaçal Tepe, magnetite in the metadiabase is typically granular and tends to form clumps and segregations suggestive of some migration and coalescing of original dusty magnetite (fig. 5*B*, *C*, *D*). Patchy sphene is common and presumably reflects reconstituted iron-titanium oxides of the original diabase (fig. 5*E*; also Desborough, 1963).

The metadiabase is a microamphibolite in the hornblende hornfels metamorphic facies (Turner, 1968, p. 193, 223). The original diabase evidently formed shallow intrusions older than the granitic rocks and either older or younger than the allochthonous limestone. Metamorphism of the diabase to amphibolite occurred either during (1) a metamorphic episode preceding contact metamorphism by the granitic intrusion or (2) an early phase of the contact metamorphism itself. The limited field evidence is inconclusive in this regard.

Phyllitic schist consisting of plagioclase, actinolite, and subordinate biotite grades to metadiabase in a few drill cores. The schist has roughly the same bulk composition as the metadiabase but bears no relict primary textures. It may have formed along localized shear zones within the diabase which were active before and (or) during metamorphism. Other planar structures in the metadiabase subparallel to the schistosity may also be of metamorphic origin.

Bordering the open pit (fig. 4) and intermittently along the crest and on the southwest flank of Bakirlik Tepe, the contact aureole is gray-green to reddish-brown hornfels which consists dominantly of an even-grained granoblastic mosaic of calcic plagioclase (approximate range An_{50-75}), diopside, and epidote, with or without hornblende, garnet, calcite, and magnetite. Epidote commonly forms crosscutting veins and aggregates, more rarely individual prisms. Magnetite tends to appear in centimeter-wide patches and veinlets in contrast to the disseminated or clotted magnetite granules in the metadiabase. In contrast to this granoblastic texture, some of the hornfels specimens retain a relict intergranular volcanic texture, but compared with the metadiabase protolith, the plagioclase laths in the hornfels are more calcic, diopside is abundant, and hornblende is subordinate or absent (fig. 7). Replacement of hornblende by diopside is sporadic. Granoblastic and intergranular texture may be gradational within any one thin section.

Homogeneous granoblastic calc-silicate hornfels grades locally to more heterogeneous coarse-grained skarn, in which the irregular distribution of minerals attests to migration and segregation. Crosscutting pods and veins, consisting mostly of epidote but locally of garnet, are ubiquitous. Magnetite, pyrite, and, more rarely, pyrrhotite and chalcopyrite form crosscutting pods, or bands and lenses, subparallel to fractures and compositional layering (fig. 6*D*). The skarn typically is adjacent and gradational to larger magnetite bodies.

The transformation of metadiabase to calc-silicate hornfels and skarn represents metamorphism from low greenschist facies to pyroxene hornfels facies. Rare isolated outcrops and scattered float of limestone suggest that some of the calc-silicate rock may have been derived from such rocks. However, neither skarn nor calc-silicate marble occurs at the only exposed contact between granodiorite and limestone, about 480 m south-southwest of the open pit.

The transition from metadiabase to hornfels follows no systematic pattern. A lateral gradation seems to occur at the surface, but transitions are irregularly distributed in many cores, hornfels being above and below. An apparent lower limit of hornfels is tentatively identified in sections $A-A'$ and $D-D'$ (fig. 4). Presumably the hornfels formed adjacent to the granitic intrusion and associated sills and dikes, but a consistent spatial relationship has not been established.

Figure 5.—Photomicrographs of metamorphosed basaltic rocks, Bakirlik Tepe area. Plane-polarized light.

A. Primary clinopyroxene (px) partly replaced by fibrous pale-green hornblende (hb) in incipiently metamorphosed basaltic dike intruded into the contact aureole of Bakirlik Tepe.

B. Plagioclase phenocrysts of original mafic volcanic rock preserved in groundmass of acicular metamorphic hornblende and magnetite.

C. Detail of same rock as photomicrograph *B*. Note aggregate of magnetite, which contrasts with dusty disseminated magnetite in less metamorphosed rocks.

D. Concentration of magnetite (right) adjacent to hornblende (hb)-plagioclase (pl) aggregate with clearly preserved diabasic texture.

E. Sharp contact between hornblende (hb)-plagioclase amphibolite (left) and diopside (di)-plagioclase hornfels (right), separated by a microshear zone containing much finely granular sphene (dark).

F. Thoroughly recrystallized calc-silicate hornfels consisting of calcic plagioclase (pl), diopside (di), and subordinate garnet (g). Texture mostly granoblastic, but note outlines of original plagioclase phenocryst (now an aggregate of smaller plagioclase crystals). No magnetite in area of thin section.

Structure

The few exposures in the part of the contact aureole east of the open pit suggest a northwest-trending synform (fig. 2). Along the mineralized crest of the hill, trends of planar structures are west to northwest, and dips are generally south to southwest. Moderate to vertical dips of planar structures are also apparent in most of the drill cores (fig. 6*D*), but their strikes are unknown. Around the open pit (fig. 4), attitudes depart from the west to northwest trends, and the overall structural pattern may well be more complex than it appears on the crest.

A

B

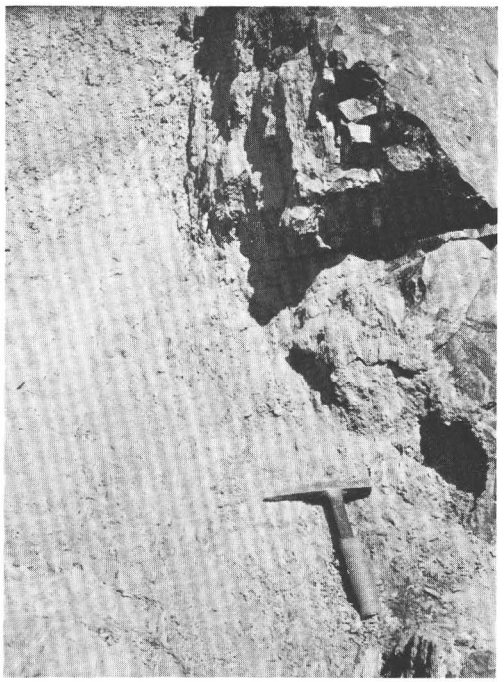

C

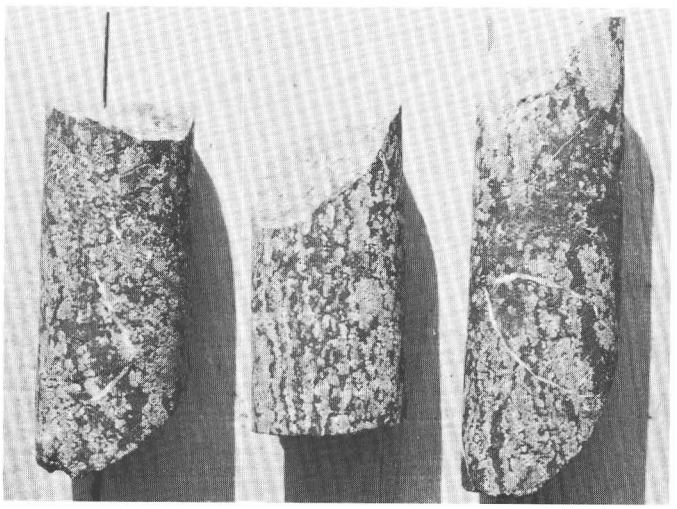

D

Figure 6.—Outcrops and drill cores of iron oxide, Bakirlik Tepe.

A. Panoramic view of open pit on Bakirlik Tepe, showing magnetite (rough blocky outcrops) in weathered calc-silicate hornfels and skarn. View is northeast from locality 1 (fig. 4); drill hole ŞA is directly above the car. The larger of the inferred northwest-trending faults (fig. 4) runs along base of cut.

B. Steeply dipping lens of magnetite in weathered calc-silicate rock. View northeast from locality 2 (fig. 4). Height of cut about 3 m.

C. Detail from photograph *B*. Sheared contact between magnetite and weathered calc-silicate rock is thought to be related to postmineralization faulting.

D. Core of vertical borehole in southeast part of mineralized zone of Bakirlik Tepe, showing mostly magnetite (dark) and epidote, both of which appear to be late replacements of original metavolcanic rock. Crude banding in center specimen shows near-vertical dip. Diameter of cores about 7 cm.

Structural elements include (1) compositional layering in skarn, accentuated by veinlets and narrow lenses of magnetite, (2) rare alinement of prismatic and platy minerals in metadiabase and granitic sills, (3) joints and fractures, some with fillings of epidote, garnet, magnetite, and sulfide minerals (fig. 6*D*), and (4) schistosity which may be accentuated by shearing. Commonly the planar structures are subparallel. As the original diabase lacks such structures, they may well have formed during intrusion of the granitic rocks.

Some tabular-appearing granitic bodies seen only in drill cores have chilled margins and sharp contacts more or less parallel to the dip of adjacent calc-silicate rocks. On this basis, all sections of granitic rock beginning and ending in drill cores have been shown as sills in the cross sections, although some of them may in fact be dikes or irregular apophyses.

Iron deposits

The iron deposits of Bakirlik Tepe are contained within the contact aureole of metadiabase (fig. 2) and are exposed mainly in the open pit (figs. 4; 6*A*, *B*, *C*). The mine has been inactive since the 1950's because of copper and other impurities in the iron oxide. The ore zone, mapped by magnetic anomalies and boreholes, strikes west-northwest and is approximately 800 m long and 100 m wide. Most bodies of iron oxide (mainly magnetite) are less than 50 m below the surface but have been penetrated down to 80 m. Figure 4 illustrates somewhat schematically the subsurface relations, based on drill cores, in the northwest end of the ore zone. Available data suggest that the iron oxide bodies approximate tabular ellipsoidal lenses but are probably irregular in detail, and the lenses each probably contain from a few hundred tons to a hundred thousand tons or more. Estimated reserves to 50-m depth are about half a million metric tons.

Thin layers and lenses of iron oxide are generally parallel to compositional layering, fractures, and other planar structures in the host rock and hence have a prevailing west to northwest strike and southwest dip within the roof pendant in the area southeast of the pit. Attitudes of the larger lenses in the same area are probably similar but could not be evaluated from the drill cores. Magnetic anomalies detected by ground magnetometer surveys suggest a west to northwest strike of iron oxide lenses at least as far west as drill hole ŞB (fig. 4). Recent additional drilling on Bakirlik Tepe suggests that several of the lenses have low to moderate southwest dips or are irregularly shaped, or both.

Attitudes of planar structures within and near the open pit tend to depart from the west-northwest trend and steep southwest dip. Some of the iron oxide lenses do dip steeply, but borehole data indicate that the largely mined out ore body was subhorizontal (fig. 4, secs. A–A', B–B'). The irregular disposition of iron oxide bodies was increased by postmineralization block faults, some of which cross the pit in a northwest direction (fig. 4). Faults are indicated by offsets of iron oxide lenses and by brecciation and shearing at the margins of some lenses (fig. 6*B*, *C*). Postmineralization faulting in various directions was also observed around Koyuntaş Tepe, Menekşelik Tepe (fig. 2), and Kale Tepe northeast of Şamli.

Composition.—The iron oxide is mostly magnetite, but commonly is mixed with subordinate hematite (martite), which evidently has formed by weathering of magnetite. Pods of sulfide (pyrite, pyrrhotite, and chalcopyrite) are irregularly distributed in the oxide, and native copper fills narrow fractures. Green hydrous copper silicate and minor copper carbonate are widespread in fractures and on weathered surfaces in outcrops and in the open pit. Pods and lenses of calc-silicate skarn and local masses of jasper constitute further impurities, especially near granitic contacts. Because of these impurities the deposit is only a marginal source of iron ore (Leo and Genç, 1972).

Processes of emplacement.—The iron oxide deposits appear to have formed in the metadiabase by mobilization and subsequent redeposition of primary magnetite. As described earlier, magnetite is increasingly concentrated and segregated during progressive transformation of diabase through metadiabase, hornfels, and skarn. Redeposition of magnetite took place at least partly along structural planes, some of which probably were temporarily open; to this extent, the redeposited magnetite represents fracture fillings and is not of metasomatic origin. Crosscutting pods and the larger irregular lenses, on the other hand, clearly indicate that metasomatic replacement probably was the dominant process.

The existence of magnetite both as metasomatic replacement bodies and as fracture fillings shows that most of the magnetite was deposited relatively late. The common association of magnetite with epidote (fig. 6*D*), in some places as veinlets cutting earlier veins and pods of epidote, supports this impression and also indicates a comparatively low temperature of deposition. The apparent sequence of events was (1) granitic intrusion, accompanied by (2) progressive metamorphism of metavolcanic rocks from metadiabase through skarn, (3) contemporaneous mobilization of iron, and (4) redeposition of magnetite. A similar sequence, under successively falling temperatures, was determined for the contact-metasomatic magnetite deposits of southwestern British Columbia (Sangster, 1969).

Although the possibility cannot be ruled out that the granitic intrusion has introduced some of the iron of the magnetite deposits on Bakirlik Tepe, as is the case at some other contacts between granite and limestone in the region, this is unlikely, as there is no apparent contact between the walls of the pluton and the iron-oxide lenses, and only an inconsistent and incidental association exists between the latter and tabular granitic apophyses (fig. 4).

The question may be raised whether there could have been enough magnetite remobilized within the contact aureole to account for the deposits. Quantitative data for a rigorous examination of this question are lacking, but an origin by remobilization is supported by a simple model. When one uses

a volume of rock of 6,400,000 m^3 (the minimum zone of mineralization, 800 m long by 100 m wide by 80 m deep) and conservatively assumes 2 percent of this volume to be mobilized magnetite, this model gives 128,000 m^3 of magnetite. At a specific gravity of 5, this amounts to 624,000 metric tons—somewhat more than the tonnage estimated on the basis of borehole data.

OTHER IRON DEPOSITS

Kocaçal Tepe

The iron mineralization of Kocaçal Tepe is a contact-metasomatic replacement deposit in limestone, and thus is in distinct contrast to that of Bakirlik Tepe. The limestone block underlying Kocaçal Tepe, interpreted as a remnant of a post-Jurassic allochthon (Krushensky and others, 1972), was intruded by a granitic pluton in early Miocene time, and a sheet of diabase apparently was emplaced between the limestone and the pluton before the latter had entirely cooled, causing incipient metamorphism of the diabase (fig. 2, secs. $B–B'$, $C–C'$). A lens of rather pure slightly magnetic iron oxide (evidently magnetite largely altered to hematite), about 12 m thick, has formed between the crystalline limestone and metadiabase near the northern margin of the limestone block (fig. 2, $C–C'$). As the relationships shown in section $C–C'$ are based on limited data from one borehole, it is not definitely known that the hematitic body is a lens, or that it lies dominantly within limestone, as shown. It is assumed, however, that the ferruginous lens formed by replacement of limestone, and that the iron was supplied by the mafic magma.

This situation differs significantly from that at Bakirlik Tepe, where iron oxide concentrations appear to have been derived from metadiabase during contact metamorphism. Such an origin is improbable for the hematite body on Kocaçal Tepe where the metamorphic grade of the diabase does not exceed greenschist or lower amphibolite facies, and neither calc-silicate hornfels nor progressive segregation of magnetite were observed.

Although the possibility exists on Kocaçal Tepe, too, that the granitic pluton was a source of the iron, this is unlikely because the only metamorphic effect at the contacts between granodiorite and limestone on the south and west sides of the hill is the local development of diopside and garnet in crystalline limestone, with no iron oxides or other mineralization.

Area northeast of Şamli

An area of about 4 km^2, northeast of Şamli village, only the western part of which is shown in figure 2, is underlain by granitic rocks, crystalline limestone, metadiabase, and calc-silicate rocks, mostly covered by younger, poorly consolidated or unconsolidated sediments. Test pits show iron oxide mineralization both in calc-silicate rocks at Koyuntaş Tepe and in crystalline limestone at Menekşelik Tepe (fig. 2). Holes drilled on magnetic anomalies near these two locations penetrated magnetite bounded by crystalline limestone and, in a few places, by granitic rocks. Magnetite is more than 40 m thick in places and contains abundant impurities, including skarn (here evidently derived from limestone) and pyrite. The deepest, and possibly largest, of the magnetite lenses is more than 300 m below the surface.

Approximately 1,500 m east of Menekşelik Tepe, beyond the mapped area (fig. 2), drilling indicates that several iron oxide lenses are bordered by calc-silicate hornfels underlain by metadiabase, as on Bakirlik Tepe.

Exposures are generally so poor that no coherent picture of the geology could be obtained, so that interpretations of these iron deposits are highly speculative. Although some features are comparable to those on Bakirlik Tepe, the fact that several large magnetite lenses have formed in limestone near granitic rocks and away from any diabase suggests that these particular deposits are genetically related to the granitic intrusions.

Demirli Tepe

On and near Demirli Tepe, about 11 km east of Şamli (fig. 1), calc-silicate hornfels and skarn locally contain abundant magnetite at the contact between granitic rocks and crystalline limestone. The skarn zone is at least several hundred meters in extent. Magnetite and epidote together form late veins, fracture fillings, and replacement bodies in skarn. Two mined-out lenses were about 15 m long, and each contained an estimated several hundred metric tons of magnetite. This example of contact-metasomatic iron mineralization is much more typical than any other described herein, and is cited mainly to point up the remarkable variety of iron deposits in the Şamli area.

DISCUSSION AND CONCLUSIONS

The iron deposits of the Şamli area are unusual in at least two respects: (1) the variety in such a small area, and (2) the mobilization and redeposition of iron within mafic host rocks (at Bakirlik Tepe).

The Şamli deposits, then, are of at least two genetic categories. Those at Kocaçal Tepe, Demirli Tepe, and some of those northeast of Şamli, are of contact metasomatic origin, or the Magnitnaya type, named after Mount Magnitnaya in the eastern Urals (Zavaritsky, 1937; Gross, 1970, p. 16, 25–26), in which magnetite generally replaces limestone at or near contacts with granitoid intrusions. Most contact-metasomatic iron deposits in Turkey are of this general type (Gümüş 1964(?); Maden Tetkik ve Arama Enstitüsü, 1964).

In some major deposits of the Magnitnaya type, for example, those of southeastern Pennsylvania (Lapham, 1968; Sims, 1968), iron is considered to have originated by fractiona-

tion or differentiation from intruding diabase sheets. Such an origin is assumed for the hematite deposit at Kocaçal Tepe.

At Bakirlik Tepe, on the other hand, no external source of iron may be involved, and the deposits are not of contact metasomatic origin in the usual sense. Hagner, Collins, and Clemency (1963, p. 758) refer to such deposits as metamorphic-metasomatic deposits.

Magnetite deposits at Sterling Lake, N.Y., which show some similarities to those at Bakirlik Tepe, have been carefully studied and analyzed by Hagner, Collins, and Clemency (1963). At Sterling Lake, iron has been liberated (1) from amphibolite "granitized" to quartzo-feldspathic gneiss, and (2) from iron-bearing silicates of unreplaced amphibolite near the ore zone. The released iron is thought to have migrated via crystal lattices, grain boundaries, and structural planes in the rock, to be redeposited as magnetite in zones of low pressure related to metamorphic recrystallization. Mobilization of the iron is considered to have been induced by the regional metamorphism and "granitization"; no nearby magmatic intrusions were involved. Calculations show that the iron thus liberated and redistributed was more than enough to account for the known magnetite deposits.

Magnetite deposits at Ausable Forks, N.Y. (Hagner and Collins, 1959), possibly provide an even closer parallel to Bakirlik Tepe, in that the iron is thought to have been provided almost exclusively by accessory magnetite in the sheared gneissic country rock. A distinct drop in the magnetite content was documented adjacent to the ore zones, and again calculations indicated that the missing magnetite would have been ample to provide the necessary iron.

Desborough (1963) has postulated formation of magnetite-hematite ore bodies by iron liberated through replacement of magnetite-ulvöspinel by sphene in hydrothermally altered Precambrian gabbro in southeastern Missouri. The presence of secondary sphene in metadiabase and hornfels of Bakirlik Tepe indicates that a similar process may account for some of the mobilized iron.

The observations presented here indicate that metamorphic-metasomatic processes have been primarily responsible for the accumulation of the magnetite deposits at Bakirlik Tepe. This occurrence underscores the probability that other metallic deposits, heretofore interpreted either cursorily or conventionally as being of magmatic or hydrothermal origin, may also have in fact originated by concentration of metals already present in the host rocks (Hagner and others, 1963, p. 758, 764–765).

REFERENCES

Aygen, Temuçin, 1956, Balya Bölgesi jeolojisinin inçelenmesi (Étude géologique de la region de Balya): Maden Tetkik Arama Enst. Yayinlarindan (Mineral Research Explor. Inst. [of Turkey] Pub.), ser. D., no. 11, 95 p.

Desborough, G. A., 1963, Mobilization of iron by alteration of magnetite-ulvöspinel basic rocks in Missouri: Econ. Geology, v. 58, no. 3, p. 332–346.

Gross, G. A., 1970, Nature and occurrence of iron ore deposits, *in* Survey of world iron ore resources, occurrence and appraisal: New York, United Nations Dept. Econ. and Social Affairs, p. 13–31.

Gümüş, A., 1964(?), Iron ore deposits of Turkey, *in* Central Treaty Organization, Symposium on iron ore, Isphanan, Iran, October 2–5, 1963: [Ankara, Turkey?], p. 61–80.

Hagner, A. F., and Collins, L. G., 1959, Host rock as a source of iron, Ausable Forks magnetite district, New York [abs.]: Geol. Soc. America Bull., v. 70, no. 12, pt. 2, p. 1613–1614.

Hagner, A. F., Collins, L. G., and Clemency, C. V., 1963, Host rock as a source of magnetite ore, Scott mine, Sterling Lake, N.Y.: Econ. Geology, v. 58, no. 5, p. 730–768.

Kaaden, Gerrit van der, 1971, Basement rocks of Turkey, *in* Campbell, A. S., ed., Geology and history of Turkey: Petroleum Explor. Soc Libya Ann. Field Conf., no. 13, p. 191–209.

Krushensky, R. D., Akçay, Yavuz, and Karaege, Erdogan, 1972, Geology of an area east of Edremit, Biga Peninsula, northwestern Turkey: Maden Tetkik Arama Enst. (Mineral Research Explor. Inst. [of Turkey] Foreign Ed.). [In press]

Lapham, D. M., 1968, Triassic magnetite and diabase at Cornwall, Pennsylvania, *in* Ridge, J. D., ed., Ore deposits of the United States, 1933–1967 (Graton-Sales Volume), v. 1: New York, Am. Inst. Mining, Metall., and Petroleum Engineers, p. 72–94.

Leo, G. W., and Genç, M. A., 1972, Geology and iron deposits of the Şamli area, Balikesir province, Turkey: U.S. Geol. Survey open-file rept., 37 p.

Maden Tetkik ve Arama Enstitüsü 1964, Iron ore deposits of Turkey: Maden Tetkik Arama Enst. Yayinlarindan (Mineral Research Explor. Inst. [of Turkey] Pub.) 118, 56 p.

Sangster, D. F., 1969, The contact metasomatic magnetite deposits of southwestern British Columbia: Canada Geol. Survey Bull. 72, 85 p.

Sims, S. J., 1968, The Grace mine magnetite deposit, Berks County, Pennsylvania, *in* Ridge, J. D., ed., Ore deposits of the United States, 1933–1967 (Graton-Sales Volume), v. 1: New York, Am. Inst. Mining, Metall., and Petroleum Engineers, p. 108–124.

Turner, F. J., 1968, Metamorphic petrology–Mineralogical and field aspects: New York, McGraw Hill Book Co., 403 p.

Zavaritsky, A. N., 1937, Mount Magnitnaya, *in* Zavaritsky, A. N., ed., Uralian excursion–Southern part: Internat. Geol. Cong., 17th, U.S.S.R., 1937, p. 92–108.

DISTRIBUTION OF EARTHQUAKES RELATED TO MOBILITY OF THE SOUTH FLANK OF KILAUEA VOLCANO, HAWAII

By ROBERT Y. KOYANAGI; DONALD A. SWANSON, and ELLIOTT T. ENDO,
Hawaiian Volcano Observatory; Menlo Park, Calif.

Abstract.—Many earthquakes at Kilauea are related to magmatic (extrusive or intrusive) events within the caldera or along the rift zones. During the early stage of a rift event, earthquakes are often concentrated near the site of extrusion or intrusion. During and after the later stage of the event, earthquakes spread southeastward across the south flank away from the site of initial seismicity. The seismic data are consistent with geodetic measurements and suggest that the south flank of Kilauea is mobile and that the north flank is relatively stable.

Fiske and Kinoshita (1969) first proposed that the entire south flank of Kilauea Volcano (fig. 1), bounded by the east and southwest rift zones and by the Koae fault system, is being displaced seaward by the wedging action that accompanies forceful injection of dikes into the rifts (principally the east rift). They suggested that the north flank of Kilauea is a relatively stable block that is undergoing little or no displacement away from the rift zones. Swanson, Duffield, and Okamura (1971a, b) examined geodetic data for this century and found them to be mostly consistent with the Fiske and Kinoshita model. Analysis of the triangulation and trilateration data for part of the south flank indicates a maximum seaward displacement of about 4.5 m since 1914, and recent geodimeter measurements have been used to key specific magmatic events along the upper east rift to measured seaward displacement of the south flank.

The large magnitude of this displacement and the fact that it is still continuing suggest that the recent record of seismicity of the south flank should show a clear relation to the magmatic events that caused the displacements. We show in this paper that such a relation does exist and that it supports the south-flank model of Fiske and Kinoshita (1969) and Swanson, Duffield, and Okamura (1971a, b).

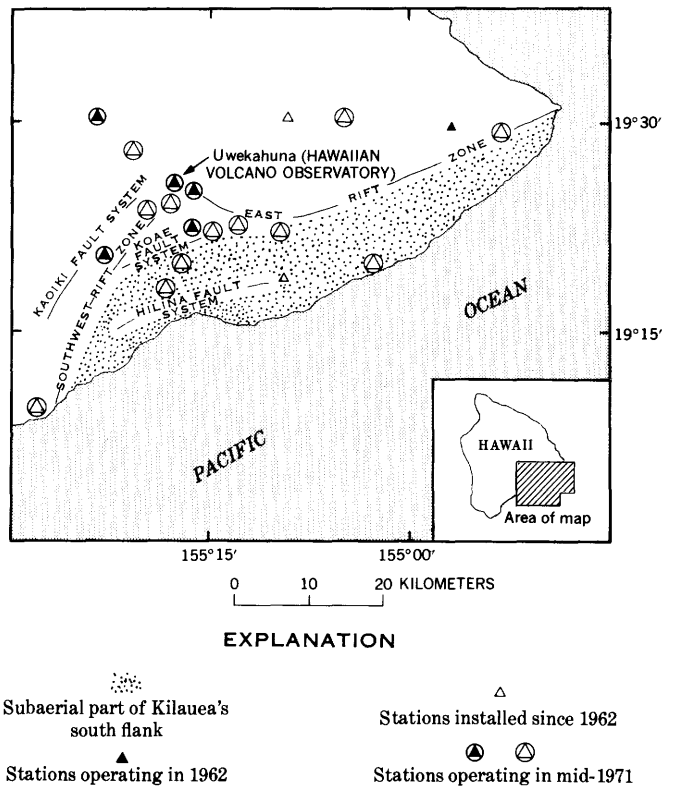

Figure 1.—Index map showing major structural features of Kilauea Volcano and locations of Hawaiian Volcano Observatory seismic stations.

THE SEISMIC NET AND OTHER TECHNICAL ASPECTS

The network of seismic stations maintained by the Hawaiian Volcano Observatory consists primarily of short-period instruments operated at high magnification to record local events (Koyanagi, 1968b). The network at Kilauea is constantly being expanded and improved, and 14 new stations have been installed since 1962, although two of these stations were operated only temporarily. As of mid-1971, 17 of the Observatory's 28 stations are located where they can extensively monitor the seismic activity of the Kilauea volcanic complex (fig. 1); their signals are telemetered to the observatory and recorded on Develocorder 16-mm strip film.

U.S. GEOL. SURVEY PROF. PAPER 800-D, PAGES D89-D97

Formerly, earthquake data were processed manually with the aid of traveltime charts. In 1969, the operation was converted to computer processing, which led to a systematic documentation of large quantities of data (Koyanagi and Endo, 1971). The determination of earthquake hypocenters is based on Eaton's Model B, a layered velocity model (Eaton, 1962):

Depth to layer (km)	*Layer velocity (km/sec)*
0.00	3.90
3.10	5.00
11.20	6.80
14.80	8.25

After most of the earthquakes considered in this paper had been processed, trial determinations were made for a selected number of events, using an alternative model based on seismic refraction data compiled by Hill (1969). For earthquakes beneath Kilauea's south flank, the two models show only slight differences in epicentral locations, but focal depths appear to be about 2 km shallower with Hill's model. Additional considerations, such as traveltime anomalies, irregular station distribution, and differences of station elevations not accounted for in our calculations, suggest that several kilometers of error should be expected in the focal-depth determination. Recently, comprehensive studies oriented toward examining the accuracy of earthquake locations in Hawaii were being made by P. L. Ward, of the U.S. Geological Survey (oral commun., 1972).

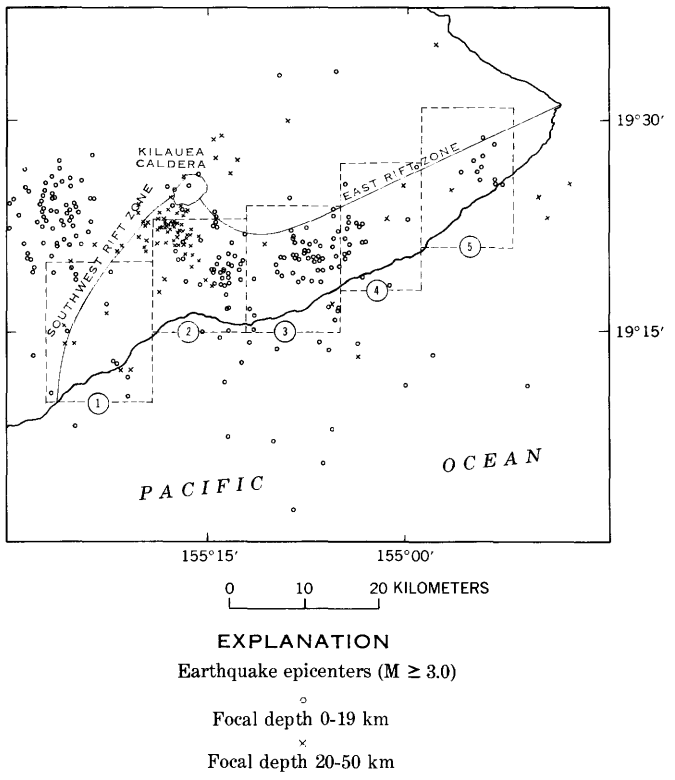

Figure 2.—Epicenters of earthquakes of magnitude 3.0 or greater located within or beneath Kilauea for the period 1965–70. The distribution of the shallow quakes along the south flank is arbitrarily subdivided into five groups, as shown by dashed lines and circled numbers. These events are heavily concentrated in groups 2 and 3 adjacent to and south of the areas of recent volcanic activity.

GENERAL SEISMIC PATTERN AROUND KILAUEA

Most of Hawaii's seismic activity is centered on the active volcano of Kilauea. Figure 2 shows the distribution of earthquakes of magnitude 3 (modified after Richter scale) or larger for the period 1965–70; the distribution of smaller quakes is nearly similar, except for somewhat more localized occurrences around the caldera complex and rift zones. The persistent seismic zones within the volcano are presumably the result of stresses ultimately generated by the continuous ingress of magma. In addition to a highly seismic region beneath the caldera, earthquakes are concentrated along the rift zones and adjacent fault systems. The high frequency of eruptions on the east rift in recent years (table 1) has been accompanied by high seismic activity in that area. The lower and more distant parts of the rift zones have recently been only spasmodically seismic, with moderate flurries occurring once or twice a year. Another source of earthquakes, 10 to 15 km west of Kilauea Caldera beneath the northwestern part of the Kaoiki fault system, may be related to the stresses generated within Kilauea because of loading by the Mauna Loa volcanic system.

Earthquakes outside the summit area of Kilauea are scattered along the southwest rift and are strongly concentrated on the south side of the central and western parts of the east rift. Earthquakes with focal depths of less than 15 km (that is, those mainly within the crust) are distributed parallel to the major rift and fault zones. However, earthquakes deeper than 15 km cluster beneath the region south of the summit and scatter quite conspicuously to the southwest; these earthquakes conform only slightly to surface traces of the rift zones and fault systems.

EFFECT OF THE RIFT ZONES ON EARTHQUAKE DISTRIBUTION

Shallow (less than 15 km deep) seismic activity on the south flank is bounded by the rift zones, particularly by the east rift (fig. 2). Many earthquakes take place along and to the south of the east rift but not to the north; the rift zone itself acts as the northern boundary of the seismic region. Consequently, a highly seismic east rift and south flank contrast strikingly with an aseismic zone north of the rift.

The asymmetric distribution is less conspicuous along the southwest rift because of moderate seismicity on both sides of the rift. The seismically active southwest rift is complemented

Table 1.—*Kilauea eruptions and seismic swarms associated with movement of magma between 1962 and 1969*

[Asterisks (*) denote well-recorded events from which earthquakes were located and plotted in figure 7]

Date	Nature of event	Approximate number of small earthquakes	Relative intensity of tremor	Relative summit deflation indicated by tiltmeter at Uwekahuna
December 1962	Eruption: east rift.	500	Moderate.	Moderate-slight.
*May 1963	Earthquake swarm: Koae fault system, southwest rift.	3,000	Weak.	Do.
*July 1963	Earthquake swarm: Koae fault system, east rift.	2,000	....do.....	Do.
*August 1963	Eruption: east rift.	1,000	Moderate.	Slight.
*October 1963	.....do.....	1,000	....do.....	Moderate.
*March 1965	.....do.....	1,000	....do.....	Do.
*December 1965	Eruption: east rift and Koae fault system.	10,000	Moderate-weak.	Do.
November 1967 to July 1968	Eruption: summit.	.....	....do.....	Slight.
*August 1968	Eruption: east rift.	500	Moderate.	Moderate.
*October 1968	.....do.....	1,000	....do.....	Do.
*February 1969	.....do.....	500	....do.....	Do.
May 1969	.....do.....	.....	Moderate-weak.	Moderate-slight.

by equally active areas to the northwest and along the adjacent Kaoiki fault system of Mauna Loa; the area about 15 km west of Kilauea Caldera makes up an especially active seismic zone (figs. 1 and 2). However, any given shallow earthquake swarm or main shock-aftershock sequence that originates on the southeast side of the rift has its epicentral distribution confined along or southeast of the rift. Conversely, earthquakes associated with usual "Kaoiki" swarms and aftershock sequences do not occur southeast of the rift. This mode of occurrence is generally suggested by quarterly and annual plots of earthquake epicenters at Kilauea (Koyanagi, 1968a; 1969a, b, c; Koyanagi and Endo, 1971), which show eipcentral concentrations either northwest or southeast of the rift, depending on the type of activity for a particular period. In general, then, the highly fractured east and southwest rifts appear to disrupt strain release patterns and significantly affect the distribution of earthquakes with depths less than 15 km.

RIFT AND SOUTH-FLANK SEISMIC EVENTS RELATED TO MAGMATIC ACTIVITY

Rift and south-flank earthquakes are related in time and space to extrusive activity or inferred intrusive activity unaccompanied by eruption (fig. 3). Earthquakes are more common during extrusive or intrusive episodes and in areas closest to the site of the magmatic activity. This association is straightforward and of utmost importance, for it virtually proves that seismicity is directly and genetically related to the intrusive and extrusive processes.

During the past 10 years, eruptive activity along the central and western part of the east rift was associated with many earthquakes, harmonic tremor, and contraction of Kilauea's summit region. The contraction is interrupted to result from transfer of magma from beneath the summit, where it is presumably held in a storage reservoir, toward the site of eruption. Several earthquake swarms have accompanied summit contraction without eruptive activity (table 1); these events are interpreted as intrusive episodes, during which magma moved from beneath the summit into the east rift and was emplaced as dikes. Earthquakes associated with such intrusive events have been located in the western part of the east rift zone and the neighboring part of the Koae fault system. In contrast, earthquake flurries that occurred along the eastern part of the east rift (area 5 in fig. 2) were unaccompanied by summit contraction and hence are not considered to have recorded migration of magma from the summit reservoir. Similarly, isolated moderate-sized earthquakes and aftershock sequences in the Hilina and Kaoiki fault systems were apparently not related directly to concurrent magmatic processes, but probably to long-term structural adjustments which indirectly result from these processes.

SEQUENCE OF EARTHQUAKES AFTER MAGMATIC EVENTS IN THE EAST RIFT

During the early stage of intrusive and extrusive events, earthquakes occur primarily at shallow depths (about 5 km or less) near the eruptive fissures, the intrusion, or active faults inferred to slip as a result of intrusion. In the subsequent period of rapidly increasing magmatic activity, earthquakes and harmonic tremor are so numerous that they largely obscure individual small earthquakes (often those of magnitude less than 2.0) on the seismograms. Such high intensities are usually short lived, persisting for less than a day during the peak times of activity. As the magmatic activity continues, the earthquakes scatter broadly throughout the south flank, but principally southeast of the initial center along an azimuth roughly perpendicular to the trend of the fissure and fault

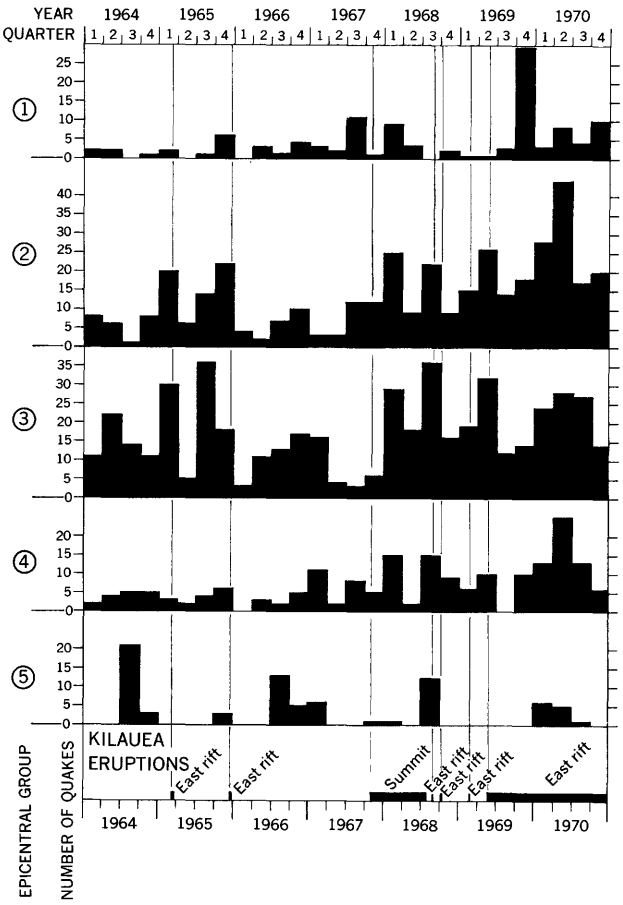

Figure 3.—Frequency of earthquakes grouped into the five geographic areas along the south flank of Kilauea shown in figure 2. The number of quakes for each group is plotted quarterly and compared with periods of extrusive activity. All earthquakes with magnitude 2.0 or greater and focal depths of less than 15 km are shown. There is a general tendency for periods of high extrusive activity to be accompanied by increased seismic activity along the upper and middle parts of the east rift zone and to some degree along the southwest rift. Periods with few or no eruptions tend to have comparatively weak seismic activity.

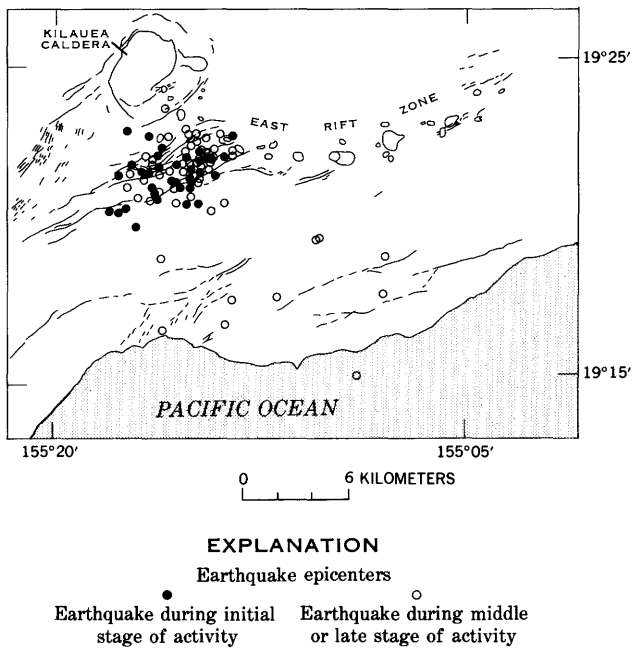

Figure 4.—Epicenters of earthquakes located during the Koae-east rift seismic episode and the Kilauea summit contraction in July 1963. These earthquakes ranged in magnitude from 1.5 to 3.8, and focal depths were generally 10 km or less. Earthquakes during the initial 4-day period of activity were located near the active major fault system and east rift; those during the later 4-day period of activity were scattered to the south and at greater depth.

zones (fig. 1; Moore and Koyanagi, 1969, fig. 1; Wright and Kinoshita, 1968, p. 3188). These later earthquakes have a wider range in depth (Koyanagi and Endo, 1971), and some are as deep as about 10 km. During the largest magmatic events, an almost immediate increase in south-flank seismicity is noticeable. In the days after the initial magmatic activity, the epicentral region spreads southeastward, sometimes for more than 18 km.

One example of such a sequence of events took place during the intrusive event of July 1963 (figs. 4 and 5), which was accompanied by marked contraction of Kilauea's summit (for a comparable event in May 1963, see Kinoshita, 1967). During the first 4 days of this event, earthquakes occurred within or very close to the Koae fault system, which was interpreted to have been affected by the intrusive event. For 4 days after the principal event, abnormally high earthquake activity took place on the south flank, some epicenters being located as far as 14 km southeast of the fault system. Several additional earthquakes occurred on the south flank during the following 2 weeks (fig. 5).

Figures 6 and 7 show compilations of nine earthquake swarms from the east and southwest rifts (table 1) similar to that of July 1963. Some of these swarms accompanied eruptions, and others, intrusive events. The compilations clearly show the same trends as the isolated July 1963 event and indicate that, as a general rule, the epicentral area enlarges southeastward away from the east rift zone and from the Koae fault system after a particular magmatic event begins.

The first southwest-rift eruption since 1920 took place on September 24 to 29, 1971, while this paper was being prepared. Numerous earthquakes occurred within the south flank south of the site of eruption. The seismic activity continued almost constantly at high levels for a month after the eruption and in sporadic swarms for several months thereafter. Seismicity was highest beneath the western part of the south flank, especially near the intersecting area of the Hilina fault system and the southwest rift. A major earthquake swarm occurred in this region in late December 1971; several dozen earthquakes of about magnitude 3 to 5 were recorded and felt by residents of southern Hawaii.

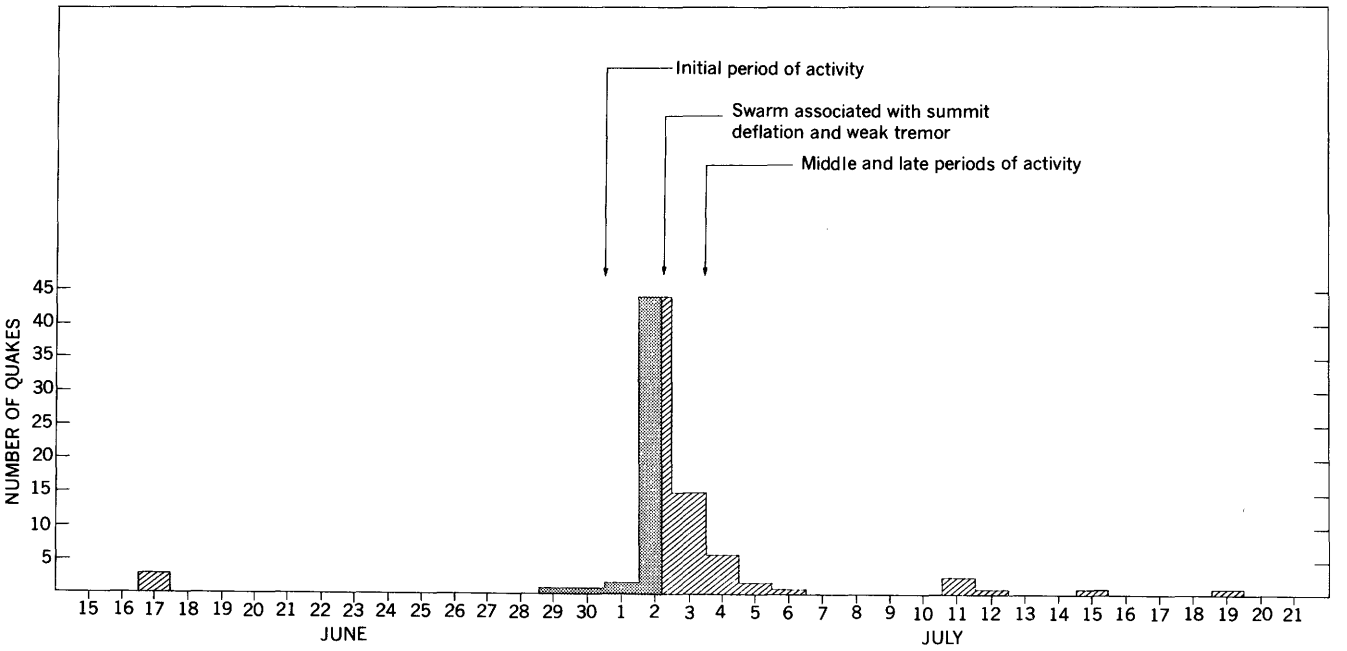

Figure 5.—Daily frequency pattern for small earthquakes during the July 1963 Koae-east rift seismic swarm. The shaded area indicates the early period when earthquake epicenters concentrated along the Koae faults and east rift; the ruled area following indicates the period when earthquake hypocenters scattered southeastward.

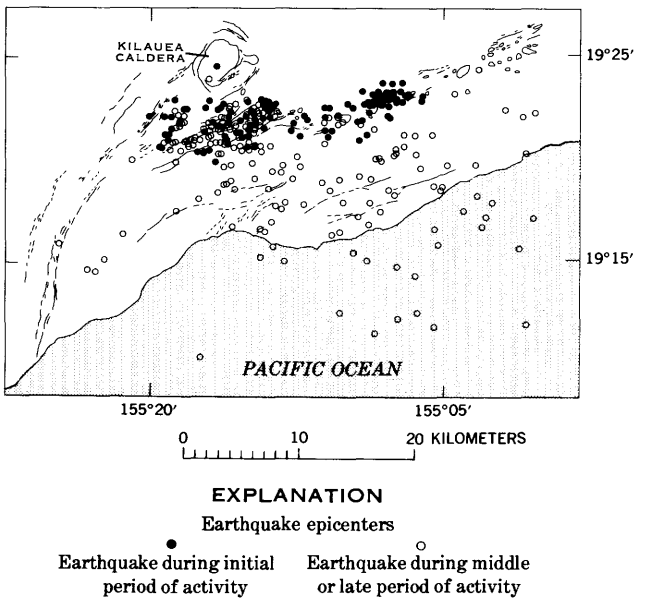

Figure 6.—Compilation of earthquake epicenters from short seismic swarms apparently associated with magmatic processes from 1963 to 1969. Earthquakes selected are of magnitude 2.0 and greater and depth less than 15 km. The epicenters were plotted according to two time categories in which they occurred. Earthquakes during the initial stages of activity were concentrated near the outbreak area along the Koae faults and east rift. Earthquakes during the middle and late stages scattered far to the south.

Preliminary focal determinations for the south-flank earthquakes of September–December 1971 suggest that depths were generally less than 10 km, using Eaton's Model B. Comparable to the earthquakes located on the eastern part of the south flank, these earthquakes also concentrated within the crust. The pattern of seismic activity after the southwest-rift eruption appears to be similar to that after east rift and Koae events, because the distribution of epicenters widened seaward with time.

AFTERSHOCK ACTIVITY WITHIN THE SOUTH FLANK

Do the widening of epicentral distribution southeastward from the site of magmatic activity and the deepening of foci simply reflect a "normal" relation between main shock and aftershocks? The asymmetry of epicentral distribution suggests otherwise. To further investigate this possibility, we examined several definite aftershock sequences on the south flank (figs. 8 and 9). Some of the largest quakes (magnitudes between 3.5 and 5.5) beneath the south flank are associated with aftershock activity. The magnitude of the main shock and the stress conditions of the rocks appear to determine the extent of the aftershocks, and as many as several hundred shocks of magnitude 0.1 to 2.5 may occur within several hours after the main shock. Most of the main shock-aftershock sequences occurred along the fault systems south of the east rift, and

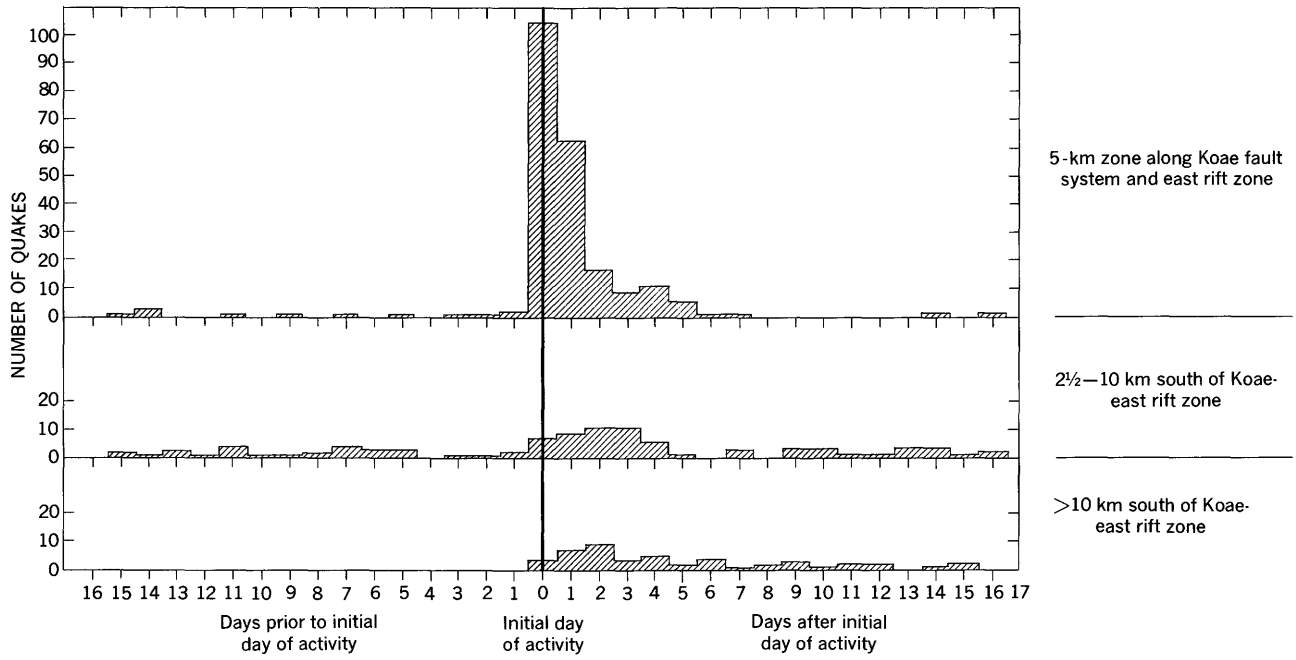

Figure 7.—Frequencies of earthquakes associated with some short extrusive or intrusive episodes between 1963 and 1969 (see table 1). The numbers of earthquakes were plotted according to various epicentral distances south of the Koae fault system and the east rift zone. Earthquakes plotted are of magnitude 2.0 or greater and depth less than 15 km. The graphs show the increased number of shallow- to intermediate-depth earthquakes along the south flank during the first and second weeks after the start of the magmatic event.

their epicentral zones were elongate parallel to the major trend of the rift and fault system, instead of broadly perpendicular to the trend, as are those of earthquakes related to magmatism. Moreover, the aftershocks occurred in a zone completely surrounding the main shock, instead of in a zone confined to the seaward side, as do magmatic earthquakes. The most extensive series of aftershocks occurred in areas of only about 50 km^2 (figs. 8 and 9). The epicentral area outlined by aftershocks after a moderate-sized earthquake is thus relatively limited compared to the wide distribution of earthquakes after magmatic episodes (compare figs. 4 and 6 with 8 and 9). The mechanisms involved in a sizable magmatic event apparently cause the release of strain across larger areas than do single earthquakes of magnitude 4 or 5 along the south flank of Kilauea.

STRESS AXES

Preliminary results of a focal mechanism study being carried out by Endo and Koyanagi suggest that the orientation and sense of stress axes of well-located south-flank earthquakes (all of which have focal depths of 5 km or more) follow a consistent pattern. Figure 10 shows that most of the maximum stress axes are oriented southeast and plunge gently seaward. The average azimuth is within 20° of a normal to the trend of east-rift fissures and Koae faults.

SUMMARY OF PRINCIPAL RESULTS

1. Earthquakes outside the summit area of Kilauea generally take place along or seaward of the rift zones and the Koae fault system.
2. Many of these earthquakes are related in space and time to magmatic events, either extrusive or intrusive.
3. Most earthquakes during the early stage of a magmatic event are located along the rifts or along the Koae fault system at depths of 5 km or less.
4. Many of the earthquakes during the later stages of or immediately after a magmatic event are located seaward of the initial activity at depths of as much as 10 km.
5. Aftershocks of "tectonic" earthquakes not immediately related to magmatic events show a different pattern of occurrence than magmatic earthquakes.
6. Maximum stress axes of most south-flank earthquakes plunge gently seaward and are oriented within 20° of a normal to the trend of east-rift fissures and Koae faults.

DISCUSSION AND COMPARISON WITH RESULTS OF GEODETIC STUDIES

The seismic data presented in this paper indicate that the south flank of Kilauea undergoes deformation during episodes of magmatic activity in or near the rift zones. The north flank, however, is not seismically active, consistent with horizontal

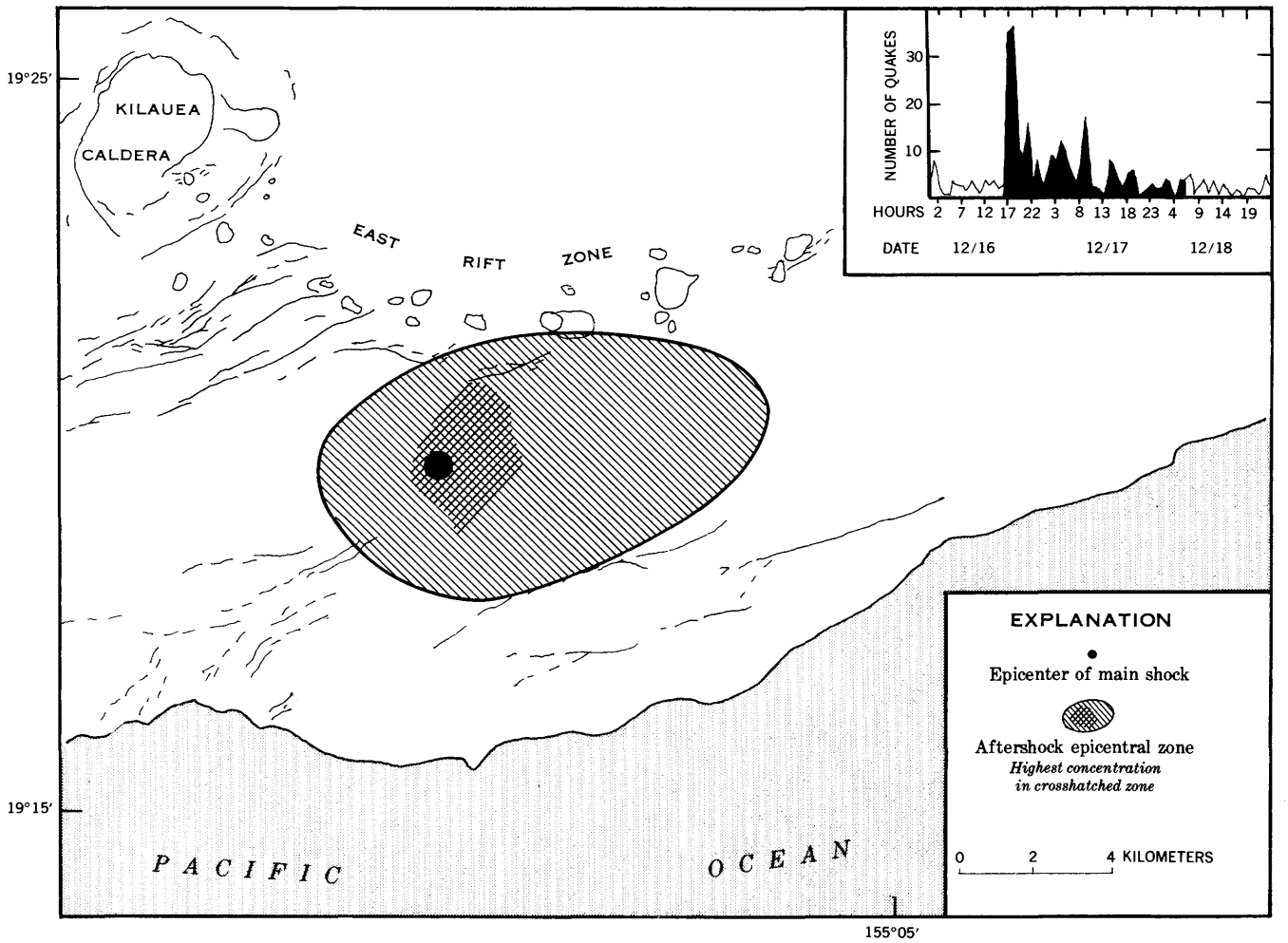

Figure 8.—Aftershock sequence from a magnitude-4.7 earthquake on December 16, 1968, located on the south flank at a depth of about 10 km. Map shows location of the main shock, the zone of concentrated aftershock activity, and the extent of the epicentral zone in relation to conspicuous structural features. Inset shows hourly frequency pattern; the darkened area indicates the period of aftershock activity.

and vertical geodetic observations (Swanson and others, 1971b) that show it is a relatively stable block in the Kilauea structure.

Flurries of south-flank earthquakes that are related directly to magmatic activity take place after, not before, the initial phase of the eruption or intrusive episode. Thus the earthquakes are a response to, and not a precursor of, the magmatism. Swanson and others (1971b) reached the same conclusion on the basis of recent geodimeter studies, which show that episodes of seaward-directed displacement of the south flank can be keyed to specific magmatic events that took place slightly earlier. These relations suggest that the south flank deforms in response to stresses induced by forceful dike intrusion, rather than in response to some process unrelated to magmatism. It thus seems reasonable that, as Fiske and Kinoshita (1969) suggested, magma injected as dikes into the rift zones makes room for itself by wedging the south flank seaward.

Over a period of a few days, earthquakes spread southeastward from the site of extrusion or intrusion, implying that an increasingly large part of the south-flank block is responding to magmatic stresses; eventually the entire block is probably displaced seaward away from the rift zone. South-flank seismicity usually peaks several days after the first day of magmatic activity (fig. 7), but abnormally high earthquake counts continue for 2 weeks or more. Geodimeter studies (Hawaiian Volcano Observatory, unpub. data), however, suggest a lag time of 2 to 4 weeks between the onset of a magmatic event and seaward displacement of the south flank at a point about 6 km southeast of the western part of the east rift. This major observed displacement event seems to be unaccompanied by significant seismic activity. Instead, the earthquakes apparently record the first stages of this displacement at depth, perhaps marking the initial opening of the fractures along which major seaward displacement ultimately takes place.

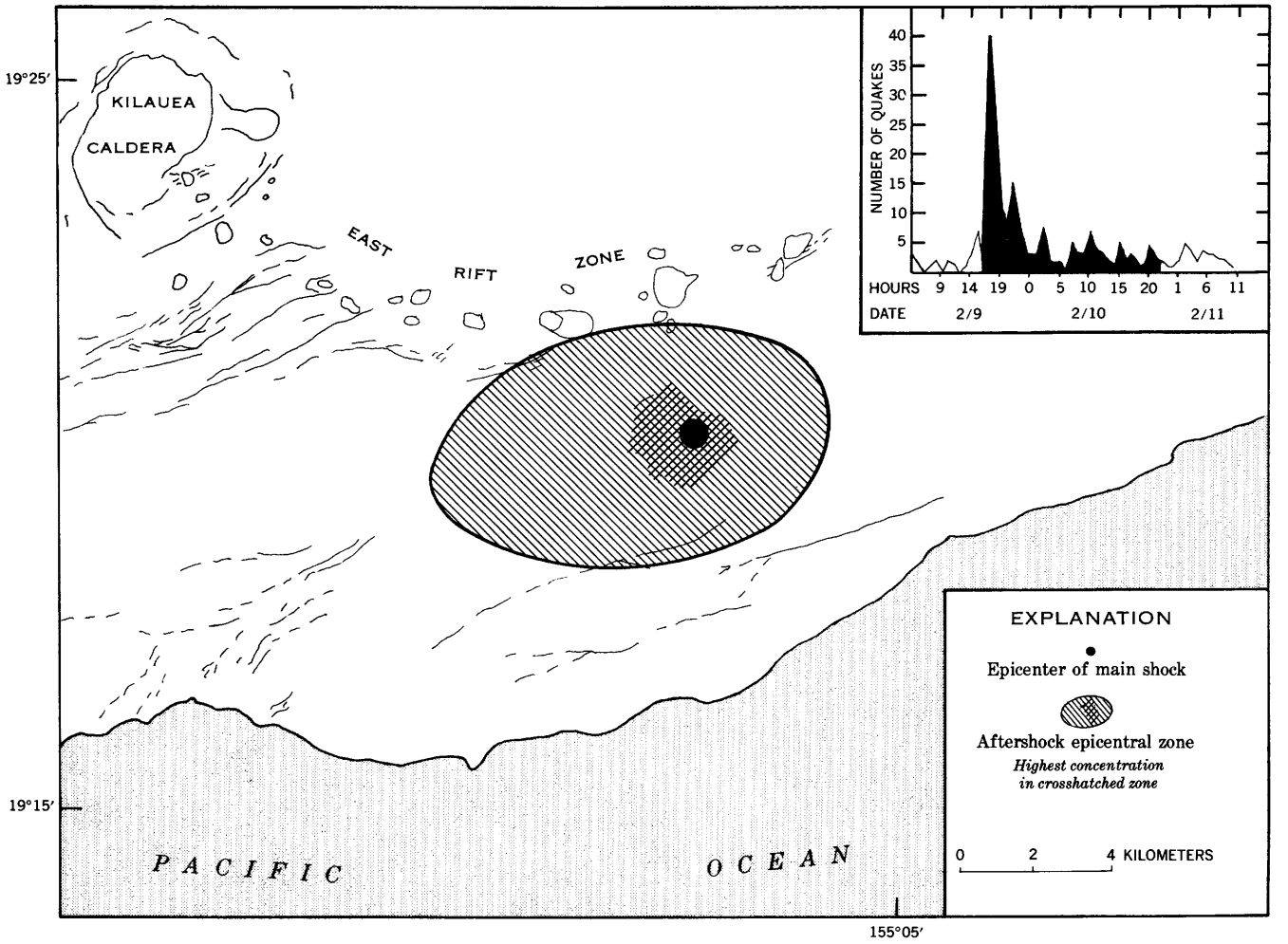

Figure 9.— Aftershock sequence from a magnitude-4.1 earthquake on February 9, 1969, located on the south flank at a depth of about 10 km. Map shows location of the main shock, the zone of concentrated aftershock activity, and the extent of the epicentral zone in relation to conspicuous structural features. Inset shows hourly frequency pattern; the darkened area indicates the period of aftershock activity.

Geodetic studies (Swanson and others, 1971a, b) indicate that the azimuth of displacement of the south flank is approximately at right angles to the trend of the east-rift fissures and Koae faults. The maximum stress axes (fig. 10) are generally within 10° to 20° of this direction. This approximate agreement in direction is surprising, considering the preliminary nature of the focal mechanism study. At present, however, the consistency of orientation of the stress axes, rather than their exact azimuth, is probably of most significance.

The south-flank earthquakes reach depths of 10 to 12 km (8 to 10 km using Hill's [1969] model), which is approximately the depth of the old sea floor on which Kilauea is built (Hill, 1969). These depths suggest that the entire south flank down to the old sea floor is being displaced away from the rest of the volcano.

A general model relating earthquakes to south-flank deformation can be suggested. With vigorous diking, probably by a process similar to hydrofracturing, rocks within the rift zone are rapidly strained beyond elastic limits, and swarms of small earthquakes exhibiting a narrow range of magnitudes are recorded. The intruding magma finally stops splitting the wallrock when magmatic pressure is relieved sufficiently, and conduits slowly widen to allow smoother passage; the earthquake swarms and, eventually, harmonic tremor diminish. To accommodate the new magma within the rift system, that part of the south-flank block adjacent to the intrusion is displaced seaward. In the subsequent stages of activity, stresses resulting from this displacement spread outward and deeper within the mobile south flank (Moore and Koyanagi, 1969), leading consequently to displacement of the entire south-flank block. The late-stage stresses are distributed over a wider area, and

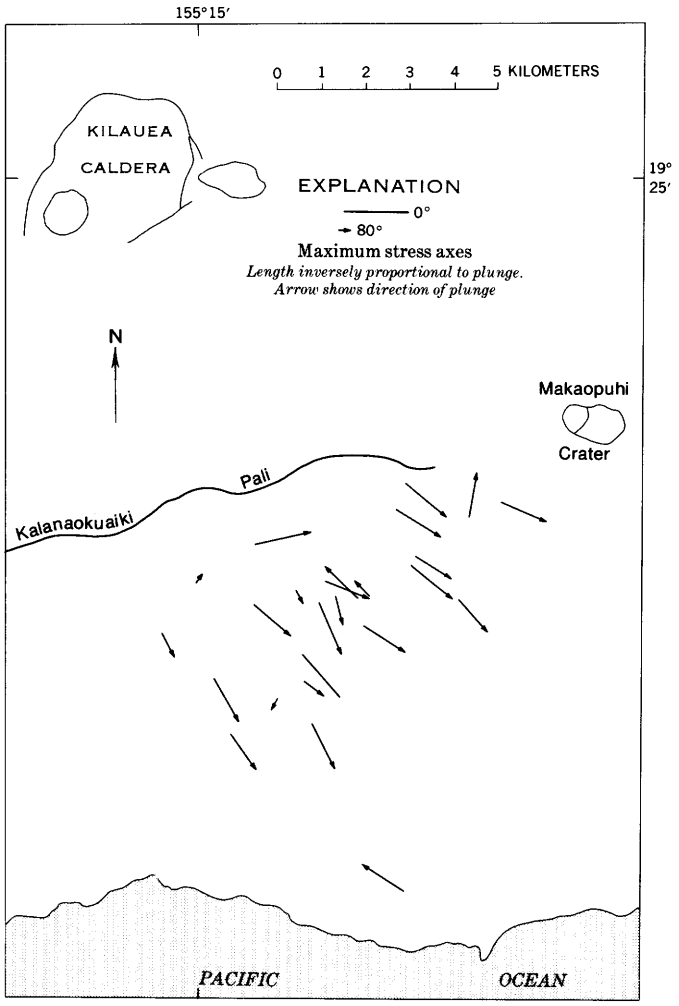

Figure 10.—Maximum stress axes for well-located south-flank earthquakes from October 1969 to March 1970 inclusive. Most axes plunge very gently southeastward. Kalanaokuaiki Pali is a cliff bounded by the southernmost fault in the Koae fault system, and Makaopuhi Crater is a conspicuous pit crater on the east rift.

the intensity of the activity is relatively reduced, so that rocks within the south flank begin to strain at slower rates. In the postmagmatic period, the earthquakes assume behavior more commonly observed in tectonic regions, displaying a wider range of magnitudes and occasional aftershock activity.

REFERENCES

Eaton, J. P., 1962, Crustal structure and volcanism in Hawaii; Am. Geophys. Union Geophys. Mon. 6, p. 13–29.

Fiske, R. S., and Kinoshita, W. T., 1969, Rift dilation and seaward displacement of the south flank of Kilauea Volcano, Hawaii, *in* Symposium on volcanoes and their roots, Oxford, England: Internat. Assoc. Volcanology and Chemistry of the Earth's Interior, p. 53–54.

Hill, D. P., 1969, Crustal structure of the island of Hawaii from seismic-refraction measurements: Seismol. Soc. America Bull., v. 59, no. 1, p. 101–130.

Kinoshita, W. T., 1967, May 1963 earthquakes and deformation in the Koae fault zone, Kilauea Volcano, Hawaii, *in* Geological Survey Research 1967: U.S. Geol. Survey Prof. Paper 575-C, p. C173–C176.

Koyanagi, R. Y., 1968a, Hawaiian seismic events during 1965, *in* Geological Survey Research 1968: U.S. Geol. Survey Prof. Paper 600-B, p. B95–B98.

—— 1968b, Earthquakes from common sources beneath Kilauea and Mauna Loa volcanoes in Hawaii from 1962 to 1965, *in* Geological Survey Research 1968: U.S. Geol. Survey Prof. Paper 600-C, p. C120–C125.

—— 1969a, Hawaiian seismic events during 1966, *in* Geological Survey Research 1969: U.S. Geol. Survey Prof. Paper 650-B, p. B113–B116.

—— 1969b, Hawaiian seismic events during 1967, *in* Geological Survey Research 1969: U.S. Geol. Survey Prof. Paper 650-C, p. C79–C82.

—— 1969c, Hawaiian seismic events during 1968, *in* Geological Survey Research 1969: U.S. Geol. Survey Prof. Paper 650-D, p. D168–D171.

Koyanagi, R. Y., and Endo, E. T., 1971, Hawaiian seismic events during 1969, *in* Geological Survey Research 1971: U.S. Geol. Survey Prof. Paper 750-C, p. C158–C164.

Moore, J. G., and Koyanagi, R. Y., 1969, The October 1963 eruption of Kilauea Volcano, Hawaii: U.S. Geol. Survey Prof. Paper 614-C, 13 p.

Swanson, D. A., Duffield, W. A., and Okamura, R. T., 1971a, Seaward displacement of the south flank of Kilauea Volcano: Am. Geophys. Union Trans., v. 52, no. 4, p. 372.

—— 1971b, Mobility of Kilauea's south flank related to rift instrusion: Gen. Assembly of Internat. Union Geodesy and Geophysics, 15th Sec. Moscow, U.S.S.R., of the Internat. Assoc. Volcanology and Chemistry of the Earth's Interior, p. 29.

Wright, T. L., and Kinoshita, W. T., 1968, March 1965 eruption of Kilauea volcano and the formation of Makaopuhi lava lake: Jour. Geophys. Research, v. 73, no. 10, p. 3181–3205.

STRONTIUM ISOTOPIC COMPOSITION OF SOME EARLY MIOCENE RHYOLITIC TUFFS AND LAVAS FROM NORTHWESTERN PART OF THE GREAT BASIN

By E. H. McKEE; D. C. NOBLE, C. E. HEDGE; and H. F. BONHAM,
Menlo Park, Calif.; Denver, Colo.; Reno, Nev.

Abstract.—Eleven rhyolitic ash-flow tuffs and lavas of early Miocene age and two tuffs of Oligocene age from the northwestern Great Basin have initial Sr^{87}/Sr^{86} ratios of 0.7046 to 0.7059, with a median of 0.7052. The values are well within the range found for late Cenozoic basalts from the central and northern Great Basin and thus are consistent with production of the silicic magmas by fractional crystallization of mafic magma. The initial Sr^{87}/Sr^{86} ratios appear to be too low to permit generation by partial melting or large-scale assimilation of pre-Cenozoic salic crustal material.

GEOLOGIC SETTING AND ROCKS STUDIED

Silicic volcanic rocks, mainly ash-flow tuffs, were erupted over a large part of the Basin and Range province during late Oligocene and early Miocene time. Most of the lower Miocene rocks in northwestern and central Nevada are highly to very highly differentiated subalkaline rhyolites with silica contents of 75 to 77 weight percent and very low MgO, CaO, Sr, and Ba contents. Ash-flow tuffs are much more abundant than lavas, although voluminous lavas are locally present in northwestern Nevada. The Fish Creek Mountains Tuff (McKee, 1970), which occupies the southern part of the Fish Creek Mountains in Lander County, was erupted from an equant vent area, and it seems likely that most or all of the ash-flow sheets of early Miocene age were erupted from either central or arcuate fissure vents. As most Basin and Range faulting did not commence until after the eruption of the early Miocene tuffs (McKee and others, 1970; Noble and others, 1970), it seems very unlikely that the tuffs were erupted from linear vents localized by normal (Basin and Range) faulting.

With the exception of the Fish Creek Mountains Tuff (fig. 1, No. 12), the exact vent locations for the ash-flow units studied here are not known. However, the approximate locations of the vent areas are known from the distribution of the units. Specimens 1–5 (table 1) were erupted from vents located in southern Washoe, Storey, Lyon, and (or) possibly western Churchill Counties (fig. 1). Specimen 6 was erupted from a vent area in west-central Hamboldt County, and specimen 9 had its source in western Lander or eastern Churchill County. The source of the Bates Mountain Tuff (specimens 10 and 11) is poorly known, but thickness and distribution relations suggest a source in central Lander County. The source of specimen 13 probably was in southern Lander or north-central Nye County.

METHODS OF ANALYSIS

Most of the analyses were made on feldspar phenocryst separates that have lower Rb/Sr ratios and higher strontium contents than whole-rock material, thereby minimizing errors resulting from uncertainties in the correction for radiogenic strontium produced since eruption. Analysis of the phenocryst fraction also eliminates errors resulting from possible groundwater addition of strontium having an isotopic composition different from that of the rock. In some silicic volcanic rocks the strontium in feldspar phenocrysts has a higher Sr^{87}/Sr^{86} ratio than that in the remainder of the rock (Noble and Hedge, 1969; Dickinson and Gibson, 1972). Thus, if isotopic disequilibrium existed prior to eruption in the rocks under study, the magmatic liquid probably was less radiogenic than the associated feldspar crystals.

Strontium isotopic composition was measured on a 6-inch, 60°-sector mass spectrometer using a triple-filament mode of ionization and digital collection of data. Measured ratios were normalized to a Sr^{86}/Sr^{88} ratio of 0.1194. The mass spectrometer used gives a value of 0.7080 for the Eimer and Amend standard $SrCO_3$. Based on numerous replicate analyses, the precision of a single analysis is ±0.0002 at the 95-percent-confidence level. Rb/Sr ratios were determined using X-ray fluorescence methods.

DATA AND DISCUSSION

Observed and calculated initial Sr^{87}/Sr^{86} ratios of 11 lower Miocene silicic volcanic rocks and two Oligocene rocks are given in table 1. The initial strontium isotope ratios of the Miocene

U.S. GEOL. SURVEY PROF. PAPER 800-D, PAGES D99-D102

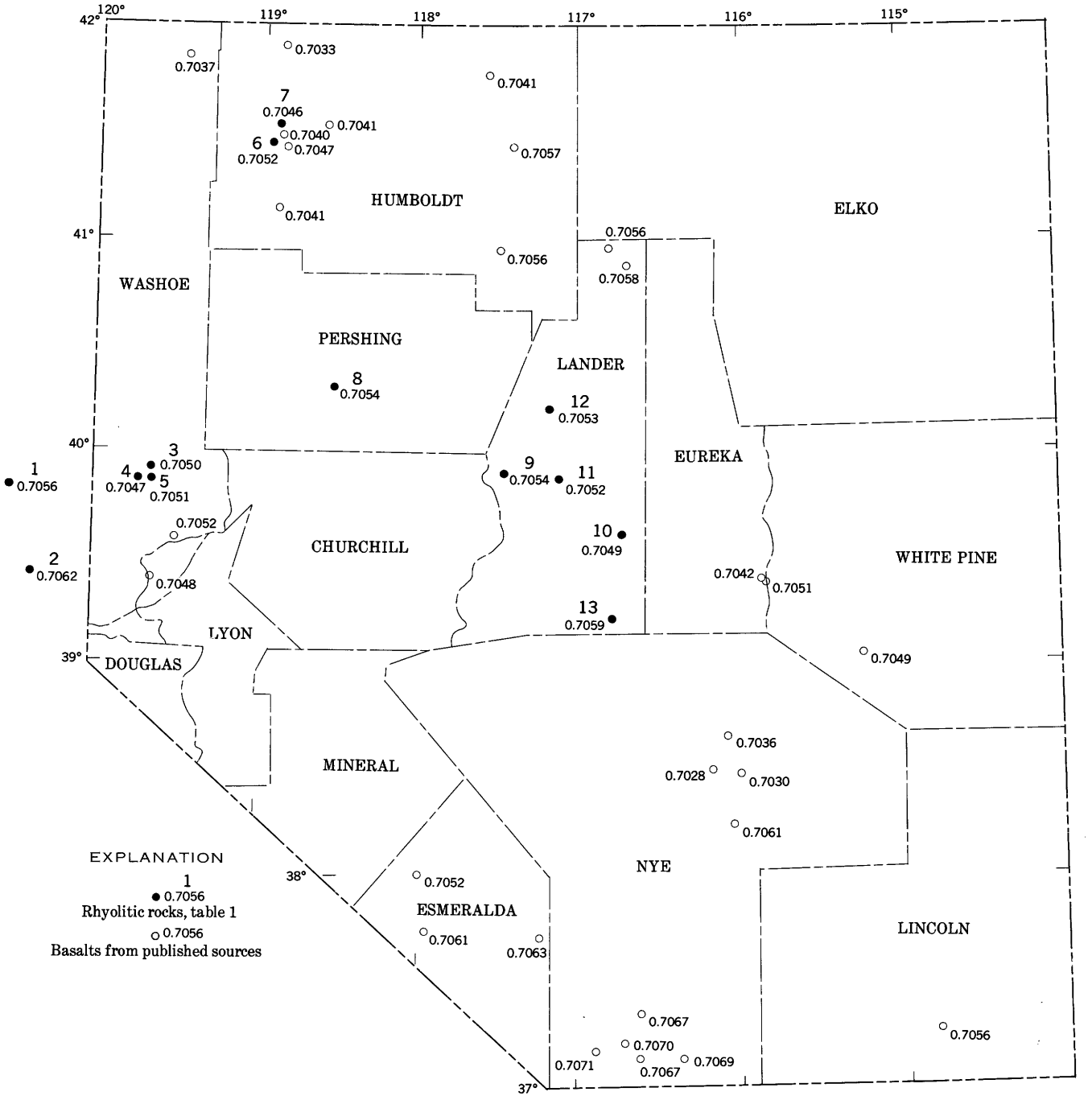

Figure 1.—Map showing sample localities and respective strontium isotopic composition (Sr^{87}/SR^{86}) of late Cenozoic basalts and silicic rocks in northern and central Nevada and in adjacent California. Basalt data from Leeman (1970), Hedge and Noble (1971), McKee and Mark (1971), Noble and others (1972), and C. E. Hedge, D. C. Noble, and R. L. Christiansen (unpub. data).

specimens, with a range of 0.7046 to 0.7059, median 0.7052 (fig. 2), are similar to those of Miocene and younger silicic tuffs and lavas from the northwestern Great Basin (Noble and others, 1972) but appreciably lower than those (0.707 to nearly 0.720) found for silicic and intermediate volcanic rocks of middle and late Cenozoic age from the southern, eastern, and east-central Great Basin and the Snake River Plain (Noble and Hedge, 1969; Hedge and others, unpub. data; Leeman and Manton, 1971; Scott and others, 1972; Noble, Hedge, and Christiansen, unpub. data).

Although a few ocean-ridge tholeiites that as a group represent the least radiogenic type of mafic magma have

Table 1.—Rb/Sr *and observed and initial* Sr^{87}/Sr^{86} *ratios of rhyolitic tuffs and lavas*

[D. C. Noble, analyst]

Sample No.	Field No.	Lat (N.)	Long (W.)	Age (m.y.)	Material analyzed[1]	Rb/Sr	Sr^{87}/Sr^{86}_o	Sr^{87}/Sr^{86}_i	$\pm(2\delta)^2$
1	KA-1126	39°48′	120°32′	[3]21	S	0.241	0.7058	0.7056	0.0002
2	KA-1131	39°19′	120°20′	[3]33	S	1.10	.7077	.7062	.0003
3	H-3	39°55′	119°41′	≈23	S	.387	.7054	.7050	.0002
4	H-4	39°54′	119°47′	≈23	P	⩽.002	.7047	.7047	.0002
5	H-8	39°54′	119°41′	≈23	S	.094	.7052	.7051	.0002
[4]6	N-SL-C3	41°30′	119°01′	24.5	S	4.91	.7101	.7052	.0008
[4]7	N9-122B	41°32′	118°55′	24	NG	.987	.7055	.7046	.0003
[4]8		40°18′	118°33′	⩾23	NG	1.80	.7072	.7054	.0003
9	8622-4	39°52′	117°27′	27	S	.275	.7057	.7054	.0002
10	15890-2	39°34′	116°45′	24	S	1.07	.7059	.7049	.0003
11	9A-66-1	39°56′	117°09′	24	S	.448	.7056	.7052	.0002
12	6805-2	40°12′	117°15′	24	S	.776	.7061	.7053	.0002
13	CC-9-2A	39°13′	116°51′	23.5	S	2.44	.7082	.7059	.0004

1,2. Unnamed ash-flow units (Dalrymple, 1964).
3, 4, 5. Hartford Hill Rhyolite Tuff (Bonham, 1969).
6. Ashdown Tuff (Noble and others, 1970).
7. Rhyolite of the Black Rock Range (Noble and others, 1970, 1972).
8. Rhyolite obsidian from U.S. Gypsum perlite pit (Noble and others, 1972).
9. Edwards Creek Tuff (McKee and Stewart, 1971).
10, 11. Bates Mountain Tuff (McKee and Silberman, 1970; Sargent and McKee, 1969).
12. Fish Creek Mountains Tuff (McKee, 1970; McKee and Silberman, 1970).
13. Unnamed crystal-poor ash-flow tuff overlying the Bates Mountain Tuff (unit 5 of Sargent and McKee, 1969).

[1] S, sanidine or anorthoclase; P, plagioclase; NG, nonhydrated glass.
[2] 2δ of calculated initial ratio.
[3] From Dalrymple (1964).
[4] From Noble and others (1972).

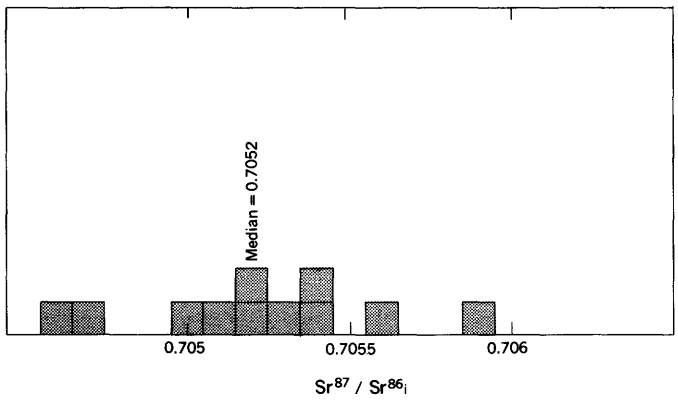

Figure 2.—Histogram showing distribution of initial Sr^{87}/Sr^{86} ratios of lower Miocene silicic ash-flow tuffs and lavas.

Sr^{87}/Sr^{86} ratios as low as 0.702, the average Sr^{87}/Sr^{86} ratio of oceanic basalt is about 0.704 (Peterman and Hedge, 1971). This value is similar (0.7035 to 0.706) to that determined for late Cenozoic basalts from the northwestern Great Basin, and it is reasonable to assume that older Paleozoic and Mesozoic plutonic and volcanic rocks in the same region have similar initial Sr^{87}/Sr^{86} ratios. Paleozoic and Mesozoic carbonate rocks in this region have Sr^{87}/Sr^{86} ratios of 0.7070 to 0.7085 (Peterman and others, 1970) as well as high absolute strontium contents. Clastic material derived from Precambrian rocks would have even higher ratios—of the order of ⩾ 0.71. If one assumes an average age of 250 million years (Permian) for the pre-Cenozoic basement of central and northwestern Nevada and an average Rb/Sr ratio of 0.33 for the noncarbonate portion of the basement (see, for example, Peterman and others, 1967; Kistler and others, 1971), by early Miocene time the average Sr^{87}/Sr^{86} ratio of the noncarbonate portion of the salic basement would have increased by 0.003 that is, to about 0.7065 to 0.709. It is therefore very unlikely that the pre-Cenozoic salic basement had an average Sr^{87}/Sr^{86} ratio of less than about 0.707 at the time that the lower Miocene silicic volcanic rocks were erupted. The relatively low initial Sr^{87}/Sr^{86} (median 0.7052) found for the early Miocene tuffs and lavas appears to rule out generation of parent magmas by partial or complete melting of pre-Cenozoic salic basement (with its relatively high Sr^{87}/Sr^{86} ratio) or by gross contamination of mafic magmas by such material.

The isotopic data are consistent with the derivation of the silicic magmas by fractional crystallization of mafic magmas isotopically similar (Sr^{87}/Sr^{86} between 0.7040 and 0.7060) to those erupted during the late Cenozoic. Some of the variation in initial Sr^{87}/Sr^{86} ratios found for the silicic volcanic rocks reflects cumulative uncertainties in determination of initial strontium isotopic composition, and some undoubtedly reflects small amounts of contamination by crustal material. The remainder can reasonably be attributed to variations in the strontium isotopic composition of the mantle material from which the primary magmas were derived.

ACKNOWLEDGMENTS

The work was partly supported by National Science Foundation grant GA-1546 and National Aeronautics and Space Administration grant NGR-22-007-103 and partly by the Nevada Bureau of Mines and Geology. G. B. Dalrymple provided splits of two dated sanidines.

REFERENCES

Bonham H. F., 1969, Geology and mineral deposits of Washoe and Storey Counties, Nevada, *with a section on* industrial rocks and mineral deposits by K. G. Papke: Nevada Bur. Mines Bull. 70, 140 p.

Dalrymple, G. B., 1964, Cenozoic chronology of the Sierra Nevada, California: California Univ. Pubs. Geol. Sci., v. 47, 41 p.

Dickinson, D. R., and Gibson, I. L., 1972, Feldspar fractionation and anomalous Sr^{87}/Sr^{86} ratios in a suite of peralkaline silicic rocks: Geol. Soc. America Bull., v. 83, p. 231–240.

Hedge, C. E., and Noble, D. C., 1971, Late Cenozoic basalts with unusually high Sr/Rb and Sr^{87}/Sr^{86} ratios from the southern Great Basin, western United States: Geol. Soc. America Bull., v. 82, p. 3503–3510.

Kistler, R. W., Evernden, J. F., and Shaw, H. R., 1971, Sierra Nevada plutonic cycle–Pt. I, Origin of composite granitic batholiths: Geol. Soc. America Bull., v. 82, p. 853–868.

Leeman, W. P., 1970, The isotopic composition of strontium in late Cenozoic basalts of the Basin-Range province, western United States: Geochim, et Cosmochim. Acta, v. 34, p. 857–872.

Leeman, W. P., and Manton, W. I., 1971, Strontium isotopic compositions of basaltic lavas from the Snake River plain, southern Idaho: Earth and Planetary Sci. Letters, v. 11, p. 420–437.

McKee, E. H., 1970, Fish Creek Mountains Tuff and volcanic center, Lander County, Nevada: U.S. Geol. survey Prof. Paper 681, 17 p.

McKee, E. H., and Mark, R. K., 1971, Strontium isotopic composition of two basalts representative of the southern Snake River volcanic province, *in* Geological Survey Research 1971: U.S. Geol. Survey Prof. Paper 750-B, p. B92–B95.

McKee, E. H., Noble, D. C., and Silberman M. L., 1970, Middle Miocene hiatus in volcanic activity in the Great Basin of the western United States: Earth and Planetary Sci. Letters, v. 8, p. 93–96.

McKee, E. H., and Silberman, M. L., 1970, Geochronology of Tertiary igneous rocks in central Nevada: Geol. Soc. America Bull., v. 81, p. 2317–2328.

McKee, E. H., and Stewart, J. H., 1971, Stratigraphy and potassium-argon ages of some Tertiary tuffs from Lander and Churchill Counties, central Nevada: U.S. Geol. Survey Bull. 1311-B, 28 p.

Noble, D. C., and Hedge, C. E., 1969, Sr^{87}/Sr^{86} variations within individual ash-flow sheets, *in* Geological Survey Research 1969: U.S. Geol. Survey Prof. Paper 650-C, p. C133–C139.

Noble, D. C., Hedge, C. E., McKee, E. H., and Korringa, M. K., 1972, Reconnaissance study of the strontium isotope composition of Cenozoic volcanic rocks in the northwestern Great Basin: Geol. Soc. America Bull., v. 83. [In press]

Noble, D. C., McKee, E. H., Smith, J. G., and Korringa, M. K., 1970, Stratigraphy and geochronology of Miocene volcanic rocks in northwestern Nevada, *in* Geological Survey Research 1970: U.S. Geol. Survey Prof. Paper 700-D, p. D23–D32.

Peterman, Z. E., and Hedge, C. E., 1971, Related strontium isotopic and chemical variations in oceanic basalt: Geol. Soc. America Bull., v, 82, p. 493–500.

Peterman, Z. E., Hedge, C. E., Coleman, R. G., and Snavely, P. D., Jr., 1967, Sr^{87}/Sr^{86} ratios in some eugeosynclinal sedimentary rocks and their bearing on the origin of granitic magma in orogenic belts: Earth and Planetary Sci. Letters, v. 2, p. 433–439.

Peterman, Z. E., Hedge, C. E., and Tourtelot, H. A., 1970, Isotopic composition of strontium in sea water throughout Phanerozoic time: Geochim. et Cosmochim, Acta, v. 34, p. 105–120.

Sargent, K. A., and McKee, E. H., 1969, The Bates Mountain Tuff in northern Nye County, Nevada: U.S. Geol. Survey Bull. 1294-E, p. E1–E12.

Scott, R. B., Nesbitt, R. W., Dasch, E. J., and Armstrong, R. L., 1972, A strontium isotope evolution model for Cenozoic magma genesis, eastern Great Basin, U.S.A.: Volcanol. Bull. [In press]

GEOCHEMISTRY OF CARBONATE ROCKS IN PHOSPHORIA AND RELATED FORMATIONS OF THE WESTERN PHOSPHATE FIELD

By K. J. MURATA[1], IRVING FRIEDMAN[2], and R. A. GULBRANDSEN[1],
[1] Menlo Park, Calif., [2] Denver, Colo.

Abstract.—Various kinds of depositional environments are represented among Permian marine formations of the western phosphate field, Idaho, Montana, Utah, and Wyoming, and the dolomites of these formations bear the imprint of their genetic environment in their isotopic composition. Dolomites of the Park City Formation formed in well-aerated waters and have carbon and oxygen isotopic compositions of normal marine carbonate; those of the carbonaceous Phosphoria Formation formed in waters of low Eh and contain light-carbon carbonate derived from organic matter. Limestones generally contain oxygen that is isotopically lighter than that of associated dolomites because they underwent isotopic exchange with percolating fresh water more readily than did dolomites. Dolomites of the Ervay Member of the Park City Formation differ from most others by having oxygen as light as that of limestones, which suggests an origin through dolomitization of nearshore limestones that had been affected by fresh water soon after deposition.

Permian sedimentary formations of the western phosphate field, and adjacent areas in Idaho, Montana, Utah, and Wyoming were deposited in widely different environments, varying from the open sea of the Cordilleran miogeosyncline (Kay, 1947) to the west through progressively shallower shelf water to evaporite basins to the east. The open-sea environment gave rise to the carbonaceous mudstones, phosphorites, and cherts of the Phosphoria Formation, whereas shallower waters yielded the carbonate rocks of the Park City Formation, the sands of the Shedhorn Sandstone, red and green beds, and evaporites (McKelvey and others, 1959; Yochelson, 1968).

We have made chemical, X-ray diffraction, and isotopic analyses of 25 dolomites and seven limestones from these formations in order to determine what information such data might provide on sedimentary and diagenetic history of the formations. Previous studies of carbonate rocks of other basins (Landergren, 1954; Clayton and Degens, 1959; Weber and others, 1965; Füchtbauer and Goldschmidt, 1965) have shown that the chemical and isotopic compositions can be sensitive indexes of the salinity and redox potential of the depositional environment. Other studies (Hodgson, 1966; Murata and others, 1969; Fontes and others, 1970; Tan and Hudson, 1971) indicate that diagenetic processes can modify original compositions and leave imprints of late postdepositional events.

Previously, the carbonate rocks of the western phosphate field received little attention, chemically or mineralogically. Gulbrandsen's X-ray examination (1960) of carbonates of the Phosphoria Formation demonstrated the general preponderance of dolomite over calcite and the presence of excess calcium in the dolomite. Campbell (1962) and Rogers (1971) made detailed petrographic analyses of carbonates of Phosphoria and correlative formations because of their importance as reservoirs for petroleum. All of the different textural types illustrated by these investigators, ranging from micrites through pelletal sands to coarse coquinas, are found among samples of the present study. Dolomitized shells and matrix are widespread and indicate that most dolomite rock probably originated through replacement of calcareous sediments.

LOCALITIES OF THE SAMPLES

The samples that we studied were obtained from sedimentary units marked with an asterisk in table 1.

We stress the fact that the three Permian formations in table 1 are characterized by different amounts of carbonate and organic matter because these differences strongly affect the isotopic compositions of the carbonates. The Phosphoria Formation is mostly carbonaceous mudstone, phosphorite, and chert that contain minor amounts of black to brown lenticular carbonate. In contrast, the Park City Formation consists mostly of gray, buff, or white carbonate rock that is poor in organic matter. The Shedhorn Sandstone is generally poor in both carbonate and organic matter.

The localities of the samples are shown on figure 1. Isopachs of the total thickness of Permian sedimentary rocks of the region (McKelvey and others, 1959) are included in the figure to outline the distribution of the sediments and to suggest the general setting of their deposition. Carbonaceous rocks of the Phosphoria Formation are predominant to the west, the limestones and dolomites of the Park City to the east, and the sands of the Shedhorn to the north, but these rocks intertongue extensively throughout most of the region.

U.S. GEOL. SURVEY PROF. PAPER 800-D, PAGES D103-D110

Table 1.—*Generalized subdivision of Permian and related formations of the western phosphate field*

[McKelvey and others (1959). Asterisks (*) denote units that were sampled for this study]

Age	Stratigraphic unit		
Triassic	Dinwoody Formation*		
Permian	Phosphoria Formation	Park City Formation	Shedhorn Sandstone
		Ervay Member*	Upper member
	Tosi Chert Member*		
	Retort Phosphatic Shale Member*		
	Cherty shale member		
	Rex Chert Member	Franson Member*	Lower member*
	Meade Peak Phosphatic Shale Member*		
	Lower chert member	Grandeur Member*	
Pennsylvanian	Tensleep Sandstone		

Samples were obtained mostly from natural outcrops or shallow trenches. Sample 5 was obtained from an underground mine, and samples 11–19 were from a deep well that was drilled to subsurface depths in excess of 14,000 feet (Sheldon, 1963, p. 241–245). Methods that we used for chemical, X-ray, and isotopic analyses have been described earlier (Murata and others, 1969, 1972).

CHEMICAL COMPOSITION

The calcium content of dolomites and the magnesium content of calcites, shown in figure 2, were estimated from the $d(10{\cdot}4)$ spacings (Goldsmith and Graf, 1958a) listed in the last column of table 2. Staining with a solution of potassium ferricyanide (Friedman, 1959) proved that the iron content of the carbonates is negligible, so the variations of $d(10{\cdot}4)$ can be attributed solely to variations in relative amounts of calcium and magnesium.

Most dolomites in figure 2*A* have a $CaCO_3$ content of 50 mole percent (Ca_{50}), only two samples containing as much as 54 mole percent. Three-quarters of the dolomites from the Park City Formation (open bars) have Ca_{50} but only half of those from the Phosphoria Formation (filled bars) have the same amount. Single samples (Nos. 15, 28, and 32) from the Shedhorn and Dinwoody Formations and from an unnamed red shale-gypsum sequence also have Ca_{50} and have been included with those from the Park City.

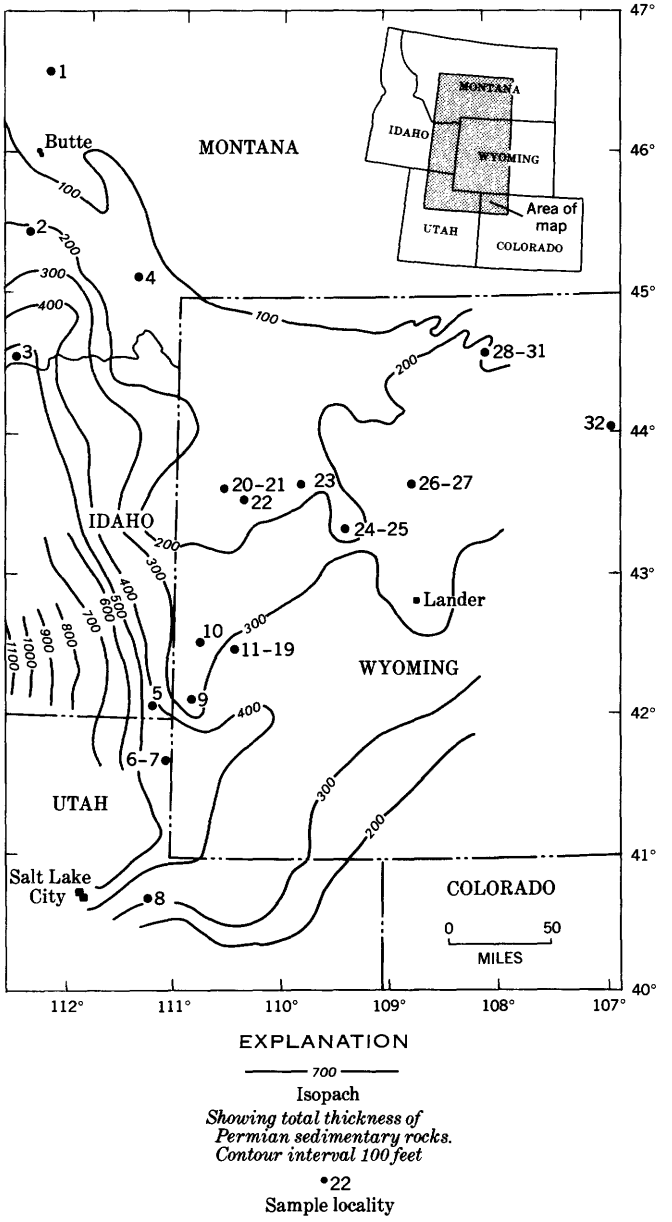

Figure 1.—Sketch map showing localities of carbonates that were studied. Numbers 1 to 32 are the sample numbers listed in table 2. Isopachs indicate the total thickness in feet of Permian sedimentary rocks (McKelvey and others, 1959).

According to Sheldon, Maughan, and Cressman (1967), the Park City Formation was deposited largely in waters of a shallow continental shelf and adjacent coastal evaporite basin in an arid region. Diagenetic dolomites now forming in an evaporite environment (Illing and others, 1965; Deffeyes and others, 1965; Müller and Tietz, 1966; Shinn and others, 1965, 1969) involve brines that are about six times more concentrated than normal sea water and have Mg/Ca atomic ratios of 10–40 compared with the normal ratio of 5.2.

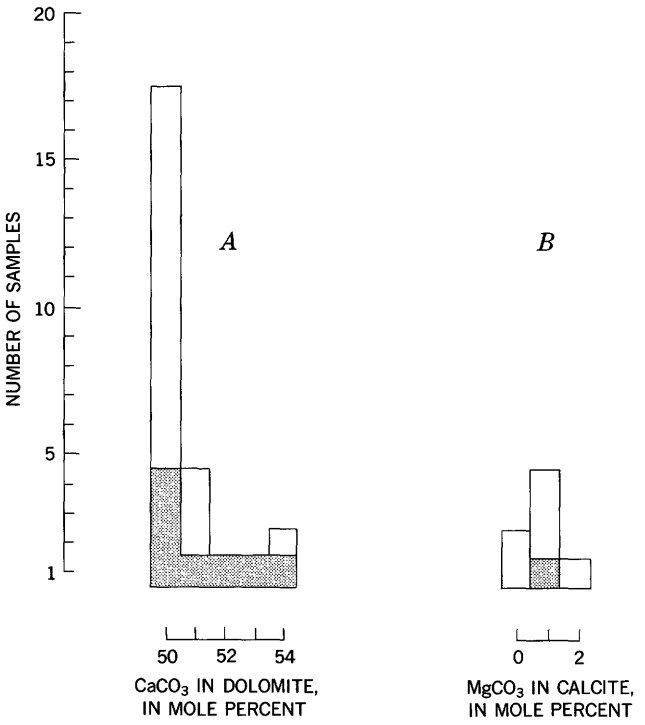

Figure 2.–Histograms showing *A*, compositional distribution of dolomites and *B*, compositional distribution of limestones. Open bars, Park City, Shedhorn, and Dinwoody Formations; filled bars, Phosphoria Formation.

Modern evaporite dolomites are richer in calcium than the samples from the Permian formations, most being in the upper part of the range of Ca_{52-60}, and those from more humid regions tend to have more excess calcium (Füchtbauer and Goldschmidt, 1965). With time, the calcium-rich dolomite inverts to the thermodynamically stable end member (Ca_{50} Mg_{50}) through a recrystallization process (Goldsmith and Graf, 1958b). The inversion probably requires the presence of a water solution (Usdowski, 1968), so it would be more likely to occur in the permeable carbonate rock of the Park City than in the less permeable mudstone of the Phosphoria.

Partial chemical analyses of five of the dolomites are given in table 3, and they confirm the low content of iron (and manganese) and the variability of calcium and magnesium. The chemically determined mole percentage of $CaCO_3$ tends to be slightly higher than that indicated by the $d(10\cdot4)$ X-ray spacing. Probably calcite, anhydrite, or other calcium minerals present in amounts below the detection limits of X-ray diffraction contributed some extraneous calcium to the acid extracts used in the analyses.

The inverse relation between δC^{13} and shade of sample color, indicated along the bottom of table 3, holds fairly well for all 32 samples. There is a surprisingly poor correlation in the table between shade of color and content of organic carbon, which suggests that organic matter is not uniformly constituted or that other materials like fine-grained pyrite contribute to the darkness of color (Frost, 1960). The black color of sample 16 seems inexplicable solely on the basis of percentage of organic carbon and must result from the presence of both pyrite and organic matter. The combined content of pyrite and organic matter can be considered a qualitative index of redox conditions of the depositional environment, and such an index would explain the correlation (to be discussed later) between color shade of the dolomite and the isotopic lightness of its carbonate carbon.

Limestones of the western phosphate field, as represented by the seven samples in figure 2*B*, contain small amounts of $MgCO_3$ (avg 1±1 mole percent). More samples were not included in the study because limestones are less attractive subjects than dolomites for the study of stable-isotopic relations, for they seem to be more readily altered isotopically than dolomites.

GENERAL FEATURES OF THE ISOTOPIC COMPOSITION

The carbon and oxygen isotope compositions are given in table 2 and are plotted one against the other in figure 3. Some distinctive groupings of points are evident in the figure. The compositions of dolomites from the Park City Formation (open circles), except those from the Ervay Member mentioned below, fall mostly within or near the compositional limits of modern marine limestone, indicated by the rectangle at (a). Single samples from the Shedhorn and Dinwoody Formations and from a Permian red shale-gypsum sequence have been grouped with those from the Park City for convenience of discussion. Dolomites 11, 12, and 26 from the Ervay Member (open circles with cross) of the Park City and all limestones (open and filled squares) except fossil 23 have oxygen that is too light for normal modern marine carbonate. Dolomites of the Phosphoria Formation (filled circles) are characterized by light carbon.

This paper attempts to explain the several compositional groupings in terms of two major processes that affected marine limestone during original deposition and subsequent diagenesis: (1) formation of carbonates with isotopically light oxygen by means of isotopic exchange with fresh water, and (2) formation of carbonates with isotopically light carbon by incorporation of carbon derived from organic matter.

The total range of δC^{13} in figure 3 is 16.6 per mil (thousand), which is only about one-third of that observed in carbonates of the California Miocene (Murata and others, 1969) and one-fifth of that in carbonates from the continental shelf of the northeastern United States (Deuser, 1970). Consequently, special processes that yield unusually heavy ($>+6$ per mil) or unusually light (<-30 per mil) carbon need not be considered.

At equilibrium, the δO^{18} of dolomite is greater than that of calcite by about 4 per mil at 25°C (O'Neil and Epstein, 1966; Northrup and Clayton, 1966; Sheppard and Schwarcz, 1970), but the two minerals occurring together in nature often show

Table 2.—*Carbon and oxygen isotopic composition and d(10·4) X-ray spacing of dolomites and limestones from Permian and related formations in the western phosphate field*

[Carbon isotopic composition is relative to University of Chicago PDB[1] standard; oxygen isotopic composition is relative to SMOW[1]. The isotopic compositions were determined by Jim Gleason and Craig Rightmere. The *d*(10·4) spacings were determined by Evelyn Druding and Karen Whiteley]

Sample	Lab. No.	Locality	County	State	Latitude (N.) and longitude (W.)	Formation	Member	Rock	Subsurface depth (feet)	δC^{13} per mil	δO^{18} per mil	*d*(10·4) (angstroms)
1	3310-10	Newman Bros. prospect	Powell	Montana	46°36′, 112°25′	Park City	Franson	Dolomite	.....	−1.8	27.1	2.887
2	3310-9	North Big Hole Canyon	Madison	...do...	45°27′, 112°39′	...do...	...do...	...do...	.....	+1.5	30.4	2.886
3	3310-11	Little Sheep Creek	Beaverhead	...do...	44°34′, 112°40′	...do...	Grandeur	Limestone	.....	−1.5	22.9	3.033
4	3310-13	Indian Creek	Madison	...do...	45°08′, 111°30′	Phosphoria	Retort	Dolomite	.....	−9.0	32.1	2.886
5	3310-15	San Francisco Hot Springs crosscut	Bear Lake	Idaho	42°07′, 111°14′	...do...	Meade Peak	...do...	.....	−8.2	24.0	2.888
6	3355-10	Brazer Canyon	Rich	Utah	41°40′, 111°05′	...do...	...do...	Limestone	.....	−4.0	25.6	3.031
7	3355-11	.....do.....	...do...	...do...	.....do.....	...do...	...do...	Dolomite	.....	−2.7	32.0	2.898
8	3310-4	Franson Canyon	Summit	...do...	40°43′, 111°14′	Park City	Franson	...do...	.....	+3.4	30.4	2.888
9	3310-5	Middlefork Pine Creek	Lincoln	Wyoming	42°07′, 110°49′	...do...	...do...	Limestone	.....	−1.4	17.5	3.035
10	3310-6	Cottonwood Canyon	...do...	...do...	42°38′, 110°50′	...do...	...do...	...do...	.....	+1.1	21.3	3.030
11	3355-1	Lakeridge Well No. 1	Sublette	...do...	42°24′, 110°28′	...do...	Ervay	Dolomite	14,269	+.5	24.5	2.888
12	3355-2	.....do.....	...do...	...do...	.....do.....	...do...	...do...	...do...	14,271	+.3	24.6	2.887
13	3355-3	.....do.....	...do...	...do...	.....do.....	Phosphoria	Tosi	...do...	14,308	−2.9	25.8	2.886
14	3355-4	.....do.....	...do...	...do...	.....do.....	Park City	Franson	...do...	14,348	+2.7	28.6	2.885
15	3355-5	.....do.....	...do...	...do...	.....do.....	Shedhorn	Lower Shedhorn	...do...	14,377	−1.0	24.3	2.885
16	3355-6	.....do.....	...do...	...do...	.....do.....	Phosphoria	Meade Peak	...do...	14,412	−5.7	26.0	2.892
17	3355-7	.....do.....	...do...	...do...	.....do.....	...do...	...do...	...do...	14,441	−9.5	28.8	2.885
18	3355-8	.....do.....	...do...	...do...	.....do.....	...do...	...do...	...do...	14,477	−11.6	27.7	2.885
19	3355-9	.....do.....	...do...	...do...	.....do.....	Park City	Grandeur	...do...	14,489	−6.4	31.9	2.885
20	3310-7	Gros Ventre slide	Teton	...do...	43°39′, 110°33′	...do...	Franson	...do...	.....	−.7	30.8	2.886
21	3310-12	.....do.....	...do...	...do...	.....do.....	...do...	Grandeur	...do...	.....	−3.6	32.0	2.886
22	3310-14	Crystal Creek	...do...	...do...	43°33′, 110°24′	Phosphoria	Retort	...do...	.....	−7.8	28.0	2.896
23	3310-20	Burroughs Creek	Fremont	...do...	43°42′, 109°39′	Park City	.....	Productid shell	.....	−3.5	27.3	3.034
24	3310-3	Dinwoody Lakes	...do...	...do...	43°22′, 109°24′	...do...	Ervay	Limestone	.....	−3.3	21.4	3.032
25	3310-8	.....do.....	...do...	...do...	.....do.....	...do...	Franson	Dolomite	.....	−4.0	30.6	2.888
26	3310-1	Embar Creek	Hot Springs	...do...	43°42′, 108°40′	...do...	Ervay	...do...	.....	+1.2	20.7	2.897
27	3310-2	.....do.....	...do...	...do...	.....do.....	...do...	...do...	Limestone	.....	+.3	23.7	3.032
28	3355-12	Sheep Mountain	Big Horn	...do...	44°32′, 108°03′	Dinwoody	.....	Dolomite	.....	−3.4	30.6	2.885
29	3355-13	.....do.....	...do...	...do...	.....do.....	Park City	.....	...do...	.....	+4.2	29.6	2.885
30	3355-14	.....do.....	...do...	...do...	.....do.....	...do...	.....	...do...	.....	+5.1	29.7	2.885
31	3355-15	.....do.....	...do...	...do...	.....do.....	...do...	.....	...do...	.....	+3.9	28.1	2.887
32	3310-19	Crazy Woman Creek	Johnson	...do...	44°02′, 106°48′	Permian red shale and gypsum sequence		...do...	.....	+2.2	31.4	2.885

[1] PDB, Pee Dee Belemnite; SMOW, Standard Mean Ocean Water.

Table 3.—*Partial analyses of dolomites from the western phosphate field*

[Analysts, Marcelyn Cremer and I. C. Frost]

Sample No. 7	16	18	26	30
Acid-soluble dolomite fraction (mole percent)				
$FeCO_3$ 0.3	0.8	0.5	0.6	0.1
$MnCO_3$ 0	.1	.2	.0	.0
$MgCO_3$ 44.6	47.4	48.8	44.0	49.2
$CaCO_3$ 55.1	51.7	50.5	55.4	50.7
$CaCO_3$ by $d(10{\cdot}4)$ X-ray spacing. 54.2	52.2	49.9	53.9	49.9
Whole sample (weight percent)				
Organic carbon 1.37	0.27	0.99	0.97	0.15
Pyrite by XRD[1] ..... Absent	Present	Present	Absent	Absent
Insoluble matter (Ignited at 900°C). 30.4	17.4	37.4	6.6	4.7
Other characteristics				
Color ..... Brown	Black	Black	Tan	White
δC^{13} per mil (PDB). . . −2.7	−5.7	−11.6	+1.2	+5.1

[1] XRD, X-ray diffraction analysis.

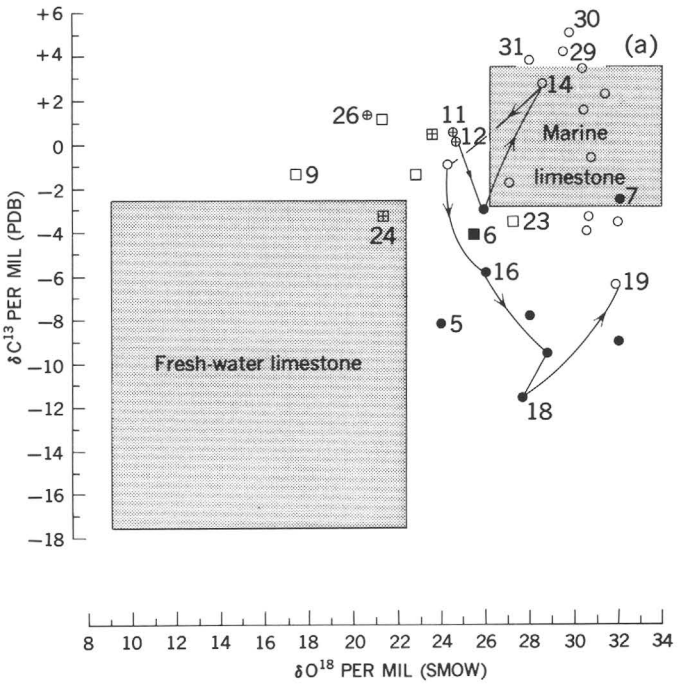

Figure 3.—Diagram showing relations between carbon and oxygen isotope compositions of carbonate rocks. Open circles denote dolomites from the Park City Formation and other formations of similar lithology; filled circles, dolomites from the Phosphoria Formation. Squares denote limestones and are open if from the Park City or filled if from the Phosphoria. Carbonates (both dolomites and limestones) from the Ervay Member of the Park City Formation are distinguished by a cross within the circle or square. Samples 11–19 from the deep Lakeridge well are linked together by an arrowed line that indicates descending stratigraphic order. The compositional limits of fresh-water and marine limestones are from Graf (1960), Keith and Weber (1964), and Degens (1969). Numbered samples are discussed in the text.

little or no difference (Friedman and Hall, 1963; Degens and Epstein, 1964). Some coexisting dolomites and calcites appear to have equilibrated at different times with different solutions (Clayton and others, 1968), so they are not isotopically comparable. Because of these uncertainties, we do not consider the equilibrium fractionation between the two minerals to explain the oxygen compositions shown in figure 3.

Samples 11–19, which are connected in figure 3 with arrows indicating downward stratigraphic direction, are drill core samples obtained in General Petroleum's Lakeridge well at subsurface depths of 14,269 to 14,489 feet (Sheldon, 1963). They, as well as sample 5 from an underground mine, are not likely to have been exposed to solutions related to the current cycle of weathering and thus provide a basis for excluding modern weathering as a factor in certain compositional changes. For example, the light oxygen in dolomites 5, 11, and 12 suggests contact with fresh water, but this contact probably occurred early in the genetic history of the dolomites.

ISOTOPIC COMPOSITION OF LIMESTONES

Six of the seven limestones in figure 3 contain oxygen that is lighter than that in normal marine limestone, sample 9 having the lightest (δO^{18} of 17.5 per mil) among all 32 carbonates. The oxygen of the limestones presumably became lighter through isotopic exchange with fresh water that percolated through them for a long time (Degens and Epstein, 1962; Keith and Weber, 1964; Tan and Hudson, 1971). Good examples of calcite so affected are also found in Miocene coastal sands of Round Mountain oil field of California (Murata and others, 1969). "Limestone" 23 is a dense shell of a productid fossil, and its oxygen has not been modified greatly.

In contrast to the limestones, most of the dolomites that we studied have the oxygen isotope composition of normal modern marine limestone. We follow Epstein, Graf, and Degens (1964) in believing that the dolomite generally inherited the isotopic composition of the precursor limestone and preserved it against later changes. The δO^{18} of the ocean during the Permian may have been 1 to 3 per mil lighter than that of the modern ocean (Perry, 1967; Knauth and Epstein, 1971). The average marine limestone of that period could have contained correspondingly light oxygen, but such a general shift in δO^{18} is not obvious in figure 3.

Fresh water contains variable amounts of light carbon as bicarbonate derived from oxidation of organic matter on land or in the sediments it pervades. Consequently, fresh water often lightens the carbon of marine carbonate as well as the

oxygen (Gross, 1964). But such an effect is not well developed among the limestones in figure 3, probably because of the generally low content of organic matter in the Park City Formation. Sample 6, which has the lightest carbon (−4.0 per mil) among the limestones, is a black Phosphoria limestone, but it is not much lighter than normal marine limestone.

PHOSPHORIA DOLOMITES

The carbonaceous chert, mudstone, phosphorite, and minor carbonate of the Phosphoria Formation were deposited in a reducing environment that allowed much organic matter to accumulate (Yochelson, 1968; Gulbrandsen, 1969). This organic matter was the ready source of the light carbon (Spotts and Silverman, 1966; Lippman, 1968) so characteristic of Phosphoria dolomite (filled circles in fig. 3). The oxygen isotope composition indicates that the incorporation of light carbon took place in sea water rather than in fresh water.

The reactions involved must have been similar to those observed by Presley and Kaplan (1968) for the bottom muds of San Pedro Basin off the southern California coast. As a result of bacterial decomposition of organic matter and reduction of sulfate, the interstitial water of San Pedro muds contained about 20 times more bicarbonate than normal sea water and only 1/200 of the sulfate; the δC^{13} of the bicarbonate was as low as −21 per mil, 5 m below the sea floor. About 10 percent of primary sedimentary carbonate (shell fragments) was present, and a systematic shift of its δC^{13} with depth in the mud (−0.6 to −3.0 per mil) indicated that isotopic exchange had taken place between the primary carbonate and dissolved biogenic bicarbonate.

The circumstances of dolomitization of the primary carbonate in the Phosphoria Formation are not clear, but dolomitization has preserved the light carbon that is typical of the earliest stage of diagenesis of carbonaceous sediments. No dolomites with heavy carbon ($\delta C^{13} > +6$ per mil) that is typical of the later stages (Murata and others, 1972) have been found. Sample 19 is from the Grandeur Member of the Park City Formation and thus is plotted as an open circle in figure 3, but it is more akin to dolomites of the Phosphoria Formation in its black color and isotopically light carbon. The common occurrence of pyrite in Phosphoria samples points to widespread bacterial reduction of sulfate accompanying the decomposition of organic matter.

PARK CITY DOLOMITES EXCLUSIVE OF SOME FROM THE ERVAY MEMBER

Park City sediments are believed to have been deposited closer to shore than those of the Phosphoria, in aerated water that did not allow much accumulation of organic matter. In some places, deposition occurred in shallow barred lagoons in which sea water became evaporated to various degrees, according to Sheldon, Maughan, and Cressman (1967).

A common feature of dolomites formed in evaporite environments, such as the Coorong Lagoon of South Australia (Clayton and others, 1968), the tidal flats of the Persian Gulf (Kinsman, 1971), and Pacific atoll lagoons (Berner, 1965), is their content of heavy oxygen (δO^{18} of 32 to 35 per mil), which reflects an enhanced content of O^{18} in evaporated sea water. The generally lighter oxygen (δO^{18} of 27 to 32 per mil) of Park City dolomites suggests that they were formed in an environment somewhat different from typical modern evaporite basins, perhaps one with a more humid atmosphere that would limit the extent of O^{18} concentration in evaporating sea water (Craig and others, 1963; Lloyd, 1966), or one more affected by incursions of fresh water. As previously mentioned, ocean water of Permian time may have been poorer in O^{18} than it is now (Knauth and Epstein, 1971), thereby possibly yielding carbonates with somewhat lighter oxygen.

The heaviest carbons (δC^{13} of +3.9 to +4.2 per mil) among the studied samples are found among Park City dolomites 29–31 from a depositional site that is well within the craton (fig. 1). The carbon isotope composition is like that of Holocene dolomites (δC^{13} of +4.0 to +4.4 per mil) of the Persian Gulf tidal flats (Kinsman, 1971), which suggests that the three Park City dolomites formed in a broadly similar environment.

SOME PARK CITY DOLOMITES FROM THE ERVAY MEMBER AND A DOLOMITE FROM THE SHEDHORN SANDSTONE

Dolomites 11, 12, and 26 from the Ervay Member of the Park City Formation and dolomite 15 from the lower member of the Shedhorn Sandstone are considered together because they all contain light oxygen. The general lightness of oxygen in limestones was previously noted and attributed to the influence of fresh water. The four dolomites under discussion are believed to have formed through dolomitization of limestones that had been affected by fresh water early in their postdepositional history (Land and Epstein, 1970). Fresh water would very likely enter a nearshore sandstone like the Shedhorn (Yochelson, 1968). The lighter oxygen in Park City dolomites of the Ervay Member compared with those of the Franson Member is also believed to result from more ready, early access of fresh water to Ervay sediments than to Franson sediments.

According to Sheldon, Cressman, Cheney, and McKelvey (1967), the Ervay Member represents the latest Permian in the region, and its complex stratigraphy involved deposition in a regressing sea with consequent overlap by continental deposits or some sequence of regional uplift, erosion, and subsequent inundation. Facies analysis of the Ervay in the Bighorn Basin of Wyoming (in the region of the locality for samples 28–31 in fig. 1) indicates a tidal-flat depositional environment (Rogers, 1971). All of these geological relations suggest a strong possibility for early entry of fresh water into Ervay sediments. More samples of Ervay dolomite need to be studied

to determine whether light oxygen is a universal characteristic of these dolomites, as suggested by this exploratory study.

REFERENCES

Berner, R. A., 1965, Dolomitization of mid-Pacific atolls: Science, v. 147, no. 3663, p. 1297–1299.

Campbell, C. V., 1962, Depositional environments of Phosphoria Formation (Permian) in southern Bighorn Basin, Wyoming: Am. Assoc. Petroleum Geologists Bull., v. 46, p. 478–503.

Clayton, R. N., and Degens, E. T., 1959, Use of carbon isotope analyses of carbonates for differentiating fresh-water and marine sediments: Am. Assoc. Petroleum Geologists Bull., v. 43, no. 4, p. 890–897.

Clayton, R. N., Skinner, H. C. W., Berner, R. A., and Rubinson, M., 1968, Isotopic compositions of recent south Australian lagoonal carbonates: Geochim. et Cosmochim. Acta, v. 32, no. 9, p. 983–988.

Craig, Harmon, Gordon, L. I., and Horibe, Y., 1963, Isotopic exchange effects in the evaporation of water: Jour. Geophys. Research, v. 68, no. 17, p. 5079–5087.

Deffeyes, K. S., Lucia, F. J., and Weyl, P. K., 1965, Dolomitization of recent and Plio-Pleistocene sediments by marine evaporite waters on Bonaire, Netherlands Antilles: Soc. Econ. Paleontologists and Mineralogists Spec. Pub. 13, p. 71–88.

Degens, E. T., 1969, Biochemistry of stable carbon isotopes, *in* Eglinton, G., and Murphy, M. T. J., eds., Organic geochemistry: Heidelberg, Springer-Verlag, p. 304–329.

Degens, E. T., and Epstein, Samuel, 1962, Relationship between O^{18}/O^{16} ratios in coexisting carbonates, cherts, and diatomites: Am. Assoc. Petroleum Geologists Bull., v. 46, no. 4, p. 534–542.

—— 1964, Oxygen and carbon isotopic ratios in coexisting calcites and dolomites from recent and ancient sediments: Geochim. et Cosmochim. Acta, v. 28, no. 1, p. 23–44.

Deuser, W. G., 1970, Extreme $^{13}C/^{12}C$ variations in Quaternary dolomites from the continental shelf: Earth and Planetary Sci. Letters, v. 8, p. 118–124.

Epstein, Samuel, Graf, D. L., and Degens, E. T., 1964, Oxygen isotopic studies on the origin of dolomites, Chap. 13 *in* Isotopic and cosmic chemistry: Amsterdam, North-Holland Publishing Co., p. 169–180.

Fontes, J. C., Fritz, Peter, and Letolle, Rene, 1970, Composition isotopique, mineralogique, et genese des dolomites du Bassin de Paris: Geochim. et Cosmochim. Acta, v. 34, no. 3, p. 279–294.

Friedman, G. M., 1959, Identification of carbonate minerals by staining methods: Jour. Sed. Petrology, v. 29, no. 1, p. 87–97.

Friedman, Irving, and Hall, W. E., 1963, Fractionation O^{18}/O^{16} between coexisting calcite and dolomite: Jour. Geology, v. 71, no. 2, p. 238–243.

Frost, I. C., 1960, Comparison of three methods for the determination of total and organic carbon in geochemical studies: Art. 217 *in* U.S. Geol. Survey Prof. Paper, 400-B, p. B480–B483.

Füchtbauer, Hans, and Goldschmidt, Hertha, 1965, Beziehungen zwischen calcium gehalt und Bildungsbedingungen der Dolomite: Geol. Rundschau, v. 55, p. 29–40.

Goldsmith, J. R., and Graf, D. L., 1958a, Relation between lattice constants and composition of the Ca-Mg carbonates: Am. Mineralogist, v. 43, nos. 1–2, p. 84–101.

—— 1958b, Structural and compositional variations in some natural dolomites: Jour. Geology, v. 66, p. 678–693.

Graf, D. L., 1960, Geochemistry of carbonate sediments and sedimentary carbonate rocks–pt. 4-A, Isotopic composition–chemical analysis: Illinois Geol. Survey Circ. 308, 42 p.

Gross, M. G., 1964, Variations in the O^{18}/O^{16} and C^{13}/C^{12} ratios of diagenetically altered limestones in the Bermuda Islands: Jour. Geology, v. 72, no. 2, p. 170–194.

Gulbrandsen, R. A., 1960, Petrology of the Meade Peak phosphatic shale member of the Phosphoria formation at Coal Canyon, Wyoming: U.S. Geol. Survey Bull. 1111-C, p. 71–146.

—— 1969, Physical and chemical factors in the formation of marine apatite: Econ. Geology, v. 64, no. 4, p. 365–382.

Hodgson, W. A., 1966, Carbon and oxygen isotope ratios in diagenetic carbonates from marine sediments: Geochim. et Cosmochim. Acta, v. 30, no. 12, p. 1223–1233.

Illing, L. V., Wells, A. J., and Taylor, J. C. M., 1965, Penecontemporary dolomite in the Persian Gulf: Soc. Econ. Paleontologists and Mineralogists Spec. Pub. 13, p. 89–111.

Kay, G. M., 1947, Geosynclinal nomenclature and the craton: Am. Assoc. Petroleum Geologists Bull., v. 31, no. 7, p. 1289–1293.

Keith, M. L., and Weber, J. N., 1964, Carbon and oxygen isotopic composition of selected limestone and fossils: Geochim. et Cosmochim. Acta, v. 28, p. 1787–1816.

Kinsman, D. J. J., 1971, Sabkhas–Studies in recent carbonate sedimentation and diagenesis, Persian Gulf: Geol. Soc. America Abs. with Programs, v. 3, no. 7, p. 772–774.

Knauth, L. P., and Epstein, Samuel, 1971, Oxygen and hydrogen isotope relationships in cherts and implications regarding the isotopic history of the hydrosphere: Geol. Soc. America Abs. with Programs, v. 3, no. 7, p. 624–625.

Land, L. S., and Epstein, Samuel, 1970, Late Pleistocene diagenesis and dolomitization, north Jamica: Sedimentology, v. 14, p. 187–200.

Landergren, Sture, 1954, On the relative abundance of the stable carbon isotopes in marine sediments: Deep-Sea Research, v. 1, no. 2, p. 98–120.

Lippman, Friedrich, 1968, Synthesis of $BaMg(CO_3)_2$ (Norsethite) at 20°C and the formation of dolomite in sediments, *in* Recent developments in carbonate sedimentology in central Europe: New York, Springer-Verlag, p. 33–37.

Lloyd, R. M., 1966, Oxygen isotope enrichment of sea water by evaporation: Geochim. et Cosmochim. Acta, v. 30, no. 8, p. 801–814.

McKelvey, V. E., and others, 1959, The Phosphoria, Park City, and Shedhorn formations in the western phosphate field: U.S. Geol. Survey Prof. Paper 313-A, 47 p.

Müller, German, and Tietz, Gerd, 1966, Recent dolomitization of Quaternary biocalcarenites from Fuerteventura (Canary Islands): Contr. Mineralogy and Petrology, v. 13, p. 89–96.

Murata, K. J., Friedman, Irving, and Cramer, Marcelyn, 1972, Geochemistry of diagenetic dolomites in Miocene formations of California and Oregon: U.S. Geol. Survey Prof. Paper 724-C.

Murata, K. J., Friedman, Irving, and Madsen, B. M., 1969, Isotopic composition of diagenetic carbonates in marine Miocene formations of California and Oregon: U.S. Geol. Survey Prof. Paper 614-B, 24 p.

Northrup, D. A., and Clayton, R. N., 1966, Oxygen-isotope fractionations in systems containing dolomite: Jour. Geology, v. 74, no. 2, p. 174–196.

O'Neil, J. R., and Epstein, Samuel, 1966, Oxygen isotope fractionation in the system dolomite-calcite-carbon dioxide: Science, v. 152, no. 3719, p. 198–201.

Perry, E. C., Jr., 1967, The oxygen isotope chemistry of ancient cherts: Earth and Planetary Sci. Letters, v. 3, no. 1, p. 62–66.

Presley, B. J., and Kaplan, I. R., 1968, Changes in dissolved sulfate, calcium and carbonate from interstitial waters of near-shore sediments: Geochim. et Cosmochim. Acta, v. 32, no. 10, p. 1037–1048.

Rogers, J. P., 1971, Tidal sedimentation and its bearing on reservoir and trap in Permian Phosphoria strata, Cottonwood Creek Field, Big Horn Basin, Wyoming: Mtn. Geologist, v. 8, no. 2, p. 71–80.

Sheldon, R. P., 1963, Physical stratigraphy and mineral resources of Permian rocks in western Wyoming: U.S. Geol. Survey Prof. Paper 313-B, p. 49–273.

Sheldon, R. P., Cressman, E. R., Cheney, T. M., and McKelvey, V. E., 1967, Middle Rocky Mountains and northeastern Great Basin, chap. H *in* Paleotectonic investigations of the Permian System in the United States: U.S. Geol. Survey Prof. Paper 515, p. 157–170.

Sheldon, R. P., Maughan, E. K., and Cressman, E. R., 1967, Sedimentation of rocks of Leonard (Permian) age in Wyoming and adjacent states, *in* Anatomy of the western phosphate field: Intermtn. Assoc. Geologists 15th Ann. Field Conf., Salt Lake City, p. 1–13.

Sheppard, S. M. F., and Schwarcz, H. P., 1970, Fractionation of carbon and oxygen isotopes and magnesium between coexisting metamorphic calcite and dolomite: Contr. Mineralogy and Petrology, v. 26, p. 161–198.

Shinn, E. A., Ginsburg, R. N., and Lloyd, R. M., 1965, Recent supratidal dolomite from Andros Island, Bahamas: Soc. Econ. Paleontologists and Mineralogists Spec. Pub. 13, p. 112–123.

Shinn, E. A., Lloyd, R. M., and Ginsburg, R. N., 1969, Anatomy of a modern carbonate tidal-flat, Andros Island, Bahamas: Jour. Sed. Petrology, v. 39, no. 3, p. 1202–1228.

Spotts, J. H., and Silverman, S. R., 1966, Organic dolomite from Point Fermin, California: Am. Mineralogist, v. 51, no. 7, p. 1144–1155.

Tan, F. C., and Hudson, J. D., 1971, Carbon and oxygen isotopic relationships of dolomites and co-existing calcites, Great Estuarine Series (Jurassic), Scotland: Geochim. et Cosmochim. Acta, v. 35, no. 8, p. 755–767.

Usdowski, H. E., 1968, The formation of dolomite in sediments, *in* Recent developments in carbonate sedimentology in central Europe: New York, Springer-Verlag, p. 21–32.

Weber, J. N., Bergenback, R. E., Williams, E. G., and Keith, M. L., 1965, Reconstruction of depositional environments in the Pennsylvanian Vanport basin by carbon isotope ratios: Jour. Sed. Petrology, v. 35, no. 1, p. 36–48.

Yochelson, E. L., 1968, Biostratigraphy of the Phosphoria, Park City, and Shedhorn Formations: U.S. Geol. Survey Prof. Paper 313-D, p. 571–660.

URANIUM, THORIUM, AND LEAD CONCENTRATIONS IN THREE SILICATE STANDARDS AND A METHOD OF LEAD ISOTOPIC ANALYSIS

By MITSUNOBU TATSUMOTO, ROY J. KNIGHT,
and MARYSE H. DELEVAUX, Denver, Colo.

Abstract.—Isotope dilution analyses of uranium, thorium, and lead in two U.S. Geological Survey rock standards, BCR-1 and AGV-1, and those in a National Aeronautics and Space Administration (NASA) basalt (from Knippa, Tex.) standard showed that concentrations in BCR-1 are 1.73 ppm U, 5.99 ppm Th, and 13.56 ppm Pb, in AGV-1 are 1.96 ppm U, 6.27 ppm Th, and 36.53 ppm Pb, and in NASA basalt are 1.87 ppm U, 6.42 ppm Th, and 5.13 ppm Pb. A comparison of lead contents for BCR-1 and the original split indicates that the standard is contaminated by lead; however, homogeneity of the sample has been established and variation of the concentration is less than 1 percent. A new technique for isotopic analysis of lead, the silica gel-phosphate method, was tested for analytical uncertainties. The lead isotopic composition for BCR-1 obtained by the method using double-spike fractionation correction is Pb^{206}/Pb^{204} = 18.794, Pb^{207}/Pb^{204} = 15.610, and Pb^{208}/Pb^{204} = 38.660.

Lead, uranium, and thorium concentrations in U.S. Geological Survey (USGS) rock standards BCR-1 (basalt) and AGV-1 (andesite) and in a basalt standard distributed by the National Aeronautics and Space Administration (NASA) were determined by the isotope dilution procedure. BCR-1 is a trachybasalt (Yakima Basalt of the Columbia River Group) from the Bridal Veil Flow quarry, Washington. AGV-1 is a trachyandesite from Guano Valley, Oreg. Sample localities and petrographic descriptions for these standards were reported by Flanagan (1967). The NASA basalt standard is from the Knippa quarry, Uvalde County, Tex., and was distributed to lunar-sample investigators by NASA. (See Levinson, 1970.)

During our analyses, we realized that the lead concentration determined for BCR-1 was significantly higher than that for comparable Miocene basalts from Oregon and Washington (Tatsumoto and Snavely, 1969), and lead contamination during preparation of the standard was suspected. A sample of the original block, from which the standard was prepared, was obtained from R. G. Coleman. This sample, hereafter referred to as BCR-chip, was pulverized and analyzed for contents of lead, uranium, and thorium for comparison with those of BCR-1.

Acknowledgments.—We thank Donald A. Morrison, NASA, Manned Spacecraft Center, and R. G. Coleman and B. R. Doe, U.S. Geological Survey, for supplying the samples.

ISOTOPE DILUTION ANALYSES FOR URANIUM, THORIUM, AND LEAD CONCENTRATIONS

Sample preparation

Most of our work dealing with uranium, thorium, and lead is an application of U^{238}/Pb^{206}, U^{235}/Pb^{207}, and Th^{232}/Pb^{208} decay schemes to lead isotopic tracer studies of lunar and terrestrial rocks. The following discussion is therefore limited to the methods used in determining uranium, thorium, and lead in volcanic rocks. The methods, however, are applicable to other silicate samples.

Because of extremely low lead concentrations in some volcanic rocks and a high concentration of lead aerosol in the atmosphere from automobile exhaust, extreme care should be exercised during the entire course of lead analyses. In general procedure for the analyses of total-rock samples, at least 1 kg of sample was collected. This large sample was sawed into small cubes (about 3/4 cu in.), and only those cubes representing the interior of the original sample were used for analyses. The surfaces of the cubes were cleaned repeatedly in an ultrasonic vibrator with distilled water, and with 6 *N* HCl for a half minute; they were then rinsed with distilled water. The cubes were next crushed by a diamond steel mortar, pulverized to about −100 mesh, and thoroughly mixed by a tungsten carbide crusher "shatterbox," capacity of about 100 g, in the lead-free laboratory of the U.S. Geological Survey.

The two USGS rock standards were split by a microsplitter, made of aluminum, to minimize the effect of inhomogeneity in the powdered material. The NASA basalt standard is distributed in small polystyrene vials (1 g each), and the entire content was used for each concentration run.

Reagents

Water.—Quintuple distilled. Secured from further distillation of triple-distilled water (Doe and others, 1967) by quartz stills.

Hydrofluoric acid (50 percent).—Commercial HF gas was filtered through a Teflon filter (9μ porosity), distilled twice, and then bubbled in quintuple-distilled water in a Teflon bottle. The purification system was all constructed of Teflon and Kel-F (Tatsumoto, 1969).

Perchloric acid (70 percent).—Commercial, vacuum triple-distilled in Vycor and shipped in Vycor. The acid was redistilled in quartz still.

Barium nitrate (saturated).—Saturated $Ba(NO_3)_2$ in water (pH about 2) was extracted first with 4-percent TTA-benzene solution three times for purification of uranium and thorium. After the pH of the solution was increased to 9 by ammonia gas, the solution was extracted for lead with dithizone-chloroform solution. Entrapped dithizone was removed by replicate chloroform extraction.

Nitric acid (concentrated).—Commercial reagent (70 percent) was purified first for lead by coprecipitation with barium. This was achieved by adding 6 ml of the purified barium-nitrate-water-saturated solution in a 5-pound reagent bottle. Only the supernatant was filtered in a quartz distiller through a Teflon filter (9μ porosity). Then the acid was distilled twice under vacuum (5 mm Hg pressure). The first 1/10 and the last 2/10 portions were discarded. The acid was kept in a Teflon bottle. Four hundred milliliters of concentrated HNO_3 was diluted with water to 1 liter to make 6.5 *N* HNO_3 for resin work.

Chloroform.—Double distilled from reagent grade.

Ammonium hydroxide and ammonium nitrate (2 percent).—Same as that of Doe and others (1967).

Ammonium citrate.—A 25-percent water solution of commercial reagent was purified by dithizone extraction (Doe and others, 1967). The dithizone extraction, including the removal of entrapped dithizone by chloroform, was repeated more than 20 times.

Potassium cyanide.—A 10-percent ammoniacal-water solution was purified by repeated dithizone extraction, as described in the ammonium citrate purification procedure.

Dithizone.—Analytical-grade dithizone was purified by extraction in ammoniacal water and by back extraction in chloroform at pH 6. The procedure was repeated.

Dowex 1 resin, NO_3^- form.—Dowex 1-chloride form, 100–200 mesh (AG grade from Bio-Rad Laboratory) was washed twice, first with pure 6 *N* HCl, then with distilled water, for 4 hours, standing by for each step. The washed resin was converted in NO_3 form by soaking the resin in 6.5 *N* HNO_3 twice.

The HF and HNO_3 were stored in Teflon bottles and $HClO_4$ was stored in a quartz dispenser. All other reagents were stored in polyethylene bottles.

Analytical technique

Analytical techniques were similar to those reported previously (Doe and others, 1967), except that the spike was added gravimetrically and decomposition was performed in a Teflon tank under nitrogen atmosphere.

The weighed sample in a Teflon beaker was gravimetrically spiked with a combined U^{235}, Th^{230}, and Pb^{206} spike solution. The sample was decomposed with HF and $HClO_4$ under nitrogen atmosphere by placing the Teflon beaker in a Teflon tank into which nitrogen is flowing. The residue was taken in a large volume (100 ml per 1-g sample) of 0.5 *N* HNO_3 in order to facilitate isotopic equilibration, and the solution was evaporated. The residue from decomposition was taken up in concentrated HNO_3, and lead was separated by $Ba(NO_3)_2$ coprecipitation (Tatsumoto, 1966). The lead was further purified by dithizone extraction (Tilton and others, 1955). The evaporated supernatant from $Ba(NO_3)_2$ coprecipitation was taken in solution with 6.5 *N* HNO_3; uranium and thorium were separated by use of an anion-exchange resin, Dowex 1-X8 NO_3^- form (Tatsumoto, 1966).

Blanks have consistently been determined for every six samples, and are as follows: 0.1–0.2 ng (nanograms) U, 0.2–0.4 ng Th, and 10–20 ng Pb for an analysis of a 1-g sample.

RESULTS

Concentrations of uranium, thorium, and lead are given in tables 1 and 2. For the replicate analyses of USGS rock standards the coefficient of variation for uranium, thorium, and lead does not exceed ±1 percent. The smaller analytical uncertainties on uranium and thorium analyses compared to those for the standard granite G-2 (Doe and others, 1967) and granodiorite GSP-1 (Peterman and others, 1967) may be due to sample inhomogeneities in the granite and granodiorite standards. The lead concentration of the split chip sample, BCR-chip, is 8.61 ppm instead of 13.56 ppm as in BCR-1, although the uranium and thorium concentrations in the two powders differ only slightly. If BCR-chip is a representative sample, it is reasonable to assume that BCR-1 was contaminated with lead during sample preparation. However, because of the small variation in the concentration, the standard still retains value as a rock standard. The replicate analyses of NASA basalt show less than 1 percent variation in uranium concentration but more than 1 percent variation in lead and thorium concentrations.

Isotopic analyses of Pb (obtained by PbS run) are given in table 3. The lead isotopic compositions for AGV-1 and BCR-1 are in the range reported for Oregon and Washington volcanic rocks (Tatsumoto and Snavely, 1969; Davis and others, 1965) even though AGV-1 and BCR-1 were presumably contaminated. The lead isotopic composition for BCR-1 is slightly less radiogenic than that of BCR-chip. On the assumption that the difference between BCR-1 and BCR-chip is due solely to one kind of lead contamination and as deduced from a material balance, the lead isotopic composition of the contaminant is Pb^{206}/Pb^{204} = 18.89, Pb^{207}/Pb^{204} = 15.69, and Pb^{208}/Pb^{204} = 38.75.

The Th/U ratios of AGV-1, BCR-1, and BCR-chip are 3.3, 3.6, and 3.6, respectively, and are in the range for volcanic rocks of this area (Tatsumoto and Snavely, 1969); however, U^{238}/Pb^{204} ratios of AGV-1 and BCR-1—3.5 and 8.2, respectively—are low compared to those ratios for similar rocks of the area. The U^{238}/Pb^{204} of BCR-chip is 12.8, suggesting that the standard basalt BCR-1, and probably AGV-1, were contaminated by lead during preparation. Other

Table 1.—*Concentrations, in parts per million, of uranium, thorium, and lead in the standard basalt BCR-1, the standard andesite AGV-1, and a separate chip of BCR-1*

Run	AGV-1 Split 18, position 13			BCR-1 Split 23, position 4			BCR-chip		
	U	Th	Pb	U	Th	Pb	U	Th	Pb
1	1.99	6.26	36.59	1.72	6.00	13.55	1.69	5.85	8.59
2	1.95	6.25	36.39	1.73	6.03	13.61	1.69	5.85	8.61
3	1.95	6.29	36.51	1.73	6.01	13.60	1.70	5.86	8.60
4	1.97	6.30	36.76	1.72	5.94	13.57	1.69	5.85	8.62
5	1.95	6.24	36.38	1.73	5.96	13.48	....	....	....
Mean	1.962	6.268	36.526	1.726	5.988	13.564	1.693	5.853	8.605
Coefficient of variation	±0.92	±0.41	±0.43	±0.29	±0.62	±0.38	±0.35	±0.10	±0.15

Table 2.—*Uranium, thorium, and lead concentrations, in parts per million, in NASA basalt standard[1] from Knippa, Tex.*

Run	Vial No.	U	Th	Pb
1	K5	1.87	6.56	5.11
2	K58	1.87	6.29	5.17
3	K60	1.86	6.32	5.17
4	K64	1.87	6.39	5.16
5	K102	1.86	6.50	5.06
6	K111	1.87	6.45	5.13
Mean		1.866	6.419	5.132
Coefficient of variation		±0.27	±1.6	±0.80

[1] Raw data of lead isotopic composition measured by PbS method are: Pb^{206}/Pb^{204} = 19.16; Pb^{207}/Pb^{204} = 15.77; Pb^{208}/Pb^{204} = 39.25.

standard samples prepared in the same manner may also have been contaminated, mostly by lead.

SILICA GEL-PHOSPHATE METHOD

More than a decade ago, Akishin and others (1957) published a new method in which silica-zirconia gel was used as an activator to effectively produce lead ions by thermal ionization in a mass spectrometer. Recently, Cameron and others (1969) adopted the method and reported that silica gel alone is useful for very small—less than 0.5 μg—samples of lead.

Because of the smallness of the lunar samples, we investigated this method. Our method, modified from that of Cameron and others, was established independently of other laboratories. Our reagent preparation was somewhat different from that of others (Cameron and others, 1969; Shields, 1970), and the method was thoroughly tested for fractionation of lead isotopes. BCR-1 was analyzed for lead isotopic composition by the silica gel-phosphate method and the result, which was corrected by the fractionation factor, was compared with the double-spike corrected value.

Reagents

Silica gel.—4.8 g of metasodium silicate ($Na_2SiO_3 \cdot 9H_2O$) was dissolved in 500 ml of water and the solution (pH ≈9) was extracted three times with dithizone in chloroform, and the entrapped dithizone was then removed by a chloroform rinse. The rinsing was repeated after the pH of the solution was adjusted to about 6. Five milliliters of clean double-distilled HNO_3 was added, and the solution was evaporated in a Teflon beaker placed in a 110°C oven overnight. The silica gel was taken up in 50 ml of 1-percent HNO_3, warmed, and was stirred well with a Teflon rod. The silica gel suspension was further vibrated by an ultrasonic vibrator to produce a finer gel. The hot solution was filtered through filter paper, and the silica gel was washed repeatedly with hot 1-percent HNO_3 and finally with hot water. The silica gel was washed into a Teflon bottle with 200 ml of water and was further vibrated by an ultrasonic vibrator for 8 hours. The suspension contained 5 μg of SiO_2 per 1 λ.

Phosphoric acid.—Sublimated P_2O_5 of Baker's "ultra-pure grade" was dissolved, and a solution of 100 μg of P_2O_5 per 1 ml was made.

Lead mounting on filaments

One milliliter of phosphoric acid was added to the lead separated from a silicate rock in a small Teflon beaker and was

Table 3.—*Lead isotopic compositions of BCR-1, AGV-1, and BCR-chip obtained by PbS method (not adjusted to absolute values)*

Run	AGV-1 Split 18, position 13			BCR-1 Split 23, position 4			BCR-chip		
	Pb^{206}/Pb^{204}	Pb^{206}/Pb^{207}	Pb^{206}/Pb^{208}	Pb^{206}/Pb^{204}	Pb^{206}/Pb^{207}	Pb^{206}/Pb^{208}	Pb^{206}/Pb^{204}	Pb^{206}/Pb^{207}	Pb^{206}/Pb^{208}
1	19.023	1.2062	0.4887	18.906	1.2009	0.4833	18.925	1.1985	0.4804
2	19.013	1.2083	.4890	18.915	1.1996	.4828	18.923	1.1985	.4807
Average	19.018	1.2073	.4889	18.911	1.2003	.4831	18.924	1.1985	.4806

evaporated. The residue made a small bead on the bottom of the Teflon beaker. The bead was taken up with 10 λ silica-gel solution using a Teflon tube (0.031 in. ID) attached to the tip of a syringe. It was loaded on about the center of a single rhenium filament (0.001 by 0.030 in.) which had been previously degassed. The drop of lead phosphate–silica gel mixture was dried with a current of 1.2 amperes through the filament. The current was increased carefully until the filament was heated to a dull-red glow.

Results

The National Bureau of Standards (NBS) equal-atom lead standard SRM-982 was analyzed in replicate by the silica-gel method (table 4). The fractionation factor of 1,285°C and 1,350°C runs was about 0.15 percent per mass unit, as can be seen from the 2.4-μg lead runs. The Pb^{206}/Pb^{207} and Pb^{206}/Pb^{208} values of the 0.24-μg lead runs (experiment 2) indicated that the fractionation was even smaller than for the 2.4-μg run. But fractionation for Pb^{206}/Pb^{204} values was larger. The large difference in Pb^{206}/Pb^{204} may be due mostly to an error in measuring the small Pb^{204} signal.

At an early stage (experiment 3) in the development of the technique, 500 μg of $(NH_4)_3PO_4$ which was purified by dithizone extraction was used. The Pb^{206}/Pb^{208} value was very close to the absolute value (Catanzaro and others, 1968); however, the Pb^{206}/Pb^{204} value was 0.3 percent per mass unit different from the absolute ratio. This difference probably resulted mostly from contamination and does not indicate real fractionation.

The lead phosphate technique (without silica gel) was further tested by the triple-filament method using a platinum ionization filament and rhenium sample filaments (Catanzaro, 1967). The 50-μg equal-atom lead gave $1-1.5\times10^{-11}$ amperes of Pb^{206} ion-beam current. The results are summarized in table 4. The 50-μg lead results are extremely close to the absolute value and indicate that the phosphate is more effective than the hydroxide for ionization by the triple-filament method because it can be applied to a smaller sample.

In table 5, we have summarized the lead isotopic compositions obtained by different methods for BCR-1. To the data obtained by the PbS method as given in table 2 were applied a 0.33-percent correction per mass unit which was obtained by comparison of replicate analyses of CIT (California Institute of Technology) shelf lead by the PbS method (Tatsumoto and Knight, 1969; Pb^{206}/Pb^{204} = 16.751, Pb^{206}/Pb^{207} = 1.0700, Pb^{206}/Pb^{208} = 0.4542) and the absolute value obtained by Catanzaro and others (1968; Pb^{206}/Pb^{204} = 16.625, Pb^{206}/Pb^{207} = 1.0743, Pb^{206}/Pb^{208} = 0.4580). Silica-gel data are listed as uncorrected and with a 0.15-percent correction per mass unit. The corrected data from both the PbS and silica-gel methods are in good agreement with results obtained by V. M. Oversby (1971, written commun. to B. R. Doe); however, these data are about 0.12 percent different in Pb^{207}/Pb^{204} value than the absolute value obtained by us using the double-spike correction method, even though Pb^{206}/Pb^{204} and Pb^{208}/Pb^{204} values agree well in all analyses.

REFERENCES

Akishin, P. A., Nikitin, O. T., and Panchenkov, G. M., 1957, A new effective ionic emitter for the isotopic analysis of lead: Geokhimiya, no. 5, p. 425–429.

Cameron, A. E., Smith, D. H., and Walker, R. L., 1969, Mass spectrometry of nanogram-size samples of lead: Anal. Chemistry, v. 41, no. 3, p. 525–526.

Table 4.—*Lead isotopic determination by silica-gel and phosphate triple-filament methods on NBS SRM-982 equal-atom lead*

[The uncertainties listed in this table are 95-percent confidence limits on the mean. Mass spectrometer operator, Maryse Delevaux]

Run	Experiment	Pb^{206}/Pb^{204}	Pb^{206}/Pb^{207}	Pb^{206}/Pb^{208}
	Absolute values (Catanzaro and others, 1968).	36.739±0.027	2.14101±0.00092	0.99984±0.00035
	Silica gel–phosphate single-filament method			
1	2.4 μg Pb:			
	Average of 5 runs at 1,285°C.	36.646±0.121	2.1446±0.0024	1.00290±0.0012
	Average of 5 runs at 1,350°C.	36.638±0.172	2.1441±0.0094	1.00283±0.0058
2	0.24 μg Pb:			
	Average of 6 runs at 1,200°C.	36.512±0.215	2.1396±0.0053	1.00026±0.0023
	Average of 6 runs at 1,285°C.	36.585±0.099	2.1393±0.0017	1.00020±0.0018
3	0.24 μg Pb with large amount $(NH_4)_3PO_4$:			
	Average of 6 runs at 1,285°C.	36.509±0.150	2.1379±0.0094	.99804±0.0058
	Average of 6 runs at 1,350°C.	36.507±0.168	2.1364±0.0100	.99759±0.0069
	Phosphate triple-filament method			
4	25 μg Pb:			
	Average of 7 runs.	36.527±0.028	2.1433±0.0044	1.00189±0.0005
5	50 μg Pb:			
	Average of 8 runs.	36.675±0.016	2.1421±0.0029	1.0005±0.0089

Table 5.—*Summary of lead isotopic composition for BCR-1*

Run	Method	Fractionation factor per mass unit (percent)	Pb^{206}/Pb^{204}	Pb^{207}/Pb^{204}	Pb^{208}/Pb^{204}	Analyst
1	PbS	−0.33	18.786	15.631	38.631	Mitsunobu Tatsumoto.
2	Silica gel	0	18.728	15.562	38.422	Do.
		+.15	18.784	15.632	38.653	Do.
3	...do...	0	18.743	15.546	38.449	Maryse Delevaux.
		Double spike correction.	18.794	15.610	38.660	Do.
		([1])	18.802	15.621	38.692	Do.
4	KI_2	Double-spike correction.	18.77	15.63	38.65	V. M. Oversby (written commun., 1971).

[1] Applied correction factors are 1.00314, 1.00480, 1.00633 for Pb^{206}/Pb^{204}, Pb^{207}/Pb^{204}, and Pb^{208}/Pb^{204}, respectively (Stacey and others, 1972).

Catanzaro, E. J., 1967, Absolute isotopic abundance ratios of three common lead reference samples: Earth and Planetary Sci. Letters, v. 3, p. 343–346.

Catanzaro, E. J., Murphy, T. J., Shields, W. R., and Garner, E. L., 1968, Absolute isotopic abundance ratios of common, equal-atom, and radiogenic lead isotopic standards: U.S. Natl. Bur. Standards Jour. Research, A. Phys. Chem., v. 72A, no. 3, p. 261–267.

Davis, G. L., Tilton, G. R., Aldrich, L. T., Hart, S. R., and Steiger, R. H., 1965, Geochronology and isotope geochemistry: Carnegie Inst. Washington Year Book 64, p. 165–171.

Doe, B. R., Tatsumoto, Mitsunobu, Delevaux, M. H., and Peterman, Z. E., 1967, Isotope-dilution determination of five elements in G-2 (granite), with a discussion of the analysis of lead, *in* Geological Survey Research 1967: U.S. Geol. Survey Prof. Paper 575-B, p. B170–B177.

Flanagan, F. J., 1967, U.S. Geological Survey silicate rock standards: Geochim. et Cosmochim. Acta, v. 31, no. 3, p. 298–308.

Levinson, A. A., ed., 1970, Proceedings of the Apollo 11 Lunar Science Conference: Geochim. et Cosmochim. Acta, Suppl. 1, v. 1–3, Pergamon Press.

Peterman, Z. E., Doe, B. R., and Bartel, Ardith, 1967, Data on the rock GSP-1 (granodiorite) and the isotope-dilution method of analysis for Rb and Sr, *in* Geological Survey Research 1967: U.S. Geol. Survey Prof. Paper 575-B, p. B181–B186.

Shields, W. R., ed., 1970, Analytical mass spectrometry section, *in* Summary of activities, July 1969 to June 1970: U.S. Natl. Bur. Standards Tech. Note 548, p. 71–74.

Stacey, J. S., Wilson, E. E., and Terrazas, R., 1972, Digital recording for mass spectrometry in geologic studies–II: Canadian Jour. Earth Sci. [Preprint].

Tatsumoto, Mitsunobu, 1966, Isotopic composition of lead in volcanic rocks from Hawaii, Iwo Jima, and Japan: Jour. Geophys. Research, v. 71, p. 1721–1733.

—— 1969, New method for preparing ultrapure hydrofluoric acid: Anal. Chemistry, v. 41, p. 2088–2089.

Tatsumoto, Mitsunobu, and Knight, R. J., 1969, Isotopic composition of lead in volcanic rocks from central Honshu with regard to basalt genesis: Geochem. Jour., v. 3, p. 53–86.

Tatsumoto, M., and Shavely, P. D., 1969, Isotopic composition of lead in rocks of the coast range, Oregon and Washington: Jour. Geophys. Research, v. 74, no. 4, p. 1087–1100.

Tilton, G. R., Patterson, Claire, Brown, Harrison, Inghram, Mark, Hayden, Richard, Hess, David, and Larsen, Esper, Jr., 1955, Isotopic composition and distribution of lead, uranium, and thorium in a Precambrian granite: Geol. Soc. America Bull., v. 66, no. 9, p. 1131–1148.

POTASSIUM-ARGON AGES FROM AREAS OF HYDROTHERMAL ALTERATION IN SOUTH CAROLINA

By HENRY BELL III; R. F. MARVIN, and H. H. MEHNERT,
Beltsville, Md.; Denver, Colo.

Abstract.—Muscovite samples from auriferous rocks representing three areas of hydrothermal alteration within the Carolina slate belt have been dated by the potassium-argon method. The apparent ages, ranging from 317 m.y. to 430 m.y., indicate that the hydrothermally altered rocks and ore deposits are not related to nearby unmetamorphosed granitic plutons, as had been previously suggested, but rather are related to early Paleozoic volcanic events.

Four unmetamorphosed granite plutons in the eastern Carolina piedmont intrude rocks which nearby contain gold deposits and areas of hydrothermal alteration. The solutions causing the alteration and the associated gold deposits have been attributed to these plutons. K-Ar ages of muscovite concentrates from the hydrothermally altered rocks, however, are older than published ages for two of these nearby plutons, the Liberty Hill pluton and the Winnsboro pluton. The older apparent ages for the muscovites suggest that the hydrothermally altered rocks and the ore deposits are not related to these unmetamorphosed granite plutons, as has been previously suggested, but rather to older plutonic or volcanic rocks.

This report discusses the samples from which the muscovites came and some implications of the results of the age determinations for prospecting in the Carolina slate belt.

THE SAMPLES

The samples of muscovite used for age determination were collected at the Brewer mine in Chesterfield County, the Blackmon mine in Lancaster County, and at Little Mountain in Newberry County, S.C. (fig. 1). The Brewer and Blackmon mines are approximately 8 miles apart, and Little Mountain is about 50 miles southwest of the Blackmon mine. The apparent ages calculated for the muscovite from these areas average 415, 358, and 319 million years, respectively (table 1). These ages are significantly older than the Permian age postulated for the granites on the basis of zircon ages (Overstreet and Bell, 1965) and older than the approximate 300-m.y. age which Fullager (1971) determined for the same granites by whole-rock Rb-Sr analysis.

Brewer mine

Two samples of muscovite for K-Ar dating came from the Brewer mine in Chesterfield County. This old gold mine is particularly noted for massive topaz. The mine is in intensely altered fragmental volcanic rocks of the Carolina slate belt about a mile south of outcrops of a granitic pluton. The volcanic rocks were probably originally rhyolitic to dacitic. Now they are principally pyritiferous quartz-sericite schists, silicified schists, and silicified breccias. In addition to free

Table 1.—*Analytical data for* K-Ar *age determinations on muscovite from altered rocks in South Carolina*

[Constants: $K^{40}\lambda = 0.585\times10^{-10}$ yr^{-1}, $\lambda_\beta = 4.72\times10^{-10}$ yr^{-1}. Abundance: $K^{40} = 1.19\times10^{-4}$ atom percent. Potassium determinations made with an Instrumentation Laboratories flame photometer with an Li internal standard. Analysts: R. F. Marvin, H. H. Mehnert, and Violet Merritt]

Sample No.	K_2O (percent)	Radiogenic argon (10^{-10} moles/gram)	Radiogenic argon (percent)	Age (m.y.,±2σ)
13-HB-15	8.42, 8.31	59.53	99	430±15
13-HB-40	7.24, 7.29	47.93	96	401±14
Blackmon 1	6.14, 6.16	36.20	97	362±13
Blackmon 2	7.78, 7.72	44.58	97	354±12
LM3-228	3.29, 3.34	17.17	94	322±11
LM3-257	6.87, 6.93	35.11	97	317±11

Location and description of samples:

13-HB-15 and 13-HB-40. Drainage tunnel, Brewer mine, Chesterfield County, S.C. (lat 34°39′06″ N.; long 80°24′48″ W.). Sample 13-HB-15 is muscovite plus some pyrophyllite; 13-HB-40 is similar to 13-HB-15, has some hematite stain, and was taken at a different place.

Blackmon 1 and 2. Blackmon mine, Lancaster County, S.C. (lat 34°39′36″ N.; long 80°35′01″ W.). Both samples are muscovite with some quartz, but were taken from different places on the mine dump.

LM3-228 and LM3-257. Little Mountain, Newberry County, S.C. (lat 34°10′56″ N.; long 81°25′40″ W.). Sample LM3-228 is impure muscovite from drill core 228 ft below the collar elevation; LM3-257 is muscovite with minor pyrite contamination from drill core 257 ft below the collar elevation.

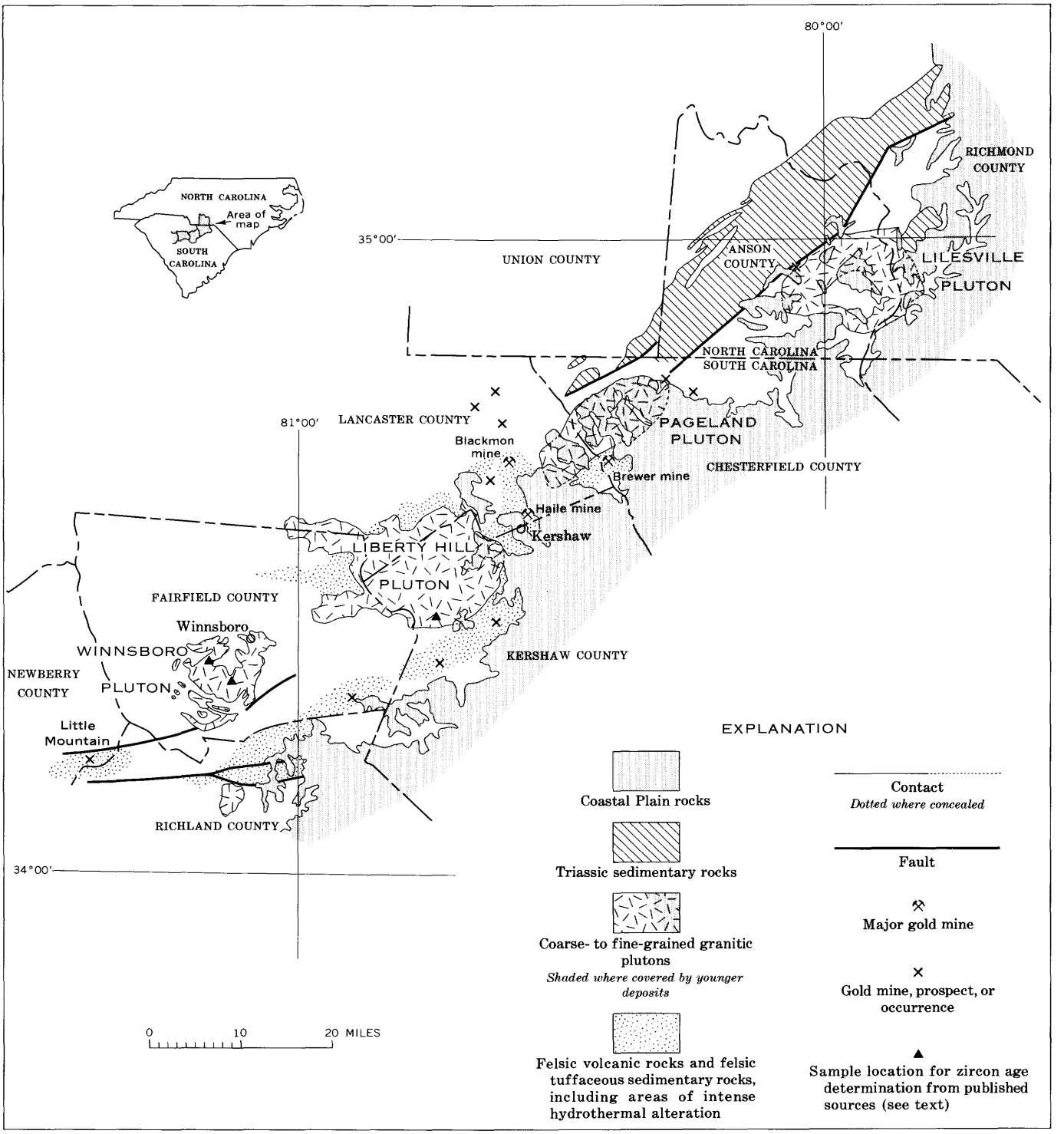

Figure 1.—Geologic map of part of North Carolina and South Carolina. Modified from Overstreet and Bell (1965), Secor and Wagener (1968), and North Carolina Div. Mineral Resources (1958).

gold, a list of minerals reported from the Brewer mine includes pyrite, pyrophyllite, ilmenite, rutile, topaz, kyanite, andalusite, enargite, covellite, cassiterite, bismutite, and native bismuth (Pardee and others, 1937; Fries, 1942; Pardee and Park, 1948).

The samples from which muscovite was obtained are a mixture of muscovite and quartz and were cut from the wall of the drainage tunnel extending out from the large open cut. They came from a depth of more than 100 feet below the

surface and appear mostly unaffected by surficial weathering. A small amount of reddish iron stain along fractures may be the result of surficial weathering but could have been deposited by the hydrothermal solutions. One sample has some small vugs, and X-ray diffraction analysis indicates that the sample also contains kaolinite and pyrophyllite. Although the specimens from which the muscovite was obtained contain no visible ore minerals and do not have features attributable to a fragmental volcanic origin, they are from the intensely altered rocks which nearby contain ore minerals. Thus, the muscovite appears to be related to the ore-forming process.

Blackmon mine

Muscovite separated from two samples collected at the Blackmon mine gave K-Ar ages of 362 m.y. and 354 m.y. The Blackmon mine, also an old gold mine, is noted for an extensive deposit of sericite schist which was mined until recently from underground workings extending more than 180 feet below the surface and now flooded. According to Graton (1906), the gold-bearing rocks are a dull-gray to pinkish, bluish, or green sericite schist containing numerous tiny red and black garnets, pyrite, siliceous lenses, and quartz veins. A porphyritic rock, foliated in part, consisting of a fine-grained mosaic of quartz, sericite, epidote, some zoisite, and large phenocrysts of quartz and turbid feldspar is in contact with the sericite schist. The Blackmon mine is about 2½ miles from outcrops of the Pageland granite. The Liberty Hill granite is about 5 miles to the southwest. A swarm of Triassic dikes trending north-northwest passes between the two granite plutons. There is much hydrothermal alteration in this area between the plutons, and both the Blackmon mine and the Haile mine, where massive pyrite and gold have been mined, are included in the altered area. Samples of coarse-grained sericite schist for age determination were collected from the freshest dump material available at the Blackmon mine. The samples consisted of muscovite, quartz, and some pyrophyllite.

Little Mountain

Two samples of muscovite from diamond drill core obtained at Little Mountain were also dated. The samples gave apparent ages of 322 m.y. and 317 m.y. Little Mountain, a syncline trending N. 70° E. (Kesler, 1972), and other nearby ridges are held up by kyanite quartzite and hematite quartzite in an area of abundant quartz sericite schists and phyllites. The major constituents of the quartzites are quartz, kyanite, and mica (McKenzie and McCauley, 1968). Muscovite, paragonite, and pyrophyllite have also been identified. Pyrite, rutile, ilmenite, hematite, lazulite, corundum, cassiterite, and garnet are accessory minerals. Gold occurs nearby but has not been mined. The kyanite occurs disseminated, as veinlets, and as elliptical pods. The pyrophyllite occurs disseminated with micas and as radial aggregates along joint surfaces with quartz veinlets. Rutile occurs as black crystals disseminated throughout the quartz-kyanite rock in minor amounts. Espenshade and Potter (1960) have described the kyanite quartzite at Little Mountain and other similar monadnocklike hills in the southeastern Piedmont. These authors consider the high-aluminum minerals to be replacement deposits in rock hydrothermally altered, perhaps by solfataric activity associated with volcanism and later subjected to regional metamorphism. The two samples of the coarsest muscovite found were separated from drill core cutting the kyanitic quartzite 228 feet and 257 feet below the collar elevation.

REGIONAL SETTING

All three areas of hydrothermally altered rocks from which the muscovite samples came are in the Carolina slate belt of low-grade metamorphic rock—largely slates, phyllites, and greenstones. Northwestward these rocks pass into higher grade metamorphic rock of the Charlotte belt. These belts of rocks have been described as resulting from different grades of regional metamorphism imposed on three thick sequences of similar sedimentary and volcanic rocks (Overstreet and Bell, 1965).

Granitic plutons

The four plutons that intrude rocks in the Carolina slate belt of South Carolina and southern North Carolina are called the Lilesville, Pageland, Liberty Hill, and Winnsboro plutons (fig. 1). These plutons have a circular or elliptical plan, are clearly intrusive into their wallrocks, and have, in general, sharp contacts. Megascopically, the intrusive rocks are similar, and coarse-grained, fine-grained, and porphyritic phases are present. They are part of an eastern subgroup of seven postmetamorphic granitic plutons discussed by Butler and Ragland (1969), who gave the following mean major-element composition, in percent, for this subgroup: SiO_2, 70.8; TiO_2, 0.47; Al_2O_3, 14.6; ΣFe, 2.64; MnO, 0.06; MgO, 0.64; CaO, 1.63; Na_2O, 3.38; K_2O, 4.68.

Gold, base-metal deposits, and areas of hydrothermal alteration have not been found in these plutons. Pardee and Park (1948), however, postulated that the mineralization at the Brewer, Haile, and other nearby mines is genetically related to one or another of these coarse-grained granitic plutons cropping out within a few miles of the mines.

Many other intrusive rocks, including stocks and dikes of gabbro, quartz monzonite, and diabase, also intrude the metamorphosed sedimentary and volcanic rocks, particularly in the Charlotte belt. Many of these rocks show evidence of metamorphism.

Age of granitic plutons

Two zircon concentrates from the pluton near Winnsboro and one zircon concentrate from the Liberty Hill pluton near

Kershaw gave lead-alpha ages of 270, 260, and 245 m.y., respectively (Overstreet and Bell, 1965). The lead-alpha age method is not as precise as the Rb-Sr age method, and it appears that these lead-alpha ages have been superseded by the whole-rock Rb-Sr ages determined by Fullager (1971) for the Liberty Hall pluton and the Winnsboro pluton and for many of the other plutons in the Carolina piedmont discussed by Butler and Ragland (1969). The rubidium-strontium ages which Fullager calculated for the Winnsboro and Liberty Hill plutons fall in a group at about 300 m.y. Eight whole-rock samples of the Winnsboro pluton yielded an isochron age of 301±10 m.y., and five samples from the Liberty Hill pluton yielded an isochron age of 299±48 m.y. The age of the Pageland granite, which is closest to the Brewer mine, has not been determined. This pluton, nevertheless, is so similar in lithology, outline, and structural setting to the other plutons that its age is probably also similar.

The ages determined for muscovite from the three areas of hydrothermal alteration are all older than the whole-rock and mineral ages from the granite plutons nearby, and a close connection between the emplacement of the granitic plutons and the alteration seems most unlikely.

VOLCANIC ROCKS

The hydrothermal alteration and mineralization are probably related to late-stage solutions that accompanied a pre-300-m.y. period of igneous activity. Worthington and Kiff (1968) have suggested that the gold mineralization in the Troy anticline area of Montgomery County, N.C., is volcanic in origin. They point out that the lode gold deposits, commonly zones of silicified and pyritic strata, are almost entirely restricted to the basal volcanic unit of that part of North Carolina. They suggest that "a volcanigenic origin for the gold deposits in the waning exhalations of the basal felsic volcanic pile seems to best account for the form, composition, and areal distribution of these deposits." Stromquist (1969) also has noted that in the Silver Hill–Gold Hill area of North Carolina, many gold prospects are richer where rhyolitic layers or tuffaceous mudstones are cut by shear zones.

These rocks in North Carolina have been divided by Stromquist and Sundelius (1969) and Conley and Bain (1965) into several groups and formations. Hills and Butler (1969) interpreted Rb-Sr isochron ages—535±50 m.y. for the Uwharrie Formation and 494±14 m.y. for the Tater Top Group—as indicating that the rocks of the Carolina slate belt in North Carolina were deposited and folded by the end of the Cambrian or, possibly, Early Ordovician. These groups and formations have not yet been correlated with rocks in the South Carolina part of the slate belt; nevertheless, the slate belt in North and South Carolina has long been recognized as similar in lithology and probably in history and origin.

The three described areas of hydrothermal alteration in South Carolina occur in similar rocks and are similar in mineralogy. At the Brewer mine and Little Mountain, pyrophyllite, rutile, and cassiterite occur associated with kyanite. The Brewer mine has andalusite and much topaz. Topaz has not been identified at Little Mountain, but it occurs commonly in other similar kyanite-pyrophyllite-bearing quartzites in the southeast. Of these minerals, only rutile and pyrophyllite have been reported from the Blackmon-Haile mine area. Sulfide minerals, principally pyrite, are abundant, however, at all three places. Copper sulfides are common only at the Brewer mine, but they do occur together with unusual amounts of molybdenum at the Haile mine. Gold is found in all three areas. These three rather widely separated areas are connected by other areas of hydrothermal alteration. Numerous occurrences of abundant thin quartz veinlets and silicified rock, disseminated pyrite and pyrite veinlets containing base metals, kaolin-rich rocks, and quartz-muscovite schist containing gold and scattered anomalous amounts of tin are found between and in the vicinity of these three areas. These occurrences all appear to be in hydrothermally altered felsic fragmental volcanic rocks and flow rocks. The Brewer mine area, Little Mountain, and the Blackmon-Haile mine area seem to represent high-temperature centers of silicification and intense argillitic alteration grading outward into sericitic alteration and propylitic alteration.

Butler and Ragland (1969, p. 173) have indicated that some of the intrusive rocks in the North Carolina piedmont are "* * *the intrusive equivalent, at least in composition if not in time, of felsic metavolcanic rocks in the Carolina slate belt * * *" and that the rocks may be part of a similar magma series. Rb-Sr isochron whole-rock ages were determined by Fullager (1971) for some of these intrusive rocks. He found that the age determinations formed two groups; one group ranges from 595 to 520 m.y. and the other, 415 to 385 m.y. Intrusive rocks of the second group have not yet been found near the areas of hydrothermal alteration. Two intrusive bodies, however, in the 595- to 520-m.y. age group are within 30 miles of the hydrothermally altered areas. These intrusive rocks have a chemical composition indicating that they could be the equivalents of the volcanic rocks in the slate belt.

Thus, Rb-Sr ages in both North and South Carolina suggest a Cambrian age for metavolcanic rocks in the Carolina slate belt. The muscovite ages from the altered rocks in the Carolina slate belt range from very Late Ordovician to Early Pennsylvanian. These are minimum ages for the altered rocks and very probably result from thermal disturbances which affected the existing K-Ar isotopic systems. A rise in the temperature of the rocks attendant on the emplacement of the nearby granitic plutons or some other geothermal event during the late Paleozoic or early Mesozoic probably reset the K-Ar isotopic systems in the altered rocks. Thus, the time of alteration has not been defined, but the radiometric ages do indicate that the hydrothermal alteration and the gold-bearing rocks are more likely to be related to lower Paleozoic plutonic rocks or other volcanic equivalents than to the nearby upper Paleozoic plutons.

REFERENCES

Butler, J. R., and Ragland, P. C., 1969, A petrochemical survey of plutonic intrusions in the Piedmont, southeastern Appalachians, U.S.A.: Contr. Mineralogy and Petrology, v. 24, no. 2, p. 164–190.

Conley, J. F., and Bain, G. L., 1965, Geology of the Carolina slate belt west of the Deep River–Wadesboro Triassic basin, North Carolina: Southeastern Geology, v. 6, no. 3, p. 117–138.

Espenshade, G. H., and Potter, D. B., 1960, Kyanite, sillimanite, and andalusite deposits of the Southeastern States: U.S. Geol. Survey Prof. Paper 336, 121 p.

Fries, Carl, Jr., 1942, Topaz deposits near the Brewer mine, Chesterfield County, South Carolina: U.S. Geol. Survey Bull. 936-C, p. 59–78.

Fullager, P. D., 1971, Age and origin of plutonic intrusions in the Piedmont of the southeastern Appalachians: Geol. Soc. America Bull., v. 82, no. 10, p. 2845–2862.

Graton, L. C., 1906, Reconnaissance of some gold and tin deposits of the southern Appalachians: U.S. Geol. Survey Bull. 293, 134 p.

Hills, F. A., and Butler, J. R., 1969, Rubidium-strontium dates for some rhyolites from the Carolina slate belt of the North Carolina Piedmont [abs.]: Geol. Soc. America Spec. Paper 121, p. 445.

Kesler, T. L., 1972, The Little Mountain syncline in the South Carolina Piedmont [abs.]: Geol. Soc. America Abs. with Programs 1972, v. 4, no. 2, p. 84.

McKenzie, J. C., and McCauley, J. F., 1968, Geology and kyanite resources of Little Mountain, South Carolina: South Carolina Div. Geology Bull. 37, 18 p.

North Carolina Div. Mineral Resources, 1958, Geologic map of North Carolina: Raleigh, N.C., North Carolina Div. Mineral Resources, scale 1:500,000.

Overstreet, W. C., and Bell, Henry, III, 1965, The crystalline rocks of South Carolina: U.S. Geol. Survey Bull. 1183, 126 p.

Pardee, J. T., Glass, J. J., and Steven, R. E., 1937, Massive low-fluorine topaz from the Brewer mine, South Carolina: Am. Mineralogist, v. 22, no. 10, p. 1058–1064.

Pardee, J. T., and Park, C. F., Jr., 1948, Gold deposits of the southern Piedmont: U.S. Geol. Survey Prof. Paper 213, 156 p.

Secor, D. T., and Wagener, H. D., 1968, Stratigraphy, structure, and petrology of the Piedmont in central South Carolina: South Carolina Div. Geology Geol. Notes, v. 12, no. 4, p. 67–84.

Stromquist, A. A., 1969, Central North Carolina, *in* U.S. Geological Survey, U.S. Geological Survey heavy metals program progress report, 1968–Field studies: U.S. Geol. Survey Circ. 621, p. 25.

Stromquist, A. A., and Sundelius, H. W., 1969, Stratigraphy of the Albermarle Group of the Carolina slate belt in central North Carolina: U.S. Geol. Survey Bull. 1274-B, p. B1–B22.

Worthington, J. E., and Kiff, I. T., 1968, A suggested volcanigenic origin for certain gold deposits in the slate belt of the North Carolina piedmont [abs.]: Mining Eng., v. 20, no. 12, p. 67.

POTASSIUM-ARGON AGES FROM WHOLE-ROCK ANALYSES OF IGNEOUS ROCKS IN THE AREA OF THE NATIONAL REACTOR TESTING STATION, IDAHO

By GEORGE H. CHASE, Washington, D.C.

Abstract.—Potassium-argon minimum ages determined by whole-rock analyses of 19 samples of basalt and silicic volcanic rocks from the vicinity of the National Reactor Testing Station, Idaho, range from 0.7±0.2 to 72±6 million years.

The National Reactor Testing Station (NRTS) in southeastern Idaho (figs. 1 and 2) is on an igneous terrane in which basaltic rocks are most widely exposed. The area, which is physiographically a part of the north-central Snake River Plain, lies in a closed basin (fig. 2). Most rock layers exposed within the basin slope toward its axis. On the north the basin is bounded by the southern ends of southeast-trending mountain ranges with intermontane fault-block valleys. Both silicic and basaltic volcanic rocks are found in the mountains at various altitudes above the margin of the plain. On the west the basin is bounded by truncated mountains consisting principally of Paleozoic sedimentary rocks, which have been rather intensely folded in some places. On the south and east the basin is bounded by moderately elevated masses of basaltic and silicic volcanic rocks. In places around the perimeter of the basin individual buttes rise from about 50 feet to more than 2,000 feet above the average altitude of the basin divides.

Geologic reconnaissance and geophysical mapping have indicated that several periods of igneous and structural activity have been involved in the development of the present geologic and physiographic situation at the surface, and that the primarily basaltic terrane is underlain by older rocks involved in fairly complex features of geologic structure and igneous tectonics. To aid in the study of aquifer geometry in the vicinity of the station, rock samples were taken to represent as much of the pertinent geologic sequence as possible. All but two of the specimens were cored from massive rocks that appeared to be unweathered; the other two consisted of cable-tool drill cuttings from two of the deepest wells on the NRTS. Selected samples were submitted to Isotopes, Inc., for dating by potassium-argon whole-rock methods (Schaeffer and Zähringer, 1966). Isotopic ages obtained from whole-rock analyses of extrusive rocks (table 1) usually represent minimum ages (Roland Kologrivov, written commun., Dec. 10, 1964) for the latest events affecting the given rocks rather than absolute ages or times of original solidification, because of the decay mechanism and the nature of the methods (Schaeffer and Zähringer, 1966, especially p. 7, 68–106, 121; Pasteels, 1968, p. 11). Future work should employ the more

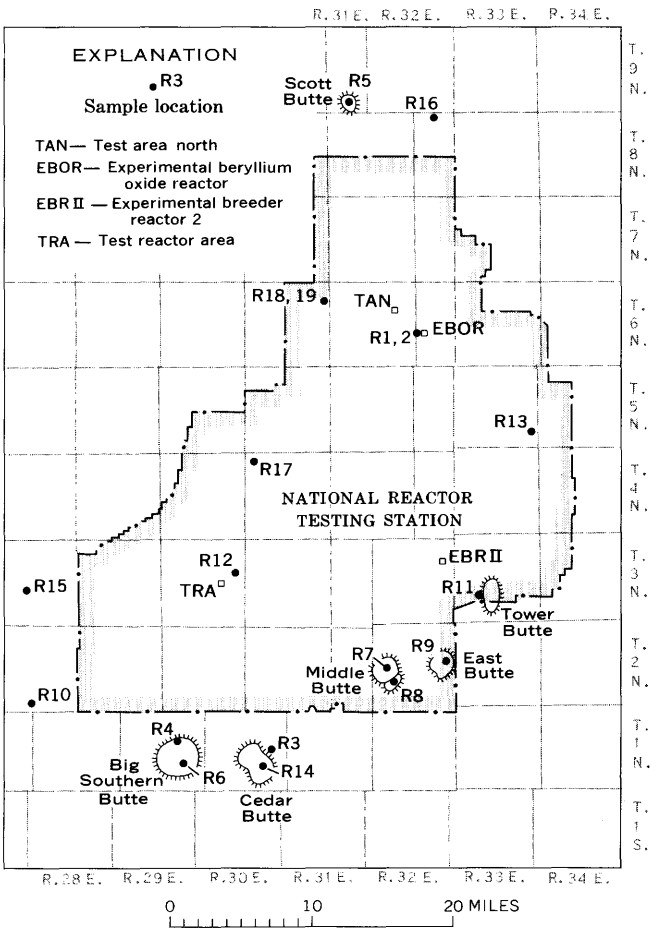

Figure 1.—Map showing sample locations, National Reactor Testing Station, Idaho, and vicinity.

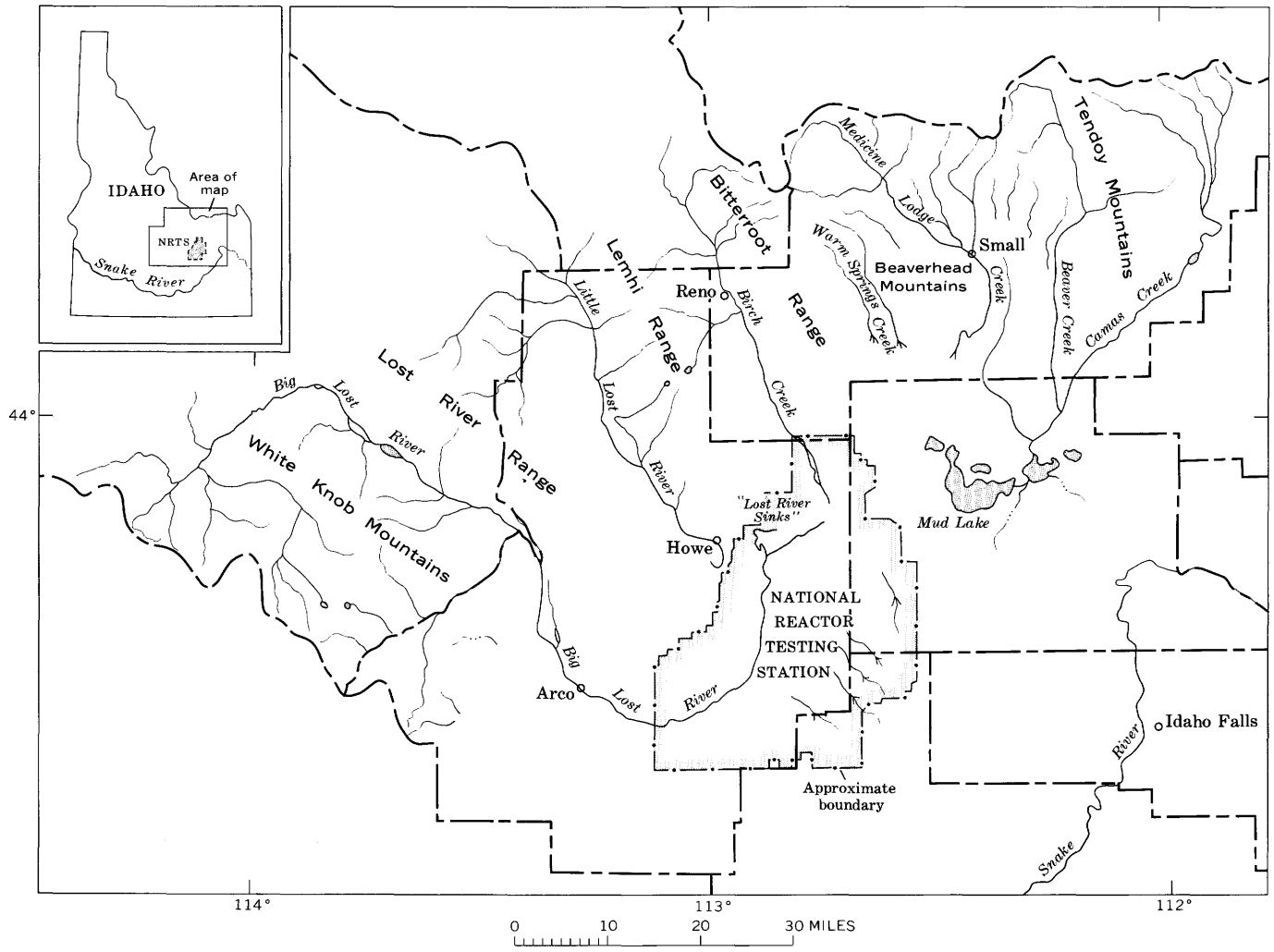

Figure 2.–Map of the surface drainage system of the National Reactor Testing Station, Idaho, and vicinity.

involved dating of mineral separates to provide more nearly absolute dates. The information in this geologic note is presented for the consideration of others working on the Snake River Plain or on other basaltic terranes in planning their programs and in interpreting results.

SIGNIFICANCE OF RESULTS

The potassium-argon isotopic ages shown in table 1 have been grouped on the basis of both geologic evidence and results of the potassium-argon dating rather than on the basis of the radioisotopic analysis alone. It seems likely that in some instances reheating during igneous or structural tectonic activity reduced the isotopic age through the partial loss of radiogenic argon-40. In general however, geologic observations and the isotopic ages–which are, of course, minimums–indicate that the various rocks of the area have been affected by numerous geologic events. The most evident of these events are of middle Pleistocene, early Pleistocene, late Pliocene, middle Pliocene, early Pliocene, Miocene, and Oligocene age. The isotopic age of sample R17, which consisted of cable-tool drill cuttings from basalt between 1,407 and 1,465 feet beneath the axis of the basin, indicated in addition an early Tertiary event. It may be of interest to note that the potassium content of the rock in the cuttings was low (0.34 percent)–well within the range for basalts. This low value would suggest that there was little or no contamination from sedimentary rocks or from silicic volcanic rocks. Repeatability of results in three analyses of different parts of the sample also supported the lack of contamination. Cores of this material should be obtained for analysis, however, before the significance of the isotopic age can be fully evaluated.

Several samples (R11, R12, and R13) were not dated with certainty even within a statistical range. (See footnote 2, table 1.) All three samples were obtained in the vicinity of features indicating local igneous activity subsequent to the emplacement of the principal surrounding masses of lava. Losses of argon-40 may, therefore, have been excessive, or the rocks

Table 1.—*Potassium-argon ages from whole-rock analyses of igneous rocks in the area of the National Reactor Testing Station (NRTS), Idaho*

[Analyses by Isotopes, Inc. Acronyms: EBR II, experimental breeder reactor 2; TRA, test reactor area; EBOR, experimental beryllium oxide reactor; TAN, test area north]

Sample No.	Location			Description, including depths of subsurface samples	Lithology	K-Ar isotopic age[1] (m.y.)
	Township (N.)	Range (E.)	Section			
R13	5	33	25	Northeast of EBR-II about 12 miles.	Basalt	[2]<1.0
R12	3	29	13	Near TRA (199 feet).	..do..	[2]<1.2
R11	3	33	28	Near Tower Butte.	..do..	[2]<1.5
R6	1	29	23	Top of Big Southern Butte.	Silicic volcanic rocks	.7±0.2
R14	1	30	26	North flank of Cedar Butte.	Basalt	.9±0.8
R3	1	30	13	Rift flow northeast of Cedar Butte.	..do..	1.7±0.8
R4	1	29	14	North flank of Big Southern Butte.	..do..	1.0±0.6
R9	2	32	13	East side of East Butte.	Silicic volcanic rocks	1.0±0.4
R1	6	32	22	Near EBOR (59 feet).	Basalt	2.7±0.6
R2	6	32	22	Near EBOR (428 feet).	..do..	2.3±0.7
R7	2	32	20	Caprock of Middle Butte.	..do..	3.5±0.4
R8	2	32	20	East lip of small crater at southeastern base of Middle Butte.	..do..	3.6±0.7
R5	9	31	35	Caprock of Scott Butte.	..do..	5.4±0.8
R19	6	30	12	Mine shaft west of TAN (115–190 feet).	..do..	10.0±5.0
R18	6	30	12	Mine shaft west of TAN (225–347 feet).	Silicic volcanic rocks	8.9±1.5
R15	3	27	21	Gorge of Big Lost River about 4 miles west of the NRTS boundary.	Basalt	26.0±15.0
R16	8	32	2	West side of mouth of Warm Springs Creek.	..do..	32.0±2.0

All samples in this table were drilled cores or blocks of unweathered material from massive rocks. Two additional samples tested consisted of cable tool drill cuttings. One of these, R10, which was obtained between depths of 1,170 and 1,200 feet in T. 2 N., R. 27 E., sec. 33, consisted of basalt with a K-Ar minimum age of 8.0±6.0 m.y.; the other, R17, which was obtained between depths of 1,407 and 1,465 feet in T. 4 N., R. 30 E., sec. 6, was basalt with a K-Ar minimum age of 72±6 m.y.

[1] Arranged in episodes as indicated by geologic and geophysical evidence, within the indicated tolerance of the method.

[2] "Samples R11, R12, and R13 were run in triplicate. All these analyses gave either zero or negative ages. Therefore, the data were analyzed statistically after setting all errors positive. The 'less than' ages reported are therefore simply an expression of the uncertainty in the measurement of the 40/38 and 40/36 ratios and are not the result of a bona fide age calculation. Thus, these 'less than' values should not be cited as ages." (Roland Kologrivov, written commun., May 24, 1966).

sampled may actually represent comparatively recent extrusions. From field observations and microscopic examination of the samples the author would suspect loss of argon-40 as the more plausible cause.

In summary, it appears that if samples are carefully selected, whole-rock radioisotope dating will furnish useful results for the igneous rocks of the area. More precise dating with mineral separates would probably involve comparatively large samples of basalt but would be extremely useful in mapping in the igneous terrane, where many structural features have been obscured by igneous activity and where the sequence of events of igneous tectonics may itself be quite important in the interpretation of the geology and hydrology. Ideally, whole-rock analyses might precede sampling for dating by the more precise methods. The work with whole-rock potassium-argon analyses has indicated a succession of geologic events spanning much of Cenozoic time for the basaltic and silicic volcanic rocks of the National Reactor Testing Station and vicinity.

ACKNOWLEDGMENTS

The writer wishes to acknowledge his deep appreciation to the U.S. Atomic Energy Commission, for which the work was done, and in particular to Bruce L. Schmalz, then Chief, Waste Management Branch, and John R. Horan, then Director, Health and Safety Division, Idaho Operations Office. Especial appreciation is also expressed for the encouragement and guidance of Donald A. Morris, then Research Project Chief, under whose supervision the technical work was done and to Jack T. Barraclough, his successor, under whose supervision most of the interpretation was completed, and who has supplied

additional supporting information obtained during drilling since the writer left the area. Roland Kologrivov, Head, Mass Spectrometry Section, Isotopes, Inc., examined many samples to evaluate their suitability for analysis and repeatedly gave valuable advice to the writer during the course of the work.

REFERENCES

Pasteels, Paul, 1968, A comparison of methods in geochronology: Earth-Sci. Rev. 4, p. 5–38.

Schaeffer, O. A., and Zähringer, J., 1966, Potassium-argon dating: New York, Springer Verlag, Inc., 234 p.

GENESIS OF MESOZONAL GRANITIC ROCKS BELOW THE BASE OF THE STILLWATER COMPLEX IN THE BEARTOOTH MOUNTAINS, MONTANA

By NORMAN J PAGE and WARREN J. NOKLEBERG[1],
Menlo Park, Calif., Fresno, Calif.

Abstract.—Granitic intrusive rocks crop out over a minimum area of 20 square miles between the Stillwater Complex and gneisses of the Beartooth Mountains, Mont. Diking and stoping relations yield the following sequence of intrusion, from oldest to youngest: (1) coarse-grained quartz monzonite, minimum age 2,750 m.y.; (2) medium-grained quartz monzonite; (3) hornblende quartz diorite; (4) fine-grained quartz monzonite; and (5) numerous aplites. The coarse-grained quartz monzonite forms dikes in, and contains inclusions of, pyroxene hornfels and gabbro of the Basal zone of the complex. The granitic rocks are therefore younger than the Stillwater Complex. A later metamorphic mineral foliation (younger than the complex) which strikes approximately east-west and dips steeply north is observed in the granitic rocks, in biotite schist pendants in the granitic rocks, and in the lower part of the Stillwater Complex. Chemical analyses, norms and modes of the rocks from granitic rocks, and electron microprobe analyses of the feldspars support a model of magmatic origin for the sequence of granitic rocks.

Previous studies of the Precambrian basement rocks below the Stillwater Complex (Butler, 1966; Jones and others, 1960) have emphasized the existence of granite gneisses, migmatitic rocks, and metasedimentary rocks on the northern border of the Beartooth Mountains, in southwestern Montana. These studies have recognized a quartz monzonite that intrudes the Stillwater Complex.

To the east and south in the Beartooth Mountains, a similar assemblage of rocks, but without extensive granitic intrusive rocks, has been described in the structural and petrologic studies of Casella (1964, 1969), Eckelmann and Poldervaart (1957), Foose, Wise, and Garbarini (1961), Harris (1959), James (1946), Larsen, Poldervaart, and Kirchmayer (1966), Poldervaart and Bentley (1958), Prinz (1964), Rowan (1969), Rowan and Larsen (1970), Skinner (1969), and Skinner Bowes, and Khoury (1969). They have shown that in the Beartooth Mountains, the Precambrian crystalline rocks are composed of granitic gneisses, migmatites, metasedimentary rocks including iron formation, cordierite-antophyllite schists and metaquartzites, biotite schists, and amphibolites. Granitic gneisses and migmatites are the most abundant rock types. These workers have found evidence for at least four deformational events, with the most dominant structure being a set of southward-plunging folds that vary from broad and open to isoclinal (F_2).

Few igneous granitic rocks other than pegmatites have been described in the southern and eastern Beartooth Mountains. Casella (1969, p. 67) stated that exposures showing large-scale intrusive relations have never been found, but Skinner, Bowes, and Khoury (1969) described a coarse-grained, nonfoliated granite near the highway between Red Lodge and Cooke City and suggested that it is a magmatic granite. Rowan and Larsen (written commun., 1971) found a 10-foot-wide dike of pink, coarse-grained granite in the Hellroaring Lakes area.

McMannis, Palmquist, and Reid (1971a, b, c) have described metamorphic equivalents of quartz-rich sandstones, impure argillaceous dolomitic sandstones, shale, siliceous dolomite, and basaltic tuffs or flows, or both, in the northwestern part of the Beartooth Mountains. Within the area they studied, they recognize at least four and possibly five periods of folding overlapping with three periods of development of felsic magmas. The granitic rocks below the Stillwater Complex must be examined within the framework of events described to the northwest and southeast in the Beartooth Mountains.

This paper (1) discusses the petrologic and structural framework of the country rocks that were intruded by the granitic rocks; (2) describes the intrusive granitic rocks, which form several stocks underlying about half of the Stillwater Complex; (3) compares them with the adjacent granitic gneisses; (4) describes the effect of the granitic rocks on the country rocks; and (5) develops lines of evidence that may suggest that the intrusive granitic rocks are mesozonal plutonic rocks. The intrusive granitic rocks crop out over a minimum of 20 square miles between the Stillwater Complex and the metasedimentary and gneissic granitic rocks of the Beartooth Mountains. The maximum original extent of the intrusive granitic rocks is unknown because they are only exposed in thrust sheets that strike east-west, parallel to the northern

[1] Fresno State College.

front of the Beartooth Mountains, but they may originally have been of batholithic dimensions. Most of the results are based on 1:12,000-scale mapping (Page and Nokleberg, 1970b) of the Basal zone of the complex and the adjacent country rocks.

Acknowledgments.—Without the support, encouragement, and use of published and unpublished mapping of E. D. Jackson, A. L. Howland, and others, the continued mapping of the Stillwater Complex would have taken many more man-years than it has. R. N. Miller and J. Adler, of the Anaconda Company, and Giles Walker, of American Mining and Metals Exploration, have facilitated and cooperated fully with this project. E. D. Jackson deserves special mention for his encouragement and support of this study.

COUNTRY ROCKS AND GEOLOGIC SETTING

Metamorphic rocks of the Beartooth Mountains (granitic gneisses, migmatites, and metasedimentary rocks), pyroxene hornfels and retrogressive hornfels, and the Basal zone of the Stillwater Complex are in contact with or adjacent to the granitic intrusive rocks. Figure 1 shows the general distribution and geologic relations between the wallrocks and the granitic intrusive rocks. This map is a greatly simplified version of Page and Nokleberg's (1970b) map. The southern boundary of the granitic rocks has not been mapped, but preliminary reconnaissance suggests that it is at least 3 miles south of the map area. The granitic rocks must therefore occupy a larger area than shown on the map. These rocks extend farther west than shown on figure 1 and underlie about the eastern half of the Stillwater Complex. These observations and the present exposure of the granitic rocks in thrust sheets between the Stillwater Complex and Beartooth metamorphic rocks (fig. 1) suggest that the granitic rocks may originally have been of batholithic dimensions.

Beartooth Metamorphic Rocks

The Beartooth metamorphic rocks form the core of the mountain range and crop out along the southern limit of the map area (fig. 1). Butler (1966) subdivided these rocks into three groups: (1) granitic gneisses and migmatites (2) amphibolites, and (3) biotite schists. We have used the same general subdivision except that we consider some of Butler's granitic gneisses to be granitic intrusive rocks. The term "granitic gneisses" in this paper (fig. 1) is restricted to foliated rocks with alternating bands and lenses of more felsic and mafic material. Common constituent minerals in the gneisses are plagioclase, potassium feldspar (commonly perthitic microcline), quartz, biotite, muscovite, epidote, and locally red garnet. Rocks in some areas, such as the block east of the Stillwater River, may contain little if any potassium feldspar. Biotite gneisses contain more than 15 modal percent biotite and are foliated quartzo-feldspathic rocks, whereas the biotite schists contain more than 25 percent biotite, sometimes contain staurolite, and have a schistose fabric. Amphibolites contain hornblende, plagioclase, quartz, garnet, and sometimes staurolite. The Beartooth metamorphic rocks are generally in fault contact with the intrusive granitic rocks (fig. 1). However, in one small part of the area, south of the West Fork of the Stillwater River, one of the younger granitic rocks, the fine-grained quartz monzonite, intrudes the biotite schist of the Beartooth metamorphic rocks.

Pyroxene Hornfelses and Retrogressive Hornfels

Hornfelses are intruded by rocks of the Stillwater Complex and by the granitic rocks (fig. 1). The hornfelses crop out between the two suites of intrusive rocks. Although locally compositionally layered, they are generally massive, fine-grained, structureless rocks. Common constituent minerals are cordierite, orthopyroxene, quartz, plagioclase, biotite, and, in some rocks, green spinel. The bulk rock composition of the hornfelses corresponds to graywackes and shales or to andesitic volcanic rocks. Lenses of quartzite and banded iron formation were probably derived from sedimentary rocks. Although sparsely distributed within the eastern part of the mapped area, blue metaquartzites and iron formation interlayered with the pyroxene hornfelses are extensive west of the mapped area.

Rocks labeled retrogressive hornfels in figure 1 occur as pendants in the intrusive granitic rocks (fig. 1) and are compositionally banded. Their mineralogy is similar to that of the pyroxene hornfelses, but most of the orthopyroxene and cordierite is altered to serpentine, chlorite, and biotite. This alteration probably occurred after granitic intrusion because both chlorite and biotite have crystallized along a plane of schistosity that cuts across the banding in the retrogressive hornfelses and across the granitic intrusive rocks.

Stillwater Complex

The ultramafic and mafic intrusive rocks of the Stillwater Complex crop out across the front of the Beartooth Mountains in the map area (fig. 1). Peoples (1933), Jones, Peoples, and Howland (1960), Hess (1960), and Jackson (1961) have subdivided the Stillwater Complex into several parts. They presented evidence that the Stillwater Complex intruded the sedimentary rocks (Jones and others, 1960) which are now the pyroxene hornfelses. For the purposes of this paper, Peoples' (1936) and Jackson's (1961) stratigraphic terminology for the Stillwater Complex has been used (fig. 1). The Ultramafic zone is split into two informally named members, the Peridotite and Bronzitite members. The Basal zone is grouped with the Peridotite member in this report. The upper noritic, gabbroic, and anorthositic parts of the complex are grouped into the Banded and Upper zones. In general, the rocks of the Ultramafic zone do not contain cumulus plagioclase, whereas those in the Basal, Banded, and Upper zones do. The Stillwater

Complex is unconformably overlain by Paleozoic and Mesozoic sedimentary rocks (fig. 1).

Structure

The Stillwater Complex and overlying Paleozoic and Mesozoic sedimentary rocks, the hornfelses, Beartooth metamorphic rocks, and granitic intrusive rocks (fig. 1) have outcrop patterns that tend to be elongate approximately east-west. Before Middle Cambrian time this group of rocks was deformed and tilted gently northward and beveled by erosion. They formed a topographic high at the beginning of Cambrian sedimentation (Jones and others, 1960). Structural history after Cambrian time is discussed by Jones, Peoples, and Howland (1960). This report is concerned only with those aspects of structural history that occurred before the tilting and that are pertinent to the granitic and metamorphic rocks.

Folds

Butler (1966) completed a structural analysis of the area south of the eastern Stillwater Complex containing mainly granitic gneisses and minor amounts of metasedimentary rocks and amphibolities. His analysis of minor fold axes, axial planes, mineral foliation, and compositional layering shows large, generally northward-plunging cylindrical folds. He observed no east-west-trending folds or foliations, nor did he sort out different generations of structures recognized elsewhere in the southeastern Beartooth Mountains. We would correlate the large folds with the large open folds described in the eastern Beartooths (F_2, Rowan, 1969). None of these structures has been observed in the area studied, except in the areas where Beartooth metamorphic rocks are exposed.

In the Mountain View area (fig. 1), the hornfelses immediately under the Stillwater contain refolded folds. At least two generations of folding have been observed. The youngest folds are isoclinal to open folds that have northeast-striking axial planes. These folds refold the axial planes of isoclinal folds, whose initial orientation is approximately east-west to northwest-southeast. Both fold sets formed before intrusion of the Stillwater Complex because norite dikes belonging to the Basal zone of the Stillwater Complex intrude both sets of folds. Both sets also formed before granitic plutonism because the folds are crosscut by dikes of granitic rocks.

Separating the Mountain View area on the north from the Beartooth metamorphic rocks on the south are a set of reverse faults (thrusts) that appear to be the extension of the Mill Creek-Stillwater fault zone (Jones and other, 1960; Butler, 1966). The earliest two generations of folds on the north side of the fault zone (Mountain View area) resemble structures to the west described by McMannis, Palmquist, and Reid (1971a, b, c). The structures on the south side are similar to those described in the southeastern Beartooths. East of the Mountain View area, intrusive granitic rocks occupy the projection of the Mill Creek-Stillwater fault zone.

Foliation

Superposed on structures on both sides of the fault zone is a metamorphic mineral foliation that strikes east-west and dips steeply north (fig. 2). The metamorphic mineral foliation is observed in the granitic intrusive rocks, in retrogressive hornfels pendants, in biotite gneiss pendants in the granitic intrusive rocks in the lower part of the Stillwater Complex, and locally, in the granitic gneisses (fig. 1). The foliation is defined in the granitic rocks by parallel elongated feldspar porphyroclasts, and parallel muscovite and biotite flakes; in the hornfelses by interbanded orthopyroxene-rich and cordierite-rich layers; in the biotite gneiss by parallel mica flakes; and in the Stillwater Complex by sheared serpentine-magnetite veins and by flattened, parallel orthopyroxene oikocrysts. The widespread extent of the foliation shown in figure 2 in rocks of diverse origins and ages supports a penetrative deformation that occurred after the emplacement of the granitic rocks, after emplacement of the Stillwater Complex, after the generation of two fold sets in the hornfelses, and after the development of F_2 folds in the Beartooth metamorphic rocks. Rowan and Mueller (1971) have assigned a tentative age of 1,600 to 1,800 m.y. (million years) to the event which formed the mineral foliation. The formation of the foliation may be correlated with 1,700-m.y. folding and a metamorphic event described by McMannis, Palmquist, and Reid (1971a, b, c).

Faults

The majority of the faults in the area are east-west-striking, southward-dipping reverse faults and steeply dipping north-south cross faults. Both fault sets crosscut, and therefore have had movement along them after the development of the metamorphic mineral foliation. Jones, Peoples, and Howland (1960) assigned a Laramide age to the movement; however, many of the faults were probably also active in Precambrian time (Jones and others, 1960), because Precambrian diabase dikes occupy some of the faults. The steeply dipping north-south faults displace the east-west faults and therefore are younger (see fig. 1). From north to south, the east-west-striking, southward-dipping faults place deeper level rocks up and over more shallow level rocks. Expressed another way, the Paleozoic sedimentary rocks are overridden by the presumably shallow level, stratiform ultramafic and mafic rocks of the Stillwater Complex, which in turn are overridden by intermediate level granitic rocks, which are in turn overridden by the Beartooth metamorphic rocks, which probably were formed at deep crustal levels.

CONSTITUTION OF THE INTRUSIVE GRANITIC ROCKS AND COMPARISON WITH ADJACENT GNEISSES

The granitic intrusive rocks are a suite of quartz monzonites, aplites, and a hornblende diorite (Page and Nokleberg, 1970a).

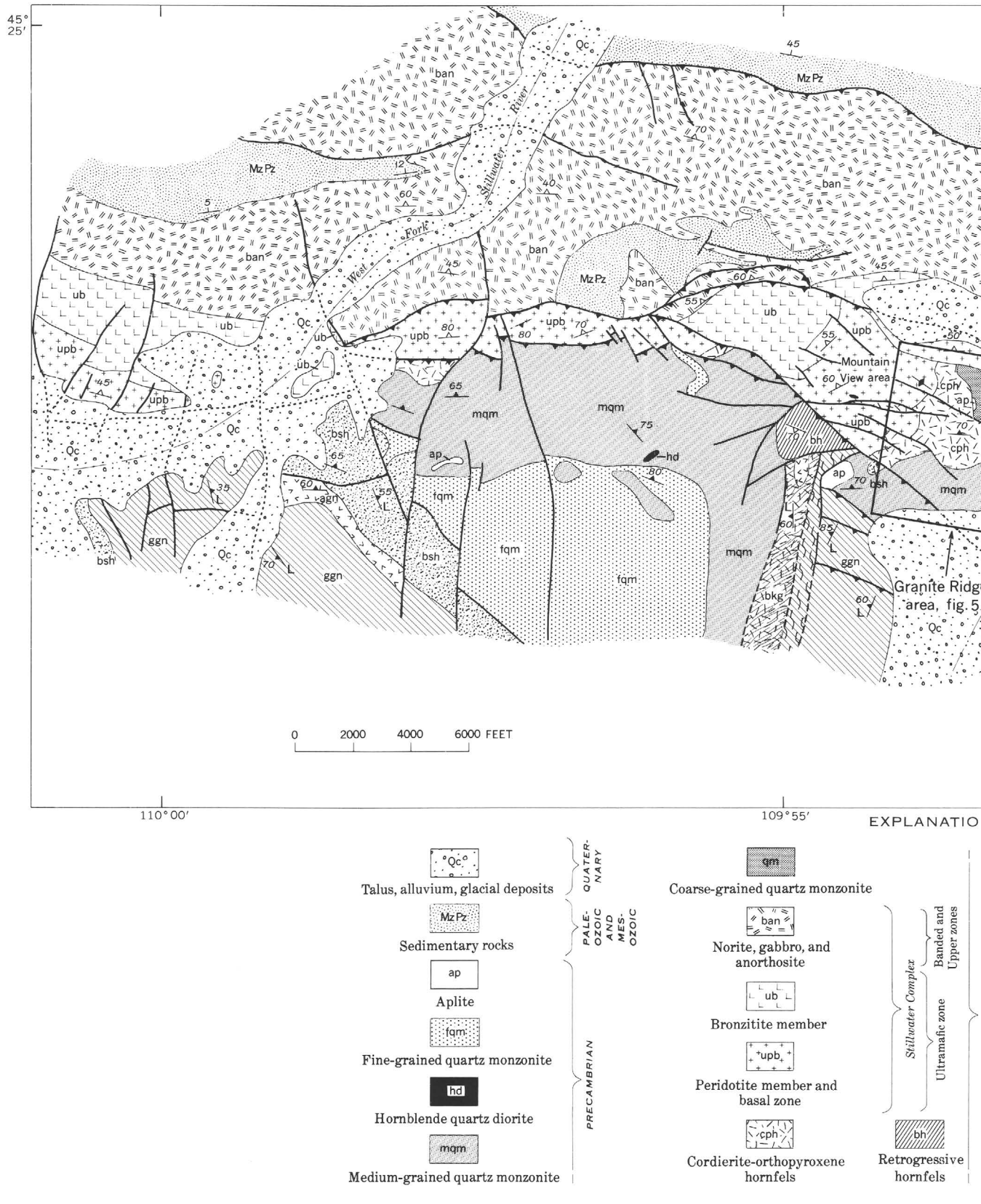
45° 25'
110° 00'
109° 55'
0 2000 4000 6000 FEET
West Fork Stillwater River
Mountain View area
Granite Ridge area, fig. 5
EXPLANATIO
QUATERNARY
PALEOZOIC AND MESOZOIC
PRECAMBRIAN
Talus, alluvium, glacial deposits
Sedimentary rocks
Aplite
Fine-grained quartz monzonite
Hornblende quartz diorite
Medium-grained quartz monzonite
Coarse-grained quartz monzonite
Norite, gabbro, and anorthosite
Bronzitite member
Peridotite member and basal zone
Cordierite-orthopyroxene hornfels
Retrogressive hornfels
Stillwater Complex
Banded and Upper zones
Ultramafic zone

Figure 1.

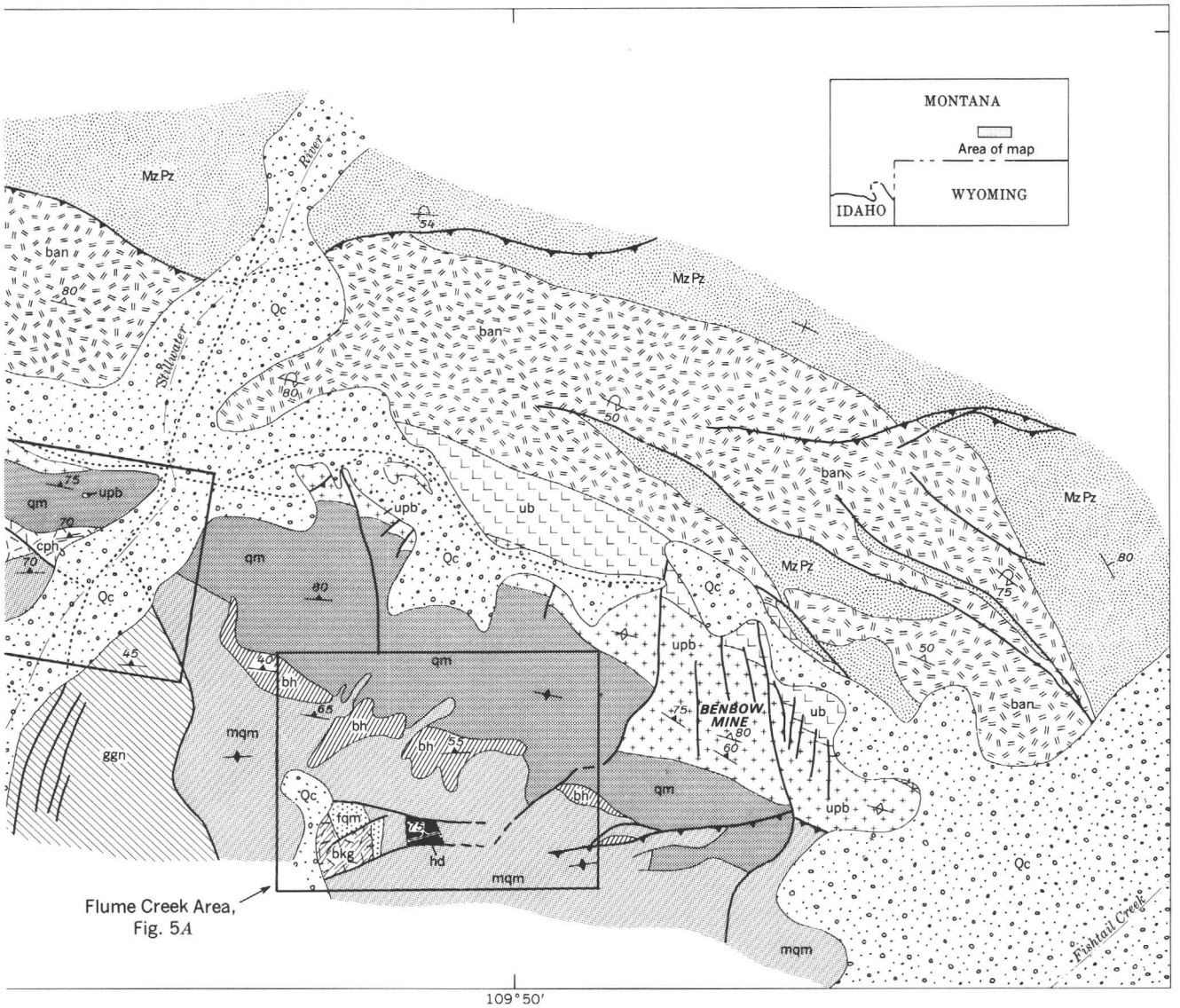

Biotite gneiss (bkg) · Amphibole gneiss (agn) · Biotite schist (bsh) · PRECAMBRIAN

Granitic gneiss (ggn)

Gneissic layering with dip

Approximate contact

Approximate fault
Dotted where concealed

Approximate thrust fault
Dotted where concealed

Zone of sheared rock

Strike and dip of beds: Inclined · Vertical · Overturned

Attitude of layering: Inclined · Vertical · Overturned

Mineral foliation: Inclined · Vertical

Figure 1.–Geologic sketch map of the eastern part of the Stillwater Complex, Montana, on the northern border of the Beartooth Mountains. Simplified from Page and Nokleberg (1970b).

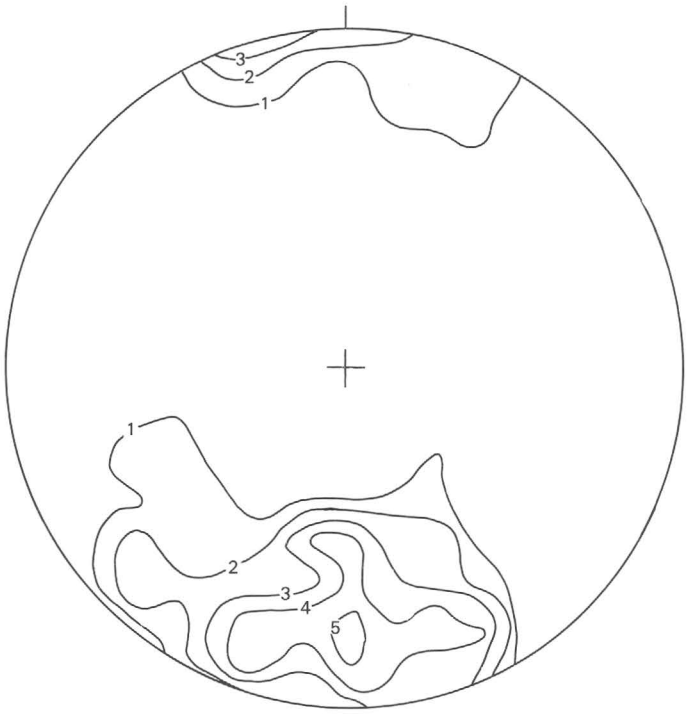

Figure 2.—Fabric diagram for metamorphic foliations. Poles to foliations in hornfels and granitic rocks of areas south of the Stillwater Complex, Montanta. Contours, in percent, are based on 269 points.

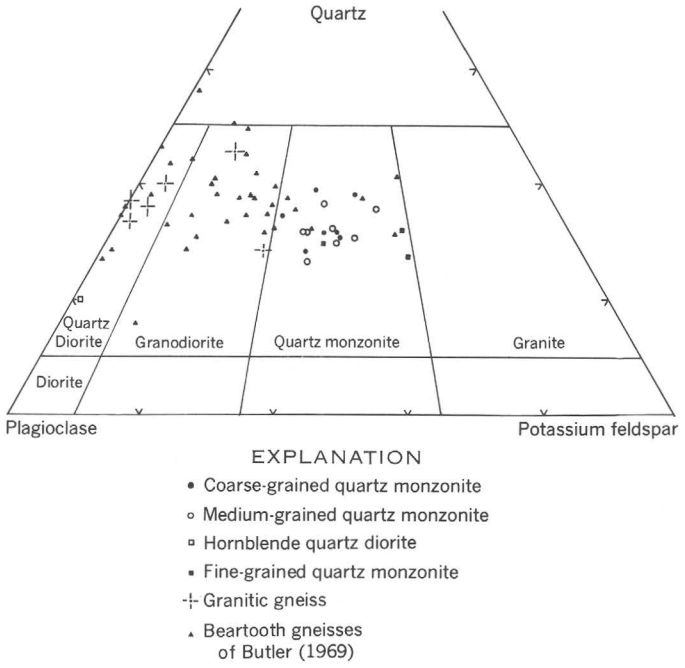

Figure 3.—Modal variation of plutonic rocks and granitic gneisses.

Quartz monzonite predominates. The following are mappable units: coarse-grained quartz monzonite, locally called the Mouat quartz monzonite; medium-grained quartz monzonite; hornblende quartz diorite; fine-grained quartz monzonite, and numerous aplites.

Lithologic and Textural Groups

The quartz monzonites exhibit relict hypidiomorphic-granular, equigranular to porphyritic textures. The most prevalent texture is of metamorphic origin and consists of seriate grain boundaries; muscovite, biotite, chlorite, quartz, and feldspar are recrystallized along feldspar-quartz grain contacts. The texture is a result of recrystallization during and after the postemplacement penetrative mineral foliation. The granitic rocks are distinguished by relict textures, major differences in grain size, and mutual intrusive relations; composition and mineralogy are minor aids for identification. For naming, a modal mineralogic classification proposed by Bateman and others (1963) is used (fig. 3). Modes of the adjacent granitic gneisses, including modes by Butler (1969), are also shown. The granitic gneisses vary widely in composition, but quartz diorite and granodiorite compositions predominate. Because of the close similarity of intrusive granitic rock modes, relative percentages of the major mineral alone cannot be used to subdivide the quartz monzonites. In order to separate the major rock types, the modes of quartz monzonites in figure 3 are grouped on the basis of grain size and mutual intrusive relations.

The coarse-grained quartz monzonite has individual grains greater than 5 mm in diameter, locally with grains greater than 5 cm, and is intruded by the medium-grained quartz monzonite, which has a grain size of between 1 and 5 mm. The fine-grained quartz monzonite has a grain size of less than 1 mm. The hornblende quartz diorite is a medium-grained rock. Each unit shows a remarkable consistency in grain size, and sharp intrusive contacts occur between units.

Mineralogy

The common minerals in the quartz monzonites are quartz, potassium feldspar (either a microcline perthite or orthoclase), plagioclase (albite to oligoclase), sometimes zoned, and biotite. Both plagioclase and microcline form phenocrysts and also occur in the groundmass of the rock. Myrmekitic intergrowths are common. Undulant quartz grains form clots up to 1 cm in diameter in the coarse-grained but not in the medium- and fine-grained quartz monzonite. Most biotite occurs as subhedral to anhedral flakes, but some forms graphic intergrowths with quartz. Both forms are partly altered to chlorite and a white mica. Usually associated with the biotite are the accessory minerals, zircon and apatite, and oxide and sulfide phases. Secondary minerals are clays, white mica, chlorite, and epidote. Hornblende occurs in the hornblende quartz diorite, and orthopyroxene and cordierite occur as xenocrysts in contaminated aplites.

Plagioclase and potassium feldspar in a number of specimens of the granitic plutonic and gneissic rocks were analyzed for sodium, calcium, and potassium with an electron microprobe analyzer.[2] Figure 4 shows the anorthite (An), albite (Ab), and orthoclase (Or) end-member compositions of each grain (several analyzed spots for each grain) for the feldspars analyzed in each sample. Grains that contained any alteration products within the area analyzed are not plotted. The presence of alteration products posed a major analytical problem, as demonstrated by plagioclase analyses from the coarse-grained quartz monzonite (74MV69). The potassium enrichment indicated by these data is probably caused by the minor amounts of fine-grained sericite in the areas analyzed in the three grains. In general, potassium feldspar is increasingly enriched in Or molecule going from coarse- to medium- to fine-grained quartz monzonites. The plagioclases do not demonstrate any simple compositional pattern related to the sequence of intrusion. Plagioclases from granitic gneisses tend to be more albitic in composition as a group than those from the intrusive granitic rocks, and the potassium feldspars tend to contain more Or molecule than those from the coarse- and medium-grained quartz monzonites. The granitic gneiss (20VC69) demonstrates another feature (fig. 4). The sample contains two plagioclases, one with an average composition $Ab_{96.5}$ $An_{2.7}$ $Or_{0.7}$ and the other $Ab_{83.2}$ $An_{16.7}$ $Or_{0.6}$. The more albitic plagioclases have oligoclase grains at their margins, and some are surrounded by the oligoclase. Oligoclase also occurs as isolated grains in the sample. The textural and compositional relations of similar occurrences of two plagioclase phases have been described by Crawford (1966) from regionally metamorphosed semipelitic schist. She interpreted the appearance of two plagioclase phases as unmixing due to the peristerite solvus. However, not enough information is available at present to evaluate the meaning of two feldspar compositions in the granitic gneisses.

Contact Relations and Sequence of Intrusion

The coarse-grained quartz monzonite and aplite dikes intrude the hornfels and the basal part of the Stillwater Complex in the Mountain View area (fig. 1). In several localities, there are inclusions of hornfels and Basal zone rocks in the coarse-grained quartz monzonite; therefore, the quartz monzonite and aplites are younger than the Stillwater Complex and the hornfels.

Stoping and diking relations between the granitic intrusive rocks are best exposed in the Flume Creek drainage (fig. 5*A*). Along the ridgeline the medium-grained quartz monzonite forms dikes and stopes in the coarse-grained quartz monzonite. Dikes of medium-grained quartz monzonite vary in size from a centimeter to about 300 feet across. All foliations present cut across the dikes of the medium-grained quartz monzonite. These outcrops cannot be interpreted as cores (central portions) of folds. Along the bottom of the Flume Creek drainage (fig. 5*A*), hornblende quartz diorite forms dikes in, and contains inclusions of, the medium-grained quartz monzonite and is in turn intruded by dikes and stopes of the fine-grained quartz monzonite. More extensive outcrops of the fine-grained quartz monzonite are found on the west side of the Stillwater River (fig. 1), where it also forms dikes and stopes in the medium-grained quartz monzonites.

Aplite dikes cut the coarse- and medium-grained quartz monzonites. Diking and stoping relations are best exposed in the Granite Ridge area (fig. 5*B*). Here, contaminated and uncontaminated aplites form a dike swarm in the hornfels and cut across both the coarse- and medium-grained quartz monzonites.

These diking and stoping relations indicate the following sequence of intrusion, from oldest to youngest: (1) coarse-grained quartz monzonite, (2) medium-grained quartz monzonite, (3) hornblende quartz diorite, (4) fine-grained quartz monzonite, and (5) numerous aplites. Wherever intrusive relations are exposed within the area mapped the sequence of events is the same.

The contact between the Beartooth metamorphic rocks and the intrusive granitic rocks is a fault in most places, but near the West Fork of the Stillwater River the fine-grained quartz monzonite intrudes biotite schists (fig. 1). The intrusive granitic rocks also contain a few biotite gneiss inclusions, one of which is shown on figure 1. The mineralogy of the inclusions excludes them from being partly absorbed cordierite-pyroxene hornfels. The biotite gneiss is more likely a still older, metamorphosed intrusive granitic or sedimentary rock. We take the existence of inclusions and stoping relations to indicate that the granitic intrusive rocks are also younger than the Beartooth metamorphic rocks.

Age of Plutonic Rocks

Although many isotopic studies have been done on rocks from the Beartooth Mountains, especially rocks in and adjacent to the Stillwater Complex, there are still conflicting age interpretations. Only those studies bearing on the age of the granitic intrusive rocks are considered here. Recent U-Pb age determinations by Nunes (1970) on euhedral zircons from the coarse-grained quartz monzonite and aplites in the Granite Ridge area gave moderately to highly discordant ages of 2,750 m.y. Cantanzaro and Kulp (1964) dated zircons from the granitic gneisses and interpreted the zircon age of these rocks to be 2,700 m.y. We conclude from these studies that the intrusive granitic rocks were emplaced about 2,750 m.y. ago

[2] An A.R.L. EXM-SM electron microprobe (analyst W. J. Nokleberg) was used with 15 kilovolts accelerating potential, sample current of 0.02 microamperes, and a 3-micron-diameter beam. All analyses were corrected for drift and background, and compositions were determined with reference to feldspar standards. The corrections program of Beeson (1967) was used for data reduction. Theoretical An, Ab, and Or end-member molecules were calculated from the partial analyses of K_2O, Na_2O, and CaO.

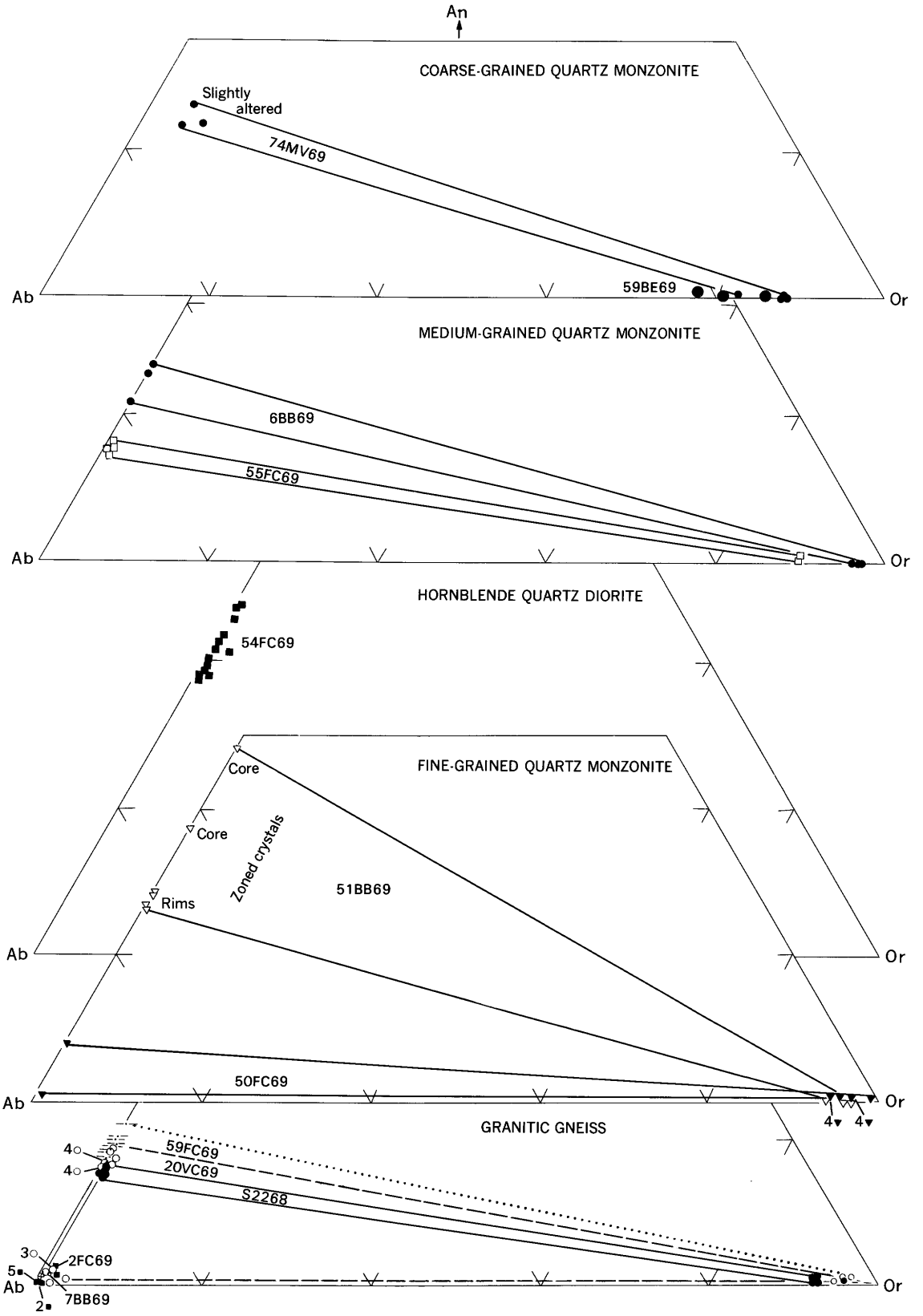

Figure 4.—Feldspar compositions determined by the electron microprobe for plutonic rocks and granitic gneiss. Sample numbers are placed near the analytical data. Diagonal lines connect points of maximum and minimum values for those samples which are quite variable.

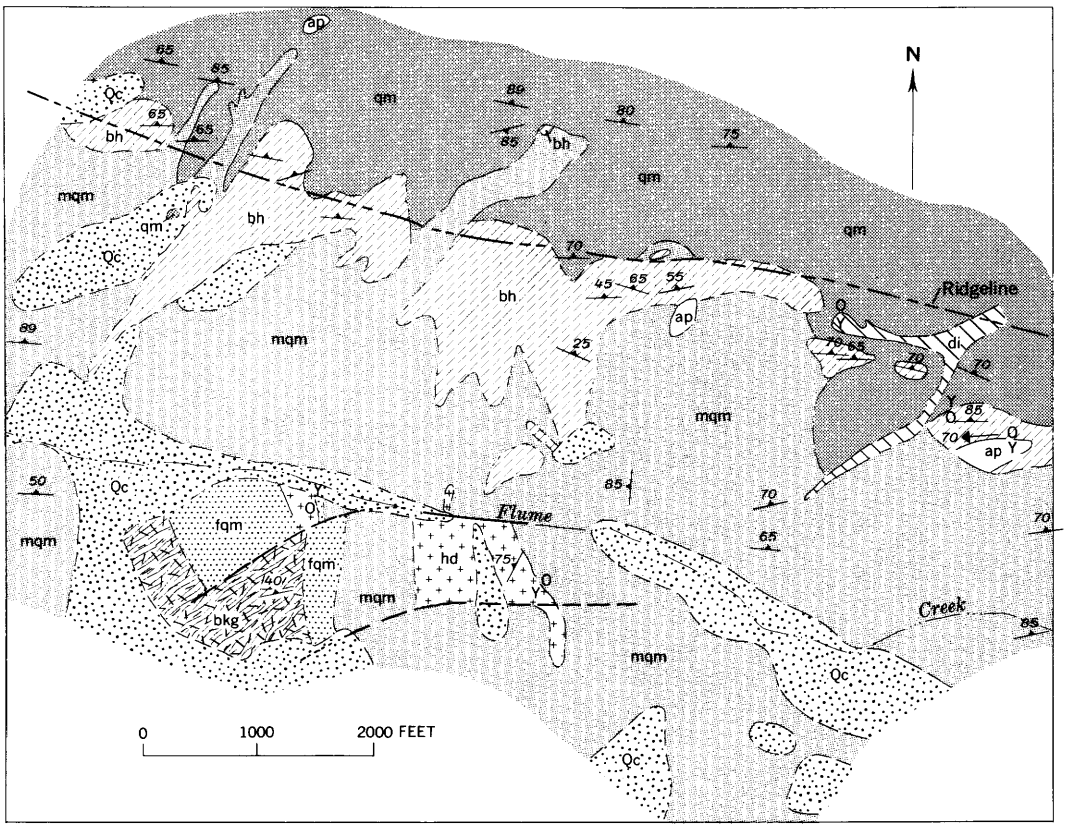

A. Flume Creek drainage

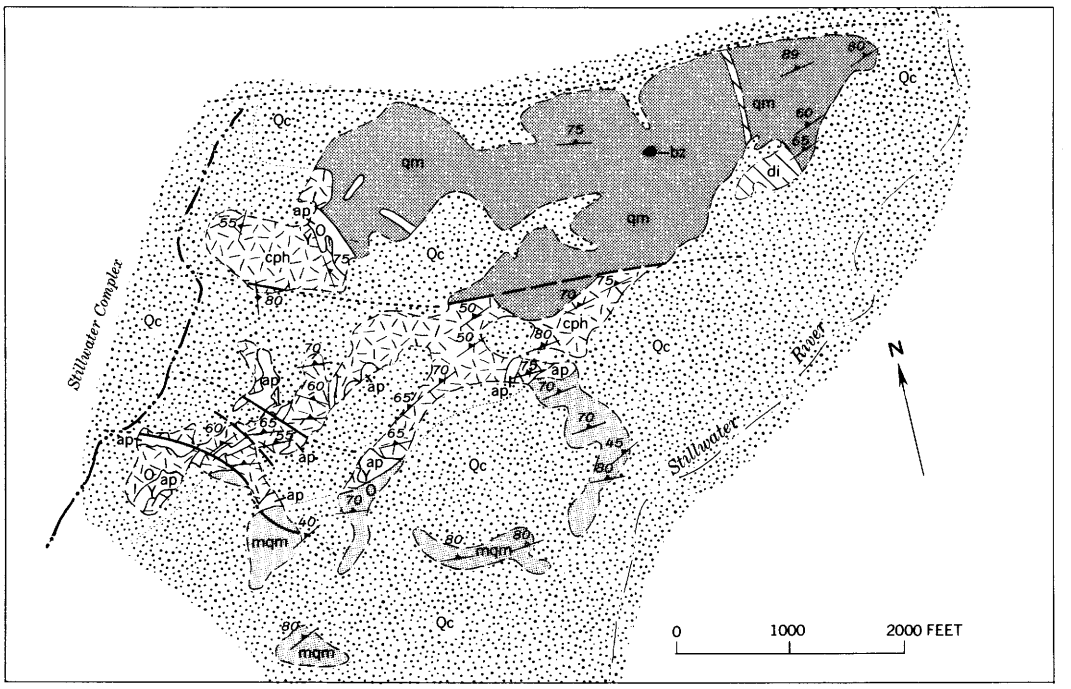

B. Granite Ridge area

EXPLANATION

QUATERNARY

Qc — Talus, alluvium, glacial deposits

di — Diabase

bz — Basal zone of Stillwater Complex

ap — Aplite

fqm — Fine-grained quartz monzonite

hd — Hornblende quartz diorite

PRECAMBRIAN

mqm — Medium-grained quartz monzonite

qm — Coarse-grained quartz monzonite

bh — Retrogressive biotite hornfels

bkg — Biotite gneiss

cph — Cordierite-orthopyroxene hornfels

Y / O — Contact
Dotted where concealed; dashed where approximately located. O, older rock; Y, younger rock

Fault
Dotted where concealed; dashed where approximately located.

75 — Mineral foliation

70 ← — Fold axis

Approximate limit of Stillwater Complex

Figure 5.—Geologic sketch maps of *A*, Flume Creek drainage; *B*, Granite Ridge area. The areas are outlined on figure 1.

and that the granitic gneisses formed around the same time. Further interpretations of the published isotopic studies concerning the age of the Stillwater Complex and adjacent rocks must consider the granitic plutonism and its effects.

Chemical and Mineralogic Trends

Three types of analytical data were obtained: (1) 12 rock analyses done by "rapid" methods (Shapiro and Brannock, 1962) for major elements and semiquantitative spectrographic analyses for trace elements; (2) 24 modes determined on stained rock slabs (Bailey and Stevens, 1960) for felsic minerals and total mafic minerals; and (3) electron microprobe partial analysis of feldspars. This information, together with CIPW norms, is given in table 1. Individual rock modes are reported for only those rocks that were chemically analyzed or for those from which the composition of the feldspar was determined. Other felsic mineral modes are depicted in figure 3. Table 1 reports average An, Or, and Ab for a number of feldspar grains from each rock. Individual values for the grains are shown in figure 4.

Examination of the chemical analyses and modes shows that the coarse-, medium-, and fine-grained quartz monzonites are quite similar in composition; in fact, there are only minor differences between the three groups of rocks. The two granitic gneisses are also very similar to the quartz monzonites, except for having higher soda values which are reflected in more albitic plagioclases. The suite of intrusive rocks is characterized by low amounts of femic oxides and high silica values, compared with other granitic rocks (for example, Bateman and Dodge, 1970). Potassium and sodium oxide contents increase slightly and calcium and femic oxides decrease in amount as silica becomes more abundant.

When the analyses and the sequence of intrusion are considered (table 1), silica, sodium, and potassium tend to increase, whereas calcium, ferric and ferrous oxide, magnesia, titania, phosphorus, and manganese decrease with each successively younger quartz monzonite, but these changes are slight. The increase in potassium with successively younger quartz monzonites is reflected modally by an increase in the amount of potassium feldspar (fig. 3), as well as by an enrichment in the Or molecule in the individual potassium feldspar grains (fig. 6). The changes in anorthite content of plagioclase (fig. 6) cannot be correlated with the sequence of intrusion but are related to the abundance of CaO in the particular rock specimen (fig. 7). The calcium content of the three quartz monzonites bears no relation to the sequence of events but ranges from 7.4 to 0.64 weight percent. These changes can be crudely correlated with increasing femic oxide contents as well.

Normative mineral calculations of the quartz monzonites and granitic gneisses (table 1) show that the total salic minerals range from 92.8 to 96.8 percent of quartz, plagioclase, and potassium feldspar. Normative An ranges from 2.53 to 12.49

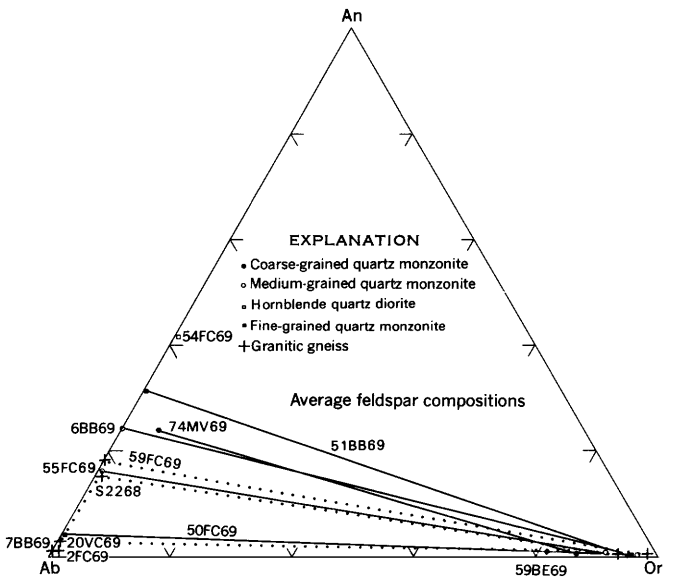

Figure 6.—Comparison of average feldspar compositions of plutonic rocks and granitic gneisses. Sample numbers are placed near the analytical data.

percent and averages 7.84 percent, excluding the hornblende quartz diorite. In all the rocks except the hornblende quartz diorite there is an excess of alumina over alkalies and calcium to form feldspars, as indicated by 0.02 to 4.23 percent corundum in the norms. In figure 8, the calculated norms are projected on the triangular diagrams of quartz (Q), albite (Ab), and orthoclase (Or), and of orthoclase (Or), albite (Ab), and

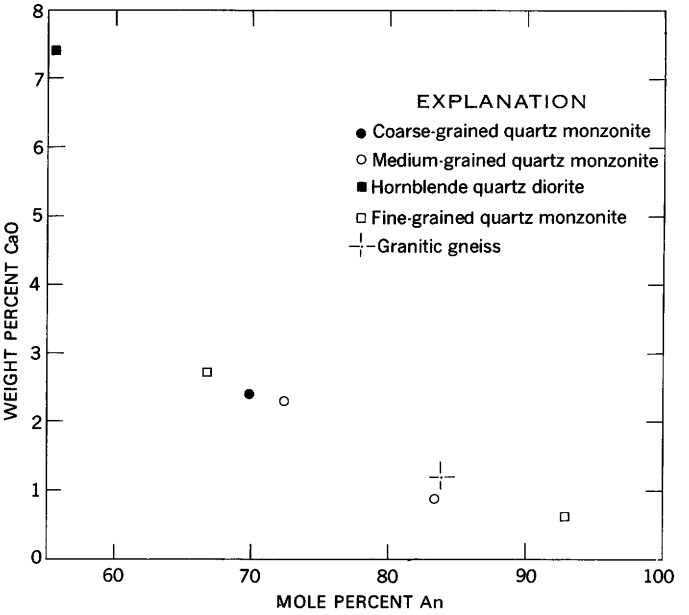

Figure 7.—Plot of weight percent CaO of rock versus respective plagioclase An content.

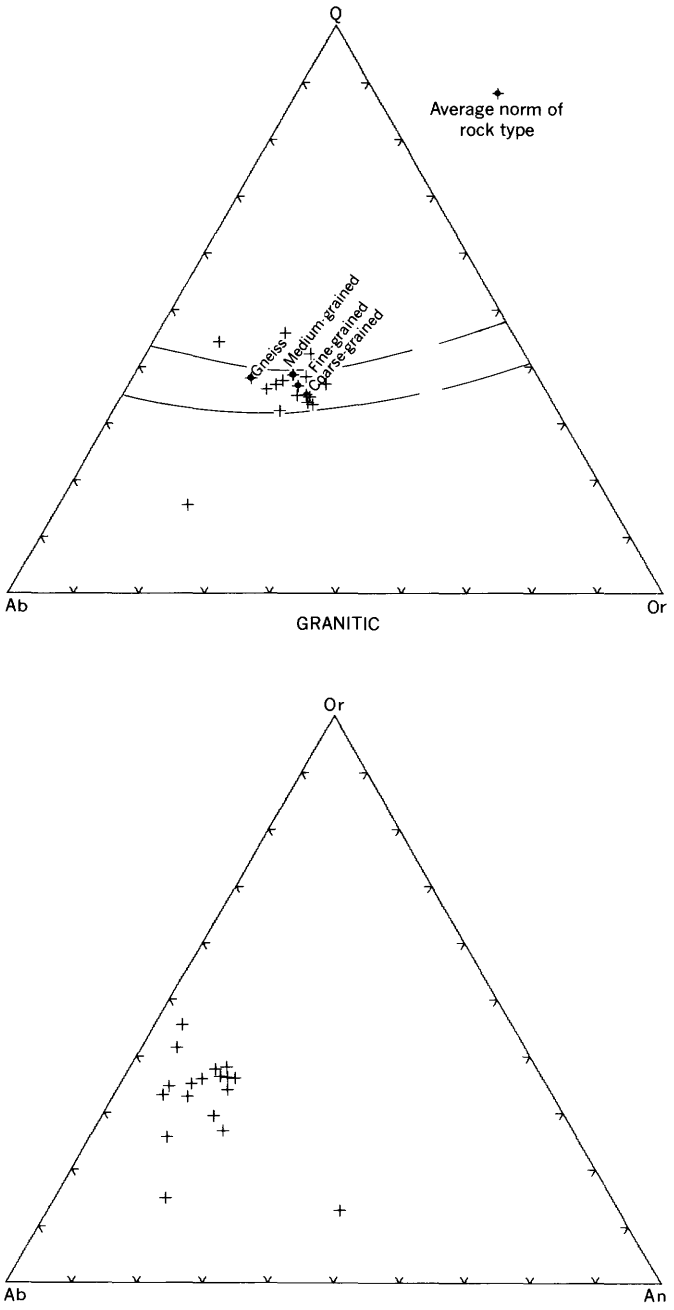

Figure 8.—Normative plots of quartz (Q), albite (Ab), and orthoclase (Or), and of orthoclase (Or), albite (Ab), and anorthite (An).

anorthite (An). Cotectic boundaries and minimums in the synthetic system Q-Ab-Or-H_2O for 0.5 kb (kilobars) and 3.0 kb water pressure are superimposed on the Q-Ab-Or diagram (Tuttle and Bowen, 1958, p. 75). The majority of the normative analyses plot between these two cotectic boundaries, but von Platen's (1965) experimental work in the system Q-Ab-An-Or-H_2O suggests that the simple system is not directly applicable to these rocks because of their An content. Von Platen (1965) studied the more complex system by increasing the An content from 0 to 15 percent and observed that the cotectic boundary positions moved toward the quartz apex. The granitic rocks with low An contents that fall between the two cotectic boundaries could have crystallized at relatively low water pressures, perhaps at higher levels in the crust. Comparison of the granitic rocks with higher An contents with von Platen's experimental system (1965, fig. 4) suggests that the minerals in them could have crystallized in different sequences as a function of the An content of the magma. The experimental work and rock compositions are consistent in suggesting a magmatic or anatectic origin for the quartz monzonites.

EMPLACEMENT OF THE GRANITIC STOCKS

Evidence for a Magma

The following observations are consistent with the idea that the granitic rocks crystallized from the melt:

1. In the Granite Ridge area, and elsewhere, the coarse-grained quartz monzonite becomes fine to medium grained within a few tens of feet of the contact with hornfels. Rocks that are finer grained than the major mass of the rock unit are also present in some dikes of the other granitic rocks.
2. Contacts of individual rock types with one another and with the wallrocks are sharp and regular, and the relative age of the rocks in contact can be determined with consistent results.
3. The four rock types are extremely homogeneous with respect to composition and texture over a large area; composition remains constant near contacts with wallrocks of diverse composition, although texture changes.
4. Compositional variations in the rock sequences are similar to variations in experimental melt systems of granitic compositions.

These four observations lead to the conclusion that the three quartz monzonites, hornblende quartz diorite, and aplites formed from magmas.

Type of Emplacement

The coarse-grained quartz monzonite probably was emplaced passively as there is no evidence of forcible emplacement. There are no indications (1) of protoclastic margins to the intrusive granitic rocks near contacts with wallrocks, (2) of foliations in the wallrocks that parallel intrusive contacts, or (3) of inclusions of wallrocks that have been stretched out into lenticular shapes by shearing. Locally, there are stoped blocks of hornfels and Basal zone rocks in the coarse-grained quartz monzonite, and there are dikes of quartz monzonite in the hornfels and Basal zone rocks. All of the foliations in the quartz monzonite, defined by parallel mica streaks and by quartz and feldspar augen, strike across intrusive contacts and are due to a later penetrative deformation. Such deformation

Table 1.—*Chemical and modal analyses of granitic rocks adjacent to the Stillwater Complex, Montana*

	Coarse-grained quartz monzonite			Medium-grained quartz monzonite					Hornblende quartz diorite	Fine-grained quartz monzonite		Granitic gneiss					Biotite gneiss
Sample number..	74MV69	51NB69	59BE69	6BB69	18VC69	57MV69	55FC69	57BE69	54FC69	51BB69	50FC69	7BB69	S2268	20VC69	1FC69	2FC69	59FC69
Chemical analyses (weight percent)[1]																	
SiO_2	70.4	69.5	70.9	71.0	73.1	73.1	75.1	74.0	54.6	71.0	75.1	....	73.5	....	73.5	....	....
Al_2O_3	14.3	15.4	14.9	14.5	14.8	14.5	14.7	13.6	17.2	15.4	13.7	....	14.5	....	14.3	....	....
Fe_2O_3	1.5	1.0	1.3	1.4	.86	.64	.16	.91	3.0	.32	.72	....	.08	....	.52	....	....
FeO	1.4	1.7	1.5	1.6	.76	.96	.64	.72	5.2	1.8	.80	....	.84	....	1.8	....	....
MgO	.91	1.0	.93	.71	.30	.41	.19	.54	5.0	.74	.34	....	.23	....	.55	....	....
CaO	2.4	2.3	2.1	2.3	.84	1.5	.89	1.7	7.4	2.7	.64	....	1.2	....	2.0	....	....
Na_2O	3.6	3.6	3.6	3.9	3.9	4.0	3.6	3.7	3.2	4.0	3.6	....	4.5	....	4.4	....	....
K_2O	4.0	3.6	4.2	3.1	4.4	3.4	2.9	4.1	1.4	2.9	4.7	....	3.9	....	1.4	....	....
H_2O+	.75	1.2	.0	.86	.71	.46	.59	.28	1.4	.57	.0	....	.32	....	1.0	....	....
H_2O-	.08	.12	.11	.09	.09	.75	.09	.14	.07	.10	.10	....	.13	....	.06	....	....
TiO_2	.34	.36	.29	.34	.16	.13	.10	.17	.69	.31	.16	....	.10	....	.23	....	....
P_2O_5	.09	.10	.09	.09	.08	.03	.04	.08	.19	.09	.05	....	.09	....	.05	....	....
MnO	.03	.04	.04	.04	.02	.04	.0	.0	.14	.03	.0	....	.0	....	.02	....	....
CO_2	.05	.05	.05	.05	.05	.05	.05	.05	.05	.05	.05	....	.05	....	.05	....	....
Sum	99.85	99.97	100.01	99.98	100.97	99.97	99.05	99.99	99.54	100.01	99.96	....	99.44	....	99.88	....	....
Semiquantitative 6-step spectrographic analyses (ppm)[2]																	
Ba	1,500	2,000	1,500	1,000	1,500	1,500	1,000	1,000	700	1,000	700	....	1,000	....	700	....	....
Be	N	N	N	N	N	N	2	N	N	1.5	N	....	N	....	N	....	....
Co	7	10	10	3	2	N	N	2	30	5	N	....	N	....	5	....	....
Cr	20	20	15	15	10	15	7	10	150	15	10	....	10	....	7	....	....
Cu	7	10	50	7	5	10	.7	7	30	1	1	....	2	....	5	....	....
La	100	50	50	N	N	N	N	N	N	70	50	....	N	....	30	....	....
Ni	10	10	50	7	7	15	3	5	70	10	7	....	7	....	2	....	....
Pb	7	7	10	30	50	30	30	30	N	50	50	....	50	....	30	....	....
Sc	10	5	7	7	N	5	N	5	30	3	5	....	N	....	N	....	....
Sr	300	300	300	300	500	200	300	150	700	200	70	....	500	....	300	....	....
V	30	30	50	30	10	20	7	15	150	20	7	....	5	....	30	....	....
Y	10	N	N	10	N	N	N	10	10	N	15	....	N	....	N	....	....
Zr	150	150	70	100	150	70	50	100	70	200	100	....	30	....	150	....	....
Ce	150	N	N	N	N	N	N	N	N	N	N	....	N	....	N	....	....
Ga	15	20	15	20	20	20	20	15	20	20	20	....	20	....	20	....	....
Yb	.7	.7	.7	1	N	N	N	1	1.5	.7	1	....	N	....	N	....	....
Modal analyses (volume percent)[3]																	
Felsic minerals:																	
Quartz	28.7	31.4	26.5	28.7	27.0	29.6	29.2	31.6	12.8	27.7	28.8	31.9	24.8	32.4	34.2	32.4	27.5
Potassium feldspar	29.4	22.0	28.7	25.8	31.8	27.5	31.5	33.2	.5	30.3	39.7	2.8	21.5	8.1	3.3	.0	1.4
Plagioclase	33.9	38.3	38.5	36.4	32.8	37.6	35.3	24.0	[4]51.1	35.3	22.5	54.4	42.1	30.9	48.4	55.6	54.5
Muscovite	....	....	....	....	....	....	....	....	....	....	....	....	....	16.5	....	....	....
Mafic minerals	8.1	8.4	6.8	9.2	8.6	5.4	4.3	11.2	[5]35.7	6.7	10.0	11.4	11.9	[6]22.1	14.4	12.6	16.6

CIPW norms

Q	27.6	27.97	27.81	30.26	31.48	32.72	40.72	....	6.62	28.96	34.29	....	29.27	....	36.56	....	....
C	.02	1.75	.94	.87	2.40	1.70	4.23	....	...	1.10	1.76	....	1.02	....	2.14	....	....
or	23.64	21.27	24.81	18.31	26.00	20.09	17.13	....	8.27	17.13	27.77	....	23.04	....	8.27	....	....
ab	30.46	30.46	30.46	33.00	33.00	33.84	30.46	....	27.07	33.84	30.46	....	38.07	....	37.23	....	....
an	11.00	10.44	9.51	10.50	3.32	6.92	3.83	....	28.43	12.49	2.53	....	5.04	....	9.27	....	....
wo	....	....	....	....	....	....	....	....	2.80	....	....	....	....	....	....	....	....
mt	2.18	1.45	1.88	2.03	1.24	.92	.23	....	4.35	.46	1.04	....	.11	....	.7	....	....
il	.65	.68	.55	.64	.30	.24	.19	....	1.31	.58	.30	....	.19	....	.43	....	....
ap	.21	.23	.21	.21	.18	.07	.09	....	.45	.21	.11	....	.21	....	.11	....	....
fs	.83	1.77	1.27	1.29	.45	1.09	.88	....	5.31	2.58	.61	....	1.31	....	2.53	....	....
en	2.26	2.49	2.31	1.76	.74	1.02	.47	....	10.69	1.84	.84	....	.57	....	1.37	....	....
hy	3.09	4.26	3.59	3.06	1.20	2.11	1.35	....	16.00	4.42	1.45	....	1.88	....	3.90	....	....
cc	.11	.11	.11	.11	.11	.11	.11	....	.11	.11	.11	....	.11	....	.11	....	....

Electron microprobe partial analyses of feldspars, average end member molecules (molecular percent)[7]

Plagioclase:																	
Or	6.1	....	....	0.0	....	....	0.8	....	0.8	0.4	0.4	0.5	0.6	0.8 0.6	....	0.6	0.1
Ab	69.9	....	....	75.4	....	....	83.6	....	57.7	68.1	95.2	98.1	83.9	96.4 83.2	....	98.6	81.4
An	23.9	....	....	24.6	....	....	15.3	....	41.4	31.4	4.4	1.4	15.4	2.7 16.2	....	.7	18.3
Potassium feldspar:																	
Or	86.6	....	81.3	96.8	....	....	89.5	....	....	95.4	96.1	....	93.0	94.9	....	....	97.9
Ab	13.0	....	18.1	3.1	....	....	9.8	....	....	4.5	3.5	....	6.3	4.7	....	....	1.8
An	.3	....	.5	.0	....	....	.6	....	....	.1	.3	....	.6	.2	....	....	.2

[1] Major-element analyses done under Leonard Shapiro by P. Elmore, G. Chloe, H. Smith, J. Kelsey, and J. Glenn using methods described by Shapiro and Brannock (1962).
[2] Semiquantitative spectrographic analyses by Chris Heropoulos; results are to be identified with geometric brackets whose boundaries are 1.2, 0.83, 0.56, 0.38, and so forth, but are reported arbitrarily as midpoints of these brackets; N = not detected, at limit of detection.
[3] Felsic modes on stained slabs, 1,000 points counted.
[4] Highly altered in thin section to epidote and fine-grained micas.
[5] Hornblende, 24.5; biotite, 5.3; chlorite, 2.2; epidote, 2.8 percent; opaque minerals, 0.9; determined by point-count analysis with 1,000 points in thin section.
[6] Epidote, 7.0; biotite, 4.5; zircon, 0.1; opaque minerals, 0.5; determined by point-count analysis with 1,000 points in thin section.
[7] Analyses by W. J. Nokleberg.

might locally account for the lack of evidence for forcible emplacement, but it is likely that a protoclastic margin and an earlier formed foliation in the hornfels would at least be preserved locally. Similar evidence can be given for each of the successive emplacements of the sequence of granitic rocks. All observations indicate that each rock unit was emplaced as a magma through stoping and assimilation.

METAMORPHIC EFFECTS OF THE GRANITIC ROCKS

One might expect to find extensive mineralogic changes in the ultramafic rocks of the Stillwater Complex along the 5 miles of strike length of the contact between those rocks and the coarse-grained quartz monzonite that intruded them. Also one might expect to find extensive retrogressive metamorphism in the pyroxene hornfels that forms the wallrocks next to the quartz monzonite. Neither of these effects has been observed. Locally, near the Bendow mine area and close to the intrusive contact, the ultramafic rocks, in particular olivine and olivine-bronzite cumulates, have been serpentinized. On weathered surfaces, the serpentinized rocks show relict cumulate textures, but on broken surfaces they present a fine-grained, granoblastic texture characteristic of hornfelses. The hornfels-textured rocks are comprised of interlocking antigorite laths (X-ray identification, Whittaker and Zussman, 1956) with minor magnetite, relict olivine, orthopyroxene, and clinopyroxene. Overprinted on the antigoritic rock is younger serpentine, consisting of lizardite and chrysotile (X-ray identification) which replace antigorite. The antigorite probably formed as a result of contact metamorphism during granitic plutonism. The development of lizardite and chrysotile appears to be closely related in space to north-south and east-west faults and the later penetrative deformation, both of which cut the granitic rocks. Therefore, the later serpentinization cannot be considered to be due to igneous plutonism. Ultramafic minerals in the country rocks within a few tens of inches to a few feet of the intrusive contact from the Benbow to Mountain View areas are also locally replaced by a chlorite. The development of chlorite could be a result of contact metamorphism during the intrusion of the quartz monzonite.

In the Granite Ridge area, at the southern contact of the coarse-grained quartz monzonite, the hornfels shows a coarsening in grain size within a few feet of the pluton. This coarsening can be attributed to contact metamorphic effects of the granitic plutonism. The hornfels pendants along the Flume Creek ridgeline (fig. 5) show minor retrogressive effects. Orthopyroxene and cordierite are altered to chlorite, serpentine, biotite, and white mica. The development of all but the biotite is ascribed to a postplutonism, penetrative deformation and recrystallization, because the minerals are crystallized along a postintrusion metamorphic foliation.

The lack of a contact metamorphic aureole or development of hydrous phases typical of the hornblende hornfels facies can be explained by a couple of models. Passive emplacement of quartz monzonites at conditions of the pyroxene hornfels facies before the country rocks cooled down from the intrusion of the Stillwater Complex could account for the lack of signs of a metamorphic aureole. Some interpretations of the isotopic ages in the area could support this argument. Nunes (1970) believes that less than 60 m.y. elapsed between the intrusion of the Stillwater Complex and the intrusion of the granitic rocks. Another model which does not require exact timing involves the intrusion of the quartz monzonitic magmas and their crystallization at conditions of undersaturation with respect to water. Under these conditions no fluids would be released to the country rocks for making hydrous phases of the hornblende hornfels facies or for causing extensive metasomatism.

CONCLUSIONS

Contrary to published opinions and observations concerning the lack of Precambrian igneous intrusive rocks in the Beartooth Mountains (Casella, 1969), detailed field mapping and laboratory study have documented the occurrence of widespread 2,700-m.y.-old granitic intrusive rocks on the northern border of the mountain range. The plutonic granitic rocks were probably emplaced after the first two episodes of folding recognized by McMannis, Palmquist, and Reid (1970a, b, c) and after the first two episodes of folding and the granitic gneiss generation in the southeastern Beartooth Mountains. Superposed on the complex sequence of events was a later deformation, which shows up as a penetrative foliation in the report area.

REFERENCES

Bailey, E. H., and Stevens, R. E., 1960, Selective staining of K-feldspar and plagioclase on rock slabs and thin sections: Am. Mineralogist, v. 45, p. 1020–1025.

Bateman, P. C., Clark, L. D., Huber, N. K., Moore, J. E., and Rinehart, C. D., 1963, The Sierra Nevada batholith, a synthesis of recent work across the central part: U.S. Geol. Survey Prof. Paper 414-D, 46 p.

Bateman, P. C., and Dodge, F. C. W., 1970, Variations of major chemical constituents across the central Sierra Nevada batholith: Geol. Soc. America Bull., v. 81, p. 409–420.

Beeson, M. H., 1967, A computer program for processing electron microprobe data: U.S. Geol. Survey open-file report, 34 p.

Buddington, A. F., 1959, Granitic emplacement with special reference to North America: Geol. Soc. America Bull., v. 70, p. 671–747.

Butler, J. R., 1966, Geologic evolution of the Beartooth Mountains, Montana and Wyoming. Part 6. Cathedral Peak area, Montana: Geol. Soc. America Bull., v. 77, p. 45–64.

—— 1969, Origin of Precambrian granitic gneiss in the Beartooth Mountains, Montana and Wyoming: Geol. Soc. America Mem. 115, p. 73–101.

Cantanzaro, E. J., and Kulp, J. L., 1964, Discordant zircons from the Little Belt (Montana), Beartooth (Montana), and Santa Catalina (Arizona) Mountains: Geochim. et Cosmochim. Acta, v. 28, p. 87–124.

Casella, C. J., 1964, Geologic evolution of the Beartooth Mountains, Montana and Wyoming. Pt. 4. Relationship between Precambrian

and Laramide structures in the Line Creek area: Geol. Soc. America Bull., v. 75, p. 969–986.

—— 1969, A review of Precambrian geology of the eastern Beartooth Mountains, Montana and Wyoming: Geol. Soc. America Mem. 115, p. 53–72.

Crawford, M. L., 1966, Composition of plagioclase and associated minerals in some schists from Vermont, U.S.A., and South Westland, New Zealand, with inferences about the peristerite solvus: Contr. Mineralogy and Petrology, v. 13, p. 269–294.

Eckelmann, F. D., and Poldervaart, Arie, 1957, Geologic evolution of the Beartooth Mountains, Montana and Wyoming. Pt. 1. Archean history of the Quad Creek area: Geol. Soc. America Bull., v. 68, p. 1225–1262.

Foose, R. M., Wise, D. V., and Garbarini, G. S., 1961, Structural geology of the Beartooth Mountains, Montana and Wyoming: Geol. Soc. America Bull., v. 72, p. 1143–1172.

Harris, R. L., Jr., 1959, Geologic evolution of the Beartooth Mountains, Montana and Wyoming. Pt. 3. Gardner Lake area, Wyoming: Geol. Soc. America Bull., v. 70, p. 1185–1216.

Hess, H. H., 1960, The Stillwater igneous complex, Montana, a quantitative mineralogical study: Geol. Soc. America Mem. 80, 230 p.

Jackson, E. D., 1961, Primary textures and mineral associations in the ultramafic zone of the Stillwater complex, Montana: U.S. Geol. Survey Prof. Paper 358, 106 p.

James, H. L., 1946, Chromite deposits near Red Lodge, Carbon County, Montana: U.S. Geol. Survey Bull. 945-F, p. 151–189.

Jones, W. R., Peoples, J. W., and Howland, A. L., 1960, Igneous and tectonic structures of the Stillwater Complex, Montana: U.S. Geol. Survey Bull. 1071-H, p. 281–340.

Larsen, L. H., Poldervaart, Arie, and Kirchmayer, Martin, 1966, Geologic evolution of the Beartooth Mountains, Montana and Wyoming. Pt. 7. Structural homogeneity of gneisses in the Lonesome Mountain area: Geol. Soc. America Bull., v. 77, p. 1277–1292.

McMannis, W. J., Palmquist, J. C., and Reid, R. R., 1971a, Precambrian geologic history, North Snowy block, northwestern Beartooth Mountains, Montana [abs.]: Geol. Soc. America, Rocky Mountain Sec., Program, v. 3, no. 6, p. 394.

—— 1971b, Origin of gneisses in North Snowy block, Beartooth Mountains, Montana [abs.]: Geol. Soc. America, Rocky Mountain Sec., Program, v. 3, no. 6, p. 395.

—— 1971c, Structural evolution of the North Snowy block, Beartooth Mountains, Montana [abs.]: Geol. Soc. America, Rocky Mountain Sec., Program, v. 3, no. 6, p. 395–396.

Nunes, P. N., 1970, U-Pb age determinations of the Stillwater igneous complex and associated rocks [abs.]: Am. Geophys. Union Trans., v. 51, p. 449.

Page, N. J, and Nokleberg, W. J., 1970a, A suite of granitic intrusive rocks below the base of the Stillwater complex, Mount Wood quadrangle, Montana [abs.]: Geol. Soc. America, Rocky Mountain Sec., Program, v. 2, no. 5, p. 342.

—— 1970b, Preliminary geologic map of the Stillwater Complex: U.S. Geol. Survey open-file report, scale 1:12,000.

Peoples, J. W., 1933, The Stillwater igneous complex, Montana [abs.]: Am. Mineralogist, v. 18, p. 117.

—— 1963, Gravity stratification as a criterion in the interpretation of the structure of the Stillwater complex, Montana: Internat. Geol. Cong., 16th, United States 1933, Rept., v. 1, p. 353–360.

Platen, H. von, 1965, Experimental analyses and genesis of migmatites, *in* Pitchers, W. S., and Flinn, G. W., eds., Controls of metamorphism: New York, John Wiley and Sons, Inc., p. 203–218.

Poldervaart, Arie, and Bentley, R. D., 1958, Precambrian and later evolution of the Beartooth Mountains, Montana and Wyoming: Billings Geol. Soc., Guidebook, 9th Ann. Field Conf., p. 7–15.

Prinz, Martin, 1964, Geologic evolution of the Beartooth Mountains, Montana and Wyoming. Pt. 5. Mafic dike swarms of the southern Beartooth Mountains: Geol. Soc. America Bull., v. 75, p. 1217–1248.

Rowan, L. C., 1969, Structural geology of the Quad-Wyoming-Line Creeks area, Beartooth Mountains, Montana: Geol. Soc. America Mem. 115, p. 1–18.

Rowan, L. C. and Larsen, L. H., 1970, Precambrian history of the Beartooth Mountains-Hellroaring Lakes area, Montana [abs.]: Geol. Soc. America Abs. with Programs, v. 2, no. 5, p. 347.

Rowan, L. C., and Mueller, P. A., 1971, Relations of folded dikes and Precambrian polyphase deformation, Gardner Lake area, Beartooth Mountains, Wyoming: Geol. Soc. America Bull., v. 82, no. 8, p. 2177–2186.

Shapiro, Leonard, and Brannock, W. W., 1962, Rapid analysis of silicate, carbonate, and phosphate rocks: U.S. Geol. Survey Bull. 1144-A, 56 p.

Skinner, W. R., 1969, Geologic evolution of the Beartooth Mountains, Montana and Wyoming. Pt. 8. Ultramafic rocks in the Highland Trail Lakes area, Wyoming: Geol. Soc. America Mem. 115, p. 19–52.

Skinner, W. R., Bowes, D. R., and Khoury, S. G., 1969, Polyphase deformation in the Archean basement complex, Beartooth Mountains, Montana and Wyoming: Geol. Soc. America Bull., v. 80, p. 1053–1060.

Tuttle, O. F., and Bowen, N. L., 1958, Origin of granite in the light of experimental studies in the system $NaAlSi_3O_8$-$KAlSi_3O_8$-SiO_2-H_2O: Geol. Soc. America Mem. 74, 153 p.

Whittaker, E. J. W., and Zussman, J., 1956, The characterization of serpentine minerals by X-ray diffraction: Mineralog. Mag., v. 31, p. 107–126.

LAYERED GABBROS IN SOUTHWEST SAUDI ARABIA

By R. G. COLEMAN[1], G. F. BROWN[2], and T. E. C. KEITH[1],
[1]Menlo Park, Calif., [2]Jiddah, Saudi Arabia

Abstract.—Layered gabbros of two distinct ages have been discovered in southwest Saudi Arabia. Numerous intrusions consisting of layered gabbro northeast of the Asir Mountains have radiometric ages ranging from 415 to 702 m.y. In contrast, a layered gabbro mass, which occupies a narrow rift zone along the eastern margin of the Red Sea near Jizan, is of Miocene (20 to 24 m.y.) age.

Mapping revealed the presence of at least 10 layered gabbro masses in southwest Saudi Arabia within the Precambrian shield between lat 17° and 21° N., and long 42° and 43° E. These layered gabbros are of two different ages in two distinct geologic settings: (1) Precambrian and possibly early Paleozoic layered gabbro masses intrude shield rocks just north of the Asir Mountains, and (2) early Miocene layered gabbro occupies a narrow rift zone at the contact between coastal plain sediments and Precambrian basement near Jizan (fig. 1, table 1).

Acknowledgment.—The work of the U.S. Geological Survey was supported by the Ministry of Petroleum and Mineral Resources of Saudi Arabia.

INTRODUCTION

In contrast to the more numerous Precambrian gabbro intrusions, a single large trough-shaped layered gabbro intrusion (Jabal at Turf) of early Miocene age is located within a narrow rift zone that marks the contact between the coastal plain sedimentary rocks and Precambrian basement. The rift zone here is approximately 3 km wide and contains numerous dikes and hypabyssal intrusives mainly of basaltic composition. A steeply dipping narrow selvage of Jurassic sandstone deposited unconformably on Precambrian metamorphic rocks is invaded by numerous dikes, and it may be the floor along which the Jabal at Turf body was emplaced. The Jabal at Turf layered complex is approximately 8 km long and 1.6 km wide. The layers of gabbro dip steeply (40°–60°) west towards the Red Sea, exposing the base and sides of the magma chamber. The actual shape of the layered body is difficult to ascertain, but it appears to be a canoe-shaped trough with a maximum thickness of 1,400 m. An associated granophyre bears the same relation to the layered gabbro as do the iron-rich granodiorites and granophyres to the Duluth Gabbro (Wager and Brown, 1967, p. 499) and probably represents a differentiate that has accumulated at the top of the magma chamber. The steep dips of the layered gabbro, granophyre, and Jurassic sandstones indicate postintrusion deformation that may be related to development of the Red Sea depression. The layered gabbro probably was formed by fractional crystallization of basaltic liquids syntectonic with the narrow rift zone. These same basaltic liquids formed dikes within the zone of fracturing, but no correlative surface flows have been observed. Strong magnetic anomalies paralleling the rift zone suggest a subsurface continuity of mafic rocks.

The Saudi Arabian layered masses are much smaller than the Stillwater, Mont.; Bushveld, South Africa; and Duluth, Minn., layered complexes (Wager and Brown, 1967). Magnetic anomalies observed in an aeromagnetic survey of the Precambrian masses are found, by use of computer modeling, to resemble those of vertical cylindrical masses rather than lopoliths or inverted cones (Andrew Griscom, oral commun., 1971).

The Precambrian gabbros have circular forms with inward dipping layers. Some seem to be a single intrusion (Jabal Shayi; figs. 2 and 3); others may be multiple coalescing intrusions, for they have lobate patterns in plan view (Jabal al Ashsha, Wadi Misyab, and Jabal Hibr; fig. 2). In plan, the maximum dimension of the largest body, Jabal Hibr, is 8 km, while that of the smallest body, Hishat al Hawi, is 1.0 km (fig. 2).

The structural control of the localization of the Precambrian gabbro intrusions is not yet clear, but they form central areas within synforms that have developed in north-trending, mobile metamorphic belts. There is no clear evidence to suggest that gabbro magma intruded during the tectonism that produced these synforms in the mobile belts. The steep dips (>60°) of the basal cumulate layers within the intrusions suggest that some downward sagging accompanied emplacement and that at least part of the synform results from the intrusion itself. No feeder dikes or necks that could be related to these intrusions, or to other probably similar but eroded bodies, have been discovered. Pegmatite and aplite dikes derived from posttectonism quartz monzonite plutons intrude the layered gabbro masses and indicate that the gabbros are earlier and are unrelated to the granites.

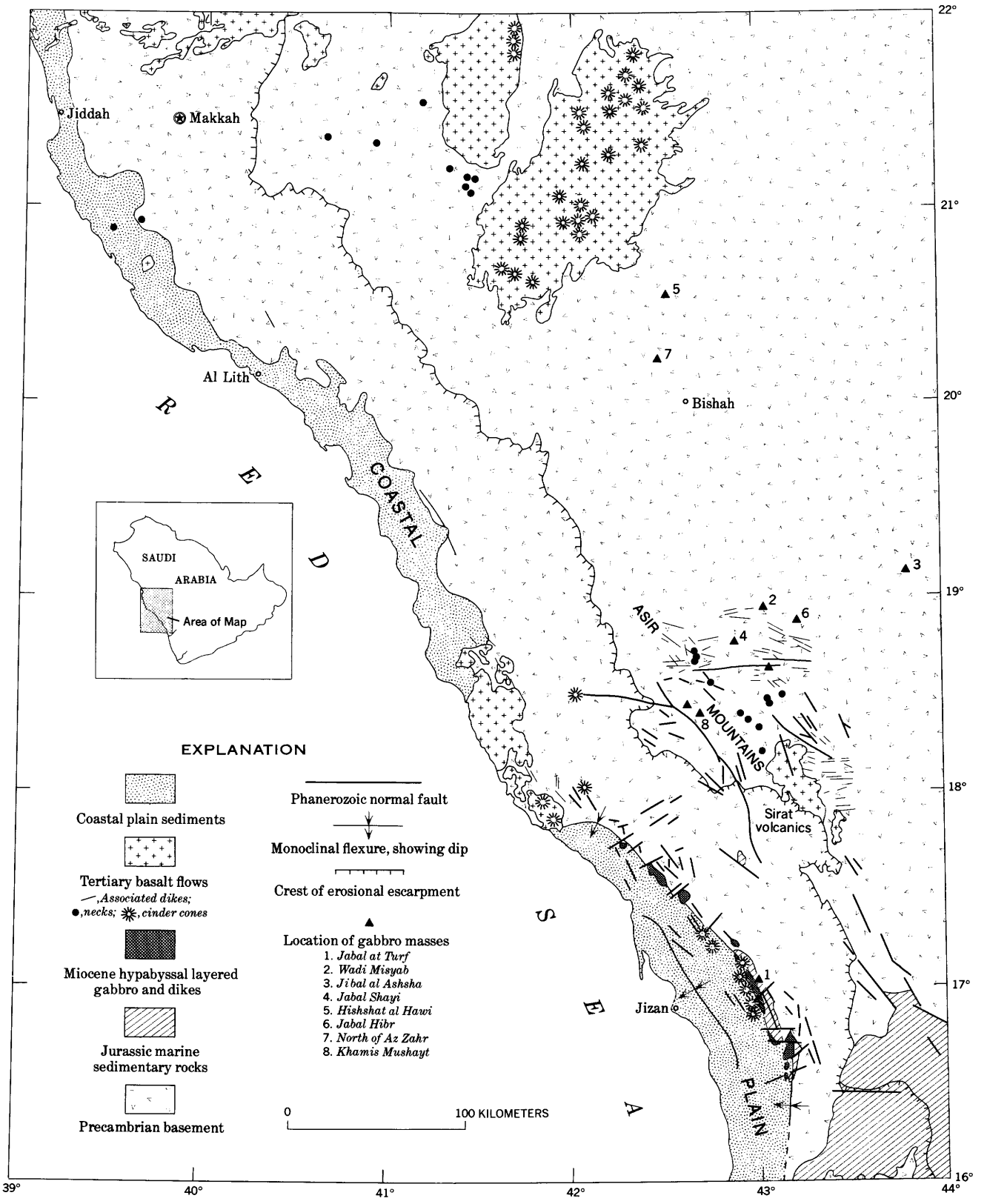

Figure 1.—Map showing distribution of layered gabbros and volcanic rocks in southwest Saudi Arabia.

Table 1.—*Characteristics of layered gabbro intrusive rocks in southwest Saudi Arabia*

Locality name and coordinates	Size and shape	Country rock and intrusive relations	Main rock types	Internal features
Jabal at Turf Lat 16°57.3′N.; long 42°57′E.	Elongated rectangle in plan view; canoe-shaped trough 8 km long, 1.6 km wide, and about 1,370 m thick.	Invades main rift zone producing hornfels and rheomorphic injections at the base. Younger dikes cut layered sequence.	Granophyre Clinopyroxene gabbro Clinopyroxene olivine gabbro	Rhythmic layering produced mostly by cumulate plagioclase (An_{57-72}) and intercumulate clinopyroxene. Phase boundaries marked by cumulate olivine and intercumulate clinopyroxene. No ultramafic zone discovered. Top part marked by extensive granophyre. Opaque material mainly magnetite and ilmenite.
Wadi Misyab Lat 18°55.8′N.; long 43°1.3′E.	Elongated and coalescing intrusion produces lobate outline in plan view 3.5 km long and 1.9 km wide.	Intrudes older gneissic granite and amphibolite. No hornfels zone found. Younger pegmatitic dikes cut layered gabbro.	Clinopyroxene gabbro Clinopyroxene olivine gabbro Norite	Rhythmic layering produced mostly by cumulate plagioclase (An_{52-73}) and intercumulate clinopyroxene. Phase boundaries marked by cumulate clinopyroxene and orthopyroxene-plagioclase cumulates. No ultramafic zone found. Granophyre not present. Opaque material mainly magnetite and ilmenite.
Jabal al Ashsha Lat 19°8.2′N.; long 43°48.8′E.	Two coalescing intrusions produce lobate outline in plan view 6 km long and 2.4 km wide.	Intrudes older gneissic granite and metamorphosed basic rocks of Precambrian age. Hornfels zone 45–90 m wide developed on north boundary. Some deformation of country rocks around northeast boundary.	Clinopyroxene olivine gabbro	Rhythmic layering inward dip produced mostly by cumulate plagioclase (An_{56-70}). Phase boundaries marked by cumulate olivine and intercumulate clinopyroxene. No ultramafic zone found. Granophyre not present. Pentlandite-pyrrhotite and magnetite-ilmenite opaque material.
Jabal Shayi Lat 18°45′N.; long 42°53′E.	Intrusive forms single ellipse in plan view 4.5 km long and 2.9 km wide.	Intrudes chlorite and amphibolite schist of Precambrian age. Occupies synform within older schists and forms concentric sills at southern border. Hornfels zone approximately 500 m wide.	Clinopyroxene gabbro Clinopyroxene olivine gabbro Norite	Rhythmic layering inward dip produced mostly by cumulate plagioclase (An_{40-75}). Phase boundaries marked by cumulate olivine and clinopyroxene. Majority of clinopyroxene is intercumulate. No ultramafic zone found. Granophyre and gabbro pegmatites are near the center of the mass. Pentlandite-pyrrhotite opaque material commonly giving way to magnetite and ilmenite in cryptic cycles.
Hishshat al Hawi Lat 20°33′N.; long 43°28′E.	Intrusive forms single ellipse, truncated through center by fault. Original major diameter 1.6 km.	Intrudes metagreenstones and gneissic diorites of Precambrian age. No hornfels zone found. Postigneous faulting truncated south half of the body and has disrupted layering.	Clinopyroxene gabbro Anorthosite Troctolite	Rhythmic layering inward dip produced mostly by cumulate plagioclase (An_{63-84}). Phase boundaries marked mainly by cumulate olivine. Minor amounts of orthopyroxene and clinopyroxene intercumulates. No ultramafic zone found. Granophyre not present. Pentlandite-pyrrhotite and magnetite-ilmenite opaque material.
Jabal Hibr Lat 18°53′N.; long 43°14′E.	Elongated coalescing intrusions 6.45 km long and 2.4 km wide.	Intrudes massive calc-alkaline granite of Precambrian age. No hornfels zone found. Postigneous basalt dikes cut granite and layered gabbro. Some country rock deformation on south side.	Clinopyroxene olivine gabbro	Rhythmic layering dips inward. Insufficient samples to characterize further.
North of Az Zahr Lat 20°13′N.; long 42°27′E.	Elongate tubular body, broadly curved with homoclinal dip, 4.8 km long and 0.8 km wide.	Intrudes Precambrian greenstone with no apparent deformation of country rock. No hornfels zone found.	Clinopyroxene olivine gabbro	Rhythmic layering dips inward. Insufficient samples to characterize further.

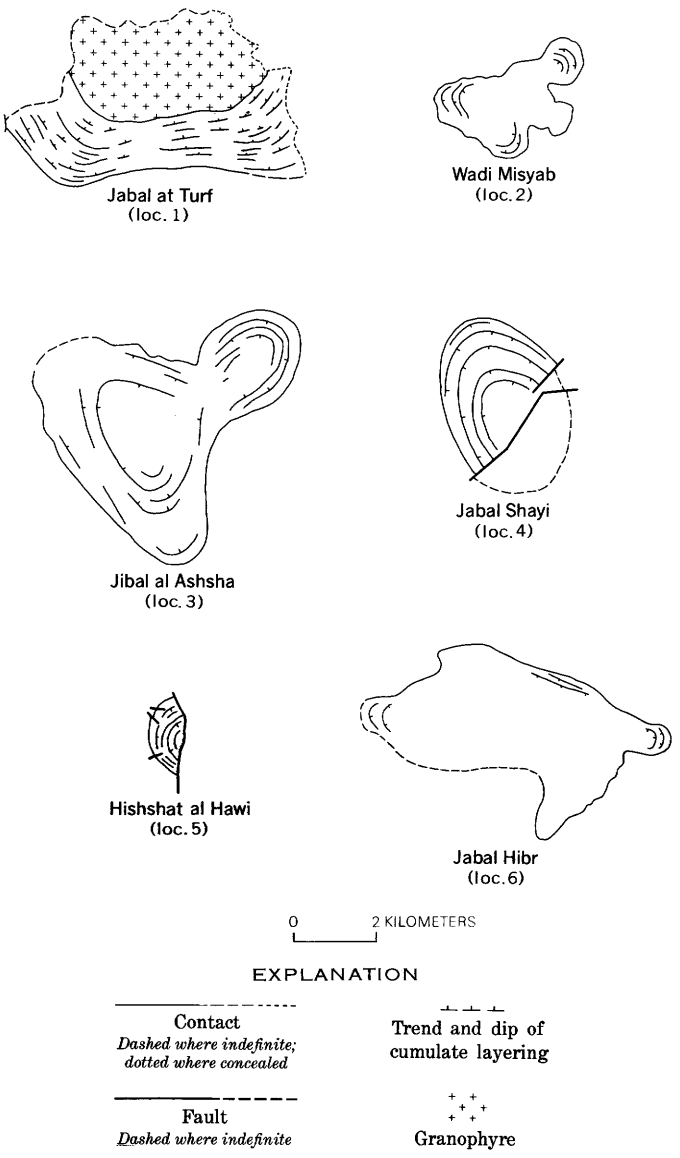

Figure 2.—Planimetric sketch maps (not oriented) showing comparative size and shape of the Saudi Arabian layered gabbro bodies. Locations shown on figure 1.

LAYERING

The Precambrian and Tertiary gabbro masses exhibit rhythmic layers produced by crystal settling from a basaltic liquid. The thickness of individual exposed layers ranges from 1 to 0.5 m (fig. 4). Differential weathering reveals a coarser layering, with layers as thick as 100 m (fig. 3). These larger layered units probably represent zones in the sense used by Jackson (1967). In other layered bodies, it has been estimated that magma chambers must have a minimum thickness of 300 m before such layering develops (Wager and Brown, 1967, p. 539). Rhythmic layering is present at all localities and is manifested by phase or ratio contacts (Jackson, 1967). In the Precambrian gabbros, layering is steep dipping at the margins, becoming flatter towards the central layers. Layering in the Tertiary rift zone gabbro has a uniform dip from center to margin, except at the narrow ends of the trough-shaped magma chamber where the strike turns and the dip steepens.

More work is needed to allow subdivision of the layered series in each intrusion on the basis of appearance of cumulus phases, according to the methods of Jackson (1967) and Wager and Brown (1967).

PETROLOGY

The Precambrian layered gabbros consist primarily of clinopyroxene gabbro with or without olivine and orthopyroxene. Plagioclase is the dominant cumulate mineral (table 1). Clinopyroxene and olivine rarely exceed more than 60 volume percent of the cumulate assemblage. Although no major ultramafic zones of olivine-, orthopyroxene-, or clinopyroxene-rich rocks have yet been discovered, the basal rocks at some phase contacts may approach 80 percent cumulate clinopyroxene or olivine. Intercumulus clinopyroxene is very common, particularly at the top of individual layers. Orthopyroxene and plagioclase cumulates (norites), and plagioclase and olivine cumulates (troctolites) are present at Jabal Shayi and Hishat Hawi, but monomineralic orthopyroxene cumulates were not found. Orthopyroxene as reaction rims and poikilitic grains are common in the middle of some layers. Postcumulate brown hornblende is present in nearly all layers irrespective of position and is accompanied by small quantities of sporadic biotite.

Magnetite and ilmenite are the common opaque minerals within the Precambrian gabbros and locally exceed 6 volume percent in some layers. Intercumulus magnetite commonly exhibits exsolution lamallae of ilmenite or ulvospinel. Pyrrhotite with exsolved pentlandite is common and may exceed several percent in certain magnetite-free layers. Presence of pyrrhotite-pentlandite droplets included within cumulate silicates in these same layers at Jabal Shayi implies changing oxygen and sulfur fugacities within the magma. Economically valuable concentrations of sulfide-rich cumulate layers in the form of pentlandite (nickel sulfide) may, therefore, exist in these layered gabbro bodies (Skinner and Peck, 1969).

Cumulus minerals within Tertiary layered gabbro mass at Jabal at Turf are similar to those previously described in Precambrian gabbros. Phase contacts are marked by abundant cumulus clinopyroxene and olivine that grade upward into predominately cumulus plagioclase with intercumulus clinopyroxene (fig. 4). Orthopyroxene was not found as a cumulus or intercumulus phase, nor was postcumulus brown hornblende or biotite. Magnetite and ilmenite accompanied by minor rutile form as intercumulus phases and show postcumulate alteration to maghemite or lepidocrocite.

Comparison of the cumulus mineral assemblages in the Saudi Arabian layered gabbros with those previously described in the literature (Wager and Brown, 1967) indicates that the exposed

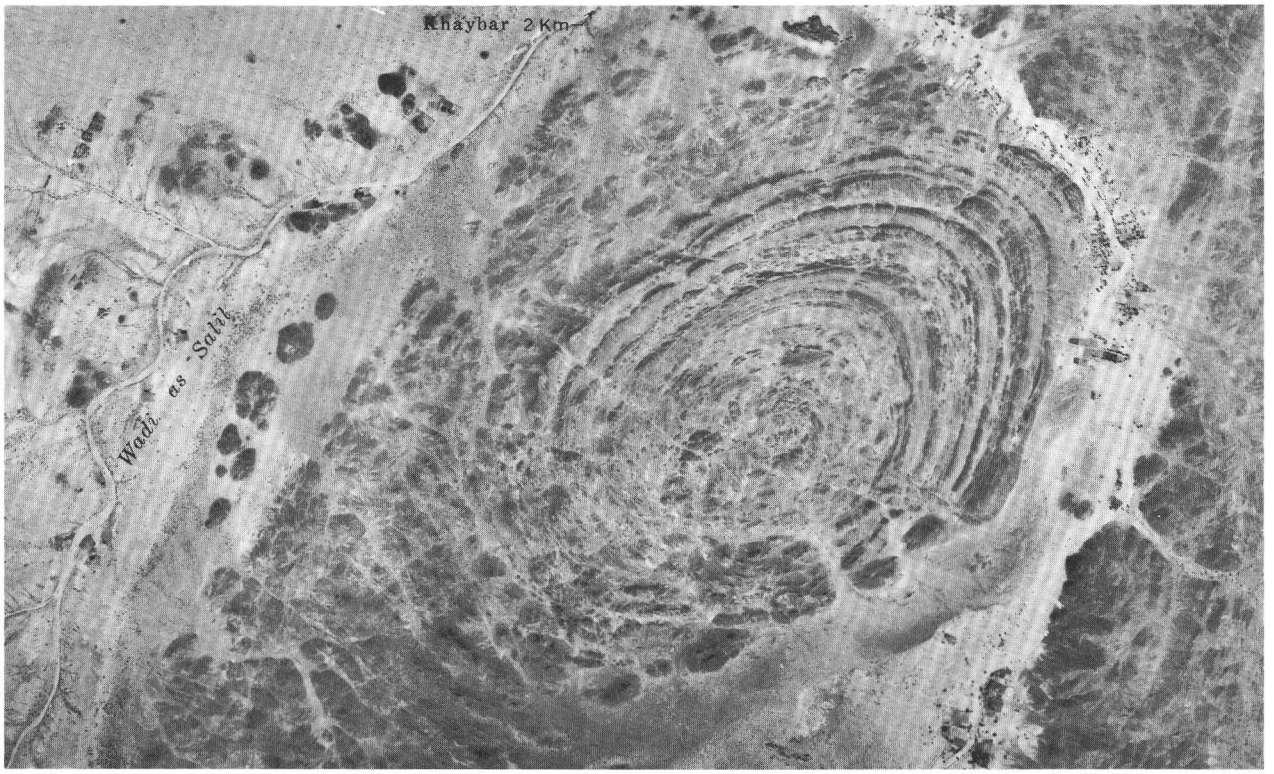

Figure 3.—Aerial photograph of Jabal Shayi, showing its lopolithic shape as expressed by weathered-out successive cumulate layers. Approximate scale 1:50,000.

levels of these fractionally crystallized rocks must be above the basal ultramafic zones if such zones are present. Cumulus plagioclase dominates; only near the basal phase contacts does olivine, clinopyroxene, or orthopyroxene exceed 60 volume percent of any one part of a single layer. Major ultramafic zones may or may not be present near the floors of these intrusions, but the present level of exposure leaves this question open. However, the lack of major ultramafic cumulates could be explained either by introduction of separate surges of "fresh" basaltic liquid or by convective overturn in the magma chamber. Thus, each layer may represent fractional crystallization of small batches of new liquid; if so, it is possible that no major basal ultramafic zones developed.

The mineralogy of these gabbros suggests that the parent liquid was tholeiitic in composition, although we have no chemical analyses of chill zones to verify this. The extremely low potassium values determined for the whole-rock radiometric determinations further suggests that these gabbros may have been derived from subalkaline basalt liquids similar to the intermediate-depth mantle melts that give rise to the subalkaline basalts of the oceanic ridges.

RADIOMETRIC AGES

Whole-rock K-Ar ages were determined on selected samples of layered gabbro from six different localities (table 2). The gabbros north of the Asir Mountains range in radiometric age from Precambrian to Ordovician. From each layered complex, two separate samples taken from distinct layers were analyzed radiometrically to establish internal consistency. Discordant ages were obtained from whole-rock pairs from Jabal Shayi and Wadi Misyab, though there is no obvious weathering or postemplacement alteration to account for the differences. East of the layered gabbros, the oldest sediments (Wajid Sandstone) deposited unconformably on the shield are Cambrian and (or) Ordovician. No gabbroic intrusive rocks have been found in these sedimentary rocks even though radiometric dates from widely scattered intrusive localities cluster around 520 m.y. (Brown, 1970). Biotite from a gabbroic plug north of Khamis Mushayt that may be related to the circular gabbroic intrusions gives a K-Ar age of 640 m.y., and muscovite from a pegmatite dike that cuts this gabbro gives an age of 607 m.y. (table 2). Perhaps the most significant age is from a soda-rich granite on the southern Red Sea coastal plain at lat 18° N. A whole-rock Rb-Sr age of 529 m.y. from this intrusive, together with a high-temperature metamorphic aureole, suggests that the magma invaded regional greenschist facies rocks after their metamorphism. The pan-African thermotectonic episode (Kennedy, 1964) has been considered a major cycle in Africa (Cahen and Snelling, 1966). This event is recognized by K-Ar radiometric dates on granites and metamorphic rocks clustering around 500 to 600 m.y. In

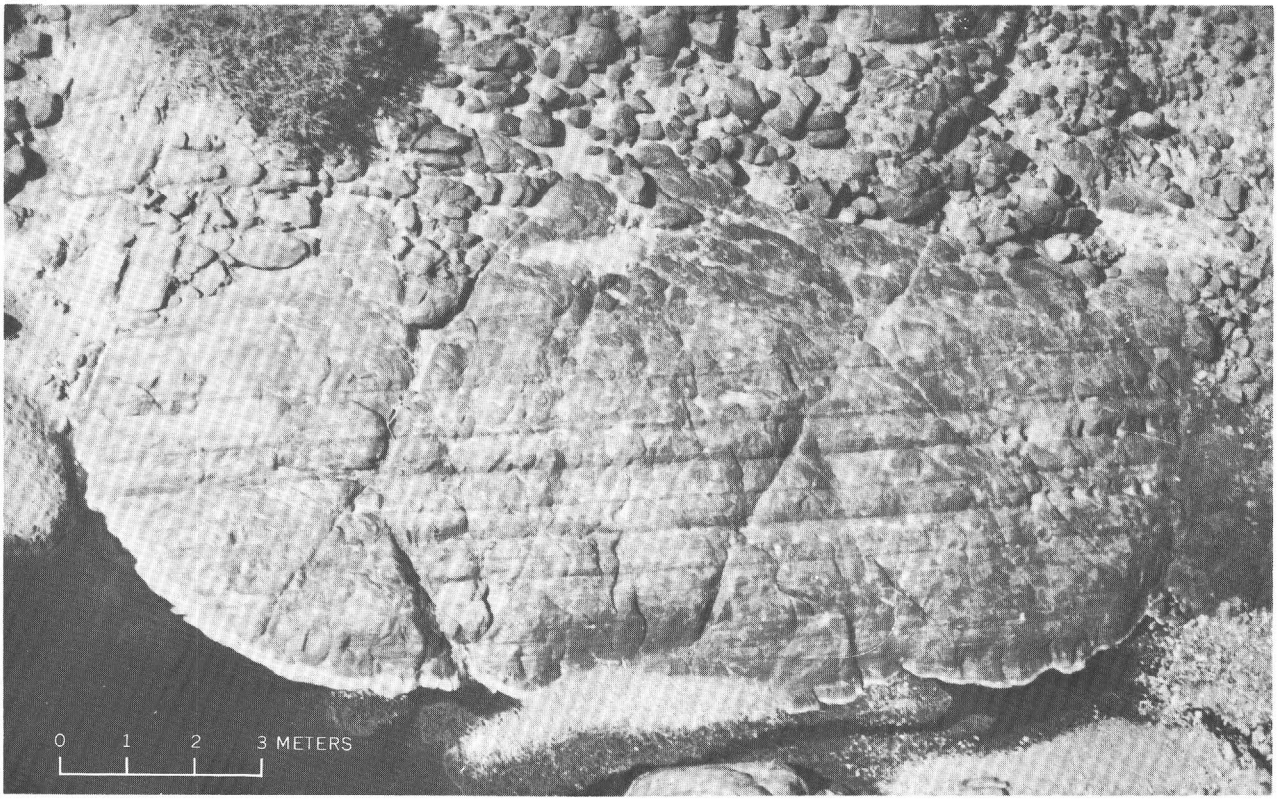

Figure 4. Photograph of rhythmic layering exposed near the top of Jabal at Turf gabbro. Sharp dark contacts mark the bottom of phase contacts where cumulate olivine and clinopyroxene predominate over plagioclase. Cumulate layers grade upward in fineness.

Africa, this thermotectonic event has reduced many older K-Ar ages by argon loss so that confusion exists as to the geologic phenomena represented. The same pattern of reduced ages can be seen in Saudi Arabia (Brown, 1970), although it is still not clear whether the pan-African event represents widespread heating, regional metamorphism accompanied by granitic intrusions, or both. If the Wajid Sandstone is considered Arenig (latest early Ordovician) or younger, as indicated by the presence of *Cruziana* in the unit northeast of the shield, then there is sufficient time for an erosional interval after a Late Cambrian invasion of gabbroic magma before deposition of the Wajid Sandstone.

Brown (1970) suggested that the pan-African event at 570 m.y. affected the older granites in Saudi Arabia in such a way that K-Ar ages represent this event rather than original igneous crystallization. If the pan-African event produced enough heat to have this effect on the granites, it may also have reset the potassium-bearing minerals within the older layered gabbros. However, the 702- to 769-m.y. age for the Hishshat al Hawi gabbro indicates either that some gabbros lost less argon than others, that some gained argon, or that there may have been a series of gabbroic magma invasions from Precambrian to perhaps as recent as Late Cambrian or Early Ordovician times.

In contrast to these older ages, Jabal at Turf gives concordant ages of 21.8±2 m.y. on granophyre and layered gabbro (table 2). Miocene K-Ar ages have also been obtained from dikes along the east margin of the Precambrian shield at its junction with the Red Sea coastal plain. Large areas of Miocene alkali olivine basalt flows (Sirat volcanics) formed at nearly the same time behind the escarpment away from the rift zone.

CONCLUSIONS

Layered gabbros intruding the Precambrian are a result of deep fracturing or foundering of the crust after the deformation and metamorphism of the mobile belts that contain them. Some of the gabbroic liquids were emplaced in local synforms where successive pulses of melt underwent fractional crystallization. The widespread occurrence of these gabbroic intrusions suggests significant shallow melting within the upper mantle during the Precambrian to Ordovician. The adherence of the intrusions to synforms and the lack of feeder dikes is puzzling. No apparent tectonic event can be clearly associated with the development of these intrusions.

In contrast to these Precambrian to Ordovician gabbros, the origin of Jabal at Turf layered gabbro seems directly related to the structural development of the Red Sea. Gillmann (1968) shows that the Jabal at Turf layered gabbro body occupies a zone of northwest-trending faults that parallel the dominant

Table 2.—*Radiometric ages of gabbros from southwest Saudi Arabia*
[Analyses by Teledyne Isotopes except as noted]

Location and rock type	Sample No.	K (percent)	Ar^{40} (moles/g)	Radiogenic Ar^{40} (percent)	Radiometric age $\pm 2\sigma$ (million years)	Geologic age
Jabal At Turf:						
Clinopyroxene gabbro	514-5	0.14	0.05506×10^{-10}	19	23±2	Miocene.
		.14	$.05952\times10^{-10}$	15		
Clinopyroxene-olivine gabbro	516-C	.093	$.02903\times10^{-10}$	13	20±2	
		.080	$.03265\times10^{-10}$	18		
Hornfels	517-C	3.12	1.350×10^{-10}	26	24.3±1	
		3.15	1.371×10^{-10}	27		
Granophyre	515-A	3.17	1.170×10^{-10}	43	20.6±.06	
		3.13	1.142×10^{-10}	43		
	515-B	1.71	$.7206\times10^{-10}$	26	23.3±1.0	
		1.70	$.7045\times10^{-10}$	29		
Wadi Misyab:						
Norite	521-E	.073	$.7255\times10^{-10}$	88	486±12	Ordovician and (or) Silurian.
		.070	$.6818\times10^{-10}$	57		
	521-F	.12	$.9803\times10^{-10}$	92	415±8	
		.12	$.9964\times10^{-10}$	92		
Jabal Al Ashsha:						
Clinopyroxene-olivine gabbro	525-1	.10	1.214×10^{-10}	82	570±12	Cambrian.
		.10	1.148×10^{-10}	60		
	525-4	.084	$.8732\times10^{-10}$	77	508±10	
		.083	$.8545\times10^{-10}$	77		
Jabal Shayi:						
Norite	511-D	.090	1.319×10^{-10}	87	684±14	Precambrian and (or) Ordovician.
		.102	1.318×10^{-10}	79		
	511-G	.15	1.442×10^{-10}	86	477±10	
		.15	1.448×10^{-10}	83		
Khamis Mushayt:						
[1] Biotite in gabbro	504-A	6.72	90.83×10^{-10}	97	[1]640±23	Precambrian.
		6.70				
[1] Muscovite in pegmatite cutting gabbro.	505	8.49	109.2×10^{-10}	94	607±12	
		8.50	107.0×10^{-10}	93		
Hishshat al Hawi:						
Troctolite	527-12	.090	1.530×10^{-10}	72	769±16	Precambrian.
		.092	1.537×10^{-10}	72		
	527-15A	.092	1.418×10^{-10}	63	702±16	
		.096	1.420×10^{-10}	70		

[1] Analyzed by the U.S. Geological Survey, Denver, Colo.

Constants: $Ar^{40}\lambda_\epsilon=0.585\times10^{-10}$/yr,
$Ar^{40}\lambda_\beta=4.72\times10^{-10}$/yr.
Atomic abundance: $K^{40}=1.19\times10^{-4}$ moles/mole.

trend of basaltic dikes within the monoclinal flexure zone (fig. 1). A second set of northeast-trending faults is manifested by magnetic anomalies off the Jizan coastal plan (G. F. Brown and D. H. Hase, unpub. map). Numerous fine-grained vertical basaltic dikes parallel to the rift zone cut the steeply dipping coarse-grained layered gabbro at Jabal at Turf. Recent alkali olivine basalt cones and associated flows cover part of the tholeiitic intrusives of the flexure zone to the west and north of Jabal at Turf. Alkali olivine plateau basalt flows at Sirat (fig. 1) occupy the back slope of the Red Sea erosional scarp 125 km north of and 2,500 m above the Jabal at Turf layered gabbro (fig. 1). Whole-rock K-Ar ages on the Sirat plateau basalts range from 24 to 29 m.y. and suggest that their emplacement along east-west feeder dikes preceded the development of the Jabal at Turf layered gabbro (22 m.y.).

A sharp monoclinal flexure along the east margin of the coastal plain sediments developed after the formation of the Jabal at Turf layered gabbro and before the deposition of the Miocene evaporites and marls. This flexure at the boundary of the coastal plain and Precambrian basement is steep enough (60° W.) to expose the magma chamber and the underlying Jurassic sedimentary rocks. These same Jurassic strata are

exposed 55 km to the north at Jabal Abu Hassan and also in Yemen to the south, where they dip gently toward the Red Sea axis. Invasion of the sea into the Red Sea depression after the flexure is recorded by a 3,000-m-thick unit of evaporites and marls of Miocene age (Gillmann, 1968; Brown, 1970). The emplacement of the Jabal at Turf layered gabbro and associated mafic dikes appears to have been part of a minor rifting event prior to the development of the Miocene Red Sea salt basin. Pliocene alkali olivine basalt volcanism within the eastern rift zone may be related to the Red Sea axial rifting and the separation of the Nubian and Arabian plates.

REFERENCES

Brown, G. F., 1970, Eastern margin of the Red Sea and the coastal structures in Saudi Arabia: Royal Soc. London Philos. Trans., sec. A., v. 267, no. 1181, p. 75–88.

Cahen, L., and Snelling, N. J., 1966, The geochronology of equatorial Africa: Amsterdam, North-Holland Pub. Co., 195 p.

Gillmann, Michel, 1968, Primary results of a geological and geophysical reconnaissance of the Jizan coastal plain in Saudi Arabia: Am. Inst. Mining Metall. Engineers, Regional Tech. Symposium, 2d, Dhahran 1968, Proc., p. 189–208.

Jackson, E. D., 1967, Ultramafic cumulates in the Stillwater, Great Dyke and Bushveld intrusions, *in* Wyllie, P. J., ed., Ultramafic and related rocks: New York and London, John Wiley and Sons, p. 20–38.

Kennedy, W. Q., 1964, The structural differentiation of Africa in the Pan-African (±500 m.y.) tectonic episode: Leeds Univ. Research Inst. African Geology 8th Ann. Rept. Sci. Results, p. 48–49.

Skinner, B. J., and Peck, D. L., 1969, An immiscible sulfide melt from Hawaii, *in* Magmatic ore deposits, a symposium: Econ. Geology Mon. 4, p. 310–322.

Wager, L. R., and Brown, G. M., 1967, Layered igneous rocks: San Francisco, W. H. Freeman and Co., 588 p.

STAUROLITE, KYANITE, AND SILLIMANITE FROM THE NARRAGANSETT BASIN OF RHODE ISLAND

By EDWARD S. GREW and HOWARD W. DAY[1],
Washington, D.C., Norman, Okla.

Abstract.—Staurolite, kyanite, and sillimanite (fibrolite) occur at several localities in the Pennsylvanian rocks of the Narragansett basin of Rhode Island, including Conanicut Island (staurolite), Stook Hill (kyanite, staurolite, sillimanite), and Tower Hill (staurolite, sillimanite). The association of kyanite and sillimanite and the partial replacement of staurolite by muscovite at Stook and Tower Hills suggest that rocks in these areas have undergone two stages of Pennsylvanian or younger metamorphism. The first stage, during which staurolite and kyanite crystallized, accompanied the burial and deformation of the basin rocks. The second stage, during which sillimanite crystallized and staurolite was replaced by muscovite, is due to the intrusion of the Narragansett Pier Granite. The pressures are estimated to have been at least 4.5 kb; the temperatures, at least 530°C during the first stage and 660°–690°C during the second. Pressures of at least 4.5 kb are equivalent to depths of burial of at least 17 km. As the estimated thickness of the basin rocks is only 3.7 km, a much thicker sequence may have been deposited and was later mostly removed by erosion.

The Narragansett basin is a synclinal area in eastern Rhode Island and southeastern Massachusetts about 90 km (55 miles) long and between 24 and 40 km (15–25 miles) wide (Shaler and others, 1899; Quinn, 1971). The basin contains four sedimentary formations of Pennsylvanian age—the Pondville Conglomerate, Wamsutta Formation, Rhode Island Formation, and Dighton Conglomerate. These formations, which have an estimated aggregate thickness of about 3,700 m (12,000 feet) (Shaler and others, 1899, p. 134), consist primarily of nonmarine shale, sandstone, conglomerate, and a few coal beds. Most of the rocks of the Narragansett basin are in the chlorite zone of regional metamorphism or in a zone of induration without the formation of metamorphic chlorite (Quinn and Moore, 1968, fig. 20-1). In the part of the basin between Attleboro, Mass., and Narragansett Pier, R.I., the metamorphic grade increases southward and reaches a maximum in the southwest corner of the basin, where the basin rocks have been intruded by the Narragansett Pier Granite.

The parts of the Narragansett basin and neighboring areas that are of interest here (fig. 1) are south and west of Williams' (1964) staurolite isograd. The Narragansett basin rocks of this area were described in some detail by Foerste (*in* Shaler and others, 1899). The 7½-minute quadrangles included in this area, namely the Wickford, Narragansett Pier, and Kingston, have been mapped at a scale of 1:31,680 or 1:24,000 by Williams (1964), Nichols (1956), and Moore (1964), respectively. The metamorphism of this area has not been studied systematically or in detail, but the general features have been described in the reports on the geology. A staurolite isograd has been mapped on the first appearance of staurolite on Conanicut Island (Williams, 1964). Staurolite-garnet schist crops out along the west shore of the island for about 5 km (3.2 miles) around Jamestown Bridge (Dale, 1885; Shaler and others, 1899; Williams, 1964). No staurolite was reported previously from the mainland west of the island, although the mainland is on the high-grade side of the isograd. Andalusite, kyanite, or sillimanite have not previously been reported from the Narragansett basin, although Quinn (1971) suggested that the rocks at Tower Hill may be in the sillimanite zone. Moore (1964, p. E11–E13, table 1) reported two occurrences of sillimanite from the Kingston quadrangle (see fig. 1) in schists that he correlated with the Rhode Island Formation, but these schists are in isolated outliers not physically continuous with the Narragansett basin.

Acknowledgments.—Part of Day's expenses was defrayed by a Penrose Bequest Research Grant from the Geological Society of America. We are deeply grateful to D. R. Wones, H. R. Dixon, D. S. Harwood, and to E-an Zen for many fruitful suggestions and for reviewing this paper. We also appreciate the advice of A. W. Quinn. Jane Graham ran some of the X-ray diffractograms on white mica from locality 71-49. Edwin Roedder very kindly helped Grew in taking the photomicrographs. G. E. Moore, Jr., generously loaned us thin sections and hand specimens from the Kingston quadrangle.

PETROGRAPHY

Kyanite, sillimanite (fibrolite), and staurolite have been found in the Rhode Island Formation. Staurolite, without kyanite or sillimanite, is abundant in mica schist on Conanicut Island (loc. 71-50, fig. 1). All three minerals occur in mica schist in a roadcut along Route 138 on Stook Hill in North

[1] University of Oklahoma.

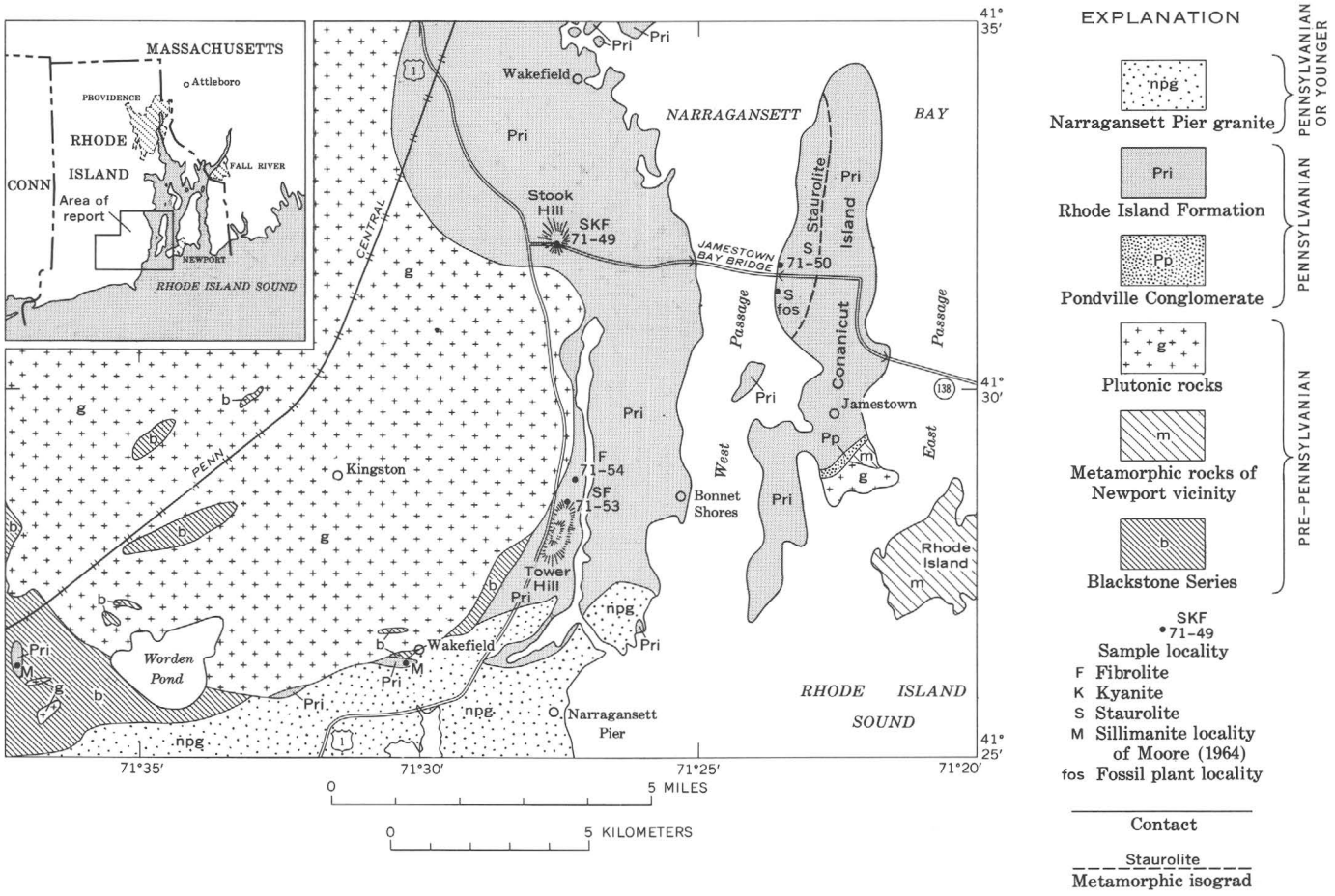

Figure 1.—Generalized geologic map (from Quinn, 1971, pl. 1) showing staurolite, kyanite, and sillimanite localities in southern Rhode Island.

Kingston, R.I., near the west border of the Narragansett basin (loc. 71-49). Fibrolite-bearing mica schist is exposed in two small abandoned graphite mines on Tower Hill in South Kingston, also near the west border of the basin (locs. 71-53 and 71-54). Staurolite is associated with the fibrolite at the southernmost of the two mines. In Wakefield, fibrolite is associated with both K-feldspar and muscovite.

The Rhode Island Formation on the west shore of Conanicut Island, (loc. 71-50, fig. 1) consists primarily of garnet-staurolite schist, sandstone, conglomerate, and a few beds of fossiliferous black slate. The bedding here trends north and dips moderately east. The garnet-staurolite schist (table 1, col. 1) is a dark-gray fine-grained rock with megacrysts of staurolite, garnet, chlorite, biotite, and ilmenite. Staurolite and garnet are locally replaced by chlorite, sericite, or limonite. The megacrysts of staurolite, chlorite, and biotite have trains of carbonaceous inclusions, which in biotite have a sigmoidal pattern. The traces of the cleavage in biotite and chlorite are at an angle to the schistosity defined by flakes of muscovite, whereas the long axes of the staurolite and ilmenite megacrysts are roughly in the plane of schistosity. The megacrysts of garnet commonly have strain shadows filled with quartz. Carbonaceous material, which has an X-ray pattern of partly disordered graphite, occurs as irregular or elongate grains generally no more than 0.01 mm across or as formless aggregates.

The fossiliferous black slate consists of quartz, muscovite, chlorite, carbonaceous material, and accessory ilmenite. The grain size of the silicates ranges from 0.01 to 0.05 mm, whereas that of the carbonaceous material, constituting about 20–25 percent of the slate by weight, rarely exceeds 0.01 mm. Fragmentary plant remains occur on splitting surfaces of the slate.

Mica schist and conglomerate of the Rhode Island Formation are exposed on Stook Hill (loc. 71–49, fig. 1) in cuts along a recently constructed part of Route 138. Scattered lenses of garnet-amphibole rock alternate with the mica schist. The strikes of the bedding and mica schistosity in the cuts trend roughly west-northwest and their moderate dip is to the north. In the cut south of the road are thin layers of mica schist, with megacrysts of biotite, garnet, staurolite, and kyanite (fig. 2*A*; table 1, col. 2). The megacrysts commonly have a sieve texture, quartz being the most abundant inclusion, but inclusions of the micas, garnet, and ilmenite also occur,

Table 1.—*Modes (visual estimates) of metamorphic rocks from the Narragansett basin, southern Rhode Island*

[(a), replacing fibrolite; (m), occurs mostly as megacrysts; tr., trace; (s), secondary]

	Sample locality (fig. 1)			
	71-50	71-49	71-53	71-54
Quartz	24	45	51	53
Andesine	-------	tr.	-------	-------
Muscovite	60	20	37	32
Biotite	5(m)	17(m)	1(m)	tr.
Chlorite	tr.(m)	tr.(s)	5(s)	8(s)
Fibrolite	-------	tr.	2	tr.
Sericite(a)	-------	-------	3	3
Kyanite	-------	tr.(m)	-------	-------
Garnet	5(m)	5(m)	tr.(m)	3
Staurolite	1(m)	13(m)	tr.(m)	-------
Apatite	-------	tr.	tr.	tr.
Zircon	tr.	tr.	tr.	tr.
Tourmaline	tr.	tr.	-------	-------
Ilmenite	2(m)	tr.	-------	-------
Carbonaceous material.	3	tr.	tr.	-------
Sphene	-------	-------	1	tr.
Opaque (unidentified).	-------	-------	-------	1
Size (mm):				
Megacrysts	0.25–10.0	0.5–10.0	0.5–5.0	-------
Groundmass	0.01–0.2	0.05–0.5	0.05–0.5	0.1–3.0
Number of thin sections examined.	1	3	1	3

Description of sample localities

71-50. Dark-gray schist. Outcrop along west shore of Conanicut Island, 400 feet north of Jamestown Bridge, Jamestown, Newport County, R.I. (Wickford 7½-minute quadrangle, lat 41°31′37″ N.; long 71°23′30″ W.).

71-49. Silvery mica schist. Roadcut on Route 138 at crest of Stook Hill, North Kingston, Washington County, R.I. (Wickford 7½-minute quadrangle, lat 41°31′49″ N.; long 71°27′05″ W.).

71-53. Light-gray mica schist. Abandoned mine for graphite on east side of Tower Hill, South Kingston, Washington County, R.I. (Narragansett Pier 7½-minute quadrangle, lat 41°28′32″ N.; long 71°27′13″ W.).

71-54. Silvery mica schist. Abandoned pit for graphite on east side of Tower Hill, South Kingston, Washington County, R.I. (Narragansett Pier 7½-minute quadrangle, lat 41°28′50″ N.; long 71°27′07″ W.).

and all four are found in staurolite. Fine inclusions, generally no more than a few microns across, are concentrated in the cores of some garnet megacrysts, giving the garnet a distinctly zoned appearance. Trains of quartz inclusions define a sigmoidal pattern in a few staurolite megacrysts. The long axes and cleavage directions of some biotite, staurolite, and kyanite megacrysts are not in the plane of schistosity defined by muscovite. Staurolite megacrysts are commonly euhedral. Some of the kyanite megacrysts are bent. Tufts and needles of fibrolite have grown in biotite, quartz, and, less commonly, garnet (fig. 2*B*), or occur along grain boundaries of these minerals with each other or with muscovite. The staurolite, garnet, and biotite are locally altered to muscovite, sericite, and chlorite, and the kyanite, to sericite. The secondary minerals form rims around or veinlets in the megacrysts. Andesine locally shows zoning or twinning. The carbonaceous material is graphite in flakes as much as 0.05 mm across. No paragonite was detected in X-ray diffraction patterns of the white mica.

Pods of massive pegmatite containing garnet and beryl, generally less than a meter thick, cut across the mica schistosity at this locality.

At the northernmost of the two abandoned graphite mines on Tower Hill in South Kingston (loc. 71–54, fig. 1), silvery fibrolite-bearing mica schist and graphite schist are exposed in a small overgrown excavation. The mica schist (table 1, col. 3) has garnet and elongated knots, 2 to 10 mm long, of sericite pseudomorphs of fibrolite. A few individual needles of fibrolite included in quartz have escaped alteration. Biotite is almost entirely replaced by chlorite with sagenitic rutile, and garnet is cut by veinlets of sericite, chlorite, and limonite. The graphite schist is composed of well-ordered graphite flakes generally 0.003 to 0.02 mm across, quartz and muscovite grains generally 0.01 to 0.07 mm across, a few megacrysts of biotite (mostly replaced by chlorite) as much as 1 mm across, chlorite pseudomorphs of garnet(?), and sphene.

At the southernmost of the two mines (loc. 71-53, fig. 1), gray fibrolite-mica schist, lustrous graphite schist, and a few pods of pegmatite have been exposed in a tunnel about 3 m (10 feet) long and in a pit. The fibrolite-mica schist has muscovite flakes generally 0.25 to 3 mm across that lack a preferred orientation, megacrysts of garnet, and elongated knots of fibrolite 1 to 10 mm long. Fibrolite (fig. 2*C*) has been largely replaced by sericite. In some of the schist (table 1, col. 4), the coarse-grained muscovite is concentrated into elongated aggregates as much as 15 mm long, which locally contain poikilitic deeply embayed staurolite grains as much as 2.8 mm across (fig. 2*D*). The aggregates, moreover, have a rhombic cross section (fig. 2*D*) suggesting that the muscovite has partly replaced euhedral staurolite megacrysts. The biotite and garnet have been altered to chlorite, sericite, and limonite. The carbonaceous material is well-ordered graphite in flakes 0.01 to 0.06 mm across. The graphite schist consists of well-ordered graphite flakes 0.003 to 0.015 mm across (rarely to 0.25 mm) and of quartz and muscovite grains 0.1 to 0.6 mm across, with accessory biotite (mostly replaced by chlorite), epidote, sphene, and rutile.

Moore (1964) reported microcline and sillimanite in the same thin section from the Rhode Island Formation in Wakefield (fig. 1). In this section, which Professor Moore generously loaned us, fibrolite mats and sillimanite needles (as much as 0.02 mm thick) are included in muscovite, biotite, quartz, plagioclase, and untwinned K-feldspar (for mode, see Moore, 1964, table 1, col. 15). The grain size of the rock ranges from 0.2 to 6 mm.

INTERPRETATION OF THE MINERAL ASSEMBLAGES AND TEXTURES

In deducing mineral assemblages in the above-described mica schists, the following criteria have been used:

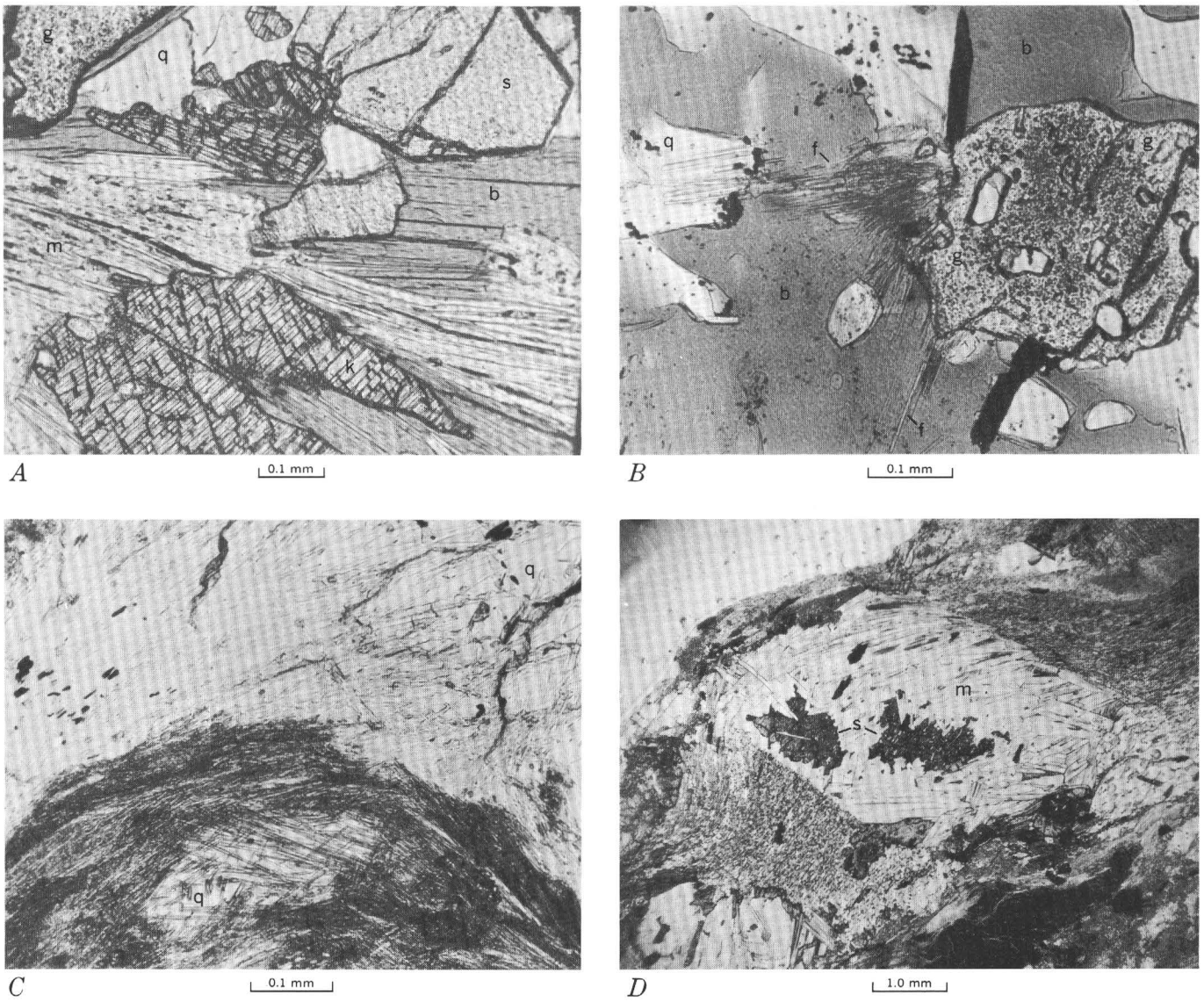

Figure 2.—Photomicrographs of mica schist of the Rhode Island Formation. Plane-polarized light.

A. Quartz (q), muscovite (m), biotite (b), garnet (g), staurolite (s), and kyanite (k). Stook Hill, North Kingston, R.I. (loc. 71-49).

B. Needles of fibrolite (f) radiate from garnet (g) into biotite (b) in two directions at 60° to each other, and into quartz (q). Stook Hill, North Kingston, R.I. (loc. 71-49).

C. Fibrolitic mica schist. Unaltered fibrolite (dark) in bottom half of photograph. Sericite (light) replacing fibrolite occupies most of upper half. Quartz (q). Tower Hill, South Kingston, R.I. (loc. 71-53).

D. Staurolite megacryst partly replaced by muscovite (m). Embayed grains of staurolite (s) near center of pseudomorph. Same thin section as *C*.

1. The assemblages include all minerals in a thin section cut from a single layer in which no compositional inhomogeneities are apparent. This does not imply that all the minerals are in physical contact.

2. Minerals, such as chlorite, sericite, and sphene, obviously formed during a late low-grade metamorphism, are not included in the assemblages, which are as follows:

Quartz-muscovite-biotite-garnet-staurolite-chlorite-ilmenite-carbonaceous material (Conanicut Island, loc. 71-50).

Quartz-muscovite-biotite-garnet-staurolite-kyanite-sillimanite (fibrolite)-ilmenite-graphite (Stook Hill, loc. 71-49).

Quartz-muscovite-biotite-garnet-staurolite-sillimanite (fibrolite)-graphite (Tower Hill, loc. 71-53; the schist from loc. 71-54 is similar, but staurolite is absent).

The replacement of staurolite by muscovite, nearly complete in the schist from Tower Hill but incipient in the schist from Stook Hill, is interpreted as textural evidence of disequilibrium. The association of kyanite and fibrolite at Stook Hill, moreover, could be an equilibrium one, only if there were

significant differences between the compositions of the two minerals. A recent study by Albee and Chodos (1969) has shown that differences in composition between kyanite and fibrolite are not large enough to stabilize the two minerals together. The association of kyanite and sillimanite is thus interpreted as mineralogical evidence of disequilibrium.

The disequilibrium texture and mineral association are thought to have resulted from two stages of metamorphism. During the first stage, rocks of appropriate composition in the Rhode Island Formation in the area under consideration recrystallized into staurolite ± kyanite schist, probably under equilibrium conditions. During the second stage, which affected the Tower Hill area to a greater extent than the Stook Hill area, staurolite was partially replaced by muscovite, and fibrolite was formed. Similar disequilibrium textures and assemblages have been explained by multiple metamorphism by some authors, notably Guidotti (1970), Chinner (1961), and Albee and Chodos (1969), whereas others (Zwart, 1962; Hollister, 1969) have explained them in terms of a single prograde metamorphism.

The rocks at all the localities studied show evidence for a low-grade metamorphism that followed the two-stage high-grade metamorphism discussed above. The alteration of staurolite, garnet, and biotite to chlorite, sericite, and limonite, and the alteration of kyanite and fibrolite to sericite are due to this late low-grade metamorphism. The sphene in the schists from Tower Hill may be derived from ilmenite.

The most intense metamorphism and the deformation of the Pennsylvanian rocks overlapped in time. All the rocks have a pronounced muscovite schistosity. Strain shadows on garnet and bent megacrysts of kyanite suggest deformation after crystal growth, whereas contemporaneous growth of staurolite and biotite is implied by the sigmoidal pattern of inclusions in these minerals. The random orientation of megacrysts of staurolite, biotite, and kyanite suggests that crystal growth continued after the deformation.

PHYSICAL CONDITIONS OF METAMORPHISM

From textural evidence, the association of kyanite, staurolite, biotite, muscovite, and quartz at Stook Hill appears to be an equilibrium assemblage. Experimental studies of the system Al_2SiO_5 (Richardson and others, 1969; Holdaway, 1971) and of staurolite in the system Fe-Al-Si-O-H (Richardson, 1968) suggest that the assemblage kyanite-staurolite-quartz crystallized at a temperature and pressure no lower than 530°C and 4.5 kb (A, fig. 3). These estimates may be too high because Richardson's (1968) curve for the formation of staurolite will be displaced toward lower temperatures by the addition of MgO to the system and by having the partial pressure of water less than that for pure water in the fluids in the rocks. The restriction that these three minerals coexist with biotite and muscovite, however, raises the estimated pressure and temperature of crystallization. According to Hess' (1969) petrogenetic grid, this five-mineral assemblage must have crystallized at a temperature and pressure of at least 590°C and 5 kb (B, fig. 3). Hess' (1969) grid is based on the Al_2SiO_5 curves of Richardson and others (1969) and, apparently, also on the assumption that the rock fluid is pure water. The minimum pressures implied by the assemblage with kyanite and staurolite and the absence of any reported andalusite in the Narragansett basin suggest that the pressure of metamorphism

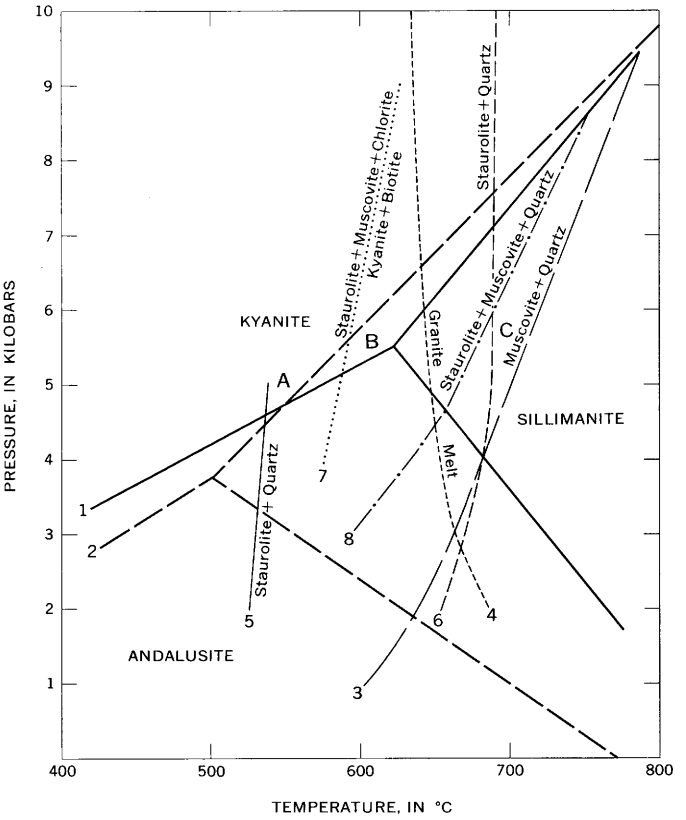

Figure 3.—Pressure-temperature curves relevant to the metamorphism of the Rhode Island Formation.

1,2 Aluminum silicates, (1, Richardson and others, 1969; 2, Holdaway, 1971).

3, Breakdown of muscovite + quartz (schematic), (Althaus and others, 1970; Day, 1970; Hess, 1969).

4, Minimum melting curve in the granite system (Luth and others, 1964).

5, Chloritoid + sillimanite = staurolite + quartz + water (Richardson, 1968).

6, Staurolite + quartz = almandine + sillimanite + water (Richardson, 1968).

7, Staurolite + muscovite + chlorite = biotite + kyanite + water (Hess, 1969).

8, Staurolite + muscovite + quartz = biotite + aluminum silicate + garnet + water (Hess, 1969).

A, Possible minimum pressure-temperature conditions for the assemblage kyanite-staurolite-quartz.

B, Possible minimum pressure-temperature conditions for the assemblage kyanite-staurolite-biotite-muscovite-quartz.

C, Possible pressure-temperature conditions for fibrolite-bearing assemblages.

during both stages probably equaled or exceeded that of the Al_2SiO_5 triple point.

The temperature of crystallization of the fibrolite, estimated to be 660°–690°C at a pressure of 4.5–5 kb (C, fig. 3), was within the stability field of muscovite + quartz and was probably on the high-temperature side of the staurolite decomposition reactions (curves 6 and 8, fig. 3). These estimates of the temperature would be the maximum possible because the fluid phase used in the experimental work on the decomposition of staurolite and muscovite was pure water. The presence of pegmatites at Stook and Tower Hills suggests, moreover, that the temperature may have been close to that for the minimum melting of water-rich granite magmas (Luth and others, 1964). The temperature of metamorphism near the contact of the Narragansett Pier Granite, as at Wakefield, was sufficient to stabilize the association K-feldspar-sillimanite-quartz, but was not sufficient to break down muscovite in the presence of quartz.

GEOLOGIC IMPLICATIONS

The increase in metamorphic grade in the Narragansett basin towards the contact with the Narragansett Pier Granite implies that the heat from the granite metamorphosed the sediments. Quinn and Moore (1968) and Nichols (1956) suggested, however, that the metamorphism may be primarily a result of deep burial of the sediments, the granite playing only a small role. The generally massive appearance of the granite, the lack of granulation, and the presence of rotated schistose inclusions are cited as evidence that the granite was intruded after the deformation and the peak of metamorphism. The lack of chilled borders in the granite, moreover, implies that the metamorphic rocks were still hot at the time of intrusion (Nichols, 1956). These conclusions are consistent with the mineralogy and textures that we observed in the metamorphic rocks. Kyanite and staurolite probably formed during the heating that accompanied deep burial and intense deformation of the rocks prior to the intrusion of the granite. Crystallization of fibrolite is interpreted to be a contact effect caused by a rise in temperature during intrusion of the granite. The occurrence of fibrolite 8 km (5 miles) north of the contact with the granite suggests that this contact may dip very gently north under the Narragansett basin rocks.

Metamorphism at a pressure of 4.5 kb is equivalent to a burial of 17 km (55,000 feet), implying that 17 km of sediment had been deposited in the Narragansett basin. The estimated thickness of Pennsylvanian sediments presently exposed in the basin, however, is 3.7 km (12,000 feet). This estimate, because of poor exposure, complex structure, and absence of distinctive marker beds, might be considerably in error (Quinn, 1971), but to be in error by a factor of five appears unlikely. A possible explanation for this discrepancy is that 17 km of sediments had been deposited in the basin, but that about 13.3 km had since been removed by erosion. This suggestion is not unreasonable, if one supposes that the Narragansett basin is the erosional remnant of a graben similar to the Fundy basin rift in southeastern Canada. As much as 4.5 km of Lower Mississippian and as much as 6 km of Upper Mississippian-Lower Pennsylvanian sediments were deposited in the Fundy basin (Belt, 1965, 1968). The similarity between the Narragansett and Fundy basins is suggested by their both belonging to the fault trough sedimentation model proposed by Klein (1968). The rocks in both basins have been metamorphosed (only to "slate grade" in the Fundy basin (Belt, 1968)) and highly deformed. The Pennsylvanian or younger metamorphism and deformation in the Narragansett basin (except for the contact effect of the granite), moreover, have only slightly affected the pre-Pennsylvanian rocks bordering the basin (Quinn, 1971); similarly the Carboniferous platform strata bordering the Fundy basin have not been metamorphosed or deformed, or only gently deformed, by the events that affected the basin rocks (Belt, 1968). On the other hand, Quinn and his coworkers have not recognized any faults bordering the basin that were active during the deposition of the Pennsylvanian rocks. Such faults, of course, might be difficult to recognize, particularly along the west border of the basin, because they could have been obliterated by the later deformation, metamorphism, and intrusion of the Narragansett Pier Granite.

Thompson and Norton (1968) suggested that the depth of burial necessary for the kyanite-sillimanite transition in the pre-Pennsylvanian rocks of southwestern New England was probably achieved by large-scale recumbent folding. The existence of these folds in the pre-Pennsylvanian rocks is well documented, but evidence for them in the Pennsylvanian rocks has not been reported.

The question of the depth of burial, in the writers' opinion, is still unresolved. Given the lack of any evidence for thickening by folding, however, the first explanation for the depth of burial, namely the deposition of a great thickness of sediments the bulk of which has since been eroded away, remains a likely possibility.

REFERENCES

Albee, A. L., and Chodos, A. A., 1969, Minor element content of coexistent Al_2SiO_5 polymorphs: Am. Jour. Sci., v. 267, no. 3, p. 310–316.

Althaus, Egon, Karotke, Ekkehard, Nitsch, K. H., and Winkler, H. G. F., 1970, An experimental re-examination of the upper stability limit of muscovite plus quartz: Neues Jahrb. Mineralogie, Monatsh., no. 7, p. 325–336.

Belt, E. S., 1965, Stratigraphy and paleogeography of Mabou Group and related middle Carboniferous facies, Nova Scotia, Canada: Geol. Soc. America Bull., v. 76, no. 7, p. 777–802.

—— 1968, Post-Acadian rifts and related facies, eastern Canada, *in* Zen, E-an, White, W. S., Hadley, J. B., and Thompson, J. B., Jr., eds., Studies of Appalachian geology—Northern and maritime: New York, Interscience Publishers, p. 95–113.

Chinner, G. A., 1961, The origin of sillimanite in Glen Clova, Angus: Jour. Petrology, v. 2, no. 3, p. 312–323.

Dale, T. N., 1885, On metamorphism in the Rhode Island coal basin: Newport Nat. History Soc., Proc., Doc. 3, p. 85–86.

Day, H. W., 1970, Redetermination of the stability of muscovite + quartz [abs.]: Geol. Soc. America, Abs. with Programs, v. 2, no. 7, p. 535.

Guidotti, C. V., 1970, Metamorphic petrology, mineralogy, and polymetamorphism in a portion of N.W. Maine, Field trip B-2, *in* New England Intercollegiate Geol. Conf., 62d Ann. Mtg., Rangeley, Maine, Oct. 2–4, 1970, Guidebook for field trips in the Rangeley Lakes–Dead River basin region, western Maine: Syracuse, N.Y., Syracuse Univ., Dept. Geology, 29 p.

Hess, P. C., 1969, The metamorphic paragenesis of cordierite in pelitic rocks: Contr. Mineralogy and Petrology, v. 24, no. 3, p. 191–207.

Holdaway, M. J., 1971, Stability of andalusite and the aluminum silicate phase diagram: Am. Jour. Sci., v. 271, p. 97–131.

Hollister, L. S., 1969, Metastable paragenetic sequence of andalusite, kyanite, and sillimanite, Kwoiek area, British Columbia: Am. Jour. Sci., v. 267, no. 3, p. 352–370.

Klein, G. deV., 1968, ed., Late Paleozoic and Mesozoic continental sedimentation, northeastern North America–A symposium: Geol. Soc. America Spec. Paper 106, 309 p.

Luth, W. C., Jahns, R. H., and Tuttle, O. F., 1964, The granite system at pressures of 4 to 10 kilobars: Jour. Geophys. Research, v. 69, no. 4, p. 759–773.

Moore, G. E., Jr., 1964, Bedrock geology of the Kingston quadrangle, Rhode Island: U.S. Geol. Survey Bull. 1158-E, 21 p.

Nichols, D. R., 1956, Bedrock geology of the Narragansett Pier quadrangle, Rhode Island: U.S. Geol. Survey Geol. Quad. Map GQ-91.

Quinn, A. W., 1971, Bedrock geology of Rhode Island: U.S. Geol. Survey Bull. 1295, 68 p.

Quinn, A. W., and Moore, G. E., Jr., 1968, Sedimentation, tectonism, and plutonism of the Narragansett Basin region, *in* Zen, E-an, White, W. S., Hadley, J. B. and Thompson, J. B., Jr., eds., Studies of Appalachian geology–Northern and maritime: New York, Interscience Publishers, p. 269–279.

Richardson, S. W., 1968, Staurolite stability in a part of the system Fe-Al-Si-O-H: Jour. Petrology, v. 9, no. 3, p. 467–488.

Richardson, S. W., Gilbert, M. C., and Bell, P. M., 1969, Experimental determination of kyanite-andalusite and andalusite-sillimanite equilibria; the aluminum silicate triple point: Am. Jour. Sci., v. 267, no. 3, p. 259–272.

Shaler, N. S., Woodworth, J. B., and Foerste, A. F., 1899, Geology of the Narragansett Basin: U.S. Geol. Survey Mon. 33, 402 p.

Thompson, J. B., Jr., and Norton, S. A., 1968, Paleozoic regional metamorphism in New England and adjacent areas, *in* Zen, E-an, White, W. S., Hadley, J. B., and Thompson, J. B., Jr., eds., Studies of Appalachian geology–Northern and maritime: New York, Interscience Publishers, p. 319–327.

Williams, R. B., 1964, Bedrock geology of the Wickford quadrangle, Rhode Island: U.S. Geol. Survey Bull. 1158-C, 15 p.

Zwart, H. J., 1962, On the determination of polymetamorphic mineral associations, and its application to the Bosost area (central Pyrenees): Geol. Rundschau, v. 52, p. 38–65.

CLAY MINERALOGY OF THE GREEN RIVER FORMATION, PICEANCE CREEK BASIN, COLORADO—A PRELIMINARY STUDY

By JOHN W. HOSTERMAN and JOHN R. DYNI, Beltsville, Md., Denver, Colo.

Abstract.—Outcrop samples of sedimentary rocks from the Garden Gulch, Parachute Creek, and Evacuation Creek Members of the Green River Formation and samples from the underlying Wasatch Formation in the Piceance Creek basin, Colorado, show selective distribution of clay minerals. The fluvial rocks of the upper Wasatch Formation and the fresh-water shales of the Garden Gulch Member contain kaolinite, illite, mixed-layer clay, and montmorillonite. Kaolinite seems to be restricted to these rocks. The lacustrine oil shales of the Parachute Creek Member contain only illite and a minor amount of mixed-layer clay. The tuffaceous sandstones of the Evacuation Creek Member contain illite and montmorillonite. The presence of kaolinite indicates that the sedimentary material was deposited in an environment containing well-oxygenated fresh water. The absence of kaolinite indicates that the sedimentary material was deposited in an environment containing reducing anaerobic brackish to saline alkaline waters.

This report describes a preliminary study of the clay minerals in 28 samples from the Green River Formation and three samples from the underlying Wasatch Formation. Both formations are Eocene in age. The purpose of this investigation was to determine if there are any differences in the clay minerals present in the several major lithofacies that compose the Green River Formation and to discuss what the clay mineralogy means in terms of depositional environments and sediment sources. Several ideas on future research are suggested.

Few studies have been published on the clay mineralogy of the Green River Formation. In a subsurface study of sodium carbonate minerals associated with the oil shale in the Piceance Creek basin, Hite and Dyni (1967, fig. 4) found, in samples from the Juhan core hole 4-1, abundant illite in the Garden Gulch Member that underlies the sodium-rich oil shale of the Parachute Creek Member. They noted that the amount of illite gradually decreased stratigraphically upward to nearly zero in the sodium-bearing section of the oil shale. Unpublished data from the Juhan core hole (J. R. Dyni, 1970) show that only trace amounts of illite are present throughout the sodium-bearing oil shale, which is about 600 feet thick in this hole. Hunt, Stewart, and Dickey (1954, p. 1678) noted that clay minerals were absent in many samples of lacustrine rocks, including oil shale and marlstones from the Green River Formation in the Uinta basin, Utah. In samples from a drill hole in southwest Wyoming, Tank (1969, p. 1593) reported illite, montmorillonite, and mixed-layer clay in tuffaceous calcareous lacustrine oil shales in the Tipton Shale Member of the Green River Formation and kaolinite in the underlying Wasatch Formation. In the same drill hole, Tank also found illite and chlorite in a sandstone unit in the middle of the Tipton (New Fork Tongue of the Wasatch Formation, according to W. C. Culbertson, oral commun., 1971). These studies and data presented in this report suggest that the kind and abundance of clay minerals found in separate lithofacies of the Green River Formation and the Wasatch Formation reflect different depositional environments and sources of sediments.

D. L. Brobst, of the U.S. Geological Survey, provided unpublished measured sections in the Piceance Creek basin which aided the authors in their study.

GEOLOGY

The Green River Formation underlies an area of about 1,600 square miles in the Piceance Creek basin between the Colorado and White Rivers in Rio Blanco and Garfield Counties, Colo. The Green River Formation and the underlying Wasatch Formation are well exposed around the periphery of the basin, which is a large structural downwarp.

The Wasatch Formation is composed of variegated claystone; shale and lenses of sandstone are present throughout the formation. The thickness of the Wasatch Formation is variable, ranging from 375 to 5,500 feet (Donnell, 1961, p. 846). Locally, the upper part of the formation contains beds of ostracodal sandstone, limestone, and shale of lacustrine origin (Snow, 1970, p. 15); however, most of this formation, as exposed around the basin edges, probably represents stream and mudflat deposits. Three samples were collected from the uppermost part of the Wasatch Formation: two samples from the north side of Logan Wash in the SW¼ sec. 28, T. 7 S., R. 97 W.; and one sample from the east side of Parachute Creek south of Granlee Gulch in the S½ sec. 4, T. 6 S., R. 96 W. (fig. 1).

The Green River Formation is composed largely of lacustrine rocks and contains the well-known thick deposits of oil

U.S. GEOL. SURVEY PROF. PAPER 800-D, PAGES D159-D163

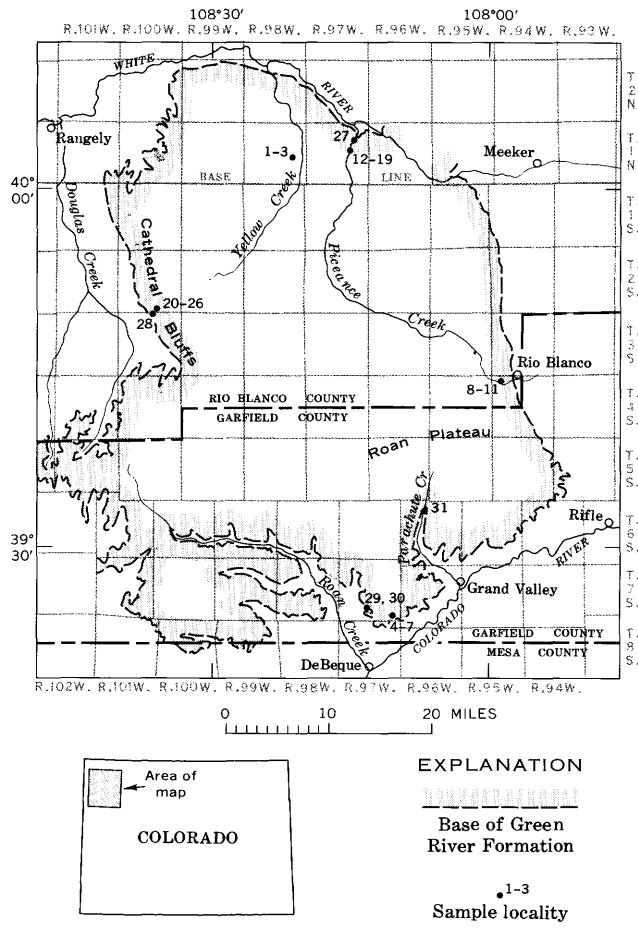

Figure 1.—Sample localities and area underlain by the Green River Formation in the Piceance Creek basin, Colorado.

shale. According to Donnell (1961, p. 847), the formation has a maximum thickness of more than 3,000 feet in the northeastern part of the area. The formation is divided into five members, the first four of which are, from oldest to youngest, the Douglas Creek, Garden Gulch, Parachute Creek, and Evacuation Creek (Bradley, 1931, p. 9); the fifth member, the Anvil Points, is present along the east side of the basin and is laterally equivalent to the Douglas Creek, Garden Gulch, and part of the Parachute Creek Members (Donnell, 1961, p. 848). The Garden Gulch, Parachute Creek, and Evacuation Creek Members were sampled and analyzed for clay minerals. Each member sampled represents a major lithofacies of the Green River Formation.

The Garden Gulch Member is characterized by abundant grayish-brown to black and greenish-gray fissile shale and siltstone of lacustrine origin. It intertongues extensively with the oil shales of the overlying Parachute Creek Member, making it a somewhat difficult unit to map in the field. Donnell (1961, p. 850) gave a range of 100 to 1,000 feet for the thickness of the member. The Garden Gulch differs from the overlying Parachute Creek Member by having a higher clay-mineral content and a lower carbonate and organic content. The upper part of this member was sampled at two localities—one sample is from lower Piceance Creek in sec. 11, T. 1 N., R. 97 W.; the other is from the section exposed along the pipeline right-of-way on Cathedral Bluffs in sec. 34, T. 2 S., R. 100 W.

The Parachute Creek Member contains the richest and thickest oil-shale beds in the Green River Formation. It is composed almost entirely of lacustrine oil shale, but thin waterlaid tuff beds are abundant in the upper part of the member. Because of extensive intertonguing of this member with the underlying Garden Gulch Member and the overlying Evacuation Creek Member, the Parachute Creek Member ranges in thickness from a minimum of 500 feet (Donnell, 1961, p. 852) to about 2,000 feet in sec. 14, T. 1 S., R. 98 W. A total of 23 samples was collected from four localities: four samples from the John Savage oil shale quarry in sec. 36, T. 7 S., R. 97 W.; four samples from a roadcut along Piceance Creek, 2 miles west of Rio Blanco, in sec. 6, T. 4 S., R. 94 W.; eight samples from a roadcut along lower Piceance Creek in sec. 14, T. 1 N., R. 97 W.; and seven samples from the pipeline right-of-way on Cathedral Bluffs in sec. 34, T. 2 S., R. 100 W.

The Evacuation Creek Member is at the surface throughout most of the Piceance Creek basin. It is composed of buff to light-brown massive sandstone and siltstone and intercalated beds of white-weathering lacustrine marlstone and shale which are low in organic materials and which locally contain saline crystal cavities. Sandstone beds increase in abundance toward the upper part of the member; along with the siltstone beds, they are typically massive and discontinuous, and bedding is generally obscure. The marlstone and shale beds tend to be more persistent laterally, and some beds are locally mappable. The maximum reported thickness of this member is 1,250 feet in a gas well in sec. 29, T. 2 S., R. 95 W. (Donnell, 1961, p. 857). The Evacuation Creek Member is probably both lacustrine and fluviatile in origin, and more than half the clastic rocks are reported to have been derived from waterlaid volcanic debris (Donnell and Cashion, 1968, p. 11). Three samples were collected from this member at a small dry wash on the north side of Pinto Creek in the NW¼ sec. 23, T. 1 N., R. 98 W.

METHOD OF INVESTIGATION

Several techniques were used in the laboratory to prepare samples for X-ray diffraction determinations of the mineral composition. The whole-rock samples were prepared by grinding approximately 200 grams of rock to pass through a 170-mesh screen. Part of the ground sample was treated with a 0.1 *M* hydrochloric acid to remove the carbonates. The acid-treatment technique consisted of continuous stirring of the sample and acid mixture over a low heat until all chemical reaction stopped, usually about 4–5 hours. The solution was then centrifuged, decanted, and washed with deionized water at least five times to remove the acid from the insoluble

residue. The residue of the acid-treated sample was oven dried at 50°C, weighed, and the weight loss was calculated as the percentage of total carbonate minerals. Small splits weighing 1–2 grams from the whole-ground sample and from the acid-treated residue were pressed into 1¼-inch-diameter disks, with a backing composed of a mixture of boric acid and methyl cellulose, in an evacuated hydraulic press for a minimum of 30 seconds at a pressure of 30,000 psi. The clay fraction was obtained from the acid-treated residue by allowing the sample to settle in water for 2 hours and 3 minutes and carefully siphoning off the upper 10 centimeters, which contained the clay-sized particles of less than 4 micrometers in diameter. This fraction was sedimented onto a 1X2X¼-inch porous ceramic tile by using vacuum to force the water out of the clay and through the tile. This method is relatively quick, and differential settling is completely eliminated.

Mineral identification by X-ray diffraction methods, using Cu$K\alpha_1$ radiation (1.54050 A) and a diffracted-beam monochromator (Hosterman, 1968, p. B117), are routine. The ratio of calcite to dolomite was determined from the major peaks at 29.4° (3.03 A) and 30.9° (2.89 A) 2θ, respectively, using a method described by Royse, Wadell, and Petersen (1971). The X-ray diffraction trace of the acid-treated residue was used to check for complete carbonate removal. Identification of the clay minerals was made by X-ray diffraction analysis of the sedimented tiles. The clay on these tiles was treated with ethylene glycol and X-rayed to detect the expandable clay minerals and heated to 300°C to detect the collapsible clay minerals.

MINERALOGY

The results of the X-ray diffraction analyses are presented in table 1. Although the samples are too few to be fully representative of the Green River and Wasatch Formations, the data suggest a selective distribution of clay minerals (except illite), carbonate minerals, and analcite in the different lithofacies analyzed. Illite and the nonclay silicates—quartz, potassium feldspar, and sodium feldspar—are present in all samples and show no apparent differences in their distribution. Some of these minerals may be authigenic in certain lithofacies; however, this possibility was not investigated. The amount of clay present in samples from the Wasatch Formation is about 30 percent and from the Green River Formation about 5–10 percent.

Samples from the Wasatch Formation and the Garden Gulch Member contain a mixed suite of clay minerals including illite, mixed-layer clay, and kaolinite; one sample from the Wasatch Formation contains montmorillonite and lacks mixed-layer clay. Samples from both units contain no analcite, a mineral that is very abundant in the overlying units. The principal difference in mineralogy between the two units seems to be the presence of dolomite and calcite in the Garden Gulch samples and the absence of these minerals in the Wasatch samples.

The only clay minerals in samples from the Parachute Creek Member are illite and small amounts of mixed-layer clay. Dolomite is abundant in all samples in amounts of as much as 55 percent; some samples contain as much as 15 percent calcite, but many samples contain little or none. Dawsonite ($NaAl(OH)_2CO_3$) is present in three samples collected about 300 feet above the base of the member from the lower Piceance Creek locality in amounts of 15 to 25 percent. Analcite, absent in the Wasatch and Garden Gulch samples, is present in all samples from the Parachute Creek Member.

The samples of silty sandstone from the Evacuation Creek Member contain illite and montmorillonite; no kaolinite or mixed-layer clay were detected. Analcite and relatively small amounts of dolomite and calcite are present in these samples. The sample of marlstone (No. 3) is similar in mineralogy to the samples of dolomitic oil shale of the Parachute Creek Member, except that calcite is much more abundant in the marlstone.

GENESIS OF CLAY MINERALS

It has been established by Bradley (1929, 1931, 1948) that the bulk of sedimentary material that makes up the Green River Formation was deposited in ancient Lake Uinta during Eocene time. The presence of kaolinite in the Wasatch Formation and the Garden Gulch Member of the Green River Formation indicates that the sedimentary material was deposited by well-oxygenated fresh water, possibly as mudflats during Wasatch time and in a fresh-water lake during the initial stage of Lake Uinta in early Green River time. In a lake that contains oxygenated fresh water, even though it may be calcareous, there is no reason for the clay minerals to be different from those transported from the source area (Millot, 1970, p. 170). The clay minerals, therefore, have been derived, without diagenetic change, from the rocks and soils of the drainage basin of Lake Uinta.

The lack of kaolinite in the Parachute Creek Member of the Green River Formation suggests that the sedimentary material was deposited in a lake that contained reducing anaerobic brackish to saline alkaline waters. It is assumed that the clay minerals derived from the source areas were the same during Green River time as they were during Wasatch time; if correct, the initial clay minerals have been subjected to diagenetic changes in the alkaline lake environment. Kaolinite was altered to illite, and montmorillonite was converted to illite and mixed-layer clay.

In Evacuation Creek time, during the waning stage of Lake Uinta, large amounts of volcanic ash were deposited in the basin. The montmorillonite in these sediments was probably derived from the alteration of the volcanic debris.

Table 1.—*Mineral composition of 31 samples from the Green River and Wasatch Formations, Piceance Creek basin, Colorado*

[Analyses by X-ray diffraction. --, not detected; tr., trace]

Description	Sample No.	Carbonates[1] (percent)			Noncarbonates[2] (percent)								Location	Remarks
		Dolomite	Calcite	Dawsonite	Quartz	Potassium feldspar	Sodium feldspar	Analcite	Kaolinite	Illite	Mixed-layer clay	Montmorillonite		
Green River Formation														
Evacuation Creek Member														
Silty sandstone (2.5Y 5/1)[3]	1	10	5	--	30	10	20	10	--	5	--	10	Sec. 22, T. 1 N., R. 98 W.	25 ft above sample 3.
Do. (10YR 6/1)	2	10	5	--	25	10	15	10	--	10	--	15		10 ft above sample 3.
Marlstone (10YR 8/1)	3	25	45	--	10	5	5	5	--	5	tr.	--		
Parachute Creek Member														
Oil shale, dolomitic (5Y 6/2)	4	55	--	--	20	5	10	5	--	5	tr.	--		15.5 ft above Mahogany bed.
Do. (2.5Y 6/2)	5	40	10	--	25	5	10	5	--	5	tr.	--	Sec. 36, T. 7 S., R. 97 W.	2.5 ft above Mahogany bed.
Do. (2.5Y 6/1)	6	40	15	--	20	5	10	5	--	5	tr.	--		3 ft below Mahogany bed.
Do. (2.5Y 4/2)	7	35	--	--	30	5	20	5	--	5	tr.	--		12.5 ft below Mahogany bed.
Do. (2.5Y 6/1)	8	30	5	--	30	15	10	tr.	--	10	tr.	--		46.5 ft above Mahogany bed.
Do. (2.5Y 6/2)	9	50	--	--	20	tr.	10	15	--	5	tr.	--	Sec. 6, T. 4 S., R. 94 W.	39 ft above Mahogany bed.
Do. (2.5Y 5/2)	10	40	10	--	20	5	10	10	--	5	tr.	--		22.4 ft above Mahogany bed.
Do. (2.5Y 4/2)	11	30	10	--	25	tr.	15	10	--	10	tr.	--		Mahogany bed.
Oil shale (5Y 4/1)	12	15	--	15	35	10	10	5	--	10	tr.	--		
Do. (5Y 5/1)	13	10	--	25	40	10	10	tr.	--	5	tr.	--		
Do. (5Y 5/1)	14	20	--	20	40	10	5	tr.	--	5	tr.	--		
Oil shale, dolomitic (2.5Y 6/1)	15	40	5	--	20	5	15	10	--	5	tr.	--	Sec. 14, T. 1 N., R. 97 W.	16.9 ft above Mahogany bed.
Do. (2.5Y 5/2)	16	40	5	--	25	5	5	10	--	10	tr.	--		4.3 ft above Mahogany bed.
Do. (5Y 4/1)	17	25	tr.	--	35	5	20	5	--	10	tr.	--		1 ft above Mahogany bed.
Do. (5Y 5/1)	18	25	5	--	35	5	10	10	--	10	tr.	--		Mahogany bed.
Do. (5Y 4/1)	19	25	--	--	40	10	5	10	--	10	tr.	--		20 ft below Mahogany bed.
Do. (5Y 6/2)	20	30	10	--	20	5	10	15	--	10	tr.	--		333.2 ft above Mahogany bed.
Do. (5Y 6/2)	21	50	tr.	--	20	5	10	10	--	5	tr.	--		200.4 ft above Mahogany bed.
Do. (2.5Y 6/2)	22	40	10	--	20	5	10	10	--	5	tr.	--		15.5 ft above Mahogany bed.
Do. (5Y 4/2)	23	30	5	--	25	5	20	10	--	5	tr.	--	Sec. 34, T. 2 S., R. 100 W.	Mahogany bed.
Do. (10YR 5/1)	24	40	--	--	15	15	15	5	--	10	tr.	--		15.7 ft below Mahogany bed.
Do. (5Y 6/2)	25	50	--	--	25	5	5	5	--	10	tr.	--		334.7 ft below Mahogany bed.
Oil shale (10YR 4/2)	26	40	--	--	35	5		5	--	10	5	--		405.3 ft below Mahogany bed.
Garden Gulch Member														
Oil shale, dolomitic (10YR 3/3)	27	45	--	--	30	tr.	5	--	5	10	5	--	Sec. 11, T. 1 N., R. 97 W.	
Shale (2.5Y 5/2)	28	5	10	--	45	5	10	--	5	15	5	--	Sec. 34, T. 2 S., R. 100 W.	60 ft below top of member.
Wasatch Formation														
Silty mudstone (5YR 4/2)	29	--	--	--	45	10	15	--	15	5	10	--	Sec. 28, T. 7 S., R. 97 W.	30–40 ft below top of formation.
Silty shale (10YR 6/1)	30	--	--	--	45	15	10	--	10	5	15	--		75–100 ft below top of formation.
Mudstone (5Y 5/1)	31	10	5	--	50	tr.	10	--	5	15	--	5	Sec. 4, T. 6 S., R. 96 W.	

[1] The percentage of total carbonates is based on weight loss after dilute HCl treatment.
[2] The percentages are based on the peak-height ratio of the major peaks on the X-ray diffraction traces.
[3] Rock color designations from Munsell Color Co. (1929–60).

ADDITIONAL RESEARCH

More samples from the Green River and Wasatch Formations need to be analyzed for their mineralogy. One approach might be to combine a stratigraphic and mineralogic study of a time-stratigraphic unit from basin edge to basin depositional center. This would include several lithofacies which represent fluviatile, near-shore, and lake-center sediments. It may be possible to recognize clastic (allogenic) and chemical (authigenic) components in the clay minerals and nonclay silicate minerals, such as quartz and feldspars. Geochemical studies could be integrated with qualitative and quantitative mineralogy, and the mineral (or organic) sites of elements might be established. This may delineate separate mineral facies and relate them to depositional environment and aid in interpreting the physical and chemical conditions of the depositional environment.

The above research may also contribute to the economic potential of the oil shale. The oil reserves in the Green River Formation of the Piceance Creek basin are well known. Other economic possibilities are sources of aluminum, sodium, and other elements. Also, preliminary tests on spent oil shale indicate that some of it would make an excellent lightweight aggregate.

REFERENCES

Bradley, W. H., 1929, The varves and climate of the Green River epoch: U.S. Geol. Survey Prof. Paper 158-E, p. 87–110.

—— 1931, Origin and microfossils of the oil shale of the Green River Formation of Colorado and Utah: U.S. Geol. Survey Prof. Paper 168, 58 p.

—— 1948, Limnology and the Eocene lakes of the Rocky Mountain region: Geol. Soc. America Bull., v. 59, no. 7, p. 635–648.

Donnell, J. R., 1961, Tertiary geology and oil-shale resources of the Piceance Creek basin between the Colorado and White Rivers, northwestern Colorado: U.S. Geol. Survey Bull. 1082-L, p. 835–891.

Donnell, J. R., and Cashion, W. B., 1968, Oil shale and related deposits of Lake Uinta (Eocene), northwestern Colorado and northwestern Utah, U.S.A., *in* United Nations symposium on development and utilization of oil shale resources, Talinn, Estonia, U.S.S.R.: published as separate, 13 p.

Hite, R. J., and Dyni, J. R., 1967, Potential resources of dawsonite and nahcolite in the Piceance Creek basin, northwest Colorado: Colorado School Mines Quart., v. 62, no. 3, p. 25–38.

Hosterman, J. W., 1968, Use of diffracted-beam monochromator in X-ray diffraction of clay minerals, *in* Geological Survey Research 1968: U.S. Geol. Survey Prof. Paper 600-B, p. B117–B118.

Hunt, J. M., Stewart, Francis, and Dickey, P. A., 1954, Origin of hydrocarbons of Uinta basin, Utah: Am. Assoc. Petroleum Geologists Bull., v. 38, no. 8, p. 1671–1698.

Millot, Georges, 1970, Geology of clays; weathering, sedimentology, geochemistry: New York, Springer-Verlag, 429 p.

Munsell Color Company, 1929–60, Munsell book of color: Baltimore, Md.

Royse, C. F., Wadell, J. S., and Petersen, L. E., 1971, X-ray determination of calcite-dolomite–an evaluation: Jour. Sed. Petrology, v. 41, no. 2, p. 483–488.

Snow, C. B., 1970, Stratigraphy of basal sandstone in the Green River Formation, northeast Piceance basin, Rio Blanco County, Colorado: Mtn. Geologist, v. 7, no. 1, p. 3–32.

Tank, Ronald, 1969, Clay mineral composition of the Tipton Shale Member of the Green River Formation (Eocene) of Wyoming: Jour. Sed. Petrology, v. 39, no. 4, p. 1593–1595.

RARE-EARTH ELEMENT FRACTIONATION IN ACCESSORY MINERALS, CENTRAL SIERRA NEVADA BATHOLITH

By F. C. W. DODGE and R. E. MAYS, Menlo Park, Calif.

Abstract.—Contents of rare earths have been determined in apatite, sphene, and garnet from rocks of the central Sierra Nevada batholith, California. The quantity sigma (Σ), the sum of the atomic percentages of La, Ce, and Pr of the total rare-earth assemblage, is a measure of rare-earth fractionation; it ranges from 12 to 81 for apatites and from 31 to 74 for sphenes from the granitic rocks. The two lowest apatite Σ values, 12 and 14, are from the extreme west side of the batholith; other apatite values are significantly greater, ranging from 35 to 81 and averaging 61. Σ values of sphene tend to increase eastward across the batholith. Chondrite-normalized distribution patterns are closely related to Σ values; patterns of apatites with lowest Σ values show no selective enrichment in any of the rare-earth elements, whereas patterns for sphenes and apatites with higher values are clearly dominated by the lighter elements. Eastward increase of lighter rare-earth elements in sphenes is consistent with both the recently advanced subduction-zone hypothesis and the anatectic hypothesis of batholithic origin. However, the presence of two strikingly different rare-earth distribution patterns of apatite suggests that both crustal and mantle sources may have played roles in origin of the batholith.

As part of a continuing program of mineralogical and geochemical studies of granitic rocks of the Sierra Nevada batholith of California, rare-earth elements (REE) in 20 sphene, 22 apatite, and three garnet separates have been determined. The batholith, which is largely a composite mass made up of numerous Mesozoic plutonic bodies of granitic rocks emplaced episodically over a period of about 100 million years (Bateman and Eaton, 1967), has been intensively studied within a wide strip across its central part between lat 36°45′ N. and 38°00′ N. Samples from which accessory minerals were recovered were taken from this strip; the same samples have been used in several other studies of the batholith (for example, Dodge and others, 1970; Naeser and Dodge, 1969; Piwinskii, 1968).

Distribution patterns of rare-earth contents of the accessory minerals that concentrate rare earths may provide clues which will aid in determining the origin of the batholith and of batholiths in general, a subject of considerable recent controversy. The value of rare-earth data in such genetic studies was shown previously by Towell and others (1965), who analyzed some rocks and constituent minerals from the southern California batholith.

ANALYTICAL METHODS

Accessory-mineral separates were prepared from carefully sized rock powders by centrifuging the powders in heavy liquids and by passing them repeatedly through an electromagnetic separator. Final sample purity of individual separates generally exceeded 98 percent. Quantities of REE were estimated by emission spectrography, by use of techniques similar to those described by Myers and others (1961). The percentages of individual elements were bracketed within intervals whose boundaries are 1.2, 0.83, 0.56, 0.38, 0.26, 0.18, 0.12, and so forth, and values were reported arbitrarily as midpoints of these intervals, that is, 1.0, 0.7, 0.5, 0.3, 0.2, 0.15, 0.1, and so forth. Precision of a reported value is approximately plus or minus one interval at 68-percent, or two intervals at 95-percent confidence. This method of data reporting has been found to be satisfactory for determining distribution patterns of rare-earth assemblages.

Σ VALUES

Grouping of the atomic percentages of the total rare-earth fraction of three elements, La + Ce + Pr, into a single value, Σ (Murata and others, 1953), is one of the many techniques that have been proposed as a means of presenting and interpreting rare-earth abundance data. This value, which is simply the content of the lighter, more basic elements relative to the entire rare-earth assemblage, has been considered a numerical index of the stage of fractionation attained by the REE (Murata and others, 1957; Lee and Bastron, 1967).

Σ values of apatite from Sierra Nevada granitic rocks range from 12 to 81. In figure 1, the Σ values of apatite and sphene are projected onto line W-E, which crosses the central Sierra Nevada batholith from southwest to northeast approximately normal to the batholith's axis. The two lowest apatite Σ values, 12 and 14, are on the extreme western side of the batholith. Elsewhere, Σ values of the mineral are considerably greater, ranging from 35 to 81 and averaging 61.

In general, sphene has significantly lower Σ values than does coexisting apatite (fig. 1). The lower proportion of the lighter, larger REE probably results from the fact that the atomic

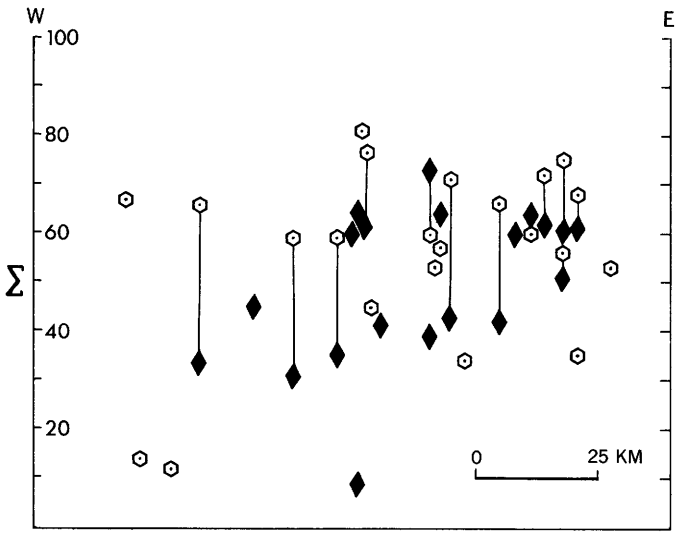

Figure 1.—Σ values (atomic percentages of La, Ce, and Pr of the total REE assemblage) of apatites (hexagons) and sphenes (diamonds) projected to line W-E, which crosses the central Sierra Nevada batholith approximately normal to its axis. Values for coexisting minerals are connected by vertical tielines.

structure of sphene provides only a seven-coordinated site for these elements (Mongiorgi and Riva di Sanseverino, 1968), whereas that of apatite additionally offers a larger, nine-coordinated site (Posner and others, 1958). Values for sphene from the granitic rocks range from 31 to 74 and average 52. We have determined an exceptionally low value of 8 on a sphene from a pegmatite; Fleischer and Altschuler (1969) have noted a tendency toward enrichment of the heavy lanthanides, that is, a tendency toward low Σ values, in sphenes from granitic pegmatites. The plot of Σ values of sphene across the batholith suggests an eastward increase of the value; however. there is considerable scatter in the data. Unfortunately, although sphene occurs throughout rocks from much of the batholith, the mineral is not present in samples from the far western flank of the batholith, including in the two samples that contained apatite with low Σ values.

Of the 29 rock samples from which sphene and (or) apatite were recovered, 26 have been analyzed for major elements. In agreement with Lee and others' (1969) observations for sphene from some granitic rocks of eastern Nevada, there is no apparent correlation of REE composition of Sierra Nevada sphenes and apatites with major-element compositions of the host granitic rocks.

The heavier REE in the three analyzed garnets show a marked enrichment over their lighter counterparts; in fact, the lighter elements were generally not detected by our methods, precluding calculation of Σ values. Other workers (see Hermann, 1970) have noted similar distributions of the REE in garnets from various geologic environments.

RARE-EARTH DISTRIBUTION PATTERNS

By plotting abundance of individual REE normalized to corresponding abundances in chondrites (using chondrite values summarized by Hermann, 1970), a widely used procedure originally described by Coryell and others (1963), it is possible to evaluate further the fractionation of the elements in accessory minerals. Examples of these plots are depicted in figure 2.

The plots for sphenes generally are dominated by the lighter members of the lanthanides to an increasing degree eastward across the batholith, as the Σ values suggest. Sphenes from samples SL-32 and FD-2, whose REE distribution patterns are presented in figure 2, are from rocks from the western and eastern parts of the batholith, respectively; their patterns also typify the changes between sphenes with relatively low Σ values and those with higher values. In contrast with the other sphenes, the distribution pattern of pegmatitic sphene, not depicted here, indicates considerable enrichment in the heavier REE.

Plots of the REE distribution patterns of the two apatites that coexist with the sphenes of figure 2 clearly show the increased relative content of the lighter rare earths in the

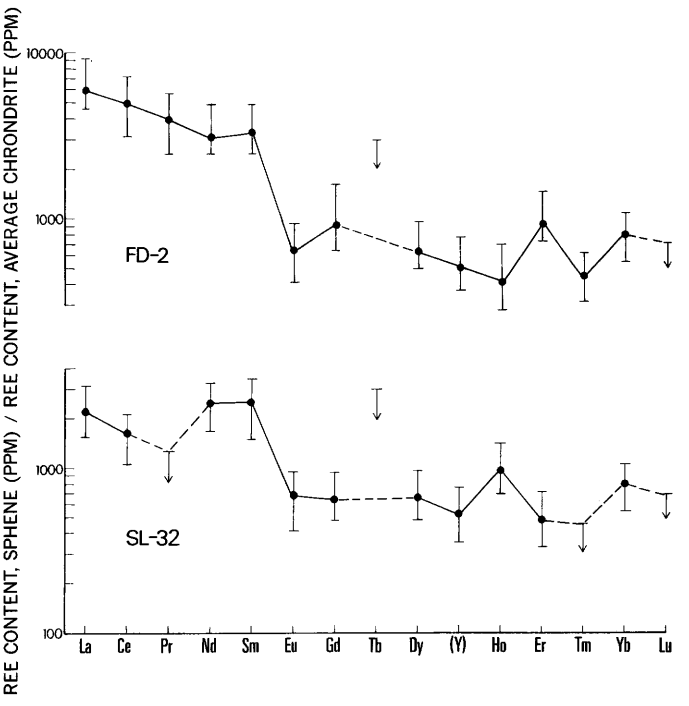

Figure 2.—Abundance of REE in typical sphenes from Sierra Nevada granitic rocks relative to chondrites. Sphene from sample FD-2 has a high Σ value (60), sphene from sample SL-32 a much lower value (34). Vertical lines are based on one spectrographic interval (see discussion of methods in text for further explanation), solid dots on reported values, and arrowheads on detectability levels, with the length of the arrow derived from that part of the interval above the detectable level. Abundance lines are dashed where they span elements present in amounts below limits of detectable levels.

apatites (fig. 3). Apatites from most rocks of the batholith generally have patterns in which the lighter elements clearly outweigh amounts of their heavier counterparts. However, the distribution patterns for the two apatites with low Σ values from rocks of the west side of the batholith (of which sample WV-1 of figure 3 is an example) show no marked trend of enrichment in any of the REE.

DISCUSSION

Relative amounts of individual REE in accessory minerals of the central Sierra Nevada batholith do not appear to be related directly to host-rock composition, thus indicating that fractionation of the rare earths is not a simple function of overall composition. Nevertheless, there is an indication that the increased fractionation of the lanthanides in sphenes eastward across the batholith parallels similar lateral variations of other chemical parameters across the batholith (Bateman and Dodge, 1970; Dodge, 1972a, b; Dodge and others, 1970). Bateman and Dodge suggested that increase of K_2O was due to progressive lateral changes in composition of the source materials from which parent granitic magmas were formed. Alternatively, Dickinson (1970) attributed K_2O variation solely to depth of magma generation along an eastward-dipping subduction zone. The suggested rare-earth fractionation trend of sphenes is compatible with either of these hypotheses.

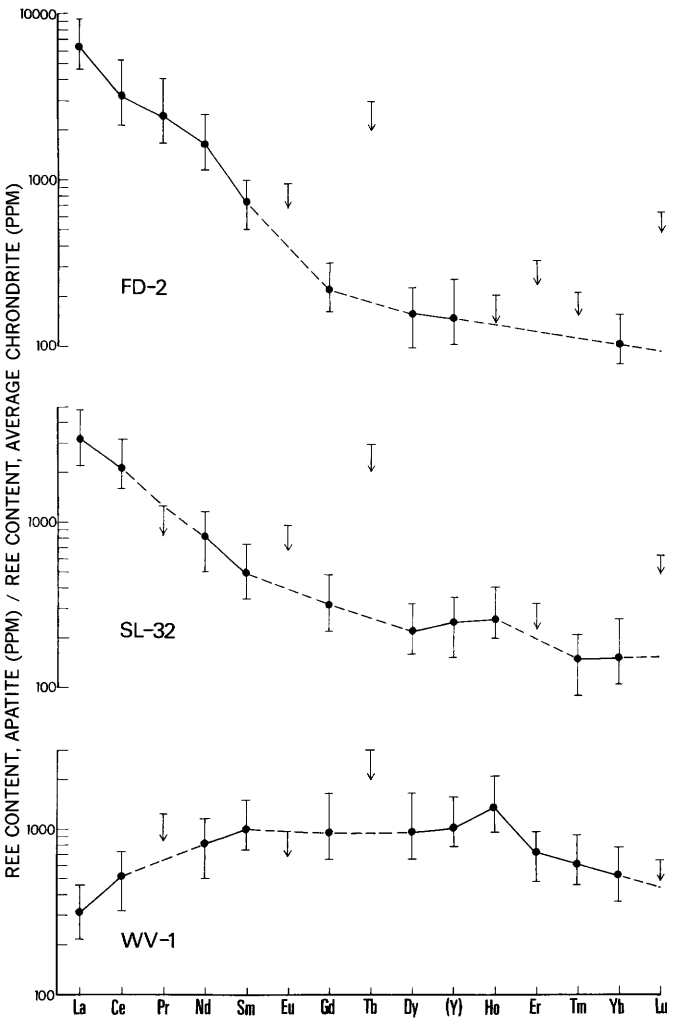

Figure 3.—Abundance of REE in typical apatites from Sierra Nevada granitic rocks relative to chondrites. Apatites from samples FD-2, SL-32, and WV-1 have high (75), intermediate (66), and low (12) Σ values, respectively; the first two apatites coexist with sphenes of figure 2. See figure 2 for further explanation.

Haskin and Frey (1966) have noted that enrichment of the lighter REE relative to chondrite abundances is characteristic of weathered portions of the earth's crust, whereas the average rare-earth pattern for the whole earth probably matches the chondritic pattern itself—presumably, the chondritic pattern is identical with that of the primordial matter from which the entire solar system developed. Thus, less fractionated rare-earth assemblages may reflect increasing amounts of juvenile, presumably mantle-derived material in the batholith's source materials, whereas the more fractionated assemblages may result from increasing amounts of crustally derived materials in eastern magmas.

Instead of ascribing K_2O variation to varying source material, Green and Ringwood (1969) have suggested that the variation of K_2O in various calc-alkaline suites generated along dipping subduction zones is controlled by a complete continuum of fractionation processes varying primarily with depth of partial melting. At shallow levels, crystal fractionation trends may be governed mainly by separation of amphibole containing small but significant amounts of K_2O. However, with increasing depth, these trends may be governed by separation of clinopyroxene and garnet, both containing negligible K_2O. Melts derived at greater depths would thus have much higher potassium contents than melts of shallower origin. According to Green and Ringwood, the proportion of garnet relative to clinopyroxene near the liquidus will increase with increasing pressure and increasing silica content. Rare-earth distribution patterns of garnets are consistently depleted in the light elements, a finding substantiated by the garnets analyzed in this study, but those of pyroxene are not. Consequently, at deeper and deeper levels along a dipping subduction zone, the generated magmas will be more and more enriched in lighter rare-earth elements. This enrichment might then in turn be reflected in the accessory minerals that concentrate rare earths. Goles (1968) has suggested that a garnet "residue" in the mantle might be responsible for the enrichment of the light rare earths in crustal materials. Even though Bateman and Dodge (1970) have presented arguments that cast doubt on the presence of a single subduction zone as the primary originating factor of the Sierra Nevada batholith, calc-alkaline magma generation along subduction zones may have been an important mechanism for originally producing rare-earth distribution patterns in the continental crust.

Although apatite from Sierra Nevada granitic rocks does not show the spatial variation of the rare earths displayed by sphene, the presence of apatites with apparently unfractionated rare-earth assemblages on the west side of the batholith is even more noteworthy. In general, the rare-earth assemblages in apatite from batholithic rocks are highly fractionated, and the change from unfractionated to fractionated is spatially abrupt. The presence of the two strikingly different distribution patterns in the same mineral is possibly a reflection of completely different sources of the rare-earth assemblages. This theory would suggest that apatites in some western plutonic bodies of the batholith may have crystallized from magmas derived entirely from mantle materials, such as oceanic tholeiite that is characterized by an unfractionated rare-earth assemblage (Haskin and others, 1966). In contrast, in other plutonic bodies, apatite crystallized from magmas derived largely from crustal materials.

REFERENCES

Bateman, P. C., and Dodge, F. C. W., 1970, Variations of major chemical constituents across the central Sierra Nevada batholith: Geol. Soc. America Bull., v. 81, p. 409–420.

Bateman, P. C., and Eaton, J. P., 1967, Sierra Nevada batholith: Science, v. 158, p. 1407–1417.

Coryell, C. D., Chase, J. W., and Winchester, J. W., 1963, A procedure for geochemical interpretation of terrestrial rare-earth abundance patterns: Jour. Geophys. Research, v. 68, p. 559–566.

Dickinson, W. R., 1970, Relations of andesites, granites, and derivative sandstones to arc-trench tectonics: Rev. Geophys. Space Physics, v. 8, p. 813–860.

Dodge, F. C. W., 1972a, Variation of ferrous-ferric ratios in the central Sierra Nevada batholith, U.S.A.: Internat. Geol. Cong., 34th, Montreal 1972, Proc., sec. 10. [In press]

—— 1972b, Trace element contents of some plutonic rocks of the Sierra Nevada batholith: U.S. Geol. Survey Bull. 1314-F. [In press]

Dodge, F. C. W., Fabbi, B. P., and Ross, D. C., 1970, Potassium and rubidium in granitic rocks of central California, *in* Geological Survey Research 1970: U.S. Geol. Survey Prof. Paper 700-D, p. D108–D115.

Fleischer, Michael, and Altschuler, Z. S., 1969, The relationship of the rare-earth composition of minerals to geologic environment: Geochim. et Cosmochim. Acta, v. 33, p. 725–732.

Goles, G. G., 1968, Rare-earth geochemistry of Pre-Cambrian plutonic rocks: Internat. Geol. Cong., 33d, Prague 1968, Proc., sec. 6, p. 237–249.

Green, T. H. and Ringwood. A. E., 1969, High pressure experimental studies on the origin of andesites, *in* McBirney, A. R., ed., Proceedings of the Andesite Conference: Oregon Dept. Geology and Mineral Industries Bull. 65, p. 21–32.

Haskin, L. A., and Frey, F. A., 1966, Dispersed and not-so-rare earths: Science, v. 152, p. 299–314.

Haskin, L. A., Frey, F. A., Schmitt, R. A., and Smith, R. H., 1966, Meteoric, solar and terrestrial rare-earth distributions, *in* Physics and chemistry of the Earth, v. 7: London and New York, Pergamon Press, p. 167–321.

Hermann, A. G., 1970, Yttrium and lanthanides, *in* Wedepohl, K. H., ed., Handbook of geochemistry, v. II: Berlin, Springer-Verlag, p. 39, 59-71-B to 39, 57-71-O.

Lee, D. E., and Bastron, Harry, 1967, Fractionation of rare-earth elements in allanite and monzonite as related to geology of the Mt. Wheeler mine area, Nevada: Geochim. et Cosmochim. Acta, v. 31, p. 339–356.

Lee, D. E., Mays, R. E., Van Loenen, R. E., and Rose, H. J., Jr., 1969, Accessory sphene from hybrid rocks of the Mount Wheeler mine area, Nevada, *in* Geological Survey Research 1969: U.S. Geol. Survey Prof. Paper 650-B, p. B41–B46.

Mongiorgi, Romano, and Riva di Sanseverino, L., 1968, A reconsideration of the structure of titanite, $CaTiOSiO_4$: Mineralog. et Petrog. Acta, v. 14, p. 123–141.

Murata, K. J., Rose, H. J., Jr., and Carron, M. K., 1953, Systematic variation of rare earths in monazite: Geochim. et Cosmochim. Acta, v. 4, p. 292–300.

Murata, K. J., Rose, H. J., Jr., Carron, M. K., and Glass, J. J., 1957, Systematic variation of rare-earth elements in cerium-earth minerals: Geochim. et Cosmochim. Acta, v. 11, p. 141–161.

Myers, A. T., Havens, R. G., and Dunton, P. J., 1961, A spectrochemical method for the semiquantitative analysis of rocks, minerals, and ores: U.S. Geol. Survey Bull. 1084-I, p. 207–229.

Naeser, C. W., and Dodge, F. C. W., 1969, Fission-track ages of accessory minerals from granitic rocks of the central Sierra Nevada, batholith, California: Geol. Soc. America Bull., v. 80, p. 2201–2212.

Piwinskii, A. J., 1968, Studies of batholithic feldspars–Sierra Nevada, California: Contr. Mineralogy and Petrology, v. 17, p. 204–223.

Posner, A. S., Perloff, Alvin, and Diorio, A. F., 1958, Refinement of the hydroxyapatite structure: Acta Cryst., v. 11, p. 308–309.

Towell, D. G., Winchester, J. W., and Spirn, R. V., 1965, Rare-earth distribution in some rocks and associated minerals of the batholith of southern California: Jour. Geophys. Research, v. 68, p. 559–566.

MINOR ELEMENTS IN COAL— A SELECTED BIBLIOGRAPHY, JULY 1972

By PAUL AVERITT[1], IRVING A. BREGER[2], VERNON E. SWANSON[1], PETER ZUBOVIC[2], and HAROLD J. GLUSKOTER[3,a], Compilers,
[1] Denver, Colo., [2] Washington, D.C., [3] Urbana, Ill.

Abstract.—A bibliography of 65 selected references on trace elements in coal is presented as a guide to available information and as an aid to further study. Most of the cited reports are in English and most are applicable to the United States.

The control or possible recovery of trace elements released on combustion of coal for generation of electric power or for manufacture of synthetic gas and liquids is of increasing environmental and economic concern. The following list of 65 selected references was prepared in response to this increased level of interest and to the increased demand for information. The compilers hope that the bibliography will be useful to those initiating studies and that it will serve as a nucleus to which new and subsidiary references can be added.

The bibliography is applicable primarily to the United States. It includes references to a few reports dealing with major ash constituents and with the geochemistry of coal; it does not include references to reports dealing exclusively with sulfur or chlorine. Most of the cited reports contain specialized bibliographies.

† † † † †

Abernethy, R. F., and Gibson, F. H., 1963, Rare elements in coal: U.S. Bur. Mines Inf. Circ. 8163, 69 p.

Abernethy, R. F., Gibson, F. H., and Frederic, W. H., 1965, Phosphorus, chlorine, sodium, and potassium in U.S. coals: U.S. Bur. Mines Rept. Inv. 6579, 34 p.

Abernethy, R. F., Peterson, M. J., and Gibson, F. H., 1969a, Major ash constituents in U.S. coals: U.S. Bur. Mines Rept. Inv. 7240, 9 p.

——1969b, Spectrochemical analysis of coal ash for trace elements: U.S. Bur. Mines Rept. Inv. 7281, 30 p.

Almond, Hy, Crowe, H. E., and Thompson, C. E., 1955, Rapid determination of germanium in coal, soil, and rock: U.S. Geol. Survey Bull. 1036-B, p. 9–17.

Bertine, K. K., and Goldberg, E. D., 1971, Fossil fuel combustion and the major sedimentary cycle: Science, v. 173, no. 3993, p. 233–235.

Bowen, H. J. M., 1966, Trace elements in biochemistry: London and New York, Academic Press, 241 p.

Breger, I. A., 1958, Geochemistry of coal: Econ. Geology, v. 53, no. 7, p. 823–841.

——ed., 1963, Organic geochemistry: Oxford, Pergamon Press, Internat. Ser. Mons. Earth Sci., v. 16, 658 p. (Distributed by Macmillan Co., New York.)

Breger, I. A., Deul, Maurice, and Meyrowitz, Robert, 1955, Geochemistry and mineralogy of a uraniferous subbituminous coal [Wyo.]: Econ. Geology, v. 50, no. 6, p. 610–624.

Breger, I. A., Deul, Maurice, and Rubinstein, Samuel, 1955, Geochemistry and mineralogy of a uraniferous lignite [S. Dak.]: Econ. Geology, v. 50, no. 2, p. 206–226.

Chow, T. J., and Earl, J. L., 1970, Lead and uranium in Pennsylvania anthracite: Amsterdam, Netherlands, Elsevier Pub. Co., Chem. Geology, v. 6, no. 1, p. 43–49.

—— 1972, Lead isotopes in North American coal: Science, v. 176, no. 4034, p. 510–511.

Corey, R. C., Myers, J. W., Schwartz, C. H., Gibson, F. H., and Colbassani, P. J., 1959, Occurrence and determination of germanium in coal ash from powerplants: U.S. Bur. Mines Bull. 575, 68 p.

Denson, N. M., and Gill, J. R., 1956, Uranium-bearing lignite and its relation to volcanic tuffs in eastern Montana and North and South Dakota, *in* Page, L. R., Stocking, H. E., and Smith, H. B., compilers, Contributions to the geology of uranium and thorium by the United States Geological Survey and Atomic Energy Commission for the United Nations International Conference on Peaceful Uses of

[a] Illinois Geological Survey.

Atomic Energy, Geneva, Switzerland, 1955: U.S. Geol. Survey Prof. Paper 300, p. 413–418.

Denson, N. M., and others, 1959, Uranium in coal in the western United States: U.S. Geol. Survey Bull. 1055, 315 p.

Deul, Maurice, and Annell, C. S., 1956, The occurrence of minor elements in ash of low-rank coal from Texas, Colorado, North Dakota, and South Dakota: U.S. Geol. Survey Bull. 1036-H, p. 155–172.

Fortescue, J. A. C., 1954, Germanium and other trace elements in some western Canadian coals: Am. Mineralogist, v. 39, nos. 5–6, p. 510–519.

Francis, Wilfrid, 1961, Coal, its formation and composition [2d ed.]: London, Edward Arnold (Publishers) Ltd., 806 p. [See especially chapter 10.]

Geer, M. R., Davis, F. T., and Yancey, H. F., 1944, Occurrence of phosphorus in Washington coal and its removal: Am. Inst. Mining and Metall. Engineers Trans., v. 157, p. 152–159; Discussion, p. 159–161.

Gluskoter, H. J., and Ruch, R. R., 1971, Chlorine and sodium in Illinois coals as determined by neutron activation analyses: Fuel, v. 50, p. 65–76.

Goldschmidt, V. M., 1935, Rare elements in coal ashes: Indus. Eng. Chemistry, v. 27, p. 1100–1102.

——1950, Occurrence of rare elements in coal ashes, *in* Bangham, D. H., ed., Progress in coal science, v. 1: London, Intersci. Pub., Ltd., p. 238–247.

Hashimoto, Yoshikazu, Hwang, J. Y., and Yanagisawa, Saburo, 1970, Possible source of atmospheric pollution of selenium: Environmental Sci. and Technology, v. 4, no. 2, p. 157–158.

Hawley, J. E., 1955, Germanium content of some Nova Scotian coals: Econ. Geology, v. 50, no. 5, p. 517–532.

Headlee, A. J. W., and Hunter, R. G., 1951, Germanium in coals of West Virginia: West Virginia Geol. Survey Rept. Inv. 8, 15 p.

——1955, The inorganic elements in coals, Pt. 5 *of* Characteristics of minable coals of West Virginia: West Virginia Geol. Survey Bull., v. 13A, p. 1–122.

Horton, L., and Aubrey, K. V., 1950, Distribution of minor elements in three vitrains from the Barnsley seam: London, Soc. Chem. Industry Jour., v. 69, suppl. 1, p. 541–548.

Joensuu, O. I., 1971, Fossil fuels as a source of mercury pollution: Science, v. 172, no. 3987, p. 1027–1028.

Kehn, T. M., 1957, Selected annotated bibliography of the geology of uranium-bearing coal and carbonaceous shale in the United States: U.S. Geol. Survey Bull. 1059-A, 28 p.

Manskaya, S. M., and Drozdova, T. V., 1968, Geochemistry of organic substances: Oxford, Pergamon Press, Internat. Ser. Mons. Earth Sci., v. 28, 345 p.

Mason, Brian, 1966, Principles of geochemistry, 3d ed.: New York, John Wiley & Sons, 329 p.

Muter, R. B., and Cockrell, C. F., 1969, The analysis of sodium, potassium, calcium, and magnesium in siliceous coal ash and related materials by atomic absorption spectroscopy: Appl. Spectroscopy, v. 23, no. 5, p. 493–496.

National Bureau of Standards, 1972, Trace mercury in coal: Natl. Bur. Standards Standard Reference Material SRM 1630. (50 g finely powdered bituminous coal provisionally certified to contain 0.13 parts per million mercury by weight, price $45.00. Office of Standard Reference Materials, Rm. B314, Chemistry Bldg., National Bureau of Standards, Washington, D.C., 20234.)

Nicholls, G. D., 1968, The geochemistry of coal-bearing strata, *in* Murchison, D. C., and Westoll, T. S., eds., Coal and coal-bearing strata: New York, Am. Elsevier Pub. Co., p. 269–307.

Ode, W. H., 1963, Coal analysis and mineral matter, *in* Lowry, H. H., ed., Chemistry of coal utilization, supplementary volume: New York, John Wiley & Sons, Inc., p. 202–231.

O'Gorman, J. V., Suhr, N. H., and Walker, P. L., Jr., 1972, The determination of mercury in some American coals: Appl. Spectroscopy, v. 26, no. 1, p. 44–48.

Pillay, K. K. S., Thomas, C. C., Jr., and Kaminski, J. W., 1969, Neutron activation and analysis of the selenium content of fossil fuels: Nuclear Applications and Technology, v. 7, no. 5, p. 478–483.

Rao, P. D., 1968, Distribution of certain minor elements in Alaskan coals: Alaska Univ. Mineral Industry Resources Lab. Rept. 15, 47 p.

Reynolds, F. M., 1948, The occurrence of vanadium, chromium, and other minor unusual elements in certain coals: London, Soc. Chem. Industry Jour., v. 67, p. 341–345.

Ruch, R. R., Gluskoter, H. J., and Kennedy, E. J., 1971, Mercury content of Illinois coals: Illinois Geol. Survey Environmental Geology Notes, No. 43, 15 p.

Schleicher, J. A., 1959, Germanium in Kansas coals: Kansas Geol. Survey Bull. 134, pt. 4, p. 163–179.

Schlesinger, M. D., and Schultz, Hyman, 1972, An evaluation of methods for detecting mercury in some U.S. coals: U.S. Bur. Mines Rept. Inv. 7609, 11 p.

Selvig, W. A., and Gibson, F. H., 1956. Analyses of ash from United States coals [2d ed.]: U.S. Bur. Mines Bull. 567, 33 p.

Stadnichenko, Taisia, Murata, K. J., Zubovic, Peter, and Hufschmidt, E. L., 1953, Concentration of germanium in the ash of American coals—a progress report: U.S. Geol. Survey Circ. 272, 34 p.

Stadnichenko, Taisia, Zubovic, Peter, and Sheffey, N. B., 1961, Beryllium content of American coals: U.S. Geol. Survey Bull. 1084-K, p. 253–295.

Szilagyi, Maria, 1971, The role of organic material in the distribution of Mo, V, and Cr in coal fields: Econ. Geology, v. 66, no. 7, p. 1075–1078.

U.S. Department of the Interior, 1972a, Composition and trace-element content of coal and power plant ash, Pt. 2 *in* Appendix J *of* Southwest energy study: Coal Resources Work Group, 61 p.

——1972b, Trace element content of the soils and vegetation in the vicinity of the Four Corners power plant, Pt. 3—Appendix J-III *of* Southwest energy study: Coal Resources Work Group, 44 p.

VanKrevelen, D. W., 1963, Geochemistry of coal, Chap. 6 *in* Breger, I. A., ed., Organic geochemistry: Oxford, Pergamon Press, Internat. Ser. Mons. Earth Sci., v. 16, p. 183–247 (distributed by Macmillan Co., New York.).

Vine, J. D., 1962, Geology of uranium in coaly carbonaceous rocks: U.S. Geol. Survey Prof. Paper 356-D, p. 113–170.

Vinikas, B., 1964, Distributions statistiques d'éléments mineurs dans les charbons nord-américains, *in* Colombo, U., and Hobson, G. D., eds., Advances in organic geochemistry: New York, Macmillan Co., p. 97–108.

Watt, J. D., 1968, The occurrence, origin, identity, distribution, and estimation of the mineral species in British coals, Pt. 1 *of* The physical and chemical behaviour of the mineral matter in coal under the conditions met in combustion plant: Leatherhead, Surrey, England, British Coal Utilization Research Assoc., 102 p., 31 illus.

Zilbermintz, V. A., 1935, On the occurrence of vanadium in fossil coal: Akad. Nauk SSSR Doklady, N.S., v. 3, no. 3, p. 117–120 [In English].

Zilbermintz, V. A., and Rusanov, A. K., 1936, The occurrence of beryllium in fossil coals: Akad. Nauk SSSR Doklady, v. 2, no. 1, p. 27–31 [In English].

Zubovic, Peter, 1966a, Physicochemical properties of certain minor elements as controlling factors in their distribution in coal, [Chap.] 13, *in* Gould, R. F., ed., Coal science: Washington, D.C., Am. Chem. Soc. (Adv. Chem. Ser. 55), p. 211–231.

——1966b, Minor element distribution in coal samples of the Interior Coal Province, [Chap.] 14, *in* Gould, R. F., ed., Coal science: Washington, D.C., Am. Chem. Soc. (Adv. Chem. Ser. 55), p. 232–247.

Zubovic, Peter, Sheffey, N. B., and Stadnichenko, Taisia, 1967, Distribution of minor elements in some coals in the Western and Southwestern regions of the Interior coal province: U.S. Geol. Survey Bull. 1117-D, 33 p.

Zubovic, Peter, Stadnichenko, Taisia, and Sheffey, N. B., 1960a, Relation of the minor element content of coal to possible source rocks: Art. 40 *in* U.S. Geol. Survey Prof. Paper 400-B, p. B82–B84.

——1960b, The association of some minor elements with organic and inorganic phases of coal: Art. 41 *in* U.S. Geol. Survey Prof. Paper 400-B, p. B84–B87.

——1960c, Comparative abundance of the minor elements in coals from different parts of the United States: Art. 42 *in* U.S. Geol. Survey Prof. Paper 400-B, p. B87–B88.

——1961a, Chemical basis of minor-element associations in coal and other carbonaceous sediments: Art. 411 *in* U.S. Geol. Survey Prof. Paper 424-D, p. D345–D348.

——1961b, Geochemistry of minor elements in coals of the northern Great Plains coal province: U.S. Geol. Survey Bull. 1117-A, 58 p.

——1964, Distribution of minor elements in coal beds of the Eastern Interior region: U.S. Geol. Survey Bull. 1117-B, 41 p.

——1966, Distribution of minor elements in coals of the Appalachian region: U.S. Geol. Survey Bull. 1117-C, 37 p.

FREMONT LAKE, WYOMING—PRELIMINARY SURVEY OF A LARGE MOUNTAIN LAKE

By DAVID A. RICKERT and LUNA B. LEOPOLD[1],
Washington, D.C., Berkeley, Calif.

Abstract.—Fremont Lake, at an altitude of 2,261 m, has an area of 20.61 km^2 and a volume of 1.69 km^3. The maximum depth is 185 m, which makes it the seventh deepest natural lake in the conterminous United States. Theoretical renewal time is 11.1 years. Temperature data for 1971 indicate that vernal circulation extended to a depth of less than 90 m. The summer heat income was 19,450 cal/cm^2. The dissolved-oxygen curve is orthograde, with a slight metalimnetic maximum, and a tendency toward decreasing concentrations at depth. At 180 m, oxygen was at 80 percent of saturation in late July 1970. The lake has a remarkably low dissolved-solids content of 12.8 mg/l, making it one of the most dilute medium-sized lakes in the world. Detailed chemical data are given for the water column at three sites in the lake and for the influent and effluent streams. Net plankton included representatives of seven genera of phytoplankters and three genera of zooplankters. A reconnaissance indicated substantially no bacteriological contamination in the lake, but there was an appreciable amount in two minor streams in the vicinity of a summer-home colony.

Fremont Lake, the largest of the many thousands of lakes which lie on the flanks of the Wind River Range, is situated 3 km north of Pinedale, Wyo. Although the beauty and angling attraction of Fremont are widely known, its limnology has been little explored.

In July 1970, a survey was made to determine its physical and chemical character. The results, together with additional information, show that Fremont is remarkedly deep and dilute, a pristine lake clearly worth preserving in its present condition as an ecological benchmark.

GEOGRAPHY

Fremont holds special limnological interest as a large, clear, glacial lake at high altitude. It lies near the northern end of the Green River Basin at an altitude of 2,261 m (fig. 1). The center of the lake is situated at lat 42°57′ N. and long 109°48′ E. The lake is elongate in a northerly direction and is bordered on both shores by steep moraines, the tops of which are at an altitude of 2,500 m. At the headwaters of the drainage basin and on the Continental Divide is Fremont Peak, altitude 4,200 m.

Valley sides in the vicinity of the lake are vegetated with sagebrush and sparse stands of aspen on slopes facing east. North- and west-facing slopes generally support mixed conifers. Where fire has destroyed the conifers, aspen has colonized the old burn. The conifer forests are a mixture of Douglas-fir, alpine fir, lodgepole pine, and Engelmann spruce. There is virtually no emergent vegetation along the shoreline, and dredging from selected shallow areas of the lake showed an absence of rooted aquatics.

GEOLOGY

Fremont Lake lies in a trough that was scoured by glacial ice into granitic rock and plugged at the downstream end by a terminal moraine.

The central core of the Wind River Range, drained by the Green River and its tributaries on the west, is composed of Precambrian crystalline rocks. In the basin of Fremont Lake the rocks are mostly gray gneisses extensively cut by quartz, pegmatite, and granite dikes. The structure of the core is that of an asymmetric anticline folded during the Laramide orogeny.

During the Pleistocene the Wind River Range was extensively glaciated. There were three glaciations before the Wisconsin age, the deposits of which either are absent from or do not compose an important part of the landscape near Fremont Lake. Two major glacier advances, the Bull Lake and Pinedale, shaped the topography in the vicinity of the lake, but since each had several stages or subdivisions, the land surface is composed of till of several different ages. The Bull Lake ice retreated from the lake basin about 60,000 years ago, and the final retreat of Pinedale ice took place about 9,000 years ago (Richmond, 1969).

The lake basin is elongate and is pinched in width at about the halfway point to form a constriction called The Narrows. Upstream from this neck, the mountain slopes bordering the lake are nearly free of glacial till, bare rock surfaces predominating. Below The Narrows, the valley slopes are mo-

[1] Department of Geology and Geophysics, University of California.

U.S. GEOL. SURVEY PROF. PAPER 800-D, PAGES D173-D188

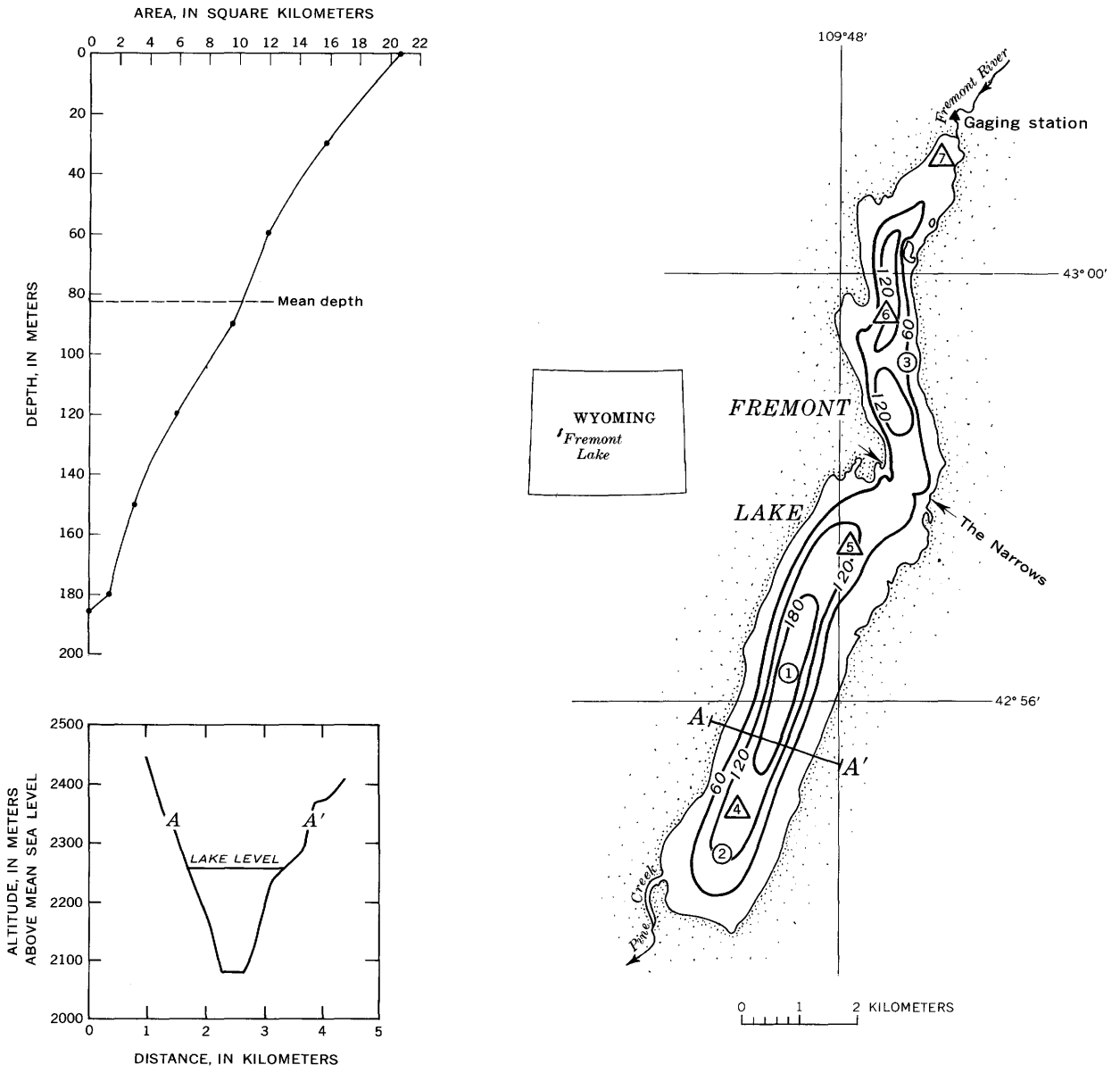

Figure 1.—Bathymetric map, hypsographic (area-depth) curve, and cross section for Fremont Lake, Wyo. All depths are in meters. Sampling sites noted on the map are 1–3, chemical analyses, 1970; and 4–7, planktonic analyses, 1969.

rainal, and there is virtually no bedrock at the surface. The outlet end of the lake is a terminal moraine made up of till of both Bull Lake and Pinedale age. Since the ice retreat, the outlet stream, Pine Creek, has incised itself into the terminal moraine only 3 or 4 m.

The glacial history has been studied by several geologists; the most detailed reports are those of Richmond (1969) and Richmond, Murphy, and Denson (1965).

Acknowledgments.—The authors wish to thank B. W. Lium for the plankton work and G. G. Ehrlich for the bacteriological analyses.

METHODS

Field measurements and samples for chemical analysis were taken at three sites in Fremont Lake and from the major inlet, the outlet, and a nearby beaver pond. Net-haul samples for plankton counts were collected at four sites in the lake. Bacteriological samples were taken just off the east and south shores of the lake, in the outlet stream, and from two ponds and two streams in the area of the Sylvan Bay summer-home colony. The sites of physical, chemical, and planktonic sampling are shown in figure 1.

Soundings were made with an oceanographic echo sounder. The bathymetric contours were drawn from 24 transects between survey-located shore stations and 350 plotted depth determinations. Lake volume was obtained by planimetering the area-depth curve.

Temperature profiles were measured with Watanabe Keike deep-sea protected reversing-thermometers.[2] Model 21912 was used in 1970, and temperatures were read to the nearest 0.1°C. The 1971 temperature data were determined with Model 21916 and were read by means of a lens to the nearest 0.01°C. All reported data have been corrected from field readings. In addition to reversing-thermometer data, several bathythermograph traces were also obtained.

Samples for all other lake water analyses were taken with a Kemmerer sampler which was lowered and lifted by a motor-operated winch. Field determinations of dissolved oxygen, pH, specific conductance, alkalinity, and hardness were made immediately after the collection of each sample. Water for laboratory analyses was stored and shipped in polyethylene bottles that were acid washed and rinsed in demineralized water. Samples for calcium, magnesium, iron, and manganese determinations were acidified to pH 2, and nutrient samples were preserved with chloroform. One sample for pesticide analysis was collected; it was stored in a specially cleaned glass bottle.

Dissolved-oxygen and stream- and pond-temperature measurements were made with a Yellow Springs Instrument Co. Model 54 oxygen-temperature meter. The meter was calibrated against the azide-modified Winkler method for dissolved oxygen and against a mercury thermometer at each use. Percentage saturation was determined from Rawson's nomograph (Welch, 1948). Specific conductance was measured with a Beckman 338 Solu-Bridge conductivity meter; pH was determined with an Orion 407 selective ion electrode meter. Measurements of alkalinity and hardness were made according to standard methods of the American Public Health Association and others (1965). Transparency of the water was measured with a 20-cm Secchi disk painted with black and white quadrants. Laboratory analyses were made on unfiltered samples according to the standard methods of the U.S. Geological Survey (Brown and others, 1970). Dissolved-solids content was determined as the sum of analyzed constituents (with bicarbonate converted to carbonate) rather than by evaporation.

Plankton collections were made with a Wisconsin-type net of No. 25 silk bolting cloth. At each of four sites a series of vertical hauls was taken from 0–3, 3–15, 15–30, and 30–45 m. The preserved plankton were identified to genus and counted in a Sedgwick Rafter slide at a magnification of X 160. Results were converted to numbers of organisms per liter as described in standard methods of the American Public Health Association and others (1965).

Bacteriological analyses were conducted using the membrane filter technique (Am. Public Health Assoc. and others, 1965). The total coliform count was determined through use of M-Endo medium, the fecal streptococci with M-Enterococcus Agar medium, and the fecal coliform count with M-Fecal Coliform medium as described by Geldreich (1966). Each incubation was started immediately after the collection of each sample.

[2]The use of brand names in this report does not imply endorsement by the U.S. Geological Survey. Equivalent products may be used for the same processes.

MORPHOLOGY AND MORPHOMETRY

The outstanding physical feature of Fremont Lake is its great depth (fig. 1). The maximum depth, 185.3 m, makes Fremont the seventh deepest natural lake in the conterminous United States (excluding the Great Lakes) and the tenth deepest with Alaska included (table 1).

For purposes of morphological description, Fremont Lake can be viewed as being divided into two oblong sections by a line drawn across The Narrows. North and south of this line there are several differences in the surficial morphology of the basin. Furthermore, the line overlies an underwater traverse ridge, so that the depth of water increases both north and south of this location.

South of The Narrows the lake has a length of 8.14 km, breadths ranging between 1.57 and 2.08 km, and a maximum depth of 185.3 m. The shoreline of this part of the lake is very regular and smooth.

In contrast, the northernmost section of the lake has a compound length (see footnote, table 2) of 6.53 km, breadths (excluding the northernmost tip) ranging between 0.75 and 1.39 km, and a maximum depth of 151 m. The shoreline here is very irregular.

The two parts of the lake are also distinguished by differences in bottom morphology. In the southern part, the depth increases in regular patterns from the three shorelines and the traverse ridge, and the bottom is exceedingly flat. In the northern part the depth patterns are much more irregular, and, instead of one basin, there are several isolated pockets of deep water which have sloping bottoms.

The extreme flatness of the bottom in the southern part of the lake is well illustrated by the bathymetric map and the

Table 1.—*Natural lakes of the United States with depths exceeding 150 m*

Name	Location	Depth (meters)
Crater	Oregon	589
Tahoe	California and Nevada	501
Chelan	Washington	489
Pend Oreille	Idaho	366
Nuyakuk	Alaska	284
Deer	...do...	267
Chauekuktuli	...do...	213
Crescent	Washington	190
Seneca	New York	188
Fremont	Wyoming	185
Clark	Alaska	184
Beverley	...do...	152

Table 2.—*Morphometric data for Fremont Lake*

Total drainage area (lake surface included)	km²	244.1
Area of lake (A)	km²	20.61
Ratio of total drainage area to lake surface area		11.9
Length (l)[1]	km	14.63
Greatest breadth (b_m)	km	2.08
Maximum depth (Z_m)	m	185.3
Volume (V)	km³	1.69
Mean depth ($\bar{Z}$)	m	82.5
Volume development ($\bar{Z}/Z_m$)		.44
Shoreline (L)	km	39.52
Shoreline development (D_L)		2.45

[1] Length refers to the total distance of lines running roughly parallel to the center of each section of the lake.

Table 3.—*Areas and volumes by depth intervals for Fremont Lake*

Depth (Z) (meters)	Area (A) (km²)	Volume (V) (km³)	Percentage of total volume
0	20.61		
10	18.97	0.20	11.8
20	17.35	.18	10.7
30	15.75	.16	9.5
60	11.90	.41	24.2
90	9.56	.32	18.9
120	5.84	.23	13.6
150	3.11	.13	7.7
180	1.42	.06	3.6
185.3	.00	.00	.0

accompanying cross section (fig. 1). The 180-m isobath covers a central area of 1.26 km² which includes, at 185.3 m, the maximum depth measured in the lake. The flat bottom is undoubtedly the result of the filling of a depression with sediment. The presence of a flat bottom only in the downstream and deepest part of the lake suggests that the sediment was deposited from density currents and consists of very fine grained material. However, no core samples have yet been taken.

Fremont Lake is a classic example of an elongate, greatly overdeepened, glacially excavated lake. From the cross section on figure 1 it can be seen that, beneath the water, the sides of the lake are of the same steepness as the hillsides bordering the lake. Because of these combined characteristics and its altitude, Fremont may be categorized as a piedmont lake according to the classification of Hutchinson (1957).

Morphometric data for Fremont Lake are summarized in table 2. The area of 20.61 km² ranks Fremont far behind Yellowstone (about 360 km²) and about equal to Shoshone in size among the large natural lakes of Wyoming (Pennak, 1963).

The shoreline development (D_L) value of 2.45 is consistent with the elongate shape of Fremont Lake and, hence, with its origin as a glacially overdeepened valley. The mean depth of Fremont Lake is 82.5 m, and the volume development (0.44) is moderately high. The volumes of different water layers are presented in table 3, along with the areas covered by selected isobaths.

HYDROLOGY

Fremont River enters the north end of Fremont Lake and is the only influent stream other than a few minor rivulets. This river contributes 5 m³/sec on the average (table 4). Annual precipitation directly on the water surface, judged from the record at the town of Pinedale (table 5), averages about 35 cm. The total drainage area is 244.1 km² (table 2). Of this total, 196.3 km² lies above the U.S. Geological Survey gaging station on Fremont River, 0.8 km above lake head. The slopes which surround the lake constitute a drainage area of 27.2 km². The ratio of total drainage area to lake surface area is 11.9.

Table 4.—*Mean monthly flow, in cubic meters per second, of Fremont River*

[Based on U.S. Geological Survey data, 1955–70]

October	1.5	April	1.0
November	.9	May	8.1
December	.7	June	23.6
January	.6	July	14.7
February	.5	August	4.6
March	.5	September	2.5
		Annual	5.0

Data pertinent to an approximate water balance are presented in table 6. Data on evaporation from other lakes of similar altitude give credence to our assumed value of 1.0 m/yr for Fremont Lake. More tenuous are the assumptions of precipitation on the lake and runoff for the drainage area below the gage. The precipitation on the lake is estimated to be somewhat greater than that at Pinedale because of the higher altitude, and still greater on the contributing area below the gaging station because this area is higher than the lake. The runoff derived from this larger value is estimated to be about the same as precipitation on the lake surface.

Table 5.—*Climatic data for Pinedale, Wyo.*

[Based on U.S. Weather Service data, 1912–70]

Jan.	Feb.	Mar.	Apr.	May	June	July	Aug.	Sept.	Oct.	Nov.	Dec.	Annual
Total precipitation (centimeters)												
1.83	1.63	1.65	2.01	3.35	3.18	2.08	2.72	2.69	2.24	1.63	2.01	27.02
Mean temperature (°C)												
-11.2	-9.4	-5.3	1.4	6.9	11.7	15.6	14.1	9.5	3.7	-3.5	-9.4	2.0

Table 6.—*Approximate water balance of Fremont Lake*

Drainage area above gaging station, Fremont River	km^2	196.3
Area of slopes below gage contributing runoff	km^2	27.2
Area of lake surface	km^2	20.6
Total area at lake outlet	km^2	244.1
Average annual flow at gage	m^3/sec	5.0
Average annual runoff depth at gage	m/yr	.80
Estimated runoff below gage	m/yr	.35
Precipitation at Pinedale	m/yr	.270
Estimated precipitation on lake surface	m/yr	.35
Estimated evaporation from lake[1]	m/yr	1.0
Runoff below gage plus precipitation on lake	m^3/yr	16.7×10^6
Runoff from area above gage	m^3/yr	157.0×10^6
Total yearly accumulation in lake	m^3/yr	173.7×10^6
Evaporation from lake	m^3/yr	20.6×10^6
Discharge from lake plus seepage	m^3/yr	153.1×10^6
Volume of water in lake	m^3	$1{,}690.0\times10^6$
Ratio—lake volume : annual contribution	years	11.1

[1] Estimate from comparison with other high-altitude lakes in Langbein (1951) and Longacre and Blaney (1962).

The estimate of theoretical renewal time, 11.1 years, is probably satisfactory because the estimated values are small compared with the measured quantities of lake volume and of runoff at the gage.

PHYSICAL CONDITIONS

Temperature

It is well known that the temperature of maximum density (T_{md}) of water is not a constant, but rather that it decreases with increasing pressure and, thus, with depth. Strøm (1945) stipulated the requirements for an empirical determination of T_{md}. He stated:

> If a holomitic lake (a lake with seasonal circulations extending to the bottom) is cooled sufficiently down before vernal full circulation, temperatures in the deep must immediately after the establishment of incipient summer stratification very nearly correspond to the T_{md} at various depths.

Fremont Lake is deep enough to exhibit the "pressure effect" and is in a climate where sufficient cooling could occur to meet Strøm's stipulation. Fremont freezes each year in mid-January, and the average date of ice breakup has been estimated to be May 15 (Dunn, 1972). To determine the relationship of temperature in Fremont to the T_{md}, a series of measurements was made at site 1 by Dunn just before and after ice breakup, May 13, 1971.

In table 7 and figure 2 the observed temperatures are shown in relation to Strøm's empirical values of T_{md}. On May 9, 4 days before ice breakup, temperatures above about 60 m were colder than the T_{md}, while those below 60 m were warmer. The upper part of the profile represented an unstable condition which changed by May 12 to one in which temperatures at most points were either very similar to or warmer than the T_{md}. The warming took place through the weakly constituted ice and affected only the upper 60 m of the profile. As expected, the data of May 17 show that further shallow-depth warming occurred immediately after ice breakup.

Table 7.—*Temperature observations, in degrees Celsius, at site 1 in Fremont Lake, 1970–71*

Depth (meters)	T_{md}[1]	1970	1971[2]				
		July 21	May 9	May 12	May 17	June 16	Sept. 9
0.1	3.94	17.6	3.88	4.17	4.01	10.80	15.30
3	3.94	....	....	....	....	10.40	15.08
5	3.93	14.7	....	....	....	9.37	14.97
10	3.93	8.0	....	....	....	7.25	14.89
12	3.93	....	....	....	....	....	13.82
15	3.92	....	3.70	....	4.38	6.20	9.13
20	3.92	5.3	....	....	....	....	6.45
25	3.91	....	....	....	....	....	5.21
30	3.90	....	3.69	3.88	....	4.78	4.81
35	3.89	4.2	....	....	....	....	4.62
50	3.88	....	....	....	....	....	4.45
60	3.87	....	3.90	....	....	4.18	4.31
90	3.83	3.8	3.88	3.88	3.88	4.07	4.10
120	3.80	....	3.88	....	....	....	4.00
150	3.77	....	3.90	....	....	....	3.95
183	3.73	3.8	3.92	3.92	3.93	3.93	3.93

[1] From Strøm (1945). [2] Ice breakup occurred on May 13.

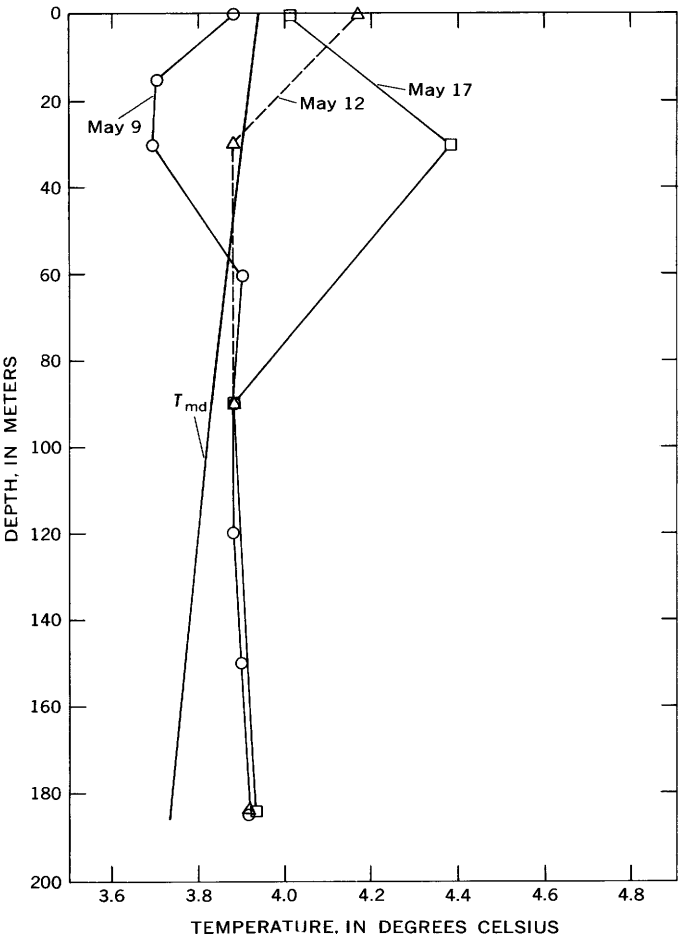

Figure 2.—Temperature curves at site 1, Fremont Lake, May 9–17, 1971 (data from Dunn, 1972).

Although the data coverage is scanty, the May 12 profile appears to closely approach the T_{md} between 30 and 90 m. Moreover, it is possible that more detailed sampling would have shown that the T_{md} was closely paralleled for much of the interval above 30 m. The important point is that, from May 9 to 17, the temperatures remained virtually unchanged at 90 m and below. Thus, vernal mixing was incomplete, extending to a depth of less than 90 m (perhaps only to about 60 m). As noted above, ice breakup on Fremont occurs during the relatively warm and calm weather of mid-May. Furthermore, steep slopes to the west and east reduce the exposure of the lake to strong winds. Apparently, in 1971, rapid warming of the upper strata quickly produced a stability so great that it prevented full vernal circulation.

The undisturbed water below 90 m probably maintained a temperature and density profile that closely reflected the conditions at fall overturn. The lake apparently circulated in late autumn or early winter at a temperature above that of maximum density for the lower depths. Strøm (1945) pointed out that when this occurs, a nearly isothermic curve will result downward from the point where the T_{md} was reached. The May 9 data show a nearly isothermic condition below 60 m.

However, the May 9 data do indicate a very slight increase in temperature below 90 m. The increase was also observed on May 12 and 17, but summer warming had erased it by June 16 (table 7). From the biological nature and depth of Fremont, it is very questionable that the higher bottom temperature resulted from either oxidation of sediments or internal heat of the earth. If either process was responsible, the bottom temperature should have increased significantly between May and September. In the absence of further data, no explanation can be given.

The stability of the lower half of the water column during May is noteworthy since the water at 90 m was more dense than that at the bottom. However, the actual differences in density were extremely small, apparently too small to overcome the shear resistance of the water and to cause rapid mixing.

The bottom temperature remained nearly constant from May 9 to September 9. In May, the temperature was momentarily fixed by the incomplete circulation and, throughout the summer, it was maintained by the considerable mean depth and depth development (table 2) of the lake.

The summer temperature profiles in Fremont are typical of those from a deep lake in a continental climate with cold winters and warm summers. Although representing two different years, the three curves in figure 3 exhibit changes of shape with time that are consistent with what would be expected for a given year. The June curve shows a moderately developed epilimnion with a gentle temperature gradient near the surface. In contrast, the July curve is typical of summer stagnation, with a layer of very warm surface water, less than 10 m thick, sitting abruptly upon the hypolimnion. By September the depth of mixing in the epilimnion extended to at least 10 m, lowering the position of the metalimnion and steepening its thermal gradient.

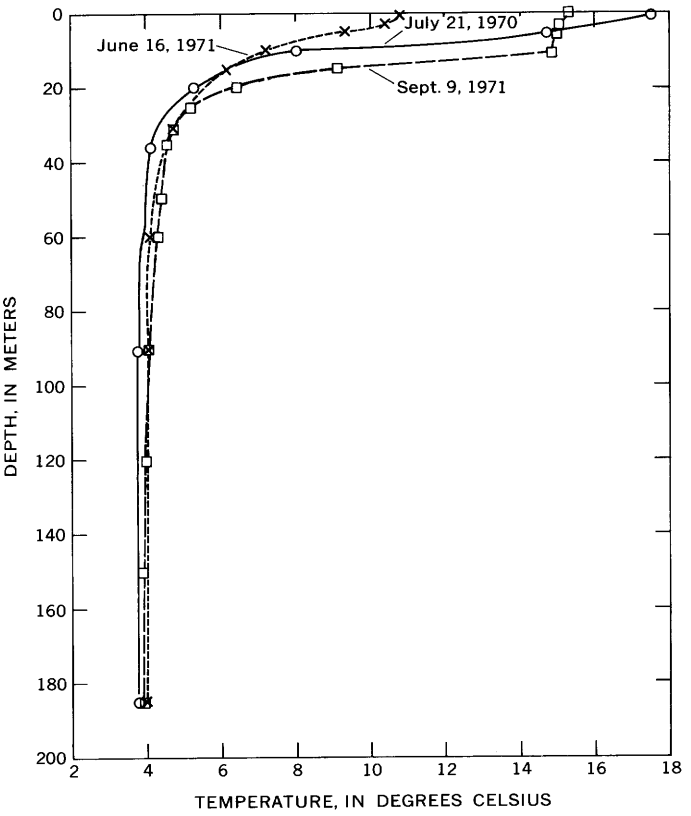

Figure 3.—Summer temperature curves at site 1, Fremont Lake, 1970–71.

Figure 4 shows the temperature profiles at sampling sites 1–3 (fig. 1) on July 21–22, 1970. Only reversing-thermometer data are plotted, but the curves are smoothed between points on the basis of bathythermograph traces. Profile 3 was to a bottom depth of 45 m, profile 2 to 120 m, and profile 1 to 183 m. Below about 30 m, the temperature curves tended to be slightly warmer in the order of decreasing profile depth. Other than this, there were no apparent trends in the curves which could be ascribed to location or depth of the profile.

The 1971 summer heat income (wind-distributed heat) was calculated for Fremont by difference (ΔT) between the May and September curves (figs. 2 and 3). The availability of the May 9 data made it possible to forgo the use of 4°C as the baseline for summer heating. While this data increased the accuracy of the determination, the lack of mid- to late-August data certainly lowered it. Both the temperatures and shape of the September curve indicated that the lake had already entered the period of surface cooling. However, although the heat loss was probably significant, the calculated summer heat income of 19,450 cal/cm^2 (table 8) should, nevertheless, be a good approximation.

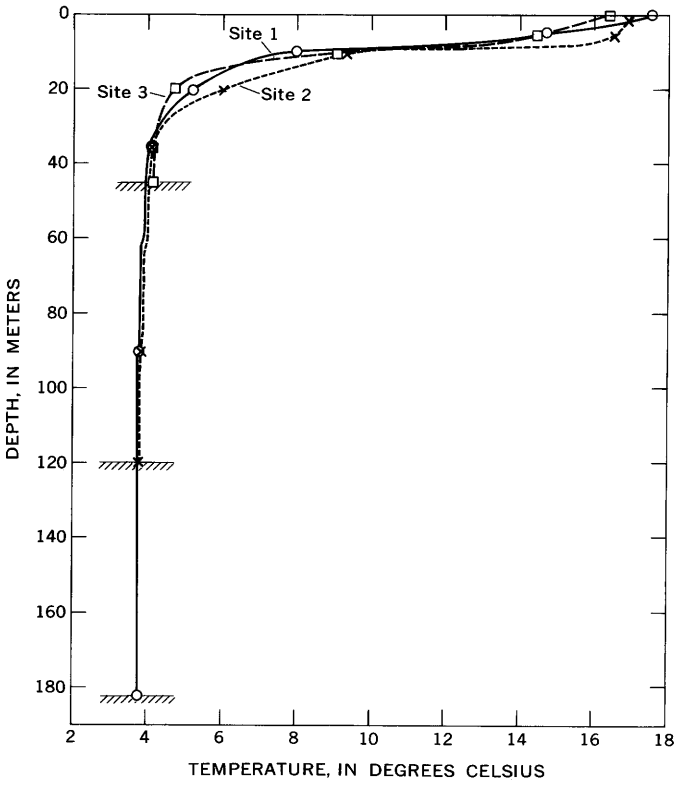

Figure 4.–Temperature curves at sites 1–3, Fremont Lake, July 21–22, 1970.

Table 8.–*Summer heat income, 1971, Fremont Lake*

Water layer (meters)	Mean increase in temperature May 9–Sept. 9 (°C)	Heat income (cal./cm²)	Percentage of total	
0–5	11.28	5,471	28	54
5–10	11.13	5,187	26	
10–15	8.28	3,691	19	28
15–20	4.09	1,726	9	
20–30	1.94	1,538	8	
30–60	.77	1,346	7	
60–90	.32	368	2	
90–120	.17	101	1	
120–150	.09	21	0	
150–183	.03	1	0	
0–183	.....	19,450	...	

As previously explained, spring heating in Fremont rapidly warms the upper strata, creating a stability so great that deep mixing by the wind is no longer possible. This manner of heating results in a relatively thin layer of warm water. During summer stagnation, the epilimnion and metalimnion are both roughly 10 m thick. It is expected, then, that most of the summer heat income would reside in the upper 20 m of the water column. The data clearly conform to expectation. The epilimnion (0–10 m) contains 54 percent (table 8) and the metalimnion (10–20 m) 28 percent, so the two together hold 82 percent of the summer heat income of the lake.

The total summer income of 19,450 cal/cm² is consistent with Hutchinson's (1957) data for temperate first-class lakes and excludes Fremont from the "mountain lake" category of Strøm (1938), who defined a high mountain lake as one with a heat budget markedly below what a comparable lake would have at sea level. In Norway, an approximate 50-percent reduction was noted at lat 61°–62°N., at altitudes in excess of 800 to 1,000 m. In the Rocky Mountains, Rawson (1942) found a comparable reduction for Lake Maligne at lat 52°40′ N. and altitude 1,663 m, while lakes at 49°–51° and up to 1,454 m exhibited normal incomes. Fremont Lake, at 2,261 m, is apparently located far enough south (42°57′) to protect it from the altitudinal effect.

Secchi disk transparency

Secchi disk readings were made at sites 1–3 and at various additional locations on July 21–22, 1970. The transparencies were nearly identical at about 9 m throughout the entire lake. A 9-m value is indicative of clear water and is within the range of 8 to 13 m found by Rawson (1942) in unsilted large alpine lakes of the Canadian Rocky Mountains.

CHEMISTRY

Dissolved oxygen

The vertical oxygen distribution (table 9) in Fremont is characteristic of oligotrophic conditions. The dissolved-oxygen (DO) concentration curve at site 1 (fig. 5) is orthograde, with a slight metalimnetic maximum (positive heterograde tendency) and small decreases below 90 m and in the warm surface layers. The corresponding percentage saturation curve shows supersaturation in the epilimnion and in the upper part of the metalimnion, slight undersaturation between 20 and 90 m, and a decrease to 80 percent at 180 m.

Besides general oligotrophic conditions, the basic form of the vertical distribution reflects a very short and, perhaps (as in 1971), incomplete vernal circulation, and slight oxygen depletion at depth. The oxygen deficit undoubtedly resulted from oxidation of organic matter, most likely within the water

Table 9.–*Dissolved oxygen in Fremont Lake, July 21–22, 1970*

	Site					
	1		2		3	
Depth (meters)	mg/l	Percentage saturation	mg/l	Percentage saturation	mg/l	Percentage saturation
0.1	7.7	106	7.9	107	7.9	106
5	8.4	108	7.9	106	8.6	110
10	9.8	108	9.0	103	9.7	110
20	9.3	97	9.2	97	9.7	99
35	9.0	91	8.8	89	9.2	92
45	...	...	...	...	9.1	91
90	8.9	88	8.8	88	...	...
120	...	...	8.6	86	...	...
180	8.0	80	...	...	...	...

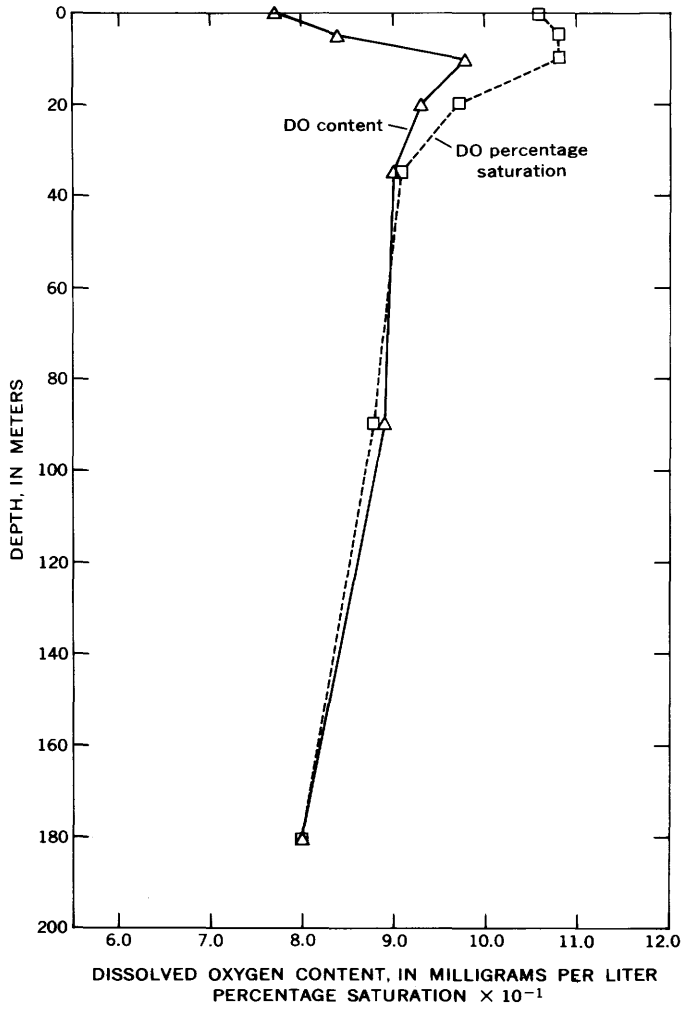

Figure 5.—Dissolved-oxygen concentration and percentage saturation at site 1, Fremont Lake, July 21, 1970.

column as well as in the bottom sediments. Although much of the deficit probably developed during summer, a considerable part may have been inherited from the previous winter. In fact, the slight undersaturation between 20 and 90 m may have resulted largely from a winter deficit which remained, in part, when the rapid onset of thermal stratification prevented sufficient turbulent exchange for complete reoxygenation below 15 m. In contrast, provided that vernal mixing was incomplete and to the same depth as in 1971, the somewhat greater deficit below 90 m represented the total oxygen depletion from the time of the last complete circulation.

The supersaturation in the upper 5 m is thought to be primarily the result of heating which occurred too close to the time of sampling to permit DO equilibration. The analyses were made on bright, warm, very calm days.

Physical causes alone, however, would seem insufficient to have caused the high DO content and supersaturation at 10 m. It is probable that the clarity of the water led to a net biological production of oxygen in the metalimnion. Yoshimura (1938) stated that if the compensation point lies within the metalimnion, a positive heterograde curve may be expected. He defined the compensation point as roughly 1.2 times the Secchi disk transparency. In Fremont Lake, this point would be about 11 m, so the fit of data to Yoshimura's hypothesis is excellent.

Ionic constituents and dissolved solids

The water in Fremont Lake was higher in mineral content than the inflow from Fremont River when sampled in July 1970. In comparing the composition of the inflow with that of the surface water at site 1 (table 10), the increase among conservative cations and anions varies from 0 percent for potassium to 64 percent for calcium. Probably the single best indicator is dissolved solids (DS), which increases 22 percent from 9 to 11 mg/l.

The DS content of the lake water, however, increases with depth (table 10; fig. 6). To determine the approximate mean content, the DS-depth distribution at site 1 was related to percentage of lake volume for the sampled depths. A DS value of 13 mg/l was assumed at 180 m on the basis of the depth profile relationships of DS and specific conductance. It was also assumed that DS stays at 12 mg/l to a depth of 20 m. The resultant mean content of DS is 12.8 mg/l, which is about 40 percent greater than in Fremont River.

The magnitude of this difference strongly suggests that the sampled inflow was more dilute than the average inflow from Fremont River. This possibility is consistent with observed DS values <13 mg/l being only in the isolated (by thermal stratification) upper 10 m of the lake (table 10; fig. 6). Further credence is lent by the fact that June and July are the months of high flow in Fremont River (table 4), and by the DS content of 12 mg/l in the lake outflow.

The factors suggest that inflow more dilute than average was passing through the upper strata of the lake, with only slight mixing with the water below. This hydraulic pattern inferred from chemical evidence, would, of course, be expected purely on the basis of temperature-induced differences in density. The river temperature was 13°C, so the inflow density was about equal to the density of water at the 6- to 9-m depth (fig. 4) in the lake.

The mean DS content of 12.8 mg/l is remarkably low for so large a lake. Lower DS contents and ion concentrations have been reported for certain lakes in northeastern Wisconsin (Juday and others, 1938) and in the Adirondack region of New York (Berg, 1963). Comparable and slightly higher values occur in some lakes in the Sierra Nevada of California (Reimers and others, 1955), in the Rocky Mountains of Colorado (Pennak, 1958), and in the Pine Barrens of New Jersey (Berg, 1963). However, Fremont is larger in area than all of the noted lakes by 1 to 2 orders of magnitude.

In arctic Alaska, the major-ion contents in Peters, Schrader, and several smaller lakes are low, but all are, nevertheless, considerably greater than in Fremont (Brown and others,

Table 10.—*Chemistry of Fremont Lake, the inflow, the outflow, and a nearby beaver pond, July 21–22, 1970*

[Data in milligrams per liter, except as noted]

Parameter	Fremont River inflow	Fremont Lake, site 1						Pine Creek outflow	Beaver pond[1]
		Depth in meters							
		0.1	5	10	35	90	180		
Calcium	1.4	2.3	2.3	2.3	2.3	2.5	2.4	2.2	12
Magnesium	.2	.3	.3	.3	.3	.3	.3	.3	6.2
Sodium	.5	.6	.7	.6	.6	1.0	...	.6	7.3
Potassium	.4	.4	.4	.4	.4	.4	...	.5	2.1
Iron	.00	.00	.00	.00	.00	.00	.02	.02	.19
Manganese	.00	.00	.00	.00	.00	.00	.00	.00	.00
Ammonia (as N)	.16	.09	.08	.07	.03	.05	...	.10	.17
Bicarbonate	7	9	9	9	10	9	...	9	81
Sulfate	1.2	1.6	2.0	2.2	2.2	2.1	...	2.0	4.0
Chloride	.2	.3	.3	.4	.3	.4	...	.3	.5
Fluoride	.1	.1	.1	.0	.1	.1	...	.1	1.0
Nitrate (as N)	.05	.02	.02	.02	.02	.02	...	.02	.14
Phosphate (as P)	.003	.003	.003	.003	.003	.003	...	.003	.033
Silica	1.1	1.1	1.1	1.3	1.5	1.5	...	1.1	.2
Organic nitrogen	.05	.02	...	.00	.01	.04	...	.00	.67
Sum of nitrogen forms	.26	.13	...	.09	.07	.11	...	.12	.98
Total organic carbon	2	1	...	2	1	1	1	2	13
Total hardness (as $CaCO_3$)	6	8	8	8	8	8	8	8	56
Dissolved solids	9	11	12	12	13	13	...	12	74
Specific conductance (μmhos/cm at 25° C)	13	18	19	19	20	21	21	19	138
pH	7.0	7.4	7.4	7.5	7.1	7.1	7.1	7.3	8.5

[1] For location, see site 12, figure 8.

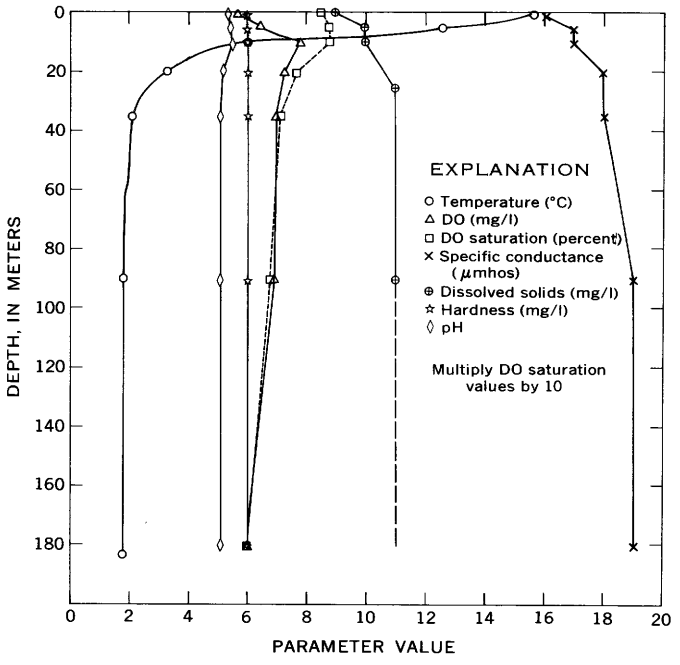

Figure 6.—Temperature and chemistry of the water column at site 1, Fremont Lake, July 21, 1970.

1962). Among larger well-known lakes, Lake Tahoe and Crater Lake, which are noted for their lack of dissolved solids, have DS contents in the range of 60–80 mg/l (Crippen and Pavelka, 1970; Edmonson, 1963). In Canada, the part of Great Slave Lake receiving drainage from the Precambrian shield has a DS content ranging between 22 and 82 mg/l (Northcote and Larkin, 1963). Great Bear Lake, astride the margin of the shield, and Lake Athabaska, almost entirely within the shield, have DS contents of 98 and 58 mg/l, respectively.

Relatively smaller lakes wholly within the Precambrian area exhibit even lower values; the DS contents in Cree and Wollaston are 32 and 31 mg/l, respectively (Rawson, 1951). Lake Superior, with much Precambrian drainage, is listed by Livingstone (1963) as having a DS content of 82.5 mg/l. In Wyoming the DS content of Yellowstone Lake is 55 mg/l, while the content in Jackson Lake is 104 mg/l (U.S. Park Service, written commun., 1972).

In North America, the most dilute large lakes reported to date are in northern New England and Oregon. Lake Winnipesaukee, N.H., has an area of 180 km^2 and a DS content of 18–21 mg/l (Brooks and Deevey, 1963). Even more striking is Moosehead Lake in Maine with an area of 331 km^2 and a DS content of only 16 mg/l. In the Cascade Mountains of Oregon, Odell Lake has a surface area of 14.4 km^2 and a DS content between 25 and 28 mg/l (Larson, 1970). The most remarkable of all, however, is nearby Waldo Lake, which, with a surface area of 25.1 km^2, has a DS range of 2–5 mg/l (Larson, 1970; Larson and Donaldson, 1970). These extremely low values for Waldo, together with the documented presence of *Sphagnum* moss, suggest that peat may be decreasing the ionic content of the water below that in atmospheric precipitation. The removal of salts from water by *Sphagnum* has been noted by several authors (Bell, 1959; Gorham, 1961; Ruttner, 1963); the primary mechanism appears to be ion exchange with release of hydrogen ions.

Thus, although Fremont Lake is not as dilute as Waldo Lake, its low DS content in relation to its large size and drainage area makes it a very remarkable lake. On a worldwide basis, Fremont and Waldo can be thought of as belonging to a special class of large, ultradilute lakes which includes the Nordfjord Lakes of Norway (Strøm, 1933).

Because the ionic concentrations in Fremont Lake are so low, it is of interest to compare the values to those in precipitation. Table 11 was compiled from the data of Junge and Werby (1958) and from the calculated mean content in Fremont Lake of the five selected ions. The precipitation data represent 1 year's average values from July 1955 through July 1956 for western Wyoming.

Column 4 of table 11 gives the concentration differences between lake water and precipitation, while column 5 shows the percentage of each ionic concentration in the lake that can be attributed to precipitation. If the values of Junge and Werby are representative of long-term composition, precipitation accounts for one-fourth of the sodium and potassium, one-third of the chloride, nearly one-half of the calcium, and over three-fourths of the sulfate in Fremont Lake.

Thus, on the basis of percentages, it appears that precipitation composition determines a considerable part of the major-ion chemistry of Fremont Lake. Further support for this conclusion is provided by the general similarity between the ionic ratios in lake water and precipitation (table 11, col. 7 and 8).

Water, as it moves through a drainage basin, is subject to changes in composition through the processes of solution, precipitation, physiochemical exchange, and biochemical uptake and release. Solution and biochemical release are the two processes most responsible for increases in mineral content. In Fremont Lake, low rates of these processes are the probable cause of the low content of DS. The low rates in turn can be attributed to three major drainage basin characteristics.

First, the general rate of solution is low because the basin is composed of highly insoluble crystalline rocks (See p. D173). Second, the glaciations which created the lake have scoured the entire basin, leaving it devoid in many places of soil and loose materials. The reduced surface area available for contact between water and minerals further slows the rate of solution. Moreover, the paucity of soil mantle greatly limits the growth of vegetation and, hence, the release of acids from the decay of organic matter. This results in very limited direct biological contributions to DS, and even more important, in little acidity to be applied to mineral solution. Third, temperatures and precipitation are quite low in the basin (table 5), further acting to slow the rates of all chemical and biochemical reactions.

Thus, conditions in Fremont Lake basin are conducive to low rates of solution and biochemical release. The low ionic content of the water is a reflection of these conditions, together with the fairly recent exposure (9,000 years ago) of the surface materials.

Calcium was the dominant cation and bicarbonate the dominant anion in all of the tested samples. At the 0.1-m depth, the concentration order of cations, on a weight basis, was calcium>sodium>potassium>magnesium. However, expressed as milliequivalents per liter, the order was calcium>sodium>magnesium>potassium. The anion order was bicarbonate>sulfate>chloride, regardless of the manner of expression.

Hardness computed from the calcium and magnesium contents averaged about 7 mg/l. In contrast, the field results, as determined by EDTA titration (total hardness), averaged 8 mg/l (table 10), a difference attributed to poor sensitivity of the field analyses.

Similarly, laboratory bicarbonate results (table 10) are slightly lower than the field-determined values (table 12). Values determined at the time of sampling would generally be accepted as the more accurate. However, at Fremont Lake, field alkalinity was determined by colorimetric titration, rather than by the inherently more accurate potentiometric method. Moreover, for such dilute water, there is probably little change in alkalinity between time of collection and laboratory analysis. Thus, the laboratory results are viewed as being more accurate in this study and were the ones used to calculate DS. The field values are used only to show the lakewide distribution of alkalinity with location and depth.

The ionic composition and specific conductance of the lake surface water was nearly identical with Rodhe's (1949) most

Table 11.—*Comparison of the content of selected ions in Fremont Lake and precipitation*

Ion	Concentration (mg/l)		C_l–C_p[2] (mg/l)	Percentage contribution of precipitation
	Lake	Precipitation[1]		
Ca^{+2}	2.3	1.0	1.3	44
Na^{+}	.8	.2	.6	25
K^{+}	.4	.1	.3	25
Cl^{-}	.3	.1	.2	33
SO_4^{-2}	2.2	1.8	.4	82
Total	6.0	3.2	2.8	

Parameter	Ratio	
	Lake	Precipitation
Cl^{-}/Na^{+}	0.4	0.5
K^{+}/Na^{+}	.5	.5
Ca^{+2}/Na^{+}	2.9	5.0
SO_4^{-2}/Cl^{-}	7.3	18.0

[1] Estimated from the concentration diagrams of Junge and Werby (1958).
[2] C_l-C_p = Concentration difference between Fremont Lake water (C_l) and precipitation C_p.

Table 12.—*Field-parameter chemistry of the water column, Fremont Lake, July 21–22, 1970*

Depth (meters)	pH Site			Bicarbonate alkalinity (mg/l) Site			Hardness (mg/l) Site			Specific conductance (μmhos/cm at 25°C) Site		
	1	2	3	1	2	3	1	2	3	1	2	3
0.1	7.4	7.5	7.3	11	11	11	8	8	7	18	18	18
5	7.4	7.6	7.3	11	10	11	8	8	8	19	18	19
10	7.5	7.5	7.4	11	11	11	8	8	7	19	18	20
20	7.2	7.2	7.2	10	11	11	8	8	8	20	20	20
35	7.1	7.1	7.2	11	10	11	8	8	8	20	20	20
45	...	...	7.2	...	...	11	...	...	8	...	...	21
90	7.1	7.1	...	11	11	...	8	8	...	21	21	...
120	...	7.1	...	...	11	...	...	8	...	...	21	...
180	7.1	...	...	11	...	...	8	...	...	21	...	...

dilute hypothetical bicarbonate water (bicarbonate converted to carbonate). The major difference was the considerably lower (0.3 versus 0.7 mg/l) chloride content in Fremont Lake.

The ratios of DS to specific conductance were very similar through the entire system. The ratio was 0.69 in Fremont River and 0.63 in Pine Creek, and it ranged randomly from 0.61 to 0.65 at different depths in the lake.

Iron and manganese concentrations were consistently low. The manganese content was below the sensitivity (0.01 mg/l) of the analytical technique in each sample. Iron was detected only twice; concentrations of 0.02 mg/l were found at 180 m in the lake and in Pine Creek below the lake. The low concentrations of iron and manganese probably resulted from a combination of (1) an iron-poor geologic environment, (2) complete lack of anaerobic conditions, and (3) a paucity of organic matter to function as a chelator. The last is important, of course, because inorganic iron and manganese are highly insoluble in well-oxygenated water.

The concentrations of silica were also low. Values ranged from 1.1 to only 1.5 mg/l within the lake and were 1.1 mg/l in the influent and effluent.

Field parameters

The vertical distributions of pH, alkalinity, hardness, and specific conductance were determined by field analyses at sites 1–3 (table 12; fig. 6). Alkalinity and hardness were strikingly consistent and showed no trends with location or depth. Alkalinity was recorded as 11 mg/l in 17 of 20 samples, while hardness was 8 mg/l in 18 out of 20.

In contrast, pH and specific conductance exhibited slight, but definite, trends with depth. Conductance increased with depth from 18 to 21 μmhos/cm at 25°C at each site. In each profile the reading increased to 20 μmhos at 20 m and to 21 μmhos at 45 or 90 m. Data for site 1 (table 10) show that the rise in conductance from 18 μmhos at 0.1 m to 20 μmhos at 35 m corresponded to a DS increase from 11 to 13 mg/l. The apparent chemical stratification undoubtedly resulted from the noted inflow dilution (see p. D180).

The pH values were more consistent than might have been expected for so dilute a water. In each profile the values exhibited a tendency toward a maximum of 7.5–7.6 between 5 and 10 m, and then a decrease to a value of 7.1 at 90 m and below. The close correspondence between the pH and DO curves near the surface (fig. 6) suggests that both are controlled by photosynthesis.

Major nutrients

The concentrations of nitrogen and phosphorus in solution are known to fluctuate with biological activity. Thus, strictly speaking, the phosphorus and nitrogen results determined for Fremont cannot be considered representative of a standard condition of the water column. As will be seen, however, most of the results are consistent with the low values found in other dilute alpine lakes of the United States.

In Fremont Lake the concentration of PO_4-P was 0.003 mg/l throughout the water column (table 10). In the Colorado Rocky Mountains, Pennak (1958) surveyed 12 dilute lakes and found that the PO_4-P content at the surface ranged from 0.001 to 0.009 mg/l, with an average of 0.0029. Reimers, Maciolek, and Pister (1955) determined middepth PO_4 concentrations for lakes of the Convict Creek basin of the California Sierra Nevada. The results, expressed as PO_4, were <0.01 mg/l (<0.003 mg/l as P) in six of the 10 lakes, and were 0.02, 0.04, 0.06, and 0.07 mg/l in the remaining four. In Waldo Lake, in the Oregon Cascades, the PO_4-P result for one sample near the surface was <0.01 mg/l (Larson and Donaldson, 1970).

Among the nitrogen species, nitrate alone exhibited the same concentration at all depths, 0.02 mg/l NO_3-N. This value corresponds very closely to the results of Reimers, Maciolek, and Pister (1955) in the Sierra Nevada. Expressing the results for the 10 lakes in terms of NO_3-N (NO_3 content was reported) gives a range of 0.009 to 0.43 mg/l, with an average of 0.020 mg/l. In Pennak's (1958) Rocky Mountain lake study, the NO_3-N content ranged from 0.009 to 0.181 mg/l, and the average of 12 samples was 0.063 mg/l.

Larson and Donaldson (1970) reported a NO_3-N value of 0.11 mg/l for Waldo Lake. This value seems too high for such extremely dilute water; an unpublished analysis (Oct. 9, 1969, district office, U.S. Geol. Survey, Portland, Oreg.)

shows the content, reported as NO_3, to be 0.0 mg/l (sensitivity of test was 0.1 mg/l).

The NH_3-N results for Fremont varied with depth from 0.03 to 0.09 mg/l. The average of the six values was between 0.06 and 0.07 mg/l. These concentrations were higher than those found by Reimers, Maciolek, and Pister (1955) and by Larson and Donaldson (1970). In the Convict Creek basin, the 10 NH_3-N values ranged from 0.016 to 0.052 mg/l, with an average of 0.026 mg/l. In Waldo Lake, the single NH_3-N determination gave a result of <0.01 mg/l.

The organic nitrogen results in table 10 were determined as the difference between total Kjeldahl nitrogen and ammonia nitrogen. The values varied with depth and ranged from <0.00 to 0.04 mg/l. Taking the lower value as 0.00 mg/l gives an average concentration of about 0.02 mg/l.

Unfortunately, no organic nitrogen data on dilute alpine lakes could be found for comparison. However, in a wide array of nondilute lakes, the organic nitrogen has been found to account for a large proportion of the total nitrogen, regardless of the trophic state (Hutchinson, 1957; Brezonik and others, 1969; Lueschow and others, 1970). Furthermore, in Fremont, organic carbon was detected in low, but definite, amounts at each depth. The precision of the total organic carbon (TOC) determination at the level of 1–2 mg/l is about 0.5 mg/l. If precision is disregarded, however, and all results are accepted at face value, C/N ratios for the depth profile would be 50:1 at 1 m, >200:1 at 10 m, and 100:1 and 25:1 at 35 and 90 m. It is obvious, except for the value of 25:1, that the ratios are much too high. Even if the organic matter were entirely of allochthonous nature, the ratios should be no greater than 45–50:1 (Hutchinson, 1957). Indeed, in water of such low organic content, the organic matter should be primarily of autochthonous nature, with C/N ratios in the range of 10–15:1.

Thus, on the basis of both nitrogen proportions and C/N ratios, it appears that the organic nitrogen results are low. Several explanations can be advanced for this observation, and they include: (1) Chloroform preservation was inadequate and some organic nitrogen was converted to ammonia nitrogen, (2) the organic nitrogen content of the ultradilute water was very low and did not account for a large proportion of the total nitrogen content, (3) the Kjeldahl nitrogen procedure (micro Kjeldahl-Nesslerization detection) lacked the sensitivity and precision to determine the low concentrations (<0.1 mg/l) of organic nitrogen, and (4) combinations of 1, 2, and 3.

Several authors have discussed the deficiencies of chloroform as a preservative for nutrients (Fitzgerald and Faust, 1967; Lee, 1969). Nevertheless, the method is still widely used for situations where prompt analysis or freezing of samples is impossible. The lake data in table 10 show higher concentrations of ammonia nitrogen than reported in previous dilute-water studies. While these results support explanation 1, the nitrogen data from the beaver pond sample (table 10, col. 10) suggest otherwise. The pond sample was collected, preserved, transported, and analyzed exactly as the lake and stream samples.

In contrast with the lake, the pond was nondilute and had a DS content of 74 mg/l. The pond water exhibited a visual abundance of algae and aquatic insects, and contained a large amount of total particulate matter. Analyses showed an organic nitrogen content of 0.67 mg/l, giving a ratio of NH_3-N to organic nitrogen of 0.25 and a C/N ratio of 19:1. These values suggest that the chloroform may have adequately preserved the sample; if so, the lake samples should also have been stabilized. In fact, stabilization would theoretically be more certain for the lake samples with their drastically lower contents of organisms and total particulate matter. However, the pond water data certainly do not preclude the possibility that some small amount of organic nitrogen was converted to NH_3-N. A small amount of conversion could conceivably have occurred without detection in the pond samples, while a similar change in the lake samples could have created the noted discrepancies. Thus, without further testing, explanation 1 remains a possibility.

Recent studies on dilute streams in Alaska (K. V. Slack, oral commun., 1972) have given nitrogen results very similar to those for Fremont Lake. The Alaskan samples were preserved with $HgCl_2$, (40 mg Hg^{+2}/l) rather than with chloroform, and the organic nitrogen was determined by the Kjeldahl-Nesslerization method. Organic nitrogen results of <0.00 mg/l were obtained on samples with NO_3-N contents ranging between 0.20 and 0.50 mg/l, NH_3-N contents between 0.17 and 0.50 mg/l, and concentrations of TOC from 3 to 5 mg/l.

The Fremont and Alaskan data could be explained by a combination of explanations 2 and 3. If the water actually contained only trace quantities of organic nitrogen, the analytical procedure may have been inadequate. Further study is needed on the determination of extremely low levels of organic nitrogen and, equally important, on the possibility that organic nitrogen may not account for a large part of the total nitrogen in ultradilute waters.

Within the lake the sum of the three nitrogen forms varied from 0.07 mg/l at 35 m to 0.13 mg/l at 0.1 m. In comparison, the sum in the effluent stream was 0.12 mg/l, but the value in Fremont River was 0.26 mg/l. The relationship of all these values suggests that Fremont Lake acts as a nitrogen trap or accumulator. In contrast, the concentration of total PO_4-P was 0.003 mg/l in the influent, the effluent, and at all sampled depths within the lake. The consistency of these values suggests that phosphorus is not being trapped. However, in relation to the large volume of the lake, the grab-sample results are far from conclusive evidence for either observation.

Pesticides

The one pesticide sample showed the presence of DDT at the concentration of 0.01 mg/l, while aldrin, DDD, DDE, dieldrin, endrin, heptachlor and lindane were not detected.

There is no agriculture within the basin, and most of the land is part of Bridger National Forest. The probable source of DDT is precipitation from wind currents which carry the material from areas of application.

BIOLOGY

Net plankton

Net-plankton samples were collected at four sites on the afternoon of August 14, 1969. Because of the one-time sampling, and the fact that net plankton are a small fraction of the total population, the results represent only a preliminary survey.

The net plankton included representatives of seven genera of phytoplankters and three genera of zooplankters. The total list is as follows:

Phytoplankton	Zooplankton
Bacillarieae:	Copepoda:
Asterionella sp.	*Cyclops* sp.
Fragilaria sp.	
Navicula sp.	Cladocera:
Synedra sp.	*Daphnia pulex*
Tabellaria sp.	
	Rotatoria:
Chlorophyceae:	*Keratella* sp.
Staurastrum sp.	
Myxophyceae:	
Nostoc sp.	

The distribution of net plankton by station and depth interval is presented in table 13. Diatoms made up 93 percent of the phytoplankton count, with *Fragilaria* sp. alone accounting for 46 percent. Pennak (1955) noted an abundance of *Fragilaria* sp. in the mountain lakes of Colorado. Among the zooplankton, *Cyclops* sp. and *Daphnia pulex* were codominant, with *Keratella* sp. only 19 percent of the count.

The desmid *Staurastrum* sp. and the blue-green algae *Nostoc* sp. were the only representatives of the Chlorophyceae and Myxophyceae, respectively. Both of these forms were low in abundance.

As shown in figure 1, plankton sampling stations 4 and 5 are in the south subbasin of Fremont Lake, while stations 6 and 7 are in the north subbasin. Comparison of the mean distribution of organisms between stations shows that the values were markedly higher at the north subbasin sites. In the 0- to 3-m interval the respective counts at stations 4 and 5 were 48,000 and 75,000 organisms per liter. In contrast, the corresponding counts at sites 6 and 7 were 102,000 and 96,000. Similar variation with location occurred in the two depth intervals between 3 and 30 m, but the trend was not observed between 30 and 45 m. Thus, if the counts are summed for the 0- to 30-m depths (which is analogous to a comprehensive vertical tow from 30 m), the distribution by station becomes 44,000 and 37,000 organisms per liter for stations 4 and 5, 66,000 at 6, and 95,000 at 7.

A striking decrease in plankton count also occurred with depth. The mean distribution of organisms by depth interval

Table 13.—*Net-plankton count distribution in Fremont Lake, August 14, 1969*

Genus	Plankton count (thousands per liter)				
	Stations				
	4	5	6	7	
Depth 0–3 m					
Asterionella	...	3	3	6	
Fragilaria	30	24	54	45	
Navicula	6	21	15	18	
Synedra	...	18	21	12	
Tabellaria	9	...	...	3	
Staurastrum	...	...	...	...	
Nostoc	...	...	6	...	
Cyclops	3	3	3	3	
Daphnia pulex	...	6	...	9	
Keratella	...	...	...	...	
Interval subtotals	48	75	102	96	
Mean plankton count per station					80
Percentage of plankton in this depth interval					34.6
Depth 3–15 m					
Asterionella	5	2	10	23	
Fragilaria	28	12	18	3	
Navicula	...	10	15	2	
Synedra	9	...	4	23	
Tabellaria	5	...	...	2	
Staurastrum	4	3	2	3	
Nostoc	...	2	2	15	
Cyclops	4	4	...	5	
Daphnia pulex	5	1	3	3	
Keratella	...	...	...	...	
Interval subtotals	60	34	54	79	
Mean plankton count per station					57
Percentage of plankton in this depth interval					24.7
Depth 15–30 m					
Asterionella	...	1	5	21	
Fragilaria	18	10	18	25	
Navicula	7	8	20	15	
Synedra	...	...	15	20	
Tabellaria	4	...	...	3	
Staurastrum	...	3	4	4	
Nostoc	...	2	3	2	
Cyclops	1	3	...	7	
Daphnia pulex	...	2	2	6	
Keratella	...	2	2	4	
Interval subtotals	30	31	69	107	
Mean plankton count per station					59
Percentage of plankton in this depth interval					25.5
Depth 30–45 m					
Asterionella	5	...	...	...	
Fragilaria	21	20	29	26	
Navicula	2	3	...	...	
Synedra	...	...	...	...	
Tabellaria	6	7	4	5	
Staurastrum	...	...	...	...	
Nostoc	...	...	3	...	
Cyclops	...	...	...	...	
Daphnia pulex	...	...	...	...	
Keratella	3	2	4	...	
Interval subtotals	37	32	40	31	
Mean plankton count per station					35
Percentage of plankton in this depth interval					15.2

shows that the 0- to 3-m zone contained 34.6 percent of the total, the 3- to 15-m and 15- to 30-m zones 24.6 and 25.6 percent, respectively, and the 30- to 45-m zone only 15.2 percent (table 13).

The zooplankters *Cyclops* sp. and *Daphnia pulex* were present in about the same total abundances in each of the three intervals through 30 m but were absent in the 30- to 45-m zone (table 13). In contrast, *Keratella* was only found in the two zones below 15 m.

It is difficult to compare the plankton data to results from other alpine lakes. One problem is the uniqueness of Fremont Lake as to size and content of dissolved materials in relation to other alpine lakes which have been studied in North America. A second problem results from use of a net for sampling. A third difficulty, of course, is that the data represent a limited, one-time sampling. However, even in the absence of direct comparison, the total of 10 genera and the magnitude of the counts seem to be very low.

Bacteriological reconnaissance

From the preceding sections it can be seen that Fremont is a pristine lake. With the exception of wind-carried DDT, the chemical and biological data indicate that man, so far, has not contaminated the water. However, bacteriological data are sometimes a more sensitive indicator of contamination than general chemical water quality and plankton counts. Moreover, the Bridger National Forest campground and the Sylvan Bay summer-home community are sources of human wastes which could pollute the lake.

To test for human contamination in the lake and in the small streams which drain the man-used areas, a bacteriological reconnaissance was conducted on July 15 and 16, 1970. Twenty-four samples were analyzed for total coliform organisms, and eight of these samples were also analyzed for fecal coliform and fecal streptococci organisms. Sample locations are indicated in figure 7, and the results are presented in table 14.

Samples 1–9 were taken from Fremont Lake at sites just off the east and south shorelines. All of the samples, with the exception of sample 6, showed either zero or very low total coliform counts. Likewise, the fecal coliform and fecal streptococci counts were very low.

Waters intended for contact sports, such as swimming, carry stringent recommendations for bacteriological standards. For this class of waters, the report of the Committee on Water Quality Criteria (Federal Water Pollution Control Adm., 1968) recommended a fecal coliform criterion. The suggested maximum permissible level is a log mean of 200 per 100 ml of water based on no less than five samples from within a 30-day period. More specifically, with regard to the Green River Basin, which includes Fremont Lake, the Wyoming Department of Public Health (1968) set a maximum permissible fecal coliform most probable number on a one-sample basis of 750 per 100 ml.

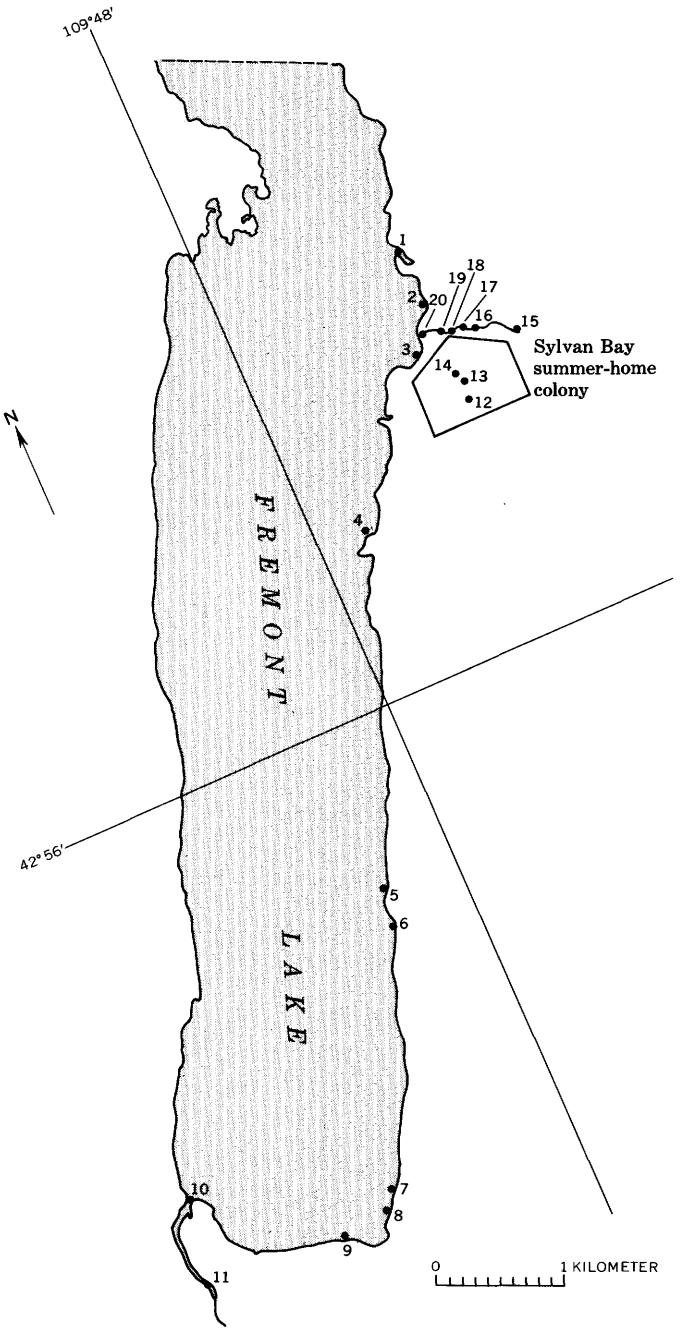

Figure 7.—Bacteriological sampling sites, Fremont Lake and vicinity, July 15–16, 1970.

Thus, on an absolute basis and in relation to criteria, the level of bacterial contamination in Fremont Lake is either zero or extremely low. The results for sample 6 indicate a significant coliform count, but the absence of fecal coliforms and fecal streptococci indicate that these may be from nonfecal sources (Geldreich, 1966). The origin of the bacteria in this sample is, therefore, uncertain.

Samples 7 and 8 were taken at points in the vicinity of U.S. Forest Service campground privies, while sample 9 was

Table 14.—*Bacteriological analyses*

Sample No.	Total coliform per 100 ml	Fecal coliform per 100 ml	Fecal streptococci per 100 ml
East and south shore of Fremont Lake			
1	0	([1])	...
2	0	...	...
3	0	...	...
4	0	1	2
5	0	...	...
6	29	0	...
7	2	...	...
8	2	...	...
9	3	4	2
Pine Creek			
10	0	0	0
11	4	7	2
Ponds and pond drainage			
12	0	...	...
13	0	...	...
14	79	...	...
Creek fed by spring drainage			
15	0	...	...
16	79	...	...
16a[2]	63	83	2
17	57	...	...
18	54	...	...
19	>80	...	...
19a[2]	60	49	4
20	>80	...	...
20a[2]	>80	>80	>80

[1] Not determined.
[2] Sampled on July 16, 1970. All other samples were collected on July 15, 1970.

collected near the pier of a boat rental establishment. In relation to criteria these samples were not polluted. However, these south-shore samples did show the presence of measurable total coliform colonies, while, excepting sample 6, no counts were obtained in the east-shore samples.

Samples 10 and 11 were taken from Pine Creek, the first just below the spillway and the second from a point near the water intake of Pinedale. The results are probably indicative of negligible contamination in Pine Creek. However, since there is some evidence for the presence of fecal coliforms and fecal streptococci at the water inlet, this site should undergo more extensive testing.

Off the lake, two abandoned beaver ponds and two streams were tested in the area of the Sylvan Bay summer-home colony (fig. 7; table 14). Sample 12 came from the larger of the ponds (see beaver pond, table 10), while samples 13 and 14 were taken from the smaller pond and from a stream about 300 feet below. Coliform bacteria were not present in either of the ponds. In contrast, sample 14 indicated significant contamination in the stream. Several summer residences built at or just below the level of the little pond may have contributed septic-tank effluent or pit-privy leachate just above the sampling site.

The water supply for the Sylvan Bay colony comes from a spring located upslope from the residential area. Excess flow from this spring and perhaps other springs and seeps eventually unites to produce a small, rapidly flowing creek which empties into Fremont Lake just north of the Sylvan Bay picnic area. The creek was sampled at six sites on July 15 and resampled at three of the sites on July 16 (fig. 7; table 14).

These results show that the spring was uncontaminated, but that the creek in the area adjacent to the summer-home colony was polluted with fecal bacteria. Unfortunately, the ratio of fecal coliforms to fecal streptococci failed to provide definitive information (Geldreich, 1966) on whether the bacteria were of human or of nonhuman origin. Moreover, animal droppings were evident in the area. More thorough sampling will be required to determine the major source of contamination.

CONCLUSION

Fremont Lake, the seventh deepest lake in the conterminous United States, has a remarkably low content of DS in relation to its size and drainage area. The dilute nature of the water, together with preliminary biological data, show that Fremont Lake fills a special, but poorly studied, limnological niche. The results of this preliminary study clearly indicate that Fremont Lake should be preserved in its present condition as an ecological benchmark.

REFERENCES

American Public Health Association, American Water Works Association, Water Pollution Control Federation, 1965, Standard methods for the examination of water and wastewater, including bottom sediment and sludges [12th ed.]: New York, Am. Public Health Assoc., 769 p.

Bell, P. R., 1959, The ability of *Sphagnum* to absorb cations preferentially from dilute solutions resembling natural waters: Jour. Ecology, v. 47, p. 351–355.

Berg, C. O., 1963, Middle Atlantic States, *in* Frey, D. G., ed., Limnology in North America: Madison, Univ. Wisconsin Press, p. 191–237.

Brezonik, P. L., Morgan, W. H., Shannon, E. E., and Putnam, H. D., 1969, Eutrophication factors in north-central Florida lakes: Gainesville, Florida Univ. Water Resources Research Center Pub. 5, 101 p.

Brooks, J. L., and Deevey, E. S., Jr., 1963, New England, *in* Frey, D. G., ed., Limnology in North America: Madison, Univ. Wisconsin Press, p. 117–162.

Brown, Eugene, Skougstad, M. W., and Fishman, M. J., 1970, Methods for collection and analysis of water samples for dissolved minerals and gases: U.S. Geol. Survey, Techniques Water Resources Inv., book 5, chap. A1, 160 p.

Brown, Jerry, Grant, C. L., Ugolini, F. C., and Tedrow, J. C. F., 1962, Mineral composition of some drainage waters from arctic Alaska: Jour. Geophys. Research, v. 67, no. 6, p. 2447–2453.

Crippen, J. R., and Pavelka, B. R., 1970, The Lake Tahoe basin, California-Nevada: U.S. Geol. Survey Water-Supply Paper 1972, 56 p.

Dunn, D. M., 1972, Ice breakup in a mountain lake, Wyoming: Water Resources Research. [In press]

Edmondson, W. T., 1963, Pacific coast and Great Basin, *in* Frey, D. G., ed., Limnology in North America: Madison, Univ. Wisconsin Press, p. 371–392.

Federal Water Pollution Control Administration, 1968, Report of the Committee on Water Quality Criteria: U.S. Dept. Interior, 234 p.

Fitzgerald, G. P., and Faust, S. L., 1967, Effect of water sample preservation methods on the release of phosphorous from algae: Limnology and Oceanography, v. 12, p. 332–334.

Geldreich, E. E., 1966, Sanitary significance of fecal coliforms in the environment: Federal Water Pollution Control Adm. Pub. WP-20-3, 122 p.

Gorham, Eville, 1961, Factors influencing supply of major ions to inland waters, with special reference to the atmosphere: Geol. Soc. America Bull., v. 72, p. 795–840.

Hutchinson, G. E., 1957, A treatise on limnology: New York, John Wiley and Sons, v. 1, 1,015 p.

Juday, Chancey, Birge, E. A., and Meloche, V. W., 1938, Mineral content of the lake waters of northeastern Wisconsin: Wisconsin Acad. Sci., Arts and Letters Trans., v. 31, p. 223–276.

Junge, C. E., and Werby, R. T., 1958, The concentration of chloride, sodium, potassium, calcium, and sulfate in rain water over the United States: Jour. Meteorology, v. 15, p. 417–425.

Langbein, W. B., 1951, Research on evaporation from lakes and reservoirs: Gen. Assembly of Brussels, Internat. Assoc. Sci. Hydrology, v. 3, p. 409–425.

Larson, D. W., 1970, On reconciling lake classification with the evolution of four oligotrophic lakes in Oregon: Corvallis, Oregon State Univ., unpub. Ph. D. thesis, 145 p.

Larson, D. W., and Donaldson, J. R., 1970, Waldo Lake, Oregon; a special study: Corvallis, Oregon State Univ., Water Resources Research Inst. Rept. 2, 21 p.

Lee, G. F., 1969, Analytical chemistry of plant nutrients, *in* Eutrophication; causes, consequences, correctives: Washington, Nat. Acad. Sci., p. 646–658.

Livingstone, D. A., 1963, Chemical composition of rivers and lakes, *in* Fleischer, Michael, ed., Data of geochemistry [6th ed.]: U.S. Geol. Survey Prof. Paper 440-G, p. G1–G64.

Longacre, L. L., and Blaney, H. F., 1962, Evaporation at high elevations in California: Am. Soc. Civil Engineers Proc., Jour. Irrigation and Drainage Div., IR2, no. 3172, p. 33–54.

Lueschow, L. A., Helm, J. M., Winter, D. R., and Karl, G. W., 1970, Trophic nature of selected Wisconsin lakes: Wisconsin Acad. Sci., Arts and Letters Trans., v. 58, p. 237–264.

Northcote, T. G., and Larkin, P. A., 1963, Western Canada, *in* Frey, D. G., ed., Limnology in North America: Madison, Univ. Wisconsin Press, p. 451–485.

Pennak, R. W., 1955, Comparative limnology of eight Colorado mountain lakes: Colorado Univ. Studies, Ser Biol., v. 2, p. 1–75.

—— 1958, Regional lake typology in northern Colorado, U.S.A.: Verh. Internat. Ver. Limnology, v. 13, p. 264–283.

—— 1963, Rocky Mountain States, *in* Frey, D. G., ed., Limnology in North America: Madison, Univ. Wisconsin Press, p. 349–369.

Rawson, D. S., 1942, A comparison of some large alpine lakes in western Canada: Ecology, v. 23, p. 143–161.

—— 1951, The total mineral content of lake waters: Ecology, v. 32, p. 669–672.

Reimers, Norman, Maciolek, J. A., and Pister, E. P., 1955, Limnological study of the lakes in Convict Creek Basin, Mono County, California: U.S. Fish and Wildlife Service Fishery Bull., v. 56, p. 437–503.

Richmond, G. M., 1969, Development and stagnation of the last Pleistocene ice cap in Yellowstone Lake Basin, Yellowstone National Park, U.S.A.: Eiszeitalter u. Gegenwart, v. 20, p. 196–203.

Richmond, G. M., Murphy, J. F., and Denson, N. M., 1965, Glacial chronology of the Wind River Mountains, Pt. C *in* Schultz, C. B., and Smith, H. T. U., eds., Guidebook for Field Conference E, Northern and Middle Rocky Mountains–Internat. Assoc. Quaternary Research, 7th Cong., U.S.A., 1965: Lincoln, Nebr., Nebraska Acad. Sci., p. 28–37.

Rodhe, Wilhelm, 1949, The ionic composition of lake waters: Verh. Internat. Ver. Limnology, v. 10, p. 377–386.

Ruttner, Franz, 1963, Fundamentals of limnology [3d ed.]: Univ. Toronto Press, 295 p.

Strøm, K. M., 1933, Nordfjord Lakes; a limnological survey: Norske Vidensk.-Akad. Oslo Skr., Mat.-Naturv. Kl. 1932, no. 8, 60 p.

—— 1938, Norwegian mountain lakes: Archiv Hydrobiol., v. 33, p. 82–92.

——1945, The temperature of maximum density in fresh waters: Geofysiske Publikasjoner, v. 16, no. 8, 14 p.

Welch, P. S., 1948, Limnological methods: Garden City, N.Y., Blakiston Co., 366 p.

Wyoming Department of Public Health, 1968, Water quality standards for interstate waters in Wyoming: Cheyenne, 14 p.

Yoshimura, Shinkichi, 1938, Dissolved oxygen of the lake waters of Japan: Science Reports Tokyo Bunrika Daigaku, sec. C. no. 8, p. 63–277.

THE HYDROLOGIC BALANCE OF LAKE SALLIE, BECKER COUNTY, MINNESOTA

By WILLIAM B. MANN IV and MARK S. McBRIDE,
St. Paul, Minn.

Abstract.—The hydrologic balance of Lake Sallie was determined for the 1969 and 1970 water years. The hydrologic balance for the 1969 water year shows that surface-water flow accounted for 77 percent of the inflow, precipitation 10 percent, and ground-water flow 13 percent; 86 percent of the outflow was surface water and 14 percent evaporation. Percentages for the 1970 water year were comparable with those for 1969; ground water accounted for 3 percent more of the inflow, 3 percent more of the outflow was by evaporation, and surface inflow and outflow were correspondingly less. To check the ground-water flows computed in the hydrologic balance, flow nets were constructed to determine the ground-water flow. The ground-water inflows determined using the flow nets were 1,730 acre-feet during a period of low ground-water levels and 1,810 acre-feet during a period of high ground-water levels. The estimated range of error for elements of the water balance is: surface-water inflow and outflow, precipitation, and change in lake storage, ±5 percent; evaporation, ±10 percent. The estimated range of error for the ground-water inflow as determined from the flow-net analysis is ±30 percent.

Lake Sallie, Minn., has been a popular recreational lake since the 1870's. Since about 1915, however, eutrophication has increased at an accelerating rate. Large increases in the growth of aquatic vegetation became apparent in the late 1940's, and objectionable growths were very apparent 10 years later. In 1968 the Water Quality Office (formerly Federal Water Quality Adm.), Environmental Protection Agency, through its research grant program, provided funds for an extensive study of the effects of aquatic-plant removal on the level of eutrophication in Lake Sallie. As part of the study, the U.S. Geological Survey was asked to determine the hydrologic budget for the lake so that nutrient budgets could be determined before and after removal of the aquatic plants. The purpose of this report is to present the hydrologic budget for the 1969 and 1970 water years.

Lake Sallie is 2 miles southwest of Detroit Lakes, Minn. (fig. 1). It lies within the Alexandria moraine complex, a broad belt of hilly country that trends north and south through west-central Minnesota. This moraine complex was formed at the western margin of the Wadena ice lobe during its Hewitt phase, the earliest Wisconsin glacial advance recognized in Minnesota

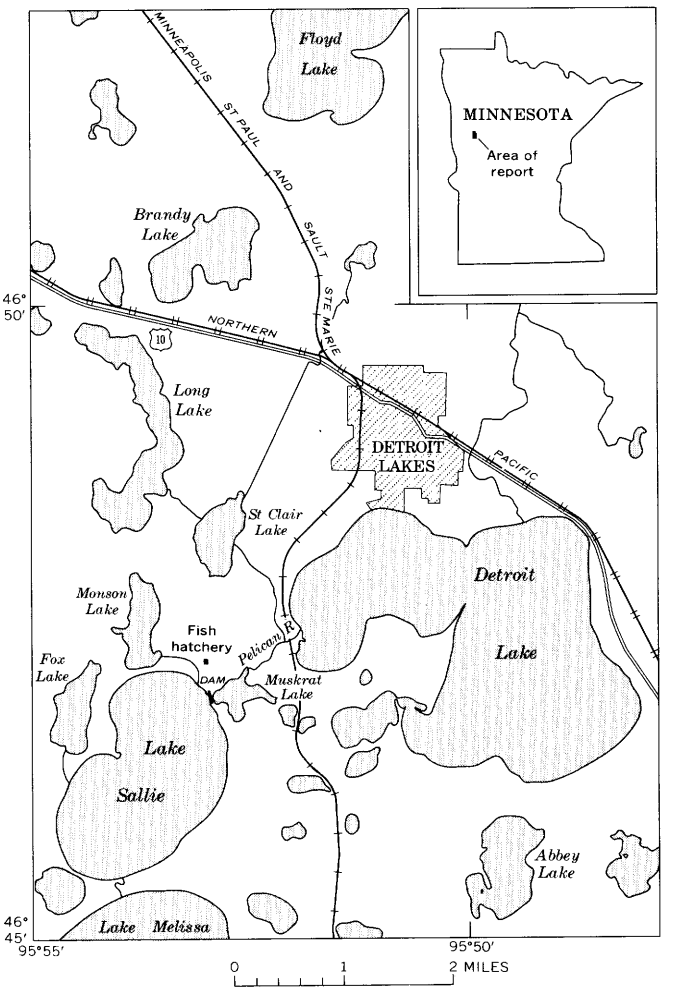

Figure 1.—Location map of Lake Sallie and Detroit Lakes, Minn., vicinity.

(Wright and Ruhe, 1965). Later, ice of the Des Moines lobe overrode the moraine from the west. Together, the two ice lobes deposited about 400 feet of silty to clayey gray till of very low permeability. As the Des Moines lobe retreated,

U.S. GEOL. SURVEY PROF. PAPER 800-D, PAGES D189-D191

coarse permeable outwash as much as 100 feet in thickness mantled the Lake Sallie area. The outwash buried many isolated ice blocks, one of which formed the Lake Sallie basin upon melting.

Acknowledgment.—Funds for this study were provided by the Water Quality Office, Environmental Protection Agency.

HYDROLOGIC SETTING

Lake Sallie is one of a chain of lakes along the course of the Pelican River. The lake is kidney shaped, approximately 2 miles long and 1 mile wide. The maximum depth of the lake is 55 feet, and the average depth is 18 feet. The surface area is 1.9 square miles, and the capacity is 22,000 acre-ft (acre-feet) at an elevation of 1,329 feet above mean sea level. In addition to the Pelican River, several small streams draining nearby lakes flow into Lake Sallie.

The Pelican River valley, including Lake Sallie, is characterized in part as an area of ground-water discharge. Regional ground-water systems within the drift are recharged in the higher parts of the moraine and discharge to the river valley and Lake Sallie. Most of the ground-water contribution comes, however, from local flow systems within the surficial outwash. Interlake ground-water flow is an important component of these systems.

THE HYDROLOGIC BUDGET

The hydrologic budget is derived by equating the water gains to the water losses, plus or minus the changes in storage. The measurement of water gains, water losses, and storage changes in a hydrologic basin involves several important factors. These are: (1) precipitation, (2) streamflow, (3) changes in surface storage, (4) ground-water flow, and (5) evaporation. These items, in relation to the Lake Sallie study area, are described in the following paragraphs. The data used to develop the hydrologic budget were collected during the 1969 and 1970 water years.

The hydrologic budget of the lake is expressed mathematically as follows:

$$\Delta S = S_I + P \pm GW - S_O - E,$$

where

ΔS = change in surface-water storage,
S_I = surface-water inflow,
P = precipitation,
GW = net ground-water flow,
S_O = surface-water outflow, and
E = evaporation.

Because of the nature of hydrologic phenomena, the components of the above equation could not be evaluated with equal accuracy.

Precipitation was measured by a National Weather Service (U.S. Weather Bureau) observer using a standard nonrecording gage 3 miles northeast of Lake Sallie. Because there was no precipitation gage at Lake Sallie, the precipitation recorded at this station was assumed to apply to Lake Sallie. Precipitation for the 1969 and 1970 water years (U.S. Dept. of Commerce, 1968–70) amounted to 21.28 and 20.26 inches, respectively. The total precipitation for the 1969 water year showed a −2.29-inch departure from the normal, and that for the 1970 water year showed a −3.31-inch departure (Baker and others, 1967).

Gaging stations to measure the surface-water inflows and outflows of Lake Sallie were installed in July 1968. The principal inflow station is on the Pelican River at the dam between Muskrat Lake and Lake Sallie adjacent to the Minnesota Department of Natural Resources fish hatchery. The outflow station is on the Pelican River channel between Lake Sallie and Lake Melissa, approximately 250 feet downstream from the outlet of Lake Sallie. Staff gages were also installed on the outlets of Fox Lake, Monson Lake, and the rearing ponds at the fish hatchery. Monthly measurements during winter and biweekly measurements during open-water periods were used to estimate the monthly mean discharges to Lake Sallie. These outlet streams contribute only a very small percentage of the total surface-water inflow to Lake Sallie; the Pelican River supplies the major part.

Direct runoff to the lake from the drainage area surrounding it is considered to be very small. This area is approximately 520 acres, or less than half the size of the lake surface. The soil is very sandy, and any direct runoff probably occurs only during the spring snowmelt. Therefore, direct runoff is considered to be insignificant.

Changes in Lake Sallie storage were determined from lake elevations obtained from a staff gage on the Lake Sallie side of the dam at the fish hatchery. A bathymetric map of the lake was furnished by the Minnesota Department of Natural Resources and was used to develop the area-capacity curves for the lake.

The estimated annual evaporation for the Lake Sallie area as reported by Meyers (1962) was 28 inches. Class A pan evaporation measurements (U.S. Dept. of Commerce, 1968–70) at Fargo, N. Dak., 43 miles northwest of Lake Sallie, were available for the 2-year period for the months May through October, except for May 1970. These data show the estimated value for evaporation to be reasonable, but accurate only to ±1 inch.

The hydrologic budget for Lake Sallie for the 1969 and 1970 water years is shown in table 1. The percentage contribution by each component of the water budget for the 2 years is shown below:

	1969	*1970*
Inflow:		
Surface water	76.9	73.3
Precipitation	10.4	10.9
Net ground-water flow	12.6	15.8
Outflow:		
Surface water	86.1	82.7
Evaporation	13.9	17.3

Table 1.—*The water budget of Lake Sallie, Minn., 1969 and 1970 water years*

[All data in acre-feet]

	Oct.	Nov.	Dec.	Jan.	Feb.	Mar.	Apr.	May	June	July	Aug.	Sept.	The year
1969 water year[1]													
Surface-water inflow	314	853	976	1,001	1,944	1,658	4,941	2,856	791	633	179	24	16,170
Precipitation	280	51	175	171	82	12	112	230	294	455	86	244	2,192
Surface-water outflow	218	796	1,170	1,420	2,270	1,960	4,270	4,400	821	834	250	7	18,416
Evaporation	179	130	45	40	40	51	170	495	390	497	609	337	2,983
Change in storage	+490	−130	0	+100	−290	−190	+1,310	−800	−210	+120	−510	−270	−380
Residual	+293	−108	+64	+388	−6	+151	+697	+1,009	−84	+363	+84	−194	+2,657
1970 water year[2]													
Surface-water inflow	25	531	708	697	529	689	2,015	4,198	3,199	1,336	149	116	14,192
Precipitation	304	33	110	17	27	96	299	190	560	161	28	282	2,107
Surface-water outflow	6	109	622	762	617	998	2,310	4,670	4,180	1,290	80	17	15,661
Evaporation	178	130	55	50	55	63	170	475	515	663	532	391	3,277
Change in storage	+120	+480	+230	0	0	+100	+440	−220	−70	−450	−430	+220	+420
Residual	−25	+155	+89	+98	+116	+376	+606	+537	+866	+6	+5	+230	+3,059

[1] October 1968–September 1969.

[2] October 1969–September 1970.

The components of the water budget vary throughout the year (see table 1). Streamflow is greatest in spring and early summer. Precipitation is greatest in spring and fall. Evaporation is greatest during the summer months. Two-thirds of the ground-water inflow occurred in the months of April to June.

In most hydrologic budget studies, the residual obtained when the total outflow is subtracted from the total inflow is assumed to represent net ground-water flow. For this study, however, direct measurement of the ground-water flow was desirable because of possible differences in nutrient concentrations between the inflow and the outflow. In addition, if ground water could be calculated directly, it would lead to better understanding of the magnitude of error in the other elements of the water budget.

Ground-water levels were measured weekly in 32 observation wells within the Lake Sallie watershed. The data showed that ground water moved into Lake Sallie everywhere except the southern end, where at certain times water moves as underflow from Lake Sallie to the next lake downstream, Lake Melissa. This underflow from the lake occurs only in the spring of the year in a very small area with low gradients and is considered to be negligible. The geometry of the saturated zone, the results of computer modeling studies, and the small differences between water levels in adjacent wells screened at different depths indicated that ground-water flow was horizontal. Thus, to calculate ground-water contribution to the lake, two flow nets were constructed using water-level data. One flow net was constructed for the winter period when levels were low, and the second was constructed for the late spring period when levels were high. The respective ground-water inflow rates calculated were 1,730 and 1,810 acre-ft per year.

The mean of these inflow rates is 1,090 acre-ft per year less than the mean residuals. The discrepancy results from errors in the flow net and in evaluating the terms of the hydrologic balance. Estimates of the percentages and magnitudes of error were made for each component individually, on the basis of the precision and adequacy of the data used. They are as follows:

Term	*Percentage error*	*Magnitude of error (acre-ft per year)*
Surface-water inflow	±5	±760
Precipitation	±5	±110
Surface-water outflow	±5	±850
Evaporation	±10	±310
Change in storage	±5	±20
Ground-water inflow from flow nets	±30	±530

It is evident that the residual, as calculated from the hydrologic budget equation, cannot be expected to agree exactly with the ground-water inflow calculated using the flow-net analysis. The results obtained in this study indicate that in this or similar hydrologic settings the flow-net analysis may give results comparable to those from the hydrologic budget equation. However, additional work is necessary before a meaningful comparison can be made between the two methods.

REFERENCES

Baker, D. G., Haines, D. A., and Strub, J. H., Jr., 1967, Precipitation facts, normals and extremes: Climate of Minnesota, Pt. V, Minnesota Univ. Agr. Expt. Sta., Tech. Bull. 254, 42 p.

Meyers, J. S., 1962, Evaporation from the 17 Western States: U.S. Geol. Survey Prof. Paper 272-D, p. 71–100, pl. 3.

U.S. Department of Commerce, Environmental Sciences Service Administration, 1968, Climatological data: Minnesota, v. 74.

——1969, Climatological data: Minnesota, v. 75.

——1970, Climatological data: Minnesota, v. 76.

——1968, Climatological data: North Dakota, v. 77.

——1969, Climatological data: North Dakota, v. 78.

——1970, Climatological data: North Dakota, v. 79.

Wright, H. E., Jr., and Ruhe, R. V., 1965, Glaciation of Minnesota and Iowa, *in* The Quaternary of the United States: Princeton, N.J., Princeton Univ. Press, p. 29–41.

AERIAL PHOTOGRAPHY OF WIND STREAKS ON ONEIDA LAKE, NEW YORK

By JANICE M. WHIPPLE and PHILLIP E. GREESON, Albany, N.Y.

Work done in cooperation with the National Aeronautics and Space Administration

Abstract.—Extensive wind streaks are visible on vertical aerial black-and-white photographs of Oneida Lake, N.Y., October 23, 1967. Development and orientation of streaks appear to be related to wind direction, fetch, and bottom topography. Massive streaks are separated by less well defined streaks, and streak directions change by parallel offsets of short segments. Streak spacing can be measured directly on vertical aerial photographs more effectively than at the water surface, and streak intensities can be discerned. The formation of wind streaks can be observed through use of repeated photography.

Mechanisms for the generation of wind streaks were first described by Langmuir (1938), who observed in Lake George, N.Y., that the wind drift of surface water had a definite structure. The structure is that of a series of parallel helices (Langmuir circulations), alternating clockwise and counterclockwise, alined with the wind. Thus, the surface of a lake can be marked by linear convergences of leaves, oil films, debris, and foam. These convergences are called wind streaks.

Subsequent discussions of wind streaks include those by Faller (1969), Myer (1969), and Scott and others (1969). Correlations of streak production with wind speed and direction as well as with water thermal convection cells have been proposed. Faller (1969, p. 511) pointed out that Langmuir circulations may not be visibly indicated by surface streaks and that streaks may have origins other than the circulations. He notes, however:

> The inconsistencies noted by Scott and others (1969) for observations of Langmuir circulations fall into three categories: (1) the angle of the windrows with respect to the wind; (2) the relation of their spacing to windspeed and other parameters [such as epilimnion depth and (or) bottom topography]; and (3) their apparent rate of formation.

Wind streaks or slicks on the ocean have been observed on visual photography and thermal-infrared imagery by McLeish (1965). Streaks have also been observed on thermal-infrared imagery of Oneida Lake. Little quantitative information has yet been presented, although general circulation patterns in other lakes have been noted (Whipple, 1971).

DESCRIPTION OF ONEIDA LAKE

Oneida Lake is about 11 miles (18 km) north of Syracuse in central New York. (See figure 1.) With a surface area of about 80 sq mi (207 sq km), it is the largest lake wholly within the State. The length of the lake is 20.9 miles (33.6 km), and its maximum width is 5.5 miles (8.8 km). Maximum depth is 55 feet (16.8 m), and mean depth is 22.3 feet (6.8 m) (Greeson and Meyers, 1969, p. 13; Greeson, 1971).

The near alinement of the long axis with the prevailing westerly winds favors wind mixing in this shallow lake. Oneida Lake does not thermally stratify during the summer, although during 1967 a stratification of dissolved oxygen was observed (Greeson and Meyers, 1969, p. 19).

AERIAL PHOTOGRAPHY

Aerial photography of Oneida Lake was provided by the Reconnaissance Branch, Rome Air Development Center (RADC), Griffiss Air Force Base, N.Y. The photographs discussed in this paper were taken during RADC mission 67-40 on October 23, 1967.

The Fairchild KC-1B camera, a standard aerial-mapping camera, was mounted in the aircraft so that the camera had a vertical line of sight. The 6-inch (152.7-mm) focal length produces a field of view of 73°44′ for each 9-inch (22.9-cm) frame. No special filter was used with the black-and-white film. Photography of this type is of standard mapping quality, and if photographs are not badly tilted, measurements between objects on a horizontal plane may be made fairly

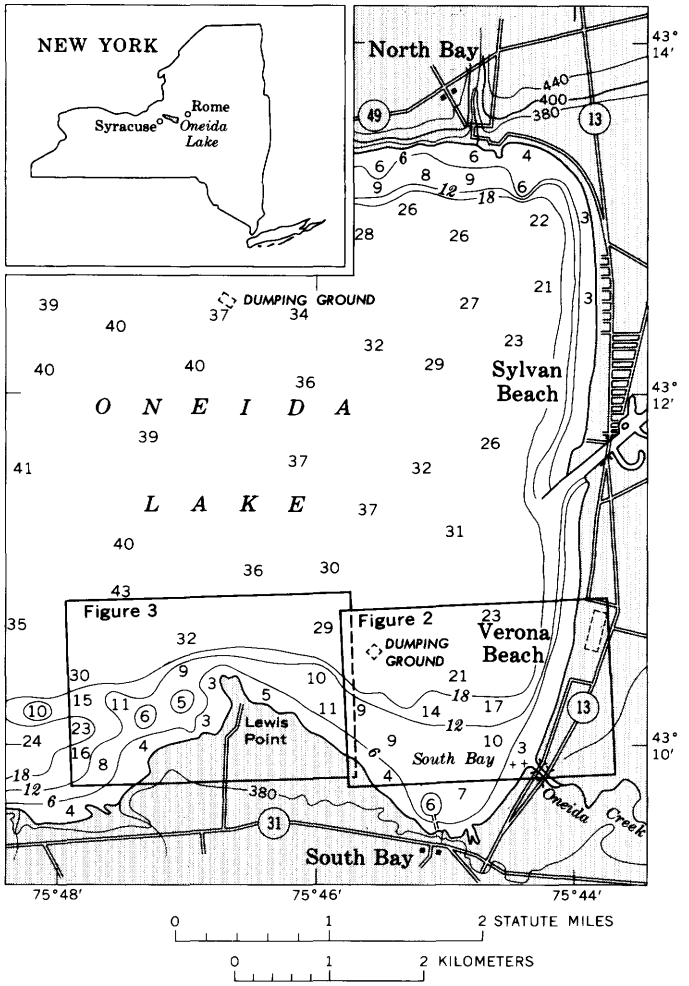

Figure 1.—Eastern part of Oneida Lake, N.Y., showing location of figures 2 and 3. Water-depth soundings are in feet. Base from U.S. Department of Commerce; Lake Survey Center-NOS Chart 180, p. E-16.

accurately by scaling directly from the prints without photographic rectification or reference to maps.

Aircraft altitude was about 7,000 feet (2,130 m) above the surface of the lake. The combination of camera focal length and altitude produced a film scale of about 1:14,000 or 1 inch ≈ 1,170 feet (1 mm ≈ 14 m).

WEATHER

Weather recording stations closest to Oneida Lake are operated by the National Weather Service at Hancock Field, Syracuse, and by the U.S. Air Force at Griffiss Air Force Base, Rome, N.Y. Weather data for the morning of October 23, 1967, are presented in table 1.

The National Weather Service at Syracuse (oral commun., 1972) reported that there is usually a difference in wind direction between Oneida Lake and Syracuse at windspeeds below about 12 knots. Similarly, temperatures may vary by an estimated 5°F or 3°C.

The Syracuse records (U.S. Dept. Commerce, 1967) show that on October 21–22, 1967, the wind shifted from south to west and northwest. Between 1600 and 1900 hours on October 22, the wind shifted again to east-southeast and varied from that to easterly through the morning of the photographic mission. Visibility was 15 miles (24 km), ceiling was unlimited, and cloud cover was zero.

Oneida Lake water temperature on October 30, 1967, was about 11°C (Greeson and Meyers, 1969).

ANALYSES OF THE PHOTOGRAPHY

Figure 2 is a vertical aerial photograph of part of eastern Oneida Lake. (See figure 1 for location.) At the upper right is the Verona Beach State Park parking lot (about 440 by 1,460 feet, or 134 by 445 m). The light-toned plume from the park area extending over land and water (A, fig. 2) is probably smoke. If so, it indicates a wind direction azimuth of 100° at the east end of Oneida Lake, compared with 90° at Syracuse and 140° at Rome.

Because of photographic-processing variables and screening necessary for halftone reproduction, recognition of small-scale, contrast-dependent photographic features is sometimes difficult. On first-generation contact prints, however, wind streaks are first discernible some 2,700 to 3,000 feet (890 to 915 m) from shore (B's, fig. 2) and are at maximum definition about 6,000 feet (1,830 m) from shore (C's). Water depths are between 20 and 30 feet (about 6 to 9 m) in this area and are shown on figure 1 as depths measured by soundings.

Table 1.—*Weather data for recording stations near Oneida Lake, October 23, 1967*

Time (hours e.s.t.)	Air temperature (°F/°C)		Relative humidity (percent)		Surface wind: Direction (az), in degrees		Surface wind: Speed (knots, m/sec)[1]	
	Syracuse	Rome	Syracuse	Rome	Syracuse	Rome	Syracuse	Rome
0700	35/1.7	29/–1.7	85	87	060	....	5, 2.6	Calm
0800	40/4.4	37/2.8	82	81	090	....	6, 3.1	Do.
0900[2]	47/8.3	43/6.1	74	71	090	140	8, 4.1	2, 1.0
1000	52/11.1	48/8.9	69	68	090	140	8, 4.1	4, 2.1
1100	59/15.0	53/11.7	49	58	160	130	8, 4.1	3, 1.5

[1] 1 knot = 1.7 feet per second = 0.515 m/sec.
[2] Time of aircraft departure from Rome: 0915 hours.

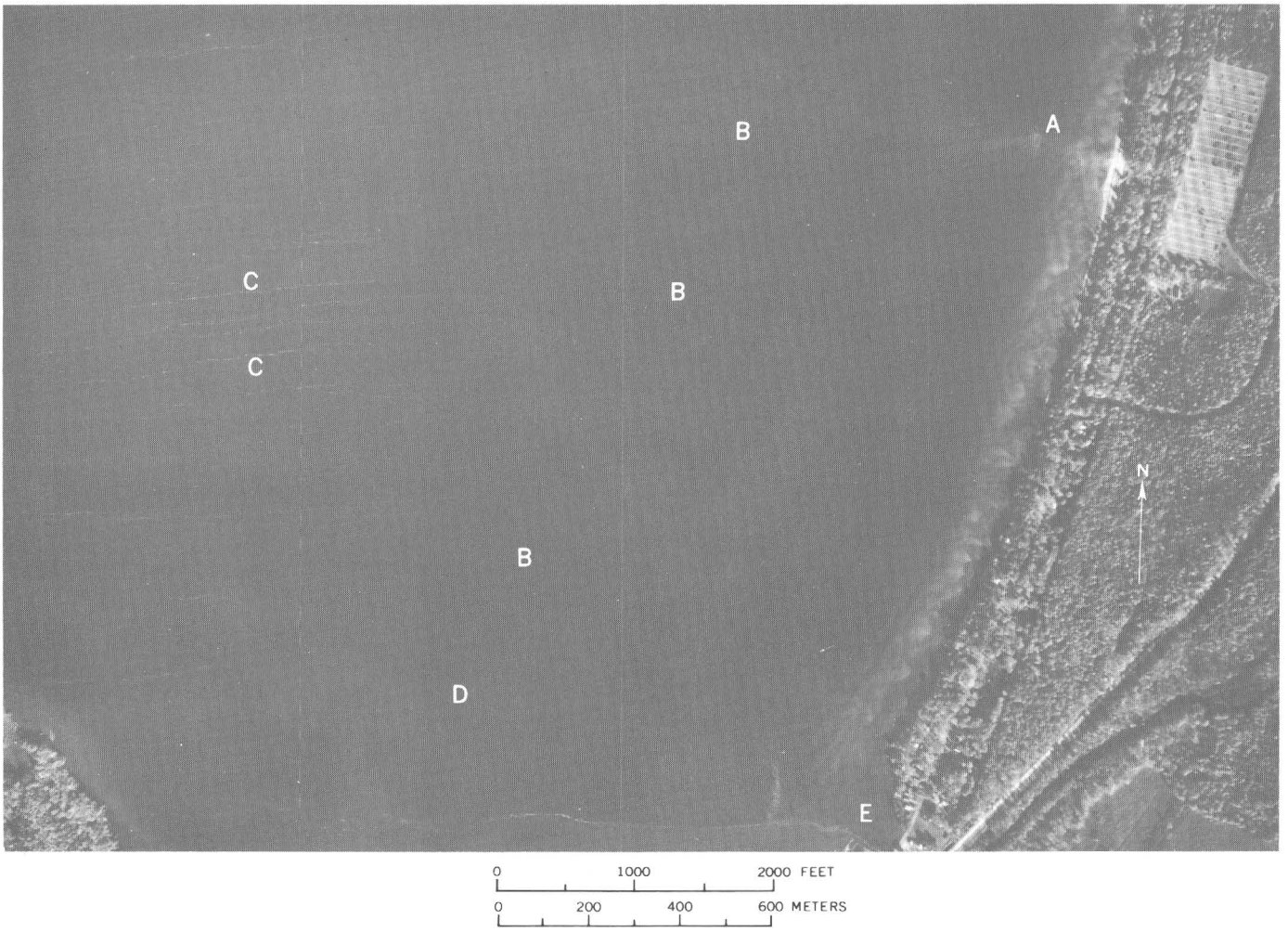

Figure 2.—Aerial photograph of Oneida Lake at Verona Beach. Courtesy of Rome Air Development Center.

Streaks vary considerably in definition (C's, fig. 2), with minor streaks interspersed between the major streaks. Photographic enlargements or lower altitude coverage could provide more detail. The general trend of the streaks appears to be approximately 10° counterclockwise from the initial direction of the plume, although the plume also drifts and disperses slightly southward. The light-toned area near D (fig. 2) is probably a shallow area, as are those near shore. The streak west of the mouth of Oneida Creek (E) is the only major one extending to shore.

Figure 3 overlaps the west end of figure 2. (See figure 1 for location and bottom contours.) East of Lewis Point, the streaks follow the same general trend developed upwind (fig. 2). There are small clockwise (northerly) offsets of streak segments at about the 18-foot (5.5-m) bottom contour (F, fig. 3) and more abrupt counterclockwise (southerly) offsets just out from the 6-foot (1.8-m) contour (G–G). The latter area is also one of darker gray tones that could represent deeper water, surface reflections or films, or submerged vegetation. Interpretation of deeper water is favored because of the continuity and the geometry of the gray tones.

A major streak develops west of Lewis Point (H, fig. 3) and offsets clockwise just north of the 12-foot (3.7-m) contour and 11-foot sounding. In the bay area leeward of Lewis Point, streaks are first discernible at K 3,700 feet (1,130 m) west of the shoreline. Major streaks are offset clockwise near L, an area of lighter gray tones that may represent shallow water. If the interpretations of depth are correct, streak offsets are probably influenced by bottom topography. This condition may be due to hydraulic changes, such as the forced scale for convective cells mentioned by Faller (1969, p. 511). However, shallow areas inferred from gray shades differ slightly from those shown on the hydrographic chart reproduced in figure 1. The interpretation of depth based on photographic gray tones may be erroneous or bottom topography may have changed. (Original soundings were made in 1912, U.S. Army Corps of Engineers, 1912a, b.)

Figures 2 and 3 are part of a continuous strip of overlapping photographs taken on October 23, 1967, that extends along the south shore of Oneida Lake to Shackelton Point, about 10

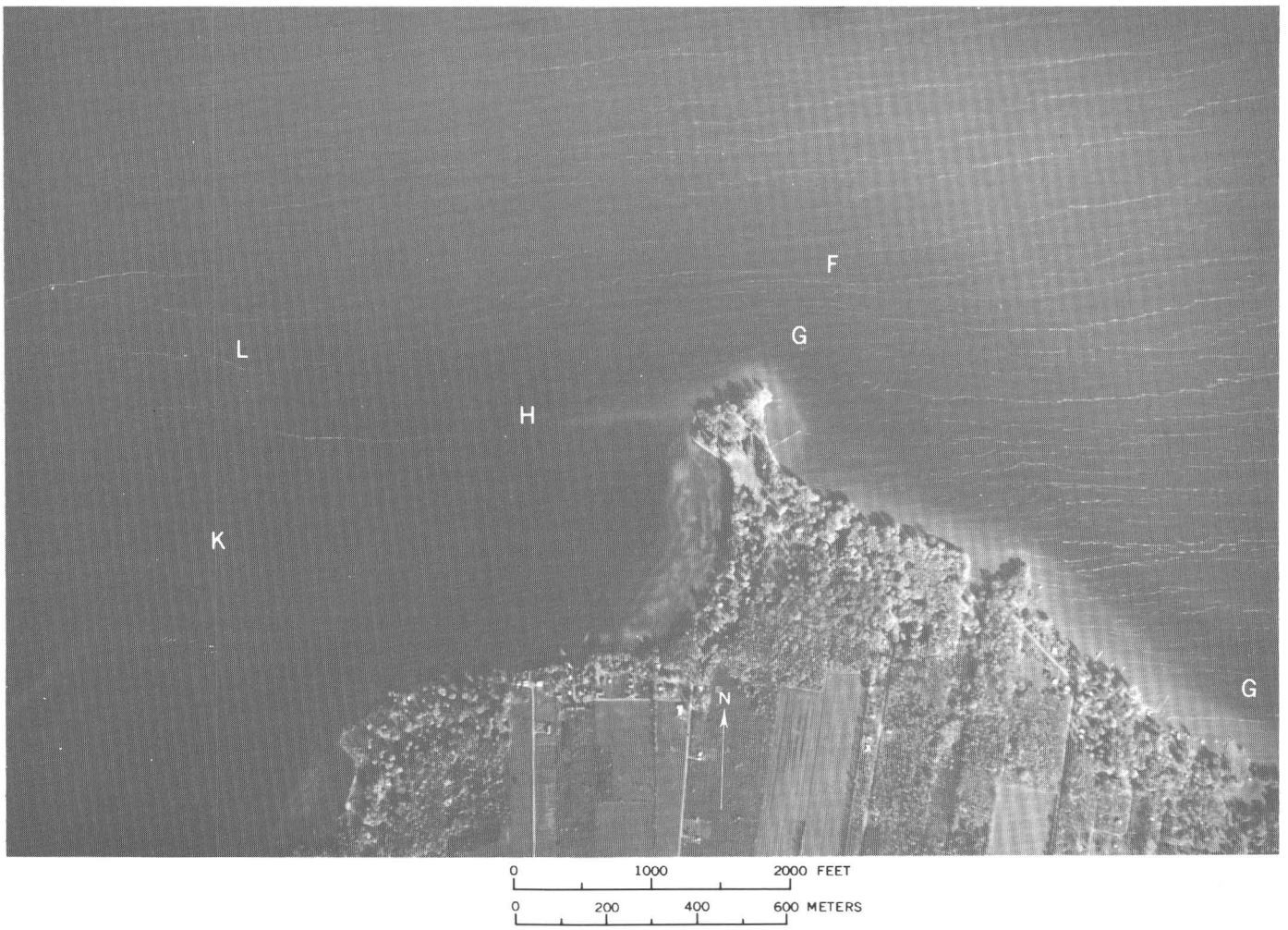

Figure 3.—Aerial photograph of Oneida Lake at Lewis Point. Courtesy of Rome Air Development Center.

miles (16 km) west of Verona Beach. A photomosaic has been made (R. R. Petroski, RADC), but it cannot easily be reduced and photographically screened for publication. It shows that the four major streaks spaced over 1,000 feet (305 m) at L (fig. 3) converge to less than 300 feet (92 m) about 3,500 feet (1,070 m) westward from L. There is no discernible streaking leeward of other shoreline projections. Other water-surface features appearing in the photomosaic are breakers, boat wakes, and refraction and diffraction patterns of surface waves. The legibility of the wave patterns depends on sun orientation.

In addition to the visual photographic data presented here, aerial thermal-infrared imagery that is thermally and geometrically calibrated may provide data for correlation with water temperatures.

CONCLUSIONS

Vertical aerial photographs can provide data suitable for field studies of wind streaks. If streak location and spacing must be measured and streak intensity must be defined, the aerial view is superior to that from the water surface. Although direct measurements of spacing can be made from the film or prints, categorization of the streak intensities can be only approximated by film density analyses. Systematic photographic coverage can provide data on streak development, decay, and pattern changes under a variety of meteorologic conditions.

The wind-streak patterns seen in this photography appear to be related to wind direction, fetch, and lake-bottom topography; major streaks are usually interspersed with less discernible streaks. Although insufficient wind data for precise correlation are available, streaks on open water trend parallel to or about 10° counterclockwise from the wind direction on land. Streaks on the windward side of land are apparent almost to the shore, whereas those on the leeward side are first discernible about 3,400 feet (1,000 m) from shore on two areas. Direction changes in streaks occur as parallel offsets of short segments. These offsets are reminiscent of shear "failures" in solid materials and are perhaps related to the torsional aspects of the fluid motion in the convection cells.

REFERENCES

Faller, A. J., 1969, The generation of Langmuir circulations by eddy pressure of surface waves: Limnology and Oceanography, v. 14, no. 4, p. 504–513.

Greeson, P. E., 1971, Limnology of Oneida Lake with emphasis on factors contributing to algal blooms: U.S. Geol. Survey open-file report, 185 p.

Greeson, P. E., and Meyers, G. S., 1969, The limnology of Oneida Lake, an interim report: New York State Water Resources Comm. Rept. Inv. RI-8, 64 p.

Langmuir, Irving, 1938, Surface motion of water induced by wind: Science, v. 87, no. 2250, p. 119–123.

McLeish, William, 1965, The use of an infrared mapper in the study of small-scale ocean circulations, *in* Symposium on remote sensing of environment, 3d, 1964, Ann Arbor, Mich., Univ. Michigan, Willow Run Labs, Proc. [2d ed.]: p. 717–736.

Myer, G. E., 1969, A field study of Langmuir circulations, *in* Conference for Great Lakes research, 12th, 1969, Ann Arbor, Mich., Proc.: Internat. Assoc. Great Lakes Research, p. 652–663.

Scott, J. T., Myer, G. E., Stewart, Ronald, and Walther, E. G., 1969, On the mechanism of Langmuir circulations and their role in epilimnion mixing: Limnology and Oceanography, v. 14, no. 4, p. 493–503.

U.S. Army Corps of Engineers, 1912a, Survey of the northern and northwestern lakes–New York State Canals, east end of Oneida Lake: U.S. [Army Corps Engineers] Lake Survey Field Sheet 1.

—— 1912b, Survey of the northern and northwestern lakes–New York State Canals, west end of Oneida Lake: U.S. [Army Corps Engineers] Lake Survey Field Sheet 2.

U.S. Department of Commerce, 1967, Local climatological data, Syracuse, N.Y., Hancock Field, Oct. 1967: U.S. Dept. Commerce, Environmental Data Service, 2 p.

Whipple, J. M., 1971, Airplanes and hydrologists–A beneficial alliance: Conservationist, v. 26, no. 2, p. 17–21.

NITROGEN CONTENT OF GROUND WATER IN KINGS COUNTY, LONG ISLAND, NEW YORK

By GRANT E. KIMMEL, Mineola, N.Y.

Work done in cooperation with the New York State Department of Environmental Conservation

Abstract.—Under native conditions virtually all the nitrogen in ground water on Long Island is in the form of nitrate. The estimated nitrate (NO_3) content of ground water in Long Island's aquifers under native conditions is 0.2 mg/l nitrate nitrogen (NO_3-N). Because the NO_3-N content of water in the upper glacial aquifer generally exceeded 0.2 mg/l, contamination by the activities of man is indicated. In 1942 and in 1970–71, the NO_3-N content of water from the upper glacial aquifer generally exceeded 0.2 mg/l in most of Kings County; locally it was as much as 28 mg/l. NO_3-N content of water in the underlying Jameco aquifer locally was as much as 9.6 mg/l in 1942. Although septic-tank and cesspool effluents were probably the chief source of the nitrogen in ground water in parts of Kings County before and during the early 1900's, continued high levels of nitrate and a possible increase in nitrate content since the widespread construction of sewers in the area suggest that leakage from sewers may now be a principal source of the nitrate and total nitrogen in the ground water of the county.

Urban development has caused widespread changes in quality of ground water in the western part of Long Island. By 1947, intensive ground-water development in Kings County (fig. 1) resulted in intrusion of salty ground water into the aquifers beneath the county. Salt-water intrusion, in turn, prompted large reductions in ground-water withdrawals for public supply (Lusczynski, 1952). In addition to changes in the chemical character brought on by the invasion of salty ground water, nitrate-nitrogen content of some of the water increased above the limit of 10 mg/l (milligrams per liter) recommended by the U.S. Public Health Service (1962) as acceptable for public supplies.

The purpose of this paper is to report the nitrate-nitrogen content of water in the upper part of the ground-water reservoir in Kings County and to suggest its origin. Some of the characteristics of the occurrence of nitrate in Kings County are relevant to present and potential ground-water-quality problems, and to the planning necessary to avoid these problems, in other parts of Long Island.

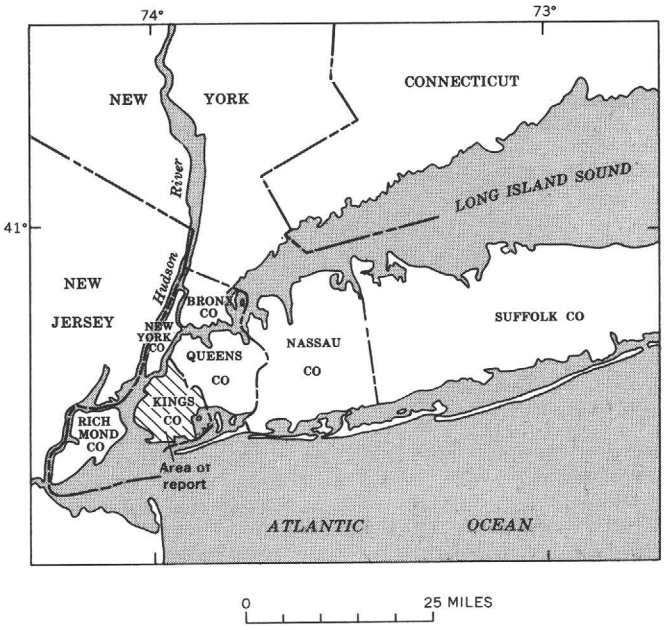

Figure 1.—Index map of Long Island, N.Y., showing area of report (diagonal lines).

HYDROGEOLOGY

Ground-water resources of Long Island have been described in numerous reports (including those by Veatch and others, 1906; Suter, 1937; Suter and others, 1949; and Cohen and others, 1968). The ground-water reservoir in Kings County, at the western end of Long Island, ranges in thickness from about 100 to 900 feet. It consists of a series of unconsolidated sedimentary deposits overlying a southeasterly sloping bedrock surface. Sedimentary deposits of the ground-water reservoir are divided into six major hydrogeologic units, which are described in table 1.

U.S. GEOL. SURVEY PROF. PAPER 800-D, PAGES D199–D203

Table 1.—*Major hydrogeologic units in Kings County, Long Island, N.Y.*

Hydrogeologic unit[1]	Approximate maximum thickness in study area (feet)	Description
Upper glacial aquifer	180	Mainly sand and gravel of high hydraulic conductivity; some thin beds of clayey material of low hydraulic conductivity.
Gardiners Clay	100	Clay, silty clay, and a little fine sand of low to very low hydraulic conductivity.
Jameco aquifer	200	Mainly medium to coarse sand and some gravel of moderate to high hydraulic conductivity.
Magothy aquifer	200	Mainly very fine sand, silt, and clay of low to very low hydraulic conductivity; some coarse to fine sand of moderate hydraulic conductivity; locally contains gravel of high hydraulic conductivity.
Raritan clay	200	Clay of very low hydraulic conductivity; some silt and fine sand of low hydraulic conductivity.
Lloyd aquifer	200	Sand and gravel of moderate hydraulic conductivity; some clayey material of low hydraulic conductivity.
Bedrock	....	Crystalline rock of very low interstitial hydraulic conductivity.

[1] Nomenclature after Cohen, Franke, and Foxworthy (1968).

Thickness of the zone of aeration in Kings County ranges from zero feet at the shoreline to 210 feet in the central part of the county and averages less than 100 feet in most of the county. Natural ground-water recharge is from precipitation; artificial recharge results mainly from leaky water and sewer pipes.

In all but the northwest edge of Kings County, the upper glacial aquifer is underlain by Gardiners Clay, which ranges in thickness from 0 to 100 feet and confines water in the underlying Jameco aquifer. Gardiners Clay is not found along the northwest edge of the county, where deposits of the upper glacial aquifer are in contact with those of the Jameco aquifer.

NITROGEN CONTENT OF NATIVE GROUND WATER

Nitrate-nitrogen (NO_3-N) content of native ground water in the upper glacial aquifer in Kings County is not known because changes in water quality began long ago. However, it can be inferred from data of eastern Long Island, where geologic and climatic conditions are similar to those in Kings County but where effects of the activities of man are minimal and, in some places, are negligible.

Shallow ground water is readily susceptible to contamination by nitrogenous wastes, and repeated sampling and analysis of water from some shallow wells on Long Island commonly reveals variations in the NO_3-N content of ground water. However, on the basis of data in a report by deLaguna (1964, table 6), the NO_3-N content of water in the upper glacial aquifer under native conditions may be inferred to have been 0.2 mg/l or less. This value is in agreement with Perlmutter and Koch's (1972) estimate that the upper limit for nitrate in the native ground water of Nassau County, Long Island, was about 1 mg/l NO_3.

NO_3-N contents of water from selected wells in nonurbanized parts of Suffolk County are listed in table 2. Nearly all the nitrogen in native ground water on Long Island is in the form of nitrate. In many older analyses, tests were made only for the nitrate ion. Thus, only the nitrate ion is reported in table 2. The wells listed in table 2 are near the ground-water divide, where flow paths are nearly vertical and, therefore, where water from the deeper wells is older than water from the shallow wells. All but one of the samples from the Magothy and the Lloyd aquifers had less than 0.1 mg/l NO_3-N. Two of the three samples from the upper glacial aquifer had a NO_3-N content slightly greater than 0.1 mg/l. Thus, the assumed value of 0.2 mg/l NO_3-N as the upper limit of the nitrate content of Long Island's ground water under native conditions is probably reasonably conservative. Values greater than 0.2 mg/l are assumed to represent nitrate-enriched water and to reflect the activities of man.

Table 2.—*Nitrate-nitrogen content of ground water from selected wells near the ground-water divide in Suffolk County, Long Island, N.Y.*

[Aquifers: ug, upper glacial; M, Magothy; L, Lloyd. Analysis by U.S. Geological Survey]

Well	Depth of well below land surface (feet)	Aquifer	Date of collection	Nitrate nitrogen (mg/l)
S 24774	110	ug	12-11-65	0.11
24771	125	ug	12-12-65	.00
22579	210	ug	8-12-64	.13
24770-1	220	M	8-6-65	.00
24773-1	234	M	10-19-65	.00
22582	296	M	5-28-64	.02
22578	402	M	8-11-64	.00
24770-2	434	M	8-10-65	.02
24773-2	442	M	11-11-65	.00
22581	450	M	7-2-64	.02
22910	642	M	5-14-64	.00
24769-2	683	M	7-9-65	.22
24772-2	688	M	9-24-65	.09
22577	734	M	8-11-64	.00
22850	802	M	7-28-64	.00
24769-3	810	M	7-7-65	.00
24772-3	838	M	10-13-65	.04
33380	850	M	10-3-68	.00
33379	1,300	L	9-20-68	.00

NITROGEN DISTRIBUTION IN KINGS COUNTY

Nitrogen data for water from representative wells tapping the upper glacial aquifer in Kings County are listed in table 3. Locations of the wells are shown in figure 2. Analyses of water from well K9 in northwestern Kings County and from wells at sites a, b, and c in the southeastern part of the county indicate that, in the early 1900's, the nitrogen content of water from the upper glacial aquifer ranged from 2.7 to 17 mg/l NO_3-N. The nitrogen species ammonium (NH_4^+), nitrite (NO_2^-), nitrate (NO_3^-), and organic nitrogen are reported in analyses of water samples collected in 1942 from 200 wells tapping the upper glacial aquifer throughout the county. The total nitrogen content of the water analyzed ranged from 0.55 to 30 mg/l.

Table 3.—*Nitrogen content of water from wells in the upper glacial aquifer in Kings County, Long Island, N.Y.*

[Results in milligrams per liter. Agency making analysis: NYC, New York City; USGS, U.S. Geol. Survey]

Well	Year of collection	Ammonia nitrogen	Nitrite nitrogen	Nitrate nitrogen	Organic nitrogen	Total nitrogen	Analyst
a[1]	Before 1903.	0.00	0.00	5.8	0.00	5.8	NYC
	1912	....	....	3.3	....	3.3	NYC
	1913	....	....	3.0	....	3.0	NYC
	1915	....	....	2.9	....	2.9	NYC
	1916	....	....	2.7	....	2.7	NYC
	1931	.01	.00	6.2	.02	6.2	NYC
b[2]	About 1900.	.01	.00	4.5	.02	4.5	NYC
c[3]	1912	....	....	4.3	....	4.3	NYC
	1913	....	....	4.5	....	4.5	NYC
	1915	....	....	4.7	....	4.7	NYC
	1916	....	....	4.2	....	4.2	NYC
	1930	.12	.03	8.5	.03	8.7	NYC
d[4]	1917	.01	.01	5.3	.01	5.3	NYC
	1920	.00	.01	5.9	.00	5.9	NYC
K3	1942	.39	.00	16	.12	17	NYC
	1971	.00	.00	12	.01	12	USGS
K9[5]	1897	.00	....	17	.00	17	NYC
K18	1970	1.2	.00	13	....	14	USGS
K36	1970	.10	.00	9.7	.22	10	USGS
K95	1942	.24	.00	22	.27	23	NYC
	1970	4.5	.10	19	....	24	USGS
	1971	.00	.00	16	.20	16	USGS
K136	1942	.16	.00	11	.08	11	NYC
	1970	.10	.00	20	....	20	USGS
	1971	.00	.00	9.5	.01	9.5	USGS
K141	1942	.34	.00	14	.12	14	NYC
	1970	.40	.00	16	....	16	USGS
K142	1970	.10	.00	20	....	20	USGS
K245	1942	.25	.00	8.5	.14	8.9	NYC
	1970	1.5	.10	12	....	14	USGS
K310	1942	.16	.05	6.0	.05	6.3	NYC
	1970	1.1	.00	20	....	21	USGS
K332	1942	.32	.00	25	.05	25	NYC
	1970	1.9	.00	28	....	30	USGS
K340	1942	.17	.02	.20	.16	.55	NYC
K501	1921	.00	.00	9.4	.01	9.4	NYC
	1938	.02	.00	8.8	.03	8.9	NYC
K503	1922	.00	.00	7.6	.00	7.6	NYC
	1924	.01	.00	12	.01	12	NYC
	1925	.01	.00	11	.01	11	NYC
	1926	.03	.03	8.0	.01	8.1	NYC
	1929	.05	.00	8.2	.02	8.3	NYC
	1939	.05	.03	7.4	.05	7.5	NYC
	1946	.08	.02	6.4	.04	6.5	NYC
K504	1934	.05	.00	5.8	.03	5.9	NYC
	1936	.03	.01	8.4	.03	8.5	NYC
	1938	.05	.00	10	.04	10	NYC
	1940	.09	.02	11	.05	11	NYC
	1942	.13	.03	12	.04	12	NYC
	1944	.13	.01	10	.05	10	NYC
	1946	.17	.01	10	.07	10	NYC
K507	1925	.07	.03	12	.03	12	NYC
	1929	.14	.01	8.7	.04	8.9	NYC
	1934	.05	.01	8.5	.03	8.6	NYC
	1936	.03	.01	10	.03	10	NYC
	1942	.13	.03	15	.03	15	NYC
	1946	.06	.02	14	.07	14	NYC
K516	1926	.03	.00	18	.02	18	NYC
	1929	.01	.00	11	.02	11	NYC
	1934	.08	.01	15	.04	15	NYC
	1936	.06	.01	18	.02	18	NYC
	1938	.06	.02	20	.04	20	NYC
	1940	.09	.03	20	.05	20	NYC
	1924	.14	.01	25	.07	25	NYC
	1946	.03	.01	20	.09	20	NYC
K576	1942	.16	.02	6.0	.26	6.4	NYC
	1970	.20	.00	17	....	17	USGS
K615	1942	.35	.00	12	.07	12	NYC
	1970	.30	.00	22	....	22	USGS
K907	1942	.32	.04	12	.07	12	NYC
	1970	1.2	.10	17	....	18	USGS
	1971	.00	.00	11	.00	11	USGS
K957	1942	.47	.04	7.0	.14	7.7	NYC
	1970	4.4	.00	13	....	17	USGS
K1029	1970	.10	2.6	17	....	20	USGS
K1046	1970	1.9	.10	19	....	21	USGS
K1153	1970	.20	.00	4.7	....	4.9	USGS
	1971	.00	.00	13	....	13	USGS
K1302	1970	.10	.00	12	....	12	USGS
K1910	1970	.10	.00	16	....	16	USGS
K2299	1971	.00	.00	11	.14	11	USGS
K2445	1971	.00	.00	5.0	.33	5.3	USGS

[1] Sample from former Gravesend pumping station, 17 wells on common suction and ranging in depth from 57 to 84 feet. First analysis from Veatch and others (1906, p. 169). Letters are used in this report to locate wells for which no formal number has been designated.

[2] Sample from former Spring Creek pumping station, 13 wells on common suction and ranging in depth from 42 to 75 feet. Analysis from Veatch and others (1906, p. 191).

[3] Sample from former Canarsie pumping station, 16 wells on common suction and ranging in depth from 63 to 161 feet in upper glacial aquifer and one well 200 feet deep in Jameco aquifer.

[4] Sample from former New York Water Service pumping station.

[5] Data from Veatch and others (1906, p. 171).

Analyses of water collected from 21 wells in 1970–71 show that the total nitrogen content ranged from 4.9 mg/l for well K1153 to 30 mg/l for well K332. Samples collected from wells K95, K136, K907, and K1153 at about 6-month intervals show variations in the total nitrogen content of up to nearly three times the lower value. The data show that chemical quality of ground water can change in short periods of time. Probably the most regionally representative analyses are those for wells K501, K503, K504, K507, and K516 in the central part of the county. Data for these wells (table 3) are averages for the year as determined from monthly samples. The average total nitrogen content of water from these wells for the years 1921–46 ranged from 5.9 mg/l for well K504 to 25 mg/l for well K516.

Although data from wells tapping the Jameco aquifer are scant, they indicate that the ammonia-nitrogen (NH_3-N)

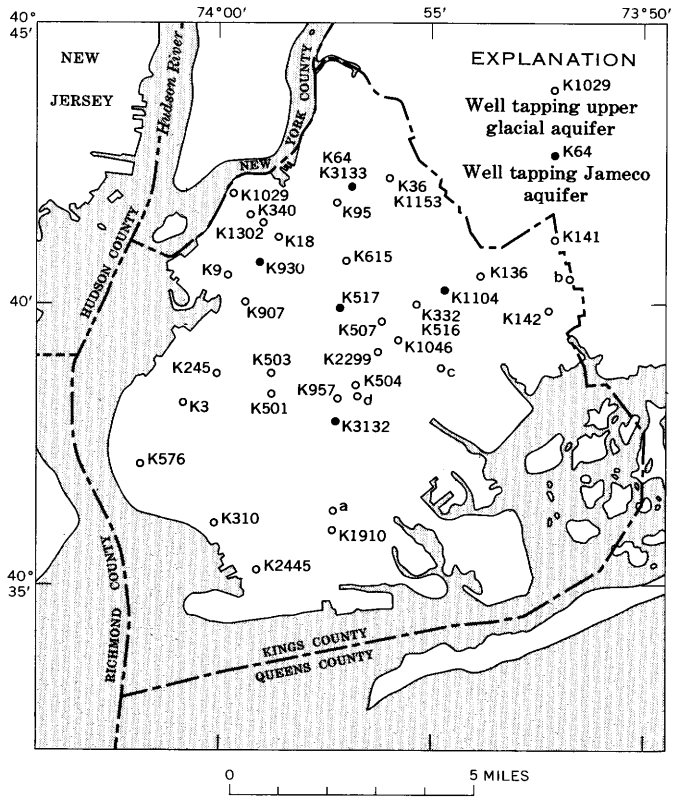

Figure 2.—Location of wells for which chemical data are given in this report, Kings County, Long Island, N.Y.

content of water from five of the six wells for which data are available (table 4) is significant. It ranges from 0.14 to 0.66 mg/l. The NH_3-N content of water from two of these six wells exceeds 0.20 mg/l. As early as 1929, water from well K517 seemingly contained dissolved nitrogen, in one form or another, in excess of the amount presumed to have been present in native ground water. For example, the NH_3-N content was 0.24 mg/l, and the total nitrogen content was 0.38 mg/l. Wells listed in table 4 are plotted on figure 2.

Table 4.—*Nitrogen content of water from wells in the Jameco aquifer in Kings County, Long Island, N.Y.*

[Results in milligrams per liter. Agency making analysis: NYC, New York City; USGS, U.S. Geol. Survey]

Well	Year of collection	Ammonia nitrogen	Nitrite nitrogen	Nitrate nitrogen	Organic nitrogen	Total nitrogen	Analyst
K64	1942	0.17	0.01	0.20	0.11	0.49	NYC
K517	1929	.24	.00	.12	.02	.38	NYC
	1934	.48	.00	.12	.11	.71	NYC
	1944	.50	.00	.49	.09	1.1	NYC
K930	1942	.66	.02	.00	.06	.74	NYC
K1104	1942	.14	.00	9.6	.11	9.9	NYC
K3132	1969	.00	.00	1.1	....	1.1	USGS
K3133	1971	.20	.00	3.0	.03	3.2	USGS

SOURCES OF NITROGEN

Although fertilizers and certain agricultural activities may be significant sources of nitrogen in water in some parts of Long Island (deLaguna, 1964; Perlmutter and Koch, 1972), domestic and industrial sewage are probably the major sources in urbanized areas. Sewage is high in ammonium ion, which in the presence of oxygen is converted to nitrite and nitrate ions. A study by the Nassau-Suffolk Research Task Group (1969) showed that the NH_3-N content of ground water near septic tanks and cesspools ranged from 51 to 115 mg/l at six sites tested. As septic-tank effluent passes through the zone of aeration, its ammonium ion content decreases with distance whereas its nitrate content increases. Nitrite was generally undetected below the water table.

According to Steel (1953, p. 407), the total nitrogen content of typical sewage ranges from 16 to 73 mg/l; the total nitrogen content of two randomly selected samples of sewage from Nassau County was 23 mg/l. As shown in table 3, the total nitrogen content of ground water from 17 widely scattered wells in Kings County is 16 mg/l or more. Also, the NH_3-N content, which is generally less than 0.02 mg/l in ground water elsewhere on Long Island, is more than 0.1 mg/l at 19 locations in Kings County. These observations, plus (1) the widespread occurrence and high concentrations of nitrate in the ground water, (2) the lack of agricultural activities and the absence of domestic waste-disposal systems in the county, and (3) the tendency of sewers to leak, indicate that leaky sewers are a major source of the nitrogen in ground water in Kings County.

At the present time, all Kings County is served by a dense network of sanitary and storm sewers. Sewerage began in the northwestern part of the county in about 1850 and increased as urbanization expanded. There were about 800 miles of common sewer lines in Kings County in 1908, 1,300 miles in 1932, and 1,700 miles in 1962 (New York City Dept. of Water Resources, written commun., 1971). No engineering and maintenance data for use in estimating total leakage from sewers in the county are available, but such leaks probably occur from time to time, and many small unreported leaks are to be expected.

The recovery of the water table throughout virtually all Kings County after a marked reduction in pumpage in 1948 seems to substantiate the premise that leaky sewers are a significant source of artificial recharge in the county. Although Kings County is highly urbanized and only a small part of the land surface is available for direct recharge of precipitation (probably less than 10 percent), the water table rose sharply from 25 feet below sea level in the 1940's (Lusczynski, 1952, p. 9) to about 9 feet above sea level in the vicinity of well K507 in 1971. Ground-water levels presently (1971) are nearly the same as they were before intensive urban development. Recharge from precipitation alone probably did not cause this rapid and marked recovery of ground-water levels. On the other hand, leaky sewers are not the only major source of

artificial recharge in Kings County. Considerable leakage probably occurs from the hundreds and perhaps thousands of miles of water mains and pipes.

CONCLUSIONS

Nitrate-rich ground water has been present in at least parts of Kings County since the early 1900's. It was found throughout the county in both 1942 and 1970. Currently, the most likely source of much of the nitrate is leakage from the sanitary sewer system.

The widespread occurrence of nitrogen-rich ground water in Kings County suggests that the value of sanitary sewer systems in alleviating or preventing contamination of ground water may be partly offset unless the sewers are carefully built and maintained.

REFERENCES

Cohen, Philip, Franke, O. L., and Foxworthy, B. L., 1968, An atlas of Long Island's water resources: New York Water Resources Comm. Bull. 62, 117 p.

deLaguna, Wallace, 1964, Chemical quality of water, Brookhaven National Laboratory and vicinity, Suffolk County, New York: U.S. Geol. Survey Bull. 1156-D, 73 p.

Lusczynski, N. L., 1952, The recovery of ground-water levels in Brooklyn, N.Y., from 1947 to 1950: U.S. Geol. Survey Circ. 167, 29 p.

Nassau-Suffolk Research Task Group, 1969, The Long Island ground water pollution study: New York State Dept. Health, 395 p.

Perlmutter, N. M., and Koch, Ellis, 1972, Preliminary hydrogeologic appraisal of nitrate in ground water and streams, southern Nassau County, Long Island, N.Y., *in* Geological Survey Research 1972: U.S. Geol. Survey Prof. Paper 800-B, p. B225–B235.

Steel, E. W., 1953, Water supply and sewerage [3d ed.]: New York, McGraw-Hill Book Co., Inc., 582 p.

Suter, Russell, 1937, Engineering report on the water supplies of Long Island: New York State Water Power and Control Comm. Bull. GW-2, 64 p.

Suter, Russell, deLaguna, Wallace, and Perlmutter, N. M., 1949, Mapping of geologic formations and aquifers of Long Island, New York: New York State Water Power and Control Comm. Bull GW-18, 212 p.

U.S. Public Health Service, 1962, Drinking water standards, 1962: U.S. Public Health Service Pub. 956, 61 p.

Veatch, A. C., Slichter, C. S., Bowman, Isaiah, Crosby, W. O., and Horton, R. E., 1906, Underground water resources of Long Island, N.Y.: U.S. Geol. Survey Prof. Paper 44, 394 p.

INVESTIGATION OF THE OCCURRENCE AND TRANSPORT OF ARSENIC IN THE UPPER SUGAR CREEK WATERSHED, CHARLOTTE, NORTH CAROLINA

By HUGH B. WILDER, Raleigh, N.C.

Abstract.—During the months of June and July 1971, the U.S. Geological Survey made a special study of the occurrence and transport of arsenic in the Sugar Creek, S.C., drainage area. It was found, during the week of June 29–July 5, that despite the fact that no known disposal of arsenic wastes had taken place in over 3 months, total arsenic concentrations ranging from 115 to 260 μg/l were still entering the tributary Irwin Creek through a sewage treatment plant, down from 1,100 μg/l in October 1970. The most contaminated phase of the aqueous system was suspended solid material in the treated sewage, which contained arsenic in amounts of 24,400 to 500,000 μg/kg by weight. Arsenic was found to be concentrating in the streambed materials, which, on June 28, contained concentrations of from 7,000 to 35,000 μg/kg. On July 29–31, 1971, samples were taken at Sugar Creek near Fort Mill, S.C., during a minor flood. These samples showed that during the flood most of the arsenic was being transported in the suspended-sediment phase and that arsenic discharge closely paralleled total suspended-sediment discharge. On February 25, 1972, dried sludge from storage beds at the treatment plant contained as much as 1,700,000 μg/kg As, 870,000 μg/kg Sb, and 120,000 μg/kg Cr.

In the fall of 1970 the U.S. Geological Survey made a reconnaissance of selected minor elements in surface waters of the United States. A sample collected from Sugar Creek near Fort Mill, S.C., was found to contain 1,100 μg/l (micrograms per liter) As, which is more than 20 times the 50 μg/l allowable in a public water supply, (U.S. Public Health Service, 1962).

The drainage area to the Fort Mill site lies primarily in the municipal and industrial complex of Charlotte, N.C. Because Sugar Creek is a tributary to the Catawba River,, which is a source of public water supplies, there was immediate concern among local officials as to the origin of the arsenic.

A second sample was taken from Sugar Creek near Fort Mill on March 23, 1971, and was found to contain 505 μg/l As—thus confirming that unusual concentrations of the element were persistent in the stream.

Federal, State, and local authorities then undertook the task of locating the source of the arsenic. The North Carolina Department of Water and Air Resources (now the Office of Water and Air Resources) sampled both Sugar Creek and its major tributaries and traced the source of arsenic to the city of Charlotte's Irwin Creek Sewage Treatment Plant. (See figure 1 for locations.) Although the primary source of the arsenic was never identified, officials of the Mecklenburg County Health Department indicated that there was a chemical company in the area, which, until March 1971, had been actively engaged in the production of arsanilic acid.

In June and July 1971, the U.S. Geological Survey undertook additional investigations to study in more detail the occurrence and transport of arsenic in the Sugar Creek drainage system. By June, when this investigation was started, concentrations of arsenic in the treatment-plant effluent were considerably less than those found in March.

There were two primary goals in this investigation. The first was to collect information that would lead to a better understanding of the local problem, and the second was to study the occurrence and transport of arsenic in a stream system. Arsenic, like most trace constituents, has been the subject of only scant attention with respect to its behavior in streams.

ARSENIC INPUT TO THE STREAMS

During June 29–July 5, 1971, the effluent from the Irwin Creek Sewage Treatment Plant was sampled at 6-hour intervals. Samples were collected with a standard USDH-59 depth-integrating suspended-sediment sampler, which is designed to collect a representative mixture of water and suspended sediment. The sampler was coated inside with white epoxy enamel and fitted with a silicone-rubber gasket to minimize the possibility of contamination from the metal body of the sampler. Several acid-washed pint milk bottles were filled each time the system was sampled, and four analytical determinations were made:

1. Total arsenic was determined on a sample which included both the liquid and the suspended-sediment phases of the aqueous mixture entering the stream channel. The purpose of this sample was to determine the total amount of arsenic being introduced into the stream.

U.S. GEOL. SURVEY PROF. PAPER 800-D, PAGES D205-D210

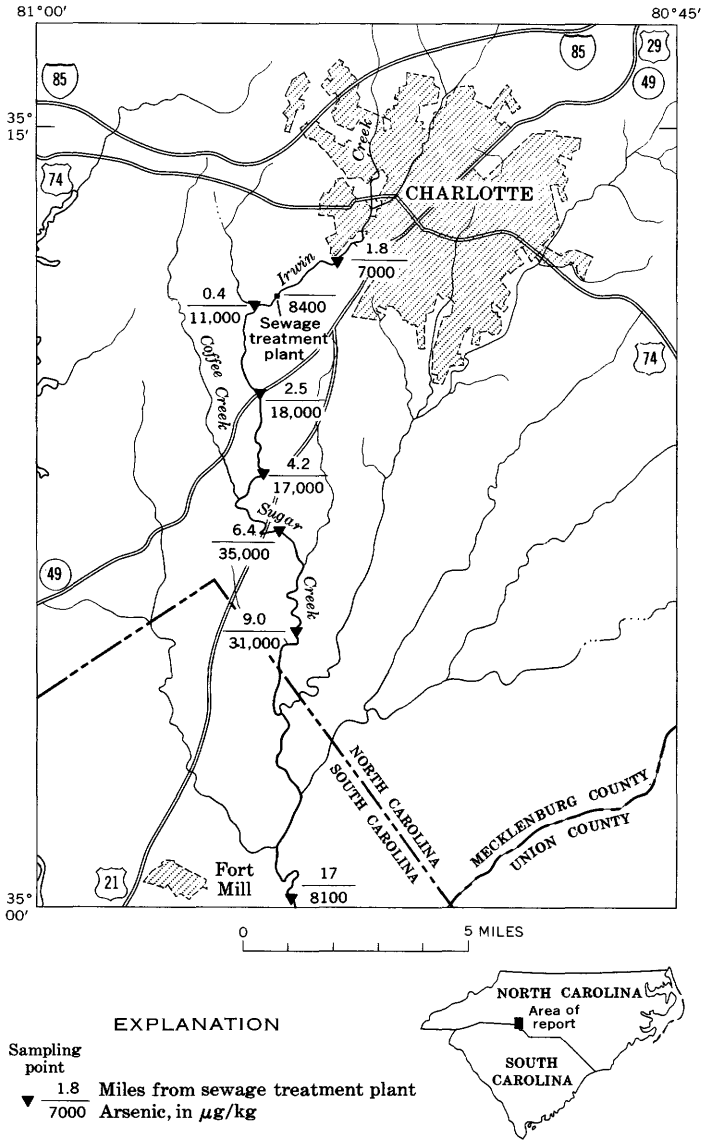

Figure 1.—Map showing sampling points, mileage from Irwin Creek Sewage Treatment Plant, and arsenic concentration for bed-material samples from Irwin and Sugar Creeks.

2. Arsenic in solution was determined on a sample from which the suspended material was removed by filtering through a 0.45μ membrane-type filter immediately after the sample was collected. This sample was to determine how much of the total arsenic was in solution.
3. The material collected on the filter from sample 2 was retained for direct analyses of arsenic contained in the suspended-sediment phase. Results of this determination are hereafter referred to as arsenic on suspended sediment.
4. Total suspended sediment was determined by filtering the suspended material from a sample collected in the same manner as the total-arsenic sample (sample 1) and weighing the material collected on the filter after drying in an oven at 130° Celsius.

Total arsenic in the plant effluent ranged from 115 to 260 μg/l during the 7-day period. The original purpose of these samples was to discover to what extent concentrations of arsenic entering the stream varied with time. As shown in table 1 the concentrations of arsenic entering the stream ranged from 115 to 260 μg/l and were erratic or "sluggy" in their chronological variations, but the then-unknown fact that no known arsenic source to the treatment plant was still active made these results much less significant than they would have been earlier when the plant was actually treating arsenic-bearing wastes. The total quantity of arsenic entering the stream system from June 29 to July 5 is shown in table 1 to have ranged from 9.3 to 17.3 lb per day (pounds per day).

The most contaminated phase of the effluent was the treated-sewage solids coming from the plant. On the basis of direct analyses, as shown by arsenic on suspended sediment in table 1, arsenic in the suspended treated-sewage solids ranged from 24,400 to 500,000 μg/kg on a dry-weight basis. The form in which this arsenic exists and the manner in which it is associated with the suspended solid materials are not known. The suspended matter in these samples was primarily a finely divided organic agglomerate, which undoubtedly was similar to the material deposited in sludge beds of the treatment plant. Thus the sludge from the plant is probably also highly contaminated with arsenic, and stockpiles of dried sludge may represent a secondary source of arsenic in the watershed that will continue to furnish arsenic to the stream.

Total suspended-sediment concentrations in the effluent ranged from 11 to 75 mg/l (milligrams per liter) (table 1). Suspended-sediment concentrations were used to determine the total dry weight of suspended material, which was needed to calculate the values reported for arsenic on suspended sediment.

ARSENIC ON BED MATERIALS

Samples of bed material from the bottom of the stream were collected on June 28, 1971. The locations of these samples and the concentrations of arsenic, in micrograms per kilogram, found in them are shown on figure 1. The data indicate a gradual buildup of arsenic in the streambed from 7,000 μg/kg, 1.8 miles upstream from the sewage outfall, to a maximum of 35,000 μg/kg, 6.4 miles downstream. At Sugar Creek near Fort Mill, S.C., which is 17 miles downstream, the concentration of arsenic in the bed materials decreased to 8,100 μg/kg.

An unexpected feature of the bed-material analyses was the high concentration upstream from the treatment plant. This remained unexplained until the Mecklenburg County Health Department (R. McMillan, oral commun., August 1971) later discovered that, in the past, arsenic-bearing wastes had probably been disposed of in a manhole, which eventually emptied into Irwin Creek above the sewage treatment plant. The overall buildup of arsenic in the streambed downstream

Table 1.—*Effluent from Irwin Creek Sewage Treatment Plant—Part 1 of investigation of June 29–July 5, 1971*

[n, noon; m, midnight]

Date	Time	Rate of effluent discharge (cfs)	Suspended sediment (mg/l)	Total arsenic		Arsenic on suspended sediment	
				(μg/l)	(lb per day)	(μg/kg)	(lb per day)
6-29-71	6 a.m.	17.9	22	115	17.3	273,000	0.5
	12 n	14.3	23	190		261,000	
	6 p.m.	17.3	34	260		176,000	
	12 m	15.5	32	250		188,000	
6-30-71	6 a.m.	14.7	16	190	15.5	500,000	.4
	12 n	13.0	27	160		74,100	
	6 p.m.	17.9	56	230		35,700	
	12 m	....	...	....		.....	
7-1-71	6 a.m.	14.2	41	205	14.2	24,400	.5
	12 n	13.6	41	160		48,800	
	6 p.m.	17.0	32	180		156,000	
	12 m	17.9	75	150		40,000	
7-2-71	6 a.m.	17.9	39	150	12.3	128,000	.7
	12 n	15.5	28	120		107,000	
	6 p.m.	17.9	30	150		100,000	
	12 m	14.3	28	120		179,000	
7-3-71	6 a.m.	14.9	29	120	10.7	138,000	.4
	12 n	12.4	32	130		62,500	
	6 p.m.	12.7	23	160		44,500	
	12 m	13.0	31	210		96,800	
7-4-71	6 a.m.	13.6	57	170	10.9	35,100	.4
	12 n	12.4	55	170		54,500	
	6 p.m.	11.4	24	170		167,000	
	12 m	11.1	21	180		238,000	
7-5-71	6 a.m.	7.7	26	150	9.3	308,000	.5
	12 n	13.9	11	170		182,000	
	6 p.m.	13.0	23	160		130,000	
	12 m	13.1	23	150		130,000	

from the treatment plant is thought by the author to be a result of the gradual settling of solid material contained in the treated effluent to the bottom of the stream during periods of low flow. It is not known if the pattern of distribution of arsenic in the bed materials shown on figure 1 is typical or if it is one view of a pattern that changes with each set of antecedent conditions.

TRANSPORT OF ARSENIC IN SUGAR CREEK

The discovery that much of the arsenic entering the stream was in the suspended organic-solids phase of the aqueous system, and that it was concentrating on the bottom sediments during periods of low streamflow, led to the hypothesis that it would be resuspended during floods. In fact, as the organic agglomerate thought to contain most of the arsenic would be the lightest (least dense) material on the bottom of the stream, it seemed logical that it would be the first solid material to go into suspension when stream velocity increased, and therefore the quantity of arsenic transported by the stream would be greatest during the early stages of a flood. To test this hypothesis, samples were collected at Sugar Creek near Fort Mill during a minor flood on July 29–31, 1971. These samples were collected and analyzed exactly the same as those collected at the sewage treatment plant as described above. Fort Mill is 17 miles downstream from the treatment plant, and the samples collected there are representative of the behavior of arsenic once it becomes a part of the natural stream environment.

Total-arsenic concentrations at Fort Mill, as shown in table 2 and on figure 2, varied from 12 to 122 μg/l. These concentrations were somewhat less than those observed in the samples of the Irwin Creek Sewage Treatment Plant effluent, because of the plant effluent's being diluted by less highly contaminated stream waters. Arsenic in solution at Fort Mill ranged from 7 to 91 μg/l.

Since July 1971, monthly measurements of total arsenic in Sugar Creek near Fort Mill, S.C., show that concentrations of the element have decreased to the point that, for the most part, they are now within acceptable limits. Analyses of these samples are tabulated below.

Date (1971)	*Arsenic (μg/l)*	*Date (1972)*	*Arsenic (μg/l)*
August 17	46	January 25	59
September 24	37	February 25	12
October 19	19	March 17	14
November 23	27	April 19	15
December 16	20		

These monthly samples were all collected when stream discharge was reasonably low (less than 500 cfs); it is possible that higher concentrations exist during at least the early stages of higher flows.

Table 2.—*Data for Sugar Creek near Fort Mill, S.C.—Part 2 of investigation of July 29–31, 1971*

Date	Time	Discharge (cfs)	Suspended sediment (mg/l)	Total arsenic		Arsenic in solution (μg/l)	Arsenic on suspended sediment	
				(μg/l)	(lb per hr)		(μg/kg)	(lb per hr)
7-29-71	11:00 p.m.	500	90	100	11	91	66,700	1.2
7-30-71	12:45 a.m.	1,100	1,530	122	27	89	27,500	8.1
	2:00 a.m.	2,000	5,720	91	40	14	17,500	35
	3:20 a.m.	2,400	3,130	51	27	17	4,470	19
	6:00 a.m.	3,000	1,490	30	22	7	9,400	16
	11:30 a.m.	4,300	840	24	22	9	14,300	15
	4:30 p.m.	4,000	564	17	14	7	10,600	9.2
	8:45 p.m.	3,000	516	17	11	4	15,500	8.3
7-31-71	6:00 a.m.	2,800	535	12	7	8	15,000	3.0
	8:00 a.m.	1,500	287	27	11	20	20,900	2.1

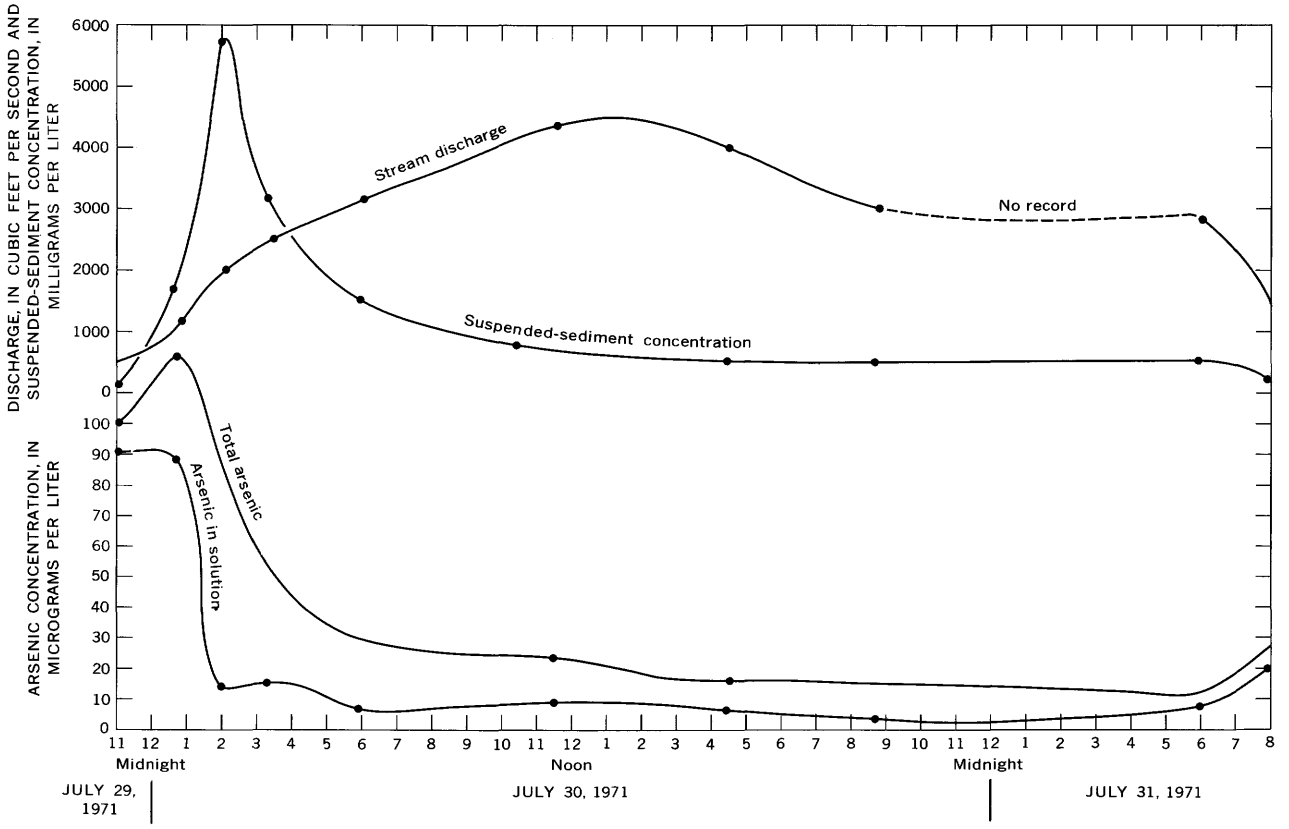

Figure 2.—Graph comparing arsenic concentrations in various aqueous phases with stream discharge and suspended-sediment concentrations, Sugar Creek near Fort Mill, S.C., July 29–31, 1971.

Arsenic-on-suspended-sediment concentrations in the samples collected at Fort Mill ranged from 10,600 to 66,700 μg/kg on a dry-weight basis, indicating that even at locations representative of typical stream conditions along Irwin and Sugar Creeks, the most contaminated phase of the aqueous environment during periods of high streamflow is the suspended-sediment phase.

Total-arsenic concentrations were increasing with stream discharge at the time the first samples were collected and continued to increase for about 2 hours, then gradually decreased to a fairly stable level after 4 to 6 hours, even though the stream discharge continued to rise throughout much of this period (fig. 2). The fact that the suspended-sediment phase contained a greater percentage of arsenic than the liquid phase suggests that the concentration of arsenic in the stream during the flood was related to the concentration of suspended sediment being transported. Figure 2 also shows a simultaneous plot of both total-arsenic and total suspended-sediment concentrations during the flood of July 29–31. It is obvious that the concentration of arsenic in the stream was indeed closely related to the concentration of sediment. It is also obvious that the total-arsenic concentration reached a

maximum slightly before the maximum sediment concentration occurred. The early peaking of total arsenic relative to sediment concentration suggests that the treated-sewage solids, being lighter than the inorganic streambed materials, are put into suspension at lower stream velocities.

A more direct appraisal of the quantity of arsenic in a stream can be made by considering the actual amount of arsenic being transported. From June 29 to July 5 the daily discharge of arsenic from the sewage treatment plant into Irwin Creek ranged from 9.3 to 17.3 lb per day. In contrast, on July 30 the floodwaters of Sugar Creek transported a total-arsenic load of 480 pounds past Fort Mill. The greater load transported during the flood represented a pickup of arsenic that had accumulated in the streambed materials during preceding periods of low flow. The discharge rate of arsenic being transported at any time is shown on figure 3 to be primarily dependent upon the suspended-sediment load being carried in the stream at that time. Stream discharge seemed to have only a minor effect on the arsenic transport rate, except as it affected the concentration of sediment in suspension.

ARSENIC IN THE WATERSHED

A short followup study was made in February 1972 to determine the extent to which certain parts of the watershed might still be contaminated with arsenic residuals left over from the period when arsenic-bearing wastes were actively produced and deposited in the basin.

This study included water samples from a drainage ditch which during rainy periods carries runoff from land surface areas around the commercial plant that had been producing arsanilic acid, and samples of solid material from two sludge beds in which the city of Charlotte stored ("disposed of") treated-sewage solids from the Irwin Creek Sewage Treatment Plant. For comparison, a sample was also collected from Charlotte's McAlpine Creek Sewage Treatment Plant, which is not known to have treated any arsenic-bearing wastes. Duplicate samples were collected from each of these sources with one set of samples being analyzed by neutron activation techniques and one set by more commonly used chemical techniques.

Results of analyses of the two sets of samples are tabulated below:

Sample	*Arsenic concentration*	
	Neutron activation	*Chemical*
Water sample from drainage ditch behind arsenic-producing plant.	1,200 μg/l	1,100 μg/l
Sludge from Irwin Creek STP bed 47 filled April 27, 1971.	1,300,000 μg/kg	1,200,000 μg/kg
Sludge from Irwin Creek STP deposited prior to March 1971.	1,600,000 μg/kg	1,700,000 μg/kg
Sludge from McAlpine STP	5,100 μg/kg	5,500 μg/kg

It is obvious that, while no disposal of arsenic is known to have occurred in the basin since March 1971, the element still is present in the upper watershed and may continue to pose a threat to the streams, particularly during periods of heavy surface runoff.

The close agreement in concentrations measured by the two independent analytical techniques enhances confidence in the validity of the results.

OTHER TOXIC SUBSTANCES

The capability of neutron activation methods to quickly "scan" for the presence of a large number of trace elements was utilized to make a search for toxic substances other than arsenic in these samples. Of these, antimony, chromium, and mercury were qualitatively identified, and later determined quantitatively. Results of these analyses are shown below:

Water from drainage ditch behind arsenic-producing plant:			
1.	Not acidified	Antimony	310 μg/l
1a.	Acidified	...do...	320
Sewage sludge from sewage treatment plant:			
2.	Irwin Creek STP sludge bed 47 collected Feb. 25, 1972 (filled Apr. 27, 1971).	Antimony	870,000 μg/kg
		Chromium	120,000
3.	Irwin Creek STP collected Feb. 25, 1972 (deposited prior to March 1971).	Antimony	650,000
		Chromium	61,000
4.	McAlpine Creek STP sludge bed 23 collected Feb. 25, 1972.	Antimony	14,000
		Chromium	100,000
		Mercury	20,000

Most significant among these results are the unexpectedly high amounts of antimony found in the samples containing large amounts of arsenic. Antimony is not an intentional component of any of the final products known to be manufactured in the basin, and its apparent association with arsenic in these samples is possibly coincidental. Because arsenic and antimony are chemically quite similar, and they frequently occur together in nature, it is possible that the antimony found here is a carryover of impurities in the raw materials brought into the basin for manufacturing purposes.

Although no standards for allowable limits of antimony in interstate waters are known to exist, it is generally considered to rank with arsenic in toxicity. These results strongly imply that, during periods when waters in the Sugar Creek watershed contain excessive amounts of arsenic, they may also contain excessive amounts of antimony.

CONCLUSIONS AND DISCUSSION

1. Arsenic concentrations in the Sugar Creek watershed have decreased considerably since the discovery of 1,100 μg/l in Sugar Creek near Fort Mill, S.C., on October 9, 1970. By June 1971, no known production of arsenic-bearing wastes had taken place in the basin since March 1971, but concentrations of arsenic ranging from 115 to 260 μg/l were still being found in the treated-sewage effluent from Charlotte's Irwin

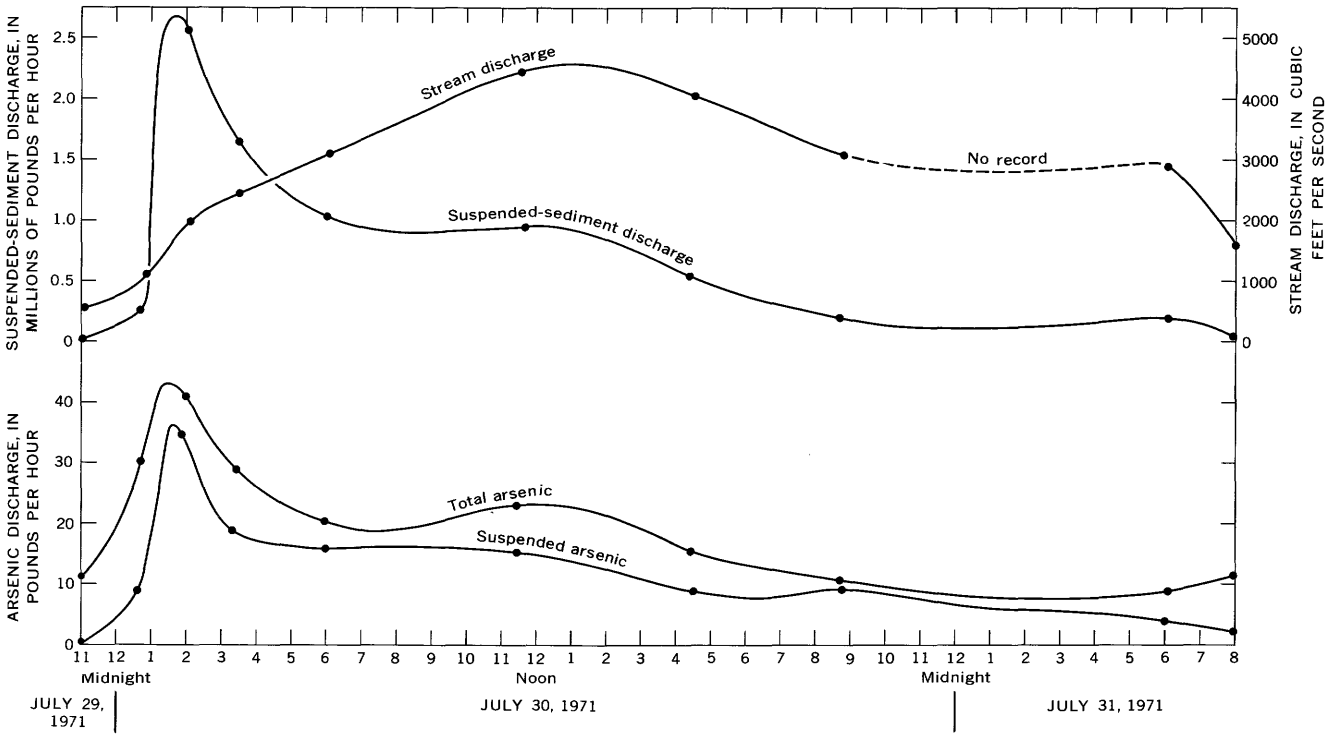

Figure 3.—Graph comparing arsenic discharge with stream discharge and suspended-sediment discharge, Sugar Creek near Fort Mill, S.C., July 29–31, 1971.

Creek Sewage Treatment Plant. It is not known whether this arsenic was residual from some earlier contaminating source; however, periodic sampling since that time has shown a steady decline in arsenic concentrations in the stream. A buildup of arsenic of 7,000 to 35,000 μg/kg was found in samples collected from streambeds in the area, and treated-sewage solids from the treatment plant were found to contain from 24,400 to 500,000 μg/kg As.

2. Samples collected from Sugar Creek near Fort Mill in July 1971 indicated that total-arsenic loads of from 7 to 40 lb per hr were being transported during a minor flood, and that 2.1 to 35 lb per hr of this was being transported in the suspended-sediment phase. The transport of arsenic during the flood correlated closely with the quantity of suspended sediment being discharged, and the effect of stream discharge was limited primarily to its effect on sediment discharge.

Monthly samples collected from August 1971 to April 1972 indicated that during low and medium flows arsenic concentrations at Fort Mill had decreased to acceptable levels.

3. The discovery that much of the arsenic was contained in the treated-sewage solids raised the possibility that sludge from the treatment plant, much of which has been disposed of on the watershed, may continue to furnish arsenic to the stream system, even though no primary source was still actively wasting arsenic to the system.

Analyses of dried sludge from the Irwin Creek Sewage Treatment Plant made in February 1972 showed that the sludge contained 1,200,000 to 1,700,000 μg/kg As and 650,000 to 870,000 μg/kg Sb. In contrast, sludge from the McAlpine Creek Sewage Treatment Plant, which is not known to have processed arsenic waters, contained only 5,100 to 5,500 μg/kg As and 14,000 μg/kg Sb.

REFERENCE

U.S. Public Health Service, 1962, Drinking water standards: Public Health Service Pub. 956, 61 p.

LAND-USE EFFECT ON THE WATER REGIMEN OF THE U.S. VIRGIN ISLANDS

By DONALD G. JORDAN, San Juan, P.R.

Work done in cooperation with the Government of the U.S. Virgin Islands and the National Park Service

Abstract.—Scattered hydrologic data collected over the past 50 years indicate that base flow of mountain streams on the three main islands of the U.S. Virgin Islands is diminishing. The decline is attributed principally to changes in land use—reversion of land from agriculture to dense brush and forest. Rainfall that once infiltrated below the shallow root zone of crops increasingly has been intercepted and transpired by deep-rooted wild growth. Recharge to the bedrock aquifer and consequent base flow thus have been reduced. The apparent long-term decline in rainfall since the early 1900's is a contributing factor.

The climate and the land are integral parts of the water cycle. The various parameters of each and the effect of these parameters on the water cycle are not readily determined, nor is it within the scope of this paper to attempt to determine them. In essence, what will be presented are some observations based primarily on the parameters of rainfall and vegetal cover of the land and their apparent effect on streamflow and ground-water levels in the mountain basins of the islands.

The U.S. Virgin Islands consist of more than 40 islands and cays located about 1,100 miles east-southeast of Miami and about 50 miles east of Puerto Rico. The islands form part of the Antilles Islands, which separate the Caribbean Sea from the Atlantic Ocean. The three largest and most important islands are Saint Croix, Saint Thomas, and Saint John, whose respective areas are approximately 80, 32, and 20 square miles (fig. 1).

HISTORICAL DEVELOPMENT OF WATER SUPPLIES

The water resources of the U.S. Virgin Islands have never been abundant. Archeological, historical, and geological evidence, however, indicates that the water resources once were greater than at present.

Scattered throughout the islands are the sites of former villages of Indian people—the Arawaks on St. Thomas and St. John, and the Caribs on St. Croix (fig. 1). Reliance on the sea for food apparently was an important factor in the location of the villages. Equally important was the need for defense, shelter from storms, and water supply. Most village sites appear to be a compromise among these factors.

Only one of the many village sites on St. Thomas and St. John is still served by a stream—that at Dorothea Bay in St. Thomas, into which Bonne Resolution Gut flows. All the other sites are within a short distance of stream courses that are now dry much of the time, but that are believed to have contained perennial streams, or at least perennial spring pools. The village sites on St. Croix are on streams that were perennial until recent years.

From comments in reports and journals of the 17th and 18th centuries, water was a precious commodity. There were complaints of drought and mention of searches made for streams and springs. Evidently the search for water was at least partly rewarding, for streams and springs no longer flowing are mentioned in the early journals and shown on maps (fig. 1).

Scattered throughout the islands, but especially on St. John, can be found the masonry remains where springs were developed or dams were built to impound water. The storage capacity of the pools formed by the dams usually was no more than a few thousand gallons each. The small storage capacity of these pools would be of little value for the retention of storm runoff for long-term use. It must be assumed that the streams were perennial and that the dams were merely diversion structures from which the flow of the streams was channeled to points of use.

More recently, water from Jolly Hill Gut on St. Croix was diverted to a sugar factory and also was used to irrigate sugarcane. A photograph taken in the 1870's, a period of severe drought, shows a fresh-water pond at the site of the baseball park north of Fredriksted that was fed by the flow of Jolly Hill Gut and its tributaries. As late as the 1920's, water was diverted from Salt River (now dry) and River Gut to supply a distillery at Christiansted and the sugar factory at Bethlehem, respectively.

U.S. GEOL. SURVEY PROF. PAPER 800-D, PAGES D211-D216

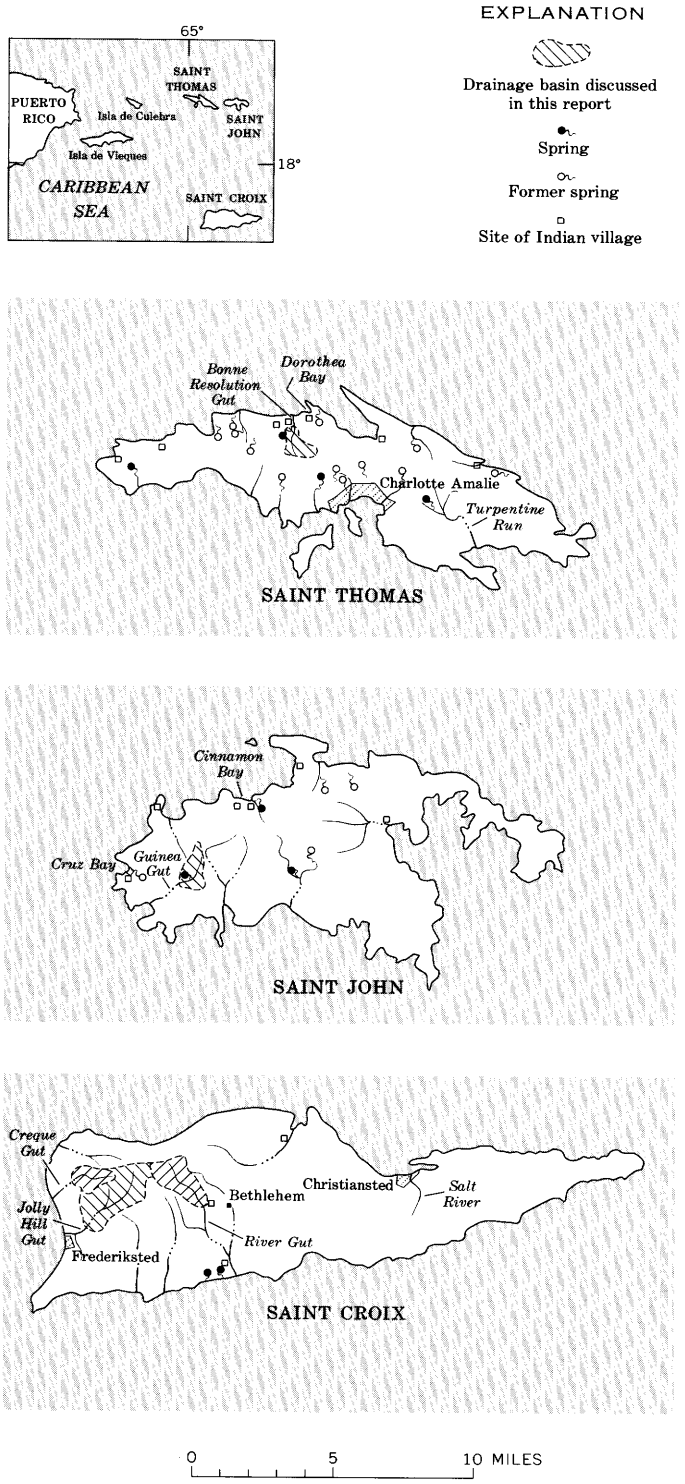

Figure 1.—Map of the U.S. Virgin Islands, showing selected streams, drainage basins, springs, and sites of Indian villages.

Calcareous tufa deposits are found in many stream channels. The deposits indicate perennial or intermittent flow in stream channels that now carry only occasional storm runoff. In Creque Gut on St. Croix, tufa covers the face of several small dams built in the 1920's or early 1930's. Tufa is being deposited at present at a small spring in Guinea Gut on St. John. Elsewhere, tufa no longer is being deposited.

The evidence points to changes in the water regime since the islands were first settled by Europeans. Such changes would be expected. Since the early 1900's, there has been a major change in the water resources, triggered, in the author's opinion, by major changes in land use and to some extent by a general decrease in rainfall. This hypothesis is based on the social and economic history of the islands, 116 years of rainfall record, the reports of early water-resources investigations, and a few years of streamflow and ground-water records.

HYDROLOGY

The islands are a study in microhydrology. River Gut on St. Croix has a drainage area of about 11 square miles, by far the largest in the islands. No other drainage basin, from headwaters to the sea, exceeds 4 square miles. The largest of the mountain drainage basins (Jolly Hill Gut on St. Croix, fig. 1) referred to in this paper has an area of 2.10 square miles—minute by continental standards.

The geology of the mountain basins is similar throughout the islands. The basins are underlain by fractured epiclastic or pyroclastic volcanic rocks covered by a thin, permeable mantle of soil generally less than 2 feet thick. River Gut on St. Croix is the only exception, with the central part of its upper basin underlain by a fractured and weathered gabbro intrusive, mantled by alluvium.

The mountain part of each basin is, in essence, a hydrologic unit. The fractured bedrock forms an aquifer whose limits are the topographic boundary of the basin. Ground-water storage in the aquifers, estimated to be only about 1 percent by volume, is replenished solely by rainfall on the basin. Streamflow from the basin also is dependent upon rainfall, either directly as storm runoff, or indirectly as base flow (ground-water discharge to the streams).

The streams are best classified as intermittent, having short reaches fed by ground-water discharge the greater part of the year. It is seldom that there is flow all the way from the headwaters to the sea. Streamflow is measured in terms of thousands of gallons per day and millions of gallons per year. Annual runoff seldom is more than 5 percent of the annual rainfall. During extreme drought, such as was experienced in 1964–68, even this small flow may cease for long periods.

CLIMATE

Little is known of the climatic history of the islands. It can only be assumed that wind direction and velocity have not changed in the past 300 years. There have been worldwide cooling and warming periods in the past 3 centuries, with associated excessive and deficient rainfall (Fairbridge, 1960).

It must be assumed that the islands also have been affected by these variations.

The only long-term climatic parameter recorded in the islands is rainfall. Rainfall was observed on St. Thomas from 1828 to 1839 by a Dr. Hornbeck (Knox, 1852). The average annual rainfall for that early period was 46.8 inches, but slightly different from the normal of 44.8 inches recorded at Charlotte Amalie in modern times.

A composite record of more than 100 years of rainfall on St. Croix is shown in figure 2. The record is believed by the author to be representative of the trend of rainfall for all the islands. Two severe droughts have occurred, one in the 1870's and the other in the 1920's. It seems that a third drought is being entered.

A 10-year moving average shows a variation of about 10 inches in rainfall between wet and dry periods—a change of about 12 percent above or below the average of 42 inches. Year to year rainfall shows large differences. In 1960, rainfall at Annas Hope on St. Croix was 56 inches. Four years later, in 1964, it was only 27 inches.

Rainfall distribution over the mountain basins ranges from 45 to 55 inches in years of average rainfall. The annual variation can be large, as is evident in a comparison of rainfall on St. Thomas and St. Croix for 1963 and 1964 (fig. 3). Rainfall on St. Croix in 1963 was near average, and distribution was similar to that of the long-term average.

In contrast, rainfall on St. Thomas in 1963 was below average in the central mountains, and distribution was in no way similar to the long-term average.

LAND USE

The U.S. Virgin Islands were covered with mature tropical forest when first settled by Europeans. Much of the forest was destroyed to clear land for crops. The cleared land, including the mountain slopes that were terraced, was planted with sugarcane and, in the drier areas, with sea-island cotton. Poorer land was used for pasture. Forest was limited to the most inaccessible areas. By the mid-1800's, the profitable sugar trade was in decline, owing to competition from other islands, and much of the planted land was converted to pasture. Between 1900 and the present, there has been wholesale abandonment of the land for any agricultural pursuit. Dense brush, primarily false tamarind and acacia, took over thousands of acres, and, locally, second-growth forest of tropical hardwoods became established.

In the five mountain basins referred to in this paper (fig. 1), the cleared land generally is in pasture now. A few acres of the Bonne Resolution Gut basin on St. Thomas are in truck crops, and in the River Gut basin on St. Croix cleared land was used about equally for sugarcane and pasture until converted to a golf course in 1965.

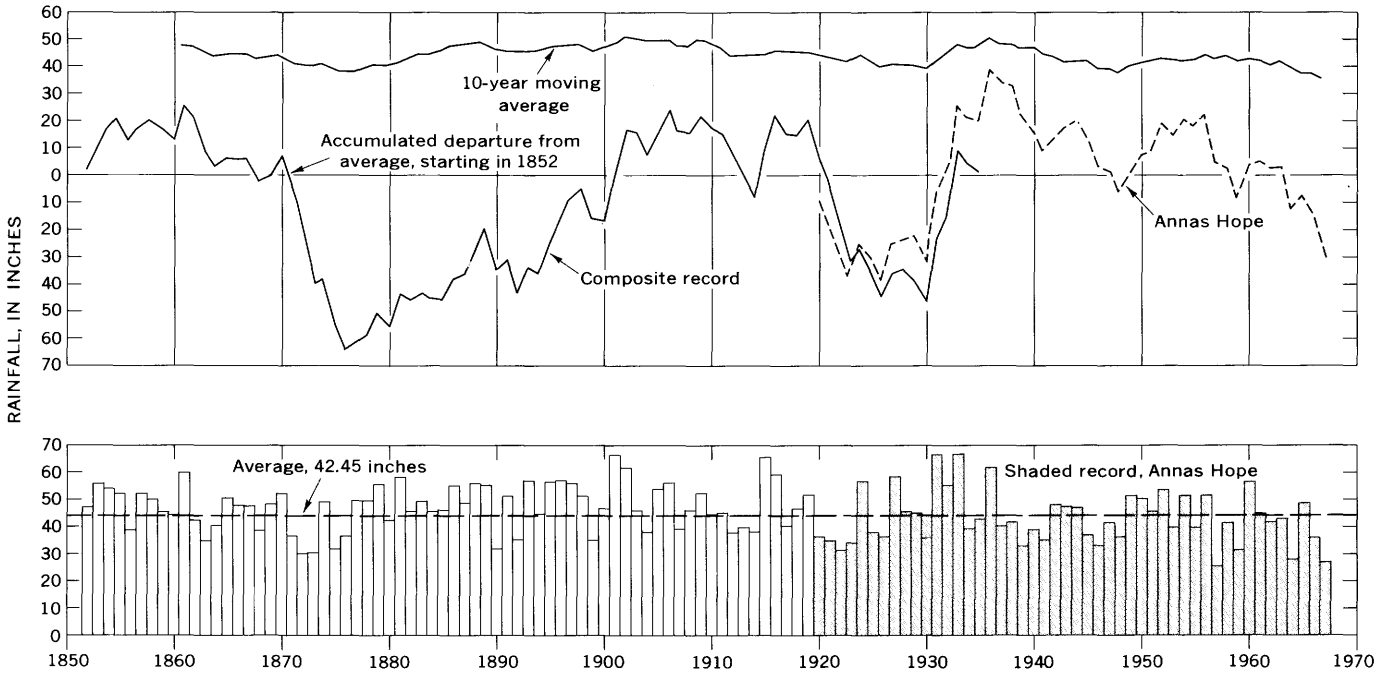

Figure 2.—Ten-year moving average, accumulative departure from average, and annual rainfall, St. Croix, 1852–1967. From composite record at Christiansted, Frederiksted, and Kingshill, 1852–1935, compiled by A. F. Johnson (1936a, b), U.S. Bureau of Reclamation, and record for National Weather Service gage at Annas Hope, 1920–67.

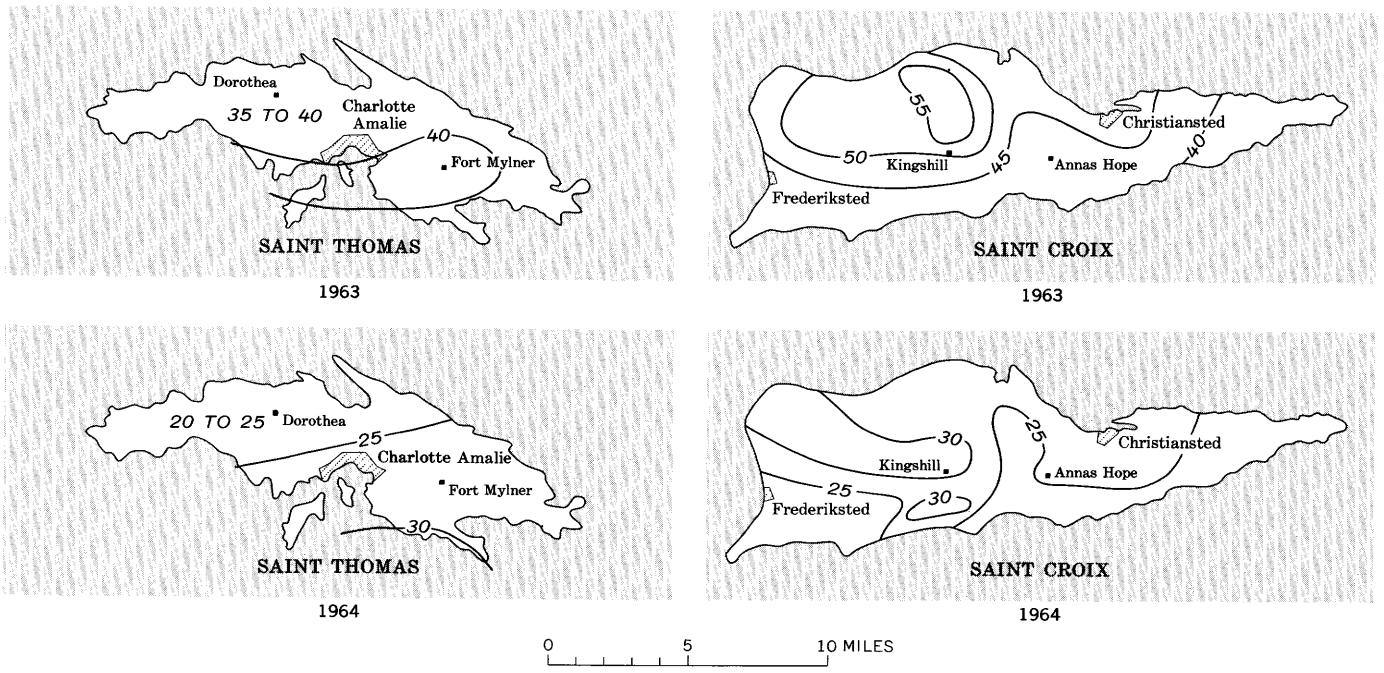

Figure 3.—Distribution of annual rainfall on St. Thomas and St. Croix, 1963 and 1964. Lines of equal rainfall in inches. Data from National Weather Service and U.S. Geological Survey gages.

LAND USE, RAINFALL, AND THE WATER REGIME

Land use in the mountain basins is believed by the author to exert greater influence on stream discharge than do topography, geology, and, to a degree, even rainfall, the ultimate source of the water.

Although the hydrogeologic features and rainfall of the major basins are similar, the flow of the streams, in terms of storm runoff, base flow, or total runoff, is not directly proportional to drainage area. For example, in 1963 the total runoff of Jolly Hill Gut on St. Croix was only about 0.5 percent of the total rainfall of 47 inches on the basin, about equally divided between storm runoff and base flow. In contrast, total runoff of Bonne Resolution Gut on St. Thomas in 1963 was about 8 percent of the total rainfall of 38 inches on the basin; storm runoff was about two-thirds of the total runoff.

Creque Gut and Jolly Hill Gut (fig. 4) drain adjacent basins in northwestern St. Croix. The basins, 0.5 and 2.1 square miles in extent, respectively, lie in terrane hydrogeologically similar. Rainfall over the basins is about 50 inches annually. Discharge of the streams would be expected to be directly proportional to drainage area, yet a comparison of instantaneous base flow of the streams in 1963 (fig. 5) shows that Creque Gut had from 6 to 10 times the flow of Jolly Hill Gut per square mile of drainage area. The difference is attributed to greater transpiration by vegetation, largely brush and forest in the Jolly Hill Gut basin.

When the base flow of the streams is related to the percentage of brush and forest cover of their watersheds, a crude pattern emerges, as shown in figure 6. No allowance has been made for variations of topography, geology, and rainfall. However, even large adjustments of base flow due to these parameters could not cause the wide differences in discharge per unit area that have been observed.

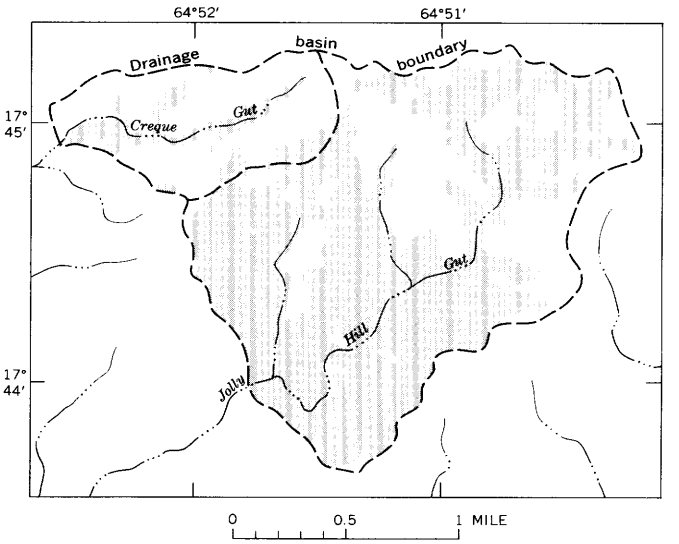

Figure 4.—Brush and forest cover (shaded) in upland parts of Creque Gut and Jolly Hill Gut basins, northwestern St. Croix (see also fig. 1). Cover information from U.S. Geological Survey topographic map, Frederiksted, V.I., 1:24,000, 1958, and updated by observation, 1963–64.

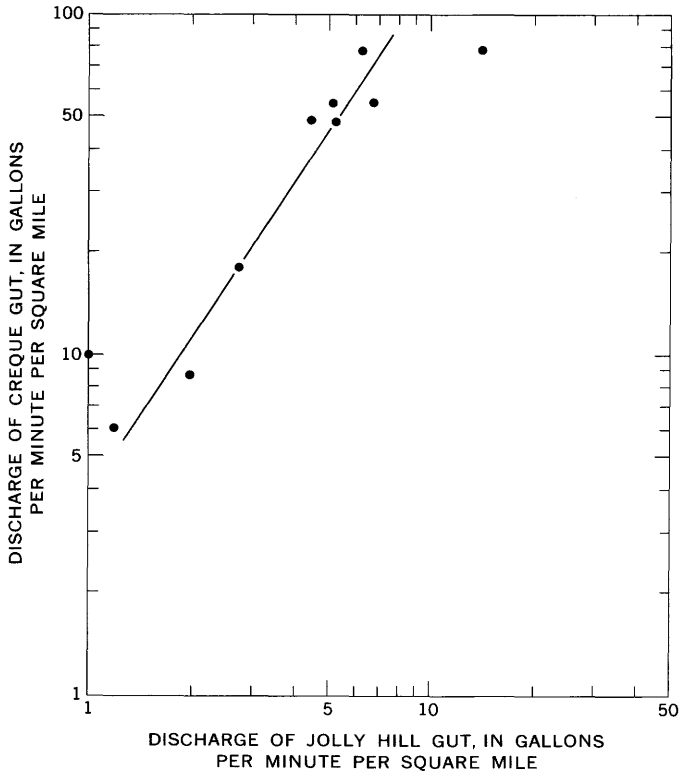

Figure 5.—Relation of base flow in Creque Gut to that in Jolly Hill Gut, St. Croix, on selected days during 1963.

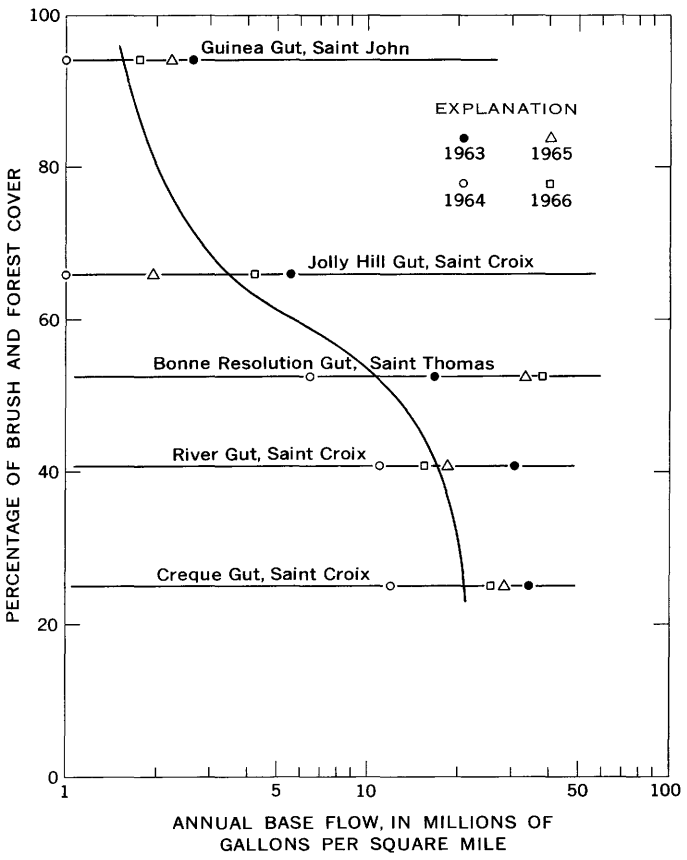

Figure 6.—Relation of annual base flow and percentage of brush and forest cover in major stream basins—also see figures 1 and 4. (Base flow obtained from separation of discharge hydrograph.)

Replenishment of the ground-water reservoir upon which base flow depends is, in turn, dependent upon the antecedent soil-moisture conditions. Even major storms may contribute nothing to the aquifer when the soil is dry, although storm runoff may be produced. In extremely dry periods, rains of as much as 3 inches have caused no recharge in some basins.

The hydrograph of a well in the Turpentine Run basin, St. Thomas, (fig. 7) shows the effect of antecedent soil-moisture conditions upon aquifer recharge. Heavy rains in September and October 1965 did little more than replenish soil moisture and satisfy the water demand of the brush and pasture land of the basin. The heavy rains in the following 2 months then were effective in recharging the aquifer.

The amount of brush cover on the mountain watershed undoubtedly is a major factor in determining ground-water recharge and the volume of base flow of a stream. The brush intercepts rainfall on its leaves in addition to being a great user of soil moisture and also of ground water where the water table is within reach of its roots. Roots of brush and trees have been observed as a dense mat at the top of the water table at a depth of 20 feet in the alluvium at Cinnamon Bay on St. John, and nearly as deep in open joints in the bedrock in roadcuts on St. Thomas. This is in contrast with grasses and crops whose roots rarely extend beyond a depth of 3 feet. Since soil moisture demand must be satisfied, or nearly so, before recharge can occur, a relatively large volume of water must go to replenish the 20 feet or so of root zone before water can replenish the aquifer.

The roots of brush not only intercept infiltrating rainwater as it moves toward the water table, but also they intercept ground water as it moves out of the aquifer to become base flow in streams. One need only look at the belt of vigorous

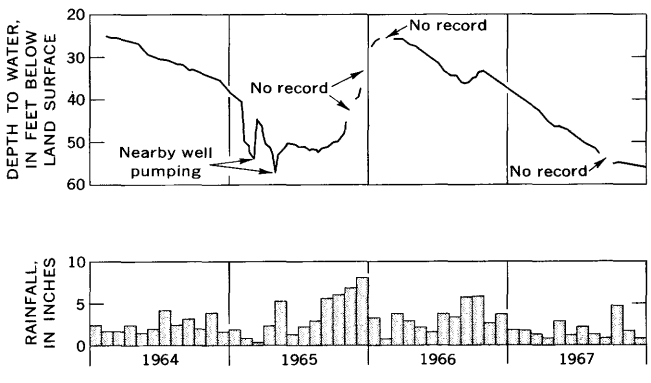

Figure 7.—Water level in well USGS-1 in Turpentine Run basin and rainfall at National Weather Service gage, Estate Fort Mylner, St. Thomas, 1964–67.

green-leafed trees adjacent to a stream to visualize the interception of ground water and also of streamflow. Observation of depletion of flow in a reach of Bonne Resolution Gut indicated that a strip of trees about 100 feet wide on each side of the stream (shown by greener foliage during dry periods) was intercepting water from the stream alone at an estimated rate of 1 million gallons per acre annually. The amount of ground water intercepted in addition was unknown.

The effect of rainfall on the water regime is considered to be short term in regard to the mountain basins, an effect that can be measured in terms of a few years rather than in decades. There appear to be two causes for this short-term effect: (1) the small storage capacity of the aquifer, and (2) the small size of the basin and its aquifer. The result is that a relatively small volume of rainfall is needed to replenish a basin aquifer—to top it off, so to speak. But, at the same time, the small volume of storage is not capable of maintaining streamflow for any prolonged length of time. It can do so for several months, as shown in figure 8 for Bonne Resolution Gut, where in 1963 there were 2 months of relatively high flow but monthly rainfall was less than ½ inch. There is, as one would expect, a definite relationship between rainfall and annual runoff, which also is illustrated in figure 8.

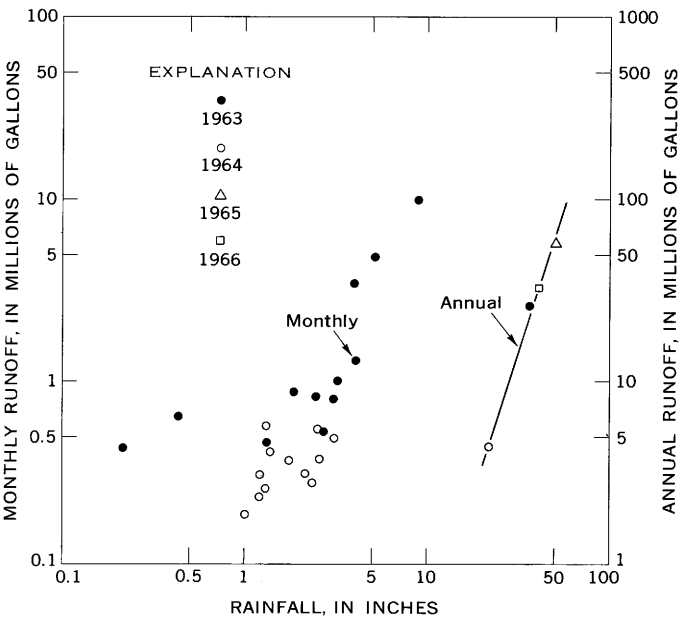

Figure 8.—Rainfall-runoff relation of Bonne Resolution Gut, St. Thomas. (Rainfall at National Weather Service gage, Estate Dorothea.)

SUMMARY

The historic and prehistoric water regime of the mountain basins of the Virgin Islands can only be surmised. There is evidence that water once was more abundant than at present and also that a major change has occurred since the turn of the century.

The lesser change in the water regime is attributed to climatic changes, in particular to a decline in rainfall. The mountain basins, with their small area and small ground-water storage capacity, are particularly sensitive to variation in rainfall, in terms of streamflow and ground-water levels. A decline in rainfall means less frequent topping off of the aquifer.

The greater change in the water regime is attributed to changes in land use. Since the turn of the century, thousands of acres have reverted from pasture and cropland to brush and second-growth forest. Transpiration by deep-rooted brush is believed to be responsible for reduction in ground-water recharge, resulting in a decline of ground-water levels, and, as a consequence, a reduction in the base flow of streams.

REFERENCES

Fairbridge, R. W., 1960, The changing level of the sea: Sci. American, May 1960, 11 p., 8 figs.

Johnson, A. F., 1936a, Water supply for St. Thomas, Virgin Islands: U.S. Bur. Reclamation open-file report, 26 p.

——1936b, Preliminary report on the water supplies for properties managed by the Virgin Islands Company, St. Croix, Virgin Islands: U.S. Bur. Reclamation open-file report, 77 p., 2 pls.

Knox, J. P., 1852, An historical account of St. Thomas, W. I.: New York, C. Scribner & Co., 271 p.

ESTIMATING LOW-FLOW CHARACTERISTICS OF STREAMS IN SOUTHEASTERN MASSACHUSETTS FROM MAPS OF GROUND-WATER AVAILABILITY

By GARY D. TASKER, Boston, Mass.

Prepared in cooperation with the Massachusetts Water Resources Commission

Abstract.—In southeastern Massachusetts the annual minimum 7-day mean flow at the 2- and 10-year recurrence intervals are significantly related, with a standard error of estimate of 50 and 70 percent, respectively, to the drainage area and the average ground water available from wells in the basin. Although a geographical bias is evident, errors in estimates of low-flow characteristics based solely on drainage area can be significantly reduced by also considering the average ground water available from wells in the basin.

A method of estimating low-flow characteristics of ungaged streams from basic geologic factors is based on low-flow measurements and ground-water availability maps resulting from recent water-resources investigations in the Taunton River basin (Williams and others, 1972) and in coastal drainage basins of southeastern Massachusetts (J. R. Williams and G. D. Tasker, unpub. data) (fig. 1). The region is characteristically of low relief; the rounded, glacier-scoured hills as much as 450 feet above sea level are separated by narrow to broad stream valleys. The southeastern part is a broad plain. Consolidated rock consists of older granitic intrusive rocks in the north and south and a central zone of younger sedimentary rocks of the Narragansett basin (Quinn and Oliver, 1962). The consolidated rock has been eroded by streams and is mantled with a few feet to several hundred feet of unconsolidated deposits of Tertiary age along Cape Cod Bay and by glacial drift of Quaternary age (Schaefer and Hartstrom, 1965). The consolidated rocks and unconsolidated deposits of Tertiary age are mantled with silty till deposited as ground moraine by the Cape Cod and Buzzards Bay lobes of the glaciers that advanced south-southeastward to end moraines on Martha's Vineyard and Nantucket. Retreat of these glacial lobes caused deposition of recessional moraines bordered by broad outwash plains in the southeastern part of the region, valley-train outwash in the narrower valleys, small to large glacial lakes characterized by fine-grained bottom deposits and sand deltaic deposits, ice-contact deposits, and eskers (Williams and Willey, 1972).

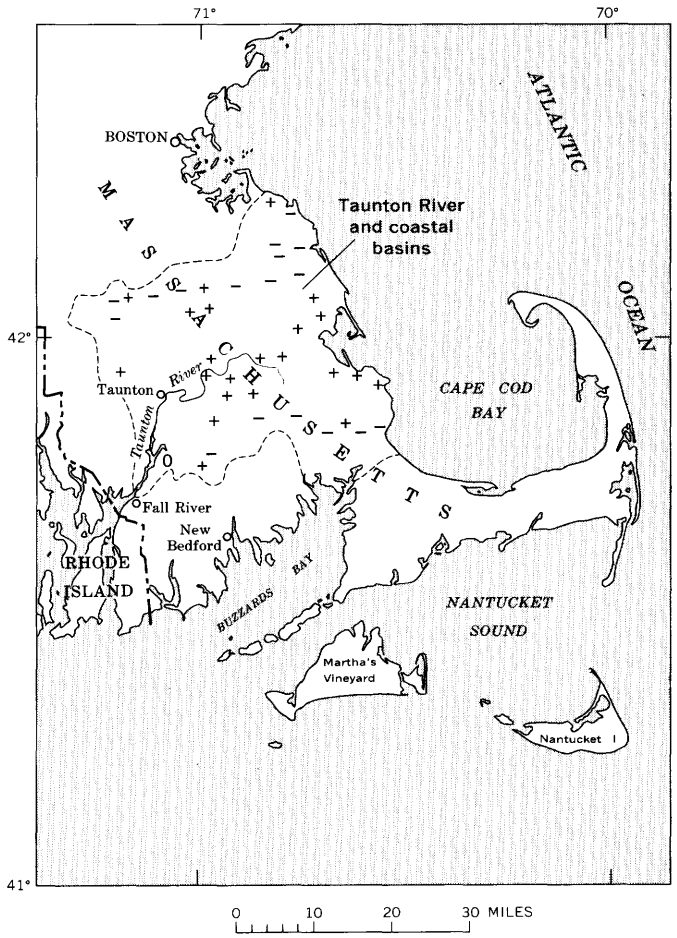

Figure 1.—Map of southeastern Massachusetts. Signs of residuals of Q_2 (table 1) are shown near the center of each basin. Zero indicates a residual of Q_2 of zero.

The coarser grained deposits laid down during retreat of the glaciers are the principal aquifers of the region.

U.S. GEOL. SURVEY PROF. PAPER 800-D, PAGES D217-D220

LOW-FLOW CHARACTERISTICS

Low-flow characteristics of streams are related both to the climate and to the geologic features of an area. By studying a relatively small area in which variations in climatologic parameters are small (mean annual precipitation ranges from 44 inches near the northern boundary to 46 inches near the southern boundary) and landforms are similar, one can minimize the influence of certain factors and amplify those influenced by the structure and lithology of the shallow geologic formations.

Many of the geologically related factors influencing the magnitudes of low flows, such as ground-water storage, infiltration capacity, and the ability of the aquifer to transmit water, are the same factors that influence the amount of ground water available from wells. For this reason low-flow characteristics can be represented by the average ground water available from wells. Maps showing the availability of ground water by Williams and others (1972) and J. R. Williams and G. D. Tasker (unpub. data) define areas where properly designed and constructed wells generally will yield (a) more than 300 gpm (gallons per minute), (b) between 100 and 300 gpm, (c) less than 100 gpm, and (d) an area of till and bedrock where virtually no water is available from stratified drift. These areas were defined from logs of wells and borings, pumping tests, seismic refraction methods, and a knowledge of the stratigraphy of glacial landforms and their history of deposition. Typically, the higher yielding areas are close to the stream channels and the lower yielding areas are close to the drainage divide. This generalization of the geologic influence on low flows allows the definition of a single ground-water factor based on maps of the availability of ground water as follows:

$$G = \frac{500 \times A_{300} + 300 \times A_{100-300} + 100 \times A_{100} + 0 \times A_0}{A_{300} + A_{100-300} + A_{100} + A_0}, \quad (1)$$

where

G is the ground-water factor,

A_{300} is the area within the basin where properly designed and constructed wells generally will yield more than 300 gpm,

$A_{100-300}$ is the area within the basin where properly designed and constructed wells generally will yield between 100 and 300 gpm,

A_{100} is the area within the basin where properly designed and constructed wells generally will yield less than 100 gpm, and

A_0 is the area of till and bedrock; no water available from stratified drift.

The constant multipliers in the numerator of equation 1 are selected to weigh the formula in favor of the higher yielding areas. The values of 500, 300, 100, and 0 are roughly equal to 1 percent of the average transmissivity in the A_{100}, $A_{100-300}$, A_{100}, and A_0 areas, respectively. Therefore, the ground-water factor is a rough approximation of the average transmissivity, in hundreds of gallons per day per foot, of the basin.

The annual minimum 7-day mean flow at the 2- and 10-year recurrence intervals, Q_2 and Q_{10}, respectively, for each basin were determined by comparison of base-flow discharge measurements with long-term gaging station records as a part of the water-resources investigations in the area. Estimates of low-flow characteristics in the Taunton River basin (table 1, station numbers 01106460–01109050) are based on seven or eight measurements in the 1966–68 water years. Estimates for station numbers 01105635–01105895 were based on six or seven measurements made in the 1969–71 water years. Stations with less than 1 square mile of drainage area and those subject to substantial regulation or diversion were not used.

REGRESSION ANALYSIS

Regression analysis (Riggs, 1968) is used to assess the amount of variation in the dependent variables Q_2 and Q_{10} caused by the independent variables, drainage area and ground-water factor. The regression equation and the standard error of estimate, using the most significant independent variable, are calculated, and then the regression equation and standard error of estimate, using both independent variables, are calculated.

To avoid zero flows, 0.1 cfs (cubic foot per second) was added to the discharges, and discharge and drainage area were converted to logarithmic units so that the regression equations summarized in table 2 are of the form:

$$\log(Q + 0.1) = a + b_1 \log A + b_2 G, \quad (2)$$

where

Q is Q_2 or Q_{10},

a is the regression constant,

b_1 is the regression coefficient for A,

b_2 is the regression coefficient of G,

A is the drainage area, and

G is the ground-water factor.

It is apparent from table 2 that substantially better estimates of Q_2 and Q_{10} at ungaged sites can be made by using ground-water availability in addition to drainage area. Q_2 was found to have the highest partial correlation with drainage area, and Q_{10} had the highest partial correlation with the ground-water factor. In both applications the addition of the second independent variable made a substantial reduction in the standard error of estimate; and, evidently, the ground-water factor, as well as the drainage area, exerts a pronounced influence upon the areal variation in low-flow characteristics in southeastern Massachusetts. The graphical representation of the regression equation for Q_2 illustrates the great effect of the availability of ground water upon low-flow characteristics

Table 1.—*Drainage area, annual minimum 7-day mean flow at 2- and 10-year recurrence intervals, and ground-water factor of southeastern Massachusetts streams*

Station No., name, and location		Drainage area, A (sq mi)	Annual minimum 7-day mean flow (cfs)						Ground-water factor, G
			2-year low-flow recurrence			10-year low-flow recurrence			
			Estimated from base-flow measurements	Computed from equation 2	Residuals (variation in estimated from computed values)	Estimated from base-flow measurements	Computed from equation 2	Residuals (variation in estimated from computed values)	
01105630	Crooked Meadow River near Hingham	5.00	0.60	0.53	+0.07	0.20	0.22	−0.02	92
01105660	Bound Brook near Cohasset	4.88	.10	.46	−.36	.0	.17	−.17	73
01105700	Indian Head Brook near Hanson	4.39	.50	.72	−.22	.20	.37	−.17	170
01105805	Pudding Brook at North Pembroke	4.53	.50	.63	−.13	.30	.30	.0	140
01105810	Third Herring Brook at Hanover	9.85	.40	1.31	−.91	.0	.55	−.55	117
01105820	Second Herring Brook at Norwell	3.22	.30	.20	+.10	.0	.05	−.05	29
01105830	First Herring Brook near Scituate	1.72	.02	.06	−.04	.0	.0	.0	33
01105845	South River at Marshfield	7.48	2.00	.86	+1.14	1.50	.35	+1.15	95
01105860	Jones River Brook at North Plympton	3.57	.90	.84	+.06	.60	.50	+.10	236
01105872	Halls Brook at Kingston	4.21	1.60	.94	+.66	1.20	.54	+.66	224
01105874	Town Brook at Plymouth	9.00	11.0	8.98	+2.02	9.00	7.10	+1.90	500
01105876	Eel River near Plymouth	14.7	18.0	12.9	+5.10	15.0	9.10	+5.90	475
01105878	Beaver Dam Brook at White Horse Beach	5.50	6.00	5.46	+.54	5.00	4.68	+.32	500
01105883	Herring River at Bournedale	7.70	4.00	7.66	−3.66	2.50	6.22	−3.72	500
01105886	Red Brook near Buzzards Bay	9.80	4.00	9.78	−5.78	2.00	7.63	−5.63	500
01105890	Agawam River at East Wareham	17.0	25.0	17.0	+8.00	20.0	12.1	+7.90	500
01105892	Wankinco River at Wareham	20.5	12.0	12.3	−.30	8.00	7.37	+.63	400
01105895	Weweantic River at South Wareham	56.1	15.0	22.3	−7.30	10.0	10.2	−.20	320
01106460	Beaver Brook near East Bridgewater	9.43	.77	.72	+.05	.24	.23	+.01	19
38	Meadow Brook at Union St., East Bridgewater.	6.24	.21	.48	−.27	.03	.16	−.13	34
01107000	Dorchester Brook near Brockton	4.67	.26	.33	−.07	.02	.10	−.08	31
01107050	Hockomock River near West Bridgewater	20.4	2.40	2.05	+.35	.81	.72	+.09	58
37	West Meadow Brook near Brockton	1.98	.19	.18	+.01	.06	.07	−.01	115
01107150	Raven Brook near Halifax	3.59	1.20	.44	+.76	.61	.20	+.41	125
01107180	Winnetuxet River near Halifax	31.3	14.0	6.32	+7.68	7.50	2.62	+5.12	189
01107220	Fall Brook at East Freetown	13.1	1.20	1.65	−.35	.40	.66	−.26	104
01107250	Black Brook near North Rochester	7.44	.31	.70	−.39	.03	.26	−.23	61
01107400	Fall Brook near Middleboro	9.34	2.80	1.40	+1.40	1.30	.62	+.58	140
01107900	Purchade Brook near Middleboro	3.12	1.00	.52	+.48	.51	.28	+.23	180
01108110	Snows Brook near North Middleboro	2.71	.45	.26	+.19	.17	.10	+.07	101
01108140	Poquoy Brook near North Middleboro	8.30	2.60	1.47	+1.13	1.20	.71	+.49	172
01108240	Dam Lot Brook near Taunton	2.97	.34	.20	+.14	.12	.05	+.07	45
01108280	Forge River near Taunton	9.19	2.10	1.40	+.70	.91	.63	+.28	143
01108300	Canoe River at East Foxboro	1.61	.14	.13	+.01	.07	.04	+.03	114
01108340	Poquanticut Brook near North Easton	4.48	.28	.40	−.12	.15	.15	.0	70
01108600	Hodges Brook at West Mansfield	3.72	.07	.31	−.24	.03	.11	−.08	64
39	Chartly Brook near Attleboro	1.40	.13	.06	+.07	.07	.0	+.07	76
01109020	Rumford River at East Foxboro	5.09	.57	.84	−.27	.32	.42	−.10	167
01109080	Assonet River near Assonet	16.2	2.30	1.62	+.68	.88	.58	+.30	59
01109090	Rattlesnake Brook near Assonet	4.22	.27	.27	.0	.08	.07	+.01	19

(fig. 2). The regression coefficients were found to be statistically significant at the 0.01 level.

The plot of Q_2 computed from the regression equation against Q_2 estimated from low-flow measurements (fig. 3) shows that the equation holds throughout a wide range in magnitude of Q_2. The residuals in table 1 show an apparent geographical bias. The plot of the algebraic sign of the residuals of Q_2 in figure 1 shows a predominance of minus signs near the northern and southern boundaries, where bedrock is near the surface but is mantled by thin till and undifferentiated stratified drift. The bias may be attributed to the arbitrary way in which the ground-water factor was defined, the fact that the ground-water factor does not consider all the effects of geology upon low flow, and poor definition of drainage areas in the southeastern quarter of the area.

Even with the apparent bias of the regression equations, the reliability of estimates of low-flow characteristics in southeast-

Table 2.—*Summary of regression analysis*

[Refer to equation 2]

Dependent variable	Constants			Standard error	
	Regression coefficient for A b_1	Regression coefficient for C b_2	Regression constant a	Percent	Percent change
Q_2	1.39	.....	−1.030	105	...
	1.00	0.0022	−1.101	55	50
Q_{10}	....	.0036	−.806	105	...
	.83	.0028	−1.340	70	35

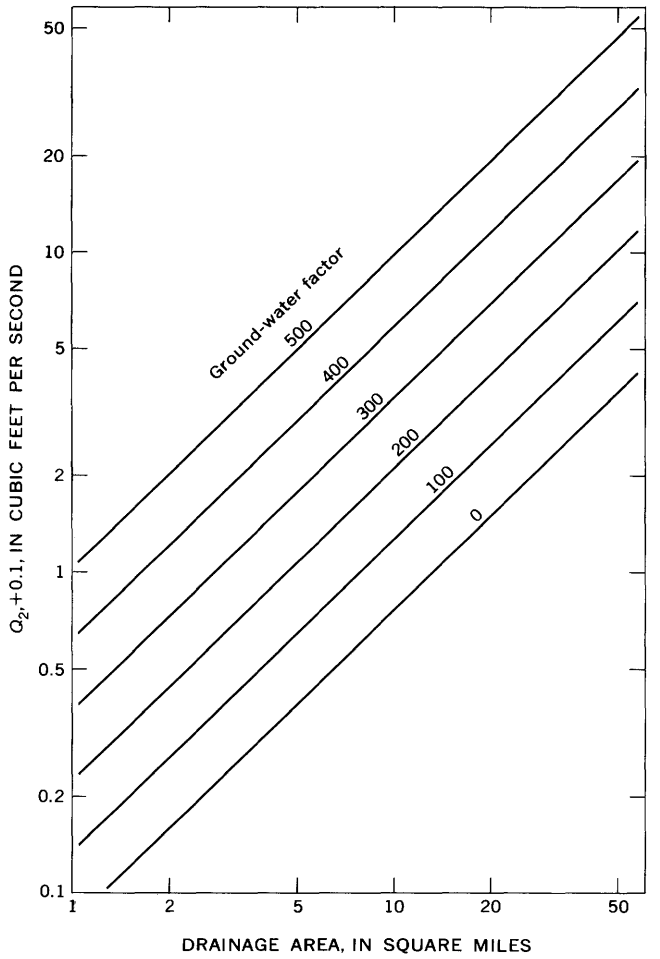

Figure 2.—Relation between Q_2 + 0.1, drainage area, and ground-water factor, where Q_2 is the annual minimum 7-day mean flow at the 2-year recurrence interval.

ern Massachusetts at ungaged sites, based on drainage area, can be significantly improved by also considering the amount of ground water available from wells.

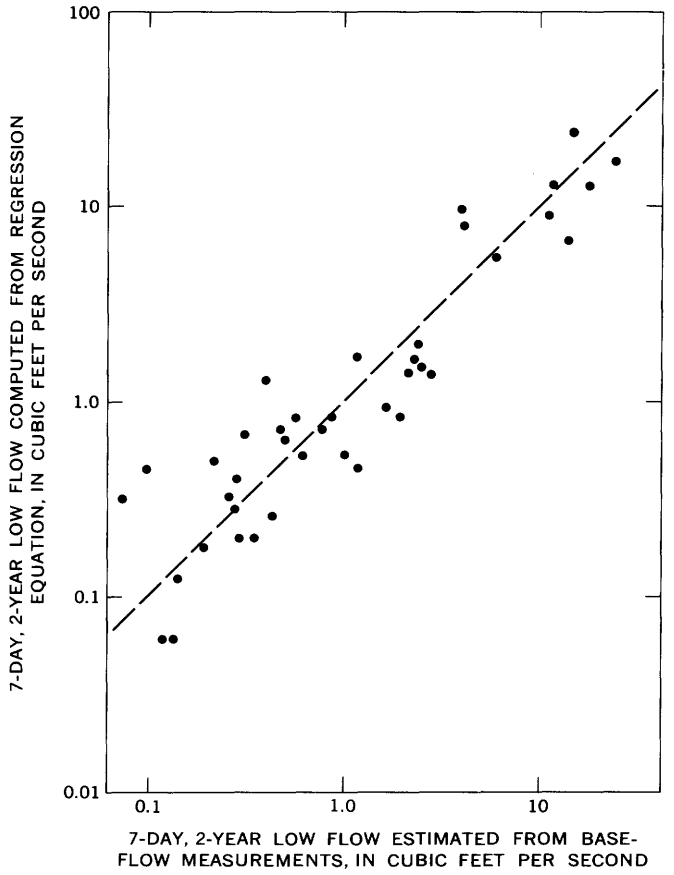

Figure 3.—Relation between Q_2 computed from regression equation and Q_2 estimated from base-flow measurements.

ACKNOWLEDGMENT

The help of J. R. Williams in describing the geology of the area is gratefully acknowledged.

REFERENCES

Quinn, A. W., and Oliver, W. A., Jr., 1962, Pennsylvanian rocks of New England, *in* Pennsylvanian System in the United States—A symposium: Tulsa, Okla., Am. Assoc. Petroleum Geologists, p. 60–73.

Riggs, H. C., 1968, Some statistical tools in hydrology: U.S. Geol. Survey Tech. Water-Resources Inv., book 4, chap. A1, 39 p.

Schafer, J. P., and Hartshorn, J. H., 1965, The Quaternary of New England, *in* Wright, H. E., and Frey, D. G. (eds.), The Quaternary of the United States—a review volume for the VII Congress of the International Association for Quaternary Research: Princeton, N.J., Princeton Univ. Press. p. 113–128.

Williams, J. R., Farrell, D. F., and Willey, R. E., 1972, Water resources of the Taunton River basin, southeastern Massachusetts: U.S. Geol. Survey Hydrol. Inv. Atlas HA-460. [In press]

Williams, J. R., and Willey, R. E., 1972, Bedrock topography and texture of unconsolidated deposits, Taunton River basin, southeastern Massachusetts: U.S. Geol. Survey Misc. Geol. Inv. Map I-742. [In press]

A METHOD FOR RAPID AND RELIABLE SCRAPING OF PERIPHYTON SLIDES

By L. J. TILLEY, Menlo Park, Calif.

Abstract.—The use of clean glass slides as a scraping tool proved to be a fast and efficient method for removal of periphyton collected on clean glass substrates. Average time to remove 99.8 percent of the periphyton from a slide was 1¼ minutes. Use of glass slides as substrates permits rapid and accurate checking of removal efficiency.

Many applications of periphyton methods in water-quality investigations require removal of the growth from a test substrate. Existing procedures for periphyton removal were found to be either too slow, ineffective, or to require the use of relatively expensive equipment. The method described below was developed while the U.S. Geological Survey was cooperating with the Municipality of Metropolitan Seattle (Metro) in a comprehensive study of the water quality of the Duwamish River estuary, Seattle, Wash.

Sampling was done by controlled exposure of artificial substrates (1- by 3-inch glass microscope slides) placed in specially fabricated slide holders. These in turn were placed either on floats, on the stream bottom, or on wooden staffs, depending on the stream conditions at the sampling points. All slides were oriented so that their faces remained vertical. Because only one investigator was available to collect and analyze about 75 samples a week, time spent in the laboratory had to be minimized.

Even though measuring quantities of periphyton in samples has not been standardized, several generalized methods have been used, such as direct counts of organisms, gravimetric (dry-weight) measurement, and plant-pigment analysis. Because apparatus for plant-pigment analysis was available at the start of the study and because autotrophic growth was primarily to be determined, it was decided to measure periphyton quantity by using the plant-pigment analysis.

Early results showed that laboratory time could be shortened only during the process of removing the periphyton from the slides. Neilson (1953), Grzenda and Brehmer (1960), King and Ball (1966), and Kevern, Wilhm, and Van Dyne (1966) all scraped slides, but they apparently were not concerned with removal time nor did they report scraping efficiency. Rubber laboratory chasers used by some investigators for removing periphyton proved to be too time consuming. King and Ball (1966) used pieces of hard rubber to remove periphyton from Plexiglas substrates, and Weber and Rasche (1966) used razor blades to scrape dried periphyton growth from glass substrates. Other investigators did not report the tool used to scrape substrates, while McConnell and Sigler (1959) and Waters (1961) extracted pigments by immersing the whole substrate (cement cylinders on rocks) in the extraction medium. Direct extraction was not used during this investigation because of the complete lack of cell disruption. Strickland and Parsons (1968) and the American Public Health Association and others (1971) recommend disruption of cells for pigment extraction.

In any case, other periphyton methods require complete removal of the growth from slides before analysis. Although the simple, rapid, and reliable method reported herein is used for pigment extraction, it is applicable for all measurements requiring removal of growth accumulation for analysis.

PROCEDURE

The microscope slides retrieved from the river were placed vertically in standard slide boxes as they were collected. The boxes were left open until the slides were nearly air dry, then placed in a secure position in the field vehicle so that jostling and vibration of the slides during the ride to the laboratory was minimized.

In the laboratory, the slides were placed in distilled water in Pyrex evaporating dishes (90 by 50 mm) long enough to allow them to become thoroughly wetted (15 to 20 minutes). Water was used so as to bring all slides to the same degree of wetness. Wet extraction is considered to be more efficient than dry extraction (Strickland and Parsons, 1968, p. 187). After the water was carefully poured out of the dishes and the slides were removed, the dishes were rinsed thoroughly with distilled water and shaken to rid them of excess drops of water. The slides were then replaced in the dishes and a few drops of 90-percent acetone were spread over them to begin extraction of pigments and to help loosen the periphyton from the slides. (Acetone is used only when pigments are to be estimated; drops of distilled water can be used in other cases.) Clean glass microscope slides were used to scrape off the encrusted

U.S. GEOL. SURVEY PROF. PAPER 800-D, PAGES D221-D222

periphyton from the sample slides. The edge of the clean slide, which was held at an oblique angle, was repeatedly run down the entire length of the periphyton slide until all visible signs of periphyton had been removed. Then both slides were rinsed with not more than 10 ml (milliliters) of 90-percent acetone solution to produce a pigment-acetone solution. This solution was then transferred to a centrifuge tube (10-ml capacity), which was shaken vigorously and then refrigerated overnight in the dark.

Chlorophylls a, b, and c and carotenoids in the pigment-acetone solutions were determined by using a Beckman (Model b) spectrophotometer, as described by Strickland and Parsons (1968, p. 185–192).

TESTS FOR RAPIDITY AND EFFICIENCY

The average cleaning time determined from the cleaning of 54 slides was 1.14 minutes per slide. Cleaning time was measured from the first spreading of acetone over a slide to the placing of the pigment-acetone solution in the refrigerator. Average cleaning time when rubber chasers were used was about 15 minutes per slide.

Cell counts per square millimeter (mm^2) of six unscraped slides were compared with the combined counts of residual cells on the scraped slides and on the slides used for scraping. The comparison shows an average 99.8-percent removal of cells and colonies from scraped slides, as shown in table 1.

Table 1.–*Test of removal efficiency by microscopic examination*

Slide number	Cells and colonies on unscraped slides (counts/mm^2)	Cells and colonies on scraped plus scraping slides (counts/mm^2)	Percentage removal
1	22.5	0.18	99.2
2	168.5	.18	99.9
3	1,033.4	.11	100.0
4	59.7	.08	99.9
5	1,333.1	.29	100.0
6	462.1	.76	99.8
Average			99.8

REFERENCES

American Public Health Association and others, 1971, Standard methods for the examination of water and wastewater [13th ed.]: New York, Am. Public Health Assoc., Inc., 874 p.

Grzenda, A. R., and Brehmer, M. L., 1960, A quantitative method for the collection and measurement of stream periphyton: Limnology and Oceanography, v. 5, no. 2, p. 190–194.

Kevern, N. R., Wilhm, J. L., and Van Dyne, G. M., 1966, Use of artificial substrate to estimate the productivity of periphyton: Limnology and Oceanography, v. 11, no. 4, p. 499–502.

King, D. L., and Ball, R. C., 1966, A qualitative and quantitative measure of aufwuchs production: Am. Microscop. Soc. Trans., v. 58, no. 2, p. 232–240.

McConnell, W. J., and Sigler, W. F., 1959, Chlorophyll and productivity in a mountain river: Limnology and Oceanography, v. 4, no. 2, p. 335–351.

Neilson, R. S., 1953, Apparatus and methods for collection of attachment materials in lakes: Progressive Fish Culturist, v. 15, no. 2, p. 87–89.

Strickland, J. D. H., and Parsons, T. R., 1968, A practical handbook of seawater analysis: Fisheries Research Board Canada Bull. 167, 311 p.

Waters, T. F., 1961, Notes on the chlorophyll method of estimating the photosynthetic capacity of stream periphyton: Limnology and Oceanography, v. 6, no. 4, p. 486–488.

Weber, C. I., and Rasche, R. L., 1966, Use of floating periphyton samples for water pollution surveillance: Water Pollution Surveillance System Application and Devel. Rept. 20, Federal Water Pollution Control Administration, 22 p.

SUBJECT INDEX

[For major headings such as "Economic geology," "Geochronology," "Limnology," see under State names or refer to table of contents]

AUTHOR INDEX